T.C.

YEDİTEPE UNIVERSITY

INSTITUTE OF HEALTH SCIENCES

DEPARTMENT OF PHARMACOGNOSY

ISOLATION OF CYTOTOXIC COMPOUNDS FROM *GLYCYRRHIZA GLABRA* AND *G. ICONICA* AND INVESTIGATION OF THEIR MECHANISMS OF ACTION

DOCTOR OF PHILOSOPHY THESIS

DİCLE ÇEVİK, Pharm.

İstanbul-2019

T.C.

YEDİTEPE UNIVERSITY

INSTITUTE OF HEALTH SCIENCES

DEPARTMENT OF PHARMACOGNOSY

ISOLATION OF CYTOTOXIC COMPOUNDS FROM *GLYCYRRHIZA GLABRA* AND *G. ICONICA* AND INVESTIGATION OF THEIR MECHANISMS OF ACTION
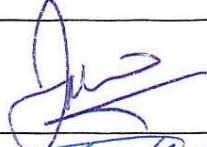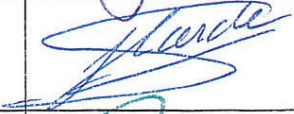
DOCTOR OF PHILOSOPHY THESIS

DİCLE ÇEVİK, Pharm.

SUPERVISOR

Prof. Dr. Hasan KIRMIZIBEKMEZ

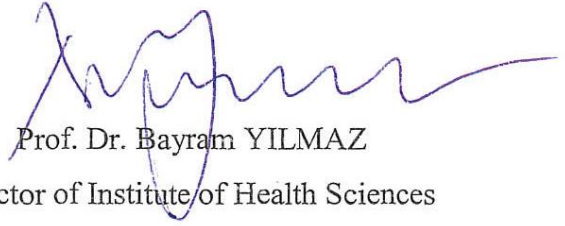İstanbul-2019

THESIS APPROVAL

Institute : Yeditepe University Institute of Health Sciences

Programme : Pharmacognosy

Title of the Thesis : Isolation of Cytotoxic Compounds from *Glycyrrhiza glabra* and

G. iconica and Investigation of Their Mechanisms of Action

Owner of the Thesis : Dicle Çevik

Examination Date : 21/02/2019

This study has been approved as a Doctorate Thesis in regard to content and quality by the Jury.

	Title, Name-Surname	Signature
Chair of the Jury:	Prof. Dr. Erdem Yeşilada Yeditepe University	
Supervisor:	Prof. Dr. Hasan Kırmızıbekmez Yeditepe University	
Member:	Prof. Dr. Fatih Demirci Anadolu University	
Member:	Assoc. Prof. Dr. Hande Sipahi Yeditepe University	
Member:	Dr. Hilal Bardakçı Acıbadem University	

APPROVAL

This thesis has been deemed by the jury in accordance with the relevant articles of Yeditepe University Graduate Education and Examinations Regulation and has been approved by Administrative Board of Institute with decision dated .01./.03./.2019. and numbered .2019./.04-01.

Prof. Dr. Bayram YILMAZ

Director of Institute of Health Sciences

DECLARATION

I hereby declare that this thesis is my own work and that, to the best of my knowledge and belief, it contains no material previously published or written by another person nor material which has been accepted for the award of any other degree except where due acknowledgment has been made in the text.

21/02/2019

Dicle Çevik

DEDICATION

This thesis is dedicated to my family with love…

ACKNOWLEDGEMENTS

TABLE OF CONTENTS

LIST OF TABLES

LIST OF FIGURES

LIST OF SPECTRA

LIST OF SYMBOLS and ABBREVIATIONS

1D	1-Dimensional
2D	2-Dimensional
Ac	Acetyl
Acet	Acetoxy
ALP	Alkaline Phosphatase
ALT	Alanine Aminotransferase
AP-1	Activator Protein-1
Apaf-1	Apoptotic Protease-Activating Factor-1
Api	Apiose
Ara	Arabinose
AST	Aspartate Aminotransferase
Bak	Bcl-2 Homologous Antagonist Killer
Bax	Bcl-2 Associated X
Bcl-2	B-Cell Lymphoma-2
Br	Broad
BuOH	Butanol
Caspase	Cysteinyl Aspartate Specific Proteinase
Calcd	Calculated
CC	Column Chromatography
CCl_4	Carbon Tetrachloride
CD_3OD	Deuterated Methanol
$CDCl_3$	Deuterated Chloroform
CDK	Cyclin Dependent Kinases
CH_2Cl_2	Dichloromethane
$CHCl_3$	Chloroform
COSY	Correlation Spectroscopy
COX	Cyclooxygenase
d	Doublet
DMEM	Dulbecco's Modified Eagle's Medium
DMSO	Dimethyl Sulfoxide
DR4	Death Receptor 4

EAT	Ehrlich Ascites Tumor
ER	Estrogen Receptor
EtOAc	Ethyl acetate
EtOH	Ethanol
F	Fluorescence indicator
FACS	Fluorescence Activated Cell Sorting
FBS	Fetal Bovine Serum
Fr / Frs	Fraction / Fractions
Gal	Galactose
gCH$_3$COOH	Glacial Acetic Acid
Glc	Glucose
GlcA	Glucuronic acid
GOT	Glutamate Oxalate Transaminase
GPT	Glutamate Pyruvate Transaminase
GSH	Glutathione
GSH-Px	Glutathione Peroxidase
GST	Glutathione S-transferase
H$_2$O	Water
HCC	Hepatocellular Carcinoma
HCl	Hydrochloric Acid
HCOOH	Formic Acid
HEGU	*n*-Hexane/EtOH Extract (9:1) of *Glycyrrhiza uralensis*
HMBC	Heteronuclear Multi-Bond Correlation
HPLC	High Performance Liquid Chromatography
HR-ESI-MS	High Resolution-Electrospray Ionisation- Mass Spectrometry
HSQC	Heteronuclear Single Quantum Coherence
IC$_{50}$	The Half Maximal Inhibitory Concentration
iNOS	Inducible Nitric Oxide Synthase
i.p.	Intraperitoneal
IR	Infrared Spectroscopy
Isopre	Isoprenyl
LDH	Lactate Dehydrogenase
LOX	Lipooxygenase

LPLC	Low Pressure Liquid Chromatography
LPS	Liposaccharide
m	Multiplet
Malo	Malonyl
MDA	Malondialdehyde
Mdm2	Mouse Double Minute 2
MeCN	Acetonitrile
MeOH	Methanol
MIC	Minimum Inhibitory Concentration
MPLC	Medium Pressure Liquid Chromatography
MS	Mass Spectrometry
mTOR	Mammalian Target of Rapamycin
MW	Molecular Weight
NF-κB	Nuclear Factor kappa B
NI	No Inhibition
NMR	Nuclear Magnetic Resonance
NOESY	Nuclear Overhauser Enhancement Spectroscopy
Nrf2	Nuclear Erythroid-Related Factor 2
$NTiO_2$	Titanium Dioxide Nanoparticles
PARP	Poly (ADP-ribose) Polymerase
PBS	Phosphate Buffered Saline
PGE_2	Prostaglandin E_2
PI	Propidium Iodide
PPAR-γ	Peroxisome Proliferator-Activated Receptor γ
pRb	Retinoblastoma Protein
PTP1B	Protein Tyrosine Phosphatase 1B
Rb	Retinoblastoma
Rha	Rhamnose
rH_2O	Remaining H_2O
RT-CES	Real Time-Cell Electronic Sensing
s	Singlet
Sh	Shoulder
SiO_2	Silica Gel

SOD	Super Oxide Dismutase
SRB	Sulforhodamine B
TBX$_2$	Thromboxane B$_2$
TCA	Trichloroacetic Acid
TCM	Traditional Chinese Medicine
TLC	Thin Layer Chromatography
TNF	Tumor Necrosis Factor
TP	Total Protein
TRAIL	Tumor Necrosis Factor-Related Apoptosis- Including Ligand
UV	Ultraviolet
†	Overlapping Signals

ABSTRACT

Çevik, D. (2019). Isolation of Cytotoxic Compounds from *Glycyrrhiza glabra* and *G. iconica* and Investigation of Their Mechanisms of Action. Yeditepe University, Institute of Health Sciences, Department of Pharmacognosy, Ph.D. Thesis, İstanbul.

Glycyrrhiza L. (licorice) species are one of the most widely used plants worldwide for their various pharmacological activities. In recent years, secondary metabolites of licorice are gaining much attention especially due to their significant cytotoxic and antitumor effects. The aim of this study was to isolate the potential cytotoxic secondary metabolites from roots of *G. glabra* L. and *G. iconica* Hub.-Mor. through bioactivity-guided fractionation procedure and to elucidate their mechanisms of action. The crude MeOH extracts of *G. glabra* (IC_{50} = 18.9 - 33.6 µg/mL) and *G. iconica* (IC_{50} = 4.3 - 12.7 µg/mL) remarkably inhibited cell proliferation in hepatocelullar (Huh7), breast (MCF7) and colorectal (HCT116) cancer cell lines. Chromatographic separations conducted on the active subextracts of *G. glabra* ($CHCl_3$ and EtOAc) and *G. iconica* ($CHCl_3$, EtOAc and *n*-BuOH) yielded 28 different secondary metabolites including a new α,β-dihydroxychalcone, namely iconichalcone (**1**). The underlying mechanisms of the most active isolates tetrahydoxymethoxychalcone (**2**), 4′-*O*-methylglabridin (**16**) and glabrene (**20**) from *G. glabra* and **2**, licoricidin (**18**), dehydroglyasperin C (**21**), iconisoflaven (**22**) and 1-methoxyficifolinol (**27**) from *G. iconica* with regard to real time-bioactivity (RT-CES) assay were investigated by Hoechst staining, cell cycle (FACS) and Western blot assays in most sensitive Huh7 cells. Compounds **2**, **16**, **18**, **20**, **21**, **22** and **27** induced apoptosis by caspase activation, increased apoptotic $subG_1$ populations and caused cell cycle arrests at G_1 and/or G_2/M phases in liver cancer cells. In addition, **21** showed increase in the expression of tumor supressor gene p53, while **2** displayed condensed nuclei in Hoechst staining assay indicating apoptotic cell death morphologically in Huh7 cells. Thus, aforementioned compounds particularly **2** and **21** established very promising results and could be potential lead molecules which deserve further *in vivo* and clinical investigations for anticancer drug development especially against hepatocellular carcinoma.

Key Words: *Glycyrrhiza glabra*, *Glycyrrhiza iconica*, cytotoxic activity, Huh7, apoptosis

ÖZET

Çevik, D. (2019). *Glycyrrhiza glabra* **ve** *G. iconica* **Bitkilerinden Sitotoksik Etkili Bileşiklerin İzolasyonu ve Etki Mekanizmalarının Araştırılması. Yeditepe Üniversitesi, Sağlık Bilimleri Enstitüsü, Farmakognozi ABD, Doktora Tezi, İstanbul.**

Glycyrrhiza L. (meyan) türleri, çeşitli farmakolojik aktivitelerinden dolayı dünya çapında en yaygın kullanılan bitkilerden biridir. Son yıllarda, meyandan elde edilen sekonder metabolitler, özellikle önemli sitotoksik ve antitümör etkileri nedeniyle ilgi çekmektedir. Bu çalışma ile *G. glabra* L. ve *G. iconica* Hub.-Mor. türlerinin köklerinden biyoaktivite rehberli fraksiyonlama tekniği kullanılarak sitotoksik etkili sekonder metabolitlerin eldesi ve etki mekanizmalarının aydınlatılması amaçlanmıştır. *G. glabra* (IC_{50} = 18.9 - 33.6 µg/mL) ve *G. iconica* (IC_{50} = 4.3 - 12.7 µg/mL)'dan elde edilen ham MeOH ekstreleri hepatosellüler (Huh7), meme (MCF7) ve kolorektal (HCT116) kanser hücre serilerine karşı önemli derecede sitotoksisite göstermiştir. *G. glabra* ($CHCl_3$ ve EtOAc) ve *G. iconica* ($CHCl_3$, EtOAc ve *n*-BuOH)'ya ait aktif alt ekstratların çeşitli kromatografik ayırımları sonucu biri yeni (iconichalcone (**1**)) olmak üzere 28 farklı sekonder metabolit elde edilmiştir. *G. glabra*'dan izole edilen tetrahydoxymethoxychalcone (**2**), 4′-*O*-methylglabridin (**16**) ve glabrene (**20**) ile *G. iconica*'dan izole edilen **2**, licoricidin (**18**), dehydroglyasperin C (**21**), iconisoflaven (**22**) ve 1-methoxyficifolinol (**27**) gerçek zamanlı sitotoksisite deneyi (RT-CES) sonuçlarına göre en güçlü bileşikler olarak belirlenmiş ve bu moleküllerin sebep olduğu hücre ölümünün moleküler mekanizmasının aydınlatılması amacıyla Huh7 hücrelerinde Hoechst boyaması, hücre döngüsü (FACS) ve Western blot deneyleri yapılmıştır. **2**, **16**, **18**, **20**, **21**, **22** ve **27** numaralı bileşikler karaciğer kanser hücrelerinde kaspaz aktivasyonu ile apoptozu indüklemiş ve apoptotik $subG_1$ fazında hücre artışına sebep olurken, hücre döngüsünü G_1 ve/veya G_2/M fazlarında durdurmuştur. Bunun yanısıra, **21** tümör supresör geni p53'ü aktive etmiştir; **2** ise Hoechst boyaması deneyinde yoğunlaşmış çekirdekler göstererek Huh7 kanser hücrelerinin apoptoz yoluyla ölümüne neden olmuştur. Dolayısıyla, ilgili bileşikler özellikle **2** ve **21** ümit vaat eden sonuçlar göstermiş olup, bu bileşiklerin daha ileri *in vivo* ve klinik deneyler ile de araştırılmayı hak eden, özellikle hepatosellüler kansere karşı antikanser ilaç gelişimi için potansiyel öncü moleküller olabilecekleri görülmüştür.

Anahtar kelimeler: *Glycyrrhiza glabra*, *Glycyrrhiza iconica*, sitotoksik aktivite, Huh7, apoptoz

1. INTRODUCTION and AIM

Cancer is a major public health problem and one of the leading cause of mortality and morbidity worldwide (1). According to GLOBOCAN 2018 statics, there are estimated 18.1 million new cancer cases, 9.6 million cancer-related deaths and 43.8 million prevalence of cancer in 2018 around the world (2). World Health Organization reported 14.1 million new cancer cases and 8.2 million cancer deaths in 2012 worldwide (3). Comparing the statics of 2012 and 2018, cancer incidence and mortality are rapidly growing due to socioeconomic development, aging and increasing of the population, as well as changes in the prevalence and distribution of the main risk factors for cancer (2).

Cancer is characterized by uncontrolled growth and multiplication of abnormal cells which is related to inadequate amount of apoptosis and thus the loss of balance between cell division and cell death (1). Apoptosis is programmed cell death that occurs both physiological and pathological conditions and dysregulation in any step of apoptosis pathway can result in cancinogenesis (4,5). Therefore, like a double-edged sword, apoptosis is a very critical target in current strategies for the anticancer drug development (6,7). Although there are some commonly used strategies in cancer treatment, these therapies have been associated with severe adverse effects as well as multidrug resistance. More effective new anticancer drugs with minimum adverse effects are needed to combat cancer (8).

Natural resources particularly medicinal plants are excellent source for the discovery of lead drug molecules. From 1940s to date, 48.6% of the total number of small anticancer drugs have been obtained by either natural resources or semi-synthesis of them (9). Today, numerous anticancer natural products are in clinical use such as vinblastine, vindesine, vincristine, paclitaxel, etoposide, teniposide, irinotecan and topotecan which are obtained from plants by isolation or produced by the semi-synthesis of the isolates (10).

The genus *Glycyrrhiza* (Fabaceae), commonly known as licorice, have been widely used traditionally in different folk medicines for many years as antiulcer, antiinflammatory and expectorant agent (11,12). The genus contains approximately 30 species distributed worldwide including *G. glabra* L. (European licorice), *G. uralensis* Fisch. (Chinese licorice) and *G. inflata* Bat. (13,14). Previous studies on different extracts

1

of the genus *Glycyrrhiza* as well as the isolated secondary metabolites revealed their antiulcer, antimicrobial, antiprotozoal, antiviral, hepatoprotective, antiinflammatory, antidiabetic, antioxidative, memory enhancing, immunomodulatory, cytotoxic and antitumor activities (15–17). Furthermore, licorice has been utilized in many Traditional Chinese Medicine prescriptions as a guide drug in order to enhance the activity of other ingredients, reduce toxicity, and modify the taste (18). Besides being one of the most commonly used remedy in phytotherapy, it is also used in food industry particularly as flavoring and sweetening agent (16). From *Glycyrrhiza* species, over 400 secondary metabolites have been isolated mainly belonging to triterpene saponins, flavonoids and isoflavonoids chemical classes (19).

In the Flora of Turkey, the genus *Glycyrrhiza* is represented by six species half of which are endemic including *G. iconica* Hub.-Mor. The roots of *Glycyrrhiza* species mainly those of *G. glabra* are utilized to treat cough, bronchitis, asthma, epilepsy, cancer, kidney stones, nephralgia and stomach problems in Turkish traditional medicine (20). In recent years, secondary metabolites isolated from *Glycyrrhiza* species most interestingly flavonoids are gaining much interest particularly due to their significant cytotoxic and antitumor effects. Based on previous reports, some phenolic compounds including isoflavones, pterocarpans and isoflavans isolated from *G. pallidiflora* and prenylated flavonoids obtained from *G. glabra*, *G. uralensis* and *G. inflata* were shown to have significant cytotoxic activities against several cancer cells (21–24).

In the light of above mentioned information, the aim of this study was to isolate and identify cytotoxic secondary metabolites from roots of *G. glabra* and *G. iconica* against hepatocellular (Huh7), breast (MCF7) and colorectal (HCT116) cancer cell lines through bioactivity-guided fractionation technique. Furthermore, elucidation of the possible molecular mechanisms of cytotoxicity of the most active compounds was aimed by using real time-bioactivity, Hoechst staining, cell cycle and Western blot assays.

2. GENERAL DESCRIPTION

2.1. General Information about *Glycyrrhiza*

2.1.1. Botanical Information

2.1.1.1. Fabaceae

Fabaceae members are woody or herbaceous. Leaves are alternate, usually stipulate, bipinnate, simply pinnate, digitate, trifoliate or simple (often unifoliate or phyllodic). Flowers are actinomorphic or zygomorphic, hypogynous or sometimes perigynous, usually hermaphrodite, and in racemes, spikes or umbels, or solitary. Sepals are (4-)5, the odd sepals are always anterior. Petals are (1-)5, valvate or imbricate in bud, free or rarely partially connivent. Stamens can be 4-many, usually 10, all united in a tube (monadelphous) or with the upper stamen free (diadelphous), or all free. Members consist of 1 carpel, which is superior, with marginal placentation. Fruits are legume (i.e. dehiscing along both ventral (ovuliferous) and dorsal (non-ovuliferous) sutures), or indehiscent, sometimes lomentum (fragmenting into 1-seeded portions). Seeds are 1-many (25).

2.1.1.2. *Glycyrrhiza* L.

Glycyrrhiza species are perennial glandular herbs. Leaves are imparipinnate; leaflets are glandotted, 4-7 paired; and stipules are minute and lanceolate. Racemes or spikes are axillary, many-flowered, lax to much conracted, even subcapitate. Bracts are small, caducous. Calyx of *Glycyrrhiza* members are campanulate, bilabiate, the upper lip is with two short teeth, while the lower is with three long teeth. Color of corolla are yellow or blue to mauve, keel obtuse to acute. Stamens are diadelphous. Fruits are smooth, glandular or echinate legume, valves are contorting on dehiscence, or indehiscent, terete or laterally compressed, 1-many seeded (25).

Glycyrrhiza L. belongs to Fabaceae family, comprises about 30 species around the world (14). *Glycyrrhiza* species are commonly distributed in Mediterranean region, central to southern Russia, North of China and Anatolia to Iran. Cultivation of some of the *Glycyrrhiza* species are now widely established throughout Europe, the Middle East

and Asia (12,26). In flora of Turkey, the genus *Glycyrrhiza* is represented by 6 species, half of which are endemic including *G. iconica, G. flavescens* and *G. asymmetrica* (25).

Dichotomous key for Turkish *Glycyrrhiza* species is as follows (25):

1. Leaves with 2-4 pairs of leaflets

    2. Flowers yellow; legume c. 4 x 1.5 cm, oblong   ***asymmetrica***

    2. Flowers lilac or bicolouredreddish-mauve and white; legume 15-30 x c. 0.3 cm

        3. Inflorescence 2-5(-6); standard 14-17 mm   ***aspera***

        3. Inflorescence 7-10 cm; standard 18-20 mm   ***iconica***

1. Leaves with 4-9 pairs of leaflets

    4. Inflorescence 2-5 cm, dense; corolla 5-7 mm; legume echinate   ***echinata***

    4. Inflorescence 5-15 cm, lax; corolla 9-18 mm; legume smooth or glandular

      5. Corolla bluish, 9-11 mm; fruit terete, c. 2 x 0.5 cm   ***glabra***

      5. Corolla yellow, 12-18 mm; fruit compressed, c. 4 x 1 cm   ***flavescens***

2.1.1.3. *Glycyrrhiza glabra* L.

Plants are sparsely pubescent, erect perennial and 30-60 cm tall. Leaflets are 5-9 paired, 15-45 x 10-20 mm and shape of the laminas are elliptic. Inflorescences are 5-9 cm, lax, elongate. Teeth of calyx are c. 3 mm. Corollas are sized 9-11 mm and colored blue to violet. Legumes are 15-25 x 4-5 mm, $\pm$ terete, red-brown, glandular (sometimes bristly) or eglandular, 1-6 seeded (25).

Flowering season: June-July

Habitat: cultivated ground, alluvial river valleys, sand dunes

Altitude: sea level to 1800 m

Distribution in Turkey:

Widespread in Anatolia including Amasya, Ankara, Antalya, Aydın, Bitlis, Çankırı, Diyarbakır, Erzurum, Gaziantep, Hakkari, Hatay, Isparta, İzmir, Kahramanmaraş, Kars, Kırşehir, Malatya, Manisa, Mardin, Muş, Samsun, Siirt, Sivas, Şanlurfa, Tunceli, Van provinces.

Worldwide distribution: South Europe, Crimea, South Russia, North Africa, Southwest, Coast and East Asia (25)

Figure 1. *Glycyrrhiza glabra* L.

2.1.1.4. *Glycyrrhiza iconica* **Hub.-Mor.**

Sparsely pubescent perennial plants, 20-30 cm in size. Leaflets are 2-4 paired, 15-23 x 10-17 mm, teeths are 2.5-4 mm. Corolla is 18-20 mm in size and its color is lilac. Ovary is glabrous, 4-seeded. Fruits are unknown (25).

Flowering season: May-June

Altitude: 900 m

Distribution: Endemic to Konya province in Turkey (25)

Figure 2. *Glycyrrhiza iconica* Hub.-Mor.

2.1.1.5. Local Names of *Glycyrrhiza* species

Glycyrrhiza name is derived from Greek words of glykos (sweet) and rhiza (root) (16).

In Turkish: Meyan (20), buyan (11), payam (27), piyan (28).

In Other Languages: Gancao (in Chineese); licorice, liquorice, glycyrrhiza and sweet wood (in English); süssholz and lakritzenwurzel (in German); reglisse and bios doux (in French); shirin bayan and mak (in Persian); jestamadh (in Indian); liquirizia (in Italian) and regaliz (in Spanish) (16).

2.1.1.6. Traditional Use of *Glycyrrhiza* species

Medicinally used licorice which is also known as "Radix Glycyrrhizae "or "Liquiritiae radix" is originated from the roots of *Glycyrrhiza glabra* L., *Glycyrrhiza uralensis* Fisch. or *Glycyrrhiza inflata* Bat (18).

Licorice has a long history as folk remedies and traditional medicines, dates back to thousands of years. Different geographical regions and time periods have demonstrated extensive traditional usages of licorice (29,30). First reports about licorice can be found in ancient Assyrian, Eyptian, Chinese and Indian cultures in which invigorating and tonic effects of licorice were used by Chinese and Hindu people. Licorice was described as a remedy to treat asthma, cough, pectoral diseases and to combat thirst by Greek botanist Theophrastus (IV-III B.C.) who was further reffered by Dioscorides in his *De materia medica*. According to his reports, it was mentioned that Scythians survived waterless 11-12 days of desert life by eating licorice roots (29). Among Romans, licorice roots were benefited to reduce hunger and thirst in addition to treat asthma and for the sterility of women as mentioned by Plinius The Elder in Naturalis Historia. The other authors of ancient Roman times (Celsus and Scribonius) also mentioned about the usage of licorice in their writings as its beneficial effects in promoting the calculi expulsion in urine as well as artery problems. Marcellus Empiricus suggested licorice for the treatment of several disturbances and pathologies of many organs including lungs, stomach, intestines, kidneys, lower back and also for fever and digestive problems (29).

In Traditional Chinese Medicine (TCM), the major theory of licorice is based on its ability to tonify the qi of heart and spleen. Furthermore, licorice has been consumed for fatigue, phlegm, cough, dyspnea, spasms, pain, toxicity and cooperation with other medicines. Combination with licorice in TCM prescriptions is very common, appears in approximately 60% of the prescriptions. Licorice is described as a "guide drug" because of its unique effect on moderating, complementing and alleviating the toxicity of the other herbs, enhancing the effectiveness of other ingredients as well as modulating its taste due to its sweet flavour (18).

G. glabra is known as "jestamadh" and "mulhati" in Ayurvedic medicine and root extract has been utilized for Addison's disease, catarrhal disorders, irritable conditions of mucous membranes of urinary organs, sore throats and gastric ulcers (31). While stems have been orally used for mental relief, diuresis and diabetes (32). In Indian Ayurveda system, *G. glabra* has been consumed as anabolic and antidote against acute and chronic poisoning as well as for the treatment of viral respiratory tract infections, wound infections, acute and chronic liver diseases like hepatitis and to improve voice (30,33).

The comparasion of traditional usage of licorice in European, Indian and Chinese medicine systems indicated that all accounts for its antiviral effects including viral induced laryngitis, pharyngitis, cough, viral hepatitis and viral skin diseases (30).

In the West Black Sea region of Turkey, *G. glabra* is called as "buyan" that has been used to treat stomach problems and cough (11). On the other hand, in Central Anatolia region of Turkey, this plant is known as "payam" and the decoction of roots have been drunk as tea for the treatment of hemorroids and internal pains (27). *G. glabra* is called as "meyan" in Eastern Anatolia region in which leaves have been directly and externally applied to sunstrokes while decocted roots have been consumed internally to treat cough, bronchitis, asthma, epilepsy, cancer, kidney Stones and nephralgia. The rhizomes of *G. echinata* (dikenli meyan) have been used for bronchitis, asthma, antitussive, stomachic, nephralgia, diuretic and antiseptic orally (20). In West Anatolia of Turkey, *G. glabra* (piyan) has been utilized to ease cough by chewing peeled roots (28).

G. glabra is used to treat malaria, peptic ulcers, asthma, pharyngitis, infections, hepatic disorders and fever in Iran (34).

In Israel, *G. glabra* fresh leaves have been used externally for wound healing while root decoction has been drunk for kidney stones, ulcers and lung ailments (35).

Aqueous root extract of *G. glabra* has been benefited for the treatment of tuberculosis in Sri Lanka (36).

2.1.2. Bioactivity Studies on *Glycyrrhiza* species

2.1.2.1. Studies on Antiulcer Activity

Jalilzadeh-Amin et al. investigated the antiulcerogenic effects of hydroalcoholic extract of *Glycyrrhiza glabra* L. (50-200 mg/kg) in mice by oral administration by using stress, ethanol, indomethacin and HCl/Ethanol-induced ulcer models. Omeprazole (30 mg/kg) and cimetidine (100 mg/kg) were used as positive controls. In HCl/Ethanol-induced ulcer model, licorice extract (50–200 mg/kg) showed significant reduction in ulcer index. Furthermore, antiulcer activity was observed in indomethacin-induced gastric lesions with licorice administration (50-150 mg/kg) in a dose dependent manner. *G. glabra* extract inhibited formation of ulcers in all tested models and at all doses significantly, but especially 150-200 mg/kg doses of extracts were found to be more effective than omeprazole and cimetidine (37).

Wittschier and colleagues studied the effect of aqueous extract and polysaccharides obtained from *Glycyrrhiza glabra* roots on the adhesiveness of the main cause of stomach ulcer, *Helicobacter pylori* to human gastric mucosa by using *in situ* adhesion assay. In addition, their cytotoxic activity against *H. pylori* was also assessed by agar diffusion assay. According to the obtained results, aqueous extract (1 mg/mL) showed significant antiadhesive property against *H. pylori*, whereas isolated polysaccharides did not show any direct cytotoxicity. Moreover raw polysaccharides from *G. glabra* exhibited strong antiadhesive effects in *Porphyromonas gingivalis*, which is a major Gram negative pathogen in development of destructive periodontal diseases (38).

In an *in vitro* study by Asha et al. anti-*Helicobacter pylori* activity of flavonoid rich extract of *G. glabra* (Gutgard®) and its probable mechanism of action were investigated. Gutgard® showed anti-*H. pylori* in agar dilution and microbroth dilution methods. Glabridin, the major flavonoid in Gutgard® showed superior activity while glycyrrhizin was found to be inactive even at 250 μg/mL. Mechanistical studies demonstrated that anti-*H. pylori* effect of Gutgard® was occured possibly by inhibiting protein sythesis, DNA gyrase and dihydrofolate reductase (39).

In another study performed by Puram et al., the effectiveness of Gutgard® was evaluated in the management of *H. pylori* gastric load by a randomized, double-blind and

placebo controlled clinical study. The urea breath and stool antigen tests results at days 0, 30 and 60 showed that Gutgard® significantly reduced *H. pylori* infection and found to have 73.2% or 3.73 times stronger activity than placebo (40).

In a randomized and controlled clinical trial conducted in patients suffering from dyspepsia, authors gave to control group a clarithromycin-based triple regimen (500 mg clarithromycin twice a day + 1 gr Amoxicillin once a day + 20 mg Omeprazole twice a day) while they gave to study group licorice extract (380 mg, twice a day) in addition to clarithromycin-based triple regimen for two weeks. According to *H. pylori* eradication tests results six weeks after therapy, peptic ulcer were treated in study and control groups by 83.3% and 62.5%, respectively. Though, combination usage of licorice increased *H. pylori* eradication in patients suffering from dyspepsia (41).

In a very recent study, Sadra et al. performed an *in vivo* study to evaluate anti-*Helicobacter* and gastric relaxing activities of AD-lico/Healthy Gut™ which is an ethanol (95%) extract of *G. inflata* containing lower level of glycyrrhizin and higher levels of phenolic contents than conventional licorice extracts. The oral application of this product (25, 50 and 100 mg/kg) significantly alleviated mucosal damage of *H. pylori* in rats, dose dependently. Its possible mechanism was explained as reduced mucosal damage of *H. pylori* as well as reduced expression of inflammatory markers (iNOS and COX-2). Authors also revealed that AD-lico/Healthy Gut™ decreased mucosal damage from water immersion stress in rats. Further, enhancement in gastric emptying and relief in gastric relaxation were also observed in normal rats using this licorice containing product (42).

The activity of *G. glabra* root powder was histopathologically investigated against aspirin induced gastric ulcer in mice by Awan et al in 2015. Thirthy-six male albino mices were divided into six groups (n=6). To the first group only normal diet, to the second group aspirin (200 mg/kg) and to the third group omeprazole (20 mg/kg) and aspirin were administered while to the each of other three groups 250 mg/kg, 500 mg/kg and 750 mg/kg *G. glabra* root powder with aspirin were given. In mices treated with licorice at highest dose (750 mg/kg) exerted no pathological changes of gastric ulcer such as edema, necrosis and sloughing. These results showed the gastroprotective activity of *G. glabra* roots in a dose dependent manner, having similar effects with omeprazole which is the most common first line therapy of gastric ulcer (43).

Choi et al. studied gastroprotective action of isoliquiritigenin which is a chalcone found in *G. glabra*, against indomethacin-induced ulcer model in mice. Briefly, pharmacokinetic and *in vivo* pharmacological studies performed by authors showed that isoliquiritigenin had a high distribution in stomach and (100 mg/kg) prevented occurance of indomethacin-induced gastric ulcers, which was considered to be possibly related with recovered cyclooxygenase-2 (COX-2) levels and thus increased gastric mucous secretion (44).

Yang et al. demonstrated the antiulcer activity of licoflavone in acetic acid-induced gastric ulcer with an *in vivo* study on rats. Licoflavone (70 mg/day) showed significant gastroprotective activity by regulating inflammatory mediators and amino acid metabolism (45).

In another study conducted by Wang et al. in 2017, the antiulcer effect of triterpenic compounds from *G. uralensis* roots against acetic acid-induced gastric ulcer and elucidation of their mechanisms of action were investigated. Rats were randomly separated into six groups including control group, model group, omeprazole group (0.8 mg/mL), high dose triterpenes group (378.0 mg/mL), middle dose triterpenes group (126.0 mg/mL) and low dose triterpenes group (42.0 mg/mL). After seven days of treatment, results demonstrated significant decrease of ulcer cases with omeprazole and high, middle, and low doses of triterpenes by 63.17%, 44.95%, 49.66% and 55.43%, respectively. As a result of HPLC-MS analysis eleven different endogenous metabolites were clarified such as tryptophan, phingosine-1-phosphate, pantothenic acid which were possibly related with regulation of the antiulcer activity of *Glycyrrhiza* triterpenes (46).

2.1.2.2. Studies on Antimicrobial Activity

Kırmızıbekmez et al. isolated six prenylated polyphenolic compounds from *G. iconica* roots and studied their *in vitro* antioxidant and antimicrobial activities against five pathogenic bacteria and one yeast. Four of the isolates (MIC= 2-8 µg/mL) especially licorisoflavan A and topazolin displayed significant activity against *Salmonella typhiurium*, compared to standard antimicrobial compounds according to *in vitro* microdilution method. Further, all of the purified compounds (IC_{50} = 0.18- 0.56 mg/mL) exerted a comparable antioxidant activity with ascorbic acid (IC_{50} = 0.07 mg/mL) as observed with *in vitro* DPPH assay (47).

In another study, inhibitory effects of *G. uralensis* and glycyrrhizin against diarrhea were demonstrated. As heat-labile enterotoxin which is the virulence factor of *Escherichia coli*, causes diarrhea by binding to G_{M1} in intestinal epithelial surfaces, the interaction between them were investigated. The results revealed that *G. uralensis* extract (73.3%) and glycyrrhizin (97.5%) attenuated the binding of heat-labile enterotoxin to G_{M1} and glycyrrhizin (10 nm) inhibited heat-labile enterotoxin induced diarrhea (48).

Bensch et al. evaluated the the antiadhesive effects of several plant extracts including *G. glabra* against *Campylobacter jejuni* which is one of the most common bacterial cause of diarrhea. Results revealed that 20% ethanol extract of *G. glabra* roots displayed significant antiadhesion activiy against *C. jejuni* ($IC_{50} = 0.65$ mg/mL) (49).

Lee et al. extracted *G. uralensis* with 80% methanol and fractionated it by organic solutions including hexane, chloroform, ethyl acetate and *n*-butanol in order to investigate their antimicrobial actions against methicillin-resistant *Staphylococcus aureus* strains. The methanol extract and all of the obtained fractions exerted antimicrobial acitivity. Hexane and chloroform fractions showed minimum inhibitory activities at doses of 0.25 mg/mL and 0.1-0.12 mg/mL, respectively. Chloroform fraction was found to be 2.5 times stronger antimicrobial activity than penicillin (50).

Badr et al. evaluated the antibacterial effect of licorice extract containing 7.5% glycyrrhizin against *Enterococcus faecalis* separately or in combination with calcium hydroxide by using agar diffusion, broth microdilution and biofilm susceptibility tests whether to compare their actions in root canal medicament. Alone and combination treatment with calcium hydroxide of licorice extract exerted significant inhibitory effect against *E. faecalis* and retained compatibility with fibroblasts in tissue culture compared to calcium hydroxide (51).

Long et al. studied the effect of 18β-glycyrrhetinic acid in survival of methicillin resistant *Staphylococcus aureus*. Regarding the results, 18β-glycyrrhetinic acid (> 0.223 μM) exerted *in vitro* bactericidal activity in a dose dependent manner and topically reduced skin lesion size *in vivo* in murine models of skin and soft tissue infection by decreasing expression of key virulence genes such as *saeR* and *hla* (52).

The antimicrobial effect of deglycyrrhizinated *G. uralensis* root was assessed against *Streptococcus mutans* which is the primary agent of human dental caries by using

time-kill kinetic, growth, adhesion, and biofilm assays. Both of minimum inhibitory concentration and minimum bactericidal concentration values against *S. mutan*s were found to be 8 µg/mL. The results exhibited that deglycyrrhizinated *G. uralensis* extract significantly supressed biofilm formation by *S. mutans* UA159 and exerted strong antimicrobial activity (53).

Antimicrobial activities of ethanolic and aqueous *G. glabra* leaf and roots extracts were studied and compared within a study of Irani and colleagues. Disc agar difussion and serial dilution methods were used against *Bacillus subtilis, Enterococcus faecalis, Klebsiella pneumoniae, Pseudomonas aeruginosa, Staphylococcus aureus, Escherichia coli* and *Candida albicans.* Root and leaf extracts were found to be active against *Candida albicans* and Gram-positive bacteria dose dependently. Ethanolic and leaf extracts (MIC= 0.31 - 5 mg/mL) showed relatively more activity than aqueous and also root extracts against *Staphylococcus aureus*, *Bacillus subtilis*, *Enterococcus faecalis*, whereas aqueous extract of *G. glabra* leaves displayed more activity (MIC= 0.625 mg/mL) than its ethanolic extract against *C. albicans* (54).

Gupta et al. performed an *in vitro* study to reveal antimicrobial compounds from *G. glabra* roots through bioactivity-guided isolation. Testing antimicrobial potential of the fractions and purified compounds against *Mycobacterium tuberculosis* H23Ra and H37Rv cells with BACTEC assay, resulted in identifying glabridin (MIC = 29.16 µg/mL) as the active content in EtOH extract (MIC= 500 µg/mL) of *G. glabra* roots (55).

Gafner et al. isolated 21 compounds by fractionating the supercritical extract of *G. uralensis.* Further, *in vitro* antimicrobial activity of the isolates were evaluated against important cariogenic and periodontopathogenic bacterial species by microplate dilution assay. Treatment with the licoricidin and licorisoflavan A showed potent activity against cariogenic *Streptococcus mutans* and *S. sobrinus* at 10 µg/mL as well as periodontopathogenic *Porphyromonas gingivalis* at 5 µg/mL. Taken together, these two compounds were found to be active in inhibiting growth of oral pathogens (13).

In another study of Tanaka et al., the compounds isolated from *G. uralensis* were evaluated against upper airway respiratory tract bacteria including *Streptococcus pyogenes, Haemophilus ifluenzae* and *Moraxella catarrhalis*. Licoricidin (MIC = 12.5 µg/mL) displayed the highest activity among the tested compounds against all tested

bacteria, followed by 3-arylcoumarins including glycyrol, glycyrin and glycycoumarin (56).

In a study performed by Demizu et al. *in vitro* antimicrobial effects of a commercially available licorice roots were investigated. Glycycoumarin and licocoumarone were obtained from active subfractions of 50% EtOH soluble subextract of total dichloromethane extract. Based on the results of *in vitro* tests, glycycoumarin and licocoumarone were found to inhibit the growth of Gram positive bacteria including *Streptococcus mutans*, *Staphylococcus aureus* and *Bacillus subtilis* with MIC values in the ranges of 3.13- 12.5 µg/mL and 6.25- 12.5 µg/mL, repectively whereas they found to be inactive against Gram negative bacteria, *Escherichia coli* (57).

2.1.2.3. Studies on Antiparasitic Activity

The antiparasitic activity of *Glycyrrhiza glabra* extract was investigated against *Plasmodium falciparum* (*in vitro*) and *Plasmodium berghei* (*in vivo*). Results revealed that *G. glabra* extract exerted *in vitro* antiplasmoidal activity and selectivity for resistant strain of *P. falciparum* K1 with IC_{50} value of 17.5 µg/mL, moreover the chlorofrom fraction of the extract showed even stronger antiplasmoidal activity with IC_{50} value of 8.9 µg/mL. Further *in vivo* antiparasitic effect of chloroform fraction was tested on mices which resulted in 86.1% supression of parasitemia at 10 mg/kg/day doses (58).

Ramazani and colleagues studied antiplasmodial activity of *G. glabra* which is traditionally used against malaria in Iran. According to *in vitro* tests against chloroquine resistant *Plasmodium falciparum* 3D7, water-methanol and EtOAc fractions of *G. glabra* were found to be active with IC_{50} values of 9.95 µg/mL and 13 µg/mL, respectively. Furthermore, in HeLa cells water-methanol fraction was found to be low toxic and showed selectivity to *P. falciparum*. Authors also conducted an *in vivo* study in mices infected with *P. berghei*, resulted in significant inhibition of parasite growth with water-methanol (72.2%) and EtOAc (65%) fractions treatment (34).

Sangian et al. examined *in vitro* and *in vivo* antimalarial activity of ethanolic extracts of ten different medicinal plants. Results obtained by authors revealed that, the crude extract of *G. glabra* showed significant *in vitro* antimalarial activity ($IC_{50} = 13.56$ µg/mL) against *Plasmodium falciparum* chloroquine-sensitive 3D7 strain and it (400

mg/kg) also found to be significantly active on *P. berghei* inoculated Swiss albino mices through reducing parasitemia (59).

In 2013, Kalani and colleagues isolated 18β-glycyrrhetinic acid from *G. glabra* roots as its one of the major constituents and evaluated its *in vitro, in silico* and *in vivo* anti-malarial activity against *Plasmodium falciparum. In vitro* studies showed the strong antimalarial potential of 18β-glycyrrhetinic acid (IC$_{50}$ = 1.69 µg/ml). While *in silico* studies indicated drug-like properties of 18β-glycyrrhetinic acid, further *in vivo* tests demonstrated antimalarial activity in the range of 68-100% (62.5-250 mg/kg) at 8th day of treatment (60).

2.1.2.4. Studies on Antiviral Activity

Ryu et al. prepared a methanol extract from *G. uralensis* roots and isolated eighteen compounds by rvH1N1 neurominidase inhibitory activity-guided fractionation technique. Results of these *in vitro* investigations concluded that isoliquiritigenin (IC$_{50}$ = 9.0 µM) and glycyrol (IC$_{50}$ = 3.1 µM) displayed strong inhibitory activities. According to structure-activity relationship analysis of the isolates, furan rings in polyphenols were essential for this activity which was increased by apiose unit in the chalcone and flavanone structures. Cyclization of C-4 and C-2' in coumestan was also found to be critical for the activitiy (61).

In an another study performed by Dao et. al in 2011, the neurominidase inhibitory activity of eight isolated compounds obtained from acetone extract of *G. inflata* on H9N2, H1N1, novel H1N1 (WT) and osetalmivir resistant novel H1N1 (H274Y) were investigated. Among the isolates, echinatin (IC$_{50}$ = 2.19 - 5.8 µg/mL) and isoliquiritigenin (IC$_{50}$ = 3.42 - 9.69 µg/mL) exhibited strong inhibitory actions on these four influenza viral strains. Moreover, a synergism was reported, increased effect of osetalmivir (52.6 fold) was reported with the combination of echinatin against tamiflu resistant novel flu H274Y neurominidase (62).

Glycyrrhizin is a triterpene saponin and the major component of licorice root. In order to examine the antiviral effects of glycyrrhizin against hepatitis C virus, Matsumoto et al. performed *in vitro* assays in hepatitis C virus infected Huh7 cells. Briefly, the results exhibited that glycyrrhizin inhibited release of hepatit C virus particles which might be due to its inhibitory effect on PLA2G1B. Authors also demonstrated that combination

therapy of glycyrrhizin with augmented interferon induced the reduction of the hepatit C virus (63).

Sasaki et al. researched effect of glycyrrhizin on HIV replication. Authors gave glycyrrhizin (100 µg/mL) to cell cultures from healthy donors and HIV+ patients for 21 days. In thirteen of forty-two samples of HIV+ cultures (31%) in which twelve of them were non-syncytium-inducing variant of HIV, glycyrrhizin showed inhibition more than 90% of HIV replication. The potential action of glycyrrhizin on inhibiting non-syncytium-inducing variant of HIV replication was considered to be occured by inducing the production of β-chemokines (64).

Kwon et al. isolated six compounds from *G. uralensis* and investigated their *in vitro* inhibitory activities against group A rotaviruses which are main pathogens causing acute dehydrating diarrhea in young children as well as various domestic animals. These tested six compounds including licocoumarone, glyasperin C, 2'-methoxyisoliquiritigenin, glycyrin, licoflavonol and glyasperin D inhibited binding of rotavirus with 50% effective inhibitory concentrations in the range of 18.7–69.5 µM and 14.7–88.1 µM against G5P and G8P rotaviruses, respectively. Licocoumarone, glyasperin C, glycyrin, licoflavonol, and glyasperin D completely stopped virus infectivity while glyasperin C and licoflavonol inhibited both virus types in virucidal assay (65).

Antirotaviral effect of *G. uralensis* extract was evaluated on rotavirus infected piglets by using fecal consistency score, fecal virus shedding and histological changes in small intestine, mRNA expression levels of inflammation-related cytokines, signaling molecules and transcription factor in the small intestine and spleen. 400 mg/mL *G. uralensis* extract supressed rotavirus infected diarrhea in piglets by regulating antiviral and antiinflammatory pathways (66).

Omer and colleagues conducted a comparative study for the evaluation of antiviral effect of *G. glabra* aqueous extract and ribavirin against Newcastle disease virus. Hemagglutination and also toxicity were not observed in 60 mg/100 mL *Glycyrrhiza* extract inoculated embryonated egg, showed similar results with 20 µg/mL ribavirin. These results revealed the potential inhibitory activity of *Glycyrrhiza* extract in replication of Newcastle disease virus (67).

Yeh et al. studied the antiviral activity of *G. uralensis* water extract, glycyrrhizin and 18β-glycyrrhetinic acid against human respiratory syncytial virus by using plaque reduction assay in upper (HEp-2) and lower respiratory (A549) tract cell lines. *G. uralensis* extract and 18β-glycyrrhetinic acid exhibited potent antiviral activity. 300 µg/mL extract significantly decreased the viral quantity and prevented viral attachment and penetration to the host cell (68).

Laconi et al. examined the ability of glycyrrhizic acid to induce Beclin 1 autophagic process activator in epithelial cells whether to evaluate its antiviral activity. HeLa cells treated with glycyrrhizic acid showed strong antiherpes simplex virus type 1 activity, while the reference compound rapamycin showed no activity. Furthermore, glycyrrhizic acid was found to be able to induce Beclin 1 production two times stronger than rapamycin (69).

Wolkerstorfer et al. investigated the effect of glycyrrhizin against influenza A virus. Authors demonstrated that glycyrrhizin treatment caused a significant reduction in influenza A virus infected human lung cells and also decreased 50% cell culture infective dose titer by 90% and reduced virus uptake into the cells (70).

Wang et al. extracted *G. uralensis* with hot water and analyzed the chemical components of extract by HPLC. Further, they evaluated the antiviral activity of the exrtact and its components against two members of *Enterovirus* genus including enterovirus 71 (EV71) and coxsackievirus A16 (CVA16) on Vero cells in order to investigate its efficacy in hand, foot and mouth diseases. According to the results the *G. uralensis* extract (1000 µg/mL) inhibited EV71 and CVA16 replication. Selective depletion of glycyrrhizic acid from extract caused loss of antiviral activity whereas addition of glycyrrhizic acid (200 µg/mL) increased the inhibitory effect of the extract. Taken together, *G. uralensis* and glycyrrhizic acid were found to be active in inhibiting viral replication of EV71 and CVA16 (71).

In a study conducted by Song et al. triterpene saponins isolated from *G. uralensis* roots were evaluated with regard to their antiviral effects against Influenza A/WSN/33 (H1N1) and HIV-1. Compounds uralsaponin M (IC_{50} = 48.0 µM), uralsaponin S (IC_{50} = 42.7 µM), uralsaponin T (IC_{50} = 39.6 µM) and 22β-acetoxyglycyrrhizin (IC_{50} = 49.1 µM) exerted significant anti-H1N1 activity comparing to osetalmivir phosphate (IC_{50} = 45.6

μM) while 22β-acetoxyglycyrrhizin (IC$_{50}$ = 29.5 μM) and 3-*O*-β-D-glucuronopyranosylglycyrrhetinic acid (IC$_{50}$ = 41.7 μM) were found to be active against HIV-1 virus (72).

Hendricks and colleagues researched immune responses of 18β-glycyrrhetinic acid in small intestinal mucosa with an *in vivo* study. 18β-glycyrrhetinic acid showed a decrease in duration of viral antigen shedding and incrase in endpoint serum antibody and orally induced lymphoid follicle maturation in intestinal mucosa (73).

Kuo et al. investigated the effect of water extract prepared from *G. uralensis* against cytopathic effects of enterovirus type 71 (EV71) in human foreskin cell line via XTT-based method. Results revealed that *G. uralensis* (0.1 μg/mL) water extract protected host cells against EV71 infection through preventing viral attachment and inhibiting virus penetration (74).

2.1.2.5. Studies on Antifungal Activity

In a study conducted by Pellati and colleagues *in vitro* effects of glycyrretinic acid was evaluated against *Candida albicans* strains obtained from patients with recurrent vulvovaginal candiasis. Authors reported that 18β-glycyrrhetinic acid (6.2 μg/mL) significantly reduced *in vitro* growth of *C. albicans* pH dependently. In low pH values (4.5, 5.0 and 5.5) the compound had stronger inhibitory activity than pH > 6.0 which could possibly make it a biological alternative for topical treatment of vulvovaginal candiasis disease (75).

Messier and Grenier investigated the effects of licochalcone A, glabridin and glycyrrhizic acid against growth, biofilm formation and yeast-hyphal transition of *C. albicans* by using microplate dilution assay, cyrstal violet staining and microscopic observation. According to the test results, both licochalcone A and glabridin were found to be equally active against *C. albicans* ATCC 28366 (MIC = 6.25 μg/mL) and *C. albicans* LAM-1 (MIC = 12.5 μg/mL) whereas glycyrrhizic acid was inactive against both strains. Further assays revealed that glabridin and licochalcone A might show synergistic effects with nystatin and either licochalcone A or glabridin (100 μg/mL) exhibited significant inhibitory activity on hyphal formation. In addition, licochalcone A (0.2 μg/mL) inhibited biofilm formation by 35-60% (76).

2.1.2.6. Studies on Antiinflammatory Activity

Inflammation is the inducer of many chronic diseases such as cardiovascular, degenerative diseases and cancer. There are various factors that involves in the experession of inflammation including cytokines, prostoglandins, COX-2 and iNOS enzymes and nuclear factors nuclear factor kappa B (NF-κB) and activator protein-1 (AP-1). Glabridin was found to be antiinflammatory according to many *in vitro* and *in vivo* studies by far which positively related to its other anti-atherogenic, neuroprotective and anti-osteoporotic activities (77).

Effects of glabridin on melanogenesis and inflammation were evaluated by using B16 murine melanoma cells and guinea pig skin. It was reported that glabridin (0.1 - 1.0 μg/mL) inhibited tyrosinase activity of cultured murine melanoma cells and decreased the T1 and T3 tyrosinase isozyme activities without affecting DNA synthesis. By topical application of 0.5% glabridin inhibited UVB-induced pigmentation and erythema in guinea pig skins. Further *in vitro* tests indicated that glabridin exerted antiinflammatry activity by inhibiting superoxide anion production and cyclooxygenase activities (78).

In another study, glabridin was demonstrated to have *in vivo* antiinflammatory effect and increased survival rate of mice in sepsis model. The possible mechanism behind this activity was studied and results showed that glabridin inhibited nitric oxide production as well as iNOS gene expression in *in vitro* cell cultures, which were important as their crucial role in endotoxin induced peptic shock and death (79) .

Thiyagarajan et al. evaluated inhibitory effects of deglycyrrhizinated extract of *G. glabra* roots and some of its contstituents including glabridin, isoliquiritigenin and glycyrrhizin against bacterial liposaccharide (LPS) induced pro-inflammatory mediators such as nitric oxide, interleukin-1 beta and interleukin-6 levels in murine macrophage cells. The results demonstated significant inhibitory effects of *G. glabra* extract and isoliquiritigenin against LPS-induced nitric oxide, interleukin-1 beta and interleukin-6 production whereas glabridin inhibited only nitric oxide, interleukin-1 beta release (80).

In an another study by Park et al. inhibitory effect of glabridin on nitric oxide, tumor necrosis factor-α and interleukin-1β levels which are the inflammatory mediators of liposaccharide induction were demonstrated in a dose dependent manner. Further studies indicated that this inhibitory activity was mediated through NF-κB and AP-1

activation. Authors suggested that glabridin might be a potential therapeutic agent for the treatment of neuroinflammatory and neurodegenerative diseases (81).

Kim et al. investigated *in vivo* antiinflammatory activity of licorice and roasted licorice extracts against murine phorbol ester-induced mouse ear edema acute inflammation model and collagen-induced arthritis model of human rheumatoid arthritis. Comparing the constituents of two licorice extracts by HPLC resulted that roasted licorice comprised five times more licochalcone content whereas two times less glycyrrhizin and isoliquitritigenin content than unroasted licorice extract. Treatment with both licorice extracts most particularly roasted licorice, dose dependently supressed mouse ear edema. The further examinations of these two extracts in chronic inflammation model displayed that oral application of licorice extracts reduced the progression of arthritis score, paw swelling and also levels of proinflammatory cytokines in serum and joints (82).

Shah et al. investigated *in vivo* antiinflammatory activity of 70% aqueous methanol extract of *G. glabra* and glycyrrhizin against corneal neovascularization. Solutions of *G. glabra* methanol extract (2% w/v) and glycyrrhizin (1% w/v) in normal saline significantly modulated neovascularization of corneal burn and showed no blood vessels in collagen fibers according to the results of digital photograph analysis and histological studies (83).

Abd and colleagues examined the effect of aqueous extract prepared from *G. glabra* against rheumatoid arthritis in antigen-induced arthritis mice model. They divided 48 male Swiss albino mices into four groups and gave no treatment to group 1 (arthritic mice, positive control), 750 mg/kg/day *G. glabra* extract to group 2, 300 mg/kg/day *G. glabra* extract to group 3 and no treatment to group 4 (non-immunized mice, negative control) for 20 days. According to the results, *G. glabra* inhibited histopathological features of antigen induced arthritis and reduced serum tumor necrosis factor-α (TNF-α) level, dose dependently (84).

In a study by Uto et al., the synergistic effect of glycyrrhizin with the other constituents in licorice extract against inflammation were evaluated. The methanol extract of licorice along with a glycyrrhizin removed extract was prepared. As a result of several assays in RAW264 murine macrophage cells, normal licorice extract showed inhibition in LPS-induced nitric oxide production and iNOS expression. Despite treatment with

glycyrrhizin alone did not show any inhibitory activity, glycyrrhizin removed extract of licorice was found to be less active than normal licorice extract. These results indicated the synergistic effect of glycyrrhizin with the other phytoconstituents in licorice (85).

In 2009 Furawasa et al. demonstrated that licochalcone A, major component of *G. inflata* significantly inhibited LPS-induced NF-κB transcriptional activation by blocking the phosphorylation of NF-κB p65 at serine 276 (86). In same year, Furawasa et al. reported the antiinflammatory mechanisms of the other chalcones from *Glycyrrhiza inflata* including licochalcone B, licochalcone C, licochalcone D, echinatin and isoliquiritigenin on LPS signalling pathway. Authors found the same inhibitory activity of licochalcone A with compounds licochalcone B and licochalcone D which also significantly decreased the LPS-induced production of nitric oxide, TNF-α and MCP-1 (87).

In a study conducted by Chandrasekaran et al. in 2011, to understand antiinflammatory mechanism behind the inhibitory activities of *G. glabra* (Gutgard™) and some of its components (glabridin, glycyrrhizin, and isoliquiritigenin), they were evaluated on both cyclooxygenase (COX) and lipooxygenase (LOX) products in murine macrophages (J774A.1) and human neutrophil (HL-60) cells. The results revealed that *G. glabra* and glabridin significantly inhibited both COX (prostaglandin E_2 (PGE_2) and thromboxane B_2 (TBX_2)) and LOX (leukotriene B_4) products, whereas isoliquiritigenin supressed only levels of COX (PGE_2 and TXB_2) products. However, glycyrrhizin did not show any inhibitory activity on both COX and LOX products up to concentration of 50 μg/mL. The dual inhibitory activity of *G. glabra* on both COX and LOX products might be explained by its glabridin and isoliquiritigenin constituents (88). On the other hand, in another study by Ohuchi in 1981, glycyrrhizin exerted inhibitory activity against PGE_2 production at dose of 100 μg/mL in macrophage cells obtained from rats (89).

In Wu and colleague's study, antiinflammatory and antioxidative stress activities and differential regulation of nuclear erythroid-related factor 2 (Nrf2) mediated genes of hexane:ethanol (9:1) extract of *Glycyrrhiza uralensis* were investigated. The tests demonstrated that *G. uralensis* extract exerted potent antiinflammatory activity by inhibiting the mRNA, nitric oxide production and protein expression levels of pro-inflammatory biomarkers including interleukin-1β, interleukin-6, COX-2 and iNOS in LPS-induced murine RAW 264.7 macrophage cells. Furthermore *G. uralensis* supressed

NF-κB luciferase activity in human HT-29 colon cancer cells and also induced the activity of Nrf2-mediated antioxidant/Phase II detoxifying enzymes. Thus, *G. uralensis* was found to be strong inhibitor against NF-κB-mediated inflammation in addition to its potent antioxidant property (90).

According to an *in vitro* comparative study by using inflammatory cell culture model, LPS stimulated inflammation mediators especially PGE_2 and TNF-α were inhibited by both unprocessed and nanoparticle suspensions of glycyrrhizic acid, dose dependently (91).

In a study performed by Wang et al. 25-75 µM glycyrrhizic acid and 18β-glycyrrhetinic acid significantly supressed LPS-induced production of nitric oxide, PGE_2, TNF-α, interleukin-1β, interleukin-6 and intracellular reactive oxygen species (ROS) in RAW 264.7 cells. Attenuation of the expression of iNOS and COX-2 genes and blockage of activation of transcription factors including NF-κB and PI3K p110δ and p110γ with the compounds glycyrrhizic acid and 18β-glycyrrhetinic acid were also observed (92).

Sasaki et al. demonstrated the antiinflammatory activity of 18β-glycyrrhetinic acid against periodotitis by an *in vivo* study conducted in interleukin-10 deficient mice. The results revealed that 18β-glycyrrhetinic acid showed strong inhibitory activity in the production of LPS-stimulated proinflammatory cytokines as well as receptor activator of nuclear factor kappa-B ligand (RANKL)-stimulated osteoclastogenesis by supressing phosphorylation of NF-κB p105 (93).

2.1.2.7. Studies on Antidiabetic Activity

A bioassay-guided fractionation of EtOH extract prepared from *G. glabra* roots by using *in vitro* GAL-4-PPAR-γ chimera assay method led to the isolation of thirty-nine compounds. Among isolates, 5'-formylglabridin, (2*R*,3*R*)-3,4',7-trihydroxy-3'-prenylflavanone, echinatin, (3*R*)-2',3',7-trihydroxy-4'-methoxyisoflavan, kanzonol X, kanzonol W, shinpterocarpin, licoflavanone A, glabrol, shinflavanone, gancaonin L and glabrone displayed significant peroxisome proliferator-activated receptor γ (PPAR- γ) ligand-binding activity. Furthermore, these compounds (10 µg/mL) were found to be three times stronger than troglitazone (0.5 µM), being licochalcone A as the most potent compound (94).

In a study performed by Gaur et al., *in vivo* antidiabetic effects of isoliquiritigenin, liquiritigenin isolated from *G. glabra* and their semi-sythetic derivatives were examined. To gain preliminary information about their antihyperglycemic effect, oral glucose tolerance test were applied to normal Swiss albino male mice treating with the compounds. As a result of test, seven of eleven tested compounds displayed significant blood glucose lowering effect. The ester and ether moiety in the stucture were found to be important for the presence of this activity. For the selected compounds including isoliquiritigenin (200 mg/kg), 2'-4'-dimethoxy-4-hydroxychalcone (50 mg/kg) and liquiritigenin-7-4'-dibenzoate (50 mg/kg), further *in vivo* experiments were conducted and the blood sugar levels were measured at 1st, 7th and 14th days of study. In conclusion, these three compounds were found to be active regarding their antidiabetic activity which might be potential candidates for the treatment of diabetes (95).

Protein tyrosine phosphatase 1B (PTP1B) is known as an insulin targeted tissue which plays critical role in regulating signalling cascades of insulin and leptin negatively. PTP1B inhibitors are gaining much attention due to their potential activities in the treatment of diabetes, obesity and cancer. In an *in vitro* study conducted by Li et al in 2010, compounds glycybenzofuran (IC_{50} = 25.5 µM) and glisoflavone (IC_{50} = 27.9 µM) obtained from *G. uralensis* inhibited PTP1B activity. In terms of the structure-activity relationship, the authors demonstrated that presence of prenyl and *ortho*-hydroxyl group were important for the activity. According to kinetic analysis results, glycybenzofuran was found to be a competitive PTP1B inhibitor whereas glisoflavone was found to be a mixed inhibitor (96).

In a similar study in 2013, screening of forty-two compounds from a library of licorice flavonoids led to the discovery of licoagrone (IC_{50} = 6.0 µM), licoagrodin (IC_{50} = 11.5 µM), licoagroaurone (IC_{50} = 23.9 µM) and isobavachalcone (IC_{50} = 27.3 µM) as inhibitors of PTP1B for the very first time. In order to elucidate their potential mechanisms of action, these active compounds were conducted to kinetic analysis in which different modes of action for each molecule were depicted. Glycybenzofuran was found to be a competitive inhibitor, exerted good inhibitory selectivity against both PTP1B and insulin-stimulated Akt phosphorylation level, which made this compound to be suggested as a new potential anti-insulin-resistant drug candidate (97).

Yoon et al. evaluated *in vitro* PTP1B inhibitory activity of six purified compounds from *G. inflata* in addition to eight semi-synthetic licochalcone A derivatives. The results exhibited that compounds with an allyl group at 5th position, licochalcone A ($IC_{50} = 19.1$ µM) and licochalcone E ($IC_{50} = 20.7$ µM) as well as methylated derivative of licochalchone A ($IC_{50} = 11.7$ µM) had significant activity (98).

2.1.2.8. Studies on Hepatoprotective Activity

Kuang and colleagues examined *in vitro* hepatoprotective activities of 180 licorice compounds obtained from *G. uralensis, G. glabra* and *G. inflata* by using MTS assay in CCl_4 and acetominophen treated HepG2 cells. According to the results, sixty-two compounds at 10 µM showed protective effects against CCl_4, increased cell viability more than 60%, using silymarin as positive control (84.6%). Amongst these, licoflavone A, 3,4-didehydroglabridin, isoliquiritigenin, 3,4,3',4'-tetrahydroxychalcone and licochalcone B exerted the most potent activities by improving cell viability by more than 80%. On the other hand, amongst the sixty-four compounds having protective effects against acetominophen, derrone, xambioona, (2S)-abyssinone I, isoliquiritigenin, licoagrochalcone A, and 2'-O-demethybidwillol B displayed the most potent activities (80%). Preliminary structure–activity analysis revealed that free phenolic compounds particularly chalcones exhibited better protective activities (99).

Hajiaghamohammadi et al. investigated the effect of licorice on non-alcoholic fatty liver disease within a double blind randomized clinical trial. 2 g aqueous licorice root extract and placebo each in capsules were given per day for 2 months to the study and control group, respectively. The authors demonstrated that licorice caused significant decreases in alanine aminotransferase (ALT) and aspartate aminotransferase (AST) levels (100).

The compounds obtained from *G. inflata* were assesed for their hepatoprotective activities with an *in vitro* assay. Against primary rat hepatocytes injured by D-galactosamine, compounds macedonoside A, licorice-saponin Q2, licorice-saponin G2, 22β-acetoxy-glycyrrhizin and glycyrrhizin (30-120 µM) exerted protective effects by lowering ALT and AST levels. Moreover, macedonoside A ($IC_{50} = 6.9$ µM), licorice-saponin Q2 ($IC_{50} = 3.6$ µM), licorice-saponin G2 ($IC_{50} = 16.9$ µM), 22β-acetoxy-glycyrrhizin ($IC_{50} = 27.1$ µM) and glycyrrhizin ($IC_{50} = 9.3$ µM) inhibited the activity of

phospholipase A$_2$, a liver cell membrane regulatory enzme which might be responsible for the possible hepatoprotective activity of these compounds (101).

Glycyrrhizin and silymarin were evaluated for their hepatoprotective effects in CCl$_4$ toxicated wistar male Albino rats by Rasool and colleagues. Results indicated that glycyrrhizin (50 mg/kg) treatment for 6 weeks improved the hepatic injury caused by CCl$_4$ through ameliorating the serum levels of liver enzymes (ALT, AST and alkaline phosphatase (ALP)) and serum total protein (TP) level. Glycyrrhizin administration also inhibited oxidative stress by elevating glutathione S-transferase (GST), glutathione (GSH), super oxide dismutase (SOD) and catalase levels. The hepatoprotective effect was even increased when glycyrrhizin (200 mg/kg) and silymarin (50 mg/kg) were given in combination, indicating their synergistic effects (102).

A retrospective study was conducted by Ikeda et al. to evaluate effect of glycyrrhizin in hepatocarcinogenesis rate in interferon-resistant hepatitis C. At 5th and 10th years, carcinogenesis rates were 13.3% and 21.5% in glycyrrhizin injected (0.2%, 20 mg, three times a week) group while it was 26.0% and 35.5% in untreated group, respectively (103).

The *in vitro* hepatoprotective and antioxidant effects of *G. glabra* extract were tested in CCl$_4$ induced carp primary hepatocytes by Yin et al. In only CCl$_4$ (8 mM) treated cells, increased lactate dehydrogenase (LDH), glutamate oxalate transaminase (GOT), glutamate pyruvate transaminase (GPT) and malondialdehyde (MDA) levels along with markedly reduced SOD and glutathione peroxidase (GSH-Px) levels were observed. Pretreatment with *G. glabra* extract (5 µg/mL) and combination of both pre- and post-treatment (5, 10 µg/mL) improved the abnormal parameters in hepatocytes compared to CCl$_4$ application alone (104) .

Chen et al. indicated the hepatoprotective effect of glycyrrhetinic acid against chronic liver inflammation by an *in vitro* study. Ethanolic crude extract of *G. uralensis* did not display cytotoxic activity at working concentrations (5-25 µg/mL) against HepG2 cells. The NF-κB activation response of *G. uralensis* on TNF-α-induced HepG2 cells were evaluated. At 25 µg/mL dose of ethanolic extract and lower doses of EtOAc subextract (10 µg/mL) reduced NF-κB activation in TNF-α-induced HepG2 cells. Bioactivity-guided isolation led to the isolation of glycyrrhetinic acid which further

showed also attenuated NF-κB activation in a dose-dependent manner (10-40 μM) according to NF-κB reporter gene assay in addition to decreased nitric oxide production and iNOS expression (105).

In another study by Zong et al. in 2013, 18α-glycyrrhetinic acid supressed the growth of the human hematopoietic stem cells cell line LX-2 and cirrhotic fat-storing cells through cell cycle arrest and apoptosis. The increased expression of PPARγ and inhibition of NF-κB activity might be the possible mechanisms behind these actions (106).

Xiao et al. studied the effect of 18β-glycyrrhetinic acid on *Propionibacterium acnes*-induced acute inflammatory liver injury in mice models with fulminant hepatitis. With regard to the results, 18β-glycyrrhetinic acid (75 mg/kg) showed antiinflammatory effects and protected hepatic injury within 7 days by supressing the liver-infiltrating CD4$^+$T cells activation, decreasing in serum ALT and pro-inflammatory cytokines (interferon-γ and TNF-α) as well as inhibiting macrophage inflammatory protein (MIP)-1α expression (107).

Orazizadeh and colleagues conducted an *in vivo* study to evaluate hepatoprotective effect of glycyrrhizic acid obtained from *G. glabra* against titanium dioxide nanoparticles (NTiO$_2$)-induced hepatic injury in rats. Autors divided Wistar rats into four groups, including a protection group treated with glycyrrhizic acid (100 mg/kg) for 7 days before intoxification with NTiO$_2$. Liver damage through centrilobular necrosis, elevated AST, ALT and ALP levels, increased oxidative stress and lipid peroxidation and reduced SOD and GSH-Px enzymes were observed with NTiO$_2$ intoxification, while in protection group glycyrrhizic acid treatment markedly decreased the hepatic injury, reduced these ALT, AST and ALP levels, oxidative stress and elevated SOD and GPx activities in hepatic tissue (108).

According to a study performed by Lin et al in 2017, seventy-seven compounds were purified from EtOAc extract of *G. inflata* roots and evaluated for their Nrf2 activation effects by using luciferase reporter assay in HepG2C8 cells and further *in vivo* hepatoprotective activities of most potent compounds were tested. Results indicated that EtOAc extract of *G. inflata* as well as some isolated chalcones including licochalcone A, licochalcone B and echinatin were found to be potent Nrf2 activators. In HepG2 cells

with CCl_4 induced cell injury, these three mentioned compounds increased viability of cells ($> 60\%$). Furthermore in CCl_4 induced liver injury mice models, 7 days of treatment with these compounds (50 mg/kg, each) and EtOAc extract (200 mg/kg) caused decreases in serum levels of ALT, AST and lactate dehydrogenase along with reduced liver lesions caused by CCl_4. Authors concluded that licochalcone A, licochalcone B and echinatin might be promising hepatoprotective agents obtained from *G. inflata* (109).

Jung and colleagues extracted *G. uralensis* with 70% ethanol and investigated its hepatoprotective effect against alcohol induced fatty liver disease. Changes because of alcohol induction (increased serum ALT, AST, triglyceride, TNF-α, lipid accumulation and reduced GSH levels) were inhibited with licorice treatment (25-200 mg/kg) in male mices. Licorice (100 mg/kg) was found to be a good candidate against chronic alcohol induced fat accumulation when compared with the same dose of silymarin (100 mg/kg) (110).

2.1.2.9. Studies on Cytotoxic and Antitumor Activity

Jo and colleagues investigated the ability of *G. uralensis* to inhibit cell proliferation in human breast cancer cell line (MCF7) by using MTT assay as well as its molecular mechanism. Cell proliferation assay results indicated that 80% ethanol extract of *G. uralensis* inhibited proliferation and induced apoptosis of MCF7 cells at 100 μg/mL concentration. According to mechanistic studies, G_1 cell cycle arrest was observed through up-regulation of p53 and p21 and down-regulation of cdk 2 and cyclin E. Furthermore, overexpression of pro-apoptotic protein Bax was observed which resulted in induced apoptosis of MCF7 cells. *G. uralensis* acted similar with 17β-estradiol and could be a natural protector against hormon dependent cancers (111).

Thu et al. screened 31 different medicinal plant extracts for their cytotoxic activities against five human cancer cell lines such as A549, MCF7, HT1080, Huh7 and HepG2 with MTT assay. Among the tested species, *G. glabra* methanol extract showed significant cytotoxicity against all of the five tested cell lines in different degrees ($IC_{50} =$ 6.6 – 15.4 μg/mL) (112).

In 2018, Fraihat and colleagues examined *in vitro* antiproliferative activity of methanol extracts of six plants including *G. glabra* against two skin cancer melanoma cell lines A375-S2 and WM136.1A by using MTT assay. The assay results demonstrated

that methanol extract of *G. glabra* supressed WM136-1A proliferation in a dose-dependent manner with IC_{50} value of 35.2 µg/mL (113).

Rasul and Ma, screened 300 ethanol extracts of medicinal plants against human gastric adenocarcinoma cells (SGC-7901) and normal spleen cells by MTT assay. Among thirty-three cytotoxically active extracts against gastric cancer cells, nine of them including *G. uralensis* exerted less cytotoxic effects against normal spleen cells (114).

In a study performed by Park et al. ethanol and aqueous extracts of roasted and unroasted *G. inflata* roots were evaluated against human prostate cancer (DU145), rat prostate cancer (MLL) and human colon cancer (HT-29) cell lines by using MTT test. Among four extracts roasted ethanol licorice extract (IC_{50} = 4.3 – 12.2 µg/mL) was found to be most potent one in inhibiting cell growth of all three tested cell lines which was followed by unroasted ethanol extract (IC_{50} = 12.0 – 31 µg/mL) while aqueous extracts showed very low effects on cell growth. Further cytotoxic activity evaluations on active ethanol extract of roasted licorice indicated that the extract (30 µg/mL) also inhibited growth of human breast cancer cells MCF7 (88%) and MDA-MB-231 (82%), mouse melanoma cancer cells B16-F10 (80%) and human skin cancer cells A375 (94%) and A2058 (93%) whereas it increased the growth of normal intestinal epithelial cells IEC-6 and fibroblasts CCD118SK. Ethanol extract of roasted licorice induced apoptosis in human prostate cancer cell line (DU145) by increasing cytochrome C, cleaved cysteinyl aspartate specific proteinase (caspase) -8, -9, -7 and -3 and cleaved poly (ADP-ribose) polymerase (PARP) levels. Furthermore, licochalcone A was isolated from the most active subfraction of dichloromethane soluble fraction of the extract against DU-145 which found to be potent cytotoxic dose dependently (2 - 8 µM) and induced apoptotic cell death by increasing cleaved caspase-8, -9, -7 and -3 as well as cleaved PARP levels. Authors also investigated *in vivo* antitumor effect of roasted ethanol extract of *G. inflata* and demonstrated that topical application of 10 mg of the extract to mouse skin decreased skin pappiloma formation by 88% (115).

In Shults and colleagues' study, twenty-one phenolic compounds were isolated from *G. pallidiflora* roots and seven of them were evaluated for their cytotoxic activity against lymphoblastoid leukaemia (CEM-13), human T-cell leukaemia (MT-4) and human monocyte (U-937) cancer cell lines by MTT assay. Results revealed that compound calycosin having an isoflavonoid structure showed potent inhibitory activity

in three tested cell lines ($IC_{50} = 2.9 - 7.6$ µM) most significantly against MT-4. Medicarpin ($IC_{50} = 4.1$ µM) and homopterocarpin ($IC_{50} = 2.7$ µM) in pterocarpan structures showed strong cytotoxicity with selectivity on U-937 cells whereas vestitol ($IC_{50} = 2.0$ µM) was found to be highly selective and more active than doxorubicin ($IC_{50} = 3.4$ µM) on CEM-13 cell lines (21).

Another study concerning the comparative cytotoxic effects of *G. glabra* roots from different geographical origins against immortal human keratinocyte (HaCaT), lung adenocarcinoma (A549) and liver carcinoma (HepG2) cells was performed by Basar et al. with an *in vitro* MTT assay. The plant material collected from Afghanistan showed the best activity among the others with IC_{50} values ranging from 158.8 to 248.5 µg/mL against three tested cell lines. Comprasion between glycyrrhizin content in licorice samples and their cytotoxic activity results indicated that glycyrrhizin might not positively contribute to the cytotoxic activity of *G. glabra* extract (116).

Yoon et al. extracted *G. inflata* roots with boiling distilled water, defatted with hexane and further partitioned with dichloromethane, ethyl acetate and *n*-butanol, respectively. Four compounds were purified from dichloromethane extract by cytotoxicity-guided fractionation. Licochalcone E was obtained as a new compound along with three known compounds which exerted different degrees of cytotoxic effects against fibrosarcoma HT1080 cells ($IC_{50} = 45.2 - 96.8$ µM), being the licochalcone E as the strongest compound among others (117).

In another study by Yoon et al., licochalcone A and licochalcone E were isolated from dichloromethane extract of *G. inflata* roots and evaluated for their cytotoxic activity in lung (A549), ovarian (SK-OV-3), melanoma (SK-MEK-2) and coloreactal (HCT-15) cancer cell lines by using sulforhodamine B assay. Licochalcone A ($IC_{50} = 2.68 - 4.83$ µg/mL) and licochalcone E ($IC_{50} = 2.86 - 5.85$ µg/mL) showed moderate cytotoxic activities against four tested cell lines comparing to doxorubicin and they inhibited DNA topoisomerase I, dose dependently (118).

Aydemir et al. reported the cytotoxic effect of aqueous extracts prepared from the leaves and flowers of an endemic species to Turkey, *G. flavescens* subsp. *antalyensis* against mouse melanoma cell lines (B16F10 and B16LNAD) and human embryo kidney cells (293T) by *in vitro* MTS test. Both extracts were found to be cytotoxic against

B16F10 (leaf IC_{50} = 67.39 μg/mL, flower IC_{50} = 49.95 μg/mL) and B16LNAD (leaf IC_{50} = 60.46 μg/mL, flower IC_{50} = 30.75 μg/mL) cells however, no cell toxicity was observed against human embryo kidney cells (293T) when compared to doxorubicin. Further mechanisms of action investigations showed that these extracts caused apoptosis by inducing TNF-α, interferon-γ and cleaved caspase-3 levels (119).

Ji and colleagues studied the cytotoxic activity of 122 compounds purified from *G. uralensis* against liver (HepG2), colorectal (SW480), lung (A549) and breast (MCF7) cancer cell lines by using MTS test. According to the obtained results, prenylated phenolic compounds showed significant cytotoxic activity, while flavonoid glycosides and triterpenoid saponins showed only weak activity. It was shown that the EtOAc extract had stronger cytotoxic effect (dose: 25 μg/mL, 76-99% inhibition) against four tested cell lines compared to the *n*-BuOH extract. Among tested isoflavones, isoangustone A and its isomer angustone A displayed the most potent effect against four tested cell lines (IC_{50} = 1.1 - 7.1 μM). The most active compound amongst the tested isoflavans was licoricidin (IC_{50} = 0.3 - 7.1 μM) which acted on liver cells (HepG2) in submicromolar level (IC_{50} = 0.3 μM) and displayed stronger cytotoxic activity than positive control irinotecan (IC_{50} = 0.9 μM). Further, the activity of flavones and coumarins were low-to-medium strength and strongest compound topazolin exerted IC_{50} values of 10.8, 16.1, 20.3 and 7.0 μM against HepG2, SW480, A549 and MCF7 cancer cells, respectively (22).

In a study in 2006 by Jung et al., the inhibitory effect of isoliquiritigenin from licorice on growth of prostate cancer cells and mechanism of cytotoxic action were investigated against rat (MLL) and human (DU145) prostate cancer cell lines. MTT, Hoechst staining and western blot assays revealed significant cytotoxic activity, increased number of apoptotic cells and induced release of cytochrom C and Smac/Diablo from mitachondria into cytosol as well as enhanced levels of cleaved caspase-9, -7, -3 and PARP. Authors demonstrated isoliquiritigenin inhibited cell growth in prostate cancer cell lines by inducing apoptosis which was mediated through mitachondrial events including caspase cascade while it did not show any growth inhibition in normal intestinal epithelal cells (120).

Lin and colleagues examined the cytotoxic activity of extracts and sixty-seven isolates obtained from *G. inflata* against liver (HepG2), colon (SW480) and breast (MCF7) cancer cell lines. Authors reported that EtOAc extract inhibited cell growth 77-

94% at 50 μg/mL concentration and eleven compounds purified from EtOAc extract including kanzonol C, gancaonin H, gancaonin Q, angustone B, 2'-hydroxyisolupalbigenin, , 6,8-diprenyl-genistein, 6,8-diprenyl-apigenin, licoflavone B, glabrol, euchrenone a_5 and euchestraflavanone A with strong cytotoxic activities (IC_{50} = 2.83 - 12.22 μM). Structure-activity relationship of the compounds revealed that the presence of the isoprenyl group in the structure increased the activity. While most of the molecules did not show cytotoxicity to normal cells (LO2, HEK293T), they were found to be selective cytotoxic to cancer cells (24).

In a study conducted by Li and colleagues, fifty-eight isolates including eleven new compounds were afforded from *G. glabra* and evaluated regarding their cytotoxic activities using HepG2, SW480, A549 and MCF7 human cancer cell lines. Glycybridin D, a new compound with an isoflavene skeleton was found to be active against all tested cancer cells (IC_{50} = 4.6 - 6.6 μM) which were further investigated by flow cytometry in A549 cells (IC_{50} = 4.6 μM) in order to understand its mechanism of action. It was shown to be a moderate tumor cell apoptosis inducer. Further, authors performed an *in vivo* experiment in nude mouse xenograft model implanted with A549 human lung carcinoma cells to evaluate antitumor effects of glycbridin D (10 mg/kg, i.p.) which resulted in significant inhibition of mass (39.7%) and volume (38.9%) of tumor at the end of 16 days of treatment with less adverse effects comparing to etoposide (5 mg/kg, i.p.). Structure-activity relationship between compounds showed that the cyclization of isoprenyl into pyran at ring A caused loss of cytotoxic activity while the absence of the isoprenyl moiety reduced activity (23).

Ji et al. in 2017 reported *in vitro* and *in vivo* anticancer activities of licoricidin against colorectal cancer and its cellular and molecular mechanisms of action. Licoricidin (IC_{50} = 7.2 μM) displayed an inhibition rate of 86% against SW480 human colorectal adenocarcinoma cells at 10 μM by using MTT assay. Furthermore it was found to be active against other colon cancer cell lines including HCT116 (IC_{50} = 5.4 μM), SW620 (IC_{50} = 4.5 μM) and LoVo (IC_{50} = 5.1 μM) cells. Further analyses indicated that on the SW480 cells licoricidin significantly increased cell cycle arrest in G_1/S phase, induced apoptosis by inhibiting cyclin/CDK1 expression and elevating cleaved caspase-3 and PARP-1 levels and promoted autophagic effect by activating the AMPK signal and inhibiting the Akt / mammalian target of rapamycin (mTOR) pathway. As a result of *in*

vivo experiments, licoricidin (20 mg/kg, i.p.) showed inhibition in the growth of SW480 xenografts in nude mice by 43.5%. In addition authors also demonstrated glycosylated product of licoricidin by microbial transformation enhanced *in vivo* antitumor activity of licoricidin (121).

Sheela et al. demonstrated that *G. glabra* methanol extract inhibited *in vivo* proliferation of Ehrlich Ascites Tumor (EAT) cell growth by 90% and water extract inhibited *in vitro* proliferation of EAT cells thus reduced cancer cell number, body weight and ascites volume. Observing decreased microvessel level in the peritoneum of EAT-bearing mice after treatment with *G. glabra* indicated blocking angiogenesis and action of cytokine vascular endothelial growth factor, which were suggested to have a crucial role in solid tumor development (122).

Hsieh et al. examined the effects of glabridin on metastasis of hepatocellular carcinoma cells. It was shown that glabridin significantly reduced *in vitro* migration and invasion abilities of human hepatoma cell lines Huh7 and Sk-Hep-1. Further analyses indicated that glabridin inhibited matrix metalloproteinase 9 (MMP9) expression, activities, protein levels and phosphorylation of ERK1/2 and JNK1/2 in Huh7 and Sk-Hep-1 cells. The effect of glabridin on tumor growth was also assesed with an *in vivo* study in SK-Hep-1 tumor xenografted nude mice model. The results showed that glabridin (10 mg/kg, i.p.) supressed tumor growth significantly (123).

Yo et al. demonstrated that *G. glabra* displayed cytotoxic activity in LNCaP human prostate cancer cells dose and time dependently and caused cell cycle arrest in G_2/M phase and accumulation of cells in subG_1 phase. *In vitro* studies on *G. glabra* and its component licochalcone A demonstrated induction of autophagy as well as caspase-dependent apoptosis which was associated by down-regulation of anti-apoptotic Bcl-2 protein and inhibition of the mTOR pathway in LNCaP cells (124).

Tamir and team conducted *in vitro* and *in vivo* studies to investigate the binding degree of glabridin, a major isoflavan found in *G. glabra*, into human estrogen receptors and the effect on breast cancer cells. Glabridin competed with estradiol and inhibited the degree of binding of estradiol to estrogen receptors in T47D human breast cancer cells at a concentration of approximately 5 μM, which is similar to activity of genistein. In order o distinguish the estrogenic agonist activity of glabridin from its antiproliferative

properties an *in vitro* cell proliferation assay was performed on estrogen receptor (ER)- (MDA-MB-468) and ER+ (T47D) human breast cancer cell lines. The activity of glabridin was found to be biphasic because glabridin exerted an estrogen receptor-dependent growth enhancing effect at low concentrations (0.1 - 10μM) whereas it showed estrogen receptor-independent antiproliferative activity at >15 μM. The effect of glabridin on anchorage-independent growth of MCF7 breast cancer cells was investigated and it was observed that colony formation was inhibited at concentrations of ≥ 25 μM while concentration at 10 μM glabridin caused increase in colony formation. Authors explained the important role of hydroxyl groups' position in estrogen receptor binding and proliferation inducing activity by comparing the activities of chemically modified derivatives of glabridin. It was found that glabridin was three to four times more active than 2'-*O*-methylglabridin and 4'-*O*-methylglabridin while 2',4'-*O*-methylglabridin had no effect in binding and cell proliferation (125).

To investigate the effect of licorice on tumor size in colon cancer, Lee et al. applied the EtOH extract of *G. inflata* alone and in combination with chemotherapeutic medicine cisplatin to BALB/C mice inoculated with colon carcinoma cells (CT-26) for 15 days. When *G. inflata* extract was administered at doses of 0.5, 1, and 2 mg/kg, tumor growth was inhibited by 38%, 57%, and 71%, respectively, while cisplatin combined treatment increased this antitumor effect. Comparasion of cisplatin alone and combination therapy revealed that licorice recovered cisplatin induced adverse effects including elevated blood urea nitrogen and creatinin as well as increased ALT and AST levels because of the kidney and liver damage. In addition, licorice extract significantly reduced oxidative stress caused by cisplatin (126).

In 2008, Choi and colleagues prepared a *n*-hexane:EtOH (9:1) extract (HEGU) to dereplicate glycyrrhizin to avoid its adverse effects such as hypertension. HEGU showed reduce in viable cell numbers of HT-29 human colon cancer cells (IC_{50} = 10.7 ± 0.3 mg/L), MDA-MB-231 human breast cancer cells (IC_{50} = 7.5 ± 0.1 mg/L), and DU145 human prostate cancer cells (IC_{50} = 4.7 ± 0.5) (127).

In a study conducted by Seon et al. in 2010, hexane/EtOH extract (9:1) of *G. uralensis* (HEGU) which contained undetectable amount of glycyrrhizin was prepared and assesed for its effects against adrogen-insensitive prostate DU145 cancer cells which was found to be most sensitive through the effect of HEGU among tested cell lines

according to previos study of Choi et al. (2008) (127). Authors demonstrated that HEGU induced apoptosis by inducing cytochrome C release and increasing levels of cleaved caspase-9, -7, -3 and PARP levels in DU145 cells in addition to increased levels of Fas, death receptor 4 (DR4), cleaved caspase-8, Mcl-1S, and cleaved Bid proteins. Further, isoangnustone A was isolated from active fraction of HEGU and structurally elucidated by NMR. Further studies on isoangustone A revealed its cytotoxic activity by increasing apoptotic cells, cleaved PARP and caspase levels in addition to DR4 and Mcl-1S levels. Taken together HEGU and isoangustone A induced apoptosis in DU145 cells via both death receptor (DR)-dependent and mitochondria-dependent apoptotic pathways (128).

Seon et al. in 2012, investigated the mechanism of inhibiting cell cycle progression of the hexane/EtOH extract (9:1) of *G. uralensis* (HEGU) and its active ingredient isoangustone A in the human prostate cancer (DU145) and murine mammary carcinoma (4T1) cells. HEGU (2.5, 5 or 7.5 μg/mL) and isoangustone A (2.5 or 5 μg/mL) inhibited DNA synthesis and induced G_1 phase arrest in both cell lines. Western blot assays revealed that HEGU reduced cyclin dependent kinases CDK2, CDK4, cylin A and cyclin D1 protein expression while isoangustone A decreased CDK2, CDK4, cylin A and cyclin E levels in both tested cells. According to the *in vivo* study results which was performed in BALC/c mice inoculated with breast cancer (4T1) cells, antiproliferative effect was observed in tumor cells in mice given HEGU (5 mg/kg/day). Further western blot analysis showed that this effect could be associated with the reduction of CDK2 and CDK4 protein expression. Based on these data, it was considered that the hexane /EtOH *G. uralensis* extract containing isoangustone A might be a potential antitumor agent (129). Isoangustone A was also studied with regards to its potential anticancer effects against colon cancer by Huang and team. It exhibited strong cytotoxic activity dose dependently (IC_{50} = 6 μM) in SW480 human colorectal adenocarcinoma cell line. Mechanistic studies showed the induction of apoptosis which was confirmed by observing fragmentation of genomic DNA in addition to presence of condensed chromatin and fragmented nuclei according to propidium iodide (PI) -Annexin V staining and Hoechst staining assays in SW480 cells. Further investigations showed that isoangustone A increased outer membrane permeabilization of mitochondria and release of cytochrome C and thus activated caspase-3 and -9 activity and caused increase in cleaved PARP and decrease in Bcl-2 protein level. Inhibition in phoshorylation of Akt was observed which is a very important pathway in preventing apoptosis (130).

According to a study by Hawthorne and Gallagher, crude *G. glabra* extract (70% ethanol) and glyryrrhetinic acid which is an *in vivo* metabolite of of glycyrrhizic acid with intestinal bacterial glucuronidase activity showed *in vitro* antiprolifetarive activity against androgen-dependent prostate cells (LNCaP) having 10.3 mg/mL and 0.5 mg/mL IC_{50} values, respectively while exerting no effect in androgen-independent prostate cells (PC3 and DU145). Additionally, they both inhibited secretion of prostate-specific antigen (PSA) (131).

Hibasami et al. demonstrated the apoptosis inducing effect of glycyrrhetinic acid by reporting presence of apoptotic body and fragmentation of DNA in human hepatoma (HLE), promyelotic leukemia (HL-60) and stomach cancer (KATO III) cells by treatment with glycyrrhetinic acid (132).

Chemopreventive effect of glycyrrhizic acid in 1,2-dimethyhydrazine- induced precancerous lesions as well as its activity on hyperproliferation, inflammation, angiogenesis and apoptosis in Wistar rat colons were investigated. Animals were divided into 5 groups. Authors administered 1,2-dimethyhydrazine (20 mg/kg) to group 2, 1,2-dimethyhydrazine and also glycyrrhizic acid (15 mg/kg orally, starting 1 week before carcinogen treatment) to group 3, 1,2-dimethyhydrazine and glycyrrhizic acid (15 mg/kg orally, starting from 2 days after carcinogen injection) to group 4 and only glycyrrhizic acid (15 mg/kg, orally, everyday) to group 5. The results showed that glycyrrhizic acid inhibited precancerous lesions development and also decreased the infiltration of mast cells, supressed Ki-67, NF-kB-p65, COX-2, iNOS and vascular endothelial growth factor (VEGF), while enhancing p53, connexin-43, caspase-9 and cleaved caspase-3 activation. Glycyrrhizin was found to reduce TNF-α level and depletion of mucous layer (133).

Park and colleagues investigated cytotoxicity and mechanism of licochalcone A against pharyngeal squamous carcinoma FaDu cell line. Within this study, licochalcone A was found to be cytotoxic against FaDu cell line with IC_{50} value of 100 μM by MTT assay. Chromatin condensation and increased number of apoptotic cells were observed with licochalcone A tretment. TRAIL (Tumor Necrosis Factor-Related Apoptosis-Including Ligand) was upregulated and apoptotic responses including caspases and PARP were significantly activated in FaDu cells with licochalcone A treatment. According to *in vivo* study conducted by authors, licochalcone A significantly inhibited FaDu cell

xenograft growth in mouse model by caspase-3 activation suggested the potential chemopreventive effects of licochalcone A (7).

Zheng and colleagues isolated eleven compounds including four new triterpene glycosides from *G. uralensis* and evaluated cytotoxic effets of selected compounds as well as their a glycones against human cervical cancer (HeLa) and MCF7 cancer cell lines by using colorimetric MTT assay. The results demonstrated that tested triterpene glycosides were not cytotoxic ($IC_{50} > 100$ µM) whereas aglycones of urolasaponin D, licorice-saponin G2 and glycyrrhizin exerted cytotoxic activities against HeLa and MCF7 with IC_{50} values of 35.3 ± 3.6, 19.9 ± 2.5, and 15.5 ± 1.4 µM; 38.5 ± 2.8, 20.5 ± 3.6, and 11.4 ± 3.0 µM, respectively (134).

Isoliquiritigenin was evaluated for its effects against cell proliferation, apoptotis as well as its mechanisms in mouse macrophage (RAW264.7), mouse colon cancer (colon 26), rat colon cancer cells (RCN-9) and human colon cancer cell (COLO-320DM). Isoliquiritigenin caused a significant decrease in PGE_2 level ($IC_{50} = 1.47$ µM) and inhibited nitric oxide production ($IC_{50} = 7.78$ µM) in RAW264.7 cells. Addtitionally expressions of COX-2 and iNOS protein were suppressed with isoliquiritigenin treatment (25 µM) by 52% and 86%, respectively. Remarkable apoptosis induction in Colon 26 cells and increase in caspase-3 activation in Colon 26 and COLO-320DM cells were observed after treatment with isoliquiritigenin. Further *in vivo* studies in male F344 rat colon indicated that oral isoliquiritigenin administration supressed the induction of preneoplastic abberant crypt foci (135). In another study, the effect of isoliquiritigenin obtained from *G. glabra* roots was investigated in breast cancer metastasis. Anoikis resistance presents in multiple key stages of metastatic cascade. The *in vitro* experiments showed that isoliquiritigenin induced anoikis in human breast cancer cells (MDA-MB-231 and BT-549) and supressed mRNA expression of phospholipase A2, COX-2 and CYP 4A and reduced PGE_2 and 20-hydroxyeicosatetraenoic acid (20-HETE) secretion in MDA-MB-31 cancer cells. Additionaly authors conducted an *in vivo* study which resulted in inhibitory action of isoliquiritigenin in lung metastasis of MDA-MB231 by decreasing intratumoral levels including PGE_2, 20-HETE and phorpho-Akt. Taken together isoliquiritigenin was found to be a promising antimetastatic agent in breast cancer by preventing anoikis resistance, migration and invasion of cancer cells via downregulation of COX-2 and CYP 4A signaling (136).

Chueh et al. studied *in vitro* antileukemia effect of glycyrrhizic acid in a mouse leukemia cell line (WEHI-3). Results showed that glycyrrhizic acid caused G_0/G_1 phase arrest, apoptosis and DNA damage in WEHI-3 cells as well as morphological changes. Furthermore, glycyrrhizic acid induced apoptosis through both intrinsic and extrinsic pathways by decreasing the mitochondrial membrane potential, activating caspase-3 activity, releasing cytochrome C, endonuclease G and apoptosis-inducing factor in WEHI-3 cells (137).

The anticancer effect of 18β-glycyrrhetinic acid which was isolated from *G. glabra* roots against MCF7 cells was investigated by Sharma et al. The authors demonstrated that 18β-glycyrrhetinic acid exerted potent cytotoxic effects against MCF7 while it did not affect normal mamary epithelial cell line (MCF10A). Apoptosis observed via phosphatidyl serine externalization and DNA fragmentation. The mechanism of apoptosis was explained by mitochondrial death cascade which was understood from increased release of cytochrome C and caspase-9 activation. Furthermore, the ratio between Bax:Bcl2 was increased along with elevated BH3 protein level. The results indicated that 18β-glycyrrhetinic acid induced apoptosis through caspase cascade as well as Akt/FOXO3a pathway (138).

2.1.2.10. Studies on Other Activities

In a study by Choi and colleagues, hexane: EtOH (9:1) extract of *G. uralensis* (HEGU) which was shown to contain no detectable glycyrrhizin was evaluated for its protective activity against doxorubicin induced cardiotoxicity. H9c2 rat cardiac myoblasts were treated with 0 – 15 mg/L HEGU which inhibited the reduction in cell viability ($34.6 \pm 7\%$) and reduced apoptosis caused by doxorubicin ($53.6 \pm 1\%$). Further mechanistic analyses showed that HEGU supressed the elevated levels of p53, phospho-p53 and proapoptotic protein Bax while caused an increase in anti-apoptotic Bcl-xL levels. HEGU also displayed inhibition in doxorubicin induced cleavage of caspase-9,-7, and -3 and PARP levels. While being cytoprotective for cardiac myoblast cells, it was found to be cytotoxic against cancer cells including HT-29 human colon, MDA-MB-231 human breast and DU145 human prostate cancer cells as mentioned previously. Taken together HEGU decreased DOX-induced apoptosis in cardiac myoblast cells (H9c2) by inhibiting of p53 activation, its downstream events including Bax expression and caspase activation (127).

G. glabra, G. uralensis, and *G. inflata* species were evaluated for their estrogenic activity. *G. inflata* showed higher estrogenic potency in alkaline phosphatase induction assay in Ishikawa cells (ERα) and an estrogen responsive element (ERE)-luciferase assay in MDA-MB-231/β41 breast cancer cells (ERβ). Bioactivity-guided fractionation of *G. inflata* resulted in the isolation of 8-prenylapigenin which showed 14-fold preferential ERβ agonist activity and was found to be 33 times more concentrated in *G. inflata* extract than other licorice extracts. 8-prenylapigenin standardized extract of *G. inflata* was suggested to be used for postmenopausal women (139).

In another study conducted by Simons et al., fifty-one fractions obtained from EtOAc fraction of *G. glabra* roots through centrifugal partition chromatography were identified by LC-MS and assesed for their estrogenic activities in yeasts. Authors revealed that many fractions showed stronger responses than 17β-estradiol, the reference compound. Furthermore glabrene rich fractions exerted estrogenic responses mainly against ERα receptors while glabridin showed no agonistic activity against any ERα or ERβ receptors and inhibited estrogenic responce of estradiol by 80% at concentration of 1 μM (140).

Dhingra and Sharma investigated antidepressant activity of *G. glabra* aqueous extract by using immobility test in mouse models. Authors gave 70, 150 and 300 mg/kg *G. glabra* extracts to divided groups of albino mices for 7 days. Forced swim test and tail suspension tests were conducted into the animal groups and it was demonstrated that 150 mg/kg licorice extract reduced the immobilization of animals regarding to the both tests through increasing brain norepinephrine and dopamine levels (141).

Effects of *G. glabra* on memory and learning were evaluated by Parle et al. with exteroceptive and interoceptive behavioral models on mices. Results showed that aqueous extract of *G. glabra* (150 mg/kg) ameliorated learning and memory of mices and supressed the amnesia caused by diazepam, scopolamine and ethanol (142).

The hypnotic effects and GABAergic mechanism of ethanol extract of *G. glabra* and glabrol, one of its major isolated flavonoids were investigated by Cho and colleagues. *G. glabra* ethanol extract showed enhancement in pentobarbital-induced sleep and increased non-rapid eye movement sleep in mice by not affecting and reducing delta activity. Further studies on glabrol indicated that it suppressed the binding of flumazenil

to GABA$_A$-BZD receptors in cerebral cortex membrane of rats and increased duration of sleep as well as reducing sleep latency dose dependently (5, 10, 25 and 50 mg/kg). These mentioned hpynotic activities of *G. glabra* and glabrol were both inhibited by GABA$_A$-BZD receptor antagonist agent flumazenil concluding that the mechanism was occured via positive modulation of GABA$_A$-BZD receptors (143).

Hoffman et al. studied the effect of glabridin on GABA$_A$ receptors and demonstrated hypnotic effect of glabridin mediated by GABA$_A$ receptor potentiating effect on α1β(1-3)γ receptors (144) .

Nerya and collagues investigated tyrosinase inhibitory activities of *G. glabra* extract, glabridin, glabrene, hispaglabridin A, hispaglabridin B and isoliquiritigenin obtained from *G. glabra* by using tyrosinase assay in human melanocyte (G361) cell culture. *G. glabra* extract showed tyrosinase inhibitory activity with IC$_{50}$ value of 0.9 µg/mL. Furthermore, authors demonstrated that glabridin (IC$_{50}$ = 0.09 µM), isoliquiritigenin (IC$_{50}$ = 3.5 µM) and glabrene (IC$_{50}$ = 8.1 µM) exerted potent monophenolase activity and these compounds could be used for skin lightening through inhibiting tyrosinase-dependent melanin biosynthesis (145).

By using an *in vitro* tyrosinase inhibition assay, the nepalese crude drugs were screened within a study of Adhikari et al in 2008. According to the obtained results, *G. glabra* methanol extract showed 78.9% mushroom tyrosinase inhibitory activity at 50 µg/mL concentration, could potentially be used to control hyperpigmentation (146).

2.1.3. Compounds Isolated from *Glycyrrhiza* species

The phytochemical studies performed on *Glycyrrhiza* species indicated that the genus comprises mainly chalcones, flavonoids, isoflavonoids and triterpene saponins. The isolated secondary metabolites from *Glycyrrhiza* species were compiled and given in the figures and tables (Table 1-103). (**A**: aerial parts, **CC**: Cell culture, **L**: leaves, **R**: roots, **Rh:** rhizomes, **S**: stems, **W**: whole plant)

2.1.3.1. Phenolic Compounds

2.1.3.1.A. Phenones Isolated from *Glycyrrhiza* species
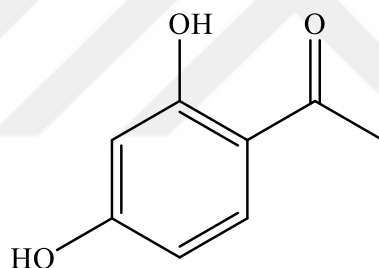
Table 1. Phenone isolated from *Glycyrrhiza* species

Compound	Species	Ref
2,4-dihydroxyacetophenone	*glabra* (S)	(147)
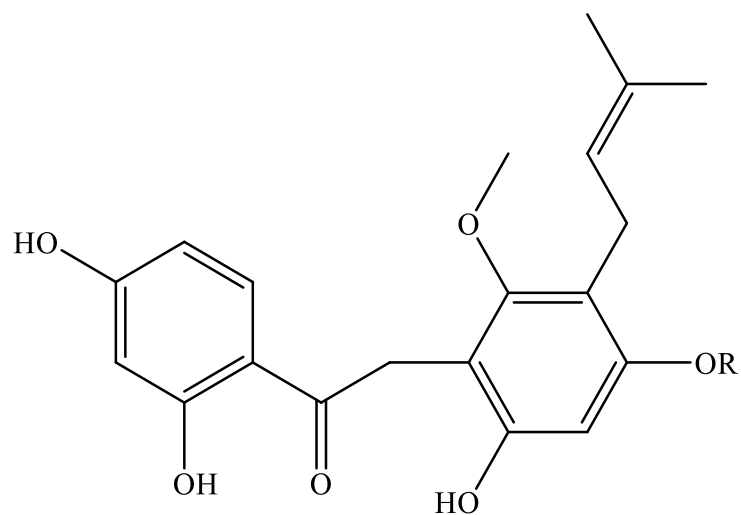
Table 2. Phenones isolated from *Glycyrrhiza* species

Compounds	R	Species	Ref
Licoriphenone	CH$_3$	*uralensis* (R)	(148)
Glicophenone	H	*uralensis* (R)	(148)
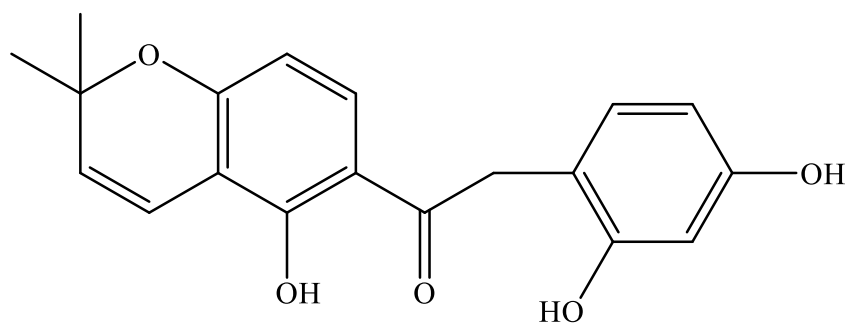
Table 3. Phenones isolated from *Glycyrrhiza* species

Compound	Species	Ref
Erybacin B	*glabra* (R)	(23)

2.1.3.1.B. Phenolic Acids and Derivatives Isolated from *Glycyrrhiza* species
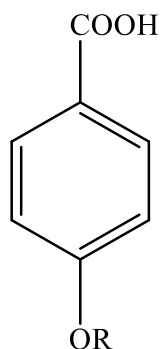
Table 4. Phenolic acids isolated from *Glycyrrhiza* species

Compounds	R	Species	Ref
Hydroxybenzoic acid	H	*inflata* (R)	(99)
Anisic acid	CH$_3$	*inflata* (R)	(99)
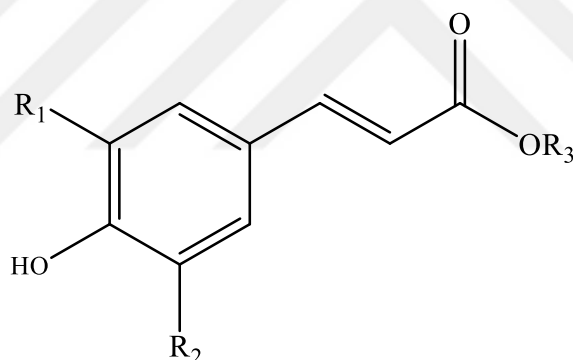
Table 5. Phenolic acids isolated from *Glycyrrhiza* species

Compounds	R$_1$	R$_2$	R$_3$	Species	Ref
Caffeic acid	OH	H	H	*glabra* (A)	(147)
Ferulic acid	OCH$_3$	H	H	*glabra* (R)	(147)
Sinapic acid	OCH$_3$	OCH$_3$	H	*glabra* (R)	(147)
Chlorogenic acid	OH	H	quinic acid	*glabra* (A)	(147)
Neochlorogenic acid	OH	H	quinic acid	*glabra* (A)	(147)
Eicosanyl caffeate	OH	H	eicosanyl	*glabra* (R)	(149)
Docosyl caffeate	OH	H	docosyl	*glabra* (R)	(149)

2.1.3.1.C. Chalcones Isolated from *Glycyrrhiza* species
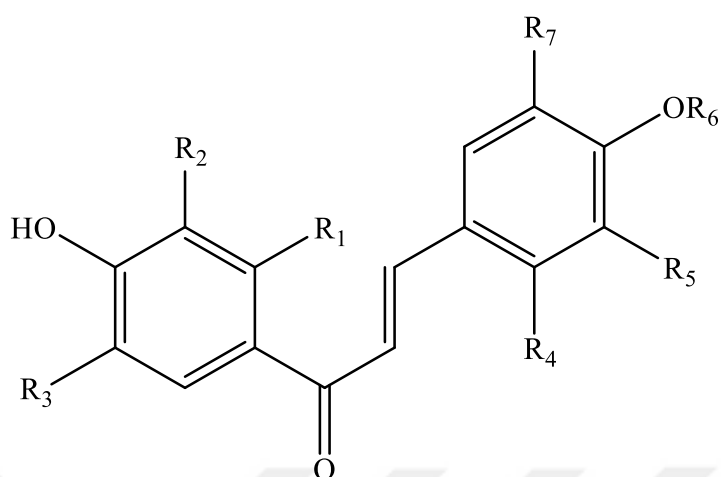
Table 6. Chalcones isolated from *Glycyrrhiza* species

Compounds	R_1	R_2	R_3	R_4	R_5	R_6	R_7	Species	Ref
Isoliquiritigenin	OH	H	H	H	H	H	H	*glabra* (R) *uralensis* (R+Rh, R) *inflata* (R) *pallidiflora* (R)	(61,88, 99,150– 152)
2'-methoxy isoliquiritigenin	OCH$_3$	H	H	H	H	H	H	*uralensis* (R)	(61,65)
Isoliquiritin	OH	H	H	H	H	β-D-Glc	H	*glabra* (R) *uralensis* (R) *eurcarpa*	(16,22,6 1,99,150, 153,154)
Isoliquiritin apioside, Licuroside	OH	H	H	H	H	β-D-Glc- 2-*O*-Api	H	*uralensis* (R) *glabra* (R)	(61,155– 157)
6''-*O*- acetylisoliquiritin	OH	H	H	H	H	6-*O*-Ac- β-D-Glc	H	*uralensis* (R)	(157)

Glc: Glucose,   Api: Apiose,   Ac: Acetyl

Table 6. Chalcones isolated from *Glycyrrhiza* species

Compounds	R$_1$	R$_2$	R$_3$	R$_4$	R$_5$	R$_6$	R$_7$	Species	Ref
Echinatin	H	H	H	OCH$_3$	H	H	H	*echinata* (R) *glabra* (R) *uralensis* (R) *inflata* (R) *pallidiflora* (R) *aspera* (R)	(21,94,99,152,158–163)
Licochalcone A	H	H	H	OCH$_3$	H	H	isopre	*inflata* (R) *glabra* (R) *uralensis* (CC, R)	(16,23,164,87,99,115,117,124,150,153,158)
Licochalcone B	H	H	H	OCH$_3$	OH	H	H	*inflata* (R) *glabra* (R) *uralensis* (R)	(87,94,99,158,159,165)
Licochalcone C	H	H	H	OCH$_3$	isopre	H	H	*inflata* (R) *glabra* (R)	(87,117,158,166)
Licochalcone D	H	isopre	H	OCH$_3$	OH	H	H	*inflata* (R)	(87,158)
Licochalcone E	H	H	H	OCH$_3$	H	H	1,2-dimethyl-2-propenyl	*inflata* (R)	(24,99,118)
Licochalcone K	H	OH	H	OCH$_3$	H	H	isopre	*inflata* (R)	(24,99)
Licochalcone I	H	H	H	OCH$_3$	OH	H	isopre	*inflata* (R)	(24,99)
Isobavachalcone	OH	isopre	H	H	H	H	H	*inflata* (R) *glabra* (CC) *uralensis* (CC)	(99,164,167)

Isopre: isoprenyl

Table 6. Chalcones isolated from *Glycyrrhiza* species

Compounds	R$_1$	R$_2$	R$_3$	R$_4$	R$_5$	R$_6$	R$_7$	Species	Ref
Licoagrochalcone A	OH	H	H	H	isopre	H	H	*inflata* (R) *glabra* (R, CC)	(24,99, 166, 168)
Licoagrochalcone C	H	OH	H	OCH$_3$	isopre	H	H	*inflata* (R) *glabra* (R)	(24,99, 109, 166)
3,4,3',4'-tetrahydroxy chalcone	H	OH	H	H	OH	H	H	*inflata* (R)	(99)
Homobutein	OH	H	H	H	OCH$_3$	H	H	*uralensis* (R)	(22)
Corylifol B	OH	isopre	H	H	OH	H	H	*inflata* (R)	(99)
Kanzonol C	OH	isopre	H	H	isopre	H	H	*inflata* (R) *glabra* (R)	(23,24, 99)
Xinjiachalcone A	H	H	H	OCH$_3$	H	isopre	H	*inflata*	(169)
Tetrahydroxymethoxychalcone	H	OH	H	OCH$_3$	OH	H	H	*uralensis* (R)	(148, 170)
3,3',4,4',-tetrahydroxy-2'-methoxy-5-prenylchalcone	H	isopre	OH	OCH$_3$	OH	H	H	*glabra* (R)	(94)
2,3',4,4',-tetrahydroxy-2-methoxy-3,5'-diprenylchalcone	OH	isopre	H	H	OH	H	isopre	*glabra* (R)	(94)
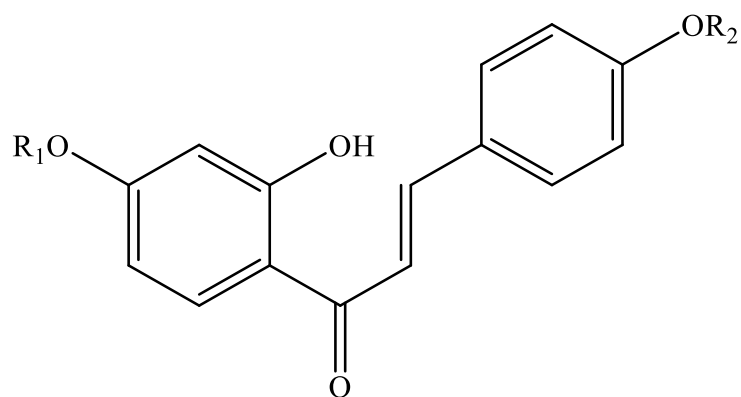
Table 7. Chalcones isolated from *Glycyrrhiza* species

Compounds	R$_1$	R$_2$	Species	Ref
Neoisoliquiritin	β-D-Glc	H	*uralensis* (R)	(157)
Neoisoliquiritin apioside, Neolicuroside	β-D-Glc-2-*O*-Api	H	*uralensis* (R) *glabra* (R)	(156,157)
Isoechinogenin	H	H	*echinata* (R)	(147)
6"-*O*-acetylneoisoliquiritin	6-*O*-Ac-β-D-Glc	H	*uralensis* (R)	(157)
Glucoisoliquiritin apioside	β-D-Glc	β-D-Glc-2-*O*-Api	*aspera* (R)	(163)
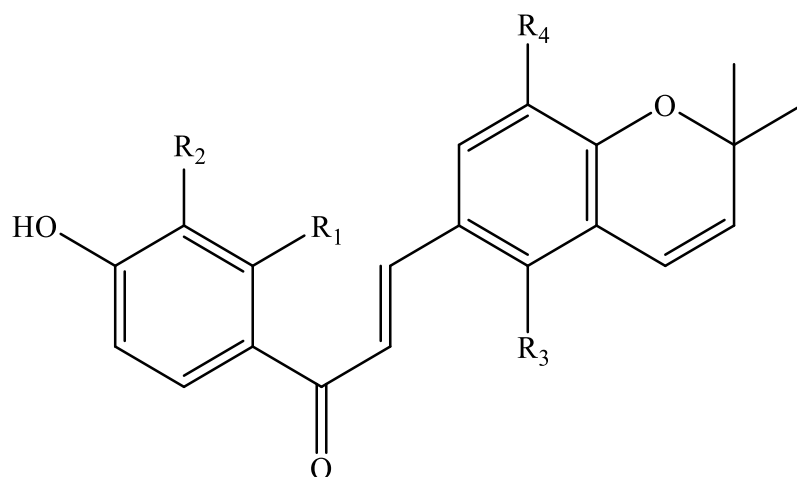
Table 8. Chalcones isolated from *Glycyrrhiza* species

Compounds	R₁	R₂	R₃	R₄	Species	Ref
Kanzonol B	OH	H	H	H	*inflata* (R) *glabra* (R)	(23,99)
[6″,6″-dimethylpyrano(2″,3″:4,5)]−3′-γ,γ-dimethylallyl-2′,3,4′-trihydroxychalcone	OH	isopre	H	OH	*glabra* (R)	(23,171)
Licoagrochalcone B	H	H	OCH₃	OH	*glabra* (R)	(166)
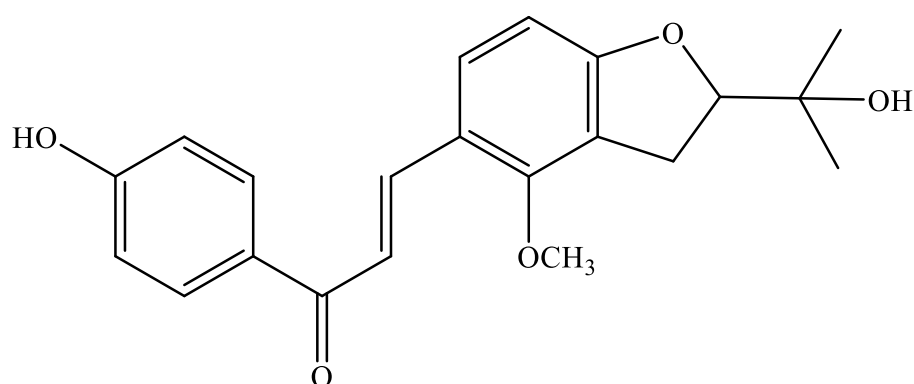
Table 9. Chalcone isolated from *Glycyrrhiza* species

Compound	Species	Ref
Licoagrochalcone D	*glabra* (R)	(166)
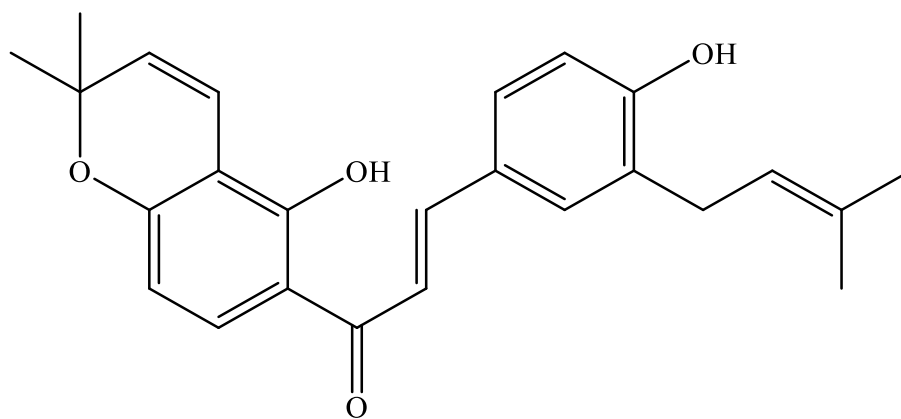
Table 10. Chalcone isolated from *Glycyrrhiza* species

Compound	Species	Ref
Paratocarpin	*inflata* (R)	(99)
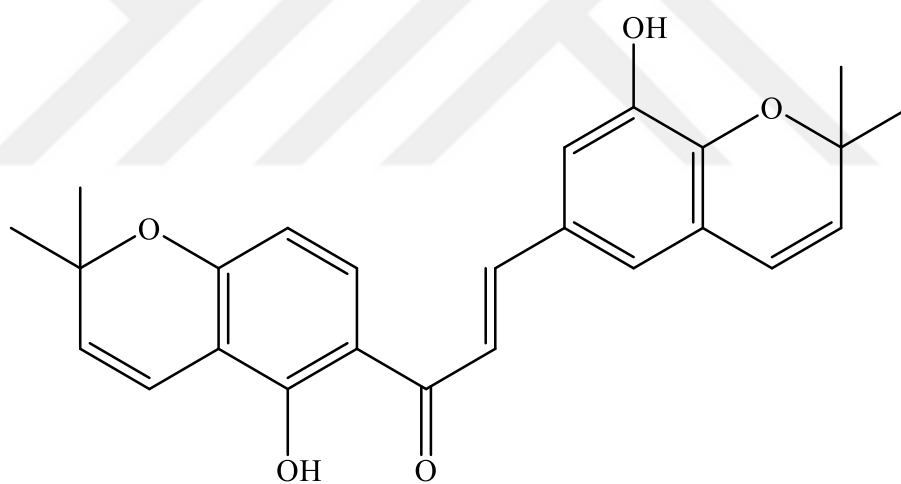
Table 11. Chalcone isolated from *Glycyrrhiza* species

Compound	Species	Ref
Glyinflanin G	*glabra* (R)	(171,172)
	inflata (R)	
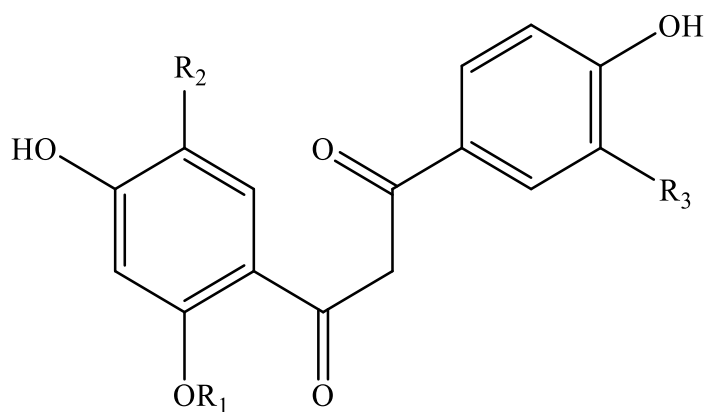
Table 12. β-Ketodihydrochalcones isolated from *Glycyrrhiza* species

Compounds	R$_1$	R$_2$	R$_3$	Species	Ref
Licodione	H	H	H	*echinata* (CC) *pallidiflora* (R)	(152,162)
2'-*O*-methyllicodione	CH$_3$	H	H	*pallidiflora* (R)	(152,173)
5'-prenyl-licodione	H	isopre	H	*inflata* *eurycarpa*	(14,174)
Glycyrdione A, Glyinflanin A	H	isopre	isoprenyl	*inflata* (R) *glabra* (R)	(14,166, 174,175)
Glyinflanin E	H	isopre	2-hydroxy-3-methyl-3-butenyl	*inflata* (R)	(172)
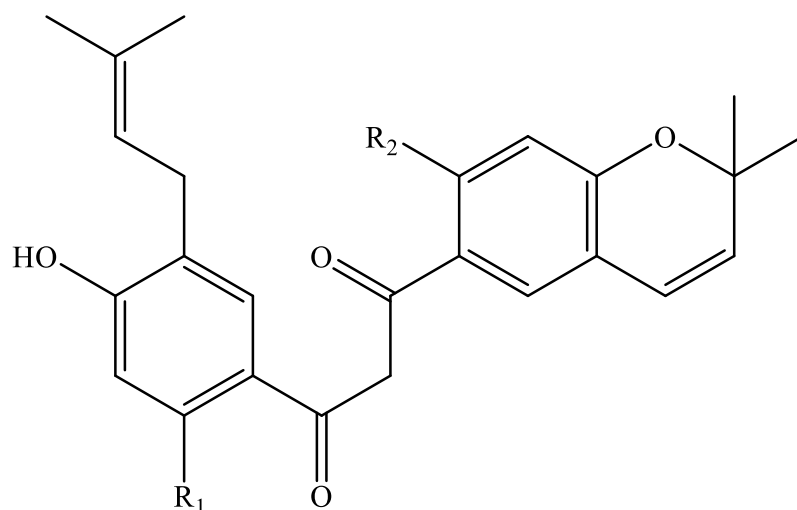
Table 13. β-Ketodihydrochalcones isolated from *Glycyrrhiza* species

Compounds	R₁	R₂	Species	Ref
Glycyrdione B	OH	H	*inflata* (R)	(174)
Glyinflanin C	H	OH	*inflata* (R)	(14,174,175)
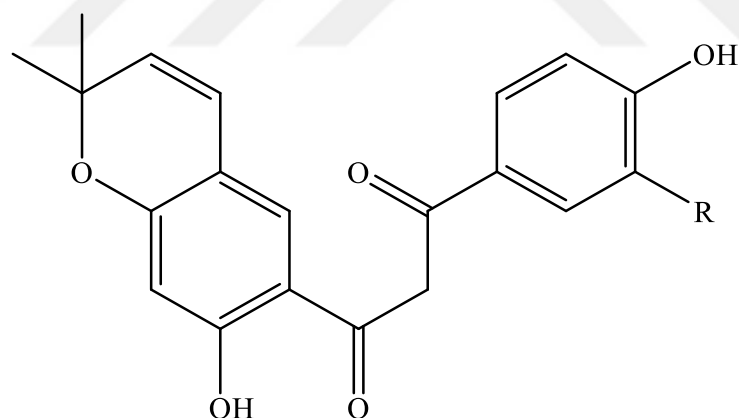
Table 14. β-Ketodihydrochalcones isolated from *Glycyrrhiza* species

Compounds	R	Species	Ref
Glycyrdione C	isoprenyl	*inflata* (R)	(176)
Glyinflanin B	H	*glabra* (R) *eurycarpa* (R) *inflata* (R)	(14,166,175)
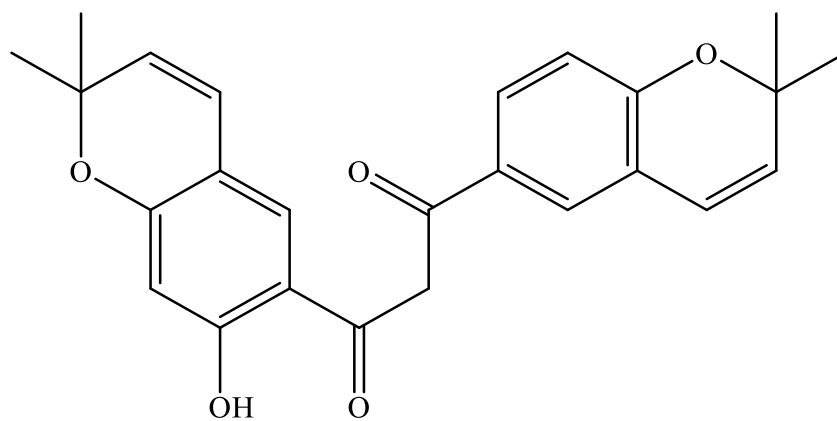
Table 15. β-Ketodihydrochalcone isolated from *Glycyrrhiza* species

Compound	Species	Ref
Glyinflanin D	*inflata* (R)	(175)
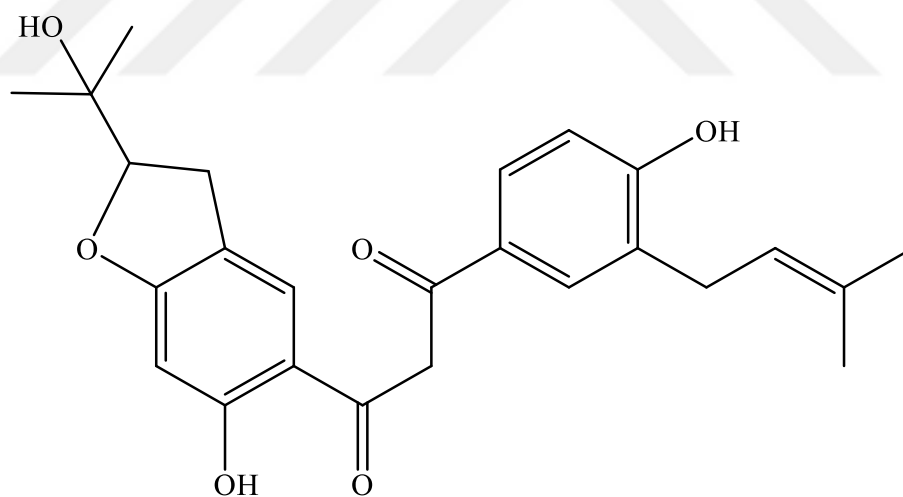
Table 16. β-Ketodihydrochalcone isolated from *Glycyrrhiza* species

Compound	Species	Ref
Glyinflanin F	*inflata* (R)	(172)
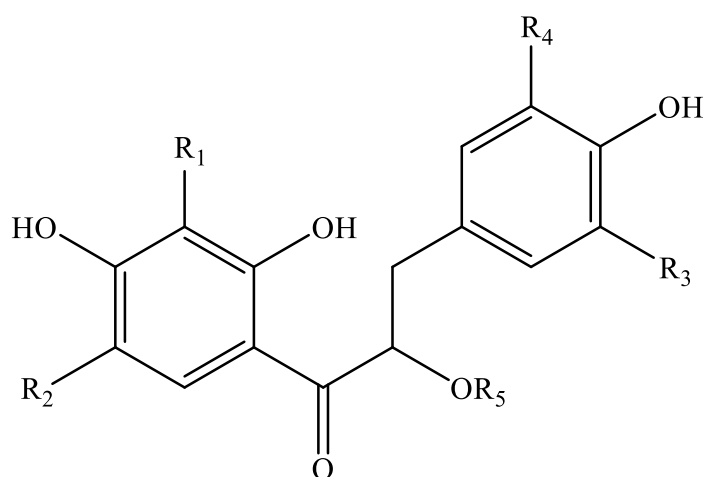
Table 17. α-Hydroxydihydrochalcones isolated from *Glycyrrhiza* species

Compounds	R₁	R₂	R₃	R₄	R₅	Species	Ref
Glycybridin B	H	H	isopre	H	H	*glabra* (R)	(23)
Glycybridin C	isopre	H	isopre	H	H	*glabra* (R)	(23,99)
Kanzonol Y	H	isopre	isopre	H	H	*glabra* (R)	(23,99, 177)
2,3',4,4',α-pentahydroxy- 3,5'-diprenyl-dihydrochalcone	isopre	H	OH	isopre	H	*glabra* (R)	(94)
2,3',4,4',α-pentahydroxy- 3-prenyl-dihydrochalcone	isopre	H	OH	H	H	*glabra* (R)	(94)
Licoagroside F	H	H	H	H	β-D-Glc	*pallidiflora* (R)	(178)
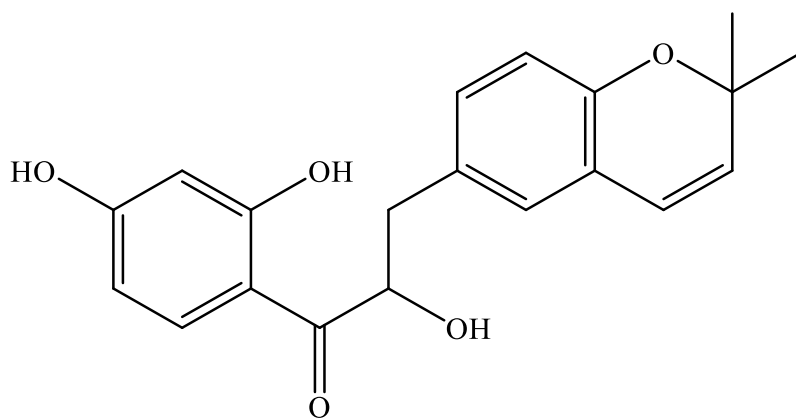
Table 18. α-Hydroxydihydrochalcone isolated from *Glycyrrhiza* species

Compound	Species	Ref
Glycybridin A	*glabra* (R)	(23)
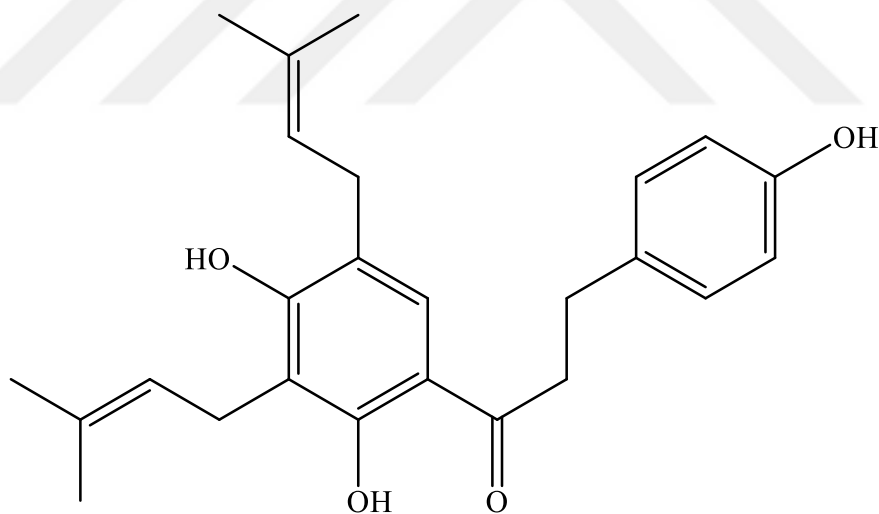
Table 19. Dihydrochalcone isolated from *Glycyrrhiza* species

Compound	Species	Ref
Gancaonin J	*pallidiflora* (R)	(173)
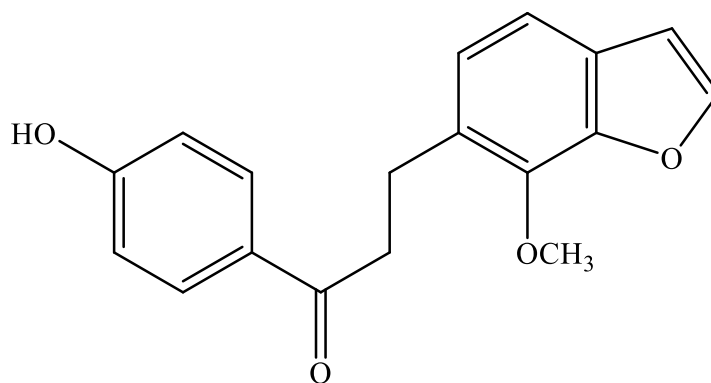
Table 20. Dihydrochalcone isolated from *Glycyrrhiza* species

Compound	Species	Ref
4'-hydroxy-2-methoxy-[2'',3'':3, 4]-furanodihydrochalcone	*uralensis* (CC)	(164)
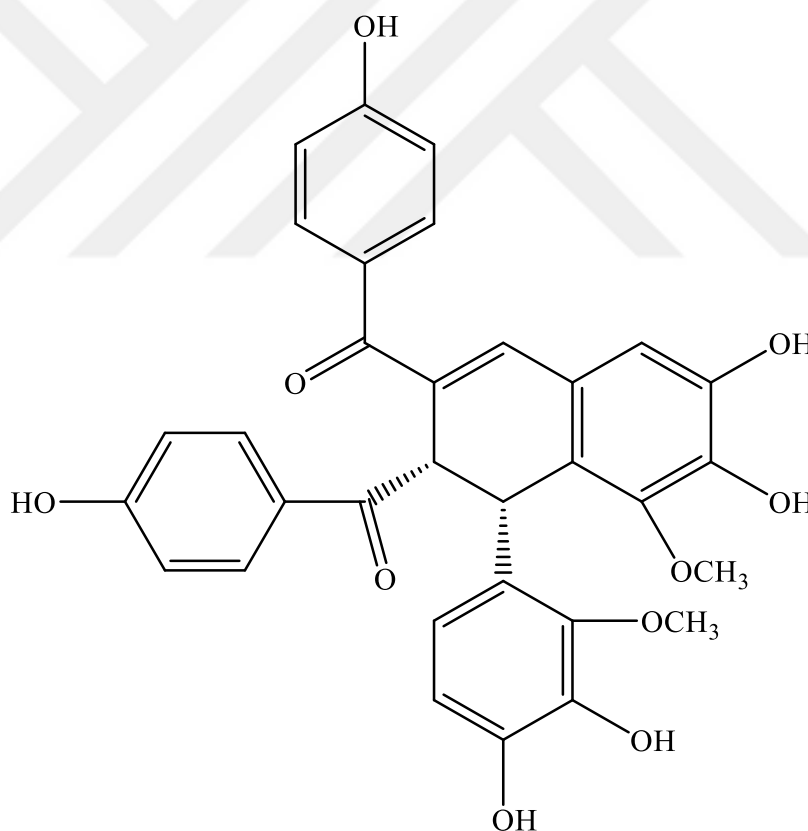
Table 21. Bichalcone isolated from *Glycyrrhiza* species

Compound	Species	Ref
Licobichalcone	*uralensis* (R)	(159)

2.1.3.1.D. Flavonoids Isolated from *Glycyrrhiza* species
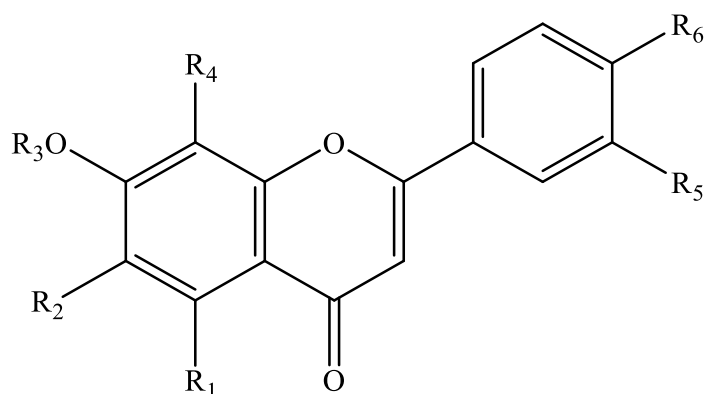
Table 22. Flavones isolated from *Glycyrrhiza* species

Compounds	R_1	R_2	R_3	R_4	R_5	R_6	Species	Ref
Apigenin	OH	H	H	H	H	OH	*pallidiflora* (R) *glabra* (R+Rh)	(21, 179)
4',7-dihydroxyflavone	H	H	H	H	H	OH	*pallidiflora* (R) *inflata* (R)	(152, 176)
Genkwanin	OH	H	CH₃	H	H	OH	*uralensis* (R)	(22)
6,8-diprenylapigenin	OH	isopre	H	isopre	H	OH	*inflata* (R)	(109)
Chrysin	OH	H	H	H	H	H	*pallidiflora* (R)	(21)
Genkwanin	OH	H	CH₃	H	H	OH	*uralensis* (R)	(22)
Licoflavone A	H	isopre	H	H	H	OH	*glabra* (R) *uralensis* (R) *inflata* (R)	(22,94, 99, 109)
Prenyllicoflavone A, Licoflavone B	H	isopre	H	H	isopre	OH	*glabra* (R) *inflata* (R)	(24,109 ,161)

Table 22. Flavones isolated from *Glycyrrhiza* species

Compounds	R₁	R₂	R₃	R₄	R₅	R₆	Species	Ref
Licoflavone C	OH	H	H	isopre	H	OH	*inflata* (R)	(109)
Gancaonin O	OH	isopre	H	H	OH	OH	*uralensis* (R)	(180)
Gancaonin Q	OH	isopre	H	H	isopre	OH	*inflata* (R) *uralensis* (R)	(24,109, 181)
Glychionide A	OH	H	β-D-GlcA	OH	H	H	*glabra* (R)	(182)
Glychionide B	OH	H	β-D-GlcA	OCH₃	H	H	*glabra* (R)	(182)
Apigenin 6,8-di-C-glucoside	OH	β-D-Glc	H	β-D-Glc	H	OH	*uralensis*	(183)
Vicenin-2	OH	β-D-Glc	H	β-D-Glc	H	OH	*glabra* (R)	(166)
Schaftoside	OH	β-D-Glc	H	α-L-Ara	H	H	*aspera* (R) *uralensis* (R) *eurcarpa*	(22,154, 163)
Isoschaftoside	OH	α-L-Ara	H	β-D-Glc	H	OH	*glabra* (R) *uralensis* (R)	(22, 166)
7-*O*-apioglucosyl-7,4′-dihydroxyflavone	H	H	β-D-Glc-Api	H	H	OH	*aspera* (R)	(163)

GlcA: Glucuronic acid,   Ara: Arabinose
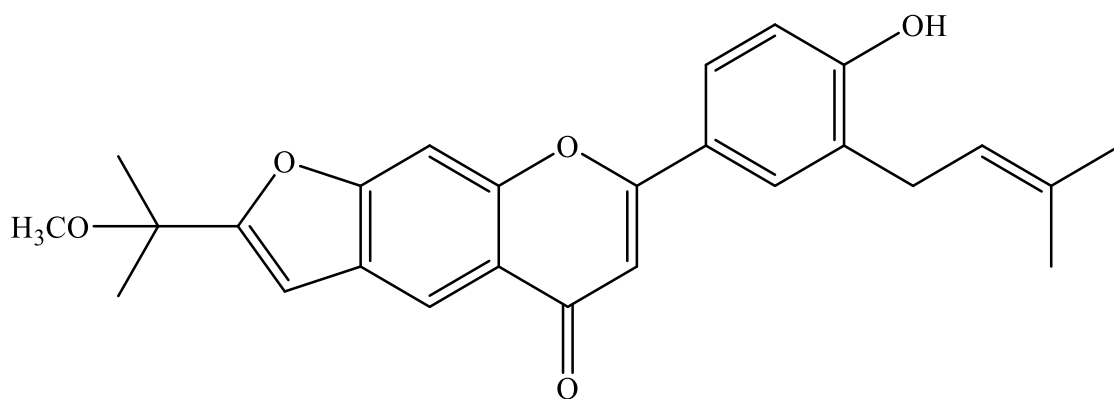
Table 23. Flavone isolated from *Glycyrrhiza* species

Compound	Species	Ref
Licoflavone D	*inflata* (R)	(109)
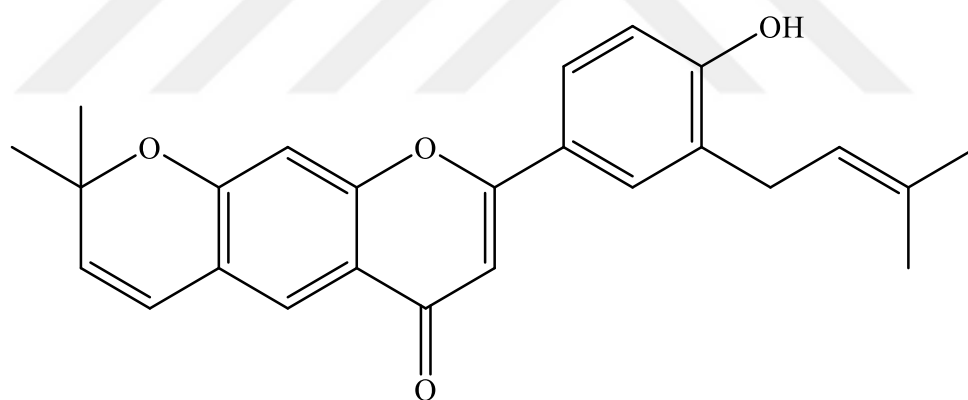
Table 24. Flavone isolated from *Glycyrrhiza* species

Compound	Species	Ref
Licoflavone E	*inflata* (R)	(109)
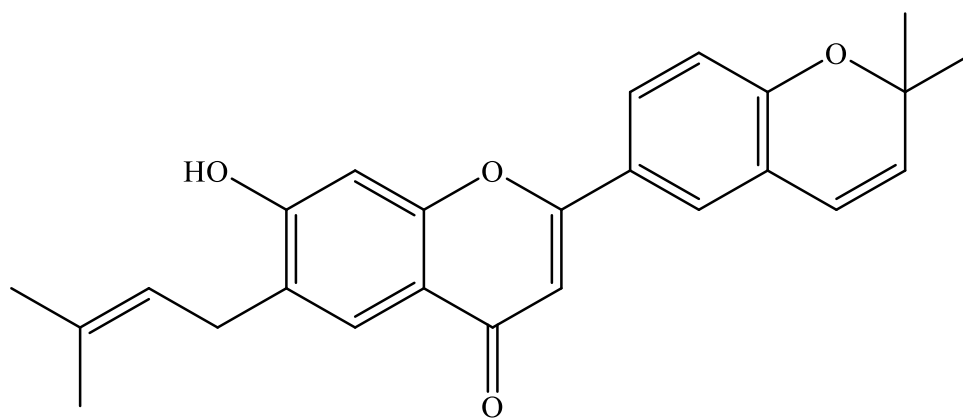
Table 25. Flavone isolated from *Glycyrrhiza* species

Compound	Species	Ref
Kanzonol E	*inflata* (R)	(109)
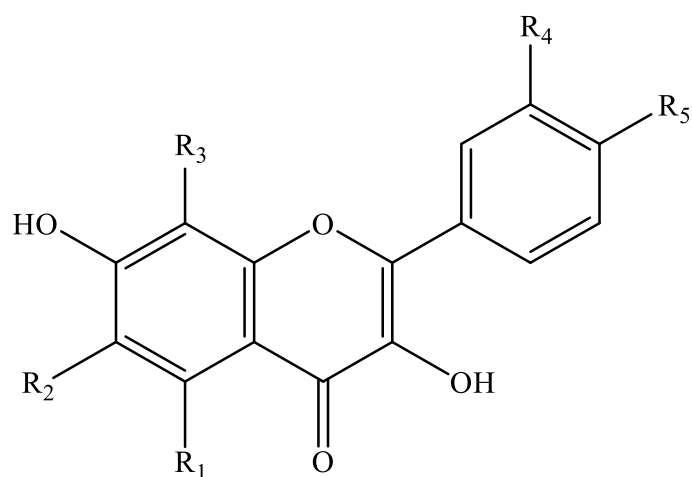
Table 26. Flavonols isolated from *Glycyrrhiza* species

Compounds	R$_1$	R$_2$	R$_3$	R$_4$	R$_5$	Species	Ref
Topazolin	OH	isopre	H	H	OH	*iconica* (R) *uralensis* (R) *aspera* (R)	(22,47, 84,185)
Glepidotin A	OH	H	isopre	H	H	*lepidota* (L)	(186)
Licoflavonol	OH	isopre	OH	H	OH	*uralensis* (R) *aspera* (R)	(61,184, 187)
Isolicoflavonol	OH	H	H	isopre	OH	*uralensis* (R)	(22,150)
Fisetin	H	H	H	OH	OH	*uralensis* (R)	(177)
Gancaonin P	OH	isopre	H	OH	OH	*uralensis* (A)	(180)
Gancaonin P-3′-methylether	OH	isopre	H	CH$_3$	H	*uralensis* (L)	(188)
Glyasperin A	OH	isopre	H	isopre	H	*aspera* (R)	(175)

Table 27. Flavonols isolated from *Glycyrrhiza* species

Compounds	R₁	R₂	R₃	R₄	R₅	R₆	R₇	Species	Ref
Isorhamnetin	H	OH	H	H	OCH₃	H	H	*glabra* (A)	(147)
Kumatakenin B	CH₃	OH	H	CH₃	H	H	H	*uralensis* (R) *inflata* (R)	(22,109)
Quercetin	H	OH	H	H	OH	H	H	*glabra* (A,R,L) *uralensis* (A, R) *Korshinskyi* (A) *inflata* (A) *aspera* (A) *echinata* (A) *pallidiflora* (A) *macedonica* (A) *lepidota* (A) *foetida* (A)	(147,189)
Quercetin-3,3'-dimethylether	CH₃	OH	H	H	OCH₃	H	H	*uralensis* (L) *eurcarpta* (A)	(190,191)
Quercetin-3,4'-dimethylether	CH₃	OH	H	H	OH	CH₃	H	*eurcarpta* (A)	(191)
6-Prenylquercetin 3-methyl ether	CH₃	OH	isopre	H	OH	H	H	*eurcarpta* (A)	(191)
Isoquercitrin	β-D-Glc	OH	H	H	OH	H	H	*glabra* (L)	(192)

Table 27. Flavonols isolated from *Glycyrrhiza* species

Compounds	R₁	R₂	R₃	R₄	R₅	R₆	R₇	Species	Ref
Hyperoside	β-D-Gal	OH	H	H	OH	H	H	*inflata* (A) *echinata* (A) *pallidiflora* (A) *macedonica* (A) *lepidota* (A)	(147)
Kaempferol	H	OH	H	H	H	H	H	*uralensis* (R, A) *glabra* (A) *Korshinskyi* (A) *inflata* (A) *aspera* (A) *echinata* (A) *pallidiflora* (A) *macedonica* (A) *lepidota* (A) *foetida* (A)	(147,185,189)
Kaempferol 3-O-methyl ether	CH₃	OH	H	H	H	H	H	*uralensis* (R)	(22,185)
6-hydroxy kaempferol	H	OH	OH	H	H	H	H	*glabra* (R)	(147)
Kaempferol 3-*O*-glucoside, Astragalin	β-D-Glc	OH	H	H	H	H	H	*glabra* (L) *uralensis* (L)	(147)
Kaempferol 3-glucobioside	β-D-Glc-(2-*O*-β-D-Glc)	OH	H	H	H	H	H	*uralensis* (A) *glabra* (A) *Korshinskyi* (A) *inflata* (A) *aspera* (A) *echinata* (A) *pallidiflora* (A) *foetida* (A)	(147)

Gal: Galactose

Table 27. Flavonols isolated from *Glycyrrhiza* species

Compounds	R₁	R₂	R₃	R₄	R₅	R₆	R₇	Species	Ref
Kaempferol 3-*O*-rhamnosylgalactoside	D-Gal-(*O*- L-Rha)	OH	H	H	H	H	H	*aspera* (L) *echinata* (L)	(147)
Nicotiflorin	β-D-Glc-(6-*O*-β-L-Rha)	OH	H	H	H	H	H	*glabra* (A) *uralensis* (A) *uralensis* (A) *glabra* (A) *Korshinskyi* (A) *inflata* (A) *aspera* (A) *echinata* (A) *pallidiflora* (A) *foetida* (A)	(147)
Rutin	β-D-Glc-(6-*O*-β-L-Rha)	OH	H	H	OH	H	H	*inflata* (A) *echinata* (A) *pallidiflora* (A) *macedonica* (A) *lepidota* (A)	(147)
Uralenol	H	OH	OH	H	OH	H	isopre	*uralensis* (L, R)	(22, 190)
Neouralenol	H	H	OH	H	OH	H	isopre	*uralensis* (L)	(190)
Uralenol-3-methyl ether	CH₃	OH	OH	H	OH	H	isopre	*uralensis* (L)	(190)
5,7,4′-trihydroxy-3′(3-methylbut-2-enyl)−3-methoxy flavon	CH₃	OH	H	H	isopre	H	H	*uralensis* (R)	(22)

Rha: Rhamnose
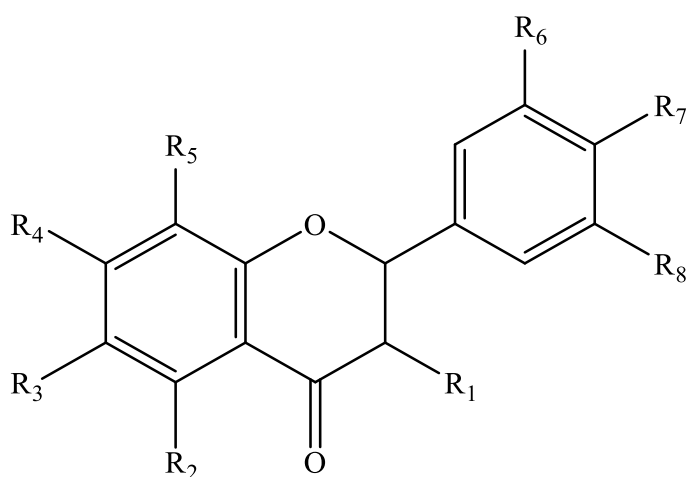
Table 28. Flavanones isolated from *Glycyrrhiza* species

Compounds	R₁	R₂	R₃	R₄	R₅	R₆	R₇	R₈	Species	Ref
Liquiritigenin	H	H	H	OH	H	H	OH	H	*uralensis* (R) *glabra* (R) *inflata* (R) *pallidiflora* (R)	(21,22,24 ,61,99,10 9,152)
Glepidotin B	OH	OH	H	OH	isopre	H	H	H	*lepidota* (L)	(186)
Echinogenin	H	OH	H	H	H	H	OH	H	*echinata* (R)	(147)
Salipurpol, Naringenin	H	OH	H	OH	H	H	OH	H	*glabra* (R) *inflata* (R) *uralensis* (R)	(23,99, 109,148)
6-prenylnaringenin	H	OH	isopre	OH	H	H	OH	H	*eurcarpa* (A) *glabra* (L)	(177,191, 193)
Sophoraflavanone B	H	OH	H	OH	isopre	H	OH	H	*eurcarpa* (A)	(191)
Pinocembrin	H	OH	H	OH	H	H	H	H	*glabra* (L,A)	(192,194, 195)
6-C-prenylpinocembrin	H	OH	isopre	OH	H	H	H	H	*glabra* (A)	(195)

Table 28. Flavanones isolated from *Glycyrrhiza* species

Compounds	R₁	R₂	R₃	R₄	R₅	R₆	R₇	R₈	Species	Ref
Eriodictyol	H	OH	H	OH	H	OH	OH	H	*eurcarpa* (A)	(191)
Glabranin	H	OH	H	OH	isopre	H	H	H	*glabra* (L)	(194)
7-*O*-methyl glabranin	H	OH	H	OCH₃	isopre	H	H	H	*glabra* (A)	(195)
Glabrol	H	H	H	OH	isopre	isopre	OH	H	*glabra* (R) *inflata* (R) *uralensis* (R)	(24,143, 157,171, 196,197)
3-hydroxyglabrol	OH	H	H	OH	isopre	isopre	OH	H	*glabra* (R)	(171,196)
Paratocarpin L	H	OH	isopre	OH	H	isopre	OH	H	*inflata* (R)	(99,109)
Licoflavanone	H	OH	H	OH	H	isopre	OH	H	*glabra* (A,L)	(192,193)
Gancaonin E	H	OH	H	OH	isopre	isopre	OH	OH	*uralensis* (A)	(177,198)
Abyssinone II	H	H	H	OH	H	isopre	OH	H	*glabra* (R) *uralensis* (R) *inflata* (R)	(23,109, 197)
Euchestraflavanone A	H	OH	H	OH	isopre	isopre	OH	H	*inflata* (R)	(24,99, 109)
Macarangaflavanone B	H	OH	isopre	OH	isopre	isopre	OH	H	*inflata* (R)	(99,109)
Liquiritin	H	H	H	OH	H	H	*O*-β-*D*-Glc	H	*uralensis* (R)	(61,157)
Neoliquiritin	H	H	H	*O*-β-D-Glc	H	H	OH	H	*uralensis* (R)	(22)

Table 28. Flavanones isolated from *Glycyrrhiza* species

Compounds	R$_1$	R$_2$	R$_3$	R$_4$	R$_5$	R$_6$	R$_7$	R$_8$	Species	Ref
6"-*O*-acetylliquiritin	H	H	H	OH	H	H	6-*O* Ac-*O*-β-*D*-Glc	H	*uralensis* (R)	(157)
Echinoside	H	*O*-β-Glc	H	H	H	H	OH	H	*echinata* (R)	(147)
Liquiritin apioside	H	H	H	OH	H	H	*O*-β-D-Glc-2-*O*-Api	H	*glabra* (R) *uralensis* (R)	(61,183,199)
Rhamnoliquiritin	H	H	H	OH	H	H	*O*-Rha	H	*glabra* (R)	(147)
Liquiritigenin 7,4′-diglucoside	H	H	H	*O*-β-D-Glc	H	H	*O*-β-D-Glc	H	*uralensis*	(183)
Sigmoidin B, Uralenin	H	OH	H	OH	H	OH	OH	isopre	*eurycarpa* (A) *uralensis* (L,A)	(190, 191, 198)
Isobavachin	H	H	H	OH	isopre	H	OH	H	*pallidiflora* (R) *uralensis* (CC)	(14, 164)
Kanzonol S	H	OH	H	OH	4-acetoxy isopre	OH	OH	H	*eurycarpa* (A)	(191)
Exiguaflavanone K	H	OH	H	OH	isopre	OCH$_3$	OH	H	*eurycarpa* (A)	(191)
7,3',5-trihydroxyflavanone	H	H	H	OH	H	OH	H	OH	*glabra* (R)	(23)
3,4',7-trihydroxy-3'-prenyl-flavanone	OH	H	H	OH	H	isopre	OH	H	*glabra* (R)	(94)
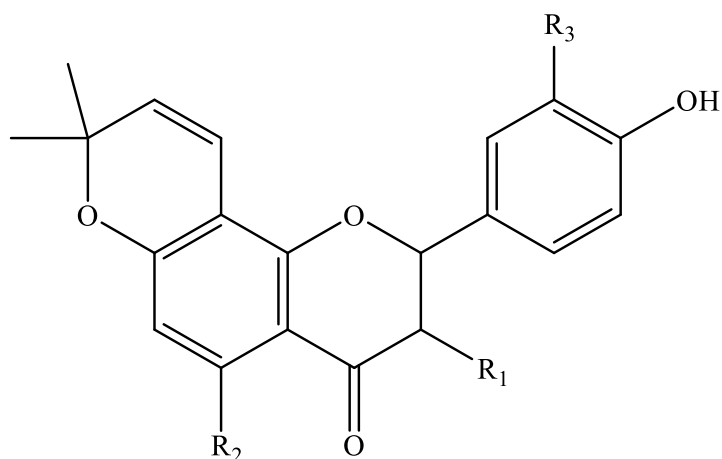
Table 29. Flavanones isolated from *Glycyrrhiza* species

Compounds	R₁	R₂	R₃	Species	Ref
Shinflavanone	H	H	isopre	*glabra* (R)	(23,94)
Kanzonol Z	OH	H	isopre	*glabra* (R)	(23,177)
Citflavanone	H	OH	H	*eurycarpa* (A)	(191)
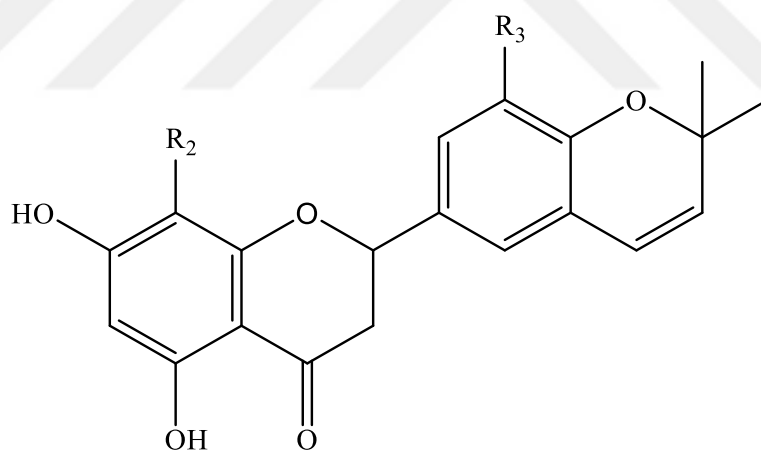
Table 30. Flavanones isolated from *Glycyrrhiza* species

Compounds	R₁	R₂	R₃	Species	Ref
(2*S*)-Abyssinone I	H	H	H	*glabra* (R)	(23)
Abyssinone III	H	H	isopre	*inflata* (R)	(109)
Euchrenone a₅	H	isopre	H	*glabra* (R) *inflata* (R)	(24,94)
Sigmoidin C	OH	H	OH	*eurycarpa* (A)	(191)

67
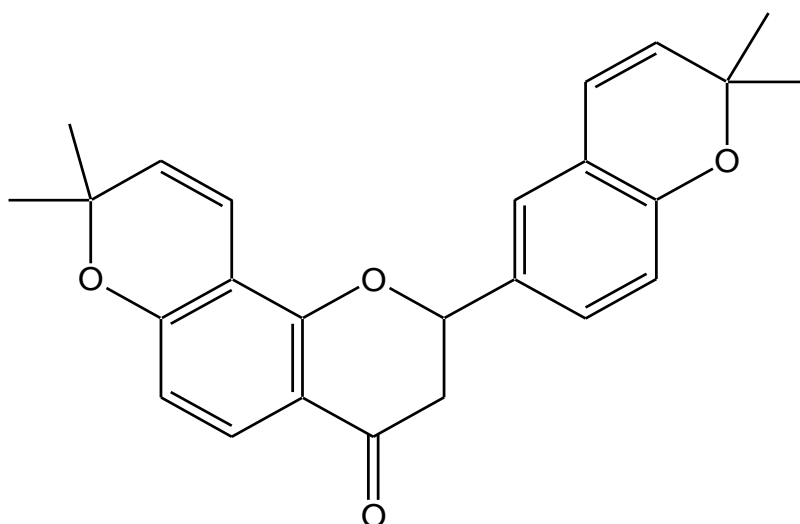
Table 31. Flavanone isolated from *Glycyrrhiza* species

Compound	Species	Ref
Xambioona	*glabra* (R)	(23,94)

2.1.3.1.E. Isoflavonoids Isolated from Glycyrrhiza species
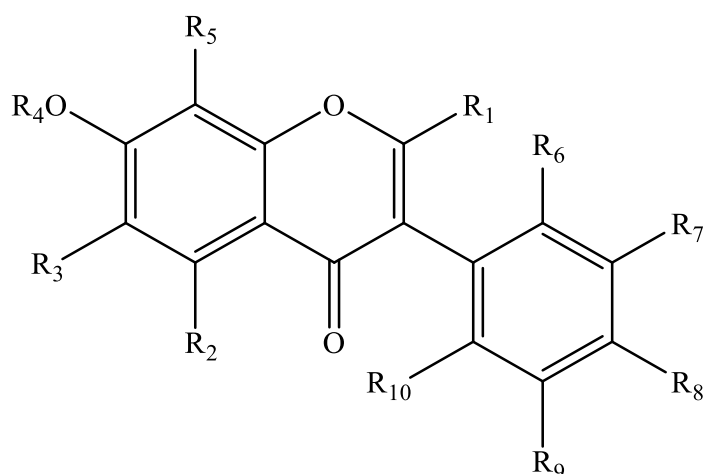
Table 32. Isoflavones isolated from *Glycyrrhiza* species

Compounds	R₁	R₂	R₃	R₄	R₅	R₆	R₇	R₈	R₉	R₁₀	Species	Ref
Daidzein	H	H	H	H	H	H	H	OH	H	H	*uralensis* (R)	(22)
Genistein	H	OH	H	H	H	H	H	OH	H	H	*uralensis* (R) *inflata* (R) *glabra* (L) *palidiflora* (R)	(22,24 ,99, 193)
3'-dimethylallyl genistein	H	OH	H	H	H	H	H	OH	isopre	H	*aspera* (R)	(187)
3',6-di-(dimethylallyl)-genistein	H	OH	isopre	H	H	H	H	OH	isopre	H	*glabra* (R)	(200)
6,8-diprenyl genistein	H	OH	isopre	H	isopre	H	H	OH	H	H	*glabra* (R) *inflata* (R) *uralensis* (R)	(22,24 ,200)

Table 32. Isoflavones isolated from *Glycyrrhiza* species

Compounds	R₁	R₂	R₃	R₄	R₅	R₆	R₇	R₈	R₉	R₁₀	Species	Ref
Formononetin	H	H	H	H	H	H	H	OCH$_3$	H	H	*palidiflora* (R) *uralensis* (CC, R, A) *echinata* (CC) *glabra* (CC, R) *inflata* (R)	(21,99 ,109,1 52,15 9,160, 164,1 92,19 8,201)
For-mononetin 7-*O*-(6"-malonyl glucoside)	H	H	H	6"-malo -Glc	H	H	H	OCH$_3$	H	H	*pallidiflora* (R)	(178)
2'-hydroxy-formononetin 7-*O*-glucoside	H	H	H	β-D-Glc	H	OH	H	OCH$_3$	H	H	*pallidiflora* (R)	(178)
3',4',7-trihydroxyisofl avone	H	H	H	H	H	H	OH	OH	H	H	*inflata* (R)	(24)
2',7-dihydroxy-4'-methoxy isoflavone	H	H	H	H	H	OH	H	OCH$_3$	H	H	*inflata* (R)	(24)
7-methoxy-2',4'-dihydroxy isoflavone	H	H	H	CH$_3$	H	OH	H	OH	H	H	*uralensis* (R)	(22)
6,8-diprenylorobol	H	OH	isopre	H	isopre	H	OH	OH	H	H	*uralensis* (R)	(202)
Eurycarpin A	H	H	H	H	H	OH	isopre	OH	H	H	*inflata* (R)	(24)

Malo: Malonyl

Table 32. Isoflavones isolated from *Glycyrrhiza* species

Compounds	R₁	R₂	R₃	R₄	R₅	R₆	R₇	R₈	R₉	R₁₀	Species	Ref
Pratensein	H	OH	H	H	H	H	OH	OCH₃	H	H	*uralensis* (R)	(22)
Glycyroside	H	H	H	β-D-Glc-2-*O*-Api	H	H	H	OCH₃	H	H	*eurycarpa*	(154)
Calycosin	H	H	H	H	H	H	OH	OCH₃	H	H	*pallidiflora* (R)	(21, 178)
Calycosin 7-*O*-glucoside	H	H	H	β-D-Glc	H	H	OH	OCH₃	H	H	*pallidiflora* (R) *glabra* (R)	(166, 178)
Ononin	H	H	H	β-D-Glc	H	H	H	OCH₃	H	H	*glabra* (R) *pallidiflora* (R)	(152, 166, 178)
6"-*O*-acetylononin	H	H	H	6-*O*-Ac-β-Glc	H	H	H	OCH₃	H	H	*uralensis* (R)	(157)
Licoagroside A	H	H	OCH₃	H	H	*O*-β-Glc	H	OCH₃	OH	H	*glabra* (R)	(166)
Wistin	H	H	OCH₃	β-D-Glc	H	H	OH	OCH₃	H	H	*glabra* (R) *pallidiflora* (R)	(21,152,166)
6"-*O*-acetyl-wistin	H	H	OCH₃	6-*O*-Ac-β-D-Glc	H	H	OH	OCH₃	H	H	*pallidiflora* (R)	(21)
6"-*O*-malonyl-wistin	H	H	OCH₃	6-*O*-malo-β-Glc	H	H	OH	OCH₃	H	H	*glabra* (L)	(166)

71

Table 32. Isoflavones isolated from *Glycyrrhiza* species

Compounds	R_1	R_2	R_3	R_4	R_5	R_6	R_7	R_8	R_9	R_{10}	Species	Ref
Luteone	H	OH	iso pre	H	H	OH	H	OH	H	H	*uralensis* (R)	(22)
7-*O*-methylluteone	H	OH	iso pre	CH₃	H	OH	H	OH	H	H	*inflata* (R) *uralensis* (R)	(22,24)
6-C-prenylorobol	H	OH	iso pre	H	H	H	OH	OH	H	H	*uralensis* (R)	(22)
Wighteone	H	OH	iso pre	H	H	H	H	OH	H	H	*glabra* (L) *inflata* (R) *uralensis* (R)	(22,24, 193)
Lupiwighteone	H	OH	H	H	iso pre	H	H	OH	H	H	*inflata* (R) *glabra* (L) *uralensis* (R,A)	(148,17 2,193,1 94,198)
Isowighteone	H	OH	H	H	H	H	isopre	OH	H	H	*uralensis* (R)	(148)
Prunetin	H	OH	H	CH₃	H	H	H	OH	H	H	*glabra* (L)	(193)
Biochanin A	H	OH	H	H	H	H	H	OCH₃	H	H	*uralensis* (R)	(22,99)
2,3-dehydro kievitone	H	OH	H	H	iso pre	OH	H	OH	H	H	*glabra* (R) *inflata* (R)	(23,24)
Licoisoflavone A	H	OH	H	H	H	OH	isopre	OH	H	H	*aspera* (R) *inflata* (R) *uralensis* (R)	(22,109 ,187)
Licoisoflavone E	H	H	iso pre	H	O H	OH	H	OCH₃	H	H	*inflata* (R)	(109)
Gancaonin L	H	OH	H	H	iso pre	H	OH	OH	H	H	*uralensis* (A,R)	(22, 180)

Table 32. Isoflavones isolated from *Glycyrrhiza* species

Compounds	R₁	R₂	R₃	R₄	R₅	R₆	R₇	R₈	R₉	R₁₀	Species	Ref
Gancaonin M	H	OH	H	H	isopre	H	H	OCH₃	H	H	*uralensis* (A)	(180)
Gancaonin N	H	OH	iso pre	H	H	OH	H	OCH₃	H	H	*uralensis* (A, R)	(180, 203)
Glyurallin B	H	OH	H	H	isopre	H	iso pre	OH	OH	H	*uralensis* (R) *inflata* (R)	(109, 203)
Isoangustone A	H	OH	iso pre	H	H	H	iso pre	OH	OH	H	*uralensis* (R)	(22)
Angustone A	H	OH	iso pre	H	H	OH	iso pre	OH	H	H	*uralensis* (R) *inflata* (R)	(22, 24)
Licoricone	H	H	H	H	H	OH	H	OCH₃	iso pre	OCH₃	*inflata* (R) *uralensis* (R)	(109, 202)
Glicoricone	H	H	H	H	H	OH	H	OH	iso pre	OCH₃	*uralensis* (R)	(148, 204)
Glisoflavone	H	OCH₃	H	H	H	H	OH	OH	iso pre	H	*uralensis* (R)	(148)
Glycyrrhisoflavone	H	OH	H	H	H	H	OH	OH	iso pre	H	*uralensis* (R) *inflata* (R) *glabra* (R)	(109, 148, 205)
Gancaonin A	H	OH	iso pre	H	H	H	H	OCH₃	H	H	*uralensis* (A)	(198)
Gancaonin B	H	OH	iso pre	H	H	H	OH	OCH₃	H	H	*uralensis* (A)	(198)
Gancaonin C	H	OH	H	H	4-hydroxy prenyl	H	H	OH	H	H	*uralensis* (A)	(198)

Table 32. Isoflavones isolated from *Glycyrrhiza* species

Compounds	R1	R2	R3	R4	R5	R6	R7	R8	R9	R10	Species	Ref
Gancaonin D	H	OH	H	H	4-hydroxy prenyl	H	OH	OCH3	H	H	*uralensis* (A)	(198)
Gancaonin G	H	OH	isopre	CH3	H	H	H	OH	H	H	*uralensis* (R)	(206)
Glabriso-flavone	H	OH	4-hydroxy prenyl	H	H	H	H	OH	H	H	*glabra* (A)	(195)
Isolupalbigenin	H	OH	H	H	isopre	H	isopre	OH	H	H	*uralensis* (R)	(22)
2'-hydroxy isolupalbigenin	H	OH	H	H	isopre	OH	isopre	OH	H	H	*uralensis* (R) *inflata* (R)	(22, 109)
Glycyuralin F	H	OH	3-hydroxy -3-methylbutyl	H	H	H	OH	OH	H	H	*uralensis* (R)	(22)
Glyzarin	CH3	H	H	H	Ac	H	H	H	H	H	*glabra* (R)	(189)
Compound A	CH3	H	H	Ac	H	H	H	H	H	H	*glabra* (R)	(189)
Compound B	CH3	H	H	CH3	H	H	H	H	H	H	*glabra* (R)	(189)
Compound C	CH3	H	H	H	H	H	H	H	H	H	*glabra* (R)	(189)
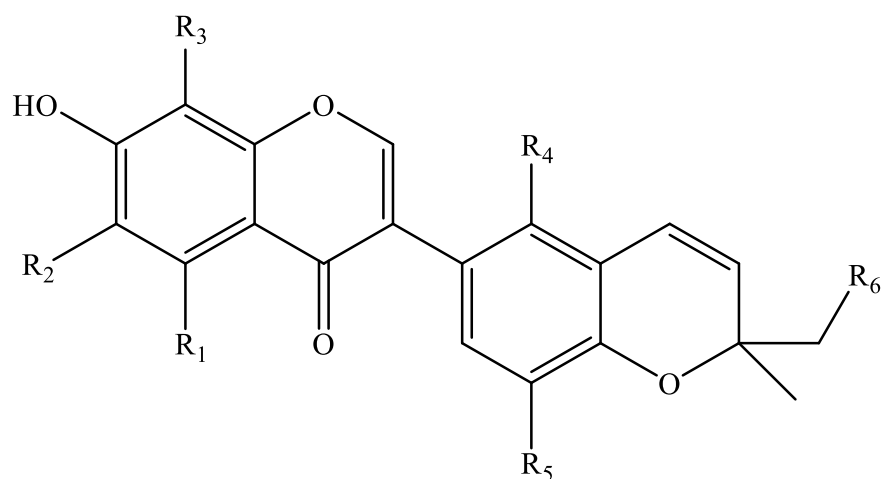
Table 33. Isoflavones isolated from *Glycyrrhiza* species

Compounds	R₁	R₂	R₃	R₄	R₅	R₆	Species	Ref
Isochandalone	OH	isopre	H	H	H	H	*inflata* (R)	(109)
Isoderrone	OH	H	H	H	H	H	*inflata* (R) *uralensis* (R)	(22, 109)
Glabrone	H	H	H	OH	H	H	*glabra* (R)	(94, 207)
Licoisoflavone B	OH	H	H	OH	H	H	*aspera* (R) *inflata* (R) *uralensis* (R) *glabra* (R)	(109,172,175,200, 202)
Licoisoflavone C	OH	H	isopre	OH	H	H	*inflata* (R)	(109)
Licoisoflavone D	OH	H	isopre	OH	H	H	*inflata* (R)	(109)
Licoisoflavone F	H	H	H	OH	H	OH	*inflata* (R)	(109)
Kanzonol T	OH	⟨OH⟩	H	OH	H	H	*glabra* (R)	(200)
Semilicoisoflavone B	OH	H	H	H	OH	H	*inflata* (R) *uralensis* (R)	(22,109,203)
Angustone B	OH	isopre	H	OH	H	H	*inflata* (R)	(109)
Glycyrrhiza-isoflavone B	OCH₃	H	H	H	OH	H	*uralensis* (R)	(151)
Erylatissin B	H	H	H	H	OH	H	*inflata* (R)	(109)

75
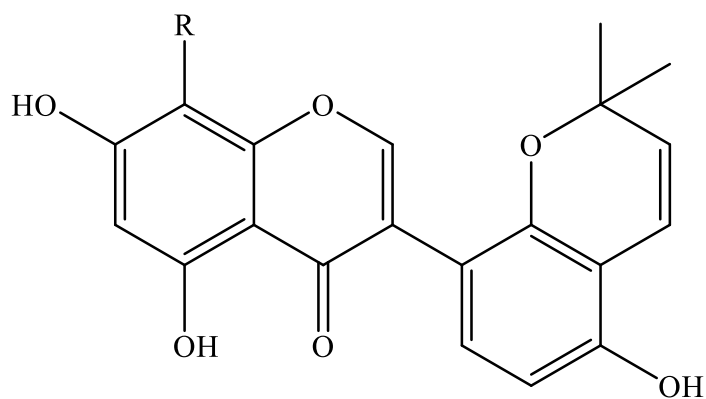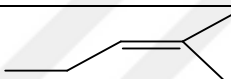
Table 34. Isoflavones isolated from *Glycyrrhiza* species

Compounds	R	Species	Ref
Sophoraisoflavone A, Allolicoisoflavone B	H	*inflata* (R) *uralensis* (R)	(22,109)
Glyasperin N		*aspera* (R)	(187)
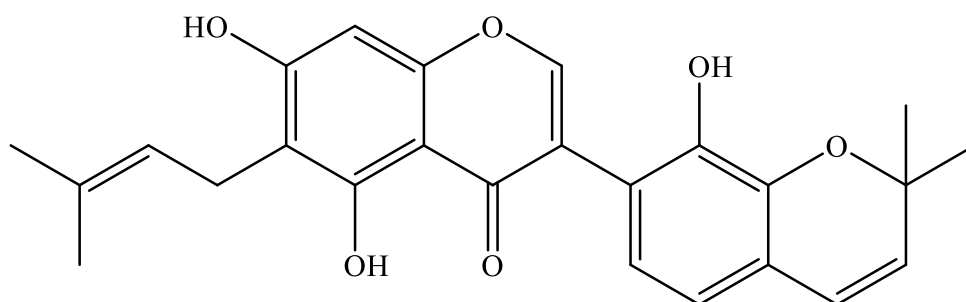
Table 35. Isoflavone isolated from *Glycyrrhiza* species

Compound	Species	Ref
Gancaonin H	*inflata* (R)	(109)
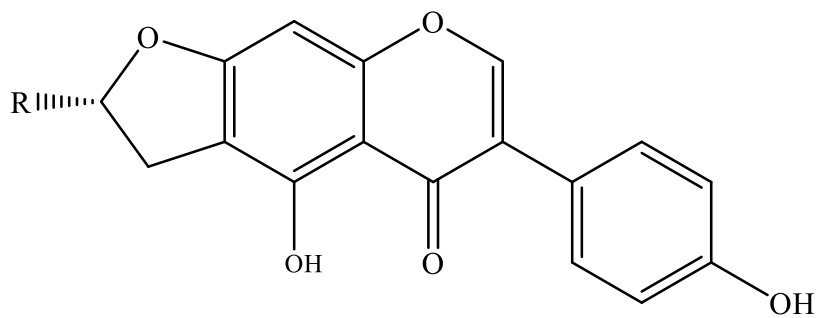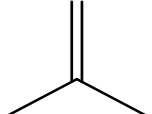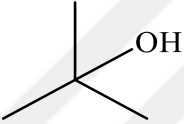
Table 36. Isoflavones isolated from *Glycyrrhiza* species

Compounds	R	Species	Ref
Licoagroisoflavone		*pallidiflora* (R)	(178)
Erythrinin		*pallidiflora* (R)	(178)
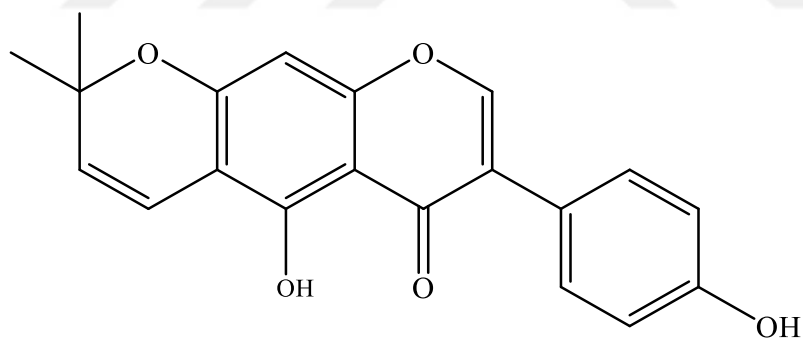
Table 37. Isoflavone isolated from *Glycyrrhiza* species

Compound	Species	Ref
Alpinumisoflavone	*inflata* (R)	(24)
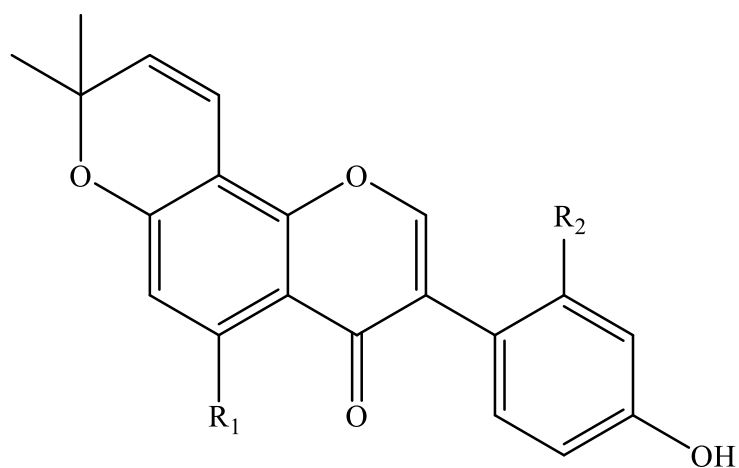
Table 38. Isoflavones isolated from *Glycyrrhiza* species

Compound	R_1	R_2	Species	Ref
Isoglabrone	H	OH	*inflata* (R) *uralensis* (R)	(22,109)
Derrone	OH	H	*glabra* (R)	(23)
Parvisoflavones A	OH	OH	*glabra* (R)	(23)
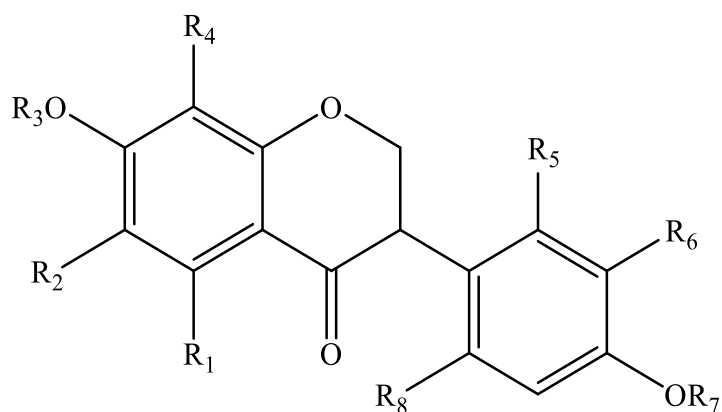
Table 39. Isoflavanones isolated from *Glycyrrhiza* species

Compounds	R_1	R_2	R_3	R_4	R_5	R_6	R_7	R_8	Species	Ref
Glyasperin B	OH	isopre	CH₃	H	OH	H	H	H	*aspera* (R) *uralensis* (R)	(204, 208)
Glyasperin K	OH	isopre	CH₃	H	OH	H	CH₃	H	*aspera* (R)	(187)
Glisoflavanone	OH	isopre	H	H	OH	isopre	H	H	*inflata* (R) *uralensis* (R)	(24, 185)
Glicoisoflavanone	H	H	H	H	OCH₃	isopre	CH₃	OH	*uralensis* (R)	(148)
Dihydrolico-isoflavone A	OH	H	H	H	OH	isopre	H	H	*uralensis* (R)	(202)
3'-(γ,γ-dimethylallyl) kievitone	OH	H	H	isopre	OH	isopre	H	H	*aspera* (R) *uralensis* (R)	(148, 208)
7,8-dihydroxy-4′-methoxy-6-prenylisoflavanon	H	isopre	H	OH	H	H	CH₃	H	*inflata* (R)	(24)
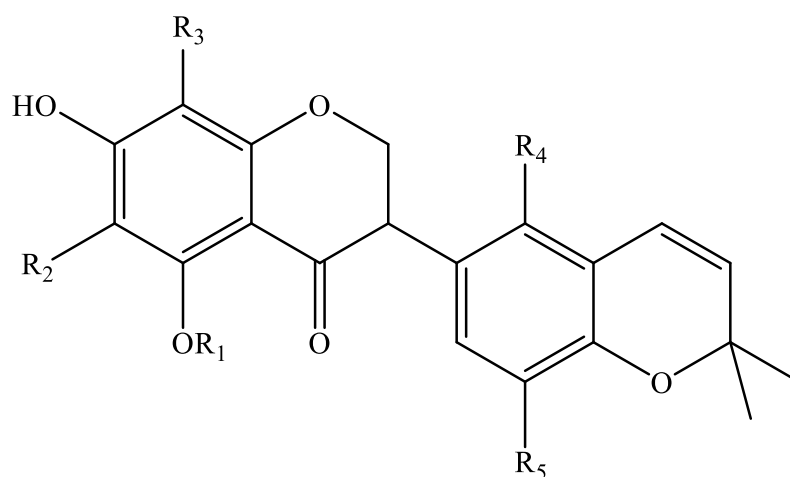
Table 40. Isoflavanones isolated from *Glycyrrhiza* species

Compounds	R$_1$	R$_2$	R$_3$	R$_4$	R$_5$	Species	Ref
Isoflavanone B	H	H	isopre	OH	H	*inflata* (R)	(109)
Isoflavanone C	H	isopre	H	OH	H	*inflata* (R)	(109)
Licoisoflavanone	H	H	H	OH	H	*aspera* (R) *uralensis* (R) *inflata* (R) *glabra*	(172,200, 203,208)
Licoisoflavanone B	H	H	isopre	OH	H	*inflata* (R)	(109)
Licoisoflavanone C	H	isopre	H	OH	H	*inflata* (R)	(109)
Glycyrrhisoflavanone	CH$_3$	H	H	H	OH	*uralensis* (R)	(148)
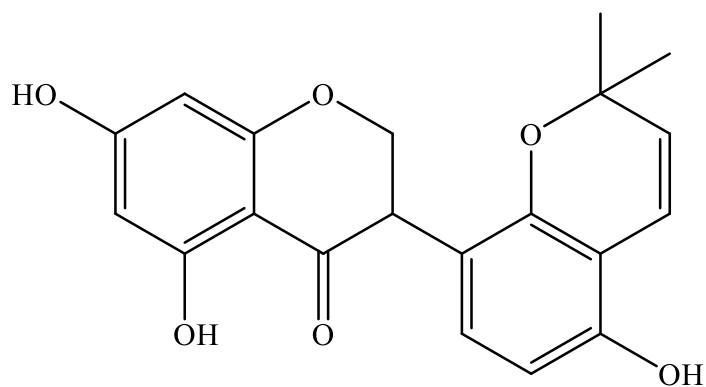
Table 41. Isoflavanone isolated from *Glycyrrhiza* species

Compound	Species	Ref
	aspera (R)	
Glyasperin F	*uralensis* (R)	(109,148,187)
	inflata (R)	
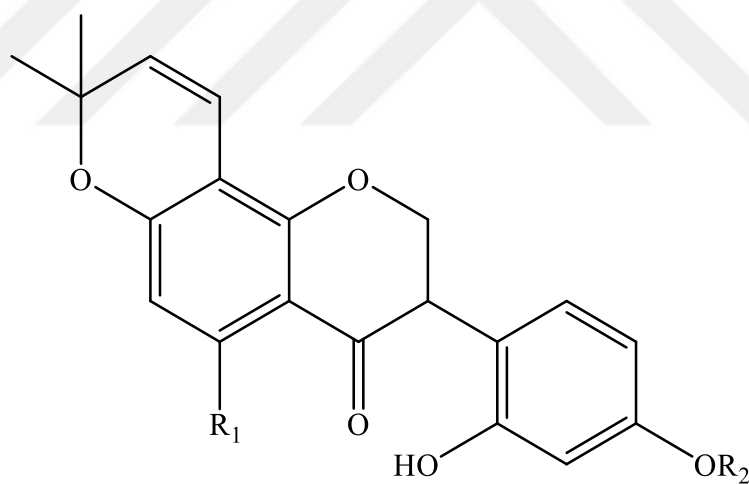
Table 42. Isoflavanones isolated from *Glycyrrhiza* species

Compounds	R_1	R_2	Species	Ref
Cyclokievitone	OH	H	*glabra* (R)	(23)
Glabroisoflavanone A	H	H	*glabra* (R)	(209)
Glabroisoflavanone A	H	CH_3	*glabra* (R)	(209)
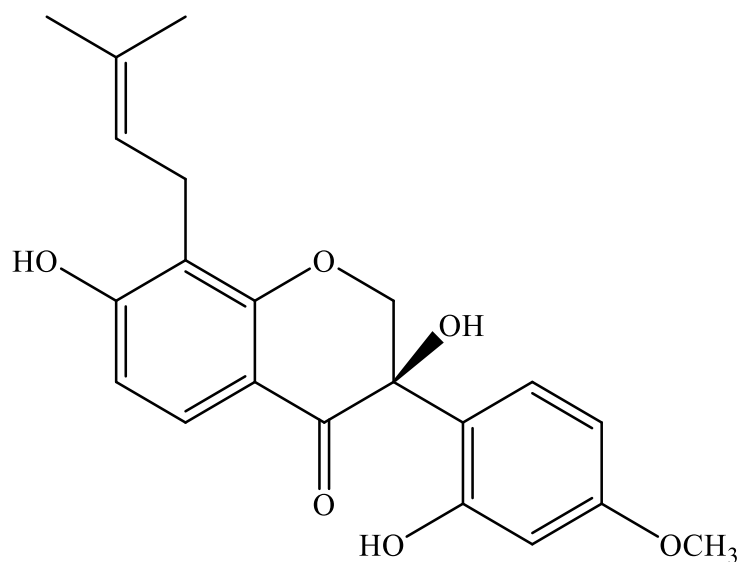
Table 43. Isoflavanone isolated from *Glycyrrhiza* species

Compound	Species	Ref
3*R*-Glycybridin J	*glabra* (R)	(23)
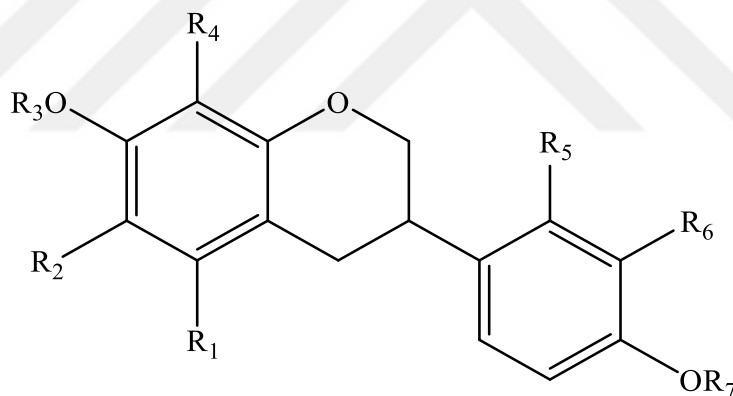
Table 44. Isoflavans isolated from *Glycyrrhiza* species

Compounds	R_1	R_2	R_3	R_4	R_5	R_6	R_7	Species	Ref
Vestitol	H	H	H	H	OH	H	CH_3	*pallidiflora* (R) *glabra* (R) *uralensis* (R)	(94,152 ,202)
Iconisoflavan	OCH_3	isopre	H	H	OH	H	CH_3	*iconica* (R)	(47)
Isomucronulatol	H	H	H	H	OH	OCH_3	CH_3	*glabra* (L)	(147)
Kanzonol X	H	H	H	isopre	OH	isopre	H	*glabra* (R)	(23,94)

Table 44. Isoflavans isolated from *Glycyrrhiza* species

Compounds	R$_1$	R$_2$	R$_3$	R$_4$	R$_5$	R$_6$	R$_7$	Species	Ref
Licorisoflavan A	OCH$_3$	isopre	CH$_3$	H	OH	isopre	H	*iconica* (R) *uralensis* (R)	(47, 151)
Glyasperin C	OCH$_3$	isopre	H	H	OH	H	H	*aspera* (R) *uralensis* (R)	(148, 208)
Glyasperin D	OCH$_3$	isopre	CH$_3$	H	OH	H	H	*aspera* (R) *uralensis* (R)	(22,61, 208)
Glyasperin I	OCH$_3$	isopre	H	H	OCH$_3$	H	H	*aspera* (R)	(210)
Licoricidin	OCH$_3$	isopre	H	H	OH	isopre	H	*iconica* (R) *uralensis* (R) *aspera* (R) *glabra* (R)	(22,47, 208, 211)
Glycybridin H	H	H	H	isopre	OH	OH	CH$_3$	*glabra* (R)	(23)
(3*R*)-2',3',7-trihydroxy-4'-methoxyisoflavan	H	H	H	H	OH	OH	CH$_3$	*glabra* (R)	(94)
(3*R*)-7,2'-dihydroxy-6-dimethylallyl-4'-methoxy-isoflavan	H	isopre	H	H	OH	H	CH$_3$	*uralensis* (CC)	(164)
7- hydroxy-3',4'-dimethoxy-isoflavan	H	H	H	H	H	OCH$_3$	CH$_3$	*uralensis* (CC)	(164)
Kanzonol R	OCH$_3$	H	H	H	OH	isopre	CH$_3$	*glabra* (R)	(212)
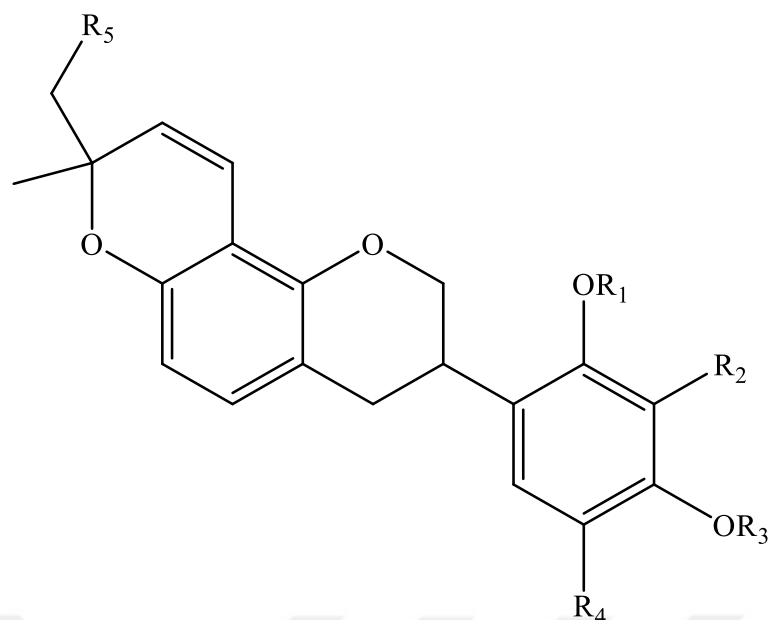
Table 45. Isoflavans isolated from *Glycyrrhiza* species

Compounds	R₁	R₂	R₃	R₄	R₅	Species	Ref
Glabridin	H	H	H	H	H	*glabra* (R) *uralensis* (CC)	(94,164, 201)
4'-*O*-methylglabridin	H	H	CH₃	H	H	*glabra* (R)	(94,201)
5'-formylglabridin	H	H	H	CHO	H	*glabra* (R)	(94)
4"- hydroxyglabridin	H	H	H	H	OH	*glabra* (R)	(94)
3'-hydroxy-4'-*O*-methylglabridin	H	OH	CH₃	H	H	*glabra* (R)	(94)
3'-methoxyglabridin	H	OCH₃	H	H	H	*glabra* (R)	(196)
Glyasperin H	CH₃	OH	CH₃	H	H	*aspera* (R)	(210)
Hispaglabridin A	H	isopre	H	H	H	*glabra* (R)	(94,196, 201)
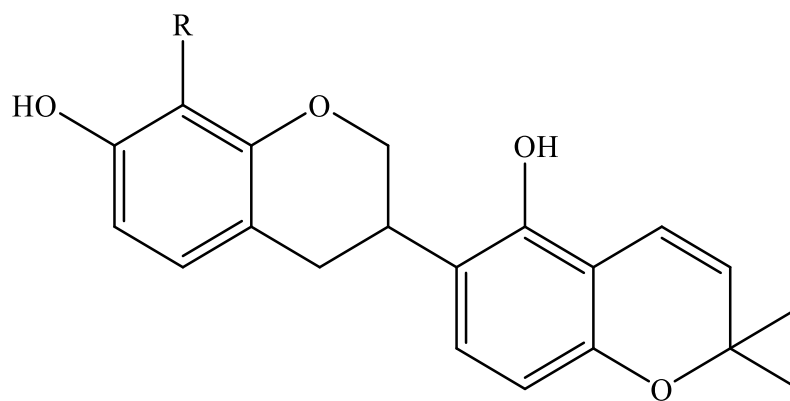
Table 46. Isoflavans isolated from *Glycyrrhiza* species

Compounds	R	Species	Ref
Phaseollinisoflavan	H	*glabra* (R)	(196)
8-prenyl-phaseollinisoflavan	isoprenyl	*glabra* (R)	(23)
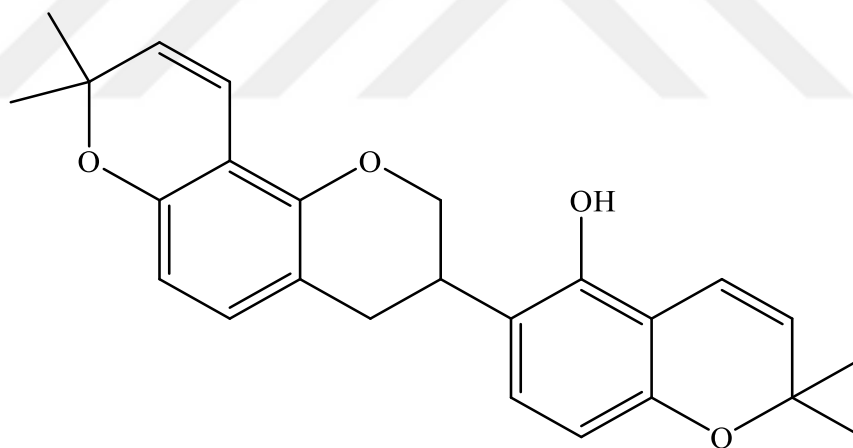
Table 47. Isoflavan isolated from *Glycyrrhiza* species

Compound	Species	Ref
Hispaglabridin B	*glabra* (R)	(94,196,201)
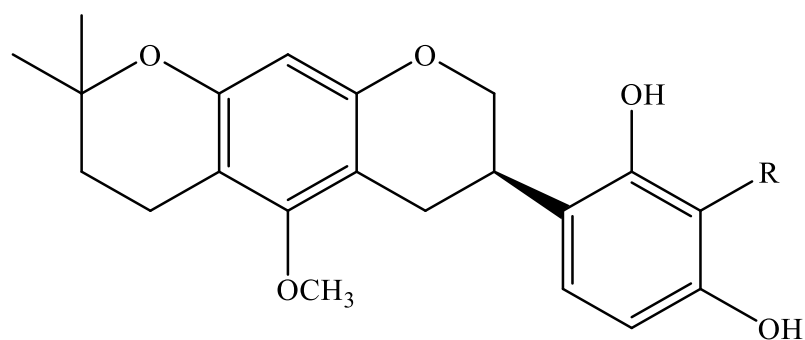
Table 48. Isoflavans isolated from *Glycyrrhiza* species

Compounds	R	Species	Ref
Glycyuralin A		*uralensis* (R)	(22)
Kanzonol H		*uralensis* (R)	(213)
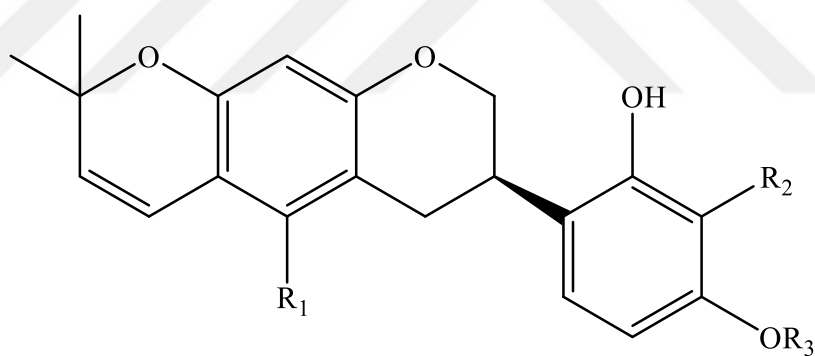
Table 49. Isoflavans isolated from *Glycyrrhiza* species

Compounds	R₁	R₂	R₃	Species	Ref
Glycyuralin C	OCH_3		H	*uralensis* (R)	(22)
Gancaonin X	H	H	CH_3	*uralensis* (CC)	(164)
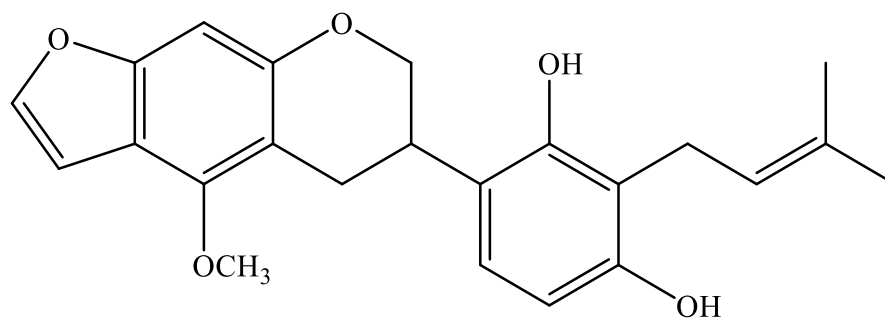
Table 50. Isoflavan isolated from *Glycyrrhiza* species

Compound	Species	Ref
Glyasperin G	*aspera* (R)	(210)
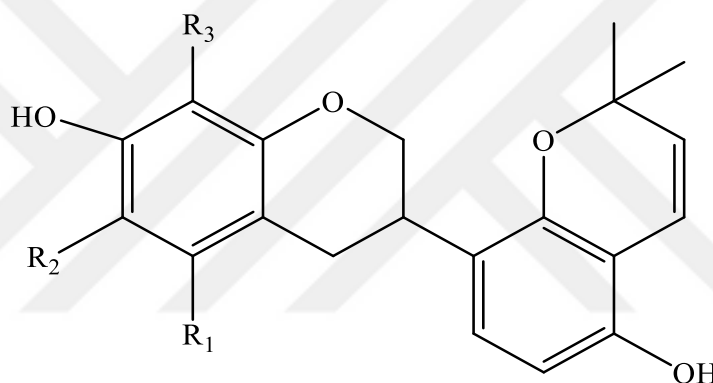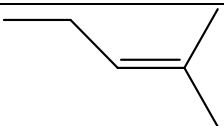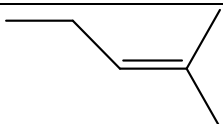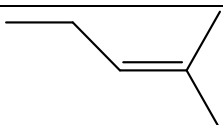
Table 51. Isoflavans isolated from *Glycyrrhiza* species

Compounds	R_1	R_2	R_3	Species	Ref
Glyasperin J	OH	H	(prenyl)	*aspera* (R)	(210)
Glyinflanin I	H	(prenyl)	H	*inflata* (R)	(172)
Kanzonol I	OCH$_3$	(prenyl)	H	*uralensis* (R)	(213)
Gancaonol C	OCH$_3$	H	H	*uralensis* (R)	(202)
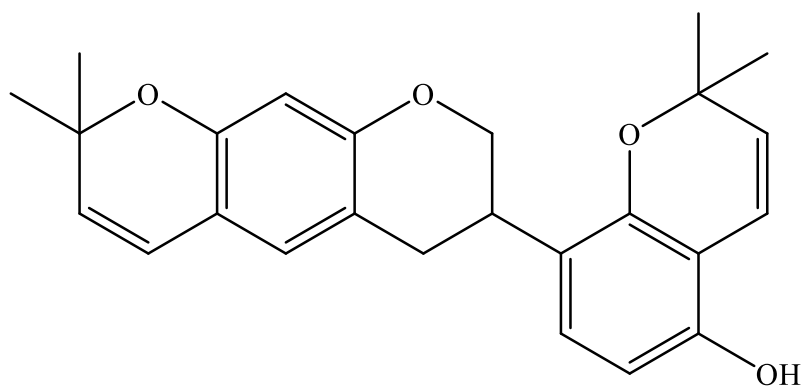
Table 52. Isoflavan isolated from *Glycyrrhiza* species

Compound	Species	Ref
Glyinflanin J	*inflata* (R)	(172)
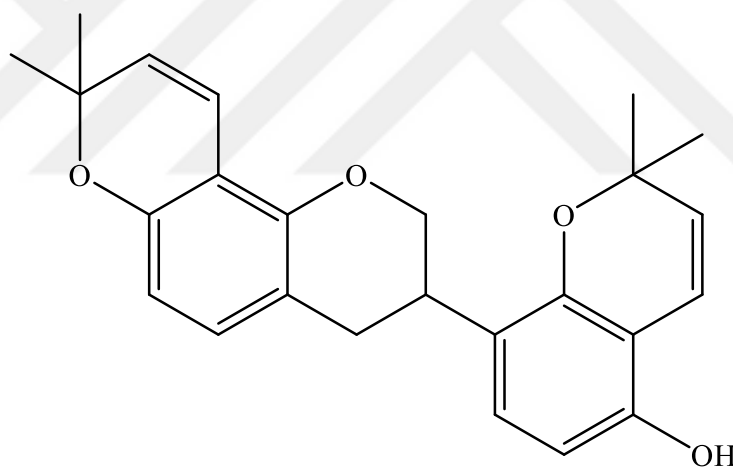
Table 53. Isoflavan isolated from *Glycyrrhiza* species

Compounds	Species	Ref
Glyinflanin K	*inflata* (R)	(172)
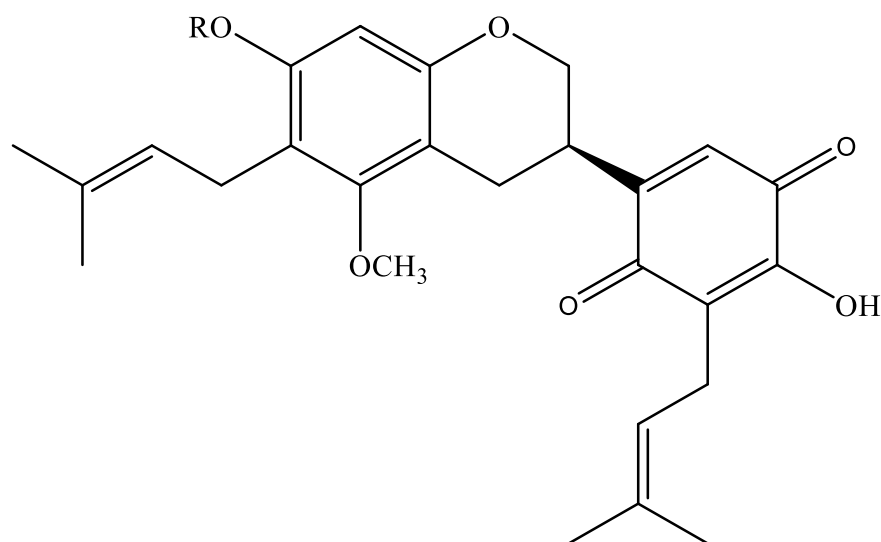
Table 54. Isoflavan-quinones isolated from *Glycyrrhiza* species

Compounds	R	Species	Ref
Licoriquinone A	CH₃	*uralensis* (R)	(13)
Licoriquinone B	H	*uralensis* (R)	(13)
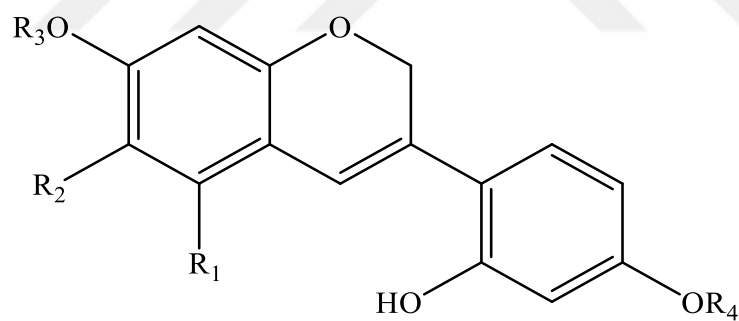
Table 55. Isoflavenes isolated from *Glycyrrhiza* species

Compounds	R₁	R₂	R₃	R₄	Species	Ref
Pallidiflorene	H	H	H	CH₃	*pallidiflora* (R)	(152)
Iconisoflavene	OCH₃	isopre	H	CH₃	*iconica* (R)	(47)
Dehydroglyasperin C	OCH₃	isopre	H	H	*aspera* *uralensis* (R)	(22,177 ,204)
Dehydroglyasperin D	OCH₃	isopre	CH₃	H	*uralensis* (R)	(204)
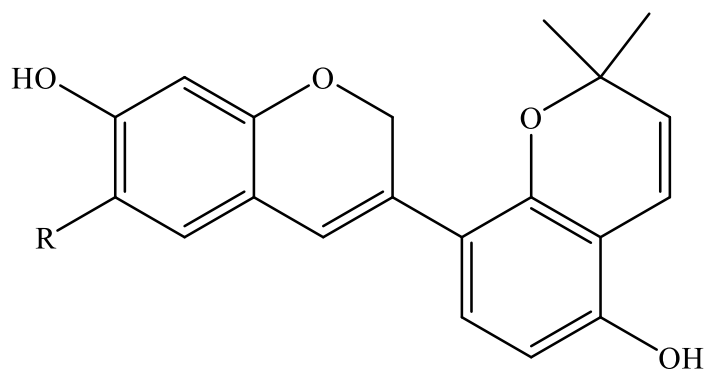
Table 56. Isoflavenes isolated from *Glycyrrhiza* species

Compounds	R	Species	Ref
Glabrene	H	*glabra* (R)	(23,145)
Glycybridin D	isopre	*glabra* (R)	(23)
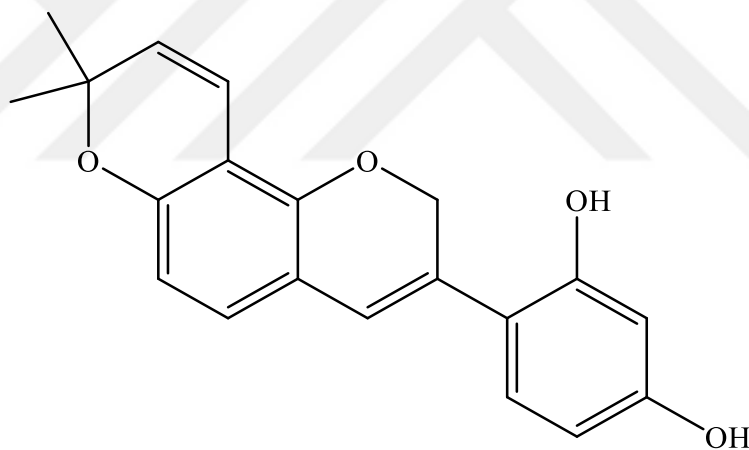
Table 57. Isoflavene isolated from *Glycyrrhiza* species

Compound	Species	Ref
3,4-didehydroglabridin	*glabra* (R)	(23)
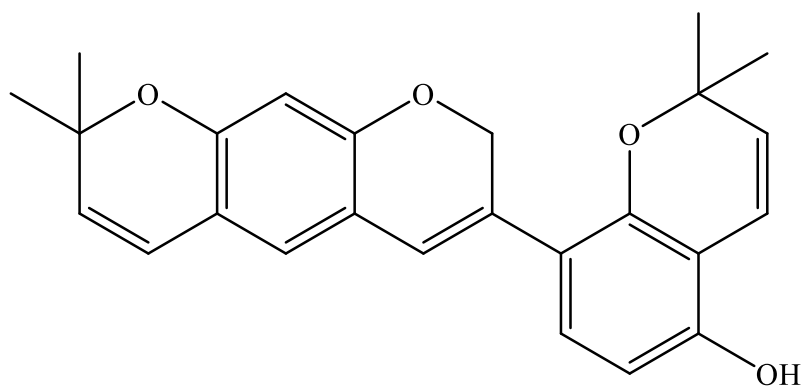
Table 58. Isoflavene isolated from *Glycyrrhiza* species

Compound	Species	Ref
Glycybridin E	*glabra* (R)	(23)
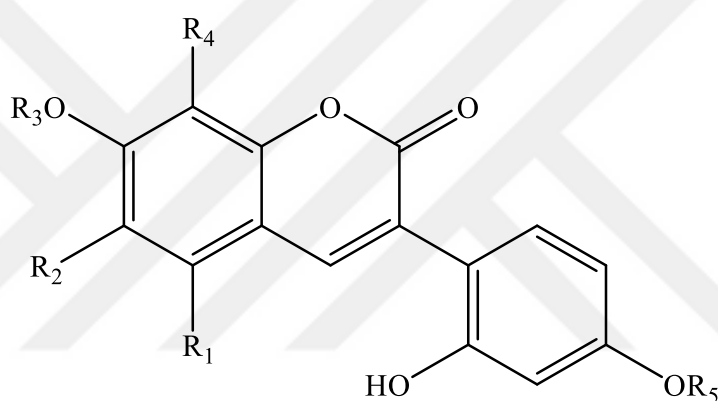
Table 59. 3-Arylcoumarins isolated from *Glycyrrhiza* species

Compounds	R₁	R₂	R₃	R₄	R₅	Species	Ref
Glycycoumarin	OCH_3	isopre	H	H	H	*uralensis* (R) *aspera* (R) *iconica* (R)	(22,47, 187)
Glycyrin	OCH_3	isopre	CH_3	H	H	*uralensis* (R)	(204,206)
Licoarylcoumarin	OCH_3	H	H	2-methylbut-3-en-2yl	H	*uralensis* (R)	(22,148)
2',7-dihydroxy-4'-methoxy-3-arylcoumarin	H	H	H	H	CH_3	*pallidiflora* (R)	(152)

91
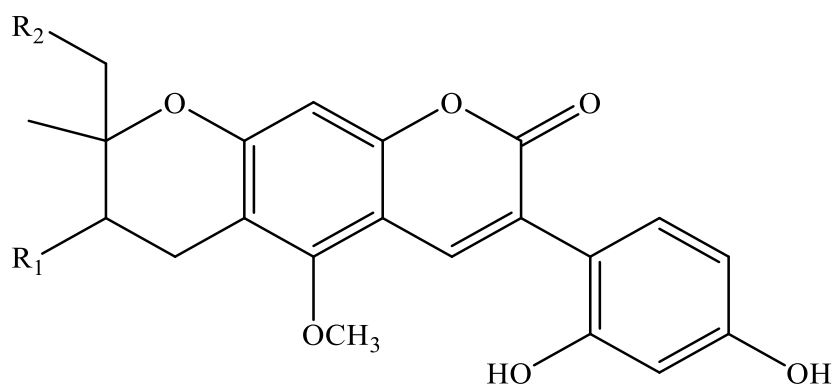
Table 60. 3-Arylcoumarins isolated from *Glycyrrhiza* species

Compounds	R₁	R₂	Species	Ref
Licopyranocoumarin	H	OH	*uralensis* (R)	(148,214)
Isolicopyranocoumarin	OH	H	*uralensis* (R)	(148)
Isoglycycoumarin	H	H	*uralensis* (R)	(22)
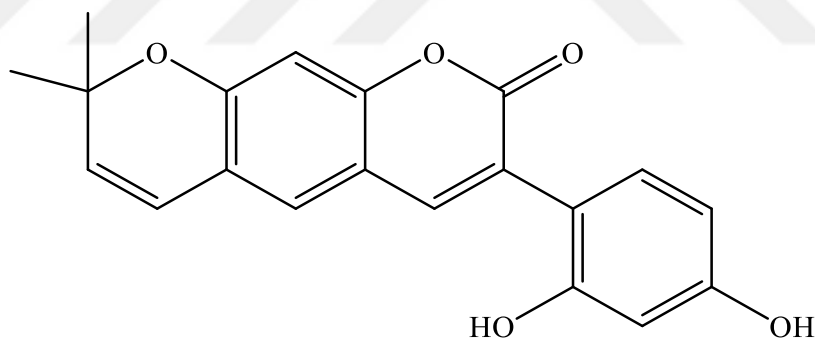
Table 61. 3-Arylcoumarin isolated from *Glycyrrhiza* species

Compound	Species	Ref
Glycybridin K	*glabra* (R)	(23)
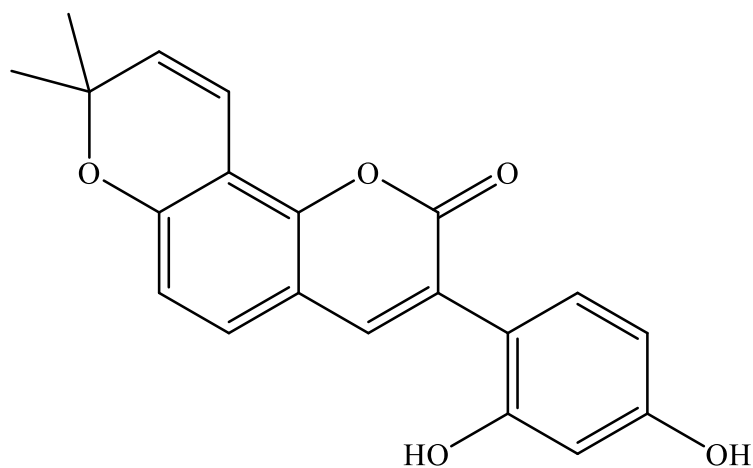
Table 62. 3-Arylcoumarin isolated from *Glycyrrhiza* species

Compound	Species	Ref
Kanzonol W	*glabra* (R)	(23)
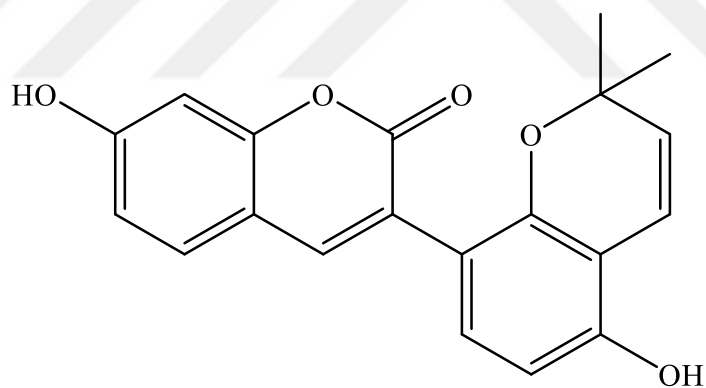
Table 63. 3-Arylcoumarin isolated from *Glycyrrhiza* species

Compound	Species	Ref
Glabrocoumarin	*glabra* (R)	(94)
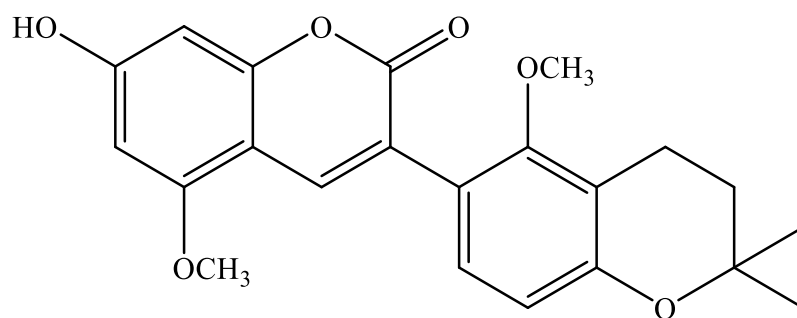
Table 64. 3-Arylcoumarin isolated from *Glycyrrhiza* species

Compound	Species	Ref
Gancaonol A	*uralensis* (R)	(202)
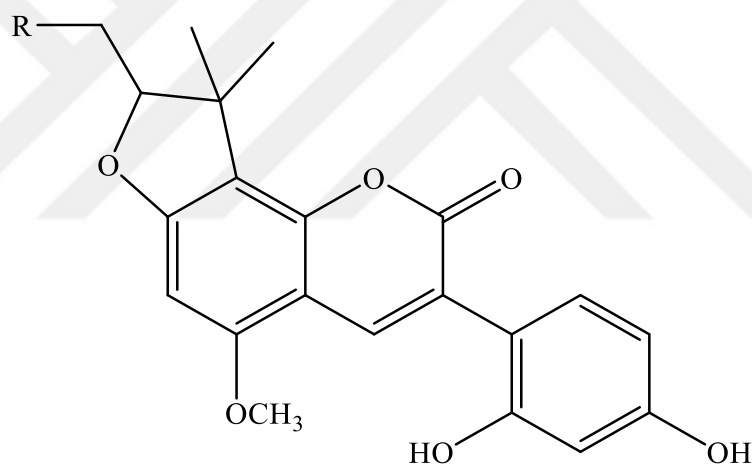
Table 65. 3-Arylcoumarins isolated from *Glycyrrhiza* species

Compounds	R	Species	Ref
Glycyfuranocoumarin A	H	*uralensis* (R)	(22)
Glycyfuranocoumarin B	OH	*uralensis* (R)	(22)
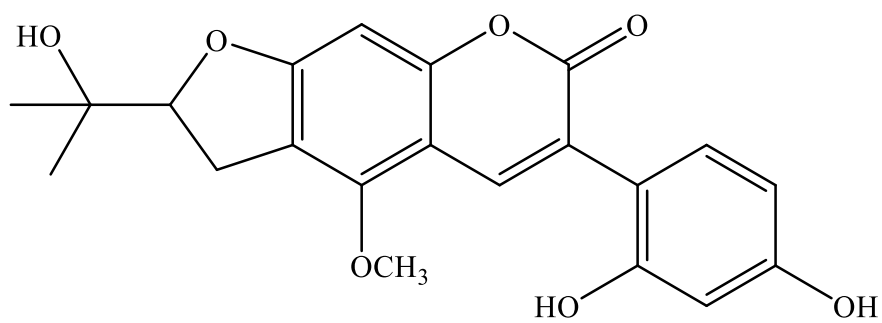
Table 66. 3-Arylcoumarin isolated from *Glycyrrhiza* species

Compound	Species	Ref
Licofuranocoumarin	*uralensis* (R)	(185)
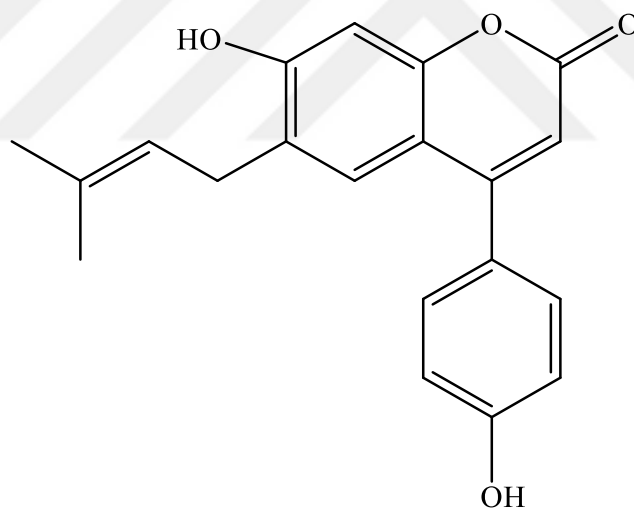
Table 67. Neoflavonoid isolated from *Glycyrrhiza* species

Compound	Species	Ref
Inflacoumarin A	*inflata* (R)	(19)
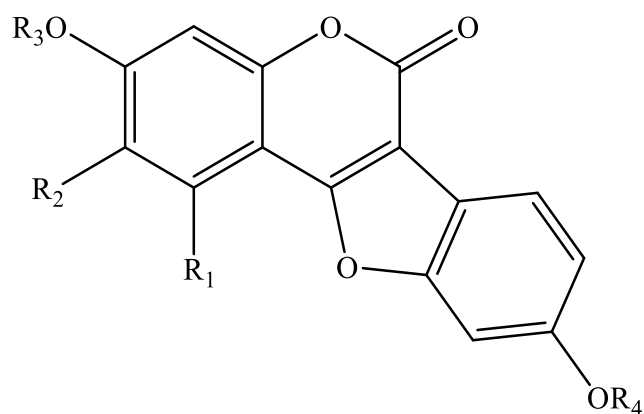
Table 68. Coumestans isolated from *Glycyrrhiza* species

Compounds	R₁	R₂	R₃	R₄	Species	Ref
Licoagroside C	H	H	β-D-Glc	CH₃	*pallidiflora* (R)	(178)
Glycyrol	OCH₃	isopre	H	H	*uralensis* (R)	(22,215,216)
3-*O*-methylglycyrol	OCH₃	isopre	CH₃	H	*uralensis* (R)	(202, 216)
Glycyrurol	OCH₃	3-hydroxy-3-methyl butyl	H	H	*uralensis* (R)	(151)
Isotrifoliol	OCH₃	H	H	H	*uralensis* (R)	(185)
9-methoxycoumestan	H	H	H	CH₃	*pallidiflora* (R)	(21)
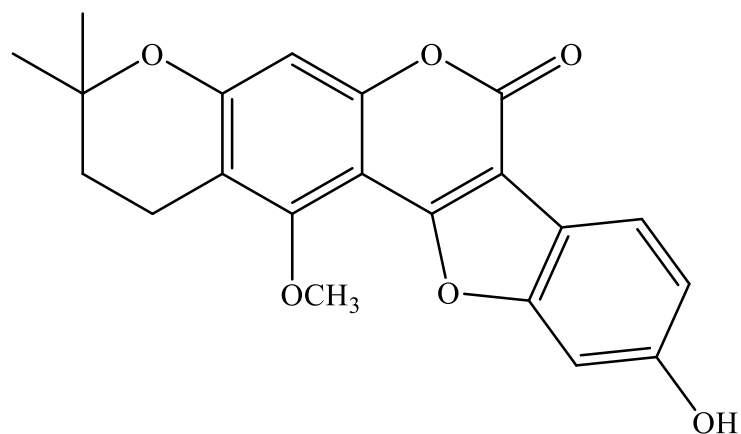
Table 69. Coumestan isolated from *Glycyrrhiza* species

Compound	Species	Ref
Isoglycyrol	*uralensis* (R) *pallidiflora* (R)	(21,22,202)
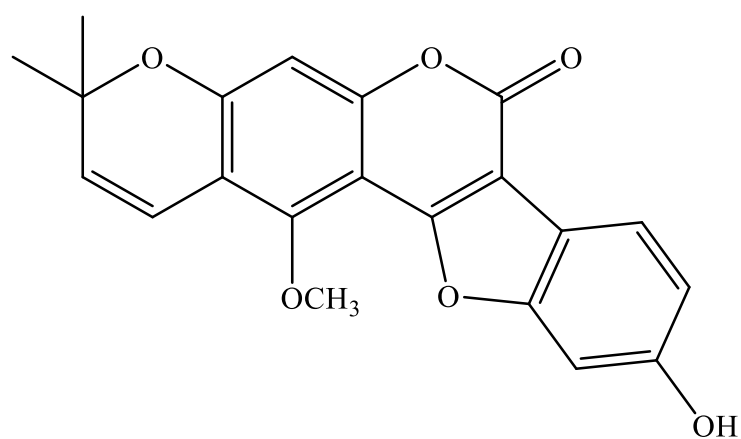
Table 70. Coumestan isolated from *Glycyrrhiza* species

Compound	Species	Ref
Gancaonin F	-	(217)
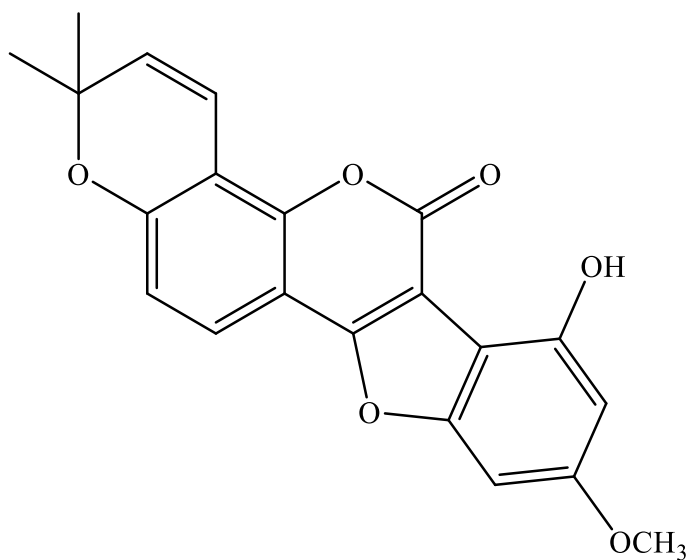
Table 71. Coumestan isolated from *Glycyrrhiza* species

Compound	Species	Ref
Gancaonol B	*uralensis* (R)	(202)
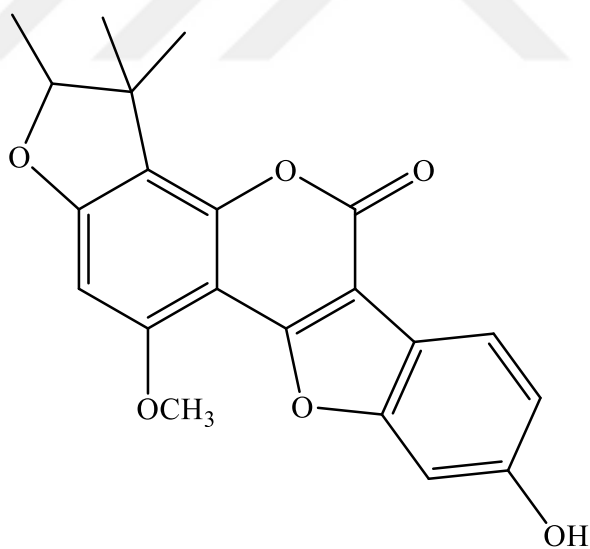
Table 72. Coumestan isolated from *Glycyrrhiza* species

Compound	Species	Ref
Glycyfuranocoumarin C	*uralensis* (R)	(22)
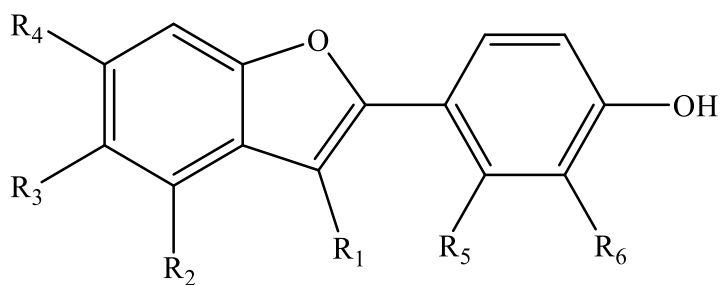
Table 73. 2-Arylbenzofurans isolated from *Glycyrrhiza* species

Compounds	R_1	R_2	R_3	R_4	R_5	R_6	Species	Ref
Licocoumarone	H	OCH_3	isopre	OH	OH	H	*uralensis* (R)	(61,204)
Gancaonin I	H	OCH_3	isopre	OCH_3	OH	H	*uralensis* (R)	(22,204)
Licobenzofuran	OH	H	OCH_3	OCH_3	H	isopre	-	(19)
2'-*O*-demethyl-bidwillol B	H	H	H	OH	OH	isopre	*inflata* (R)	(109)
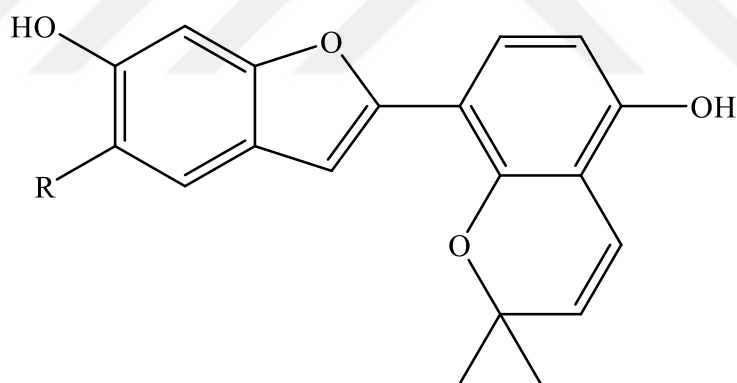
Table 74. 2-Arylbenzofurans isolated from *Glycyrrhiza* species

Compounds	R	Species	Ref
Kanzonol U, Glabrocoumarone A	H	*glabra* (R)	(94,171,209)
Kanzonol V	isoprenyl	*glabra* (R)	(171)
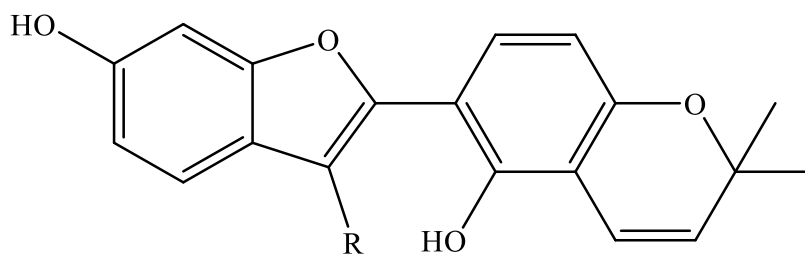
Table 75. 2-Arylbenzofurans isolated from *Glycyrrhiza* species

Compounds	R	Species	Ref
Glabrocoumarone B, Glyinflanin H	H	*inflata* (R) *glabra* (R)	(24,209)
Glycybridin F	CHO	*glabra* (R)	(23)
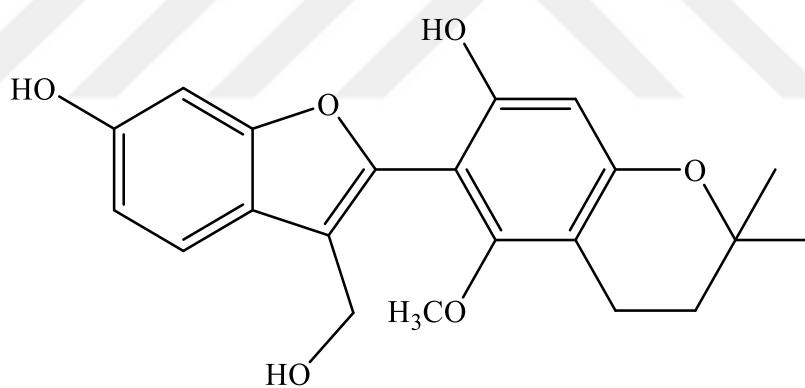
Table 76. 2-Arylbenzofuran isolated from *Glycyrrhiza* species

Compound	Species	Ref
Glycyuralin E	*uralensis* (R)	(22)
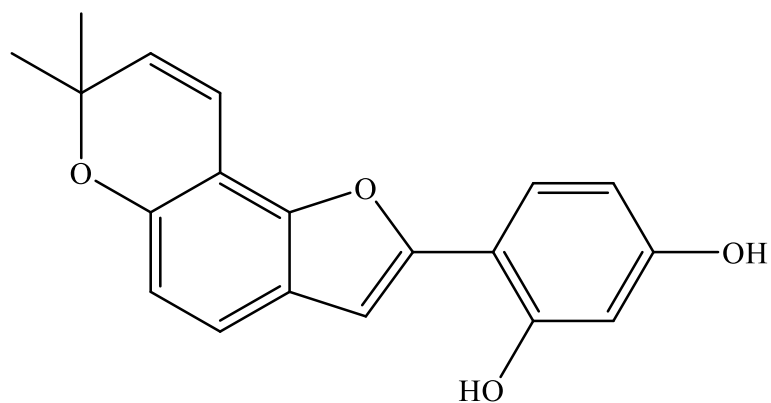
Table 77. 2-Arylbenzofuran isolated from *Glycyrrhiza* species

Compound	Species	Ref
Glycybridin G	*glabra* (R)	(23)
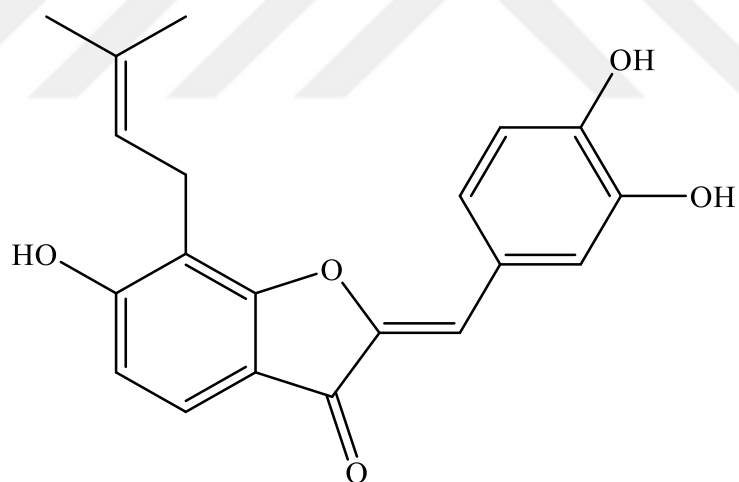
Table 78. Aurone isolated from *Glycyrrhiza* species

Compound	Species	Ref
Licoagroaurone	*glabra* (R)	(166)
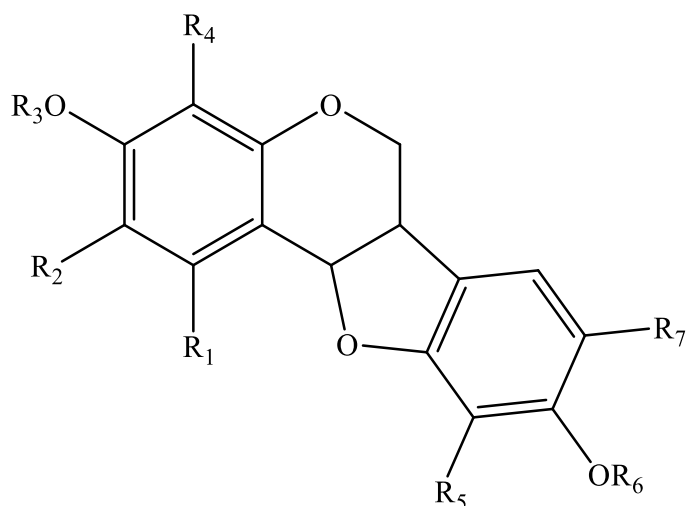
Table 79. Pterocarpans isolated from *Glycyrrhiza* species

Compounds	R$_1$	R$_2$	R$_3$	R$_4$	R$_5$	R$_6$	R$_7$	Species	Ref
Medicarpin	H	H	H	H	H	CH$_3$	H	*aspera* (R) *pallidiflora* (R)	(21, 163)
Medicarpin 3-*O*-β-D-glucopyranoside	H	H	β-D-Glc	H	H	CH$_3$	H	*uralensis* (R)	(159)
Homopterocarpin	H	H	CH$_3$	H	H	CH$_3$	H	*pallidiflora* (R)	(21)
1-Methoxy-phaseollidin	OCH$_3$	H	H	H	isopre	H	H	*aspera* (R) *uralensis* (R)	(163, 202)
Asperopterocarpin	OCH$_3$	H	isopre	H	H	H	H	*aspera* (R)	(163)
Phaseollidin	H	H	H	H	isopre	H	H	*aspera* (R)	(163)
Licoagropin	H	H	H	isopre	H	CH$_3$	H	*glabra* (CC)	(167)
Glycyuralin B	OH	1,1-di-methyl-2-propenyl	H	H	H	CH$_3$	H	*uralensis* (R)	(22)
1-Methoxyficifolinol	OCH$_3$	isopre	H	H	H	H	iso pre	*aspera* (R) *uralensis* (R)	(13, 163)
Edudiol	OCH$_3$	isopre	H	H	H	H	H	*glabra* (R) *uralensis* (R)	(13, 177)
3-methoxy-9-hydroxypterocarpan	H	H	CH$_3$	H	H	H	H	*inflata* (R) *uralensis* (R)	(22, 109)
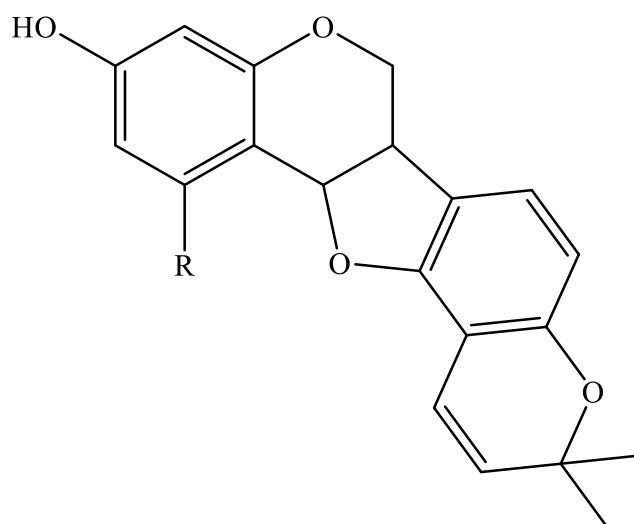
Table 80. Pterocarpans isolated from *Glycyrrhiza* species

Compounds	R	Species	Ref
Phaseolin	H	*glabra* (R)	(23)
1-Methoxyphaseollin	OCH$_3$	*aspera* (R) *uralensis* (R)	(22,163)
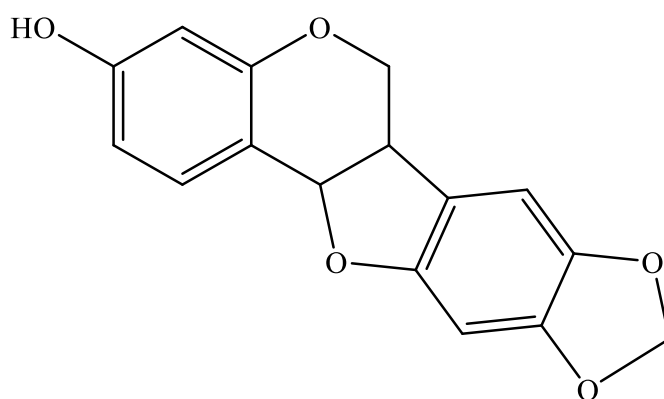
Table 81. Pterocarpan isolated from *Glycyrrhiza* species

Compound	Species	Ref
Maackiain	*pallidiflora* (R)	(21,178)
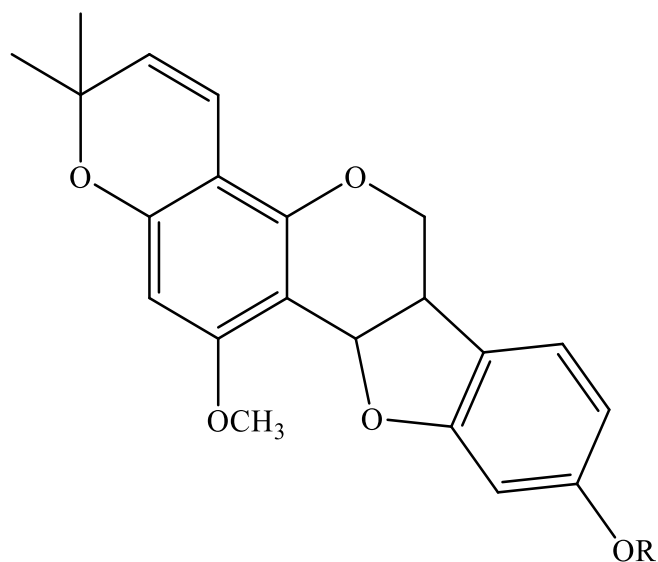
Table 82. Pterocarpans isolated from *Glycyrrhiza* species

Compounds	R	Species	Ref
Shinpterocarpin	H	*glabra* (R)	(94)
O-methylshinpterocarpin, ent-(-)-Hemileiocarpin	CH₃	*glabra* (R)	(94)
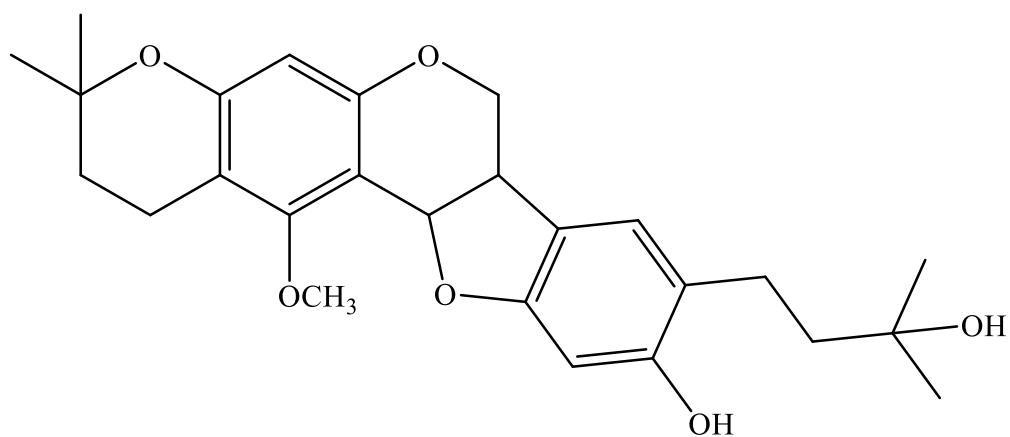
Table 83. Pterocarpan isolated from *Glycyrrhiza* species

Compound	Species	Ref
Glycycarpan	*uralensis* (R)	(13)
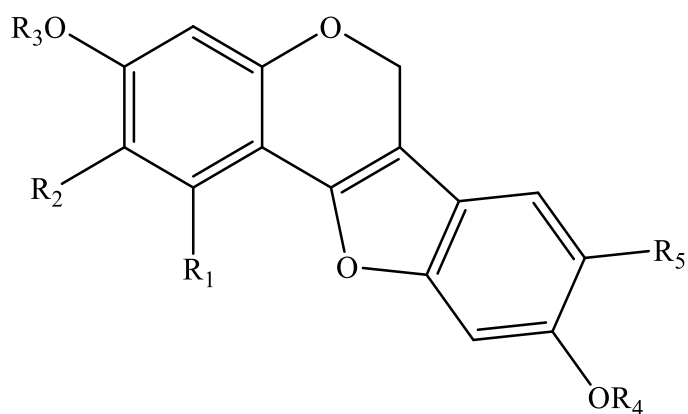
Table 84. Pterocarpenes isolated from *Glycyrrhiza* species

Compounds	R₁	R₂	R₃	R₄	R₅	Species	Ref
Glyurallin A	OCH₃	isopre	H	H	H	*uralensis* (R)	(203)
Glycyrrhizol A	OCH₃	isopre	H	H	isopre	*uralensis* (R)	(218)
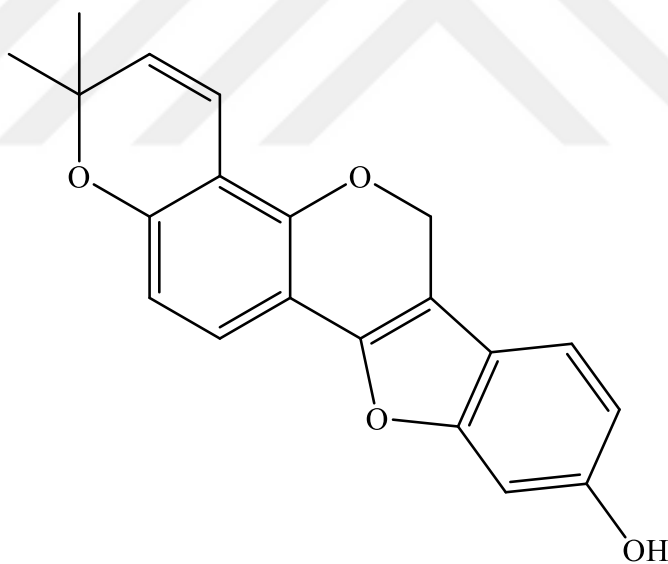
Table 85. Pterocarpene isolated from *Glycyrrhiza* species

Compound	Species	Ref
Dehydroglyceollin I	*glabra* (R)	(23)
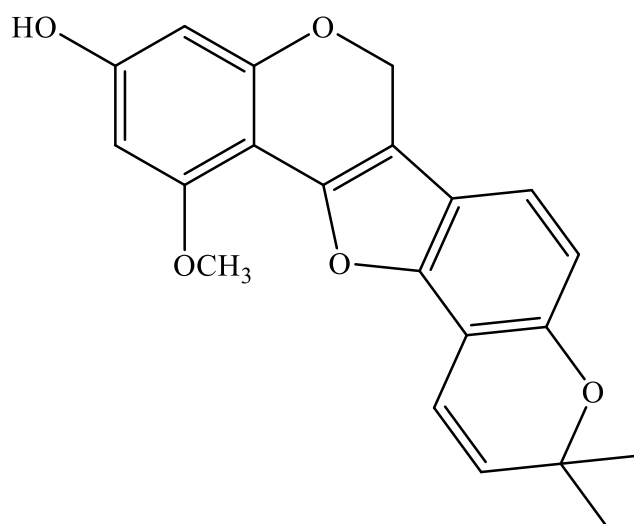
Table 86. Pterocarpene isolated from *Glycyrrhiza* species

Compound	Species	Ref
Glycyrrhizol B	*uralensis* (R)	(218)
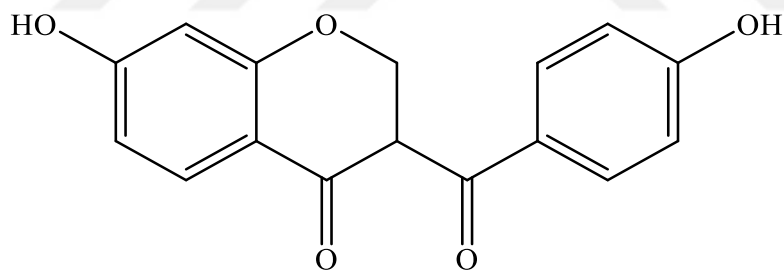
Table 87. Homoisoflavanones isolated from *Glycyrrhiza* species

Compound	Species	Ref
Gancaonin K	*pallidiflora* (R)	(173)
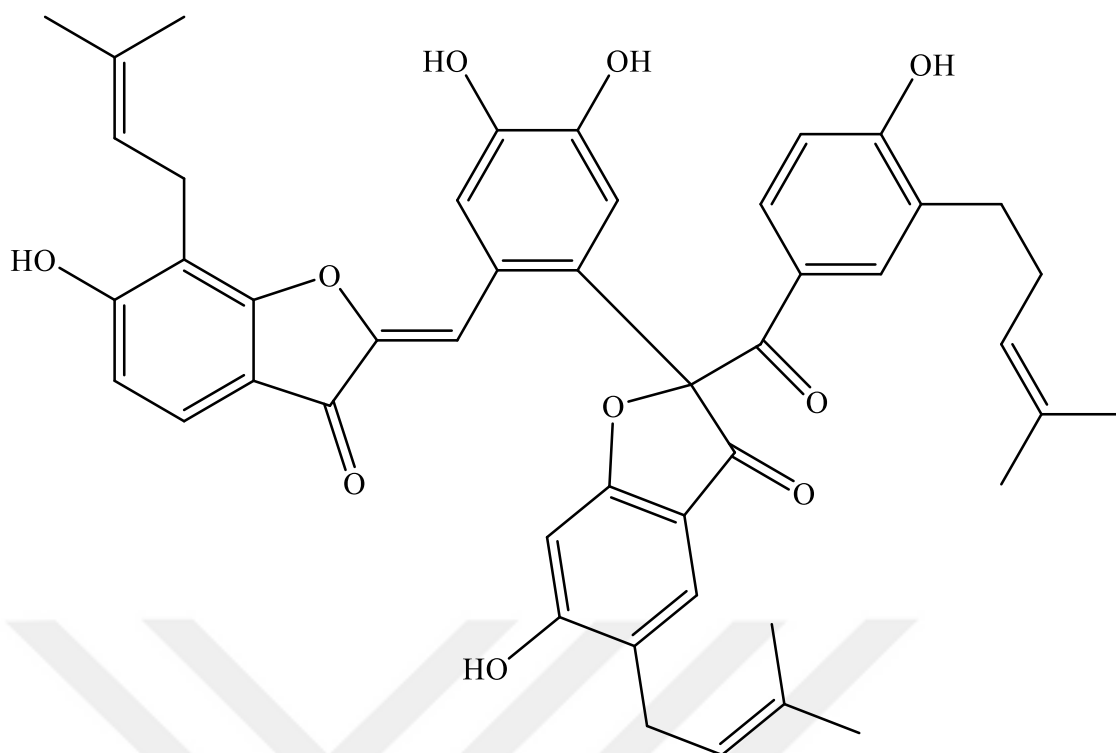
Table 88. Biaurone isolated from *Glycyrrhiza* species

Compound	Species	Ref
Licoagrone	*glabra* (R)	(168)
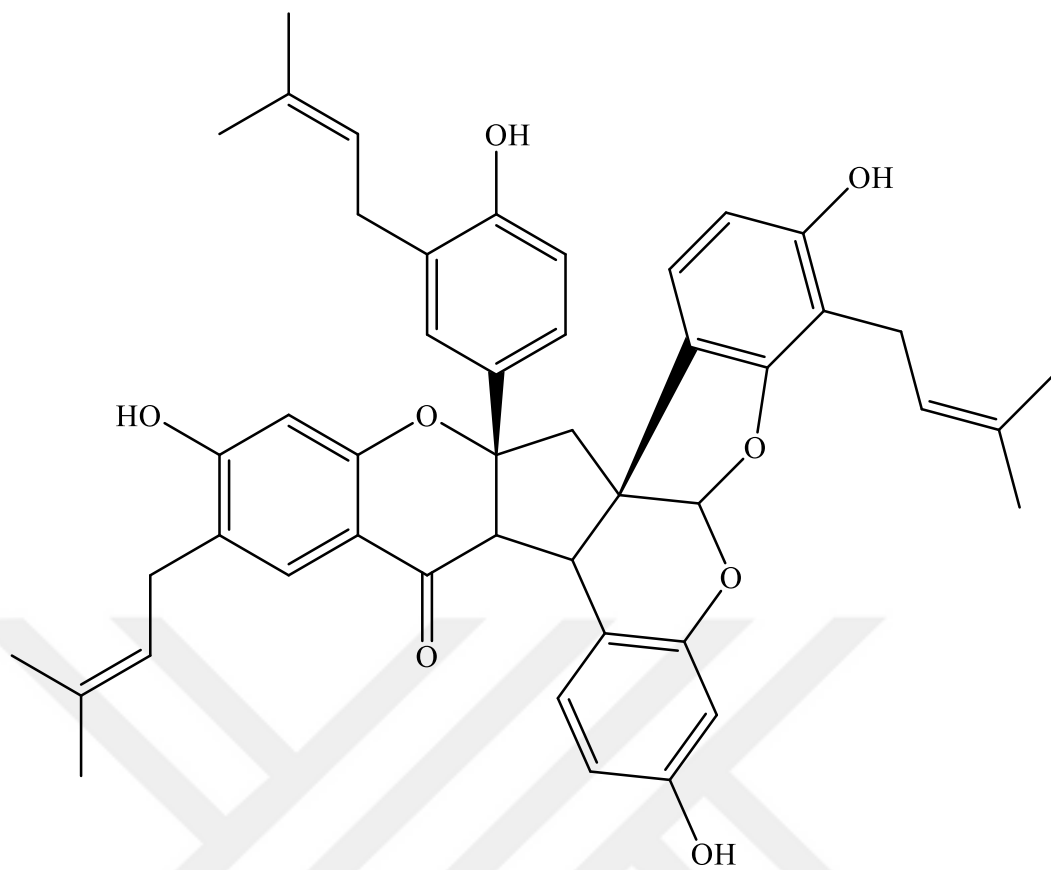
Table 89. Biflavonoid isolated from *Glycyrrhiza* species

Compound	Species	Ref
Licoagroside	*glabra* (R)	(166)

2.1.3.1.F. Chromones Isolated from *Glycyrrhiza* species
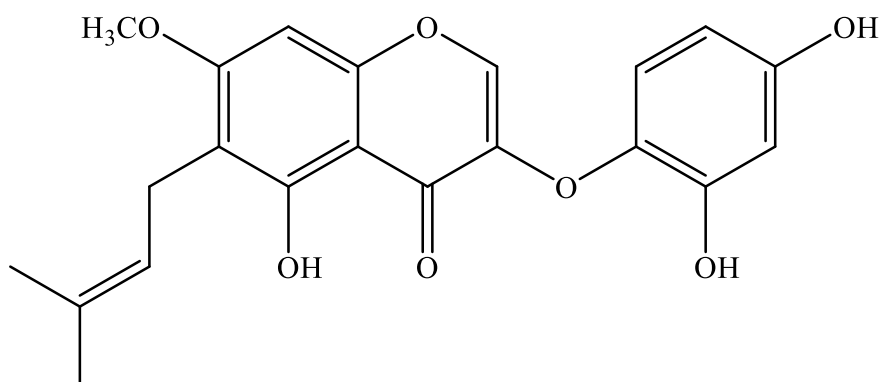
Table 90. 3-Oxygenated chromen-4-one isolated from *Glycyrrhiza* species

Compound	Species	Ref
Glyasperin E	*aspera*	(14)
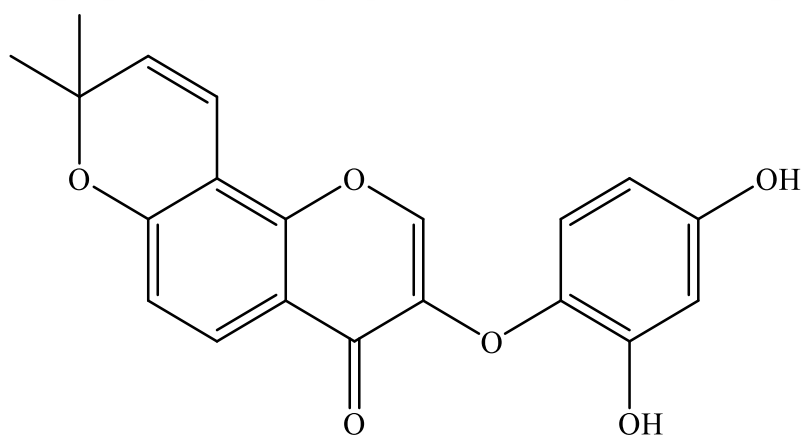
Table 91. 3-Oxygenated chromen-4-one isolated from *Glycyrrhiza* species

Compound	Species	Ref
Glycybridin I	*glabra* (R)	(23)

2.1.3.1.G. Stilbenes Isolated from *Glycyrrhiza* species
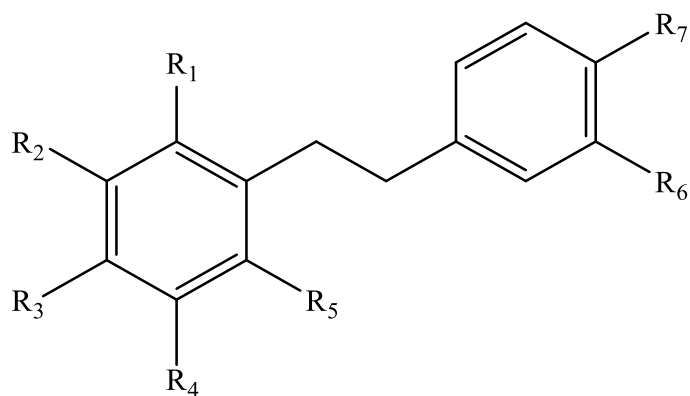
Table 92. Dihydrostilbenes isolated from *Glycyrrhiza* species

Compounds	R₁	R₂	R₃	R₄	R₅	R₆	R₇	Species	Ref
Gancaonin R	isopre	OH	H	OH	isopre	OH	OH	*uralensis* (A)	(181)
Gancaonin S	isopre	OH	isopre	OH	H	OH	OH	*uralensis* (A)	(181)
Glepidotin C	H	OH	2-hydroxy-3-methyl-but-3-enyl	OH	H	H	H	*lepidota* (L)	(186)
Glepidotin C	H	OH	isoprenyl	*O*-isopre	H	OH	H	*lepidota* (L)	(186)
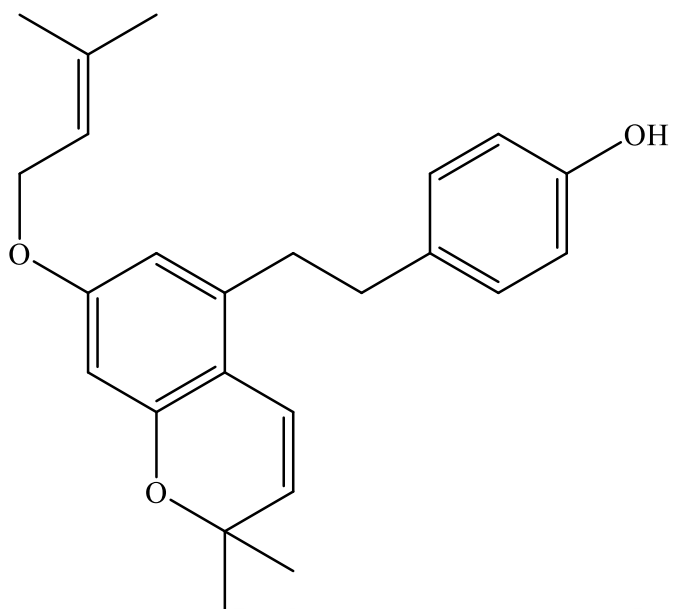
Table 93. Dihydrostilbene isolated from *Glycyrrhiza* species

Compound	Species	Ref
Xinjiastilbene A	*inflata*	(169)
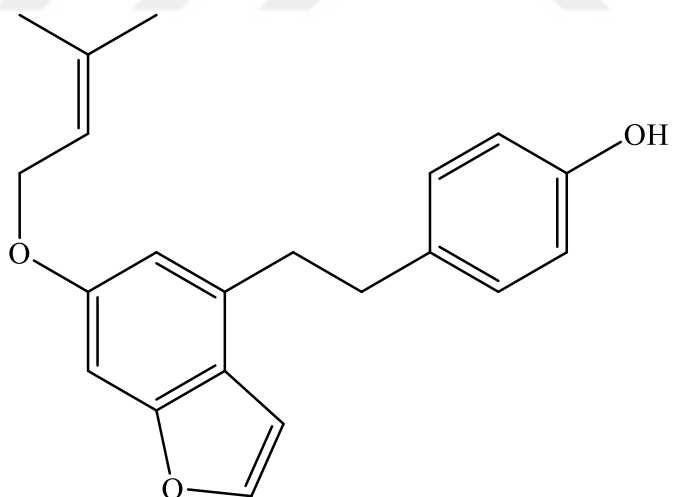
Table 94. Dihydrostilbene isolated from *Glycyrrhiza* species

Compound	Species	Ref
Xinjiastilbene B	*inflata*	(169)
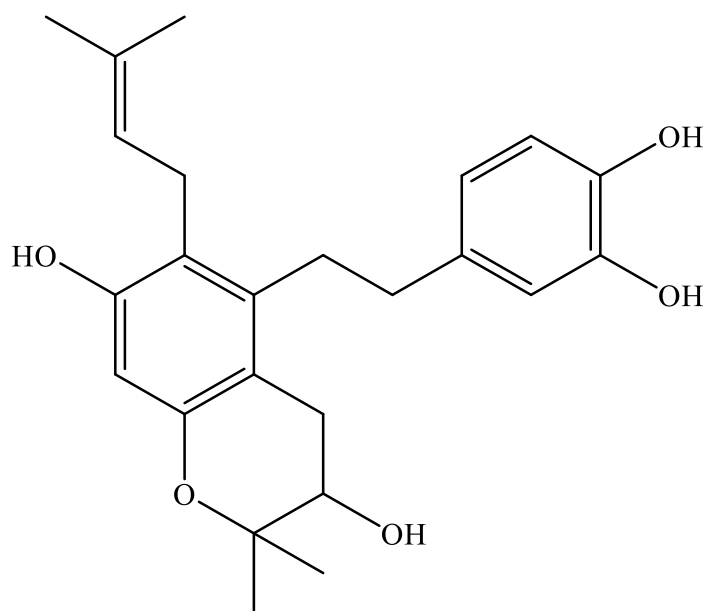
Table 95. Dihydrostilbene isolated from *Glycyrrhiza* species

Compound	Species	Ref
Gancaonin T	*uralensis* (A)	(181)

2.1.3.1.H. Phenanthrenes Isolated from *Glycyrrhiza* species
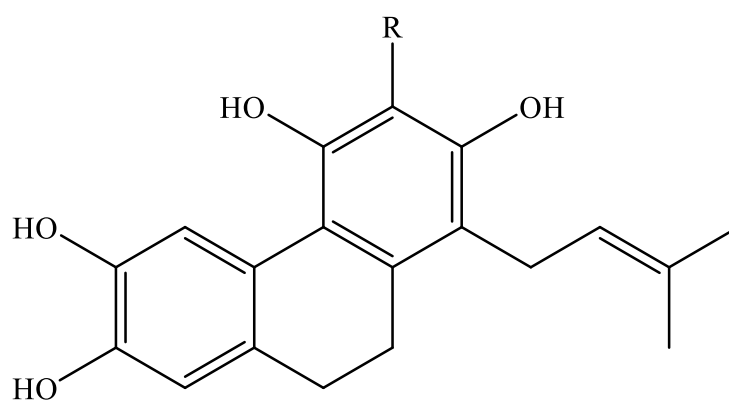
Table 96. Dihydrophenanthrenes isolated from *Glycyrrhiza* species

Compounds	R	Species	Ref
Gancaonin U	H	*uralensis* (A)	(181)
Gancaonin V	isoprenyl	*uralensis* (A)	(181)

2.1.3.2. Terpenic Compounds

2.1.3.2.A. Triterpene Saponins Isolated from *Glycyrrhiza* species
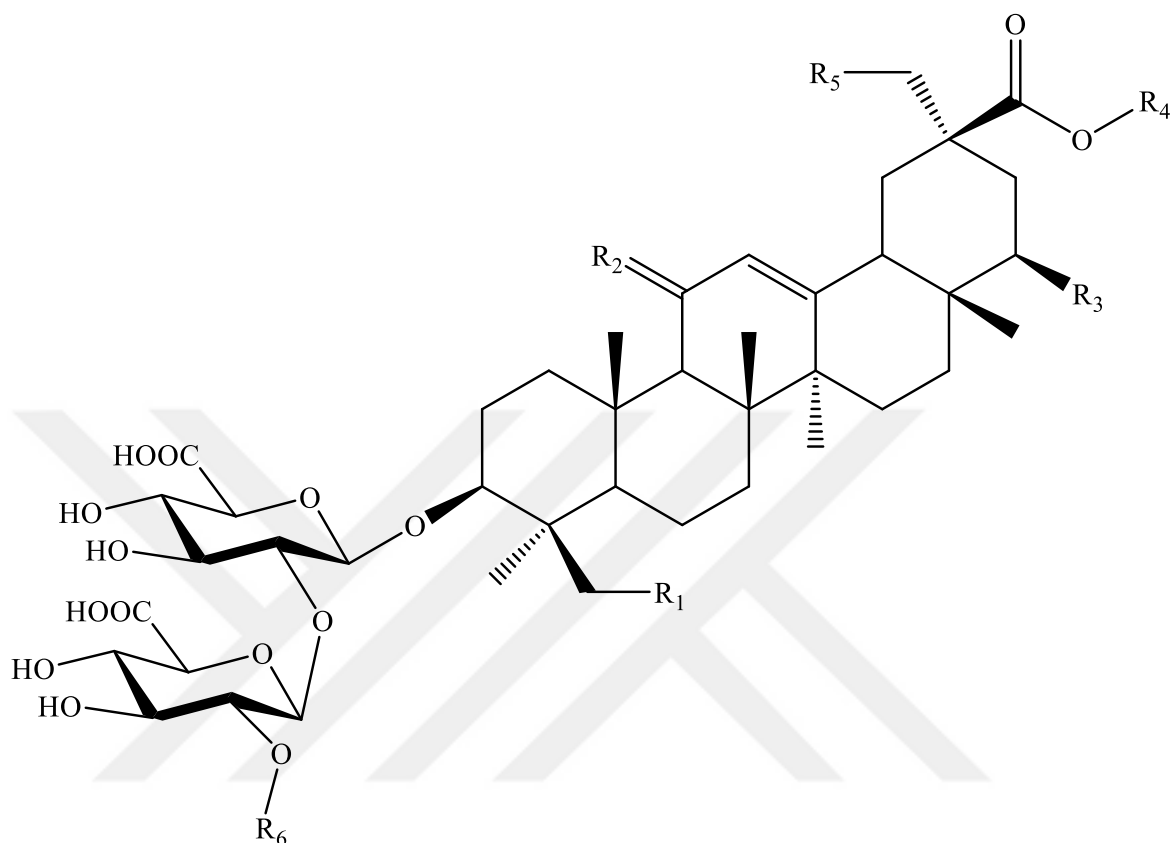
Table 97. Triterpene saponins isolated from *Glycyrrhiza* species

Compounds	R$_1$	R$_2$	R$_3$	R$_4$	R$_5$	R$_6$	Species	Ref
Glycyrrhizic acid, Glycyrrhizin	H	O	H	H	H	H	*glabra* (R) *inflata* (R) *uralensis* (R)	(22,134, 219)
Licorice-saponin A3	H	O	H	β-D Glc	H	H	*inflata* (R) *uralensis* (R)	(22,101)
Licorice-saponin B2	H	H$_2$	H	H	H	H	*uralensis* (R)	(22)
Licorice-saponin D3	H	H$_2$	Acet	H	H	α-L- Rha	*uralensis* (R)	(220)
Licorice-saponin G2	OH	O	H	H	H	H	*inflata* (R) *uralensis* (R)	(22,101)

113

Table 97. Triterpene saponins isolated from *Glycyrrhiza* species

Compounds	R₁	R₂	R₃	R₄	R₅	R₆	Species	Ref
Licorice-saponin J2	OH	H₂	H	H	H	H	*uralensis* (R)	(72)
Licorice-saponin L3	OH	H₂	Acet	H	H	α-L-Rha	*glabra* (R)	(165)
Licorice-saponin P2	H	O	H	H	OH	H	*inflata* (R)	(101)
Licorice-saponin Q2	OH	O	H	H	H	H	*inflata* (R)	(101)
Rhaoglycyrrhizin	H	O	H	H	H	α-L-Rha	*glabra* (R)	(219)
22β-acetoxyglycyrrhizin	H	O	Acet	H	H	H	*inflata* (R) *uralensis* (R)	(101,134)
Uralsaponin F	OH	O	Acet	H	H	H	*uralensis* (R)	(134)

Acet: Acetoxy
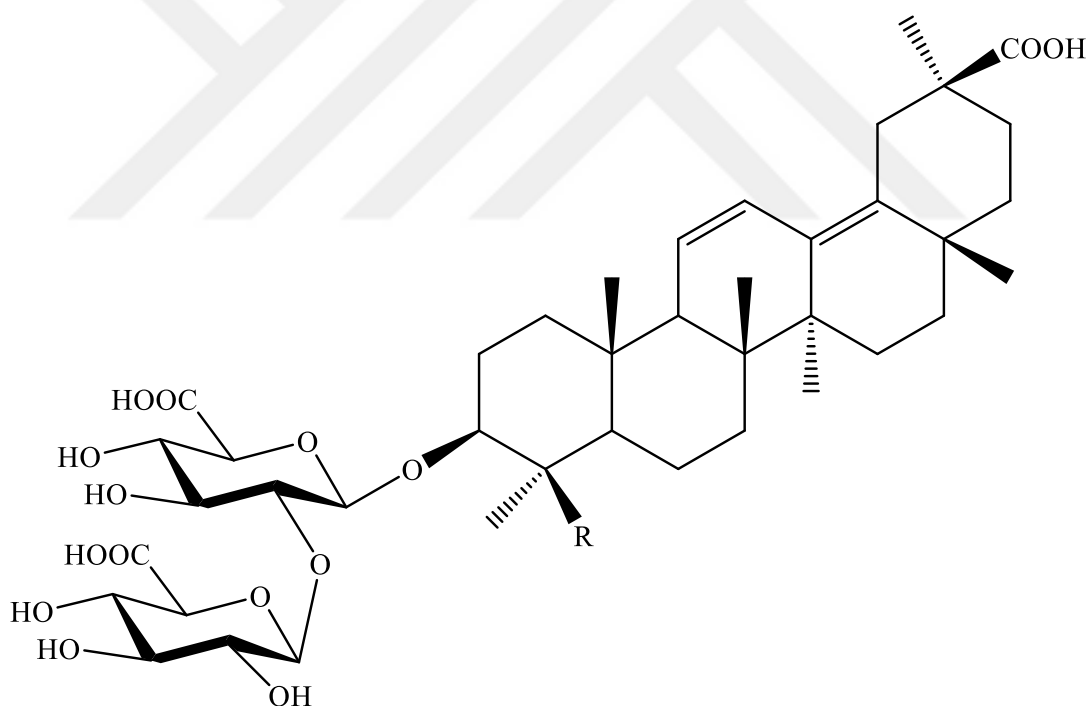
Table 98. Triterpene saponins isolated from *Glycyrrhiza* species

Compounds	R	Species	Ref
Licorice-saponin C2	CH₃	*uralensis* (R)	(220)
Licorice-saponin K2	CH₂OH	*uralensis* (R)	(221)
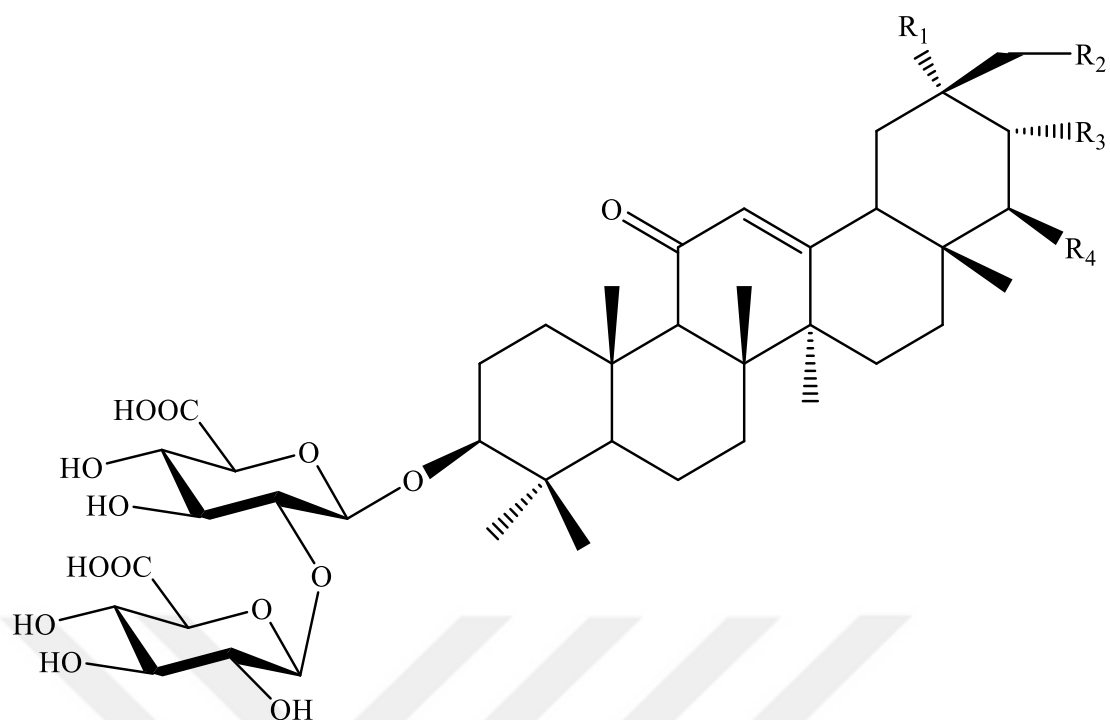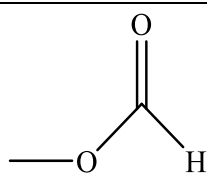
Table 99. Triterpene saponins isolated from *Glycyrrhiza* species

Compounds	R$_1$	R$_2$	R$_3$	R$_4$	Species	Ref
Macedonoside A	COOH	H	OH	H	*inflata* (R)	(101)
Licorice-saponin H2	COOH	H	H	H	*uralensis* (R)	(22)
30-hydroxyglycyrrhizin	CH$_3$	OH	H	H	*glabra* (R)	(219)
Glycyrrhizin 20-methanoate	CH$_3$	(see structure)	H	H	*glabra* (R)	(219)
Uralsaponin C	CH$_3$	OH	H	OH	*uralensis* (R)	(134)
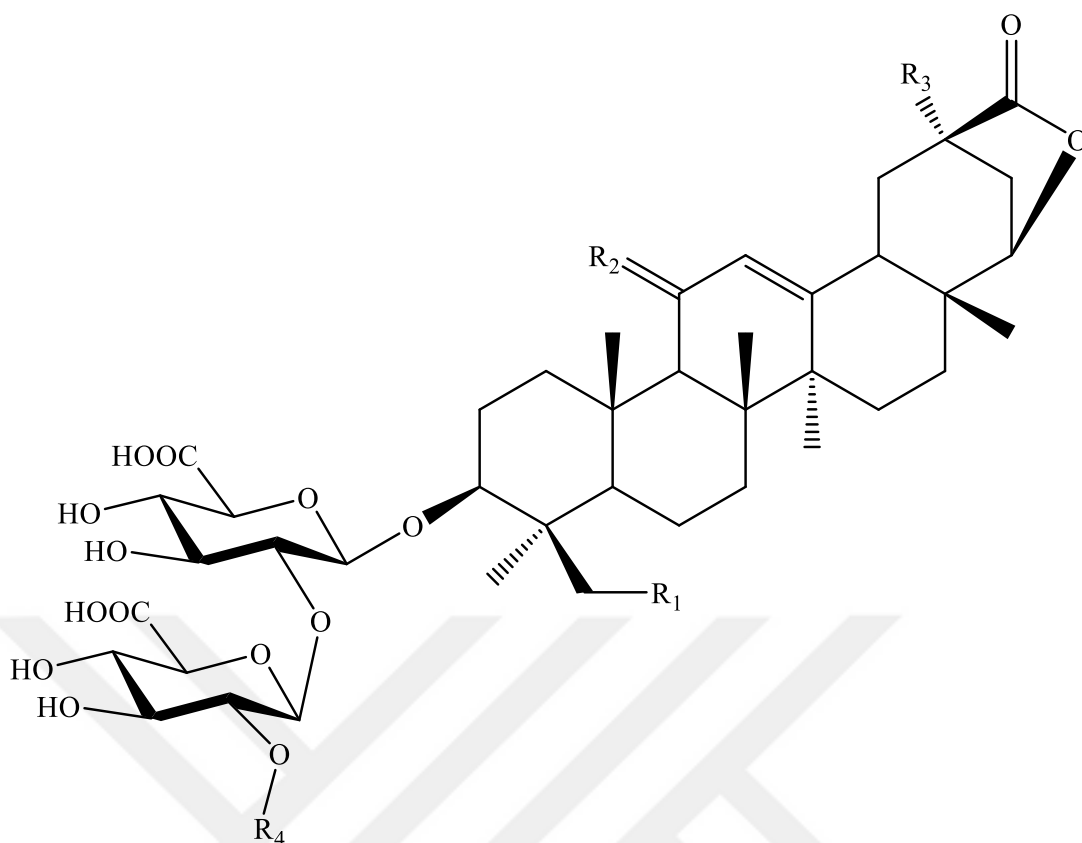
Table 100. Triterpene saponins isolated from *Glycyrrhiza* species

Compounds	R_1	R_2	R_3	R_4	Species	Ref
Licorice-saponin E2	H	O	CH_3	H	*inflata* (R) *uralensis* (R)	(22,101)
24-hydroxylicorice-saponin E2	OH	O	CH_3	H	*inflata* (R)	(101)
Licorice-saponin F3	H	H_2	CH_3	α-L-Rha	*uralensis* (R)	(221)
Uralsaponin D	H	O	COOH	H	*inflata* (R) *uralensis* (R)	(101,134)
Uralsaponin E	H	O	CH_2OH	H	*uralensis* (R)	(134)
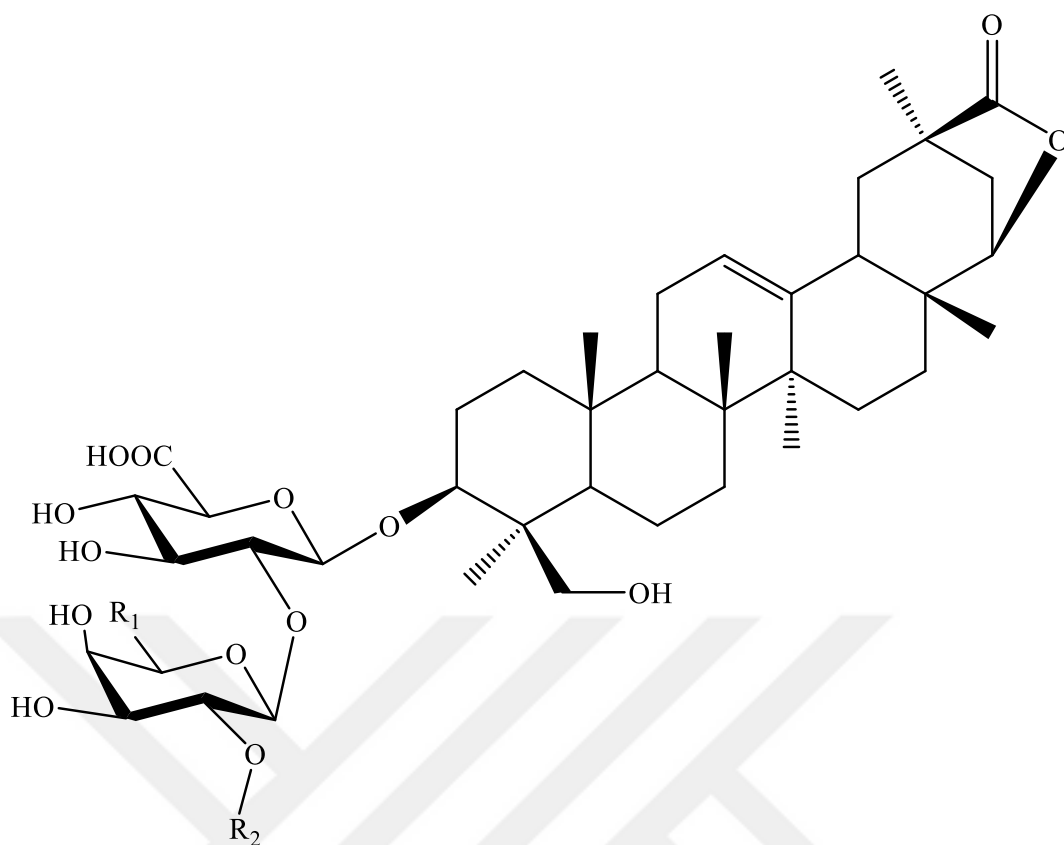
Table 101. Triterpene saponins isolated from *Glycyrrhiza* species

Compounds	R₁	R₂	Species	Ref
Glycyrflavoside A	CH₂OH	α-L-Rha	*flavescens* (R)	(222)
Glycyrflavoside B	H	α-L-Rha	*flavescens* (R)	(222)
Glycyrflavoside C	CH₂OH	H	*flavescens* (R)	(222)
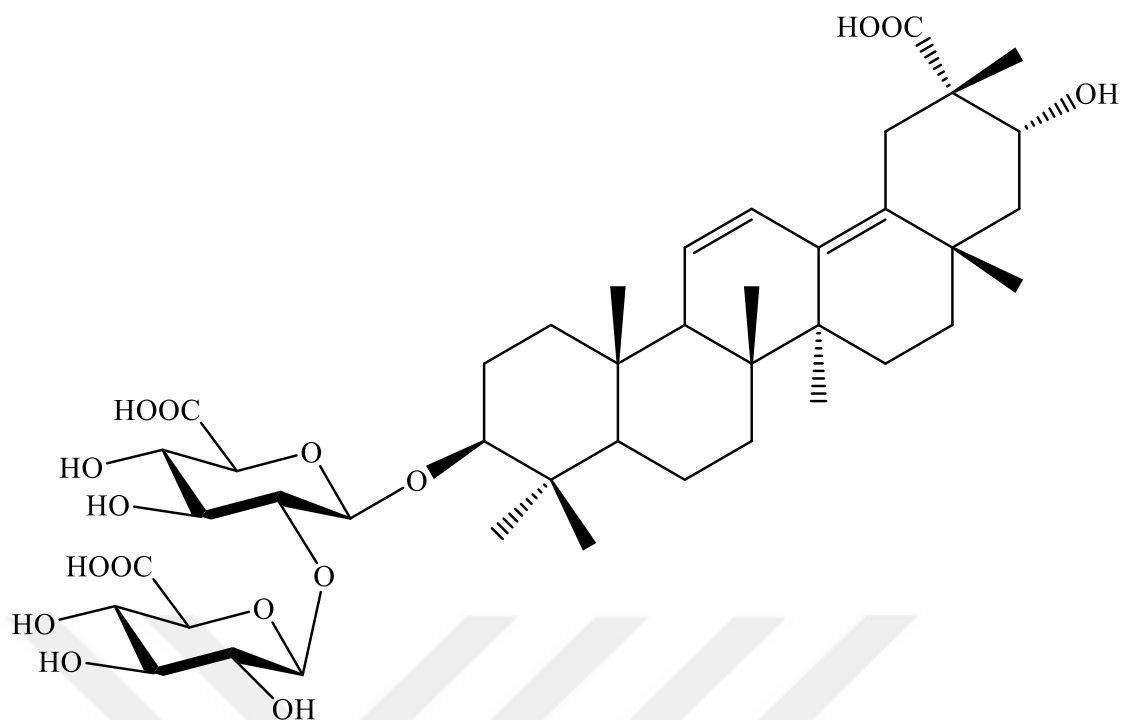
Table 102. Triterpene saponin isolated from *Glycyrrhiza* species

Compound	Species	Ref
Macedonoside C	*echinata* (R) *macedonica* (R) *pallidiflora* (R)	(147)
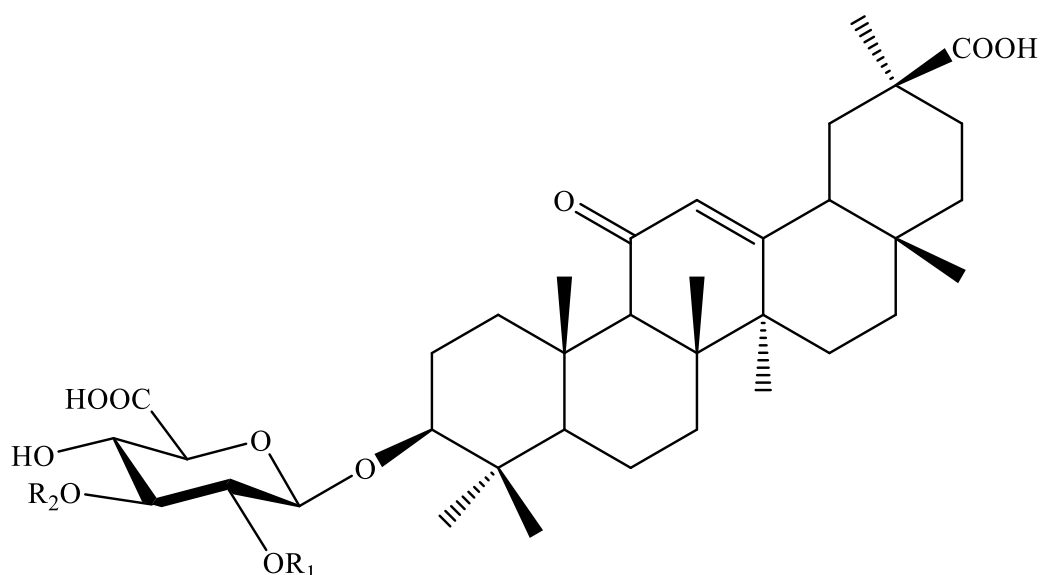
Table 103. Triterpene saponins isolated from *Glycyrrhiza* species

Compounds	R₁	R₂	Species	Ref
3-*O*-β-D-glucuronopyranosyl-glycyrrhetinic acid	H	H	*uralensis* (R)	(72)
Uralsaponin B	H	β-D-GlcA	*uralensis* (R)	(19)
Apioglycyrrhizin	β-D-Api	H	*glabra* (R) *inflata* (R)	(219)
Araboglycyrrhizin	α-L-Ara	H	*glabra* (R) *inflata* (R) *uralensis* (R)	(22,219)
Rhaogalactoglycyrrhizin	-β-D-Gal-(2-*O*-α-L-Rha)	H	*glabra* (R)	(219)
Rhaoglucoglycyrrhizin	-β-D-Glc- (2-*O*-α-L-Rha)	H	*glabra* (R)	(219)

2.2. General Information about Cancer and Apoptosis

Cancer is a major public health problem and one of the leading cause of mortality and morbidity worldwide. With regard to GLOBOCAN 2018 statics, there have been estimated 18.1 million new cancer cases, 9.6 million cancer-related deaths and 43.8 million prevalence of cancer in 2018 across globe. Breast cancer has the highest incidence rate among women, followed by colorectal cancer. Among men, colorectal cancer has been ranked as third while, liver cancer has been the fifth common site of cancer (223). Cancer is identified by uncontrolled growth and multiplication of abnormal cells which is related to the evasion of apoptosis as being one of the most significant hallmarks of cancer (1,128).

Apoptosis is natural mechanism of cell for programmed cell death, that occurs both physiological and pathological conditions (4,5). Since it gives insights both about the pathogenesis and treatment of the diseases, understanding of its underlying mechanism is one of the most studied topics among cell biologist. Apoptosis is considered as a double edged sword, besides being a cause it can also be a treatment (4). New drugs target different aspects of apoptosis including apoptotic genes or pathways (6). Accelerated apoptosis results in infertility, immunodeficiency as well as acute and chronic degenerative diseases. In carcinogenesis, inadequate apoptosis or resistance to it plays a vital role, resulting malignant cells because of the loss of balance between cell division and cell death. A problem in any step of apoptosis signalling pathway can cause cancer. These can be generally divided into three main reasons including imbalance between pro-apoptotic and anti-apoptotic proteins, reduced caspase function, and impaired death receptor signalling (4,5).

Morphological changes in apoptosis are chromatin condensation and nuclear fragmentation in cell nucleus followed by rounding up of the cell, cell volume reduction and retraction of pseudopodes. Chromation condensation begins from the nuclear membrane which further becomes a crescent or ring-like structure followed by breaking up called karyorrhexis. Membrane blebbing, ultrastructural changes of cytoplasmic organelles and loss of membrane integrity are observed at later stage of apoptosis. Mostly, apoptotic cells are engulfed by phagocytic cells before apoptotic bodies ocur (224).

Caspases are cysteine protease enzymes, accepted as central mechanisms of apoptosis as being both the initiators and executioners. Caspase activation includes three initiation pathways described as intrinsic (or mitochondrial), extrinsic (or death receptor) and intrinsic endoplasmic reticulum pathways. There are four initiator caspases such as caspase -2, -8, -9 and -10 and three executioner caspases such as caspase -3, -6 and -7 (4,225).

Initiation of intrinsic pathway occurs within the cell. Internal stimuli including hypoxia, irreperable genetic damage, high concentrations of cytosolic Ca^{2+} and severe oxidative damage can trigger the initiation of intrinsic mitochondrial pathway (4). This pathway is the consequence of increased permeability of mitochondrial membrane and release of pro-apoptotic molecules such as cytochrome C into cytoplasm which is regulated by B-cell lymphoma-2 (Bcl-2) protein family. There are two main groups of Bcl-2 family that regulates apoptosis by promoting or blocking mitochondrial release of cytochrome C into cytosol, named as pro-apoptotic proteins and anti-apoptotic proteins, respectively. Apoptosis initiation is determined with respect to the balance between these pro- and anti-apoptotic proteins of Bcl-2 family (4,5,226).

Upregulation of pro-apoptotic BH3-only proteins is observed upon various apoptotic stimuli that inhibit anti-apoptotic Bcl-2 proteins and activate pro-apoptotic Bcl-2 proteins, known as Bcl-2 associated X (Bax) and Bcl-2 homologous antagonist killer (Bak) proteins. Activated Bax and Bak proteins oligomerize and lead to mitochondrial outer membrane permeabilization and thus induce release of mitochrondrial proteins such as cytochrome C (5,226). Released cytochrome C in cytosol interacts with Apaf-1 (apoptotic protease-activating factor-1), pro-caspase-9 and dATP to form a complex called "apoptosome" which further dimerizes and activates caspase-9 (4). Activated caspase-9 subsequently stimulates proteolytic activity of other downstream caspases including executioner caspase-3 and -7 which leads to cleavage of various proteins such as PARP and cascade results in breaking down of cellular proteins and cell death. The other mitochondrial proteins that released in order to promote apoptosis are apoptotic inducing factor (AIF), Smac/Diablo, Endonuclease G, Omi/HtrA2 (5,227–229).

Extrinsic pathway is regulated by extracellular signals for inducing apoptosis. Cell death ligands (or death ligands) including Fas ligand (Fas-L), TNF-related apoptosis-inducing ligand (TRAIL) and tumor necrosis factor (TNF), bind to TNF family death

receptors. An adaptor protein, Fas-associated death domain (FADD) or TNF receptor-associated death domain (TRADD) recruited to the death receptor. Death-inducing signalling complex (DISC) is formed by binding initiator pro-caspases -8 and -10 to adaptor protein which activated caspases -8 and -10. Executioner caspases -3, -6 and -7 are then activated and lead to cell death. Moreover, activated caspase-8 cause activation of one of a BH3-only protein which further activates and oligomerizes Bax and Bak proteins and apoptosis occurs by the intrinsic apoptotic pathway (5,226).

The third and less well known pathway is the intrinsic endoplasmic reticulum pathway which is considered to be caspase 12- dependent and mitochondria- independent. It is occured by unfolding of proteins and decreased protein synthesis as well as dissociating of TNF receptor associated factor 2 (TRAF2) from pro-caspase-12 in the cell when there is an injure in endoplasmic reticulum by cellular stresses (4).
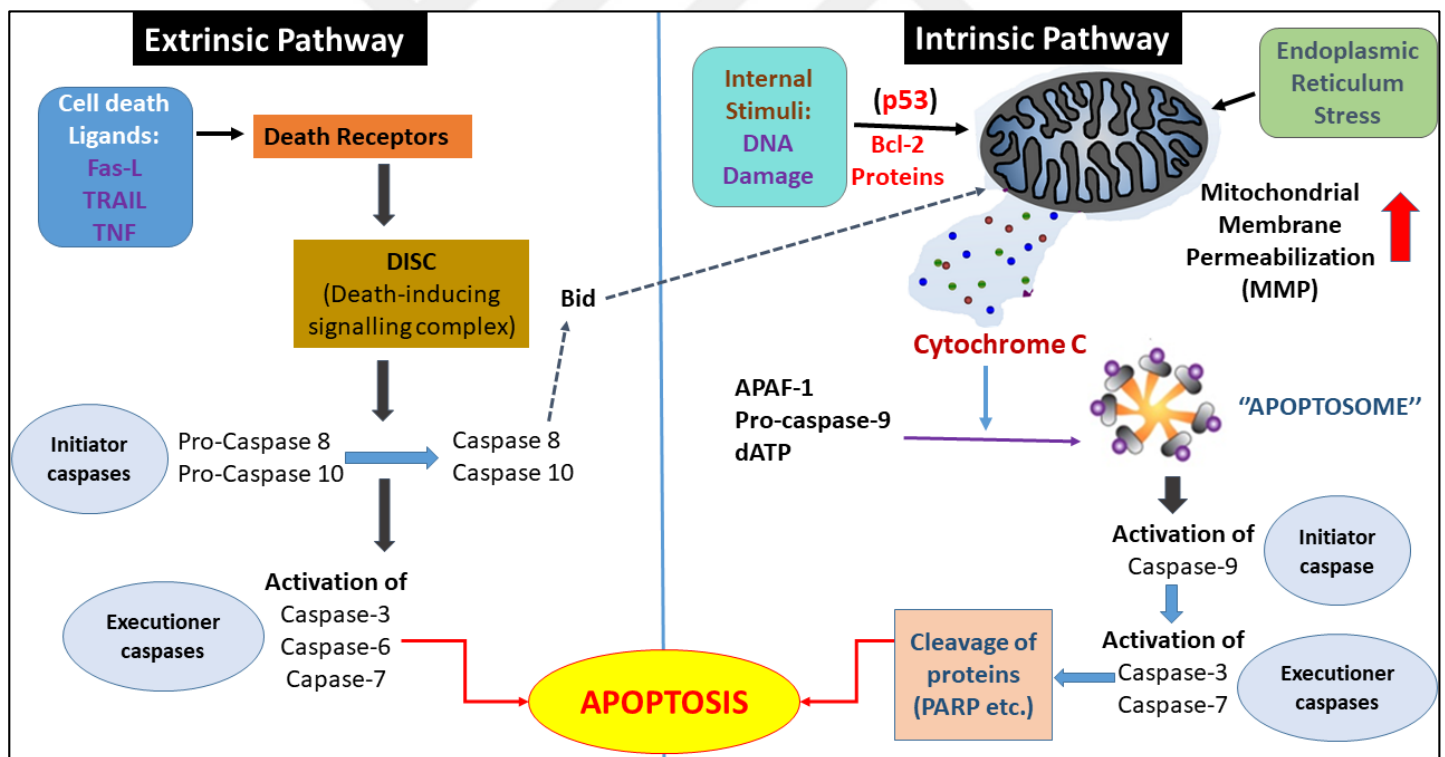
Figure 3. Mechanism of apoptosis through caspase cascade

The p53 is a tumor supressor gene which is known as "guardian of genome", acts in various cellular processes including cell cycle regulation, induction of apoptosis, development, differentiation, gene amplification, DNA recombination, chromosomal segregation and cellular senescence (230). Among these cellular responses regulated by p53, the most pivotal abilities of p53 are to induce cell cycle arrest and apoptosis. p53 is known to play a vital role in every type of human cancers by eliminating and inhibiting the proliferation of abnormal cells, whereas mutation or loss of p53 is found in more than 50% of human cancer cases (231,232). In normal conditions of cells, p53 gene remains in "standby" mode (233). Upon the intracellular or extracellular stimuli such as DNA damage, heat shock, hypoxia or oncogene overexpression, phosphorylation of p53 and further activation of p53 through increasing its expression are observed (232).

p53 can induce apoptosis through both intrinsic and extrinsic pathways by regulating apoptotic gene products. Intrinsic pathway consists modulating the expression of pro-apoptotic proteins (Bax, Bad, Bid, Puma, Noxa, p53AIP1 and Apaf-1) which controls mitochondrial membrane permeability and release of mitochondrial proteins. For example, in response to DNA damage in cell activated p53 transcriptionally activates pro-apoptotic Bad protein which further inhibits anti-apoptotic Bcl-2 protein by directly binding to it. Inactivation of Bcl-2 rescues pro-apoptotic protein Bax from prevention of Bcl-2 protein (234). Bax increases the permeability of mitochondrial membrane causing cytochrome C release and finally leads to p53 mediated and caspase dependent apoptosis (232,234,235). On the other hand, p53 also directly and transcriptionally activates pro-apoptotic Bax gene and down regulates Bcl-2. The relative ratio between Bcl-2/Bax proteins that determines whether the cell will undergo apoptosis or not, decreases and eventually promotes programmed cell death (235). p53 also regulates the expression of Apaf-1, which is a key constituent of apoptosome formation. Through extrinsic pathway, p53 promotes apoptosis by activating death receptors in the plasma membrane (232).

Besides being an inducer of apoptosis, p53 is also a key player in cell cycle regulation (230) and has an important role in G_1 and G_2 phases of cell cycle (234). Overexpression of p53 inhibits the cells entering to mitosis by causing cell cycle arrest in G_1 and G_2/M by controlling G_1 and G_2 checkpoints acting or inhibiting genes involved in cell cycle, apoptosis and DNA repair (231,232,235). Among several p53 target genes, the best known is p21 that is a primary mediator of p53-dependent cell cycle arrest in G_1 phase. P53 upregulates p21 expression which further inibits cyclin-dependent kinases and cyclin E/CDK2-mediated phosphorylation of retinoblastoma protein (pRb) (230–232).

Moreover, p21 has a dual activity in apoptosis that its downregulation or overexpression supresses the cellular proliferation, hence promotes apoptotic processes and leads to G_2 phase arrest (236).

Retinoblastoma (Rb) protein (pRb) is a tumor suppressor and negative regulator of cell growth that is neccesary for the continuation of cell cycle. Besides being a negative regulator, it is also an anti-apoptotic factor and clevead during apoptotic pathways. This fragmentation impairs the interaction of pRb with Mdm2 which acts as an apoptosis inhibitor together with pRb (231). Rb proteins function in G_1 phase for the phosphorylation of transcriptional genes. Decrease in the phosphorylation of retinoblastoma protein (phosho-Rb) is indicator of cell cycle arrest in G_1 phase (231).

Activity of p53 is regulated by several cellular proteins particularly by mouse double minute 2 (Mdm2) which is an oncogene product of various types of human cancer. Mdm2 inhibits transcriptional activator actions of p53 and targets p53 for rapid degredation, thus acts as a potent physiological antagonist. Besides, Mdm2 establishes a negative autoregulatory feedback loop where p53 activates its own inhibitor Mdm2 by being a direct target for transcriptional activation through p53 (230).

3. MATERIALS and METHODS

3.1. Materials

3.1.1. Plant Materials

The roots of *Glycyrrhiza glabra* L. (Figure 4) and *G. iconica* Hub.-Mor. (Figure 5) were collected in June 2015 from Medicinal Plant Experimental Garden, Faculty of Agriculture, Selçuk University, Konya, Turkey where the plant species were cultivated. Plant materials were authenticated by Prof. Dr. Yüksel Kan before any process. Voucher specimens for *G. glabra* L. (YEF 15005) and *G. iconica* Hub.-Mor. (YEF 15006) have been deposited at the Herbarium of the Department of Pharmacognosy, Faculty of Pharmacy, Yeditepe University, İstanbul, Turkey.

Figure 4. *Glycyrrhiza glabra* roots

Figure 5. *Glycyrrhiza iconica* roots

3.1.2. Chemicals and Solvents

Table 104. Chemicals and solvents

Chemicals and Solvents	Trademark
Acetic Acid	Merck
Acetonitrile	Merck
Chloroform	Merck
Cleaved caspase-3	Cell Signaling
Cleaved caspase-9	Santa Cruz
Cleaved PARP	Cell signalling
Cytochrome C	Santa Cruz
Dichloromethane	Merck
Dimethyl Sulfoxide (DMSO)	Sigma-Aldrich
Dulbecco's Modified Eagle's Medium (DMEM)	Gibco
EtOAc	Sigma-Aldrich
EtOH	Sigma-Aldrich
Fetal Bovine Serum (FBS)	Gibco
Formic Acid	Merck
Hoechst 33258	Sigma-Aldrich
Mdm2	Calbiochem
MeOH	Sigma-Aldrich
n-Butanol	Fluka
n-Hexane	Sigma-Aldrich
p21	Calbiochem
p53	Millipore
Penicillin	Gibco
Phospho-p53	Cell signalling
Phospho-Rb	Cell signalling
Polyamide (for column chromatography)	Fluka
Propidium iodide	Merck Millipore
Redisep MPLC columns (C_{18} and SiO_2)	Teledyne Isco
Reverse phase (C_{18}) column for HPLC	Agilent
Reverse phase (C_{18}) F_{254} Aluminium sheet	Merck
Sephadex LH-20	Sigma-Aldrich
Silica gel 60 F_{254} Aluminium sheet	Merck
Silica gel 60 (for column chromatography)	Merck
Sulforhodamine B	Sigma-Aldrich
Sulphuric Acid (98%)	Riedel de Haen
Trichloroacetic acid (TCA)	Merck
Vanillin	Fluka
β-actin	Sigma-Aldrich

3.1.3. Equipments and Instruments

Table 105. Equipments and instruments

Equipments and Instruments	Trademark
Airdryer	Arçelik
Balance	Ohaus Explorer
FACS Cell Analyzer	Novocyte Flow Cytometer
Filter	Sartorius Stedim
Filter paper	Munktell
Florescence Microscope	Nikon Eclipse 50i
Gel Electrophoresis system	Novex NuPAGE
Glass basic laboratory equipments (beaker, erlenmeyer, pasteur pipette, test tubes etc.)	Isolab
HPLC	Agilent 1100 Series
HPLC vials	HP Agilent
HR-ESI-MS	HP Agilent
IR spectrometer	Perkin-Elmer
Laminar Flow Cabinet	Flores Valles
Lyophilizator	Christ Alpha 2-4 LD
MilliQ H_2O device	Millipore
MPLC	Buchi
NMR device (^{1}H: 400 MHz, ^{13}C: 100 MHz)	Varian Mercury
Oven	Binder
Refrigerator	Arçelik
Rotatory evaporator	Buchi, Heidolph
TLC chamber	Camag
Ultrasonic bath	Sonorex
UV lamb	Camag
UV Spectrophotometer	HP Agilent
Vortex	Heidolph
xCELLigence System	Roche Applied Sciences

3.2. Methods

3.2.1. Phytochemical Studies

3.2.1.1. Thin Layer Chromatography (TLC)

SiO_2 and C_{18} coated aluminium plates were used in TLC analyses during chromatographic studies. SiO_2-TLC was used to gain a preliminary estimation about secondary metabolite profiles of the extracts and the main fractions as well as to choose the most proper mobile phases for preperative studies.

Stationary Phases:

Normal Phase: Silica gel 60 F_{254} aluminium plates 9.5–11.5 μm (Merck)
Reverse Phase: C_{18} F_{254} aluminium plates 9.5–11.5 μm (Merck)

Developing Solvents:

Mobile phases contained different ratios of solvents (Table 106). In some cases one drop of acetic acid or formic acid were added into mobile phase mixture to prevent tailing and to obtain better resolution of spots.

Table 106. Mobile phases used in TLC

Mobile Phases	Ratio
$CHCl_3$:MeOH:H_2O or CH_2Cl_2:MeOH:H_2O	90:10:1, 80:20:2, 70:30:3, 61:32:7
CH_2Cl_2:MeOH	90:10, 85:15, 80:20
EtOAc:MeOH:HCOOH:gCH_3COOH:H_2O	100:25:10:10:11
EtOAc:MeOH:H_2O	100:16:13, 100:10:5
n-hexane:EtOAc	4:1, 7:3, 3:2, 2:1, 1:1, 1:2, 3:7
MeCN:H_2O	1:1, 7:3
MeOH:H_2O	1:2, 1:1, 7:3

Developing Distance: 7-10 cm

Derivatization: 1% Vanillin/H_2SO_4 (105°C)

Visualization: UV light at short and long wavelengths (254 and 366 nm)

3.2.1.2. Column Chromatography

3.2.1.2.A. Polyamide Column Chromatography

Polyamide column chromatography was used for the main fractionation of EtOAc and *n*-BuOH subextracts of *G. glabra* and *G. iconica* to separate group of different compounds such as phenolics and terpenics from each other. The adequate amount of polyamide material was weighed, dispersed with distilled water and kept at room temperature over night for the swelling of polyamide. The glass column with cotton in the bottom was filled with polyamide and washed with certain amount of water to get rid of monomeric impurities. After equilibration of column with initial mobile phase (distilled water), sample was applied on the top of column. Elution was started with H_2O, and continued by increasing the MeOH proportion in H_2O in a stepwise manner and finally with 100% MeOH.

3.2.1.2.B. Sephadex LH-20 Column Chromatography (Gel Filtration)

Gel filtration chromatography is a technique that provides separation of molecules with regard to their different sizes. Sephadex LH-20 which is a gel filtration material, was preferred in the preliminary fractionation of $CHCl_3$ subextract of both plants as well as separation of different groups and mostly in purification of compounds. Proper amount of Sephadex LH-20 according to the quantity of sample was weighed, suspended with MeOH and left for one day before separation procedure in order to provide swelling. After loading and settling suspended Sephadex LH-20 mixture into glass column, the column was equilibrated with the starting mobile phase and further the sample which was dissolved in the starting mobile phase was applied to the top of column. Mostly, isocratic elution was carried out in gel filtration separations with MeOH or CH_2Cl_2:MeOH (1:1) mobile phases, however stepwise gradient elutions ($CHCl_3/CH_2Cl_2$:MeOH, 1:1 to 0:1) were also performed in the main fractionation of $CHCl_3$ subextracts.

3.2.1.2.C. Silica Gel Column Chromatography

Silica gel column chromatography was performed in order to separate the fractions and purify the compounds with different polarities. The appropriate amount of silica gel (SiO_2) was dispersed in starting solvent system and poured to the glass column with cotton in the bottom. Before the application of sample, column was waited to be settled. When the solvent system was aligned with the silica gel surface, the sample was loaded which was previously dissolved in starting solvent system. Stepwise gradient elution was conducted with increasing polarities of solvent systems with different proportions of mixtures during separation process. The appropriate solvent selection throughout elution was done with regard to TLC chromatograms.

Table 107. Mobile phases used in silica gel column chromatography

Mobile Phases	Ratio
$CHCl_3$:MeOH or CH_2Cl_2:MeOH	100:0, 97.5:2.5, 95:5, 93:7, 90:10, 85:15, 80:20, 75:25, 70:30, 60:40, 50:50
CH_2Cl_2:MeOH:H_2O	98:2:0, 97:3:0, 95:5:0, 93:7:0, 90:10:0, 90:10:1, 87:13:1, 85:15:1, 80:20:2, 75:25:2, 70:30:3, 61:32:7
n-hexane:EtOAc	100:0, 95:5, 90:10, 85:15, 80:20, 75:25, 70:30, 65:35, 60:40, 50:50, 55:45, 40:60, 30:70, 25:75, 20:80, 0:100

3.2.1.2.D. Medium Pressure Liquid Chromatography (MPLC)

MPLC was applied for fractionation and purification processes by using both normal (SiO_2) and reverse phase (LiChroprep C_{18}) pre-packed plastic flash columns in various sizes. Gradient elution system was used during separations. In MPLC studies, conditioning was performed with the solvent system in which the elution was started and the sample was dissolved before injection. Most commonly, reverse phase MPLC elutions were initiated with H_2O and went on with stepwise increasing ratios of MeOH or MeCN in H_2O and finally terminated with MeOH or MeCN. In normal phase MPLC studies, elutions were started with CH_2Cl_2 or *n*-hexane and continued with different proportions of CH_2Cl_2:MeOH or *n*-hexane: EtOAc in a stepwise manner. Generally, *n*-hexane:EtOAc and CH_2Cl_2:MeOH solvent systems were used as mobile phases in the separation of nonpolar fractions.

3.2.1.2.E. Semi-preperative High Performance Liquid Chromatography (Semi-prep HPLC)

Semi-preperative HPLC was conducted in order to purify a compound from the subfractions of the chloroform subextract of *G. glabra*. HPLC on Zorbax Eclipse XDB-C_{18} column (9.4×250 mm) was used as stationary phase which were eluted with H_2O:MeCN mixture (10–50%, MeCN).

3.2.1.3. Extraction and Partition

3.2.1.3.A. Extraction and Partition of *G. glabra*

The air-dried and powdered *G. glabra* (370 g) roots were macerated for one week at room temperature with 2.5 L of MeOH and further extracted at 45°C for 4 hours. After filtering, the same extraction procedure for the plant pulp was repeated with the same amount of solvent under the same conditions. The pooled extracts were concentrated to afford crude extract of *G. glabra* by using rotary evaporator under reduced pressure at 45 °C. Then, the crude MeOH extract was dispersed in 200 mL of H_2O and partitioned against $CHCl_3$ (3 x 200 mL), EtOAc (3 x 200 mL) and H_2O saturated *n*-BuOH (3 x 200 mL), respectively. The $CHCl_3$, EtOAc and *n*-BuOH phases were evaporated to dryness, while H_2O phase was freeze-dried to yield subextracts.

3.2.1.3.B. Extraction and Partition of *G. iconica*

The air-dried roots of *G. iconica* (210 g) were powdered and left for maceration with 2.3 L of MeOH at room temperature for five days. Then, the extraction was done twice at 45 ºC for 4 hours. The combined extracts were concentrated under reduced pressure to obtain crude MeOH extract which was dispersed in 150 mL of H_2O and partitioned three times with equal volumes of (each 150 mL x 3) $CHCl_3$, EtOAc and *n*-BuOH, respectively. The $CHCl_3$, EtOAc and *n*-BuOH phases were evaporated to dryness, while H_2O phase was lyophilized in order to yield subextracts.

3.2.1.4. Main Fractionation and Isolation

3.2.1.4.A. Main Fractionation and Isolation Studies on *G. glabra*

CHCl$_3$ subextract (3.92 g) of *G. glabra* was subjected to Sephadex LH-20 (90 g) column chromatography eluting with CH$_2$Cl$_2$:MeOH (1:1, 400 mL) and MeOH (200 mL), respectively to yield three main fractions (frs. A-C). EtOAc subextract (5.4 g) was loaded onto polyamide (40 g) column eluted with H$_2$O and stepwise gradient of MeOH in H$_2$O (25-100% in steps of 25%, each 100 mL) to obtain frs.1-4. The isolation schemes of *G. glabra* are given in Figures 6 and 7.

3.2.1.4.B. Main Fractionation and Isolation Studies on *G. iconica*

G. iconica CHCl$_3$ subextract (4.2 g) was loaded onto Sephadex LH-20 (100 g) column chromatography eluted with CHCl$_3$:MeOH (1:1, 400 mL) and MeOH (350 mL), respectively to yield three main fractions (frs. A-C). EtOAc subextract (9.7 g) was fractionated over poliamide column (75 g) eluting with H$_2$O and stepwise gradient of MeOH in H$_2$O (25-100% in steps of 25%, each 150 mL) to afford four main fractions (frs.1-4). In order to fractionate *n*-BuOH subextract, 7.8 g of this extract was submitted to polyamide (65 g) column chromatography eluted with H$_2$O and then stepwise gradient of MeOH in H$_2$O (25-100% in steps of 25%, each 150 mL) to obtain four main frs. D-G. Isolation and purification studies conducted on *G. iconica* are illustrated in Figures 8-10.
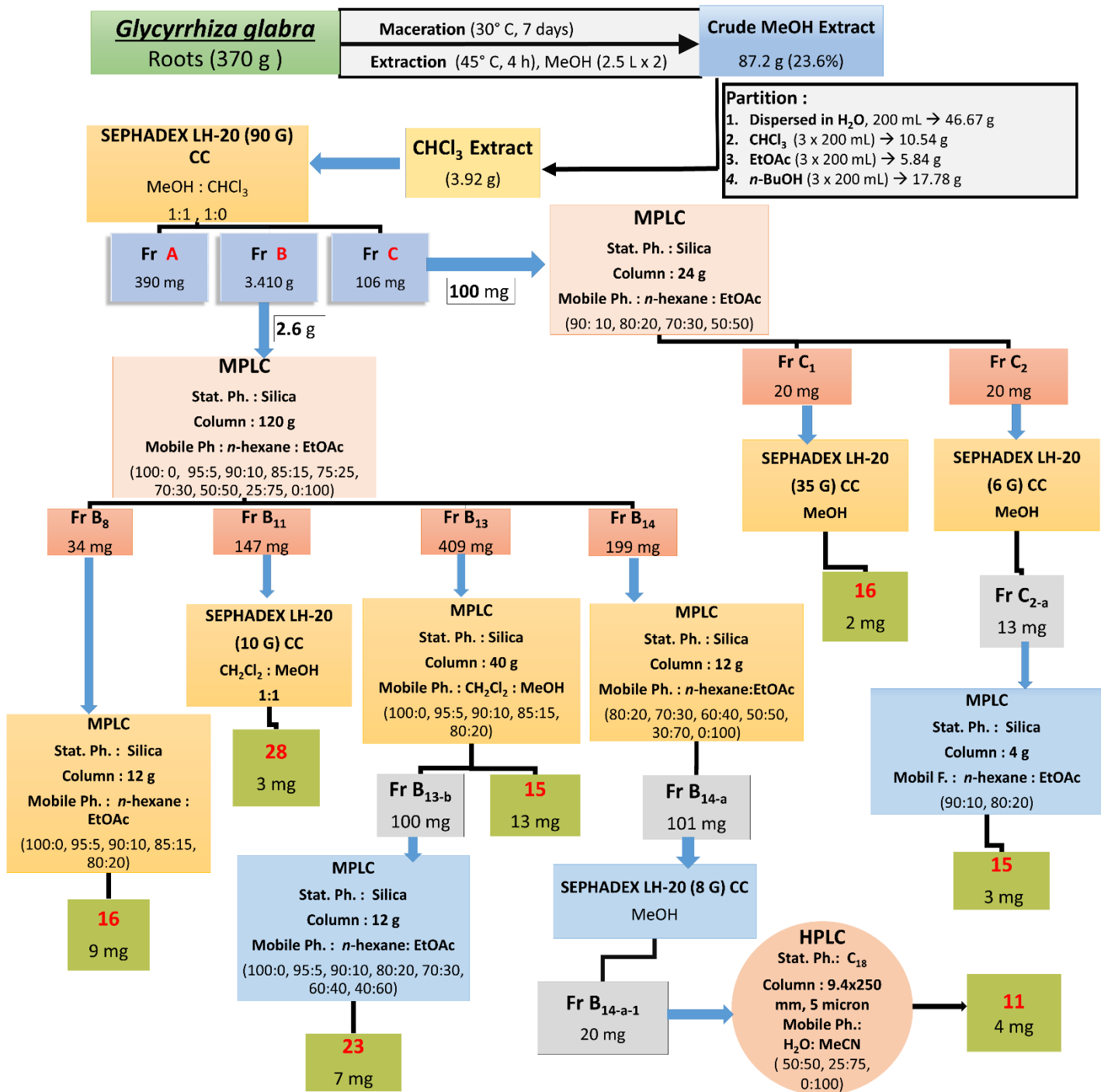
Figure 6. Isolation of compounds from *G. glabra*
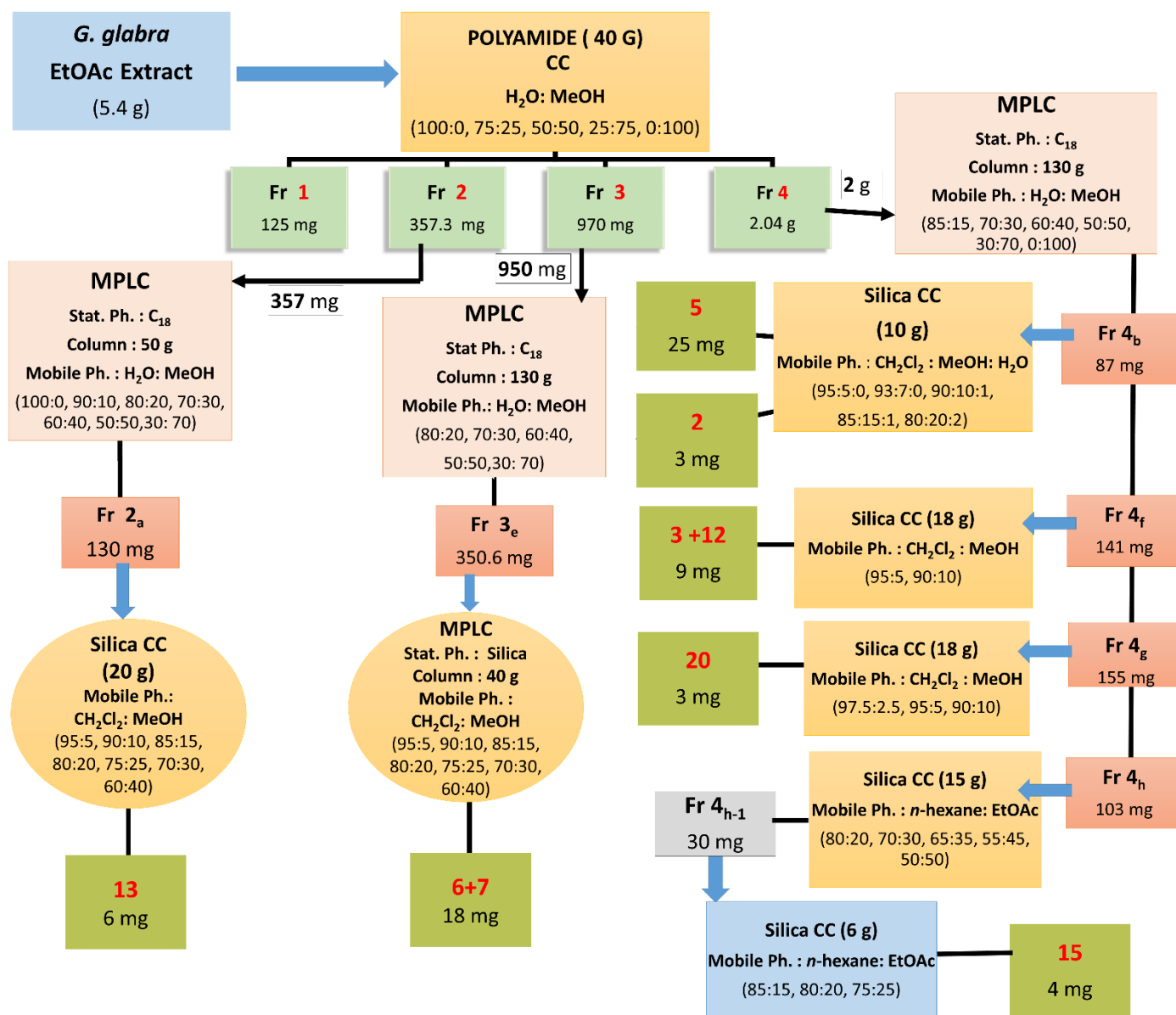
Figure 7. Isolation of compounds from *G. glabra*
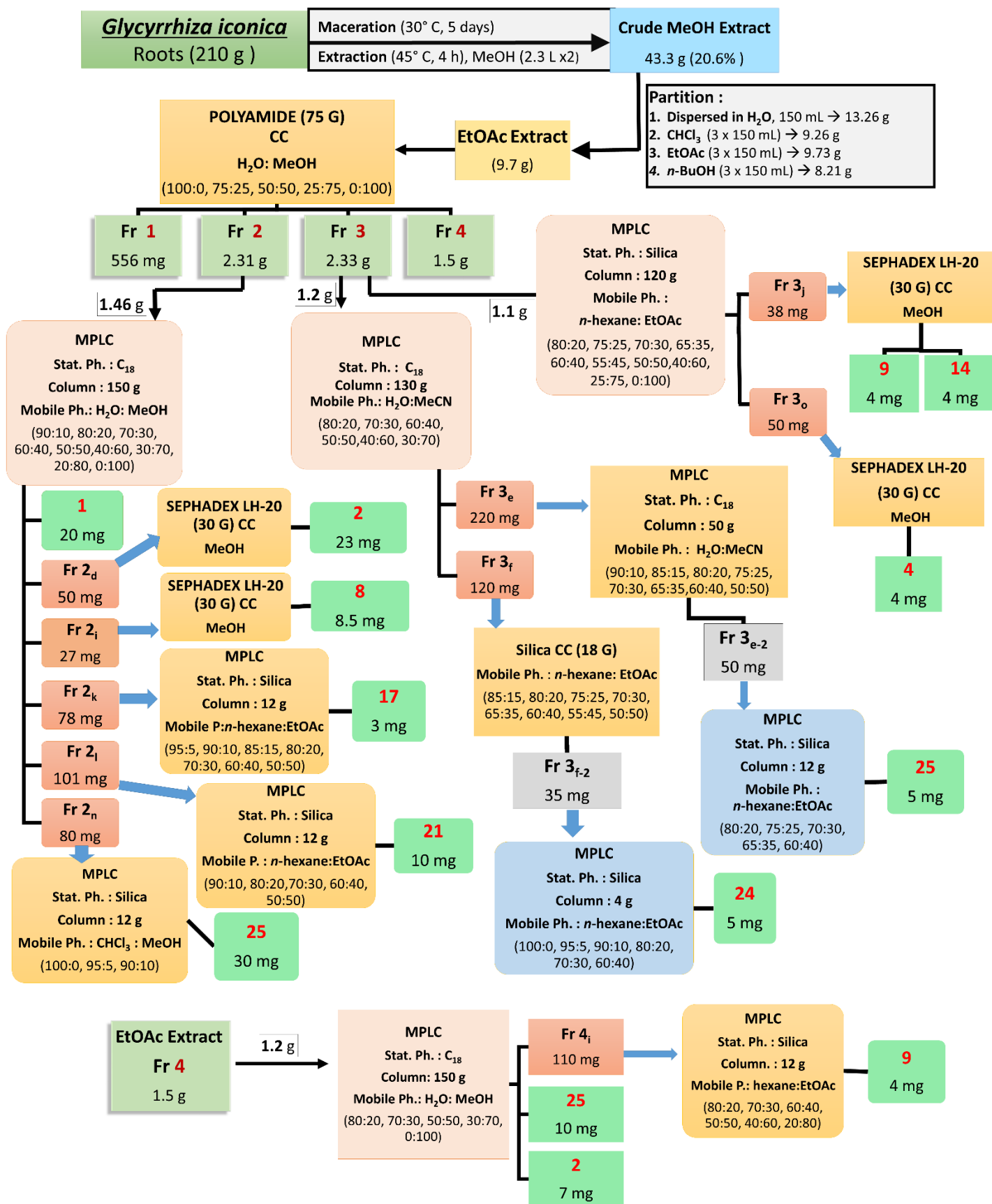
Figure 8. Isolation of compounds from *G. iconica*
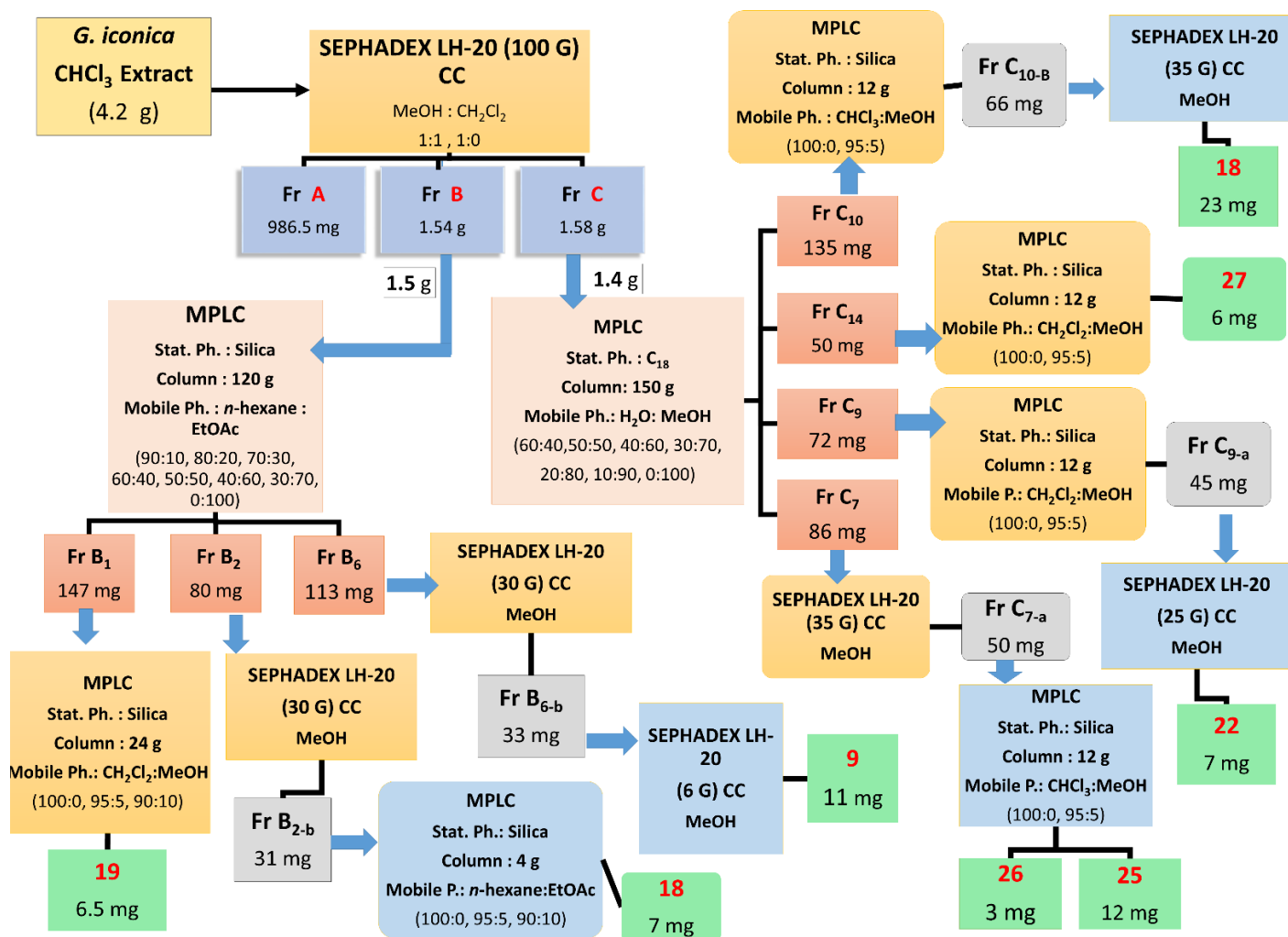
Figure 9. Isolation of compounds from *G. iconica*
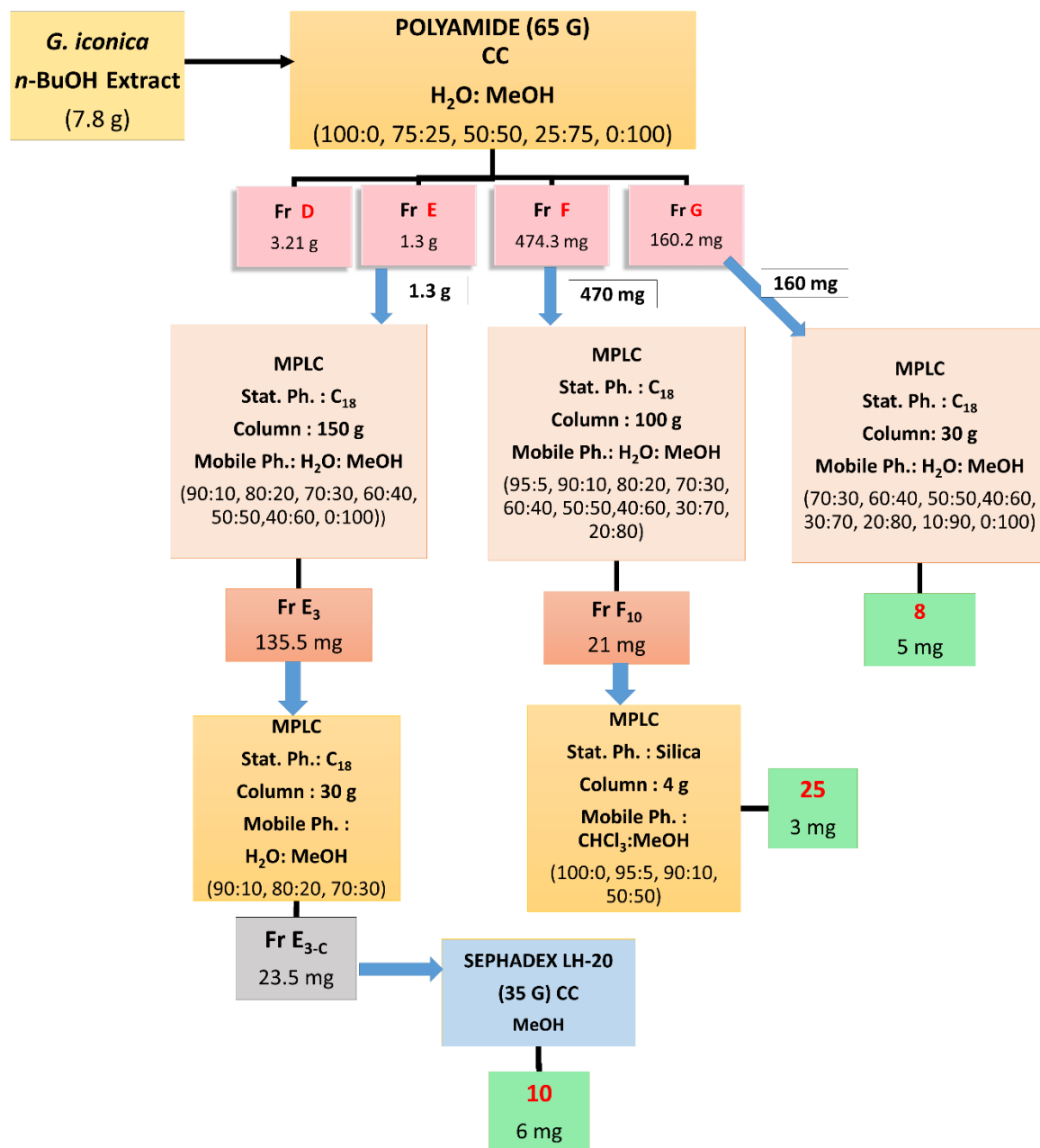
Figure 10. Isolation of compounds from *G. iconica*

3.2.1.5. Structure Elucidation Methods

As a result of sequential chromatographic techiques, the exact chemical structures of the purified compounds were elucidated based on spectroscopic methods including UV, IR, 1D (^{1}H and ^{13}C) and 2D (COSY, HSQC, HMBC, NOESY) NMR and MS/HR-ESI-MS.

3.2.2. *In vitro* Activity Studies

3.2.1. Cell Lines and Cell Culture

Human liver (Huh7), colon (HCT116) and breast (MCF7) cancer cell lines were grown in Dulbecco's Modified Eagle's Medium (DMEM) supplemented with 10% fetal bovine serum (FBS) and 1% penicillin and cell lines were maintained in an incubator at 37°C under 5% CO_2 (237).

3.2.2. Sulforhodamine B Assay

The sulforhodamine B (SRB) assay was performed to evaluate the cytotoxic effects of crude extract, subextracts, main fractions as well as purified compounds. SRB assay was developed by US National Cancer Institute (NCI) as a rapid, sensitive and inexpensive method, based on the measurement of cellular protein content and used for cell density determination (238). Human cancer cell lines (MCF7/Huh7: 2000 cell/well, HCT116: 3000 cell/well in 150 µl/well DMEM) were plated in 96-well plates and incubated for 24 hours at 37°C followed by treatment with different concentrations of extracts, main fractions (1.875, 3.75, 7.5, 15 and 30 µg/mL or 0.4, 1.6, 6.25, 25 and 100 µg/mL) or compounds (2.5, 5, 10, 20 and 40 µM) dissolved in DMSO by serial dilution method. If IC_{50} value was found to be beyond 1.875 µg/mL or 2.5 µM, the assays were repeated with lower concentrations. 72 hours post-treatment at 37 under 5% CO_2, the cells were washed with 1xPBS (phosphate buffered saline, $CaCl_2$-, $MgCl_2$-free) and fixed with 100 µL 10% (v/v) ice-cold trichloroacetic acid (TCA) and further incubated in dark at 4°C for one hour. Then TCA was washed away with ddH_2O for two times and plates were air-dried. Finally, staining process was perfomed by applying 100 µL of 0.4% (m/v) of SRB in 1% acetic acid solution into each well for 30 minutes. In order to remove excess unbound SRB, cells were washed repeatedly with 1% acetic acid solution for four times and left for air drying. The bound SRB was further solubilized using 100 µL 10 mM Tris-base before absorbance measurement. The absorbance was read at 515 nm. The experiments were done in triplicates and IC_{50} values were calculated from the cell growth inhibition curves obtained from the treatments with different concentrations of extracts, fractions (µg/mL) or isolated compounds (µM).

3.2.3. Real Time Bioactivity Assay (RT-CES xCELLigence)

The real time growth inhibitory effect of the most active compounds according to SRB assay were monitored in Huh7 cells by the xCELLigence System (Roche Applied Sciences) which has a microelectronic biosensor technology to do dynamic, real-time, label-free and non-invasive analysis of cellular events, including cell number change, cell adhesion, cell viability, cell morphology, and cell motility (239). Huh7 cancer cell lines (2000 cells/well) were seeded into 96-well E-plates. The proliferation of cells were recorded every 30 minutes for 24 hours after seeding, then treatments with the compounds with their IC_{50} concentrations found in SRB assay were performed in log growth phase of the cells. The cell index (CI) values were continuously monitored and recorded for 72 hours (every 10 minutes for the first 24 hours and then every 30 minutes for the remaining 48 hours). The cell growth ratios were calculated by CI_{drug}/CI_{DMSO}.

3.2.4. Apoptotic Cell Death Assay (Hoechst Staining)

The presence of apoptotic cells were identified by Hoechst staining assay. Huh7 cells were seeded onto coverslips in 6-well plates. After 24 hours of culture, cells were treated with the compounds with their IC_{50} concentrations at 48th hour in RT-CES assay. After 48 hours, coverslips were washed twice with PBS, fixed with 1 mL of ice-cold 100% methanol for 10 minutes. Further, incubation with Hoechst 33258 stain for 5 minutes in darkness was conducted. Cells were analyzed and images of them were taken by using the fluorescence microscope (Nikon Eclipse 50i).

3.2.5. Cell Cycle Assay (Fluorescence-Activated Cell Sorting (FACS))

The effects of the cytotoxic isolates on cell cycle progression were investigated by Fluorescence-activated cell sorting (FACS) assay by using Propidium Iodide (PI) dye which binds to DNA in the presence of a cytotoxic agent. With regard to this method the cell cycle phases were determined by different type of DNA of cells after staining with PI (240). Huh7 cells were inoculated into 100 mm culture dishes and maintained for 24 hours. After 24 hours, cells were treated with the compounds with their IC_{50} concentrations based on the RT-CES results at 48th hour except for compound **2**. Since IC_{50} value of compound **2** distrupted the cell cycle distribution of Huh7 cells, IC_{25} concentration of **2** at 48th hour was used. Following 48 hours of incubation, cells were

141

fixed with ice-cold 70% ethanol for 3 hours at -20 ºC. Cell cycle analysis was performed by staining with PI and using Fluorescence-activated cell sorting (FACS).

3.2.6. Cell Protein Assay (Western Blot)

Immunoblotting (western blotting) is a technique that has been used to for the identification of specific antigens recognized by polyclonal or monoclonal antibodies. It gives information about the identity of the specific proteins, the change of their amounts and phosphorylation character of them (241). Huh7 cancer cell lines were seeded into 150 mm culture dishes and incubated for 24 hours, followed by treatment with the compounds (IC_{50} concentrations based on the RT-CES results at 48th hour) or DMSO control for 48 hours. Novex® NuPAGE® Bis-Tris Electrophoresis system was utilized according to the manufacturer's protocol for the western blotting analysis. 20-50 µg of protein was used for each well for gel electrophoresis (NuPAGE). Then the proteins were transferred to nitrocellulose membrane via XCell IITM Blot Module. Antibodies including p53 (#05-224, Millipore), phospho-p53 (Ser15) (#9284, Cell signalling), phospho-Rb (Ser807/811) (#9308S Cell Signaling), cytochrome C (sc-7159, Santa Cruz), Mdm2 (OP46, Calbiochem), p21 (OP64, Calbiochem), cleaved caspase-9 (sc-22182, Santa Cruz), cleaved caspase-3 (#9661, Cell Signaling) and cleaved PARP (#9532, Cell Signaling) were used in 1:200 to 1:500 5% BSA-TBS-T. DMSO was used as a negative control and β-actin (#A5441, Sigma) antibody was used for equal loading (237).

4. RESULTS

The aim of this study was to isolate cytotoxic secondary metabolites from *G. glabra* and *G. iconica* through bioactivity guided fractionation technique. For this purpose, first crude MeOH extracts and then their subextracts were obtained from *G. glabra* and *G. iconica* roots which were evaluated for their cytotoxic activities by using sulforhodamine B assay against Huh7, MCF7 and HCT116 cancer cell lines. The main fractions obtained from the active subextracts were also assessed for their cytotoxic activities in the same cancer cell panel. Based on the SRB assay results, cytotoxically active main fractions were selected for further phytochemical studies in order to isolate the compounds that were responsible for the cytotoxic activity. The *in vitro* cytotoxic effects of the isolates were also evaluated and underlying mechamisms of most active ones were elucidated.

4.1. Extraction

4.1.1. Extraction of *G. glabra*

The dried and powdered roots of *G. glabra* (370 g) were extracted with MeOH to yield crude MeOH extract (87.2 g, 23.6%). From crude extract, $CHCl_3$ (10.5 g), EtOAc (5.8 g), *n*-BuOH (17.8 g) and rH_2O (46.6 g) subextracts were yielded as described previously.

4.1.2. Extraction of *G. iconica*

G. iconica (210 g) roots were macerated and extracted with MeOH in order to yield crude MeOH extract (43.3 g, 20.6%). The $CHCl_3$ (9.3 g), EtOAc (9.7 g), *n*-BuOH (8.2 g) and rH_2O (13.3 g) subextracts were obtained from crude MeOH extract as described previously.

4.2. *In vitro* Cytotoxic Activity Results of Extracts

The *in vitro* cytotoxic acitivities of the crude extracts and subextracts obtained from *G. glabra* and *G. iconica* roots were evaluated against human hepatocellular (Huh7), breast (MCF7) and colon (HCT116) cancer cell lines by Sulforhodamine B (SRB) assay.

4.2.1. *In vitro* Cytotoxic Activity Results of *G. glabra* Extracts

The SRB assay results (Table 108) indicated that crude MeOH extract of *G. glabra* showed cytotoxic activity markedly with IC_{50} values of 18.9, 28.8 and 33.6 µg/mL against hepatocellular (Huh7), breast (MCF7) and colorectal (HCT116) cancer cell lines, respectively. Moreover, $CHCl_3$ and EtOAc subextracts obtained from the crude MeOH extract of *G. glabra* roots exhibited considerable cytotoxic activity against Huh7, MCF7 and HCT116 cancer cell lines with IC_{50} values in the range of 5.6-29.3 µg/mL whereas *n*-BuOH and remaining H_2O subextracts were not cytotoxic (Table 108).

Table 108. *In vitro* cytotoxic activity results of the extracts obtained from *G. glabra*

	Huh7		MCF7		HCT116	
	IC_{50}(µg/mL)	R^2	IC_{50}(µg/mL)	R^2	IC_{50}(µg/mL)	R^2
MeOH	18.9	0.6	28.8	0.6	33.6	0.7
$CHCl_3$	13.3	0.9	29.3	0.6	8.2	0.9
EtOAc	5.6	0.9	9.1	0.9	7.4	0.9
***n*-BuOH**	NI		NI		NI	
rH_2O	NI		NI		NI	

NI: No Inhibition

4.2.2. *In vitro* Cytotoxic Activity Results of *G. iconica* Extracts

As illustrated in Table 109, the crude MeOH extract of *G. iconica* roots showed cytotoxic activity against Huh7, MCF7 and HCT116 cancer cell lines (IC_{50} = 12.7, 7.4 and 4.3 µg/mL, respectively). $CHCl_3$, EtOAc and *n*-BuOH subextracts displayed strong cytotoxic effects against three tested cell lines with IC_{50} values in the range of < 0.4 – 7.7 µg/mL, while remaining H_2O subextract was found to be active only against MCF7 cancer cells.

Table 109. *In vitro* cytotoxic activity results of the extracts obtained from *G. iconica*

	Huh7		MCF7		HCT116	
	IC_{50}(µg/mL)	R^2	IC_{50}(µg/mL)	R^2	IC_{50} (µg/mL)	R^2
MeOH	12.7	0.9	7.4	0.9	4.3	1
CHCl₃	7.0	0.9	0.9	0.8	2.4	0.8
EtOAc	6.4	0.9	1.1	0.9	< 0.4	0.9
***n*-BuOH**	7.7	0.9	0.6	0.9	2.1	0.9
rH₂O	NI	0.8	2.6	0.8	NI	0.8

NI: No Inhibition

4.3. Main Fractionation of Active Subextracts

The cytotoxically active subextracts according to Sulforhodamine B assay results obtained from *G. glabra* and *G. iconica* were subjected to chromatographic techniques including Polyamide and Sephadex LH-20 column chromatography for the main fractionation. While CHCl₃ subextracts were loaded to Sephadex LH-20 column, EtOAc and *n*-BuOH subextracts were separated by Polyamide column chromatography.

4.3.1. Main Fractionation of *G. glabra* Subextracts

CHCl₃ and EtOAc subextracts of *G. glabra* roots were fractionated by Sephadex LH-20 and Polyamide column chromatography, respectively as described before. Amounts of the obtained main fractions from both subextracts are given in Table 110.

Table 110. The amount of the main fractions obtained from *G. glabra* subextracts

Subextract	Fraction	Amount
	Fr. A	0.39 g
CHCl₃ subextract	Fr. B	3.41 g
	Fr. C	0.106 g
	Fr. 1	0.125 g
	Fr. 2	0.357 g
EtOAc subextract	Fr. 3	0.97 g
	Fr. 4	2.04 g

4.3.2. Main Fractionation of *G. iconica* Subextracts

The CHCl₃, EtOAc and *n*-BuOH subextracts were separated into fractions by Sephadex LH-20 and Polyamide CCs. Amounts of the main fractions are given in Table 111.

Table 111. The amount of the main fractions obtained from *G. iconica* subextracts

Subextract	Fraction	Amount
CHCl₃ subextract	Fr. A	0.986 g
	Fr. B	1.54 g
	Fr. C	1.58 g
EtOAc subextract	Fr. 1	0.556 g
	Fr. 2	2.31 g
	Fr. 3	2.33 g
	Fr. 4	1.5 g
_n_-BuOH subextract	Fr. D	3.21 g
	Fr. E	1.3 g
	Fr. F	0.474 g
	Fr. G	0.160 g

4.4. *In vitro* Cytotoxic Activity Results of Main Fractions

The main fractions obtained from the active subextracts of *G. glabra* ($CHCl_3$ and EtOAc) and *G. iconica* ($CHCl_3$, EtOAc and *n*-BuOH) were also tested against Huh7, MCF7 and HCT116 cancer cell lines in order to determine bioactive fractions.

4.4.1. Cytotoxic Activity Results of Main Fractions Obtained from *G. glabra*

Amongst the main fractions obtained from EtOAc and $CHCl_3$ subextracts, fraction 4 (IC_{50} = 1.3 - 4.9 µg/mL) of EtOAc subextract and fractions B (IC_{50} = 14 - 18.5 µg/mL) and C (IC_{50} = 8.9 - 14.9 µg/mL) of $CHCl_3$ subextract showed remarkable cytotoxic activity against Huh7, MCF7 and HCT116 cancer cell lines as shown in Table 112. Due to their similar secondary metabolite profiles with their following fractions (fr. B and fr. 2, respectively) according to TLC results, fr. A of $CHCl_3$ subextract and fr. 1 of EtOAc subextract were not tested.

Table 112. Cytotoxic activity results of the main fractions obtained from *G. glabra* against Huh7, MCF7 and HCT116 cancer cell lines

Fractions	Huh7		MCF7		HCT116	
	IC_{50} (µg/mL)	R^2	IC_{50} (µg/mL)	R^2	IC_{50} (µg/mL)	R^2
$CHCl_3$						
Fr. B	14	0.8	14.6	0.8	18.5	0.8
Fr. C	9.2	0.7	8.9	0.6	14.9	0.6
EtOAc						
Fr. 2	NI	-	NI	-	NI	-
Fr. 3	NI	-	NI	-	NI	-
Fr. 4	4.9	0.9	2.5	0.9	1.3	0.7

NI: No Inhibition

4.4.2. Cytotoxic Activity Results of Main Fractions Obtained from *G. iconica*

According the cytotoxic activity results by SRB assay, amongst the main fractions obtained from EtOAc (frs. 1-4), CHCl₃ (frs. A-C) and *n*-BuOH (frs. D-G) subextracts of *G. iconica*; main fractions 1-4 (IC$_{50}$ = < 0.4 - 12.8 µg/mL), A-C (IC$_{50}$ = < 0.4 - 11.7 µg/mL) and F-G (IC$_{50}$ = 5.9 - 20.3 µg/mL) were found to be cytotoxically active against all tested cell lines. On the other hand, fr. E from *n*-BuOH subextract showed cytotoxicity only against Huh7 and MCF7 cell lines (IC$_{50}$ = 16.4 and 23.7 µg/mL, respectively), while fr. D was not cytotoxic (Table 113).

Table 113. Cytotoxic activity results of the main fractions obtained from *G. iconica* against Huh7, MCF7 and HCT116 cancer cell lines

Fractions	Huh7		MCF7		HCT116	
	IC$_{50}$ (µg/mL)	R^2	IC$_{50}$ (µg/mL)	R^2	IC$_{50}$ (µg/mL)	R^2
CHCl₃						
Fr. A	10.1	0.9	< 0.4	0.9	11.7	0.9
Fr. B	4.4	0.9	0.4	0.9	4.1	0.8
Fr. C	5.3	0.9	< 0.4	0.9	6.0	0.9
EtOAc						
Fr. 1	4.3	0.8	6.7	0.7	4.8	0.9
Fr. 2	4.0	0.9	< 0.4	0.8	3.0	0.9
Fr. 3	12.8	0.9	10.4	0.9	5.8	0.7
Fr. 4	11.6	0.9	9.0	0.9	3.0	0.7
***n*-BuOH**						
Fr. D	NI	-	NI	-	NI	-
Fr. E	16.4	0.7	23.7	0.7	NI	-
Fr. F	8.5	0.9	13.1	0.9	20.3	0.8
Fr. G	7.9	0.8	12.1	0.8	5.9	0.7

NI: No Inhibition

4.5. Phytochemical Study Results

Sequential chromatographic techniques were conducted on the bioactive main fractions of *G. glabra* (frs. B-C and fr. 4) and *G. iconica* (frs. 2-4, frs. E-G and frs. B-C) to isolate compounds that were responsible for the cytotoxicity (Figures 6-10). Moreover, some major compounds of the inactive fractions of *G. glabra* (frs. 2 and 3) were also isolated in order to have an idea about the main constituents of the Turkish licorice species. As a result, thirteen compounds were obtained from *G. glabra*, while sixteen compounds were afforded from *G. iconica*. Compounds **3**+**12** and **6**+**7** were obtained as mixtures. The isolates (**1**-**28**) were categorized into 11 subclasses inluding chalcones (**1**-**7**), flavonols (**8** and **9**), flavone (**10**), flavanones (**11**-**13**), isoflavone (**14**), isoflavans (**15**-**19**), isoflavenes (**20**-**22**), 2-arylbenzofurans (**23** and **24**), 3-arylcoumarin (**25**), pterocarpans (**26** and **27**) and triterpene (**28**). The isolated compounds are presented in Table 114.

Table 114. Isolated secondary metabolites from *G. glabra* and *G. iconica*

Compound No	Compound Name	Species
1	Iconichalcone	*G. iconica*
2	Tetrahydroxymethoxychalcone	*G. glabra & G. iconica*
3	Isoliquiritigenin	*G. glabra*
4	2'-*O*-Methylisoliquiritigenin	*G. iconica*
5	Isoliquiritigenin 4'-*O*-β-glucopyranoside	*G. glabra*
6	Licuroside	*G. glabra*
7	Neolicuroside	*G. glabra*
8	3-*O*-Methylkaempferol	*G. iconica*
9	Topazolin	*G. iconica*
10	Violanthin	*G. iconica*
11	Abyssinone II	*G. glabra*
12	(2*R*,3*R*)-3,4',7-trihydroxy-3'-prenylflavanone	*G. glabra*
13	Liquiritin apioside	*G. glabra*
14	Glycyrrhisoflavone	*G. iconica*
15	Glabridin	*G. glabra*
16	4'-*O*-Methylglabridin	*G. glabra*
17	Glyasperin C	*G. iconica*
18	Licoricidin	*G. iconica*
19	Licorisoflavan A	*G. iconica*
20	Glabrene	*G. glabra*
21	Dehydroglyasperin C	*G. iconica*
22	Iconisoflaven	*G. iconica*
23	Kanzonol U	*G. glabra*
24	Licocoumarone	*G. iconica*
25	Glycycoumarin	*G. iconica*
26	Edudiol	*G. iconica*
27	1-Methoxyficifolinol	*G. iconica*
28	β-amyrin	*G. glabra*

4.5.1. Structure Elucidation of Isolated Compounds

4.5.1.1. Chalcone Derivative Compounds
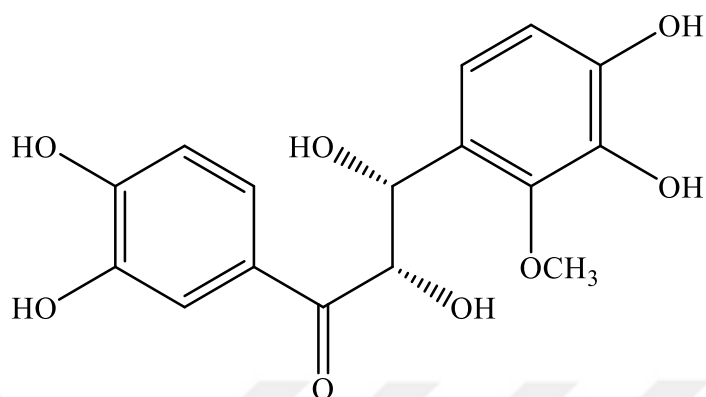
ICONICHALCONE (1): $C_{16}H_{16}O_8$ (MW: 336.296)

UV λ_{max} (MeOH) nm:	231, 283
IR υ_{max} (KBr) cm^{-1}:	3433 (OH), 1648 (C=O), 1597,1512, 1472 (aromatic ring)
HR-ESI-MS m/z :	359.0790 [M+Na]$^+$ (calcd for $C_{16}H_{16}O_8Na$, 359.0743), 319.0820 [(M+H) − H_2O]$^+$ (calcd for $C_{16}H_{15}O_7$, 319.0812), 341.0648 [(M+Na) − H_2O]$^+$ (calcd for $C_{16}H_{14}O_7Na$, 341.0632)
^{1}H NMR:	Table 115, Spectrum 1
^{13}C NMR:	Table 115, Spectrum 2
COSY:	Spectrum 3
HSQC:	Spectrum 4
HMBC:	Spectrum 5
NOESY:	Spectrum 6

ICONICHALCONE (1)

Compound **1** was obtained as yellowish amorphous powder from EtOAc subextract of *G. iconica*. The HR-ESI-MS of **1** exhibited $[M+Na]^+$ ion at *m/z* 359.0790 (calcd for $C_{16}H_{16}O_8Na$, 359.0743), $[(M+Na) -H_2O]^+$ ion at *m/z* 341.0648 (calcd for $C_{16}H_{14}O_7Na$, 341.0632) and $[(M+H) -H_2O]^+$ ion at *m/z* 319.0820 (calcd for $C_{16}H_{15}O_7$, 319.0812), supporting a molecular formula of $C_{16}H_{16}O_8$. The UV spectrum of **1** showed absorption maxima at 231 and 283 nm, while its IR spectrum displayed absorption bands at 3433 (hydroxyl groups), 1648 (ketone C=O), 1597, 1512 and 1472 (aromatic rings) cm^{-1}.

The ^1H NMR spectrum (Table 115, Spectrum 1) of **1** displayed three aromatic signals ascribable to an ABX system at δ_H 7.21 (d, *J* = 2.1 Hz), 7.05 (dd, *J* = 8.4, 2.1 Hz) and 6.57 (d, *J* = 8.4 Hz). Moreover, two aromatic proton signals as an AB system were detected at δ_H 6.93 (d, *J* = 8.5 Hz) and 6.61 (d, *J* = 8.5 Hz). In addition, signals for two oxymethines at δ_H 5.58 (d, *J* = 8.6 Hz) and 4.84 (d, *J* = 8.6 Hz) as well as one methoxy signal at δ_H 3.65 (s, 3H) were observed. The ^{13}C NMR spectrum (Table 115, Spectrum 2) contained sixteen resonances including one ketone (δ_C 199.8), two oxymethine (δ_C 82.5 and 59.6), one methoxy (δ_C 61.5) and twelve aromatic ring signals. Detailed analysis of COSY (Spectrum 3), HSQC (Spectrum 4) and HMBC (Spectrum 5) spectra, revealed that **1** was a dihydrochalcone derivative. Two oxymethine signals were corresponded to the hydroxylation of C-α and C-β positions. Long range heteronuclear correlations of C=O signal (δ_C 199.8) with H-2' (δ_H 7.21) and H-6' (δ_H 7.05) supported this foreseen structure. The location of methoxy unit was determined to be at C-2 by the cross-peaks between δ_C 148.1 (C-2) and methoxy at δ_H 3.65 in the HMBC experiment (Spectrum 5). The NOE correlations between H-α/H-β, H-α/H-2', H-α/H-6' and H-β/H-6 in the NOESY spectrum (Spectrum 6) suggested α configuration for both hydroxyl groups at C-α/β. On the basis of the above evidence, the structure of **1** was established to be 3,4,3',4'-tetrahydroxy-2-methoxy-α,β-dihydroxychalcone and named as **iconichalcone**.

Table 115. ^{1}H and ^{13}C NMR spectroscopic data of iconichalcone (**1**) (CD$_3$OD; ^{1}H: 400 MHz, ^{13}C: 100 MHz)^a

C/H atom	Multiplicity	δ_H (ppm), J (Hz)	δ_C (ppm)
α	CH	4.84 d (8.6)	59.6
β	CH	5.58 d (8.6)	82.5
C=O	C	-	199.8
1	C	-	125.7
2	C	-	148.1
3	C	-	139.4
4	C	-	147.8
5	CH	6.61 d (8.5)	112.5
6	CH	6.93 d (8.5)	118.9
1'	C	-	130.5
2'	CH	7.21 d (2.1)	116.4
3'	C	-	146.2
4'	C	-	152.7
5'	CH	6.57 d (8.4)	115.9
6'	CH	7.05 dd (8.4, 2.1)	124.3
2-OCH$_3$	CH$_3$	3.65 s	61.5

^{a} Resonances were assigned by the help of 2D NMR (COSY, HSQC, HMBC and NOESY).
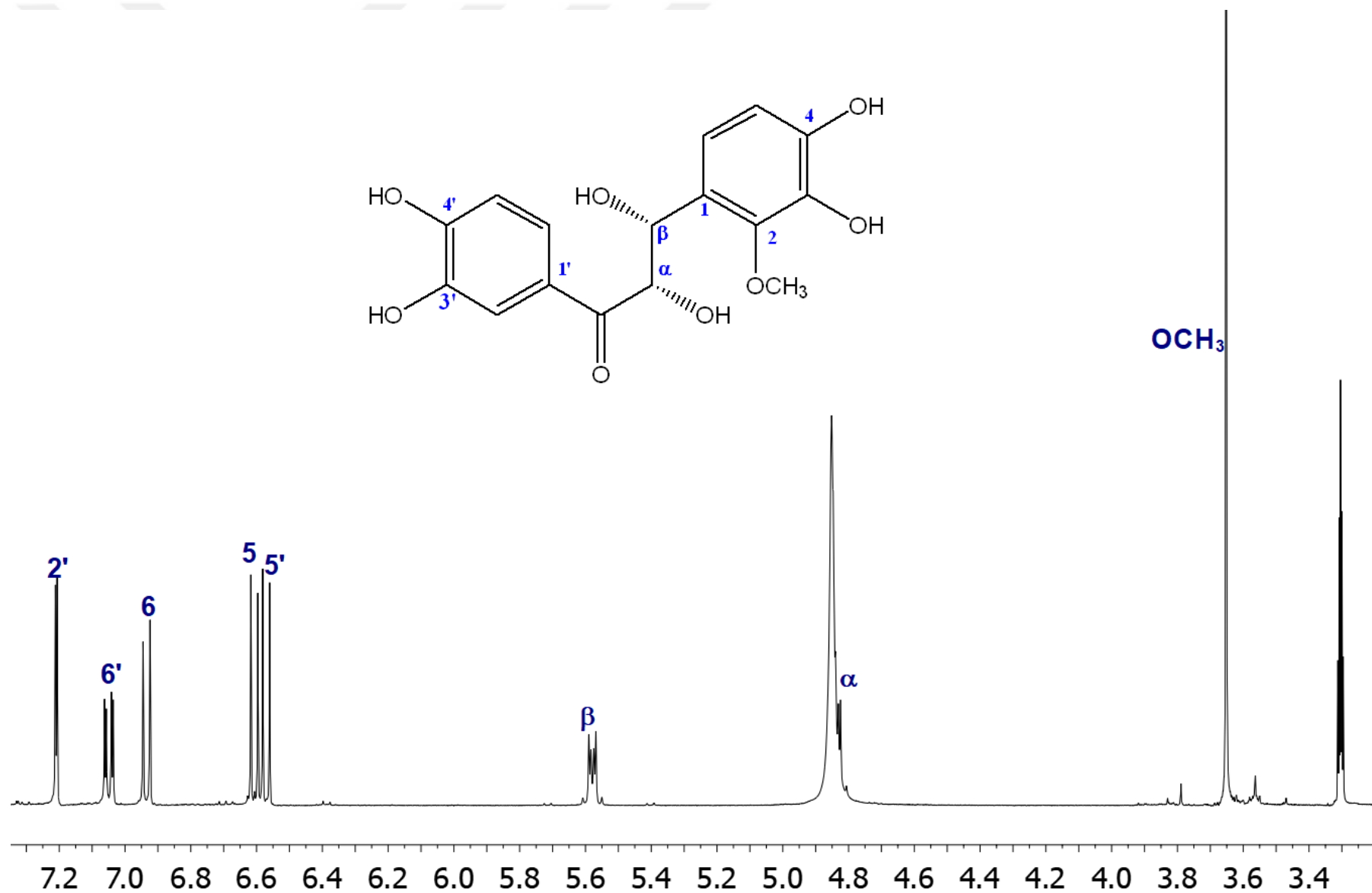
Spectrum 1. ^{1}H NMR Spectrum of Iconichalcone (**1**) (CD$_3$OD, 400 MHz)
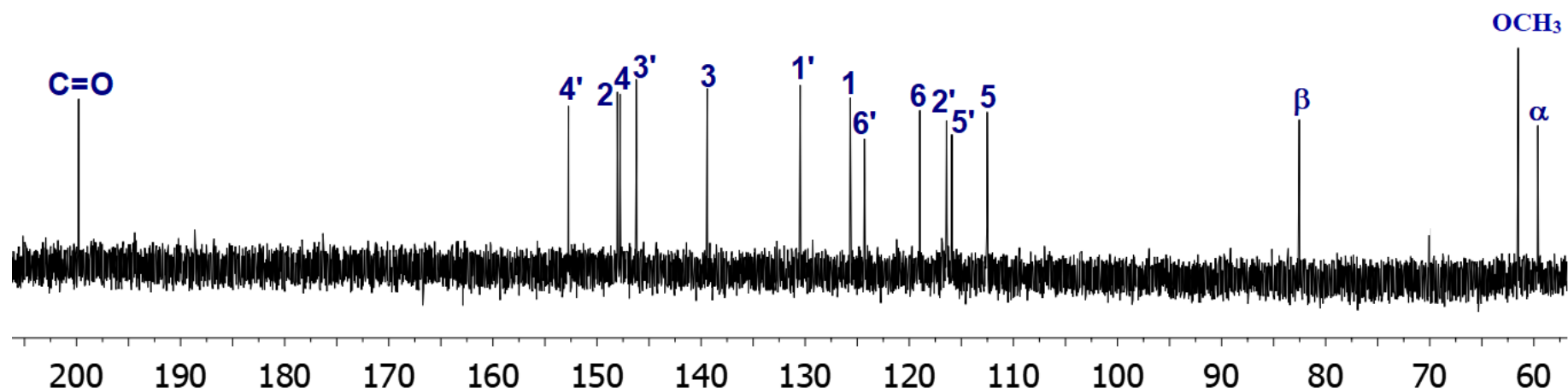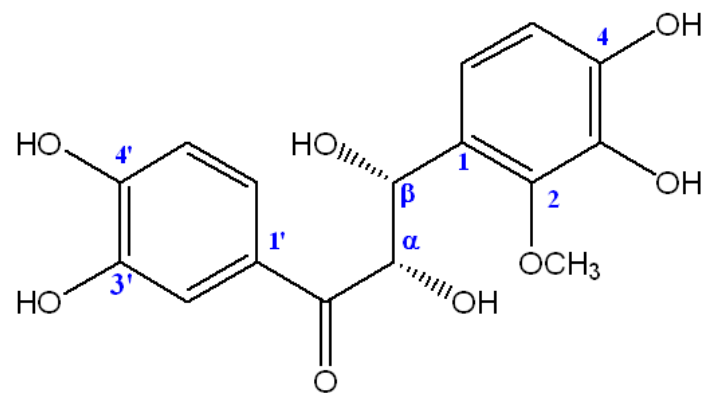
Spectrum 2. ^{13}C NMR Spectrum of Iconichalcone (**1**) (CD$_3$OD, 100 MHz)
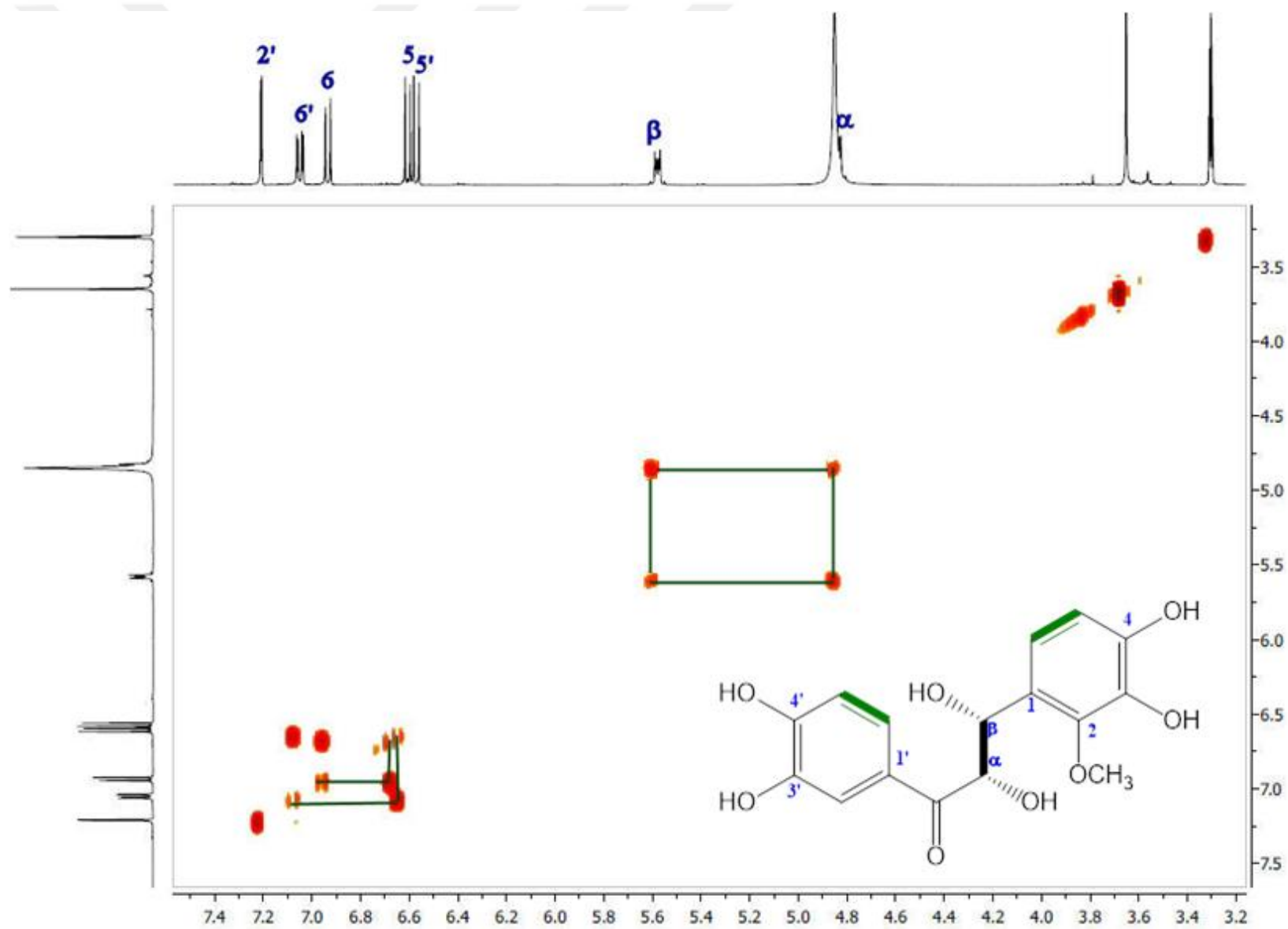
Spectrum 3. 2D-^{1}H,^{1}H-Homonuclear Correlation Spectrum (COSY) of Iconichalcone (**1**)

157
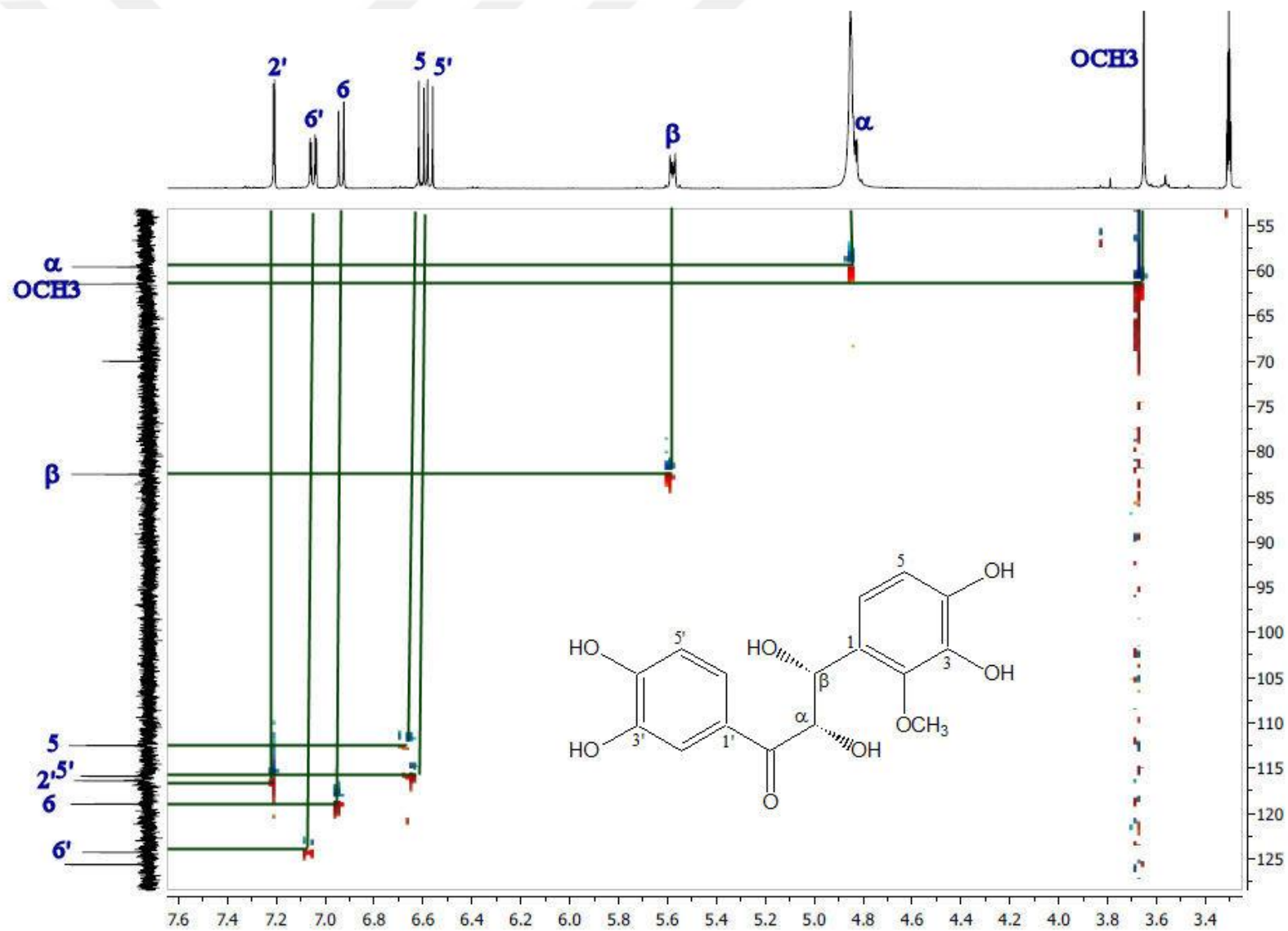
Spectrum 4. Heteronuclear 2D-^{1}H,^{13}C Correlation Spectrum (short range) of Iconichalcone (**1**) (HSQC)
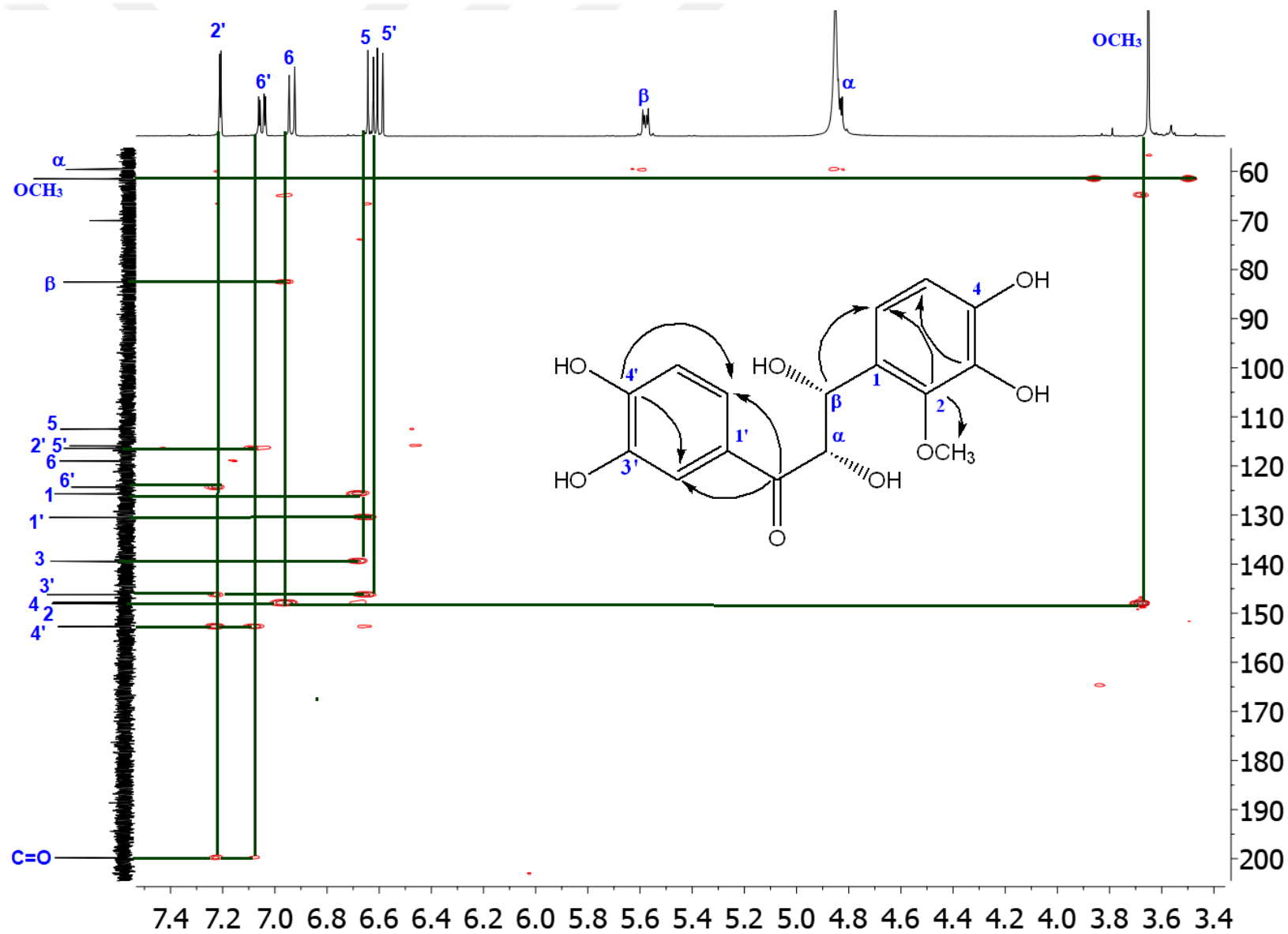
Spectrum 5. Heteronuclear 2D-^{1}H,^{13}C Correlation Spectrum (long range) of Iconichalcone (**1**) (HMBC)
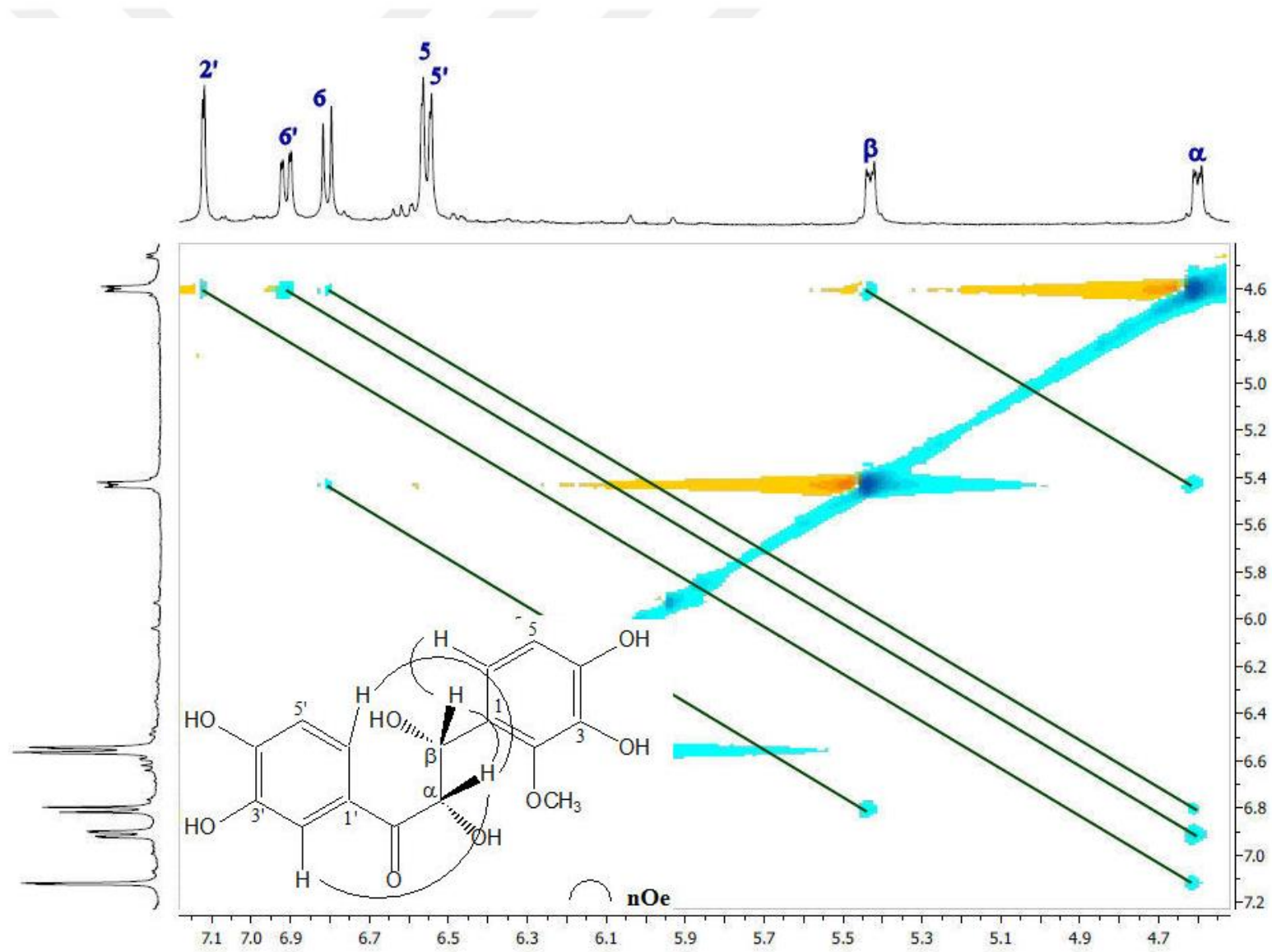
Spectrum 6. 2D-^{1}H,^{1}H-Homonuclear Overhauser Enhancement Spectrum (NOESY) of Iconichalcone (**1**)
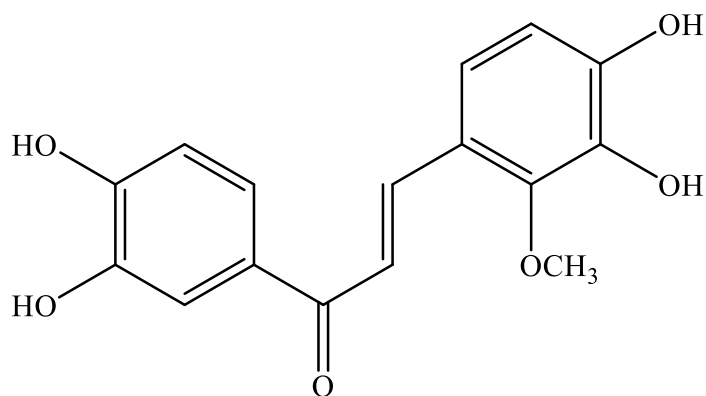
TETRAHYDROXYMETHOXYCHALCONE (2): C$_{16}$H$_{14}$O$_6$ (MW: 302.28)

UV λ_{max} (MeOH) nm:	206, 255, 366
IR υ_{max} (KBr) cm^{-1}:	3334 (OH), 1638 (α,β-unsaturated ketone C=O), 1599, 1566 (conjugated C=C), 1509 (aromatic ring)
^{1}H NMR:	Table 116, Spectrum 7
COSY:	Spectrum 8
NOESY:	Spectrum 9

TETRAHYDROXYMETHOXYCHALCONE (2)

Compound **2** was purified from EtOAc subextracts of both *G. glabra* and *G. iconica* roots as a yellow amorphous powder. In its UV spectrum, bands at 206, 255 and 366 nm were detected, while absorption peaks at 3334 (OH), 1638 (α,β-unsaturated ketone C=O), 1599, 1566 (conjugated C=C) and 1509 (aromatic ring) were observed in IR spectrum of **2**.

^{1}H NMR (Table 116, Spectrum 7) of compound **2** showed a pair of *trans*-olefinic signals at δ_H 7.61 (d, J = 15.7 Hz) and 7.94 (d, J = 15.7 Hz) ascribable to H-α and H-β, respectively. Besides, the spectrum contained five aromatic signals as systems of ABX at δ_H 7.53 (dd, J = 8.3, 2.1 Hz), 7.50 (d, J = 2.1 Hz) and 6.87 (d, J = 8.3 Hz) indicating a tri-substituted benzene ring and AB at δ_H 7.19 (d, J = 8.6 Hz) and 6.64 (d, J =8.6 Hz) arising from a tetra-substituted benzene ring. Taken together, these above signals were characterisitic for a chalcone derivative. Besides, one methoxy signal was observed at 3.85 (3H, s) ppm. COSY spectrum (Spectrum 8) contained three spin systems; one between H-5 and H-6, the other between H-5' and H-6' and also between H-α and H-β. The location of the methoxy unit was determined to be at C-2 on ring B by NOESY spectrum (Spectrum 9) in which NOE correlations were observed between H-α/OCH$_3$ and H-β/OCH$_3$. Based on the above NMR findings the structure of compound **2** was elucidated as 3,4,3',4'-tetrahydroxy-2-methoxychalcone which is also known as **tetrahydroxymethoxychalcone** in the literature (170).

Table 116. ^{1}H NMR spectroscopic data of tetrahydroxymethoxychalcone (**2**) (CD$_3$OD, 400 MHz)^a

C/H atom	Multiplicity	δ_H (ppm), J (Hz)
α	CH	7.61 d (15.7)
β	CH	7.94 d (15.7)
1	C	-
2	C	-
3	C	-
4	C	-
5	CH	6.64 d (8.6)
6	CH	7.19 d (8.6)
1'	C	-
2'	CH	7.50 d (2.1)
3'	C	-
4'	C	-
5'	CH	6.87 d (8.3)
6'	CH	7.53 dd (8.3, 2.1)
OCH$_3$	CH$_3$	3.85 s

^{a} Signals were assigned by the help of COSY and NOESY experiments.
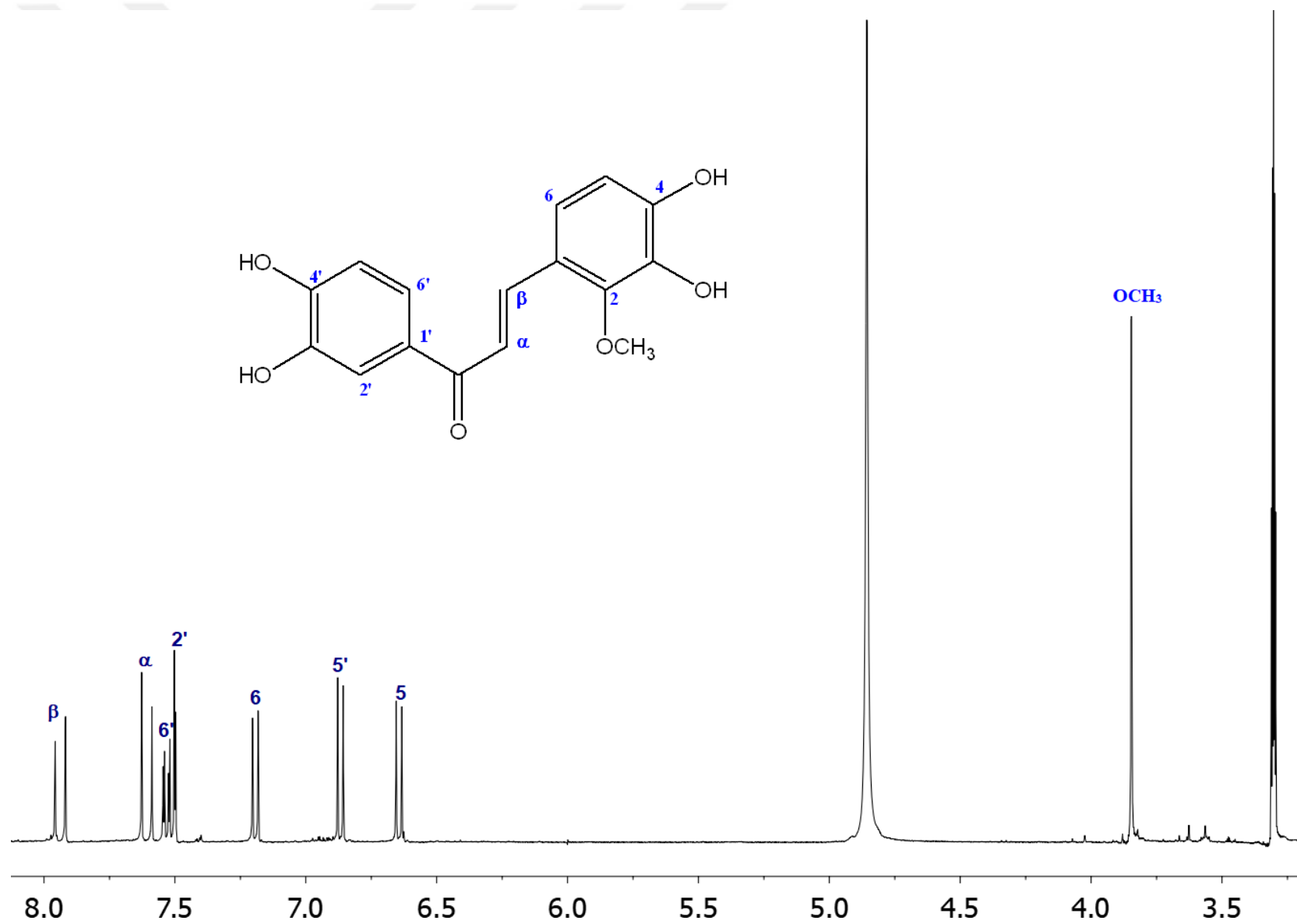
Spectrum 7. ^1H NMR Spectrum of Tetrahydroxymethoxychalcone (**2**) (CD$_3$OD, 400 MHz)

164
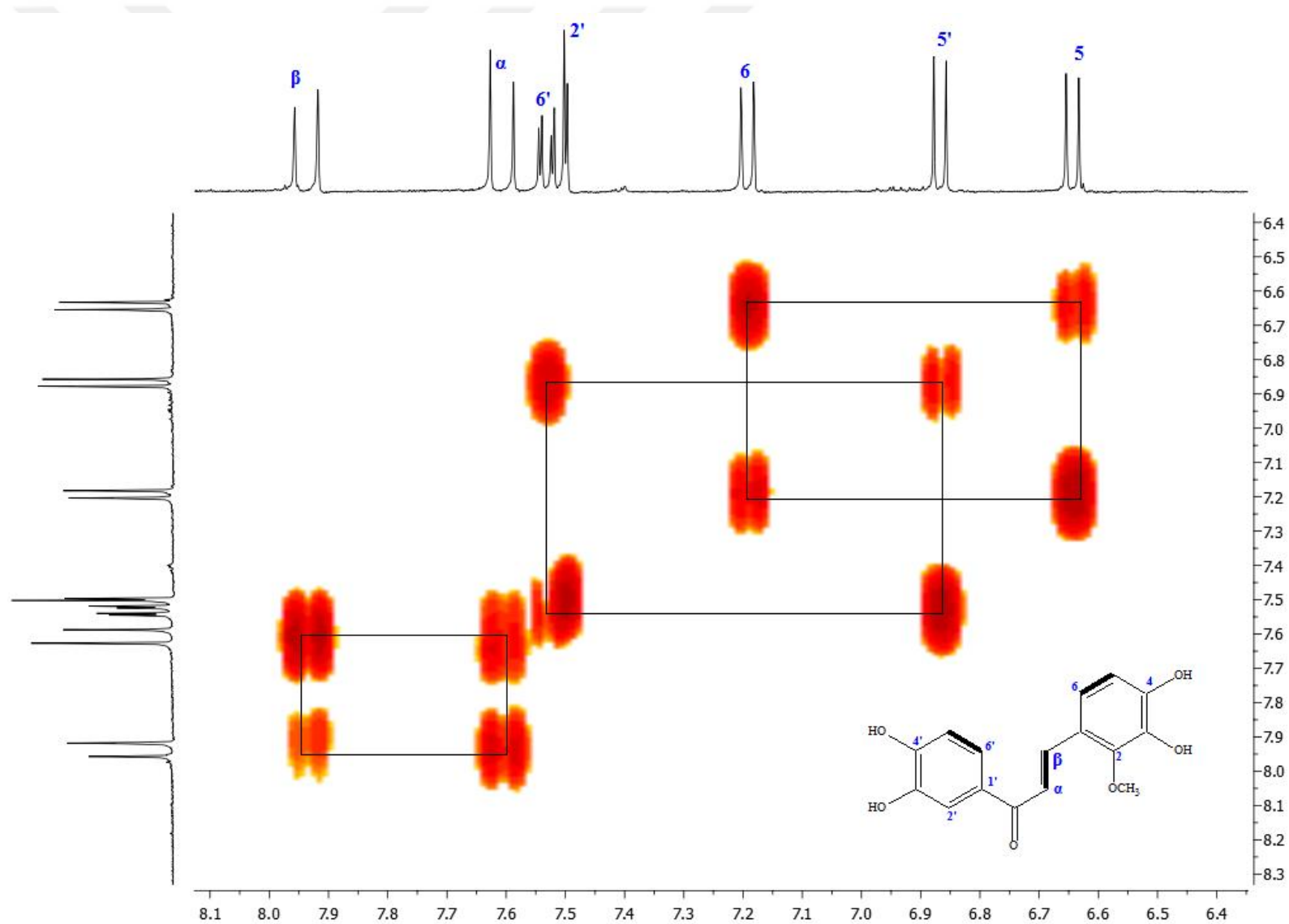
Spectrum 8. 2D-^{1}H,^{1}H-Homonuclear Correlation Spectrum (COSY) of Tetrahydroxymethoxychalcone (**2**)

165
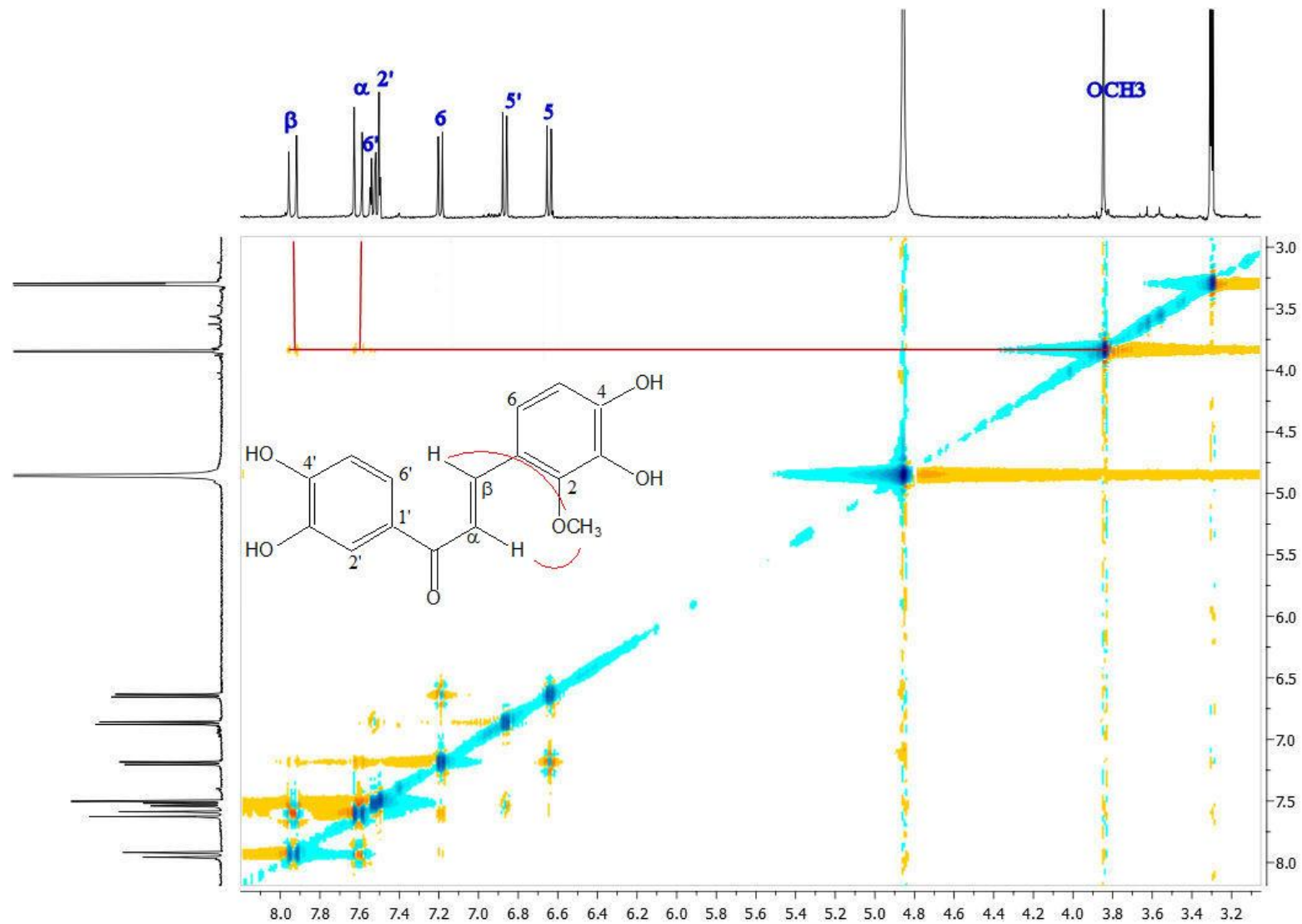
Spectrum 9. 2D-^{1}H,^{1}H-Homonuclear Overhauser Enhancement Spectrum (NOESY) of Tetrahydroxymethoxychalcone (**2**)
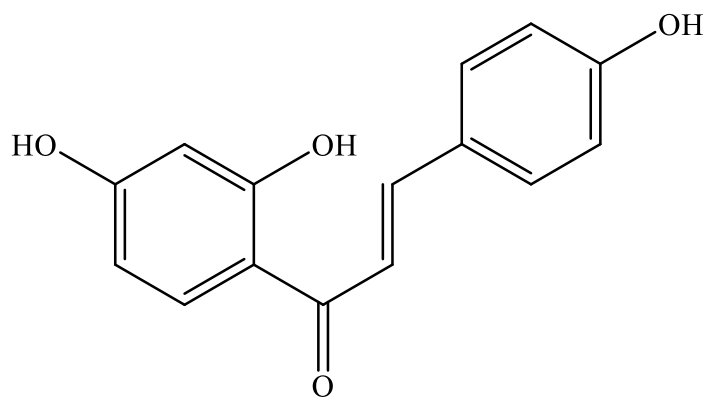
3
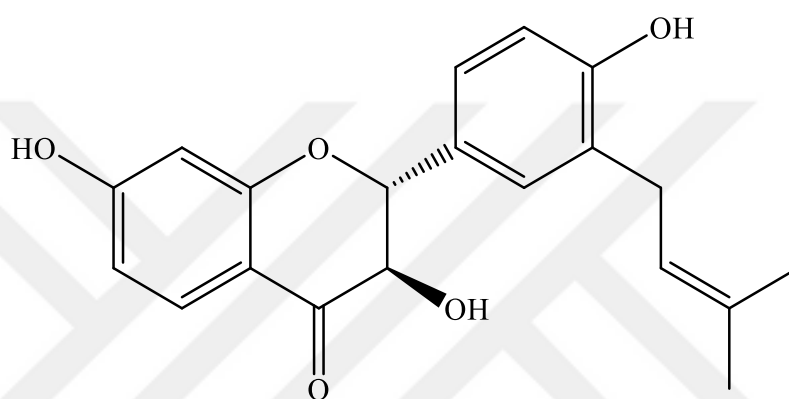
12

ISOLIQUIRITIGENIN (3): C$_{15}$H$_{12}$O$_4$ (MW: 256.25)

(2*R*,3*R*)-3,4',7-TRIHYDROXY-3'-PRENYLFLAVANONE (12): C$_{20}$H$_{20}$O$_5$ (MW: 340.37)

	Isoliquiritigenin (3)	**(2*R*,3*R*)-3,4',7-trihydroxy-3'-prenylflavanone (12)**
^{1}H NMR:	Table 117 Spectrum 10	Table 118 Spectrum 10
^{13}C NMR:	Spectrum 11	Spectrum 11
COSY:	Spectrum 12	Spectrum 12

167

ISOLIQUIRITIGENIN (3) and (2*R*,3*R*)-3,4',7-TRIHYDROXY-3'-PRENYLFLAVANONE (12)

Compounds **3**+**12** were obtained from the EtOAc subextract of *G. glabra.* As these compounds were obtained as a mixture, their UV and IR spectroscopy could not be conducted.

In ^{1}H NMR spectrum (Table 117, Spectrum 10), five aromatic signals between 7.97 - 6.29 ppm were observed arising as AA'BB' and ABX coupling systems. Proton resonances at δ_H 7.97 (d, *J* = 9.0 Hz, H-6'), 6.41 (dd, *J* = 9.0, 2.4 Hz, H-5') and 6.29 (d, *J* = 2.4 Hz, H-3') indicated 1,2,4- trisubstitution in benzene ring. While, AA'BB' system at δ_H 7.62 (d, *J* = 8.8 Hz, H-2/6) and 6.84 (d, *J* = 8.8 Hz, H-3/5) ascribed to *para*-substitution in the other benzene ring. Additional *trans*-olefinic proton signals at δ_H 7.79 (d, *J* = 15.4 Hz, H-β) and 7.61 (d, *J* = 15.4, H-α) along with carbonyl signal at 193.6 ppm in ^{13}C NMR (Table 117, Spectrum 11) suggested the presence of a chalcone nucleus. In COSY experiment (Spectrum 12), two-dimensional (2D) ^{1}H/^{1}H correlations from H-α to H-β, from H-5' to H-6' as well as from H-2/6 to H-3/5 were detected. Comparing NMR data with those of published literatures led to the identification of compound **3** as a 4,2',4'-trihydroxychalcone, namely **isoliquiritigenin** (242)**.**

Inspection of the remaining signals in ^{1}H NMR (Table 118, Spectrum 10) displayed proton signals ascribable to a prenyl group at δ_H 5.34 (1H, m), 3.32 (2H, br d, *J* = 7.3 Hz) in addition to two overlapped methyl signals at δ_H 1.72 (6H, s). Moreover, aromatic signals containing two ABX-type spin coupling systems were detected. One of the ABX system signals at δ_H 7.72 (d, *J* = 8.7 Hz), 6.52 (dd, *J* = 8.7, 2.2 Hz) and 6.33 (d, *J* = 2.2 Hz) were assigned to 7-monosubstituted A ring, while the other ABX type signals at δ_H 7.21 (d, *J* = 2.3 Hz), 7.18 (dd, *J* = 8.2, 2.3 Hz) and 6.79 (d, *J* = 8.2 Hz) indicated existence of 3,4-disubstitution in B ring. Furthermore, *ortho*-coupled proton signals at 4.96 (d, *J* = 11.8 Hz) and 4.49 (d, *J* = 11.8 Hz) ppm and their corresponding carbon resonances (Spectrum 11) at 85.8 and 74.6 ppm suggested the presence of two oxygenated methine signals arising from C-2 and C-3, respectively. A carbon signal at δ_C 194.5 (C-4) showed presence of a ketone function according to ^{13}C NMR spectrum (Table 118, Spectrum 11). COSY spectrum (Spectrum 12) indicated 2D-^{1}H,^{1}H homonuclear correlations between H-2/H-3, H-5/H-6 as well as between protons of isoprenyl unit. With regard to these findings, compound **12** was elucidated as a dihydroxyflavanon-3-ol

derivative with a prenyl unit. The above data were superimposible with those of **(2R,3R)-3,4',7-trihydroxy-3'-prenylflavanone** (94).

Table 117. ^{1}H and ^{13}C NMR spectroscopic data of isoliquiritigenin (**3**) (CD$_3$OD, ^{1}H: 400 MHz, ^{13}C: 100 MHz)^a

C/H atom	Multiplicity	δ_H (ppm), J (Hz)	δ_C (ppm)
α	CH	7.61 d (15.4)	118.4
β	CH	7.79 d (15.4)	145.7
C=O	C	-	193.6
1	C	-	127.9
2/6	CH/CH	7.62 d (8.8)	131.9
3/5	CH/CH	6.84 d (8.8)	116.9
4	C	-	161.6
1'	C	-	114.7
2'	C	-	166.4
3'	CH	6.29 d (2.4)	103.8
4'	C	-	166.9
5'	CH	6.41 dd (9.0, 2.4)	109.2
6'	CH	7.97 d (9.0)	133.4

^{a} Resonances were assigned by the help of COSY experiment.

Table 118. ^{1}H and ^{13}C NMR spectroscopic data of (2R,3R)-3,4',7-trihydroxy-3'-prenylflavanone (**12**) (CD$_3$OD, ^{1}H: 400 MHz, ^{13}C: 100 MHz)[a]

C/H atom	Multiplicity	δ_H (ppm), J (Hz)	δ_C (ppm)
2	CH	4.96 d (11.8)	85.8
3	CH	4.49 d (11.8)	74.6
4	C	-	194.5
5	CH	7.72 d (8.7)	130.3
6	CH	6.52 dd (8.7, 2.2)	112.1
7	C	-	167.5
8	CH	6.33 d (2.2)	103.8
9	C	-	165.2
10	C	-	113.5
1'	C	-	130.1
2'	CH	7.21 d (2.3)	131.9
3'	C	-	129.3
4'	C	-	156.8
5'	CH	6.79 d (8.2)	115.6
6'	CH	7.18 dd (8.2, 2.3)	127.6
1"	CH$_2$	3.32 br d (7.3)	31.2
2"	CH	5.34 m	123.9
3"	C	-	133.1
4"	CH$_3$	1.72 s	29.4
5"	CH$_3$	1.72 s	26.0

[a] Resonances were assigned by the help of COSY experiment.
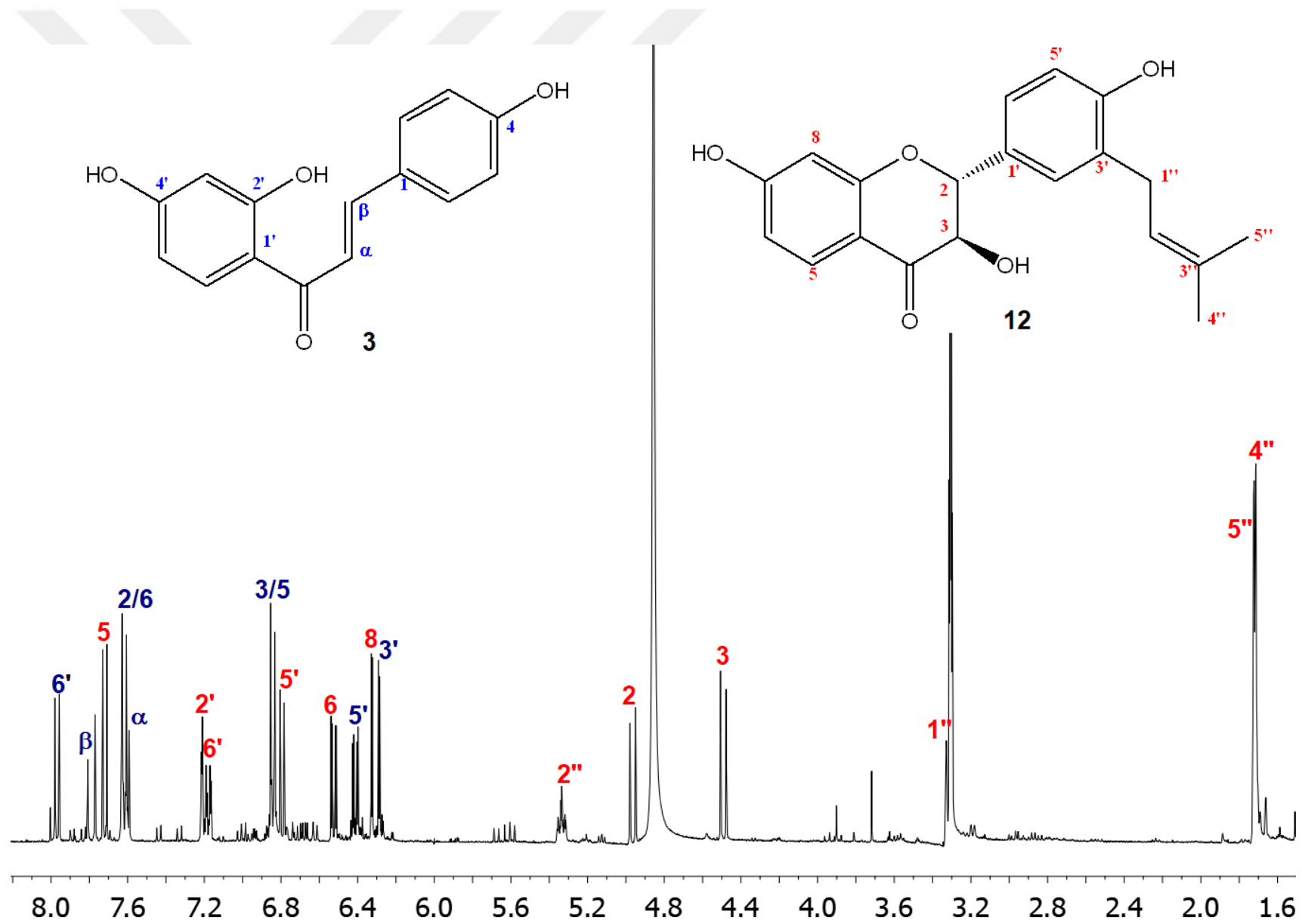
Spectrum 10. ^{1}H NMR Spectrum of Isoliquiritigenin (**3**) and (2*R*,3*R*)- 3,4',7-trihydroxy-3'-prenylflavanone (**12**) Mixture (CD$_3$OD, 400 MHz)

172
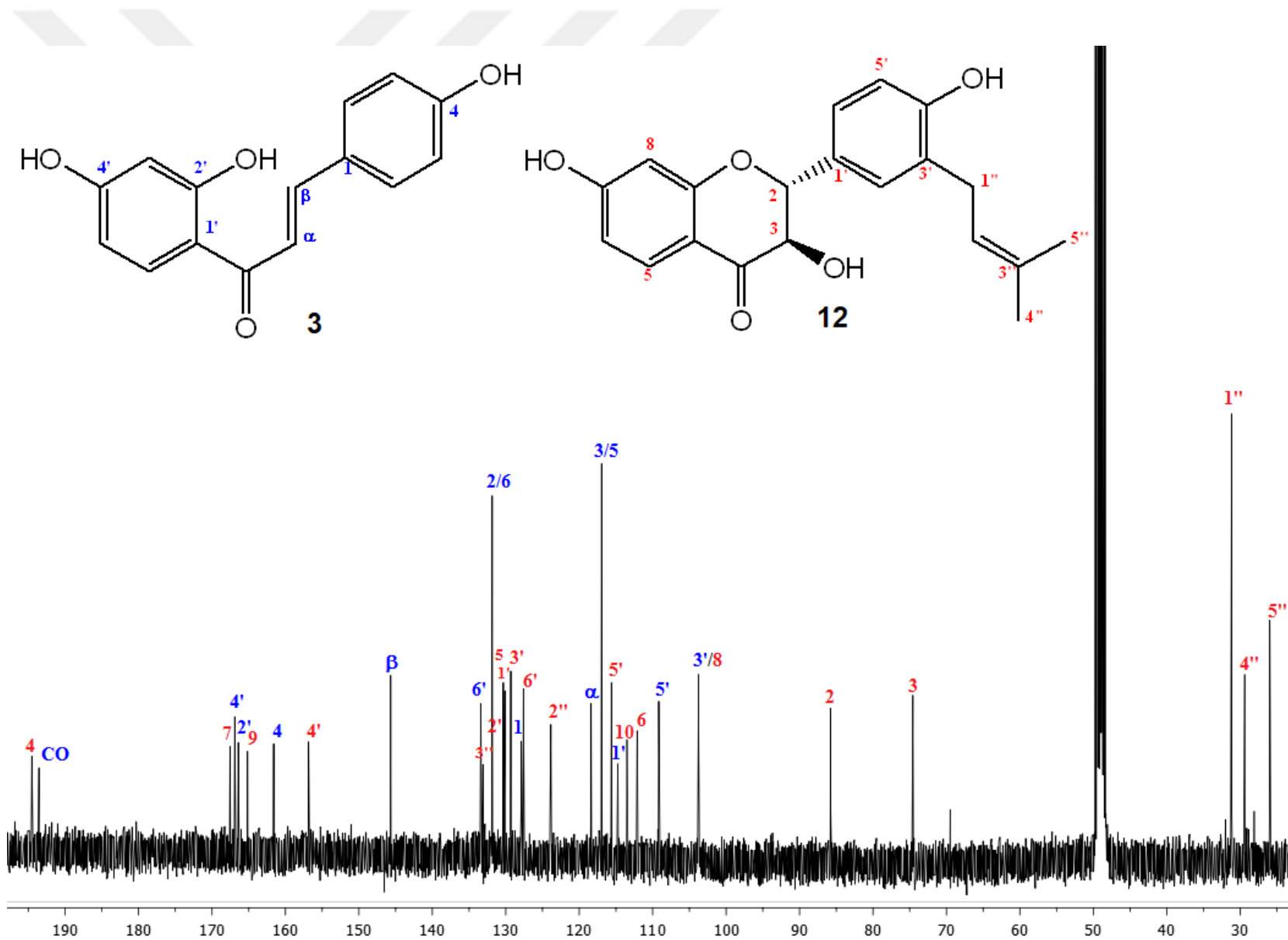
Spectrum 11. ^{13}C NMR Spectrum of Isoliquiritigenin (**3**) and (2R,3R)- 3,4',7-trihydroxy-3'-prenylflavanone (**12**) Mixture (CD$_3$OD, 100 MHz)

173
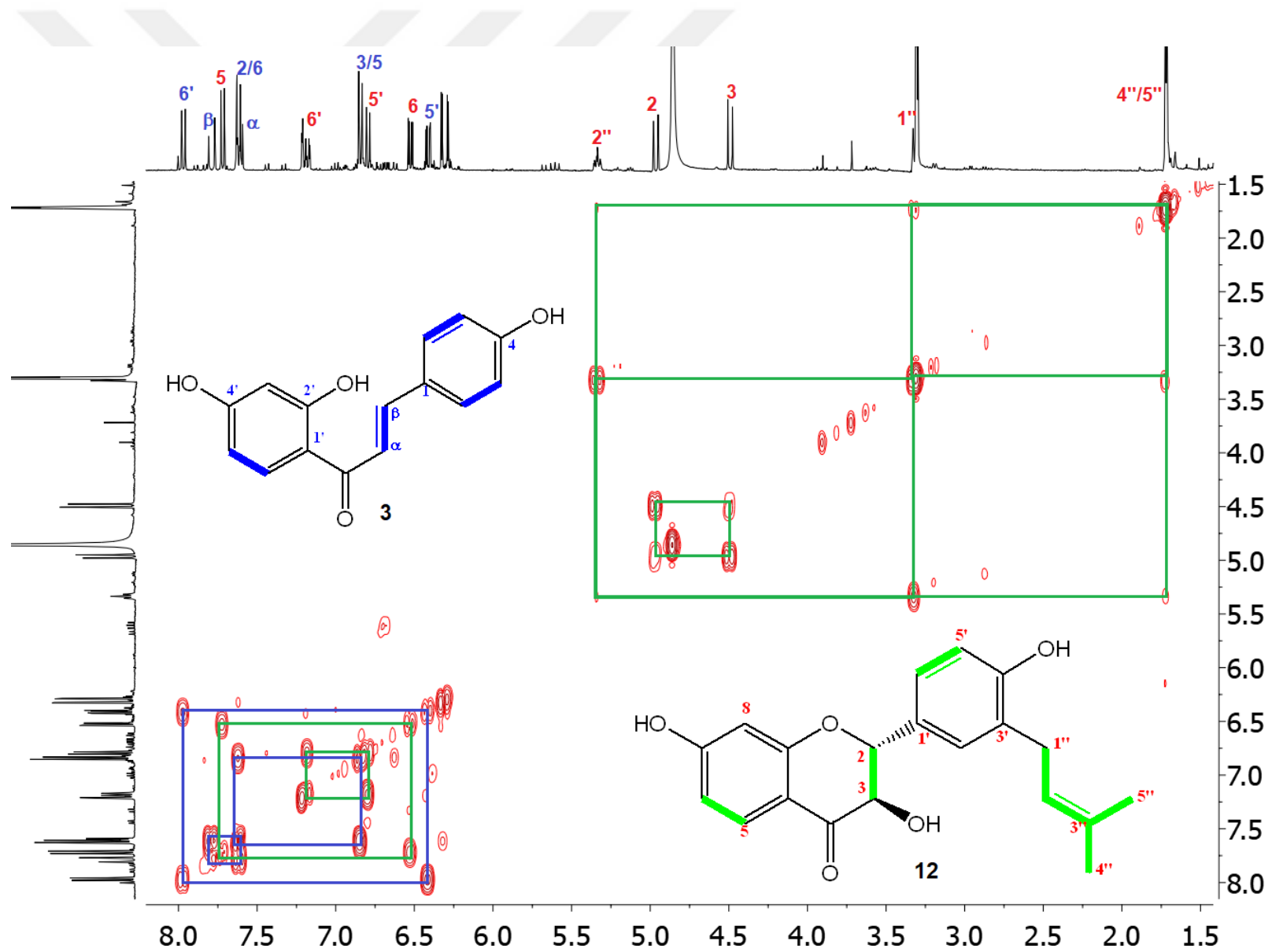
Spectrum 12. 2D-^{1}H,^{1}H-Homonuclear Correlation Spectrum (COSY) of **3** and **12** Mixture

174
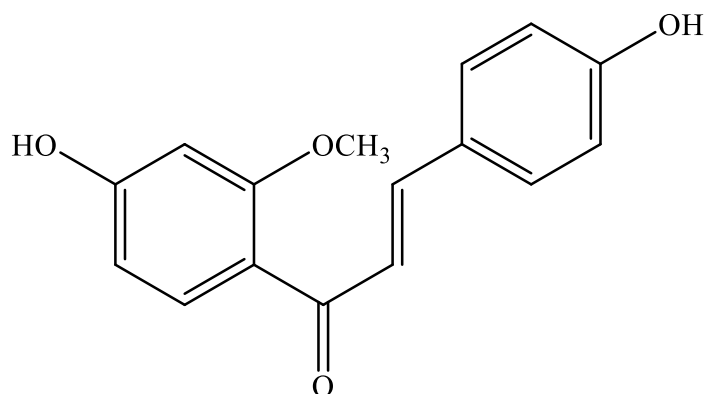
2'-*O*-METHYLISOLIQUIRITIGENIN (4): $C_{16}H_{14}O_4$ (MW: 270.28)

UV λ_{max} (MeOH) nm:	288, 351
IR υ_{max} (KBr) cm^{-1}:	3435 (OH), 1606 (α,β-unsaturated ketone C=O)
^{1}H NMR:	Table 119, Spectrum 13
COSY:	Spectrum 14
NOESY:	Spectrum 15

2'-*O*-METHYLISOLIQUIRITIGENIN (4)

Compound **4** was isolated from EtOAc subextract of *G. iconica* as yellow amorphous powder, having a $C_{16}H_{14}O_4$ molecular formula. UV spectrum of it showed absorption maxima at 277 and 251 nm, while its IR spectrum showed bands at 3435 and 1606 cm^{-1} indicating hydroxyl and α,β-unsaturated ketone groups, respectively.

In its ^{1}H NMR spectrum (Table 119, Spectrum 13), two aromatic signals were observed as an AA'BB' system at δ_H 7.96 (d, J = 8.8 Hz) and 6.88 (d, J = 8.8 Hz) revealed a *para*-substituted benzene ring that were assigned to H-2/6 and H-3/5, respectively. In addition, signals at δ_H 7.60 (d, J = 8.4 Hz), 6.45 (dd, J = 8.4, 2.3 Hz) and 6.47 (d, J = 2.3 Hz) were indicative of an ABX system in the molecule. Presence of *trans*-olefinic proton signals at δ_H 8.03 (d, J = 15.6 Hz, H-β) and 7.61 (d, J = 15.6 Hz, H-α) as an AX system together with above mentioned AA'BB' and ABX type aromatic signals concluded that the main core of this compound was a chalcone. Moreover, proton resonance of a methoxy unit at 3.89 (3H, s) was detected. ^{1}H/^{1}H cross peaks in COSY experiment (Spectrum 14) showed the spin systems from H-α to H-β and from H-5' to H-6' as well as from H-2/6 to H-3/5. Moreover, the NOE correlations between H-3'/OCH$_3$, H-6'/H-5' and H-2/6/H-3/5 in the NOESY spectrum (Spectrum 15) indicated that methoxy group was attached from C-2' and also confirmed the exact structure of the compound as, 4,4'-dihydroxy-2'-methoxychalcone, namely **2'-*O*-methylisoliquiritigenin** (243).

Table 119. ^{1}H NMR spectroscopic data of 2'-*O*-methylisoliquiritigenin (**4**) (CD$_3$OD, 400 MHz)^a

C/H atom	Multiplicity	δ_H (ppm), *J* (Hz)
α	CH	7.61 d (15.6)
β	CH	8.03 d (15.6)
1	C	-
2/6	CH/CH	7.96 d (8.8)
3/5	CH/CH	6.88 d (8.8)
4	C	-
1'	C	-
2'	C	-
3'	CH	6.47 d (2.3)
4'	C	-
5'	CH	6.45 dd (8.4, 2.3)
6'	CH	7.60 d (8.4)
OCH$_3$	CH$_3$	3.89 s

^{a} Resonances were assigned by the help of COSY and NOESY experiments.
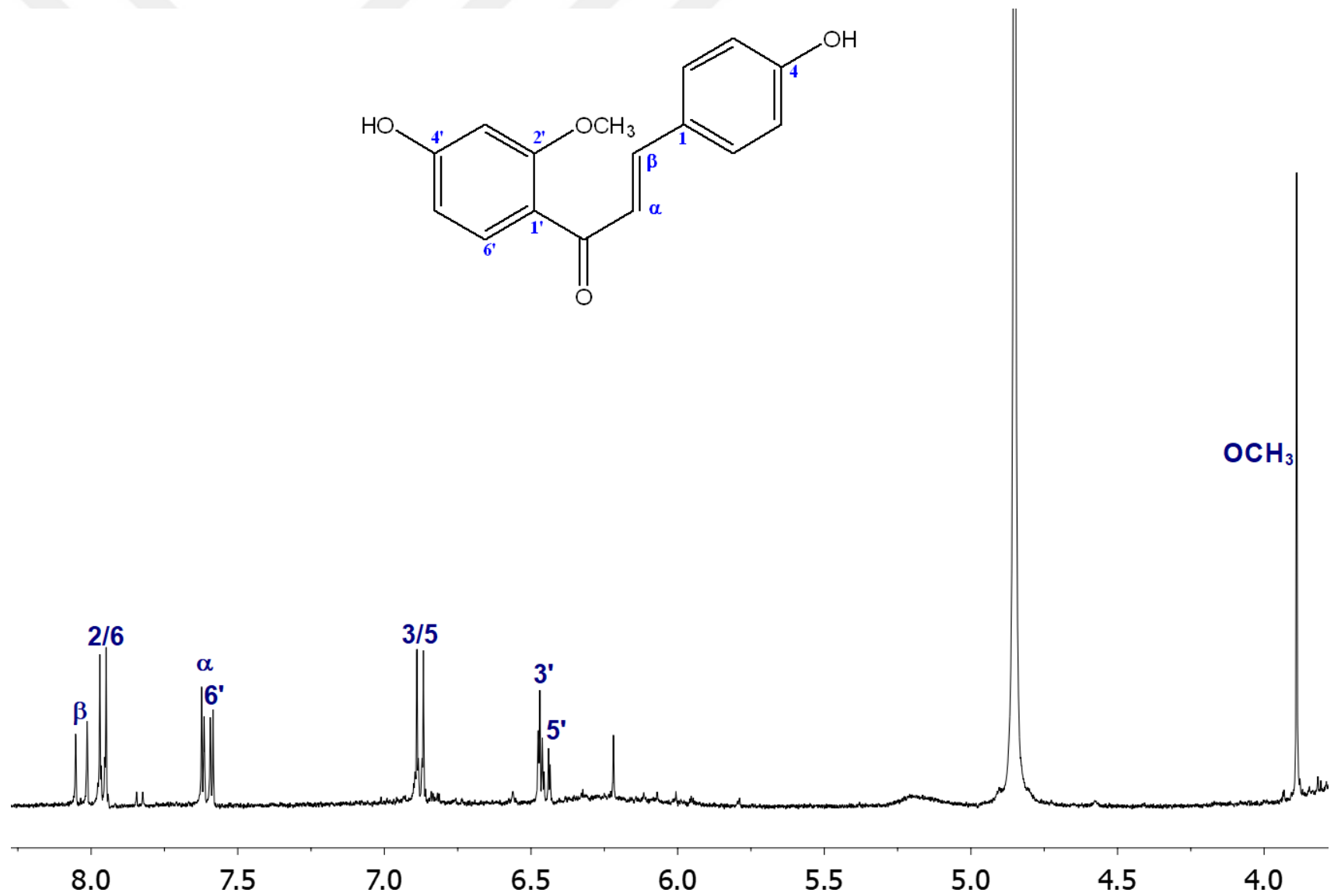
Spectrum 13. ¹H NMR Spectrum of 2'-*O*-Methylisoliquiritigenin (**4**) (CD₃OD, 400 MHz)
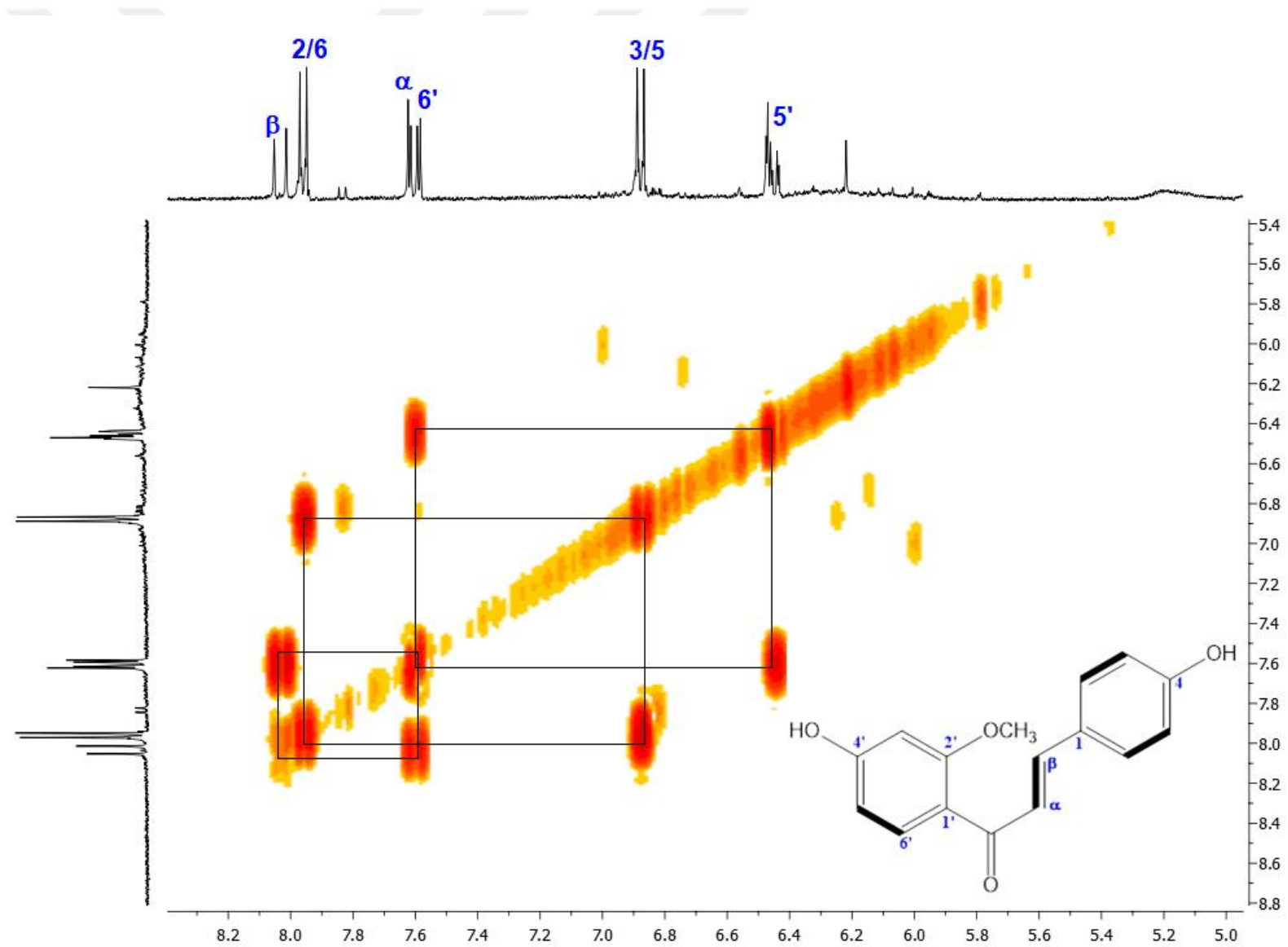
Spectrum 14. 2D-^{1}H,^{1}H-Homonuclear Correlation Spectrum (COSY) of 2'-O-Methylisoliquiritigenin (**4**)
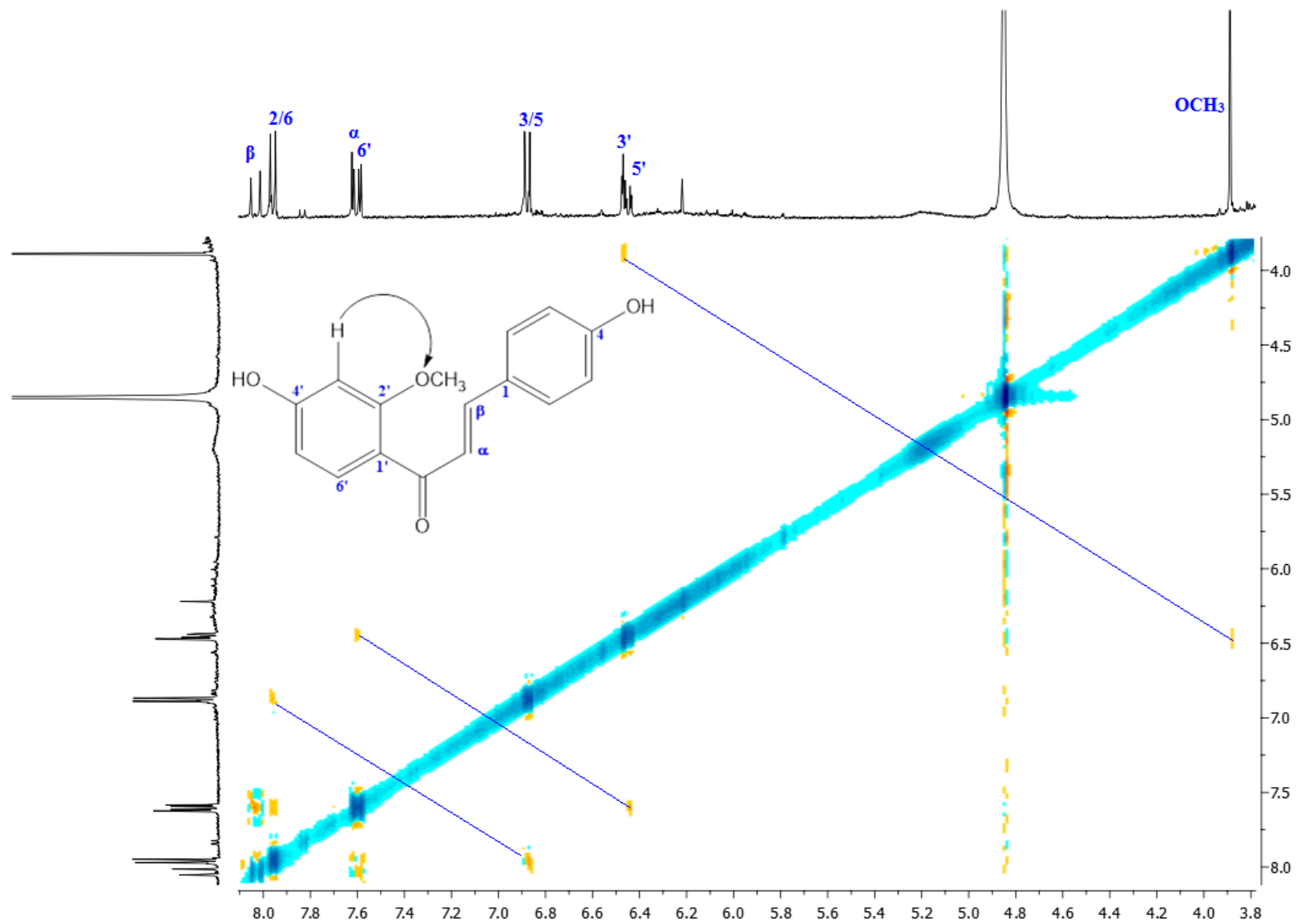
Spectrum 15. 2D-^{1}H,^{1}H-Homonuclear Overhauser Enhancement Spectrum (NOESY) of 2'-*O*-Methylisoliquiritigenin (**4**)
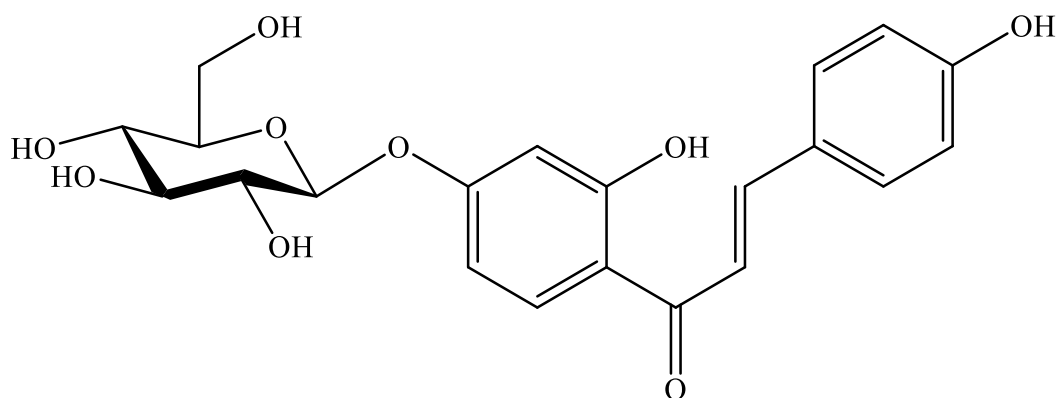
ISOLIQUIRITIGENIN 4'-*O*-β-GLUCOPYRANOSIDE (5): $C_{21}H_{22}O_9$ (MW: 418.4)

UV λ_{max} (MeOH) nm:	203, 366
IR υ_{max} (KBr) cm^{-1}:	3428 (OH), 1635 (α,β-unsaturated ketone C=O), 1606 (conjugated C=C), 1513 (aromatic ring)
^{1}H NMR:	Table 120, Spectrum 16
NOESY:	Spectrum 17

ISOLIQUIRITIGENIN 4'-*O*-β-GLUCOPYRANOSIDE (5)

Compound **5**, a yellow amorphous powder with a $C_{21}H_{22}O_9$ molecular formula was obtained from *G. glabra* EtOAc subextract. Absorption maxima at 203 and 366 nm in UV spectroscopy and bands at 3428 (OH), 1635 (α,β-unsaturated ketone C=O), 1606 (conjugated C=C), and 1513 (aromatic ring) cm^{-1} in IR spectoscopy were observed which were consistent with a chalcone nucleus.

Chalcone skeleton was deduced from ^1H NMR spectrum (Table 120, Spectrum 16) of compound **5** by presence of an α,β-*trans* olefinic proton signals along with five aromatic proton signals as AA'BB' and ABX systems. *Trans*-olefinic signals were detected at $δ_H$ 7.83 (d, *J* =15.2 Hz, H-β) and 7.64 (d, *J* =15.2 Hz, H- α), while AA'BB' type aromatic signals were seen at $δ_H$ 7.63 (d, *J* = 8.6 Hz, H-2/6) and 6.85 (d, *J* = 8.6 Hz, H-3/5) due to *para*-substitution. ABX type proton resonances at $δ_H$ 8.06 (d, *J* = 8.9 Hz), 6.69 (dd, *J* = 8.9, 2.3 Hz) and 6.62 (d, *J* = 2.3 Hz) indicated trisubstitution in one of the benzene rings of the chalcone. Additional proton resonances arising from β-glucopyranose were detected. One anomeric signal at $δ_H$ 5.03 (d, *J* = 7.2 Hz) together with signals between 3.91 - 3.41 ppm revealed a monoglucosidic structure. The 7.2 Hz coupling constant of anomeric proton indicated the β-configuration. By the aid of NOESY experiment (Spectrum 17), the position of β-glucopyranose unit was determined to be at C-4' by NOE correlations of H-1'' with both H-3' and H-5'. All these data led to the characterization of compound **5** as **neoisoliquiritin** or **isoliquiritigenin 4'-*O*-β-glucopyranoside** (242).

Table 120. ^{1}H NMR spectroscopic data of isoliquiritigenin 4'-*O*-β-glucopyranoside (**5**) (CD$_3$OD, 400 MHz)

C/H atom	Multiplicity	δ$_H$ (ppm), *J* (Hz)
Aglycone		
α	CH	7.64 d (15.2)
β	CH	7.83 d (15.2)
1	C	-
2/6	CH/CH	7.63 d (8.6)
3/5	CH/CH	6.85 d (8.6)
4	C	-
1'	C	-
2'	C	-
3'	CH	6.62 d (2.3)
4'	C	-
5'	CH	6.69 dd (8.9, 2.3)
6'	CH	8.06 d (8.9)
Glucose		
1"	CH	5.03 d (7.2)
2"- 4"	CH	3.47 - 3.52 †
5"	CH	3.41 m
6"	CH$_2$	3.91 dd (12.0,1.5) 3.72 dd (12.0, 5.3)

†: Overlapping signals
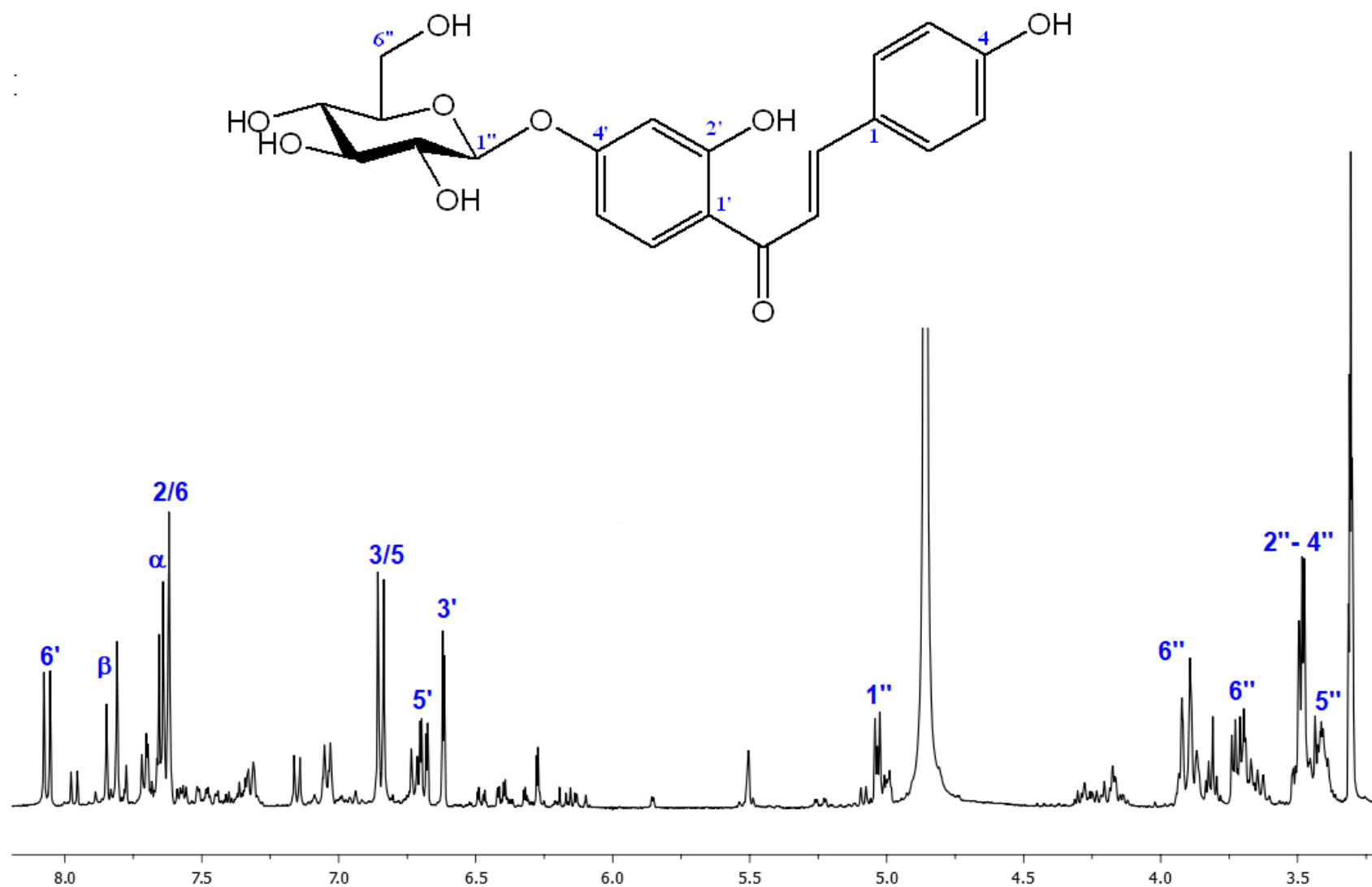
Spectrum 16. ^{1}H NMR Spectrum of Isoliquiritigenin 4'-O-β-glucopyranoside (**5**) (CD$_3$OD, 400 MHz)
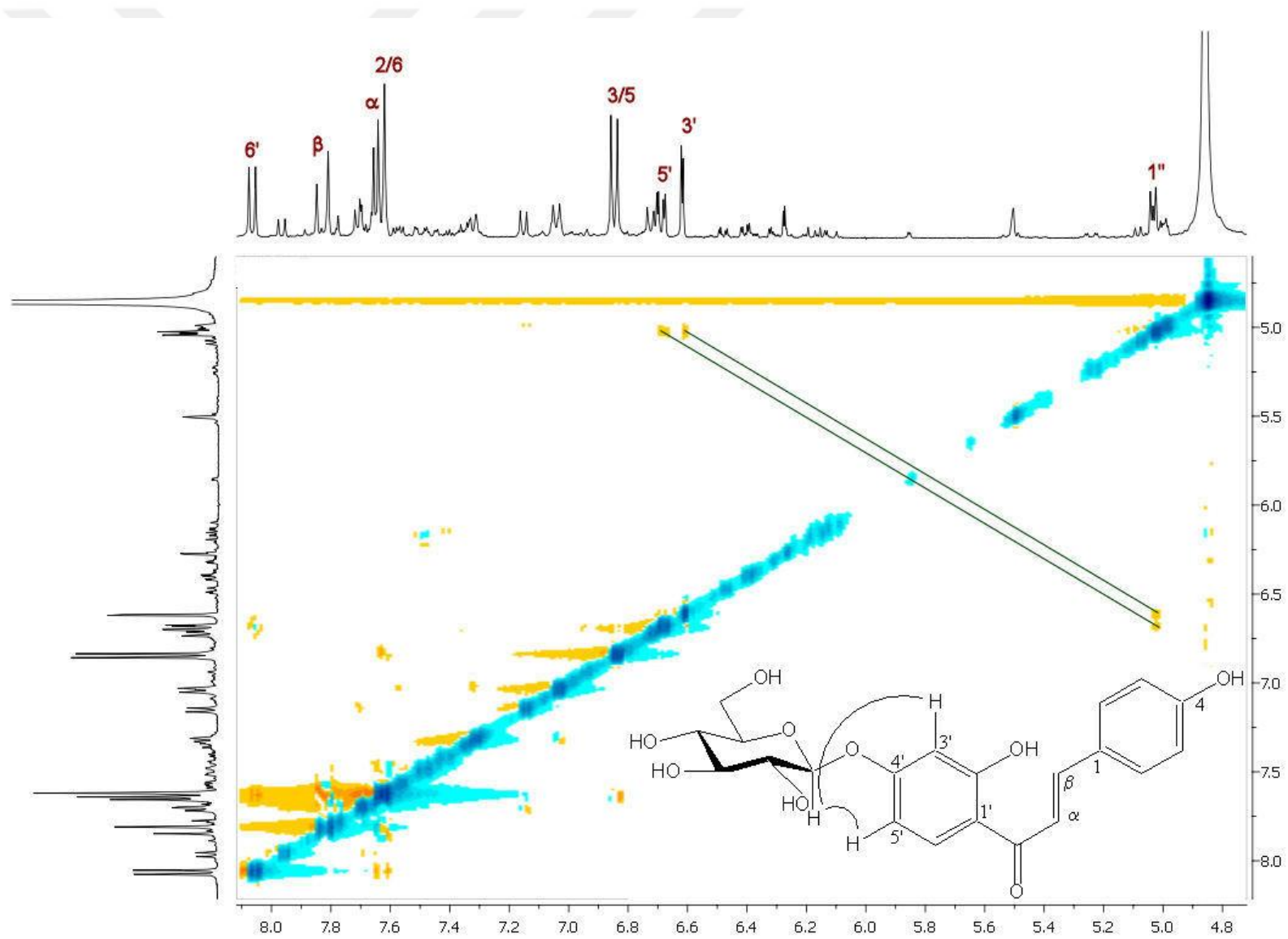
Spectrum 17. 2D-^{1}H,^{1}H-Homonuclear Overhauser Enhancement Spectrum (NOESY) of Isoliquiritigenin 4′-*O*-β-glucopyranoside (**5**)
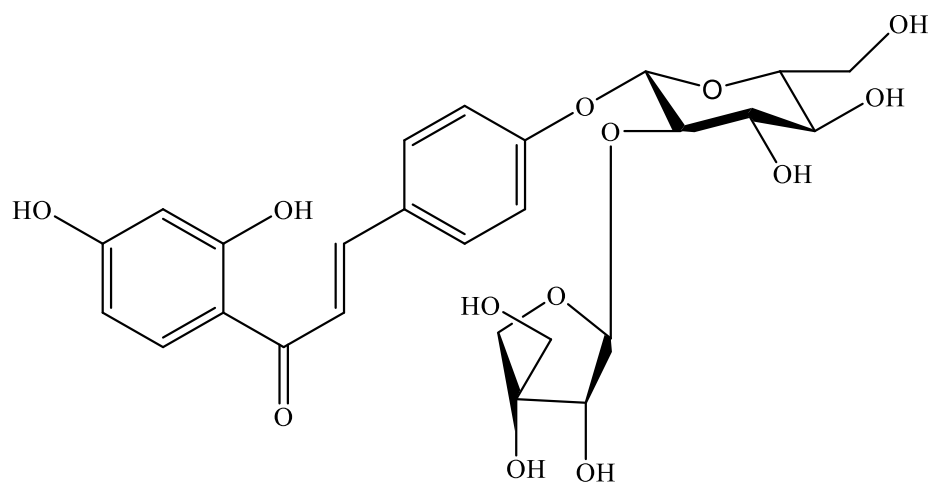
6
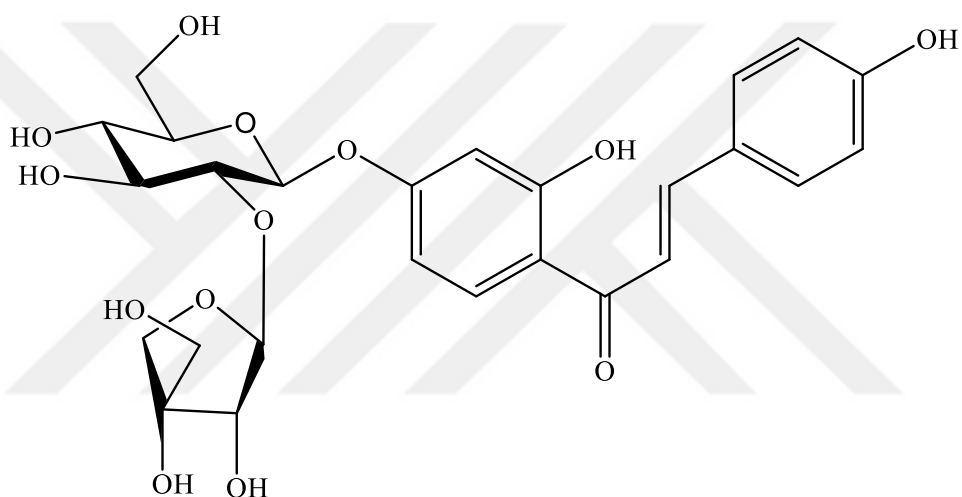
7

LICUROSIDE (6): C₂₆H₃₀O₁₃ (550.51)

NEOLICUROSIDE (7): C₂₆H₃₀O₁₃ (550.51)

UV λ$_{max}$ (MeOH) nm:	203, 365
IR υ$_{max}$ (KBr) cm^{-1}:	3306 (OH), 1635 (α,β-unsaturated C=O), 1509 (aromatic ring)
MS m/z:	549.57 [M-H]$^+$, 551.44 [M+H]$^+$
^{1}H NMR:	Table 121, Spectrum 18

186

LICUROSIDE (6) and NEOLICUROSIDE (7)

Inseparable mixture of compound **6** and **7** was obtained from EtOAc subextract of *G. glabra*. Molecular formula was found to be $C_{26}H_{30}O_{13}$ based on the ion peaks at *m/z* 549.57 $[M-H]^+$ and 551.44 $[M+H]^+$. IR spectrum displayed absorption bands at 3306 (OH), 1635 (conjugated C=C), 1509 (aromatic ring) cm^{-1}, while UV spectrum showed absorption maxima at 203 and 365 nm.

The ^1H NMR spectrum (Table 121, Spectrum 18) of **6** displayed proton resonances at δ_H 7.80 and 7.63 (each d, *J* = 15.4 Hz) due to an α,β-*trans* olefinic protons. Moreover, AA'BB' type signals at δ_H 7.71 (d, *J* = 8.8 Hz) and 7.12 (d, *J* = 8.8 Hz) showed *para* substitution in one benzene ring, while ABX type signals at δ_H 7.97 (d, *J* = 8.9 Hz), 6.42 (dd, *J* = 8.9, 2.4 Hz) and 6.29 (d, *J* = 2.4 Hz) revealed 1,2,4-trisubstitution in another benzene ring. Two anomeric signals at δ_H 5.05 (d, *J* = 7.4 Hz) and 5.47 (d, *J* = 1.6 Hz) along with signals between 4.05-3.38 indicated a diglycosidic structure. The large coupling constant of anomeric proton at 5.05 ppm showed β-configuration of glucopyranose. Besides, characteristic signals for β-apiofuranose moiety were observed. These resonances were consistent with a trisubstituted chalcone nucleus containing β-apiofuranosyl-(1→2)-β-glucopyranosyl moiety. The location of diglycoside chain was determined to be at C-4 by the chemical shift observed in H-3/5 comparing to isoliquiritigenin (242). From these observations, the structure of **6** was assigned as **licuroside** (156).

Chalcone skeleton of the compound **7** was identified from remaining proton signals in ^1H NMR spectrum (Table 121, Spectrum 18) by presence of an α,β-*trans* olefinic proton signals at 7.82 (d, *J* = 15.4 Hz) and 7.64 (d, *J* = 15.4 Hz) and aromatic signals having AA'BB' and ABX coupling systems. AA'BB' type aromatic signals were detected at δ_H 7.71 (d, *J* = 8.7 Hz, H-2/6) and 6.85 (d, *J* = 8.7 Hz, H-3/5) due to *para*-substitution in ring B, while ABX type resonances at δ_H 8.06 (d, *J* = 9.1 Hz), 6.65 (dd, *J* = 9.1, 2.5 Hz), and 6.58 (d, *J* = 2.5 Hz) were ascribed to H-6', H-5' and H-3' in ring A, respectively. Furthermore, anomeric proton resonances were observed at δ_H 5.10 (d, *J* = 7.4 Hz) and 5.45 (d, *J* = 1.6 Hz) which were assigned to β-glucopyranose and β-apiofuranose, respectively with regard to signals between 4.02 – 3.38 ppm and their corresponding coupling constants. The attachment point of sugar moiety was found to be at C-4' by chemical shifts of H-3' and H-5' comparing to isoliquiritigenin (**3**) and

licuroside (**6**) (242). All these data led to the elucidation of the structure of compound **7** as **isoliquiritigenin-4'-*O*-β-apiofuranosyl-(1→2)-β-glucopyranoside** or **neolicuroside** (156).

Table 121. ^{1}H NMR spectroscopic data of licuroside (**6**) and neolicuroside (**7**) (CD$_3$OD, 400 MHz)

C/H atom	Multiplicity	6 δ$_H$ (ppm), J (Hz)	7 δ$_H$ (ppm), J (Hz)
Aglycone			
α	CH	7.63 d (15.4)	7.64 d (15.4)
β	CH	7.80 d (15.4)	7.82 d (15.4)
1	C	- -	-
2/6	CH/CH	7.71 d (8.8)	7.71 d (8.7)
3/5	CH/CH	7.12 d (8.8)	6.85 d (8.7)
4	C	-	-
1'	C	-	-
2'	C	-	-
3'	CH	6.29 d (2.4)	6.58 d (2.5)
4'	C	-	-
5'	CH	6.42 dd (8.9, 2.4)	6.65 dd (9.1, 2.5)
6'	CH	7.97 d (8.9)	8.06 d (9.1)
Glucose			
1"	CH	5.05 d (7.4)	5.10 d (7.4)
2"	CH	3.38- 3.67 †	3.38- 3.67 †
3"	CH	3.38- 3.67 †	3.38- 3.67 †
4"	CH	3.38- 3.67 †	3.38- 3.67 †
5"	CH	3.38- 3.67 †	3.38- 3.67 †
6"	CH$_2$	3.90 dd (12.1, 1.9) 3.70 dd (12.1, 5.5)	3.90 dd (12.1, 2.0) 3.71 dd (12.1, 5.3)
Apiose			
1'''	CH	5.47 d (1.6)	5.45 d (1.6)
2'''	CH	3.95 d (1.6)	3.95 d (1.6)
3'''	C	-	-
4'''	CH$_2$	4.05 d (9.6) 3.80 d (9.6)	4.02 d (9.6) 3.80 d (9.6)
5'''	CH$_2$	3.53 d (2.5)	3.53 d (2.5)

†: Overlapping signals

189
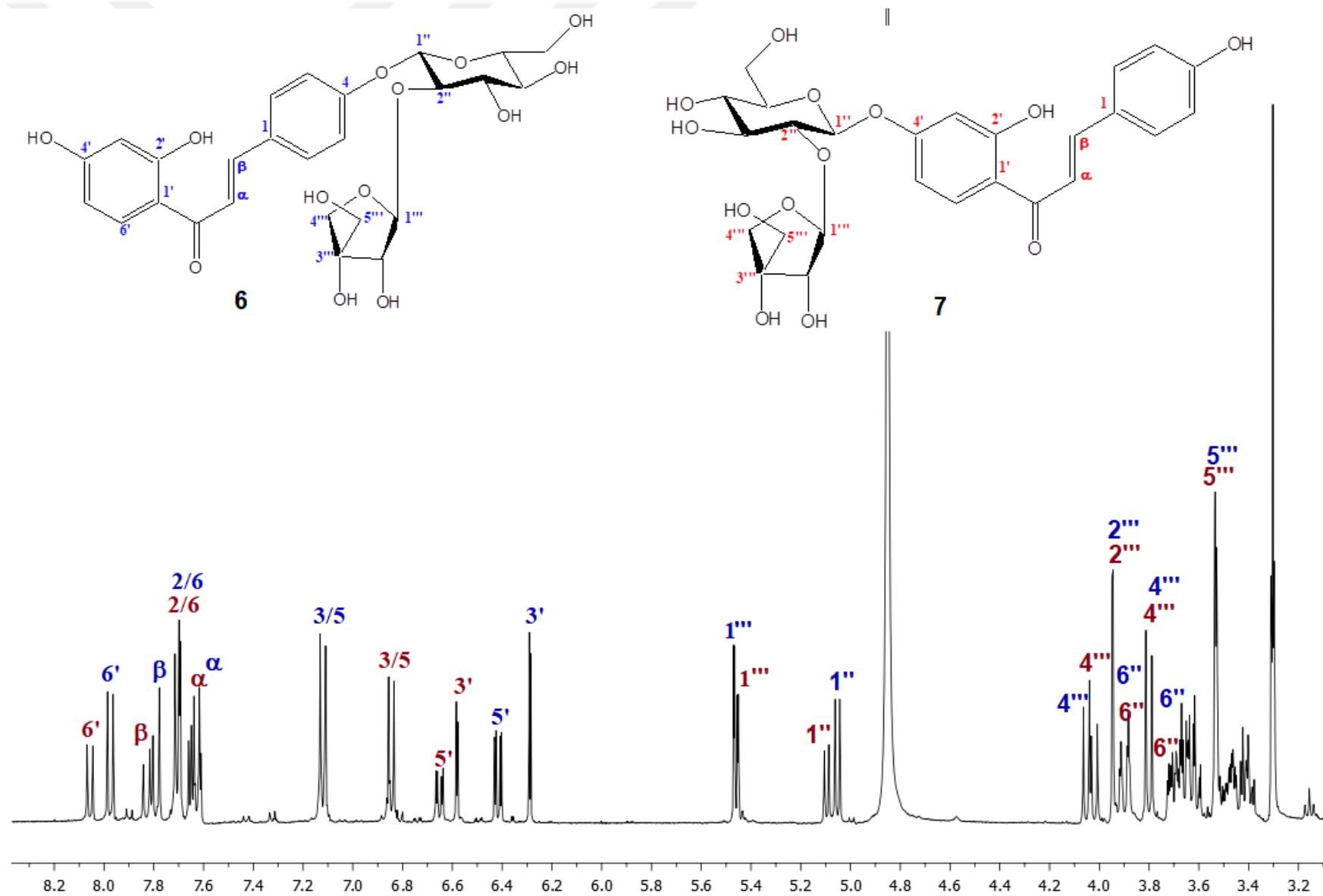
Spectrum 18. ^{1}H NMR Spectrum of Licuroside (**6**) and Neolicuroside (**7**) Mixture (CD$_3$OD, 400 MHz)

4.5.1.2. Flavonols
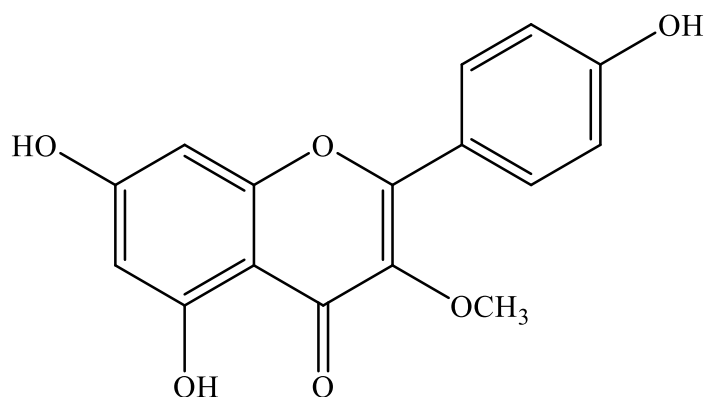
3-*O*-METHYLKAEMPFEROL (8): C$_{16}$H$_{12}$O$_6$ (MW: 300.27)

UV λ$_{max}$ (MeOH) nm:	267, 346
IR υ$_{max}$ (KBr) cm^{-1}:	3434 (OH), 1654 (γ-pyron C=O), 1609 (conjugated C=C), 1506 (aromatic ring)
^{1}H NMR:	Table 122, Spectrum 19
^{13}C NMR:	Table 122, Spectrum 20
HMBC:	Spectrum 21

3-*O*-METHYLKAEMPFEROL (8)

Compound **8** was purified as yellow amorphous powder from both EtOAc and *n*-BuOH subextracts of *G. iconica*. UV spectra showed characteristic bands (λ_{max} 267, 346 nm) of a flavonoidal structure. The hydroxyl group (3434 cm^{-1}), γ -pyrone carbonyl (1654 cm^{-1}), signals of aromatic ring (1506 cm^{-1}) and conjugated C=C bands (1609 cm^{-1}) were observed in its IR spectrum.

^{1}H NMR spectrum (Table 122, Spectrum 19) displayed aromatic signals ascribable to AA'BB' system at δ_H 7.98 (d, *J* = 8.9 Hz, H-2'/6') and 6.97 (d, *J* = 8.9 Hz, H-3'/5') revealed the presence of *para*-substitution in B ring of flavonoid. Additional aromatic proton signals of two *meta*-coupled doublets at δ_H 6.45 (d, *J* = 2.0 Hz, H-8) and 6.25 (d, *J* = 2.0 Hz, H-6) in the ^{1}H NMR spectrum were the indicative of a 5,7-disubstituted A ring. The ^{13}C NMR spectrum (Table 122, Spectrum 20) contained a ketone moiety at 180.0 ppm (C-4) and an oxygenated olefinic carbon signal at 139.5 ppm (C-3). Above findings led to the presence of a flavonol core in **8**. Moreover, additional resonances arising from methoxy unit were observed at δ_H 3.76 (3H, s) and δ_C 61.0. The location of methoxy unit were determined by HMBC experiment (Spectrum 21). The long range couplings from C-3 (δ_C 139.5) to methoxy (δ_H 3.76) elicited the position of methoxy unit at C-3. The data were superimposible with those reported for 5,7,4'-trihydroxy-3-methoxyflavone namely **3-*O*-methylkeampferol** or **3-methoxyapigenin** (214).

Table 122. ^{1}H and ^{13}C NMR spectroscopic data of 3-*O*-methylkaempferol (**8**) (CD$_3$OD, ^{1}H: 400 MHz, ^{13}C: 100 MHz)[a]

C/H atom	Multiplicity	δ_H (ppm), *J* (Hz)	δ_C (ppm)
2	C	-	158.4
3	C	-	139.5
4	C	-	180.0
5	C	-	162.6
6	CH	6.25 d (2.0)	100.2
7	C	-	166.0
8	CH	6.45 d (2.0)	95.3
9	C	-	158.5
10	C	-	105.9
1'	C	-	122.7
2'/6'	CH/CH	7.98 d (8.9)	131.6
3'/5'	CH/CH	6.97 d (8.9)	116.8
4'	C	-	161.4
3-OCH$_3$	CH$_3$	3.76 s	61.0

[a] Resonances were assigned by the help of HMBC experiment.
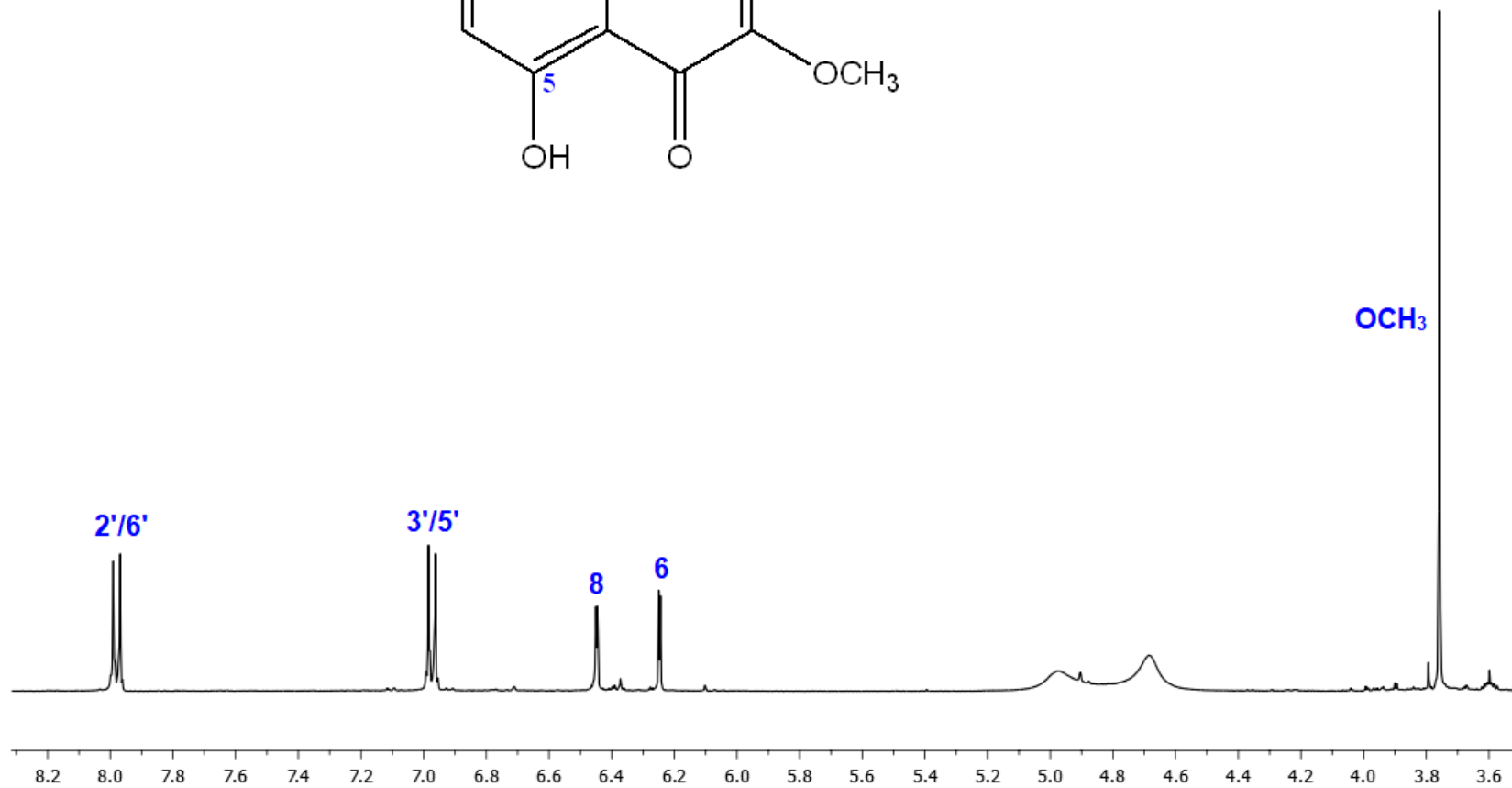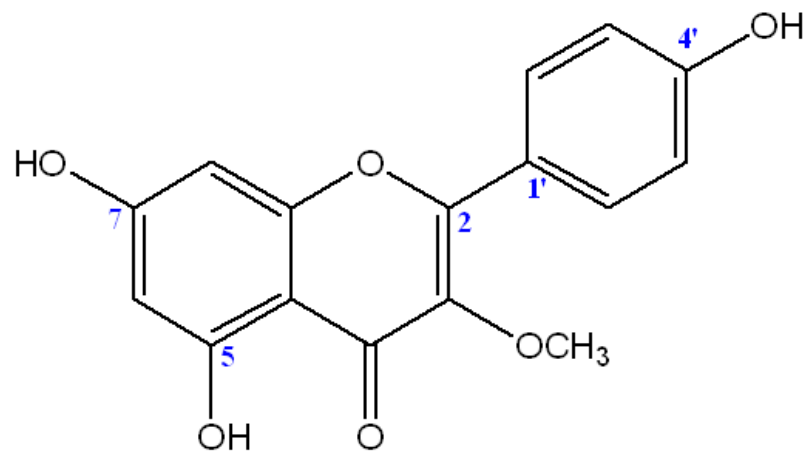
Spectrum 19. ^{1}H NMR Spectrum of 3-*O*-methylkaempferol (**8**) (CD$_3$OD, 400 MHz)
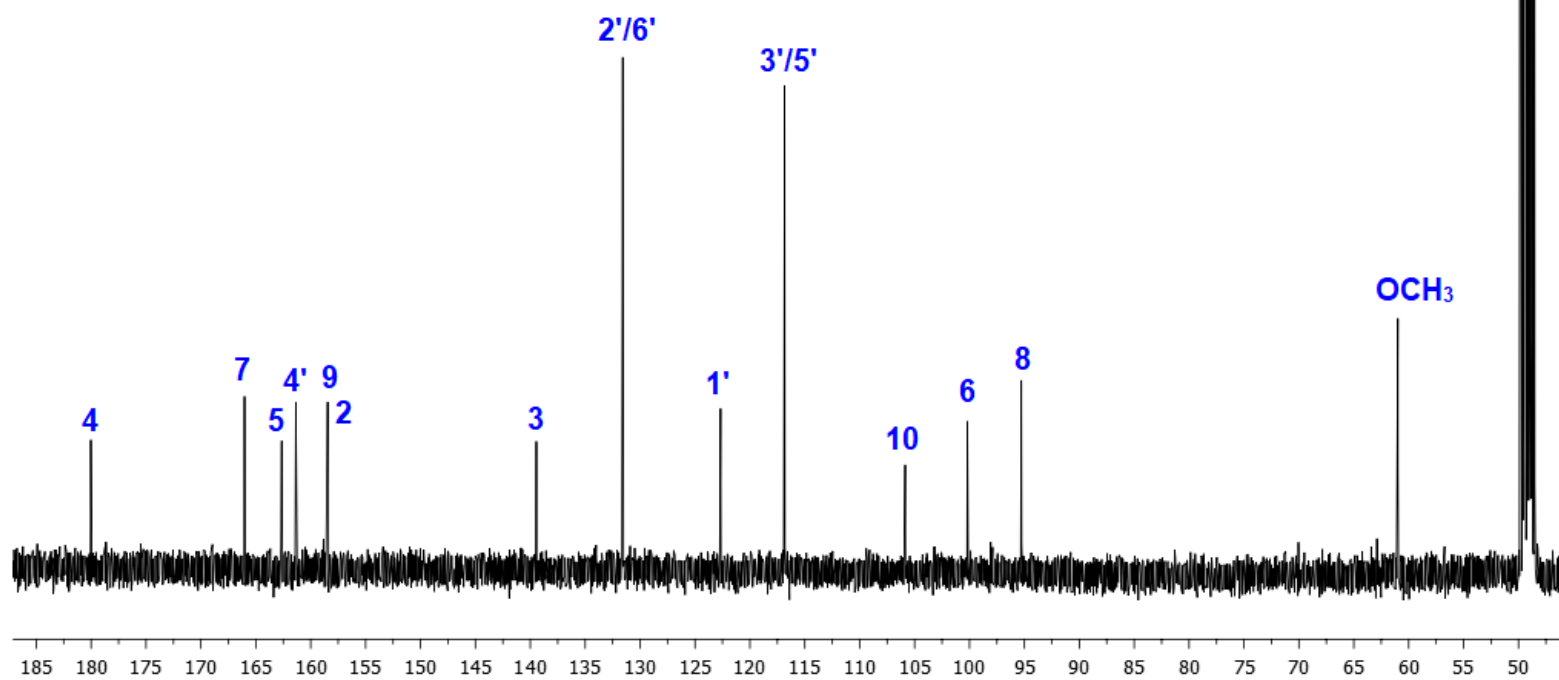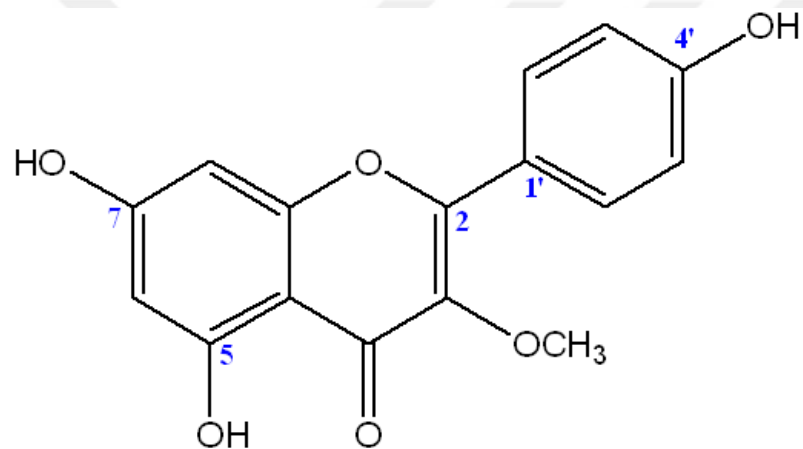
Spectrum 20. ^{13}C NMR Spectrum of 3-*O*-methylkaempferol (**8**) (CD$_3$OD, 100 MHz)
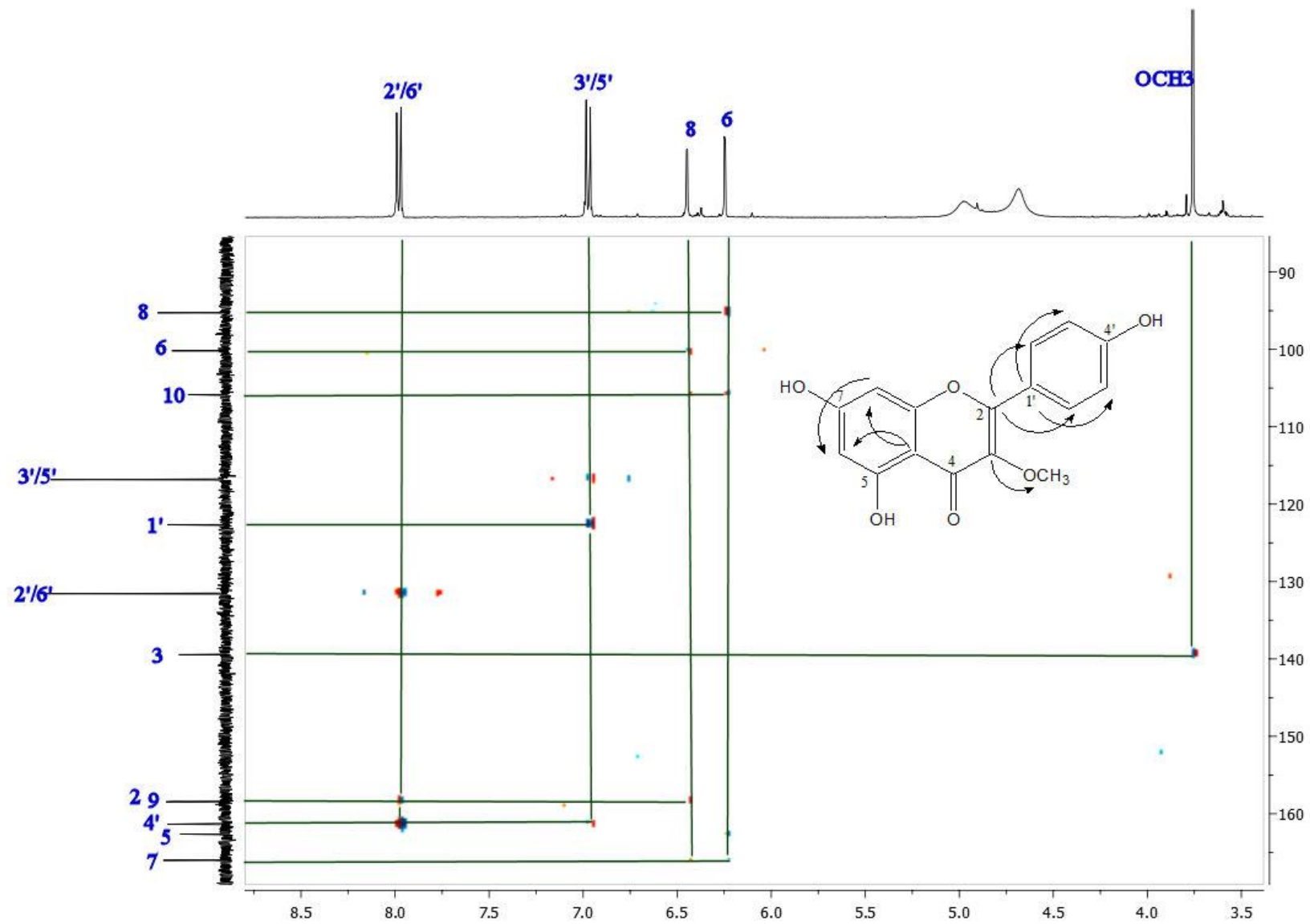
Spectrum 21. Heteronuclear 2D-^{1}H,^{13}C Correlation Spectrum (long range) of 3-*O*-methylkaempferol (**8**) (HMBC)
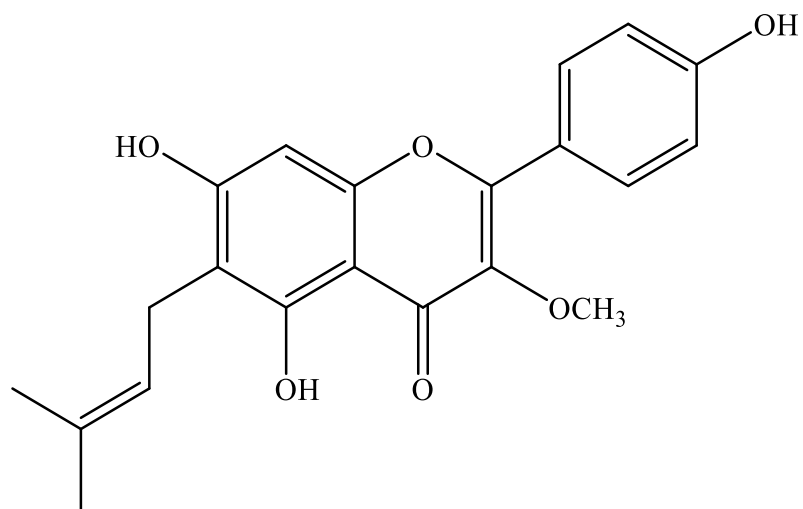
TOPAZOLIN (9): $C_{21}H_{20}O_6$ (MW: 368.39)

UV λ_{max} (MeOH) nm:	272, 336
IR υ_{max} (KBr) cm^{-1}:	3414 (OH), 1646 (γ-pyron C=O), 1609 (conjugated C=C), 1472 (aromatic ring)
^{1}H NMR:	Table 123, Spectrum 22

TOPAZOLIN (9)

Compound **9** was obtained from both EtOAc and CHCl₃ subextracts of *G. iconica* as yellow amorphous powder. The absorption bands at 272 and 336 nm were the characteristics of a flavonoid backbone. Its IR spectrum displayed bands at 3414 (OH), 1646 (γ-pyron C=O), 1609 (conjugated C=C) and 1472 (aromatic ring) cm^{-1}.

In ^{1}H NMR spectrum (Table 123, Spectrum 22), the signals at δ$_H$ 7.97 (d, J = 9.0 Hz, H-2'/6') and 6.92 (d, J = 9.0 Hz, H-3'/5') indicated a *para*-substituted benzene in ring B of flavonoid core. One isolated aromatic singlet proton signal at δ$_H$ 6.43 (H-8) in the ^{1}H NMR spectrum elicited 5,6,7-trisubstitution in ring A. Absence of singlet proton signal of H-3 at around 6.60 ppm revealed the structure of **9** as a flavon-3-ol. Moreover, proton resonances at δ$_H$ 3.31 (2H, br d, J = 7.3 Hz), 5.23 (1H, m), 1.66 and 1.78 (each 3H, s) were characteristic for an isoprenyl chain. In addition, a signal at 3.76 ppm (3H, s) showed the presence of a methoxy unit. All these findings and comparasion of NMR data with published values unambigously concluded that compound **9** was 5,7,4'-trihydroxy-3-methoxy-6-prenylflavone which is known as **topazolin** (244).

Table 123. ^{1}H NMR spectroscopic data of topazolin (**9**) (CD$_3$OD, 400 MHz)

C/H atom	Multiplicity	δ_H (ppm), J (Hz)
2	C	
3	C	-
4	C	-
5	C	-
6	C	-
7	C	-
8	CH	6.43 s
9	C	-
10	C	-
1'	C	-
2'/6'	CH/CH	7.97 d (9.0)
3'/5'	CH/CH	6.92 d (9.0)
4'	C	-
1"	CH$_2$	3.31 br d (7.3)
2"	CH	5.23 m
3"	C	-
4"	CH$_3$	1.66 s
5"	CH$_3$	1.78 s
3- OCH$_3$	CH$_3$	3.76 s
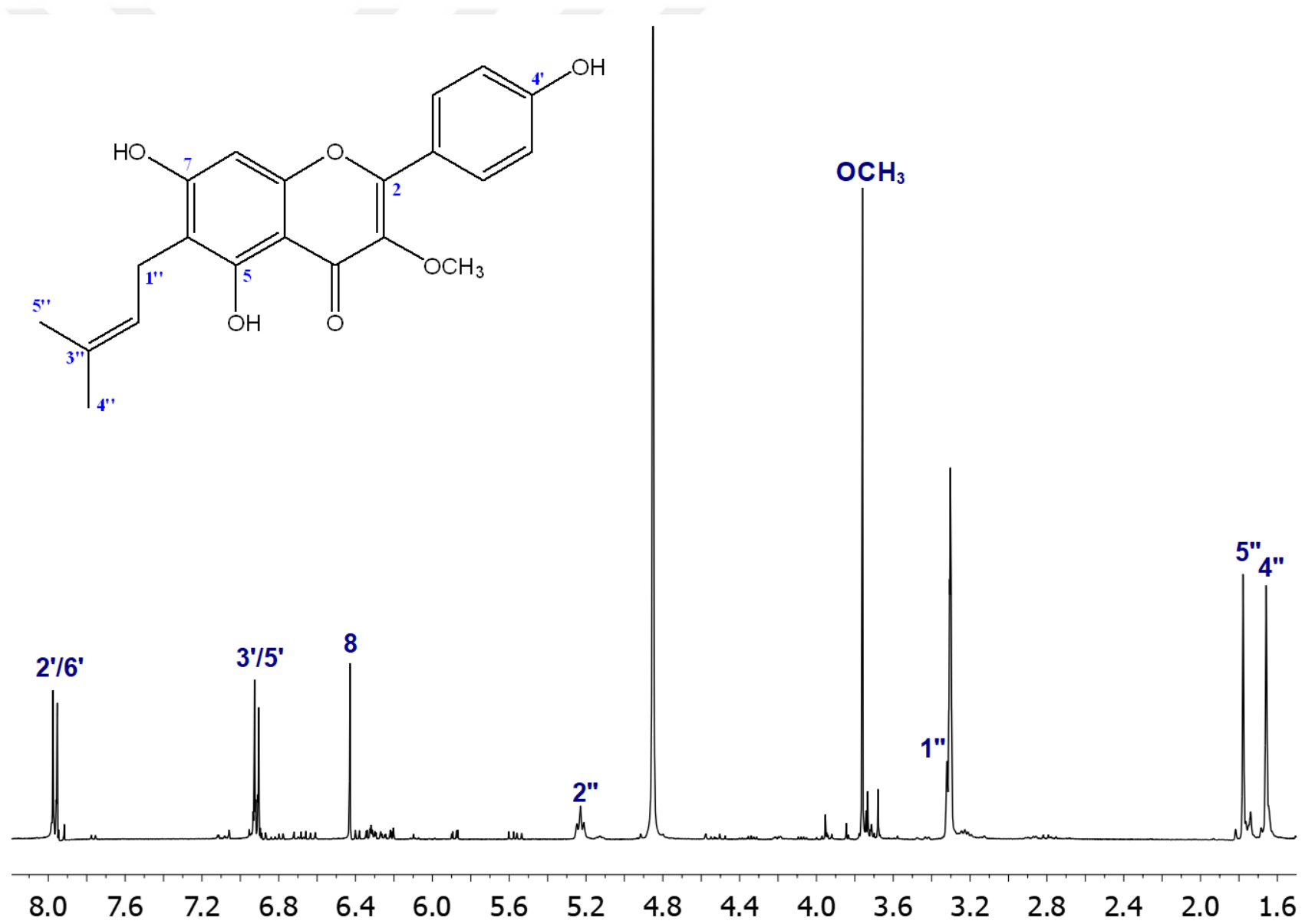
Spectrum 22. ¹H NMR Spectrum of Topazolin (**9**) (CD₃OD, 400 MHz)

4.5.1.3. Flavone
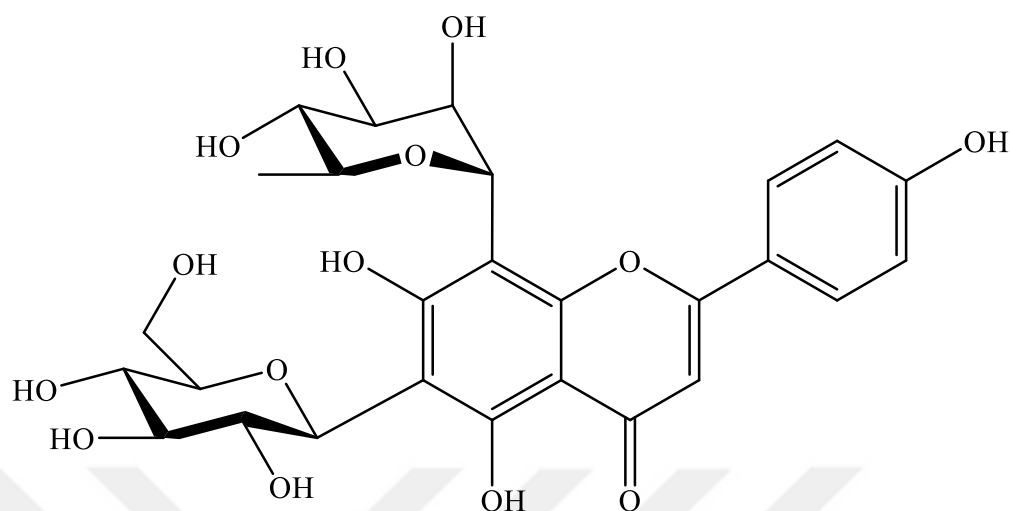
VIOLANTHIN (10): C$_{27}$H$_{30}$O$_{14}$ (MW: 578.52)

UV λ_{max} (MeOH) nm:	205 (sh), 217, 273, 334
IR υ_{max} (KBr) cm^{-1}:	3412 (OH), 1630 (γ-pyron C=O), 1579, 1511, 1448 (aromatic ring)
MS m/z:	577.8 [M-H]$^+$, 579.4 [M+H]$^+$, 601.7 [M+Na]$^+$
^{1}H NMR:	Table 124, Spectrum 23
^{13}C NMR:	Table 124, Spectrum 24
COSY:	Spectrum 25
HMBC:	Spectrum 26

VIOLANTHIN (10)

Compound **10** was obtained as yellow amorphous powder from *n*-BuOH subextract of *G. iconica.* Mass spectrum showed ion peaks at *m/z* 577.8 [M-H]+, 579.4 [M+H]+, 601.7 [M+Na]+ indicating the molecular formula of **10** as $C_{27}H_{30}O_{14}$. Characteristic absorption bands for flavonoid skeleton were observed at 205 (sh), 217, 273 and 334 nm along with IR absorption bands at 3412 (OH), 1630 (γ-pyron C=O), 1579, 1511 and 1448 (aromatic ring) cm⁻¹.

Inspection of ^{1}H NMR spectrum (Table 124, Spectrum 23) of compound **10** led to the assignment of resonances at δ_H 7.97 (d, *J* = 9.0 Hz, H-2'/6') and 6.92 (d, *J* = 9.0 Hz, H-3'/5') arising from a *para*-substituted B ring system. In addition, olefinic singlet proton signal at δ_H 6.50 (H-3) together with the corresponding carbon resonance (Table 124, Spectrum 24) appeared at δ_C 103.5 (C-3) were consistent with a 5,6,7,8,4'-pentasubstituted flavone skeleton as aglycone. Moreover, two anomeric proton signals were detected at 5.01 (d, *J* = 9.8, H-1") and 5.16 (br s, H-1''') indicating two sugar molecules were attached to flavone. The anomeric carbon resonances were found to be at δ_C 75.8 (C-1") and 77.3 (C-1''') which were chemically shifted to upfield, and the proton resonances arising from protons of second carbon atoms (H-2" and H-2''') of sugar moieties were shifted to downfield when compared to *O*-glycosylated sugars. These findings demonstrated that both sugar units were directly bonded to aglycone through C-C bonds. The ^{13}C NMR signal at δ_C 107.9 was assigned to be the carbon atom of the C-6, while carbon resonance at δ_C 105.6 was ascribed to C-8 which proposed a 6,8-di-*C*-glycosyl apigenin structure together with above findings. The large coupling constant of the anomeric proton signal at 5.01 ppm (*J* = 9.8 Hz, H-1") along with the other signals between 4.10-3.40 ppm suggested that one of the sugar moiety was *β*-glucopyranose. Another anomeric proton signal at 5.16 ppm (br s, H-1''') and secondary methyl resonance at δ_H 1.38 (3H, d, *J* = 5.9 Hz) and carbon signal at δ_C 18.5 elicited the other sugar molecule as *α*-rhamnose. COSY spectrum (Spectrum 25) secured the other proton resonances of sugar molecules. According to HMBC experiment (Spectrum 26), the long range correlations from C-8 (δ_C 105.6) to H-1''' (δ_H 5.16) placed *α*-rhamnose moiety at C-8 which consequently indicated that *β*-glucopyranose was attached to C-6. All the spectral data were compared with those published and the structure of the compound **10** was elucidated as apigenin-6-C-*β*-glucopyranosyl-8-C-*α*-rhamnopyranoside, namely **violanthin** (245).

Table 124. ^{1}H NMR spectroscopic data of violanthin (**10**) (CD$_3$OD, ^{1}H: 400 MHz, ^{13}C: 100 MHz)

C/H atom	Multiplicity	δ$_H$ (ppm), J (Hz)	δ$_C$ (ppm)
Aglycone			
2	C	-	166.2
3	CH	6.50 s	103.5
4	C	-	184.1
5	C	-	157.2
6	C	-	107.9
7	C	-	162.9
8	C	-	105.6
9	C	-	162.9
10	C	-	103.5
1'	C	-	123.4
2'/6'	CH/CH	7.97 d (9.0)	130.1
3'/5'	CH/CH	6.92 d (9.0)	117.0
4'	C	-	159.1
Glucose			
1"	CH	5.01 d (9.8)	75.8
2"	CH	4.10 t (9.8, 9.1)	72.4
3"	CH	3.51 t (9.1)	82.9
4"	CH	3.40 - 3.50 †	73.0
5"	CH	3.40 - 3.50 †	80.3
6"	CH$_2$	3.93 dd (12.0, 1.9) 3.77 dd (12.0, 5.4)	63.2
Rhamnose			
1'''	CH	5.16 br s	77.3
2'''	CH	4.05 br d (2.5)	73.8
3'''	CH	3.60 dd (2.5, 9.0)	75.3
4'''	CH	3.40-3.50 †	73.5
5'''	CH	3.40-3.50 †	78.9
6'''	CH$_3$	1.38 d (5.9)	18.5

[a] Resonances were assigned by the help of COSY and HMBC experiments. †: Overlapping signals
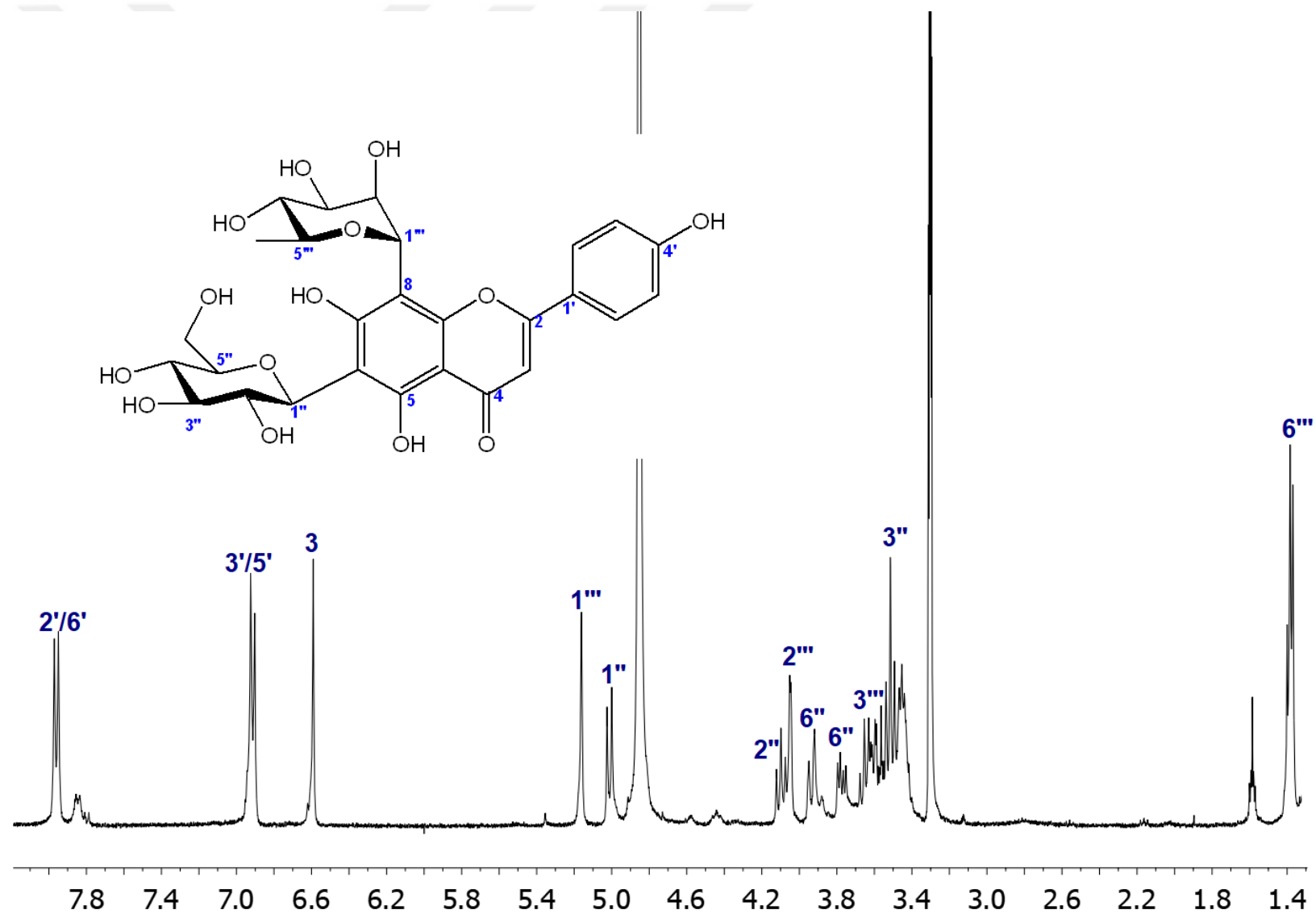
Spectrum 23. ^{1}H NMR Spectrum of Violanthin (**10**) (CD$_3$OD, 400 MHz)
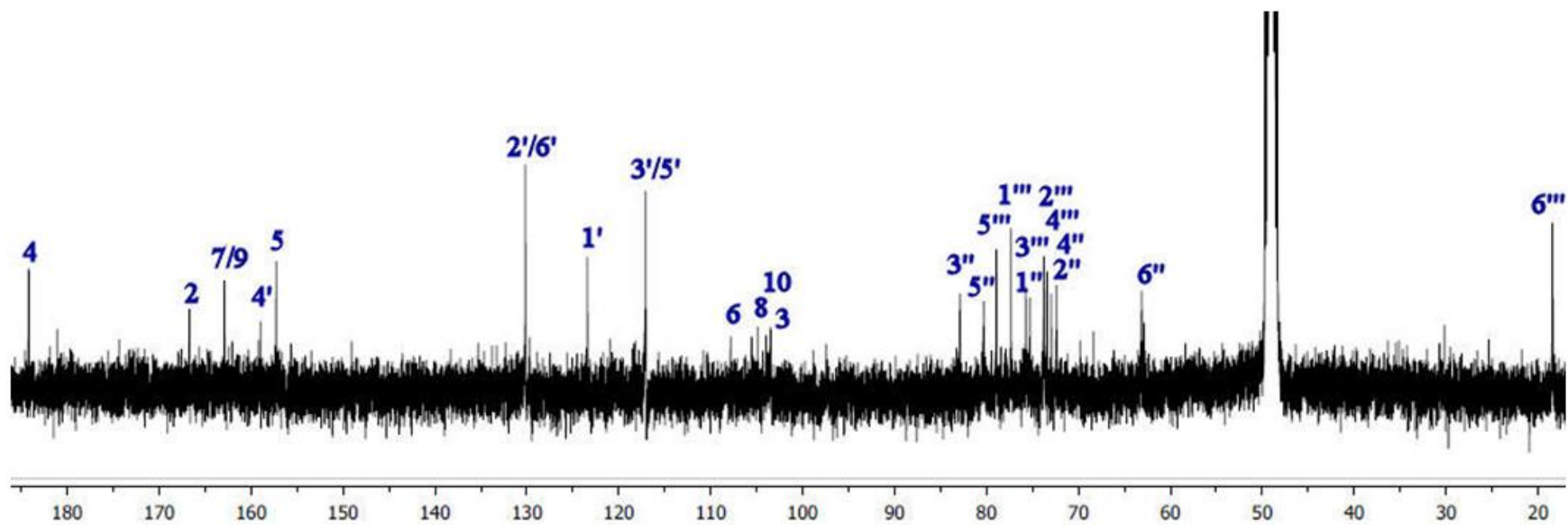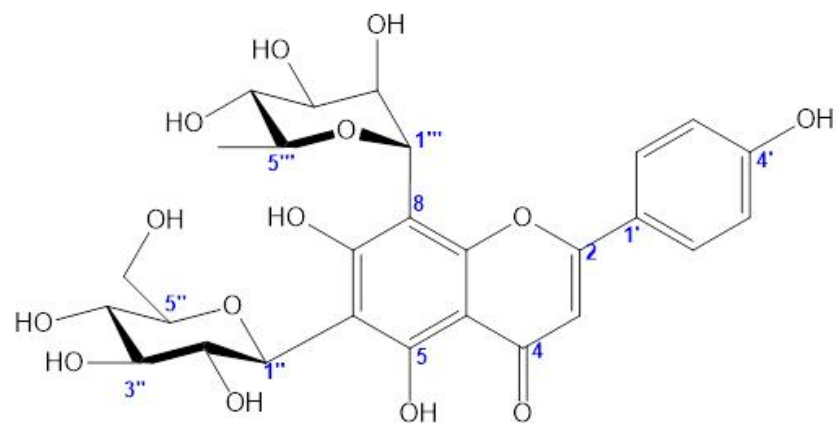
Spectrum 24. ^{13}C NMR Spectrum of Violanthin (**10**) (CD$_3$OD, 100 MHz)
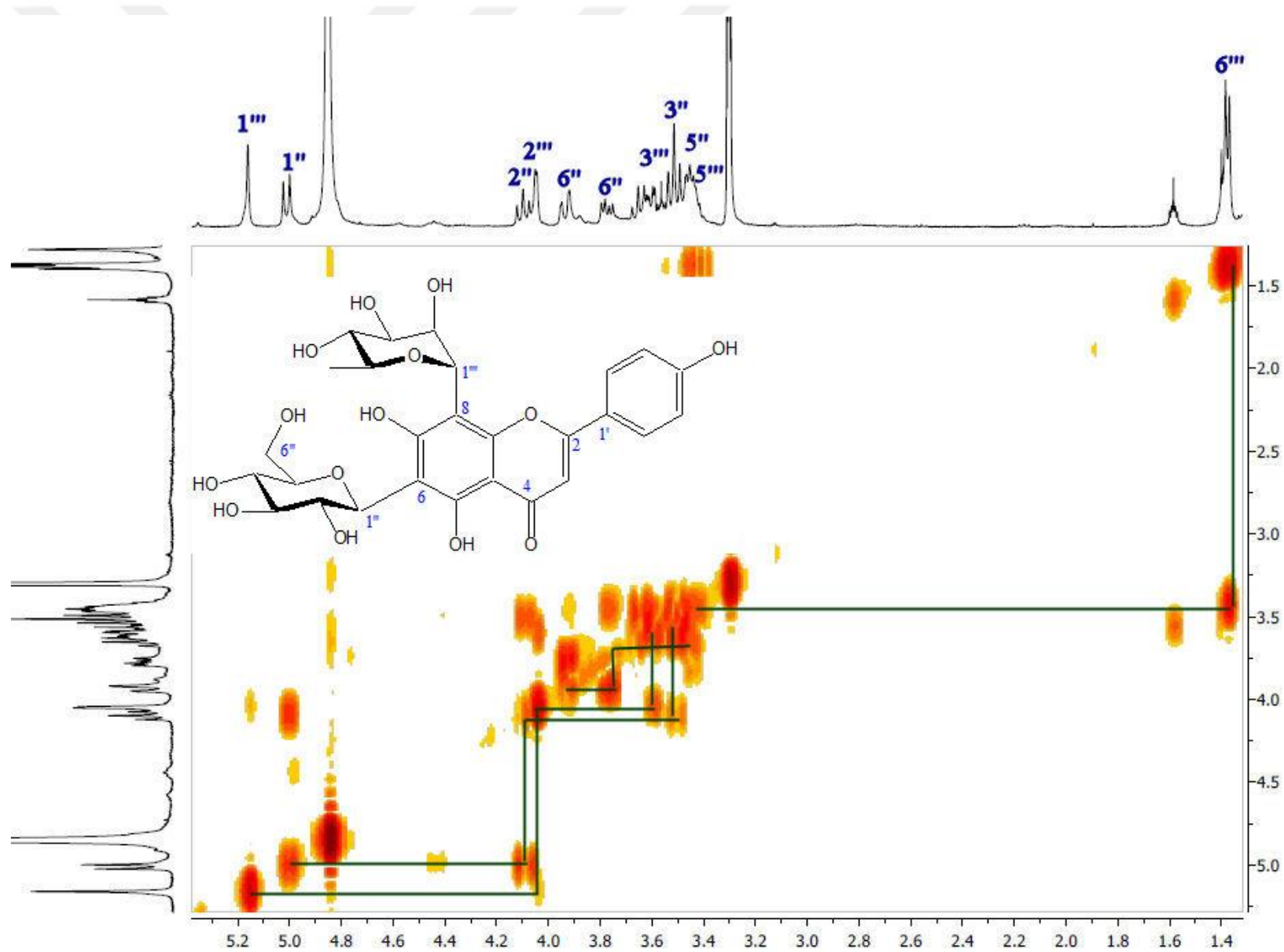
Spectrum 25. 2D-^{1}H,^{1}H-Homonuclear Correlation Spectrum (COSY) of Violanthin (**10**)
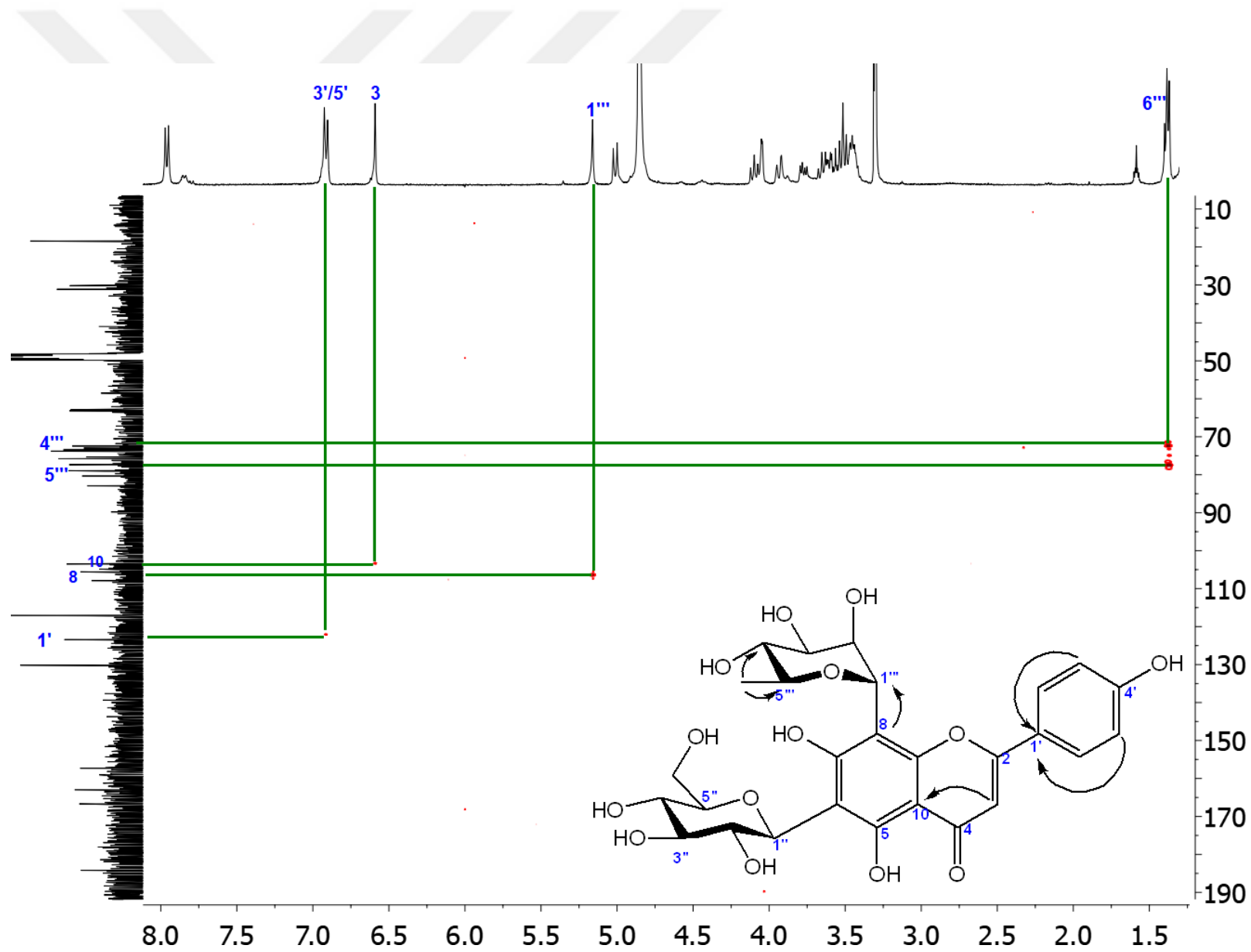
Spectrum 26. Heteronuclear 2D-^{1}H,^{13}C Correlation Spectrum (long range) of Violanthin (**10**) (HMBC)

4.5.1.4. Flavanones
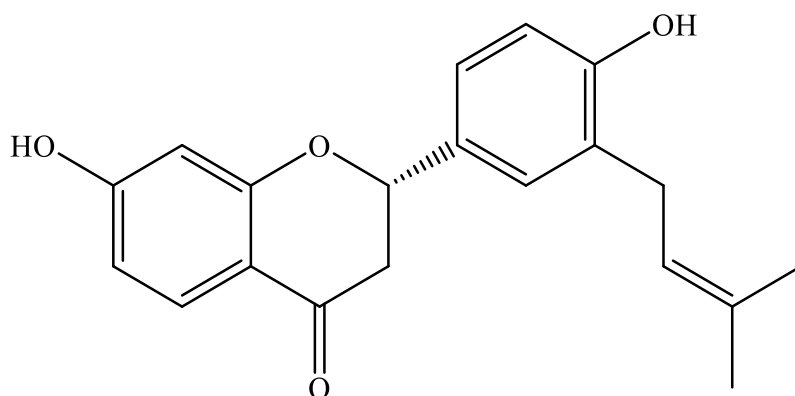
ABYSSINONE II (11): $C_{20}H_{20}O_4$ (MW: 324.38)

UV λ_{max} (MeOH) nm:	277, 313
IR υ_{max} (KBr) cm^{-1}:	3399 (OH), 1606 (C=O), 1511, 1462 (aromatic ring)
^{1}H NMR:	Table 125, Spectrum 27
COSY:	Spectrum 28

ABYSSINONE II (11)

Compound **11** was isolated from $CHCl_3$ subextract of *G. glabra* as a white colored powder. Its UV spectrum exhibited bands at 277 and 313 nm, characteristic of flavanones. Its IR spectrum showed absorption bands due to hydroxyl group (3399 cm^{-1}), carbonyl group (1606 cm^{-1}) and aromatic rings (1511 and 1462 cm^{-1}).

^{1}H NMR (Table 125, Spectrum 27) spectrum of **11** displayed a methylene signal at δ_H 3.05 (dd, J = 16.9, 13.4 Hz) and 2.78 (dd, J = 16.9 and 2.8 Hz) in addition to an oxymethine signal at δ_H 5.36 (dd, J = 13.4, 2.8 Hz). Moreover, six aromatic proton resonances were detected as ABX systems. One of the ABX system signals were observed at δ_H 7.85 (d, J = 8.6 Hz), 6.53 (dd, J = 8.6, 2.4 Hz) and 6.44 (d, J = 2.4 Hz) which were the typical signals for 7-monosubstituted A ring and ascribed to H-5, H-6 and H-8, respectively. The other ABX type proton signals were seen at δ_H 7.24 (†),7.20 (br s) and 6.85 (d, J = 8.0 Hz), suggesting a 3,4-disubstitution in B ring. All these above mentioned findings were consistent with an 7,3',4'-trisubstituted flavanone core. Additional signals arising from an isoprenyl moiety were detected [δ_H 3.38 (br d, J = 7.2 Hz, H_2-1''), 5.25 (m, H-2'') and 1.78 (6H, s, H-4''/5'')]. COSY (Spectrum 28) experiment was conducted to confirm the structure which contained four spin systems between H-5/H-6, H-5'/H-6', H-2/H-3 as well as between H-1''/H-2''. Taken together, the exact chemical structure of compound **11** was deduced to be 7,4'-dihydroxy-3'-prenylflavanone, namely **abyssinone II** by comparing the NMR data with those of published in the literature (246).

Table 125. ^{1}H NMR spectroscopic data of abyssinone II (**11**) (CDCl$_3$, 400 MHz)[a]

C/H atom	Multiplicity	δ_H (ppm), J (Hz)
2	CH	5.36 dd (13.4, 2.8)
3	CH$_2$	3.05 dd (16.9, 13.4)
		2.78 dd (16.9, 2.8)
4	C	-
5	CH	7.85 d (8.6)
6	CH	6.53 dd (8.6, 2.4)
7	C	-
8	CH	6.44 d (2.4)
9	C	-
10	C	-
1'	C	-
2'	CH	7.20 br s
3'	C	-
4'	C	-
5'	CH	6.85 d (8.0)
6'	CH	7.24 †
1"	CH$_2$	3.38 br d (7.2)
2"	CH	5.25 m
3"	C	-
4"	CH$_3$	1.78 s
5"	CH$_3$	1.78 s

[a] Resonances were assigned by the help of COSY experiment.
†: Overlapping signals
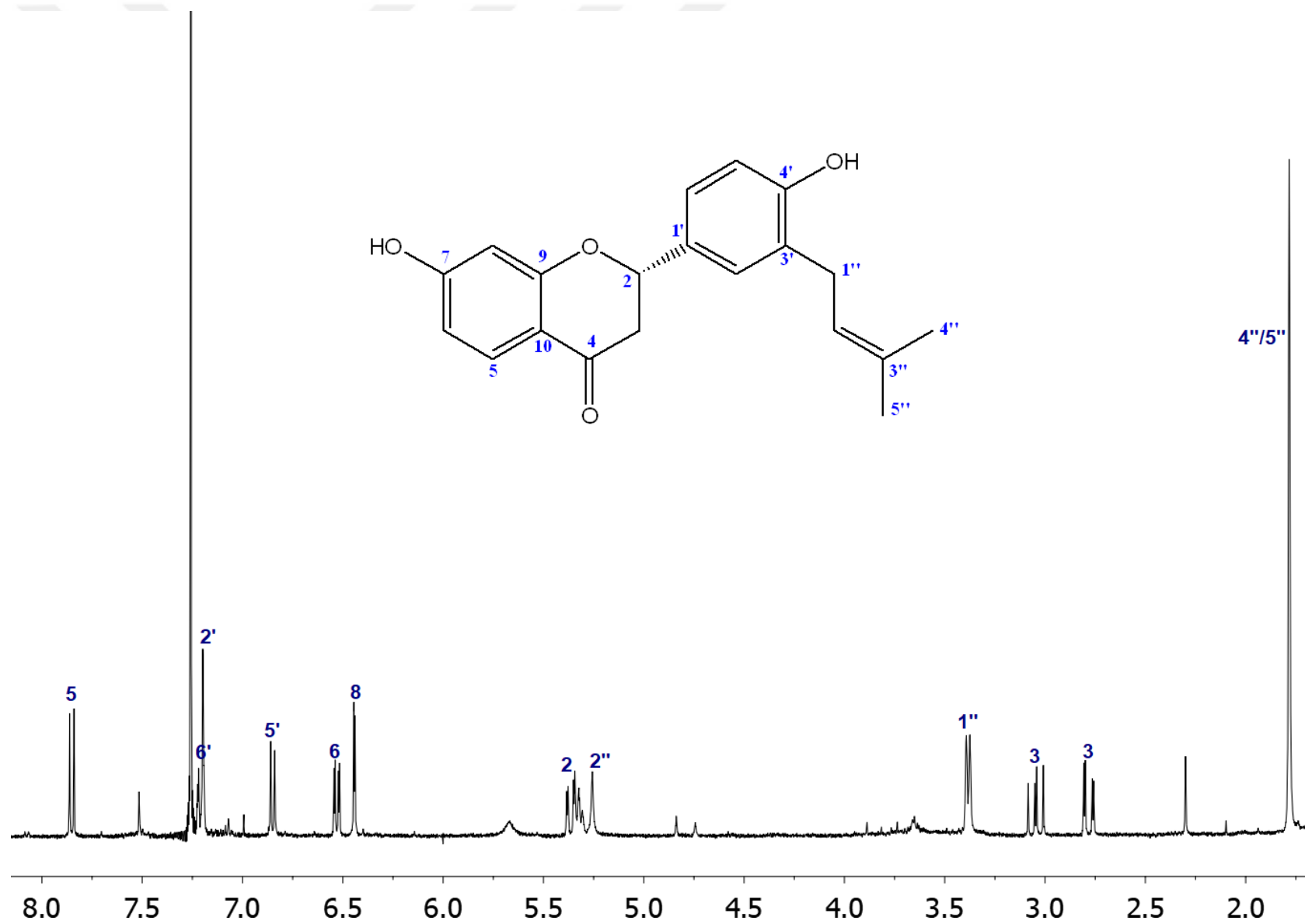
Spectrum 27. ^{1}H NMR Spectrum of Abyssinone II (**11**) (CDCl$_3$, 400 MHz)
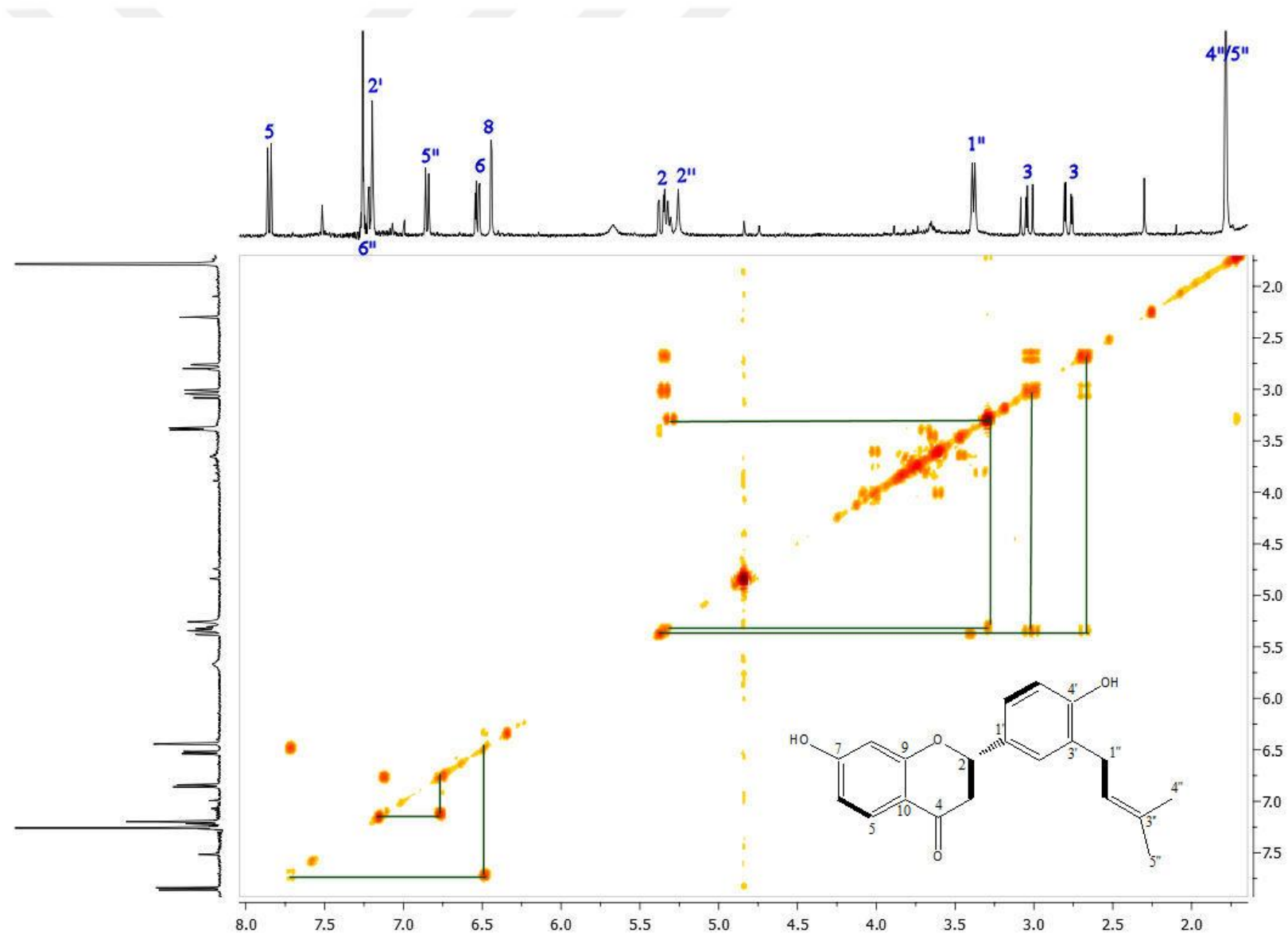
Spectrum 28. 2D-^{1}H,^{1}H-Homonuclear Correlation Spectrum (COSY) of Abyssinone II (**11**)
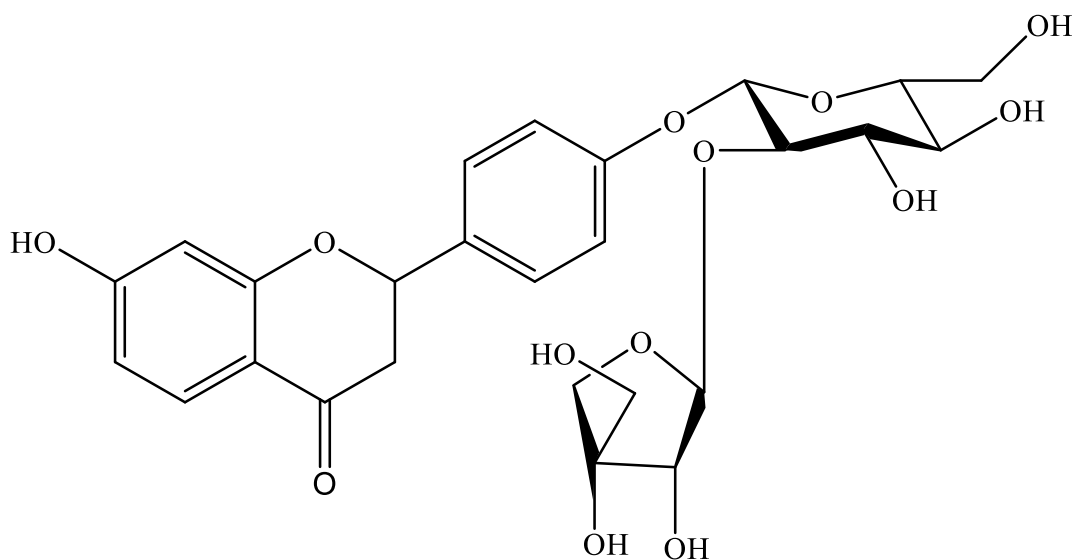
LIQUIRITIN APIOSIDE (13): C$_{26}$H$_{30}$O$_{13}$ (MW: 550.513)

UV λ_{max} (MeOH) nm:	350
IR υ_{max} (KBr) cm^{-1}:	3428 (OH), 1617 (C=O), 1511 (aromatic ring)
HR-ESI-MS *m/z*:	573.1579 [M+Na]$^+$ (calcd for C$_{26}$H$_{30}$O$_{13}$Na, 573.1584), 551.1737 [M+H]$^+$ (calcd for C$_{26}$H$_{31}$O$_{13}$, 551.1765)
^{1}H NMR:	Table 126, Spectrum 29
^{13}C NMR:	Table 126, Spectrum 30
COSY:	Spectrum 31
HSQC:	Spectrum 32
HMBC:	Spectrum 33

LIQUIRITIN APIOSIDE (13)

Compound **13** was isolated from *G. glabra* EtOAc subextract as a yellow amorphous powder. HR-ESI-MS of **13** showed pseudomolecular ion peaks at *m/z* 573.1579 [M+Na]$^+$ (calcd for $C_{26}H_{30}O_{13}Na$, 573.1584) and 551.1737 [M+H]$^+$ (calcd for $C_{26}H_{31}O_{13}$, 551.1765) that revealed the molecular formula of **13** as $C_{26}H_{30}O_{13}$. Its UV spectrum exerted band at 350 nm, whereas IR spectrum had absorption bands at 3428, 1617 and 1511 cm^{-1} indicating hydroxyl, ketone groups and aromatic ring, respectively.

^{1}H NMR spectrum of compound **13** (Table 126, Spectrum 29) showed signal of one methine bearing an oxygene function at δ_H 5.45 (dd, *J* = 12.8, 3.0 Hz) as well as methylene signals at δ_H 3.04 (dd, *J* = 16.8, 12.8 Hz) and 2.73 (dd, *J* = 16.8, 3.0 Hz). Furthermore, five aromatic signals comprising one AA'BB' and one ABX-type spin coupling systems at δ_H 7.44 (2H, d, *J* = 8.7 Hz) and 7.11 (2H, d, *J* = 8.7 Hz); δ_H 7.72 (d, *J* = 8.6 Hz), 6.49 (dd, *J* = 8.6, 2.3 Hz) and 6.36 (d, *J* = 2.3 Hz) were respectively assigned to *para*-substituted B ring and 7-monosubstituted A ring. Two anomeric proton signals were detected at δ_H 5.00 (d, *J* = 7.4 Hz) and 5.47 (d, *J* = 1.6) along with proton resonances at 4.06-3.39 ppm. From the above data, compound **13** was deduced to be a flavanone derivative with two sugar units. One of the sugar unit was identified as *β*-glucopyranose due to the anomeric proton signal at 5.00 ppm with a large coupling constant (*J* = 7.4 Hz) together with six other proton resonances between 3.39-3.89 ppm. The other sugar unit was established as an β-D-apiofuranose due to specific proton signals such as anomeric proton at δ_H 5.47 (d, *J* = 1.6 Hz, H-1''), oxymethine signal at δ_H 3.95 (d, *J* = 1.6 Hz, H-2''), oxymethylene signals at δ_H 4.06 and 3.79 (each d, *J* = 9.6 Hz, H$_2$-4'') and another oxymethylene signal at δ_H 3.54 (2H, d, *J* = 1.4 Hz, H-5''). Further two dimensional NMR experiments (COSY, HSQC and HMBC) were conducted to elucidate the exact structure of **13**. Seven spin systems were identified by 2D-^{1}H,^{1}H-Homonuclear Correlation Spectroscopy (Spectrum 31). The protons were matched with the corresponding carbon resonances (Table 126, Spectrum 30) by HSQC experiment (Spectrum 32). The connections between the subunits were unambigiously determined by HMBC experiment (Spectrum 33). Long-range correlations between C-2 and H-2'/H-6' secured the existing flavanone core. Besides, cross peaks of C-4' (δ_C 159.3) with anomeric proton signal H-1'' (δ_H 5.00) indicated the glycosylation site of aglycone. The glycosidation site of β-apiose was found to be at C-2'' (OH) of β-glucopyranose based on the long-range correlation from δ_C 110.9 (C-1''') to δ_H 3.64 (H-2'') as well as the dowfield shift of C-2'' signal around

5 ppm in ^{13}C NMR spectrum. The data were superimposible with those reported for **liquiritin apioside** in the literature (199).

Table 126. ^{1}H and ^{13}C NMR spectroscopic data of liquiritin apioside (**13**) (CD$_3$OD, ^{1}H: 400 MHz, ^{13}C: 100 MHz)[a]

C/H atom	Multiplicity	δ$_H$ (ppm), *J* (Hz)	δ$_C$ (ppm)
Aglycone			
2	CH	5.45 dd (12.8, 3.0)	80.9
3	CH$_2$	3.04 dd (16.8, 12.8) 2.73 dd (16.8, 3.0)	45.0
4	C	-	193.3
5	CH	7.72 d (8.6)	130.0
6	CH	6.49 dd (8.6, 2.3)	112.1
7	C	-	165.6
8	CH	6.36 d (2.3)	104.1
9	C	-	167.3
10	C	-	115.1
1'	C	-	134.6
2'/6'	CH/CH	7.44 d (8.7)	129.0
3'/5'	CH/CH	7.11 d (8.7)	117.8
4'	C	-	159.3
Glucose			
1"	CH	5.00 d (7.4)	101.0
2"	CH	3.64 dd (7.4, 9.2)	78.8
3"	CH	3.60 t (9.2)	78.8
4"	CH	3.39 m	71.6
5"	CH	3.44 m	78.2
6"	CH$_2$	3.89 dd (12.1, 2.0) 3.69 dd (12.1, 5.2)	62.6
Apiose			
1'''	CH	5.47 d (1.6)	110.9
2'''	CH	3.95 d (1.6)	78.2
3'''	C	-	80.8
4'''	CH$_2$	4.06 d (9.6) 3.79 d (9.6)	75.6
5'''	CH$_2$	3.54 d (1.4)	66.2

[a] Resonances were assigned by the help of 2D NMR (COSY, HSQC and HMBC) techniques.
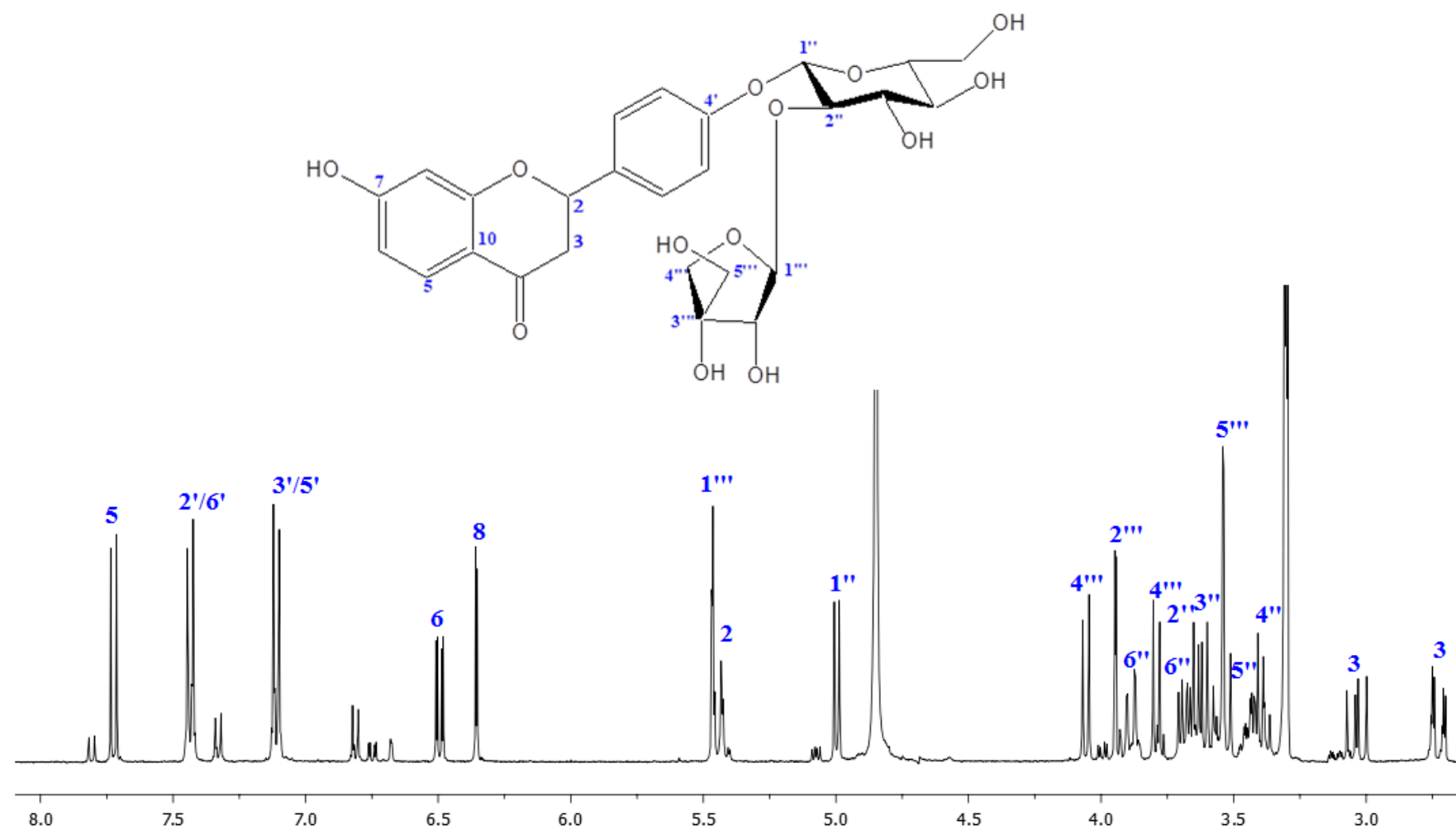
Spectrum 29. ^{1}H NMR spectrum of Liquiritin apioside (**13**) (CD$_3$OD, 400 MHz)
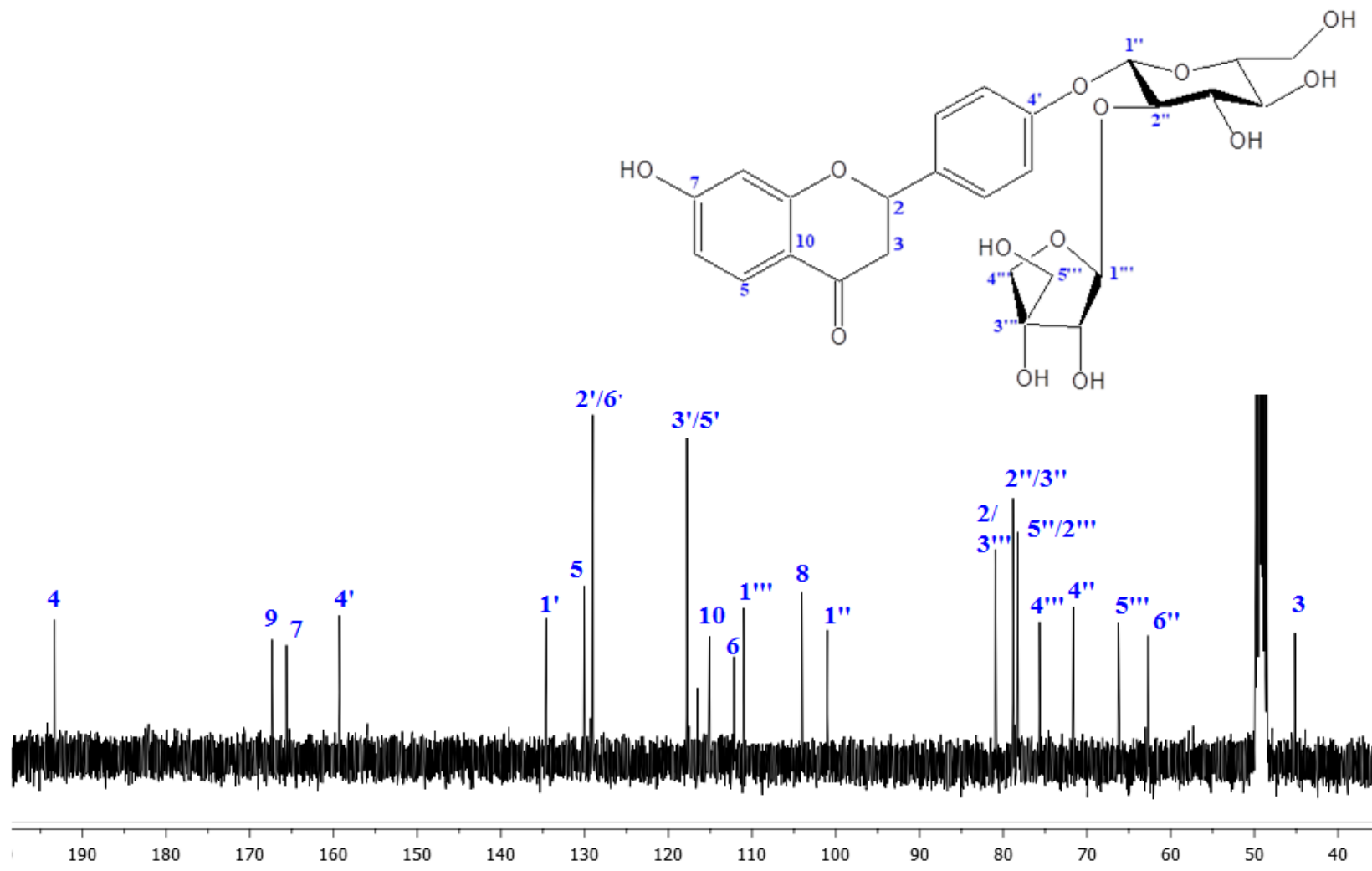
Spectrum 30. ^{13}C NMR spectrum of Liquiritin apioside (**13**) (CD$_3$OD, 100 MHz)
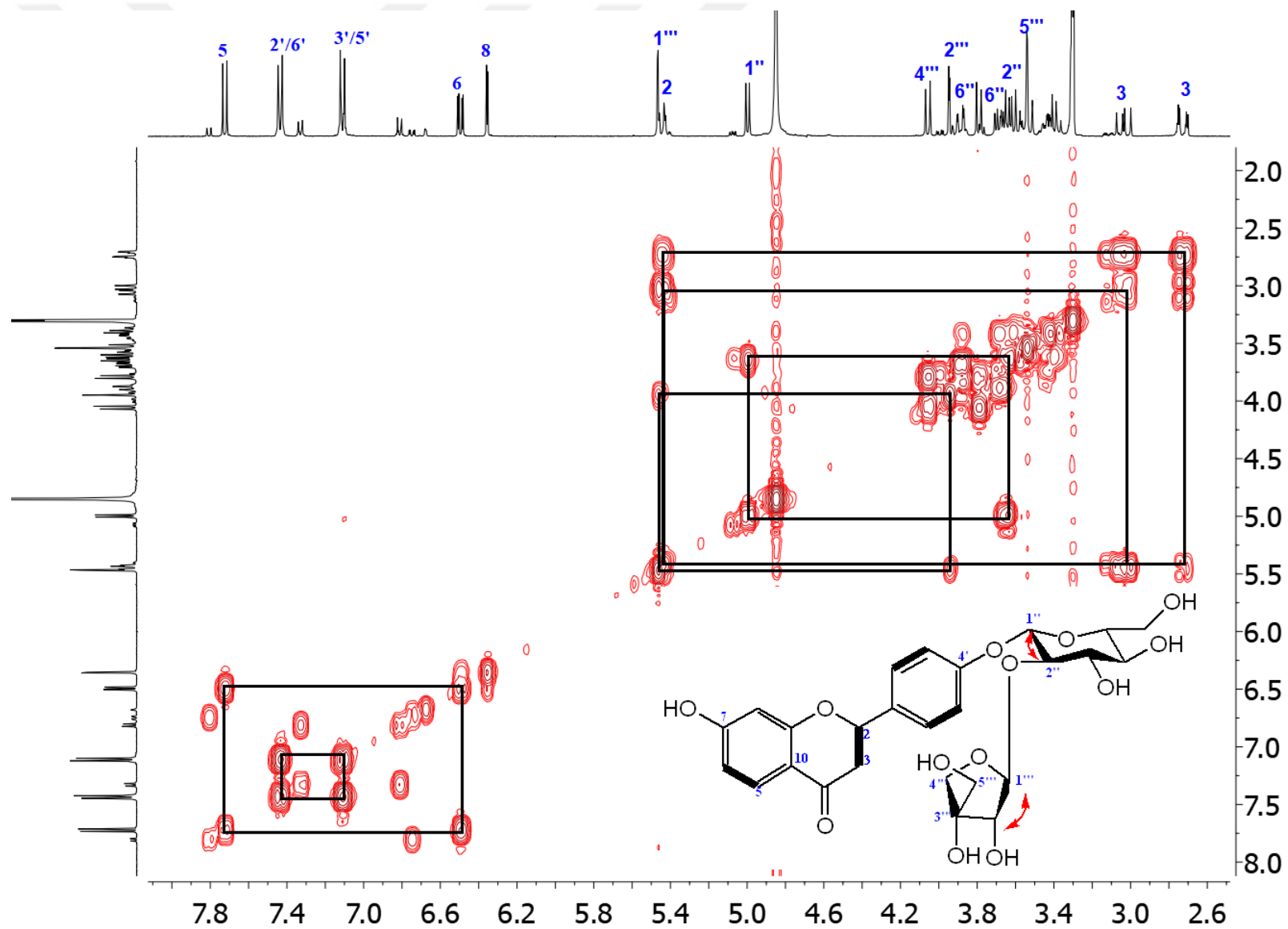
Spectrum 31. 2D-^{1}H,^{1}H-Homonuclear Correlation Spectrum (COSY) of Liquiritin apioside (**13**)
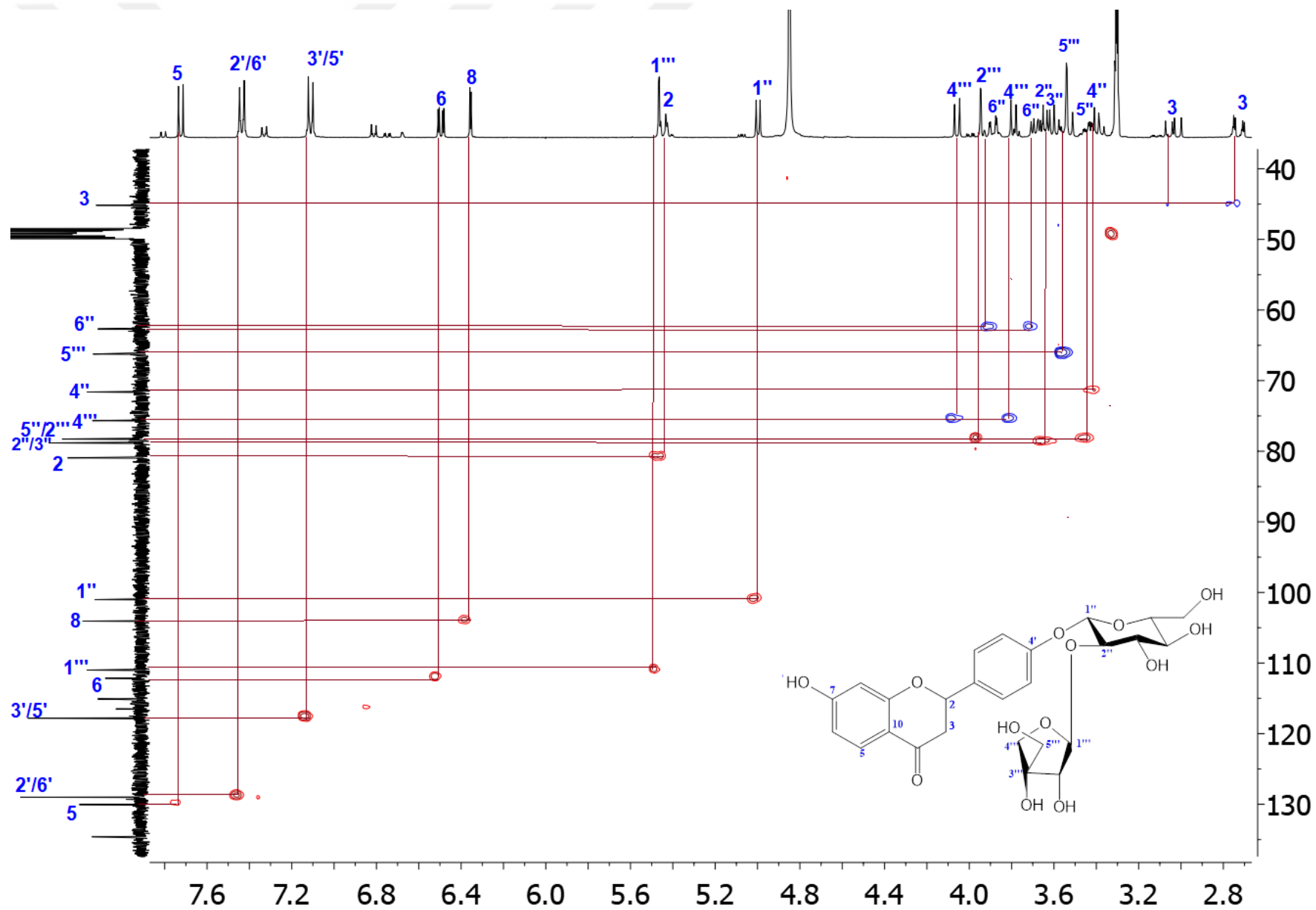
Spectrum 32. Heteronuclear 2D-^{1}H,^{13}C Correlation Spectrum (short range) of Liquiritin apioside (**13**) (HSQC)
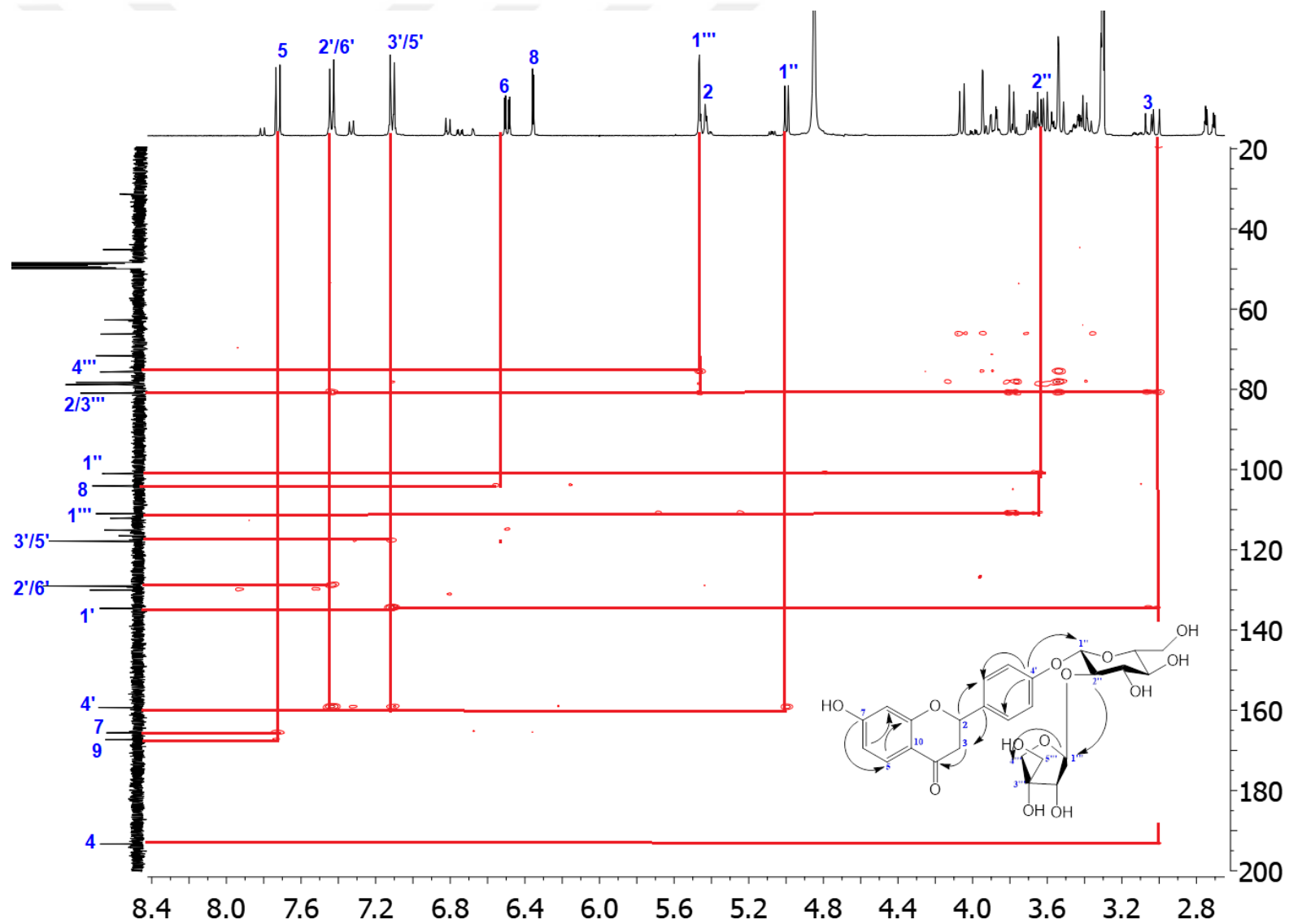
Spectrum 33. Heteronuclear 2D-^{1}H,^{13}C Correlation Spectrum (long range) of Liquiritin apioside (**13**) (HMBC)

4.5.1.5. Isoflavones
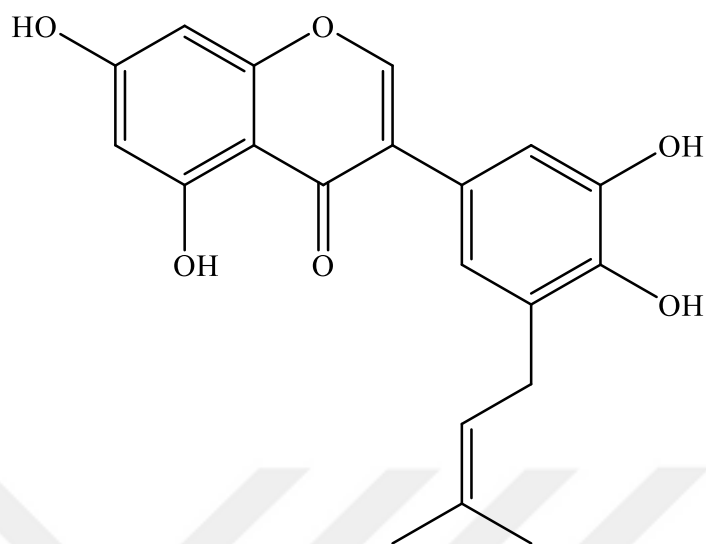
GLYCYRRHISOFLAVONE (14): $C_{20}H_{18}O_6$ (MW: 354.36)

UV λ_{max} (MeOH) nm:	263
IR υ_{max} (KBr) cm^{-1}:	3358 (OH), 1630 (γ-pyron C=O), 1578, 1541, 1472 (aromatic ring)
HR-ESI-MS m/z:	355.1175 [M+H]$^+$ (calcd for $C_{20}H_{19}O_6$, 355.1182)
^{1}H NMR:	Table 127, Spectrum 34
^{13}C NMR:	Table 127, Spectrum 35
COSY:	Spectrum 36
HSQC:	Spectrum 37
HMBC:	Spectrum 38
NOESY:	Spectrum 39

GLYCYRRHISOFLAVONE (14)

Compound **14**, an amorphous yellowish powder, obtained from EtOAc subetract of *G. iconica*. Based on the ion peaks at *m/z* 355.1175 [M+H]$^+$ (calcd for $C_{20}H_{19}O_6$, 355.1182) in HR-ESI-MS, the molecular formula was elucidated as $C_{20}H_{18}O_6$ (MW: 354.36). Compound **14** showed absorption maxima bands at 263 nm in UV spectrum. The IR spectrum suggested the presence of hydroxyl (3358 cm^{-1}), γ-pyrone C=O (1630 cm^{-1}) and aromatic rings (1578, 1541 and 1472 cm^{-1}).

The main core of compound **14** was deduced to be an isoflavone by presence of a sharp singlet at δ_H 7.99 in ^{1}H NMR spectrum (Table 127, Spectrum 34) and corresponding carbon signal at δ_C 154.7 as well as presence of a ketone signal (δ_C 182.3) in ^{13}C NMR spectrum (Table 127, Spectrum 35) and aromatic proton resonances. Two pairs of *meta*-coupled proton signals at δ_H 6.21 (d, *J* = 2.1 Hz, H-6) / 6.32 (d, *J* = 2.1 Hz, H-8) and 6.71 (d, *J* = 2.1 Hz, H-2') / 6.86 (d, *J* = 2.1 Hz, H-6') were assigned to 5,7-disubstituted A ring and 3,4,5-trisubstituted B ring, respectively. Additional signals arising from an isoprenyl moiety were detected in ^{1}H NMR spectrum at δ_H 3.33 (br d, *J* =7.4 Hz), 5.33 (m) and two overlapped methyl signals at 1.72 ppm (each 3H, s). Corresponding carbon resonances were elucidated by HSQC experiments (Spectrum 37). COSY spectrum (Spectrum 36) revelaed the spin system between protons of isoprenyl unit (H-1''/H-2''/H4''-5''). The attachment site of isoprenyl moiety as well as the interfragmental connections were determined by the help of HMBC (Spectrum 38) and NOESY (Spectrum 39) experiments. The long-range couplings of C-4' (δ_C 144.7), C-5' (δ_C 129.7) and C-6' (δ_C 122.2) with methylene protons of prenyl unit (δ_H 3.33, H-1'') led the location of isoprenyl unit to be at C-5' in ring B. Furthermore, ^{13}C/^{1}H correlations of C-9 (δ_C 159.7) and C-1' (δ_C 123.0) with H-2 (δ_H 7.99, s) as well as correlations from C-3 (δ_C 125.2) to H-6' (δ_H 6.71) helped us determine the structure as depicted. NOESY spectrum contained cross peaks between H-2/H-2', H-2/H-6', H-6'/H-1'' and H-1''/H-2'' secured the final structure of compound unambigously as 5,7,3',4'-tetrahydroxy-5'-prenylisoflavone, which is known as **glycyrrhisoflavone** (150).

Table 127. ^{1}H and ^{13}C NMR spectroscopic data of glycyrrhisoflavone (**14**) (CD$_3$OD, ^{1}H:400 MHz, ^{13}C:100 MHz)[a]

C/H atom	Multiplicity	δ$_H$ (ppm), J (Hz)	δ$_C$ (ppm)
2	CH	7.99 s	154.7
3	C	-	125.2
4	C	-	182.3
5	C	-	166.2
6	CH	6.21 d (2.1)	100.2
7	C	-	163.9
8	CH	6.32 d (2.1)	94.8
9	C	-	159.7
10	C	-	106.2
1'	C	-	123.0
2'	CH	6.86 d (2.1)	114.8
3'	C	-	145.9
4'	C	-	144.7
5'	C	-	129.7
6'	CH	6.71 d (2.1)	122.2
1"	CH$_2$	3.33 br d (7.4)	29.3
2"	CH	5.33 m	124.0
3"	C	-	132.9
4"	CH$_3$	1.72 s	17.9
5"	CH$_3$	1.72 s	25.9

[a] Resonances were assigned by the help of 2D NMR (COSY, HSQC, HMBC and NOESY) techniques.
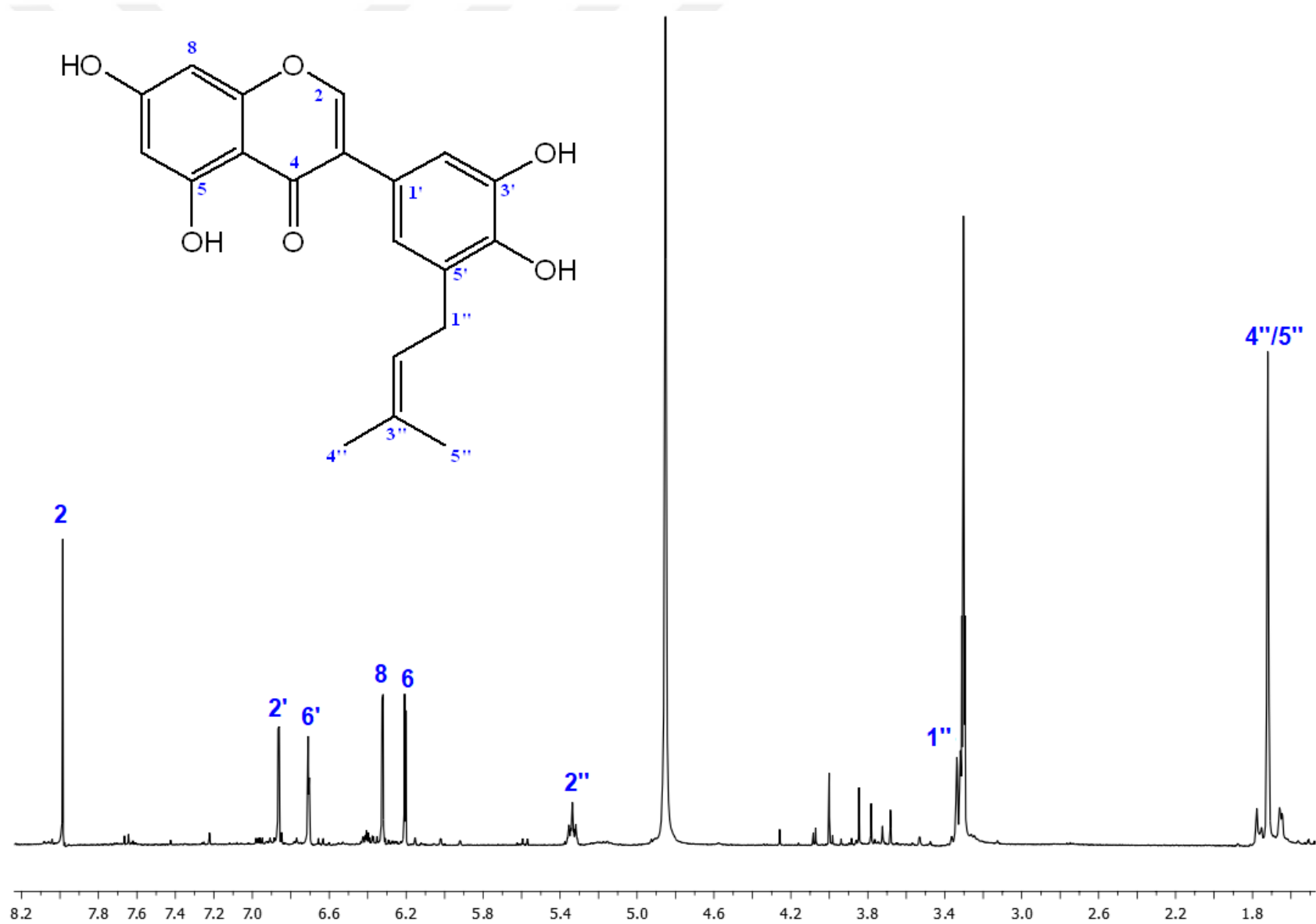
Spectrum 34. ^{1}H NMR Spectrum of Glycyrrhisoflavone (**14**) (CD$_3$OD, 400 MHz)
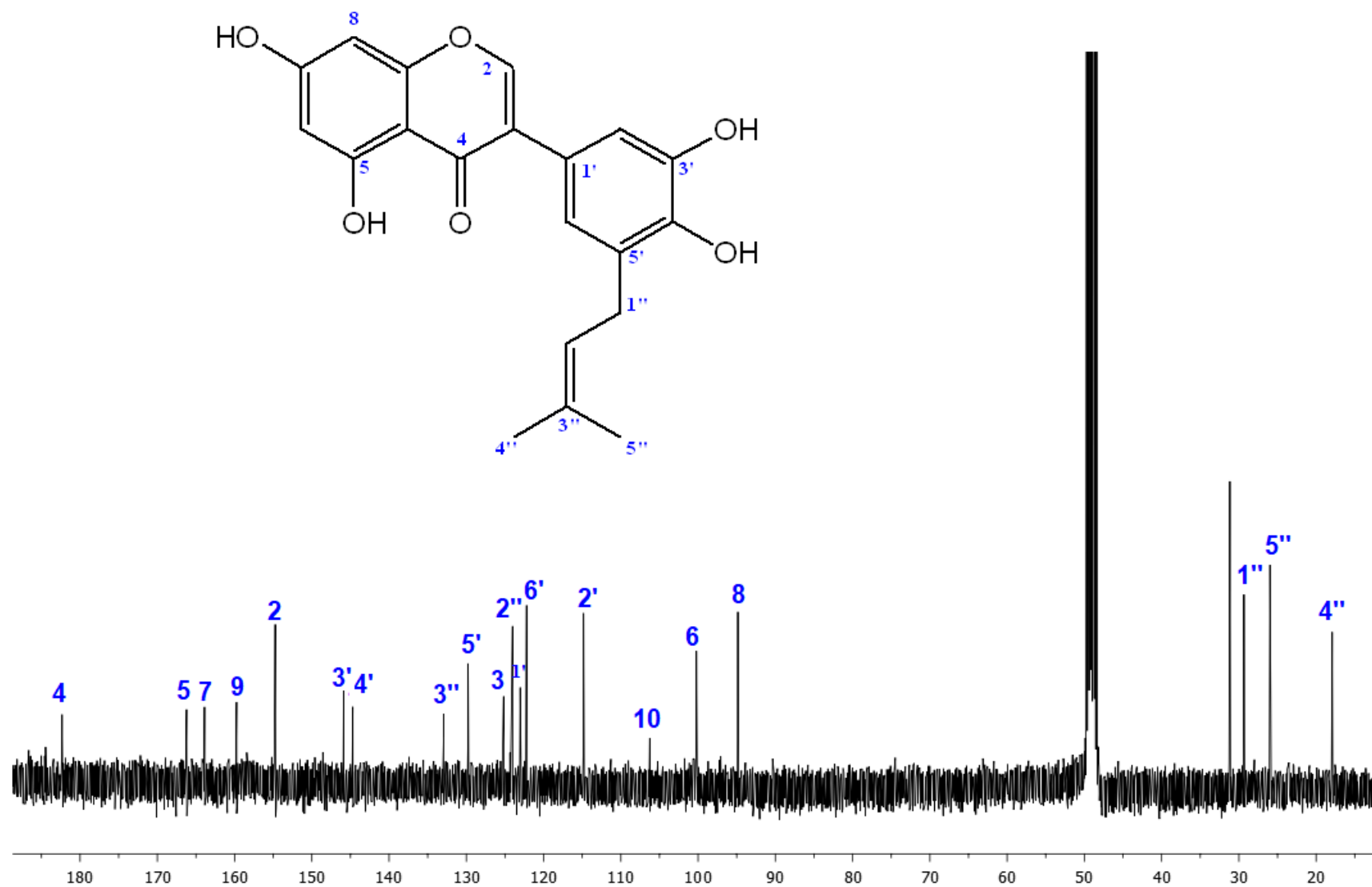
Spectrum 35. ^{13}C NMR Spectrum of Glycyrrhisoflavone (**14**) (CD$_3$OD, 100 MHz)
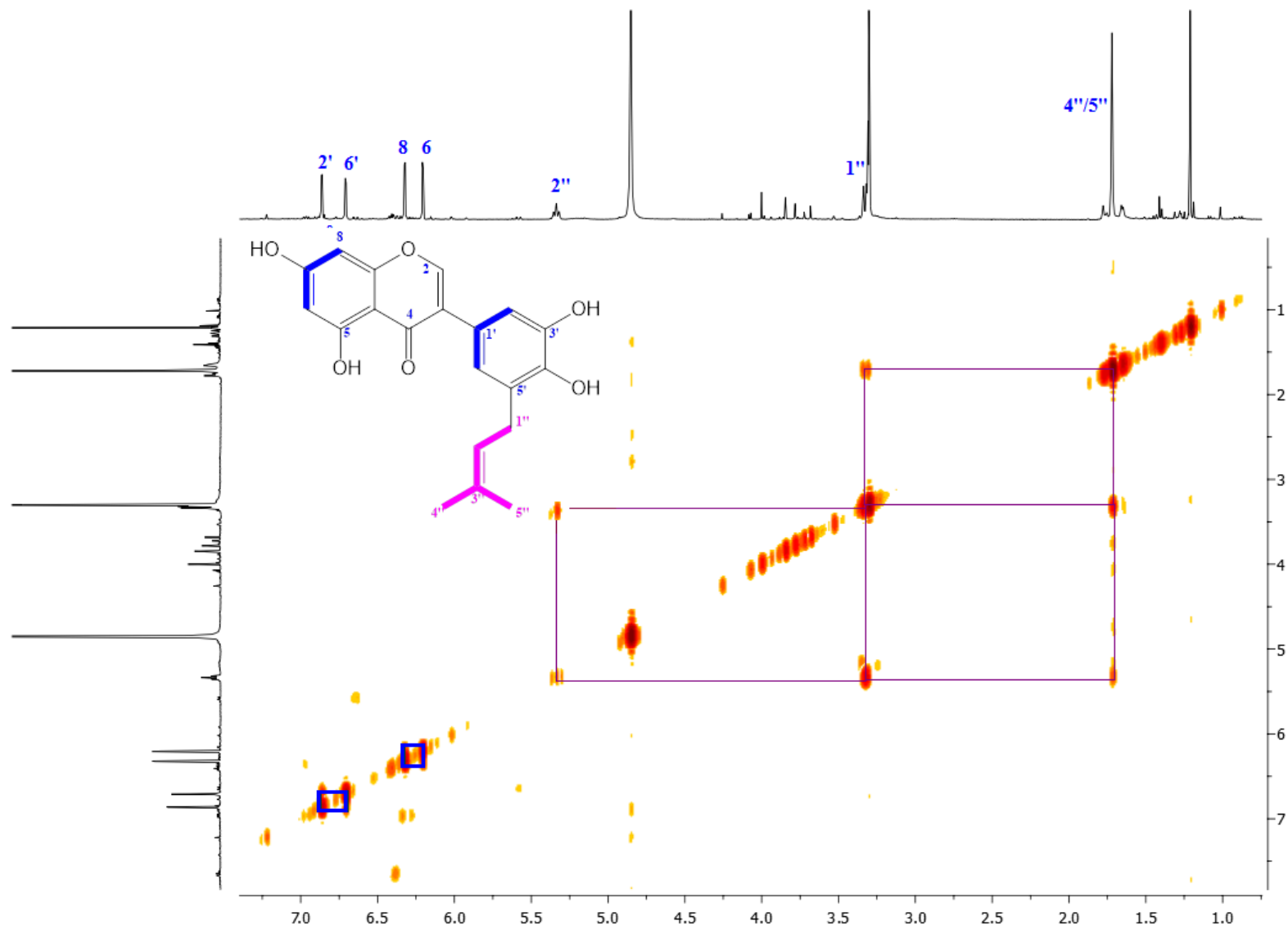
Spectrum 36. 2D-^{1}H,^{1}H-Homonuclear Correlation Spectrum (COSY) of Glycyrrhisoflavone (**14**)
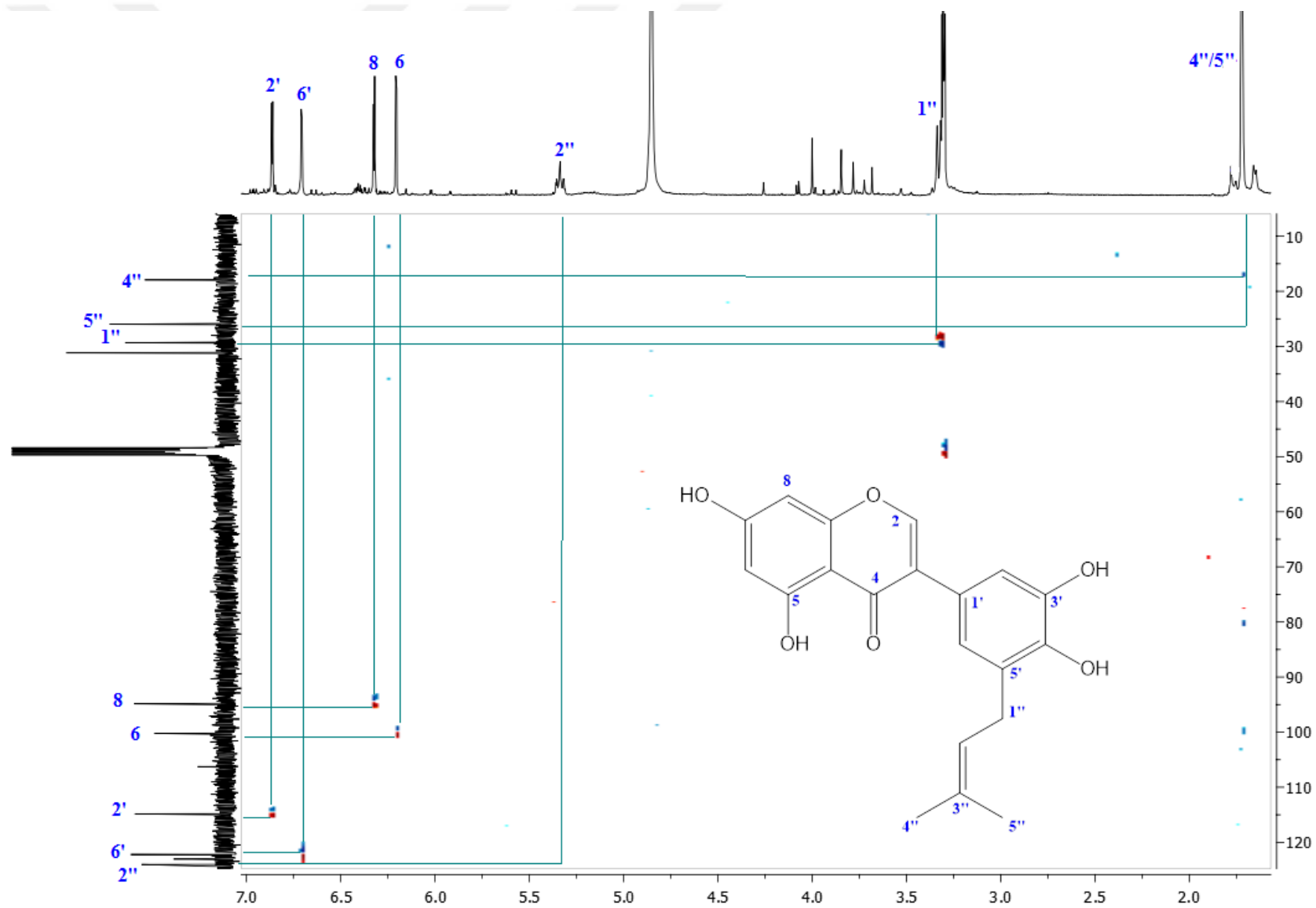
Spectrum 37. Heteronuclear 2D-^{1}H,^{13}C Correlation Spectrum (short range) of Glycyrrhisoflavone (**14**) (HSQC)

228
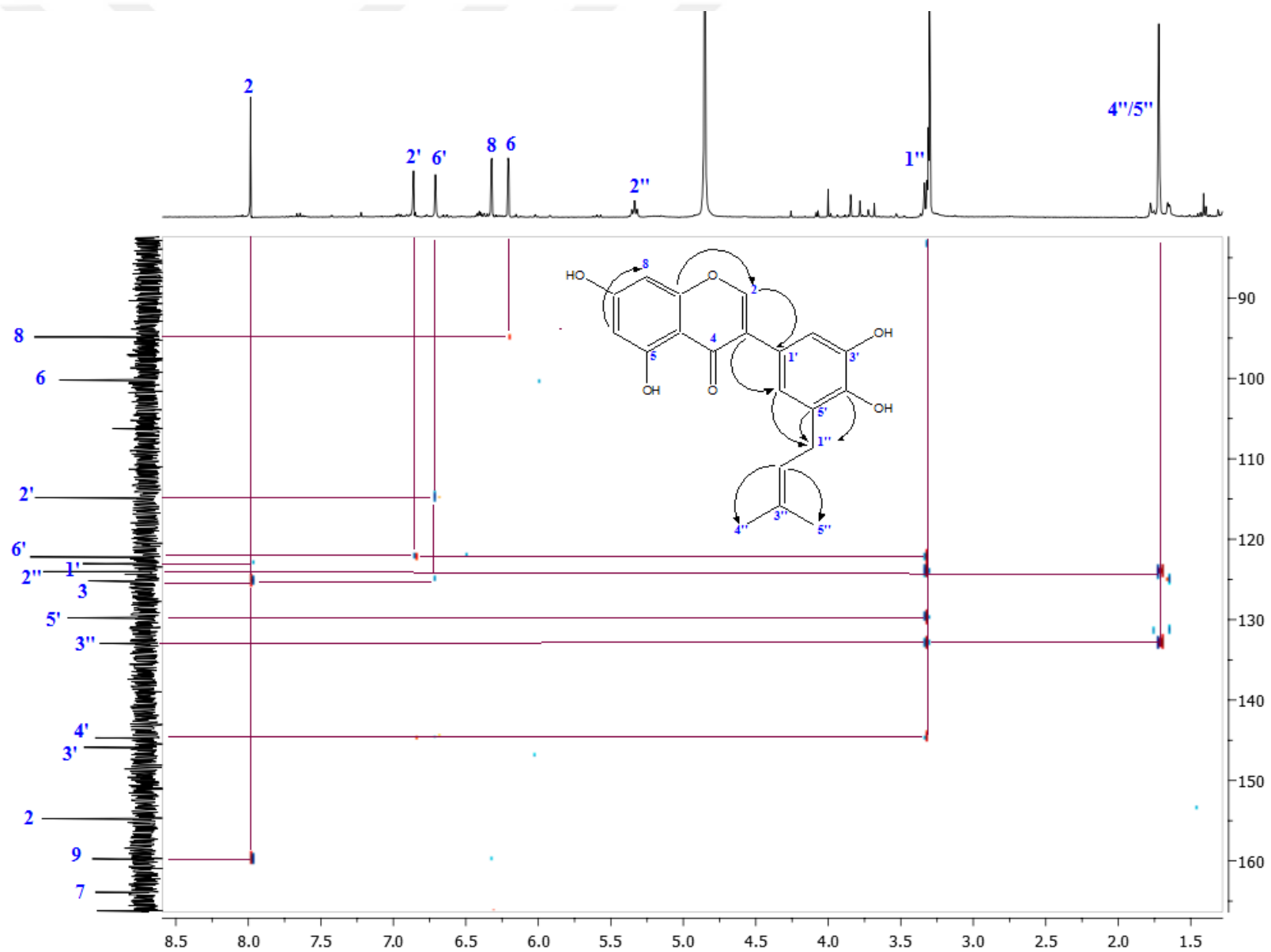
Spectrum 38. Heteronuclear 2D-^{1}H,^{13}C Correlation Spectrum (long range) of Glycyrrhisoflavone (**14**) (HMBC)
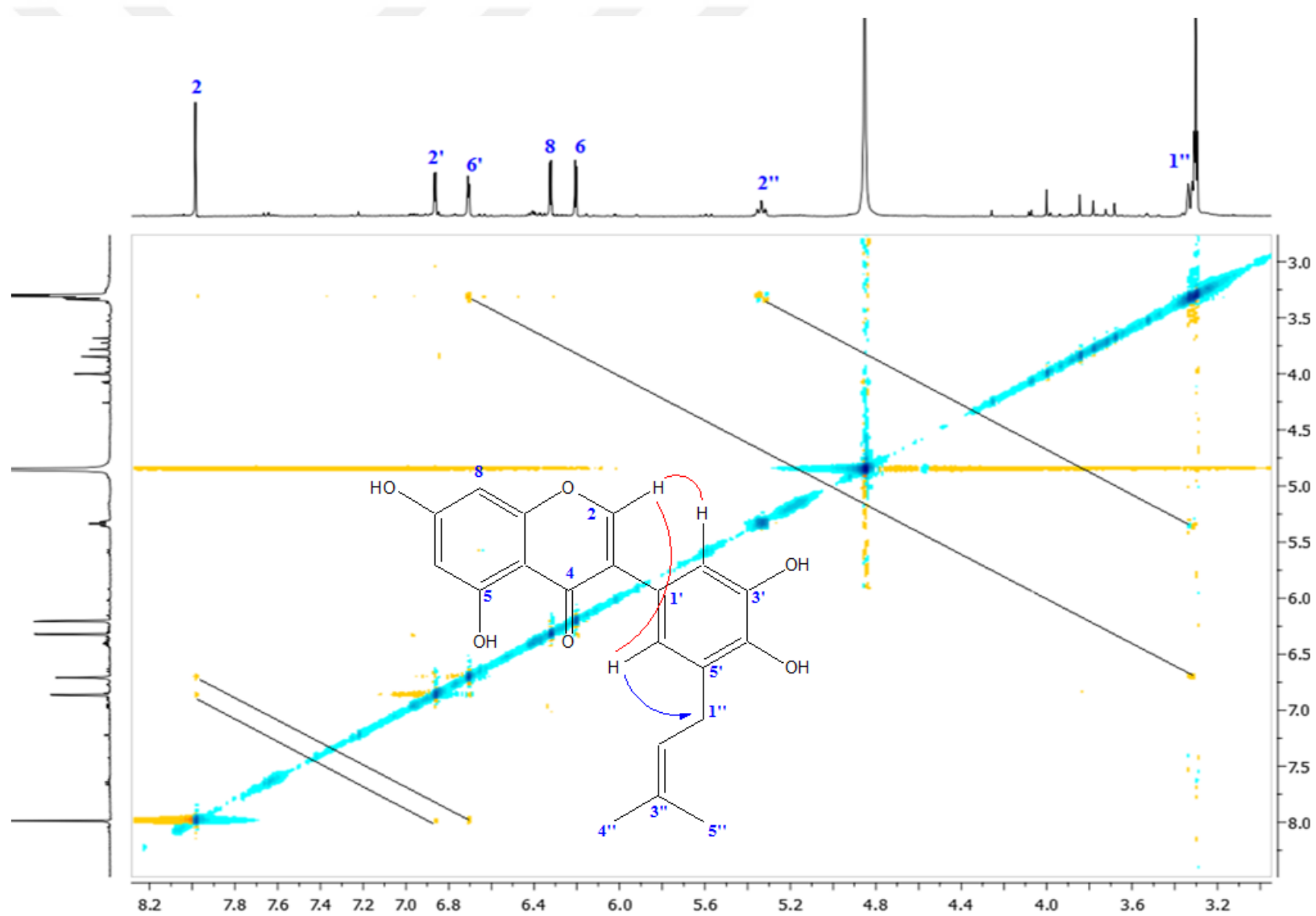
Spectrum 39. 2D-^{1}H,^{1}H-Homonuclear Overhauser Enhancement Spectrum (NOESY) of Glycyrrhisoflavone (**14**)

4.5.1.6. Isoflavans
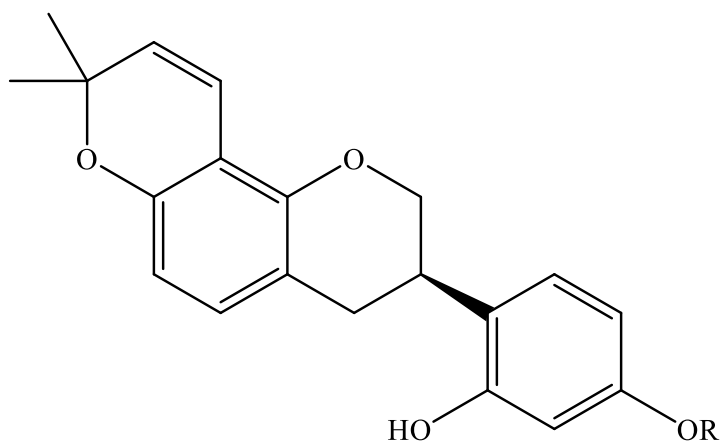
15 R = H
16 R = CH$_3$

GLABRIDIN (15): C$_{20}$H$_{20}$O$_4$

4'-*O*-METHYLGLABRİDİN (16): C$_{21}$H$_{22}$O$_4$

	Glabridin (15)	**4′-*O*-Methylglabridin (16)**
UV λ_{max} (MeOH) nm:	229, 281	229, 285
IR υ_{max} (KBr) cm^{-1}:	3350 (OH), 1620 (conjugated C=C), 1608, 1519 (aromatic ring)	3427 (OH), 1618 (conjugated C=C), 1584, 1520 (aromatic ring)
^{1}H NMR:	Table 128 Spectrum 40	Table 128 Spectrum 43
^{13}C NMR:	Spectrum 41	-
COSY:	Spectrum 42	-

GLABRIDIN (15)

Compound **15** was obtained as an amorphous, pale orange colored powder from both CHCl$_3$ and EtOAc subextracts of *G. glabra.* In its UV spectrum, absorption maxima at 229 and 281 nm were observed, while bands at 3350 (OH), 1620 (conjugated C=C), 1608 and 1519 (aromatic ring) cm^{-1} were detected in its IR spectrum.

^{1}H NMR spectrum (Table 128, Spectrum 40) of **15** showed oxygenated methylene signals at δ_H 4.37 (ddd, *J* = 10.4, 3.5, 1.9 Hz, H$_2$-2) and 4.01 (t, *J* = 10.4 Hz), a methine signal at δ_H 3.48 (m, H-3) and methylene signals at δ_H 2.97 (dd, *J* = 15.7, 10.8 Hz, H$_2$-4) and 2.85 (ddd, *J* = 15.7, 5.3, 1.9 Hz) which were characteristic of an isoflavan skeleton. The corresponding carbon resonances of ring C were observed at δ_C 70.0 (C-2), 31.7 (C-3) and 30.6 (C-4) in ^{13}C NMR spectrum (Table 128, Spectrum 41). Additionaly, ^{1}H NMR spectrum contained two aromatic *ortho*-coupled doublet signals at 6.82 ppm (*J* = 8.3 Hz, H-5) and 6.36 ppm (*J* = 8.3 Hz, H-6) revealed the signals of AB system due to 7,8-disubstitution in ring A. Moreover, three aromatic proton signals were detected as an ABX system at δ_H 6.95 (d, *J* = 8.3 Hz, H-6'), 6.38 (dd, *J* = 8.3, 2.4 Hz, H-5') and 6.31 (d, *J* = 2.4 Hz H-3'). A pair of olefinic doublets at δ_H 6.64 (1H, *J* = 10 Hz) and 5.55 (1H, *J* = 10 Hz) along with two singlet proton signals at δ_H 1.42 and 1.41 (each 3H, s) as well as two olefinic carbon resonances at δ_C 128.4 and 116.9 and two methyl signals at δ_C 27.8 and 27.5 indicated the presence of a 2,2-dimethylpyran ring occured by cyclization of an isoprenyl moiety. In COSY spectrum (Spectrum 42), spin systems were seen between H$_2$-2/H-3/H$_2$-4, H-5/H-6, H-5'/H-6' and H-1''/H-2''. The above data were superimposible with those of 4-[(*3R*)-8,8-dimethyl-3,4-dihydro-2H-pyrano[2,3-f]chromen-3-yl]benzene-1,3-diol, namely **glabridin** (201).

4'-*O*-METHYLGLABRIDIN (16)

Compound **16** was isolated from CHCl$_3$ subextract of *G. glabra* as an amorphous, pale orange colored powder. Its molecular formula was established as C$_{21}$H$_{22}$O$_4$. Its UV spectrum exerted bands at 229 and 285 nm, whereas IR spectrum displayed absorption bands at 3427, 1618, 1584 and 1520 cm^{-1} indicating hydroxyl groups, olefinic carbon atoms as well as aromatic rings.

^{1}H NMR spectrum of compound **16** (Table 128, Spectrum 43) displayed the signals of a characteristic isoflavan core by containing signals at δ_H 4.38 (ddd, *J* = 10.3, 3.5, 1.9 Hz, H-2), 4.03 (t, *J* = 10.3 Hz, H-2), 3.49 (m, H-3), 2.99 (dd, *J* = 15.7, 10.2 Hz, H-4) and 2.86 (ddd, *J* = 15.7, 5.3, 1.9 Hz, H-4). Two aromatic *ortho*-doublet signals were ascribed to H-5 (δ_H 6.83, *J* = 8.3 Hz) and H-6 (δ_H 6.37, *J* = 8.3 Hz) in A ring of isoflavan. Moreover, ABX system signals arising from ring B were observed at δ_H 7.02 (d, *J* = 8.5 Hz, H-6'), 6.48 (dd, *J* = 8.5, 2.4 Hz, H-5') and 6.36 (d, *J* = 2.4 Hz, H-3') due to 2',4'-disubstitution. The ^{1}H NMR spectrum of compound **16** showed very similar proton resonances to those of compound **15**, except for the presence of a methoxy signal in **16** at δ_H 3.77. The downfiled shifting in the signal of H-5' in B ring for 0.1 ppm revealed the location of methoxy group in 4'. Comparison of all the spectral data with the published literature, led to the characterization of compound as **4'-*O*-methylglabridin** (201).

Table 128. ^{1}H and ^{13}C NMR spectroscopic data of glabridin (**15**)[a] and 4'-*O*-methylglabridin (**16**) (CDCl$_3$, [1]H: 400 MHz, [13]C: 100 MHz)

C/H atom	Multiplicity	15 δ$_H$ (ppm), *J* (Hz)	δ$_C$ (ppm)	16 δ$_C$ (ppm), *J* (Hz)
2	CH$_2$	4.37 ddd (10.4, 3.5, 1.9) 4.01 t (10.4)	70.0	4.38 ddd (10.3, 3.5, 1.9) 4.03 t (10.3)
3	CH	3.48 m	31.7	3.49 m
4	CH$_2$	2.97 dd (15.7, 10.8) 2.85 ddd (15.7, 5.3, 1.9)	30.6	2.99 dd (15.7, 10.2) 2.86 ddd (15.7, 5.3, 1.9)
5	CH	6.82 d (8.3)	129.1	6.83 d (8.3)
6	CH	6.36 d (8.3)	108.7	6.37 d (8.3)
7	C	-	151.9	-
8	C	-	109.9	-
9	C	-	149.7	-
10	C	-	114.3	-
1'	C	-	119.9	-
2'	C	-	154.4	-
3'	CH	6.31 d (2.4)	103.1	6.36 d (2.4)
4'	C	-	155.2	-
5'	CH	6.38 dd (8.3, 2.4)	107.9	6.48 dd (8.5, 2.4)
6'	CH	6.95 d (8.3)	128.9	7.02 d (8.5)
1"	CH	6.64 d (10.0)	116.9	6.65 d (10.0)
2"	CH	5.55 d (10.0)	128.4	5.56 d (10.0)
3"	C	-	75.6	-
4"	CH$_3$	1.42 s	27.8	1.43 s
5"	CH$_3$	1.41 s	27.5	1.41 s
4'-OCH$_3$	CH$_3$	-	-	3.77 s

[a] Resonances were assigned by the help of COSY experiment.

234
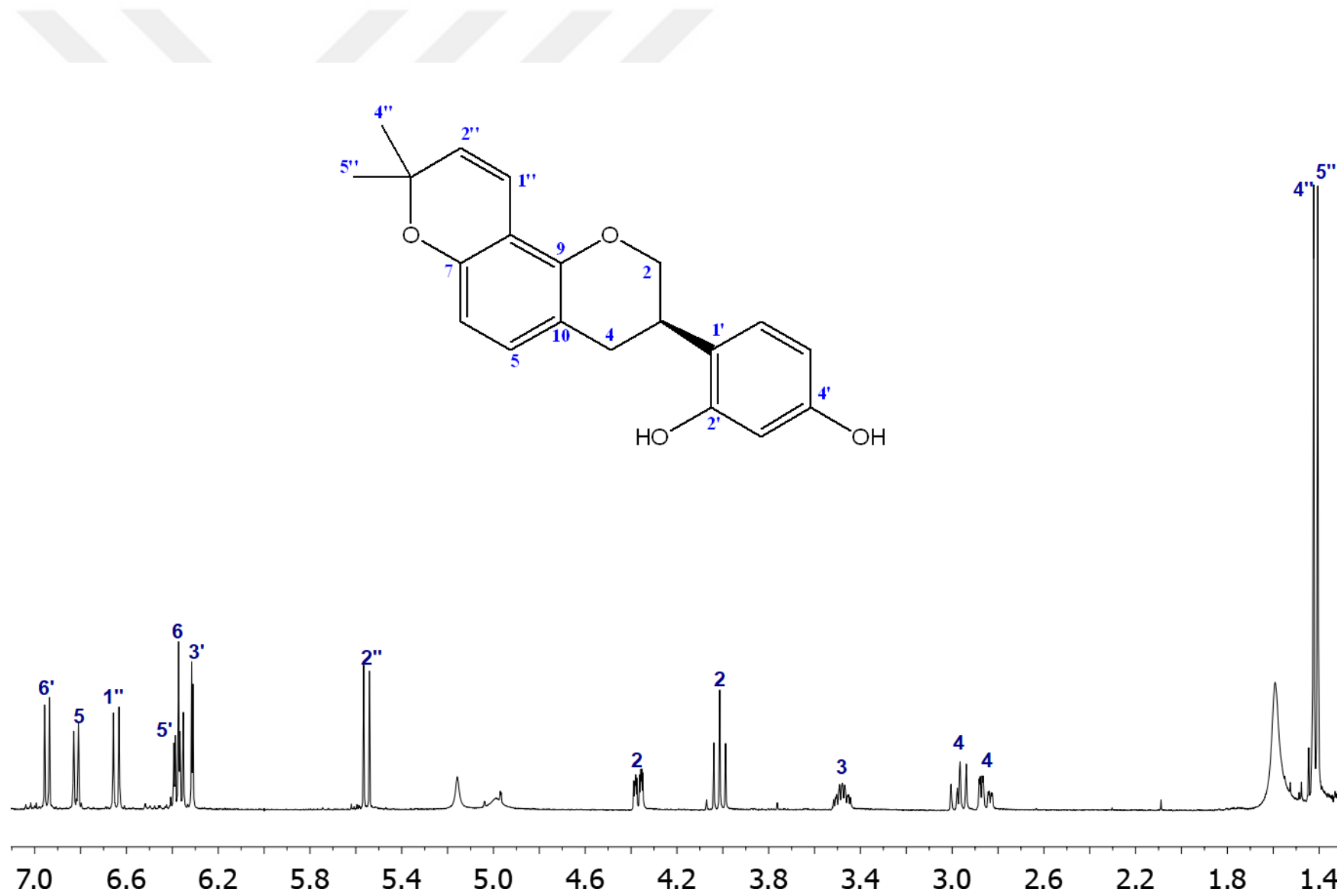
Spectrum 40. ^{1}H NMR Spectrum of Glabridin (**15**) (CDCl$_3$, 400 MHz)
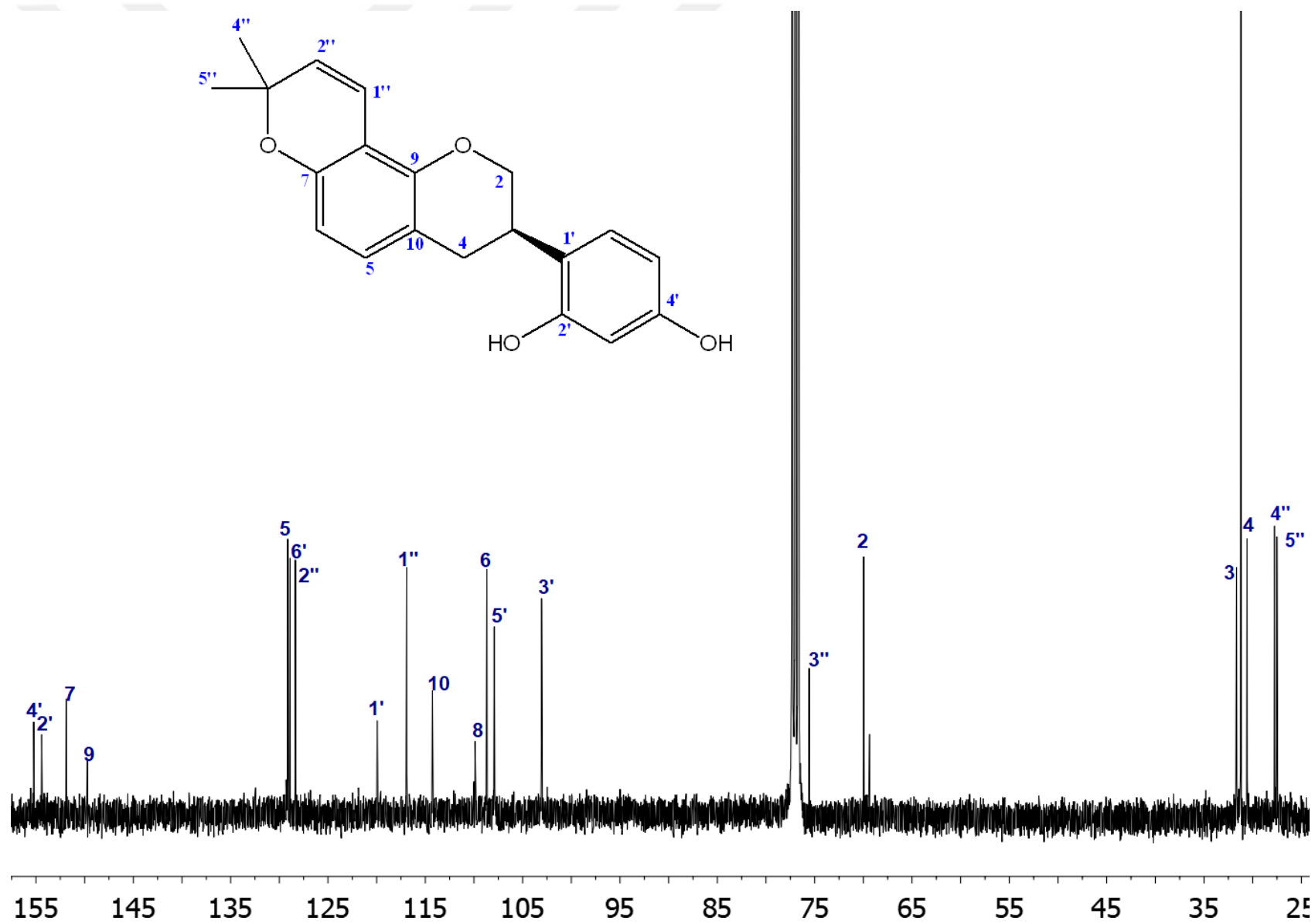
Spectrum 41. ^{13}C NMR Spectrum of Glabridin (**15**) (CDCl$_3$, 100 MHz)
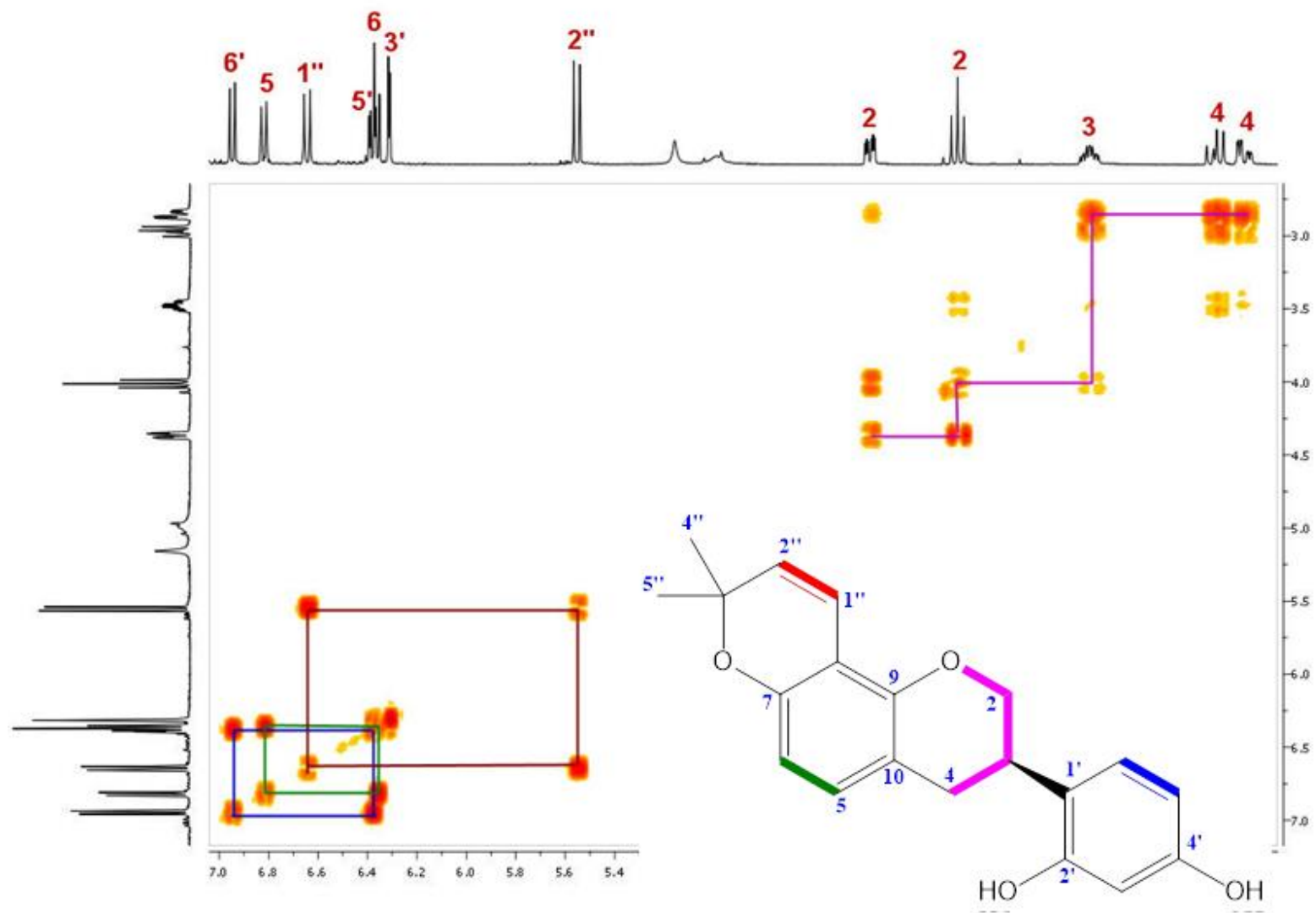
Spectrum 42. 2D-^{1}H,^{1}H-Homonuclear Correlation Spectrum (COSY) of Glabridin (**15**)

237
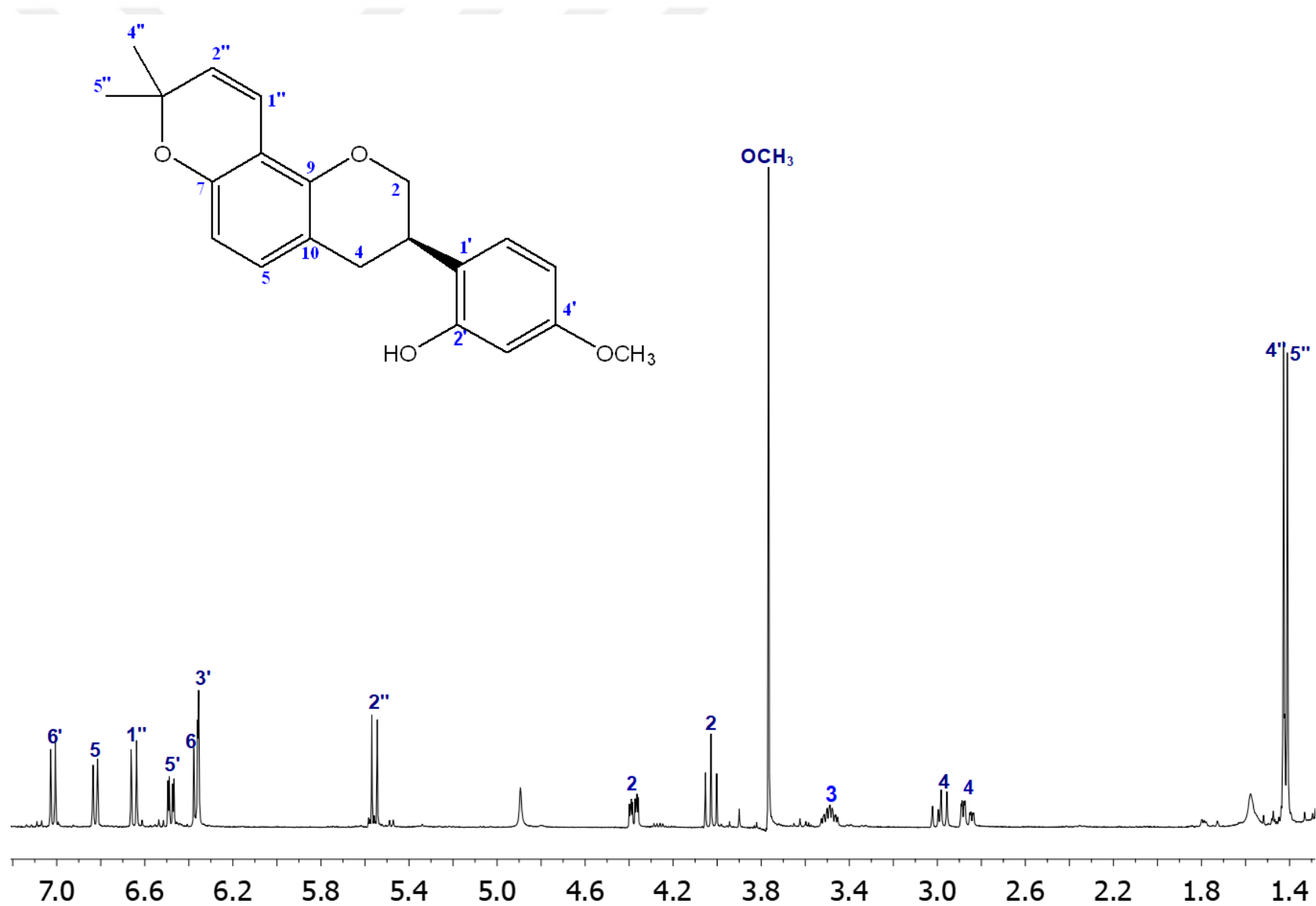
Spectrum 43. ^{1}H NMR Spectrum of 4′-O-Methylglabridin (**16**) (CDCl$_3$, 400 MHz)
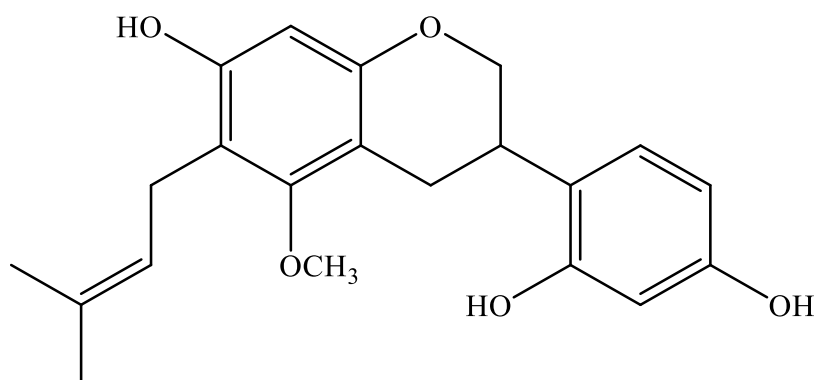
GLYASPERİN C (17), C$_{21}$H$_{24}$O$_5$ (MW: 356.42)

UV λ_{max} (MeOH) nm:	208, 283, 321
IR υ_{max} (KBr) cm^{-1}:	3433 (OH), 1621 (C=C), 1459 (aromatic ring)
^{1}H NMR:	Table 129, Spectrum 44
COSY:	Spectrum 45
NOESY:	Spectrum 46

GLYASPERİN C (17)

Compound **17** was isolated from EtOAc subextract of *G. iconica* as white colored amorphous powder. UV spectrum of **17** contained maxima at 208, 283, 321 nm; while IR spectrum showed absorption bands at 3433 (OH), 1621 (C=C) and 1459 (aromatic ring) cm^{-1}. The molecular formula of compound **17** was determined as $C_{21}H_{24}O_5$.

In ^{1}H NMR spectrum (Table 129, Spectrum 44) of compound **17**, three aromatic signals ascribable to an ABX system were seen at δ_H 6.88 (d, J = 8.4 Hz, H-6'), 6.26 (dd, J = 8.4, 2.4 Hz, H-5') and 6.31 (d, J = 2.4 Hz, H-3') along with a singlet aromatic signal at δ_H 6.08 (s, H-8). Furthermore, signals for one oxymethylene at δ_H 4.17 (ddd, J = 10.2, 3.4, 1.9 Hz) and 3.91 (t, J = 10.2 Hz), one methine at δ_H 3.34 (m) and one methylene at δ_H 2.87 (ddd, J = 16.0, 5.4, 1.9 Hz) and 2.76 (dd, J = 16.0, 10.8 Hz) were observed. These signals were typical for proton resonances of C ring in an isoflavan nucleus. COSY spectrum (Spectrum 45) confirmed that these proton signals (H$_2$-2/H-3/H$_2$-4) were in the same spin system. Moreover, proton signals of an isoprenyl moiety at δ_H 5.20 (1H, m), 3.24 (2H, br d, J = 7.0 Hz), 1.75 and 1.66 (each 3H, s) as well as methoxy group at δ_H 3.68 (3H, s) were detected. The locations of isoprenyl and methoxy units were established to be at C-5 and C-6, respectively by NOe couplings of methoxy group (δ_H 3.68) with H$_2$-4 (δ_H 2.87 and 2.76) and H-1" (δ_H 3.24) (Spectrum 46). The above findings deduced the structure of compound **17** as 7,2',4'-trihydroxy-5-methoxy-6-prenylisoflavan, namely **glyasperin C** (208).

Table 129. ^{1}H NMR spectroscopic data of glyasperin C (**17**) (CD$_3$OD, 400 MHz)[a]

C/H atom	Multiplicity	δ$_H$ (ppm), J (Hz)
2	CH$_2$	3.91 t (10.2) 4.17 ddd (10.2, 3.4, 1.9)
3	CH	3.34 m
4	CH$_2$	2.76 dd (16.0, 10.8) 2.87 ddd (16.0, 5.4, 1.9)
5	C	-
6	C	-
7	C	-
8	CH	6.08 s
9	C	-
10	C	-
1'	C	-
2'	C	-
3'	CH	6.31 d (2.4)
4'	C	-
5'	CH	6.26 dd (8.4, 2.4)
6'	CH	6.88 d (8.4)
1"	CH$_2$	3.24 br d (7.0)
2"	CH	5.20 m
3"	C	-
4"	CH$_3$	1.66 s
5"	CH$_3$	1.75 s
5- OCH$_3$	CH$_3$	3.68 s

[a] Resonances were elicited with the help of 2D NMR (COSY and NOESY) techniques.

241
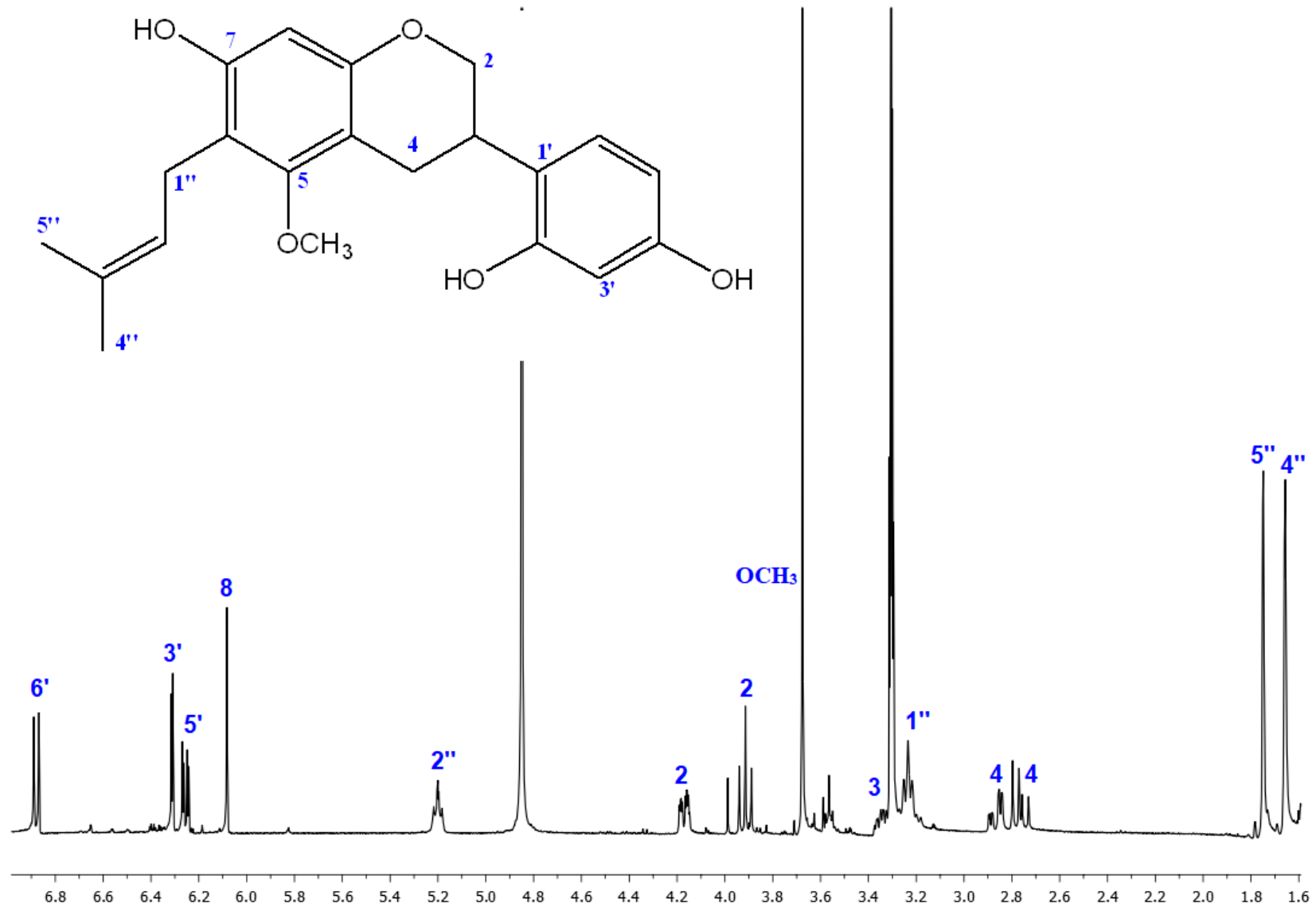
Spectrum 44. ^{1}H NMR Spectrum of Glyasperin C (**17**) (CD$_3$OD, 400 MHz)
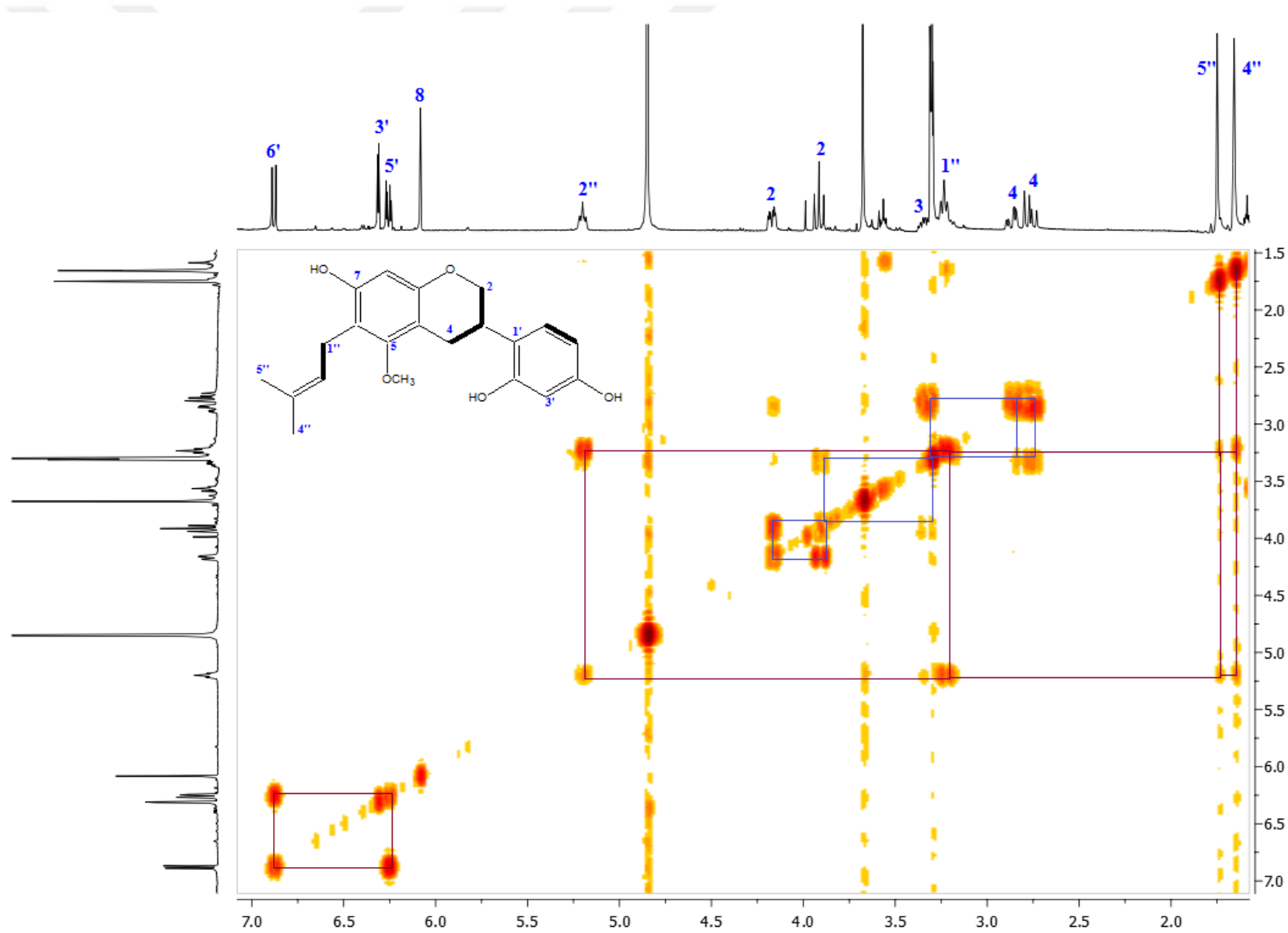
Spectrum 45. 2D-^{1}H,^{1}H-Homonuclear Correlation Spectrum (COSY) of Glyasperin C (**17**)
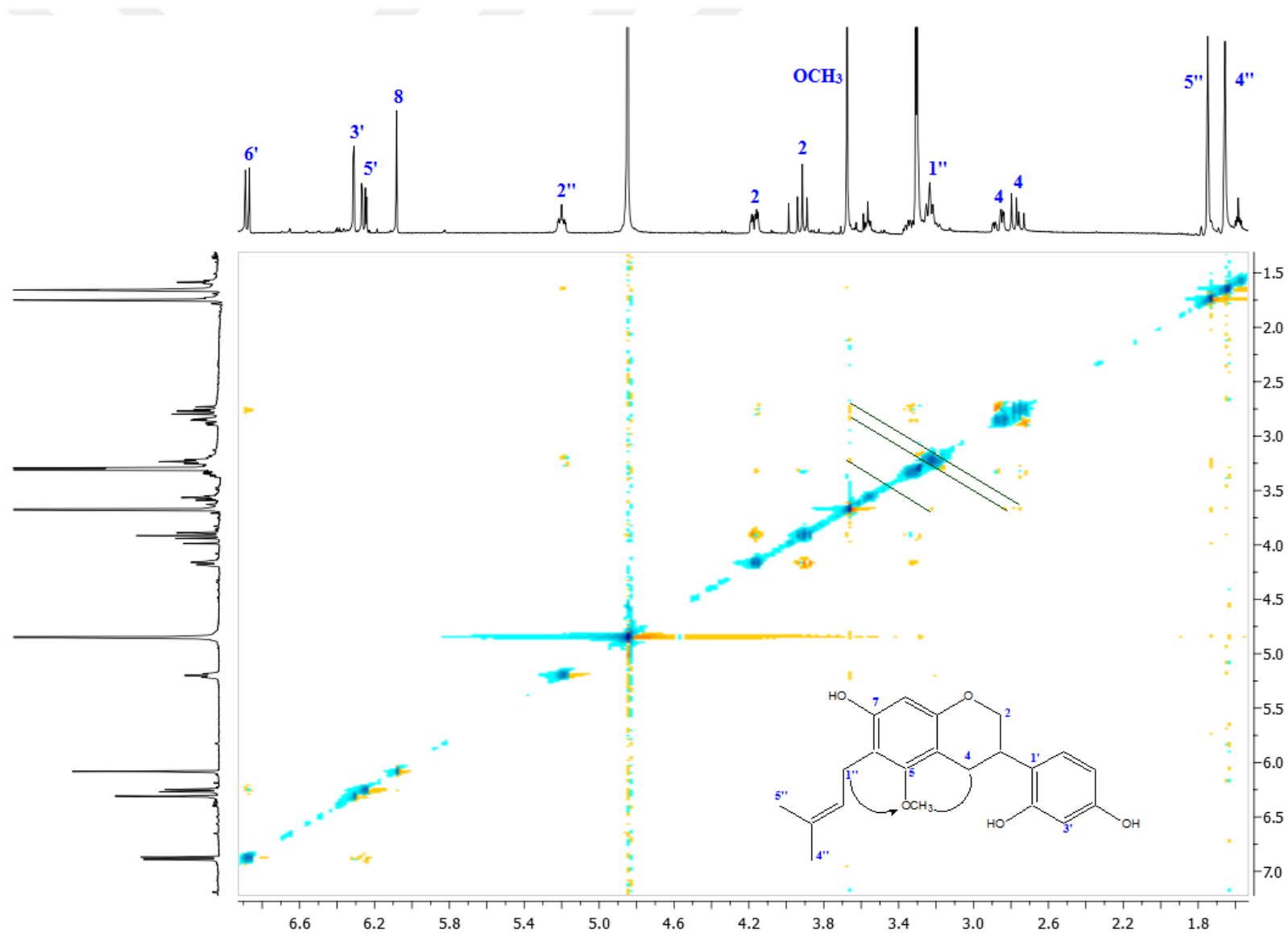
Spectrum 46. 2D-^{1}H,^{1}H-Homonuclear Overhauser Enhancement Spectrum (NOESY) of Glyasperin C (**17**)

18 R = H
19 R = CH$_3$
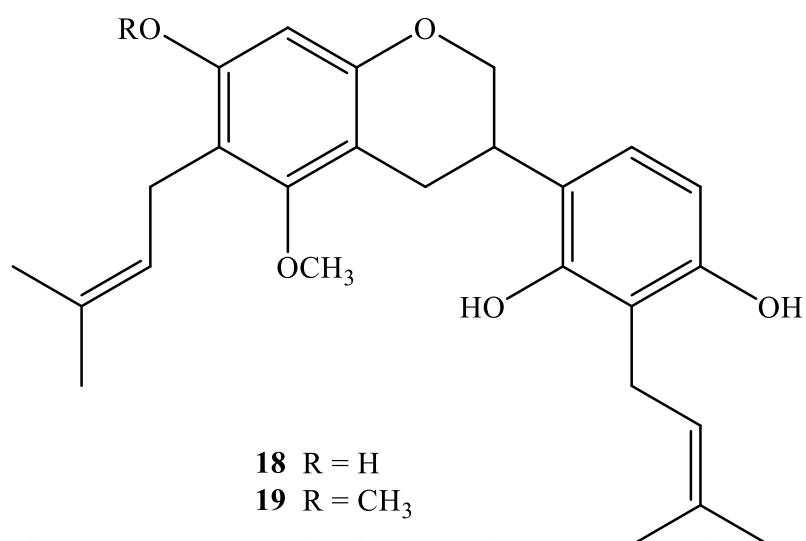
LICORICIDIN (18): C$_{26}$H$_{32}$O$_5$ (MW: 424.54)

LICORISOFLAVAN A (19): C$_{27}$H$_{34}$O$_5$ (MW:438.56)

	Licoricidin (18)	Licorisoflavan A (19)
UV λ_{max} (MeOH) nm:	208, 283	208, 283
IR υ_{max} (KBr) cm^{-1}:	3434 (OH), 1617 (C=C), 1496, 1455 (aromatic ring)	3434 (OH), 1614 (C=C), 1448 (aromatic ring)
^{1}H NMR:	Table 130 Spectrum 47	Table 130 Spectrum 48

LICORICIDIN (18)

Compound **18** was obtained as white colored amorphous powder from the $CHCl_3$ subextract of *G. iconica*. Bands at 208 and 283 nm were observed in UV spectroscopy. IR spectrum showed hydroxyl bands (3434 cm^{-1}), conjugated carbon atoms (1617 cm^{-1}) and benzene (1455 cm^{-1}). The molecular formula of the compound **18** was found to be $C_{26}H_{32}O_5$.

^1H NMR spectrum (Table 130, Spectrum 47) of **18** showed characteristic signals of an isoflavan derivative including one oxymethylene at δ_H 4.17 (ddd, J = 10.2, 3.4, 1.95 Hz) and 3.89 (t, J = 10.2 Hz), one methine at δ_H 3.39 (m) and one methylene at δ_H 2.89 (ddd, J = 16.0, 5,2, 1.95 Hz) and 2.72 (dd, J = 16.0, 11.0 Hz) which were assigned to H_2-2, H-3 and H_2-4, respectively. Besides, one singlet aromatic signal at 6.09 (1H, s) was indicative for 5,6,7-trisubstituted A ring. Moreover, two aromatic signals ascribable to AB system were observed at δ_H 6.35 (d, J = 8.4 Hz) and 6.75 (d, J = 8.4 Hz) which revealed trisubstitution in ring B. Additional signals were detected arising from one methoxy unit at 3.67 ppm (3H,s) along with two isoprenyl chain moieties at δ_H 5.20 (each 1H, m, H-2" and H-2‴), 3.36 (2H, br. d, J =7.2 Hz, H-1‴), 3.23 (2H, br t, J =7.2 Hz, H-1"), 1.77 (3H, s, H-5‴), 1.75 (3H, s, H-5"), 1.67 (3H, s, H-4‴) and 1.66 (3H, s, H-4"). The NMR findings were found to be superimposible with those of **licoricidin** (7,2',4'-trihydroxy-5-methoxy-6,3'-diprenylisoflavan) (211). TLC comparision also supported this assumption.

LICORISOFLAVAN A (19)

Compound **19** was isolated from $CHCl_3$ subextract of *G. iconica* as white amorphous powder, having molecular formula of $C_{27}H_{34}O_5$. In UV spectroscopy, absorption maxima at 208 and 283 nm were observed, whereas IR spectrum showed absorption bands at 3434 (OH), 1614 (C=C), 1448 (aromatic ring) cm^{-1}, indicating very similar results with compound **18**.

^{1}H NMR signals (Table 130, Spectrum 48) at δ_H 4.21 (ddd, J = 10.2, 3.4, 2.0 Hz, H-2), 3.92 (t, J = 10.2 Hz, H-2), 3.41 (m, H-3), 2.91 (ddd, J = 16.0, 5.2, 2.0 Hz, H-4), and 2.74 (dd, J = 16.0, 10.9 Hz, H-4) were typical for the C ring of an isoflavan skeleton. Additionally, the spectrum revealed signals for three aromatic proton including an AB coupling system at δ_H 6.75 (d, J = 8.4 Hz) and 6.35 (d, J = 8.4 Hz) and one singlet aromatic signal at δ_H 6.21, belonging to H-6' and H-5' in B ring and H-8 in A ring, respectively. Moreover, signals of two methoxy (δ_H 3.74 and 3.68, each 3H) and two isoprenyl moieties [at δ_H 5.13 (1H, m), 3.23 (2H, br t, J = 7.3 Hz), 1.67 and 1.64 (each 3H, s) and at δ_H 5.21 (1H, m), 3.36 (2H, br d, J = 7.3 Hz), 1.77 and 1.74 (each 3H, s)] were also observed. These spectroscopic data were found to be very close to those of **18** except for the additional methoxy signal at δ_H 3.74 (3H) in the ^{1}H NMR spectrum of **19**. Chemical shifting to downfield in proton resonance of H-8 in ^{1}H NMR spectrum of compound **19** placed these second methoxy unit at C-7. Thus, compound **19** was characterized as 2',4'-dihydroxy-5,7-dimethoxy-6,3'-diprenylisoflavan, namely **licorisoflavan A** (247).

Table 130. ^{1}H NMR spectroscopic data of licoricidin (**18**) and licorisoflavan A (**19**) (CD$_3$OD, 400 MHz)

C/H atom	Multiplicity	18 δ$_H$ (ppm), *J* (Hz)	19 δ$_H$ (ppm), *J* (Hz)
2	CH$_2$	3.89 t (10.2) 4.17 ddd (10.2, 3.4, 1.95)	3.92 t (10.2) 4.21 ddd (10.2, 3.4, 2.0)
3	CH	3. 39 m	3.41 m
4	CH$_2$	2.72 dd (16.0,11.0) 2.89 ddd (16.0, 5.2, 1.95)	2.74 dd (16.0, 10.9) 2.91 ddd (16.0, 5.2, 2.0)
5	C	-	-
6	C	-	-
7	C	-	-
8	CH	6.09 s	6.21 s
9	C	-	-
10	C	-	-
1'	C	-	-
2'	C	-	-
3'	C	-	-
4'	C	-	-
5'	CH	6.35 d (8.4)	6.35 d (8.4)
6'	CH	6.75 d (8.4)	6.75 d (8.4)
1"	CH$_2$	3.23 br t (7.2)	3.23 br t (7.3)
2"	CH	5.20 m	5.13 m
3"	C	-	-
4"	CH$_3$	1.66 s	1.64 s
5"	CH$_3$	1.75 s	1.67 s
1'''	CH$_2$	3.36 br d (7.2)	3.36 br d (7.3)
2'''	CH	5.20 m	5.21 m
3'''	C	-	-
4'''	CH$_3$	1.67 s	1.74 s
5'''	CH$_3$	1.77 s	1.77 s
5- OCH$_3$	CH$_3$	3.67 s	3.68 s
7- OCH$_3$	CH$_3$	-	3.74 s
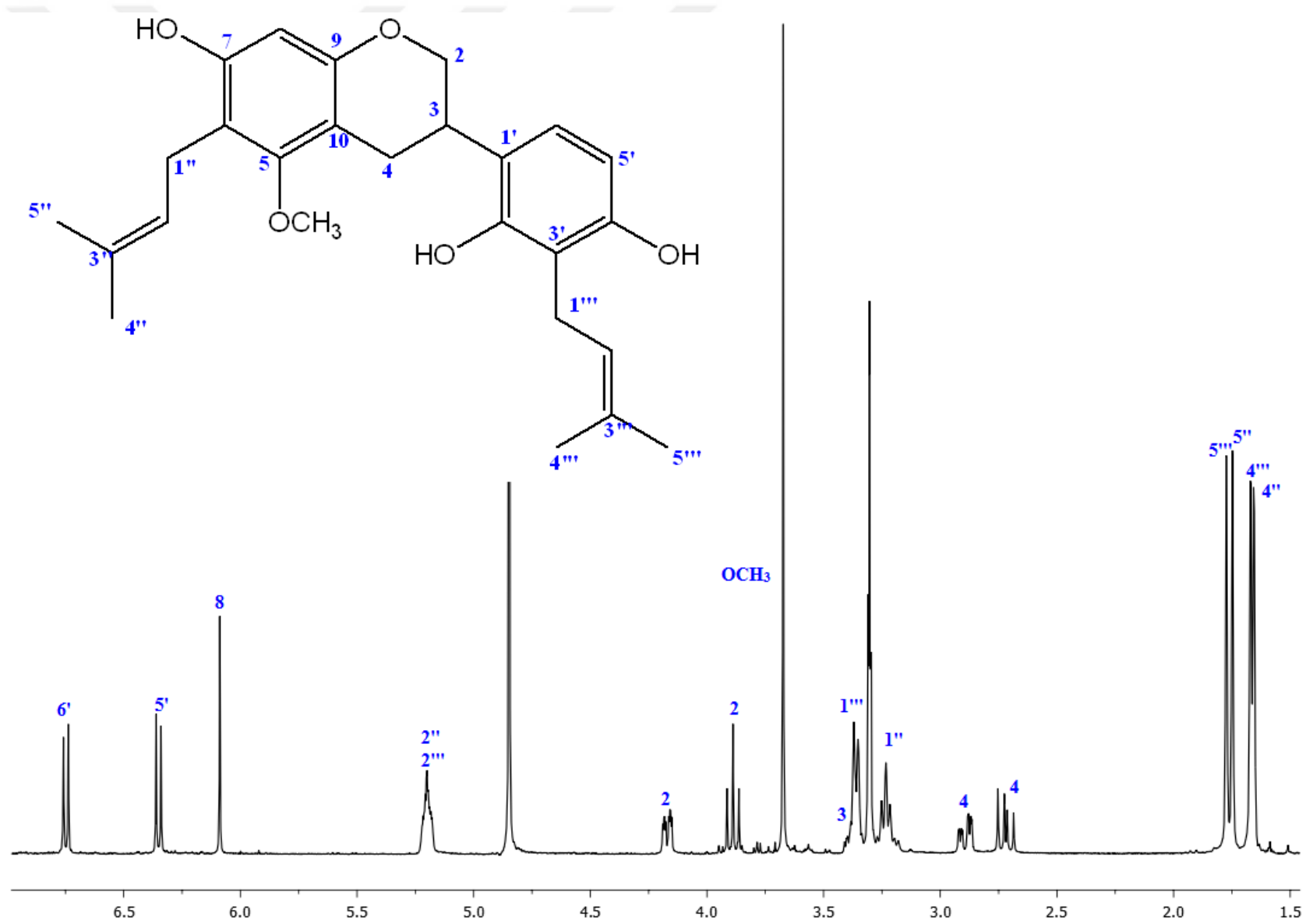
Spectrum 47. ^{1}H NMR Spectrum of Licoricidin (**18**) (CD$_3$OD, 400 MHz)

249
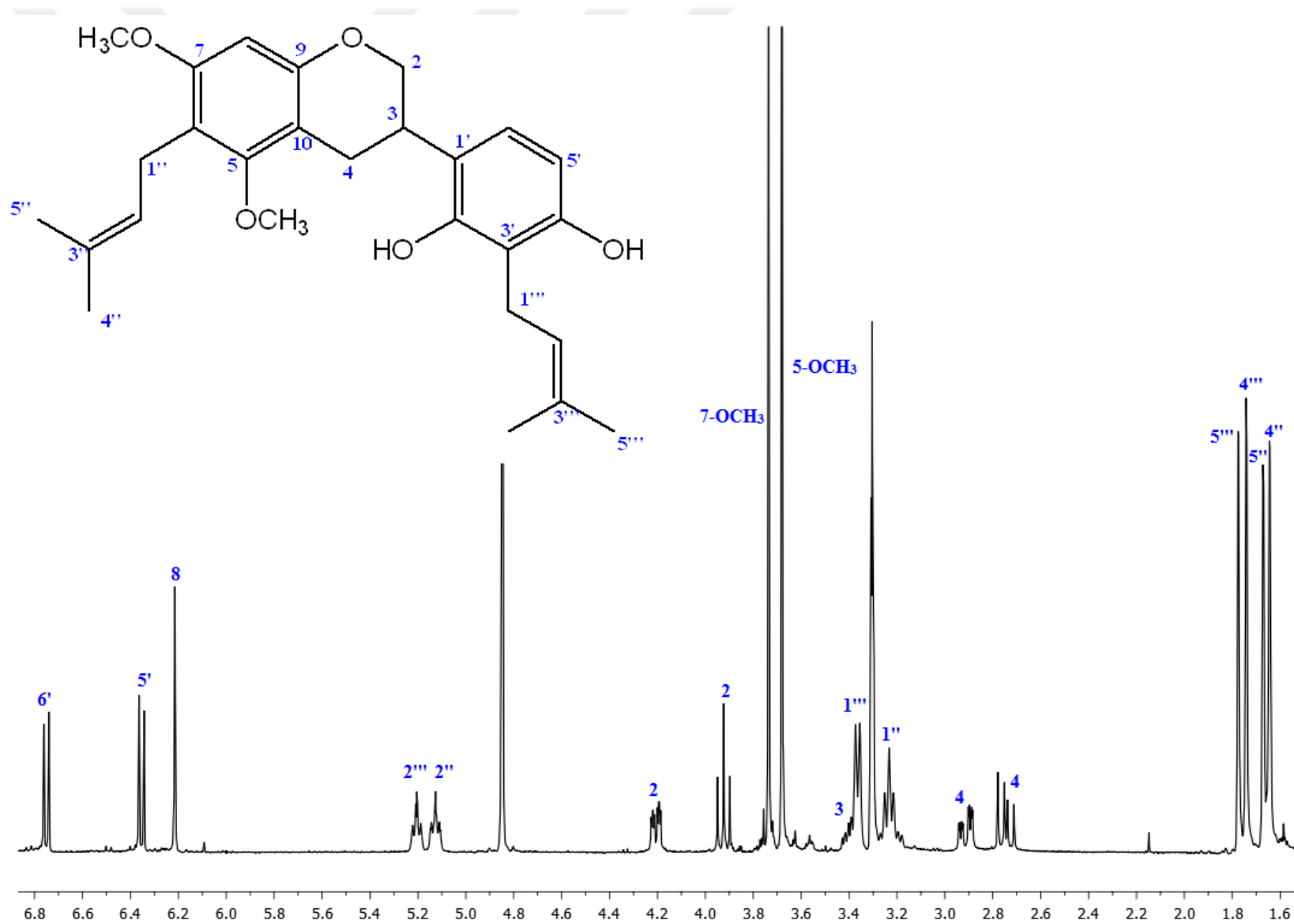
Spectrum 48. ^{1}H NMR Spectrum of Licorisoflavan A (**19**) (CD$_3$OD, 400 MHz)

4.5.1.7. Isoflavenes
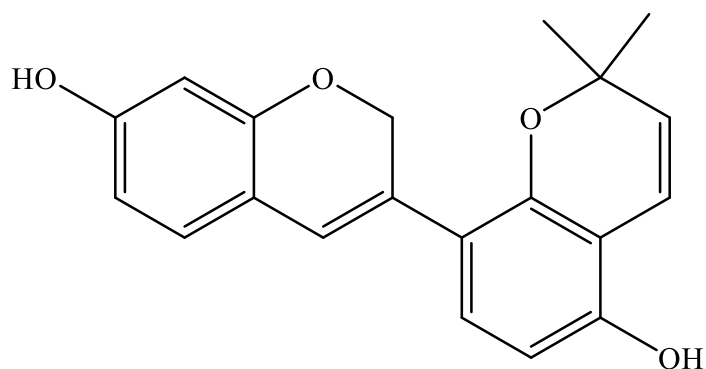
GLABRENE (20): C$_{20}$H$_{18}$O$_{4}$ (MW: 322.36)

UV λ$_{max}$ (MeOH) nm:	285, 295, 322
IR υ$_{max}$ (KBr) cm^{-1}:	3337 (OH), 1615 (conjugated C=C), 1505 (aromatic ring)
^{1}H NMR:	Table 131, Spectrum 49
^{13}C NMR:	Table 131, Spectrum 50
COSY:	Spectrum 51
HSQC:	Spectrum 52
HMBC:	Spectrum 53

GLABRENE (20)

Compound **20** was isolated from EtOAc subextract of *G. glabra* as an orange colored amorphous powder, having molecular formula of $C_{20}H_{18}O_4$. IR spectrum displayed absorption bands at 3337 (OH), 1615 (conjugated C=C), 1505 (aromatic ring) cm^{-1}, while UV spectrum showed absorption maxima at 285, 295 and 322 nm.

^{1}H NMR spectrum (Table 131, Spectrum 49) of compound **20** displayed an ABX system at δ_H 6.87 (d, *J* =8.2 Hz), 6.34 (dd, *J* = 8.2, 2.3 Hz) and 6.26 (d, *J* =2.3 Hz) due to 7-monosubstitution pattern of ring A. Moreover, a pair of doublet aromatic signals at 6.99 and 6.35 (each 1H, *J* = 8.5 Hz,) suggested the presence of 2',3',4'-trisubstituted ring B. Additional proton resonances arising from dimethylated pyran ring were observed at δ_H 6.65 (d, *J* = 10.0 Hz) and 5.59 (d, *J* = 10.0 Hz) along with two methyl signals at δ_H 1.41 (each 3H, s). Trisubstituted olefinic signals at δ_H 6.47 (br s, H-4) and δ_C 121.3 (C-4), oxymethylene signal at δ_H 4.93 (br s, H$_2$-2) and δ_C 69.6 (C-2) as well as carbon data of C-3 at δ_C 129.9 (Table 131, Spectrum 50) suggested the presence of an unsaturation between C-3 and C-4 in ring C. 2D NMR experiments (COSY, HSQC and HMBC) were conducted to identify the exact structure of compound. Four spin systems were detected according to COSY experiments (Spectrum 51) by ^{1}H/^{1}H cross peaks between H-2/H-4, H-5/H-6, H-5'/H-6' as well as between H-3"/H-4". Corresponding carbon data of proton signals were elucidated by HSQC (Spectrum 52) and HMBC (Spectrum 53) spectra. The site of hydroxylation and pyran ring were unambiguously established by HMBC experiments. ^{13}C/^{1}H long range correlations from C-7 (δ_C 159.1) to H-5 (δ_H 6.87) as well as from C-4' (δ_C 154.4) to H-6' (δ_H 6.99) placed the hydroxyl groups at C-7 and C-4'. Additionally, cross peaks between carbon resonance at δ_C 110.8 (C-3') and proton signal at δ_H 5.59 (H-3") indicated the pyran ring was attached from C-2' and C-3'. Thus, the structure of **20** was found to have an isoflav-3-ene core. Consequently, comparison of all the spectroscopic data with the published data of glabrene (2',7-dihydroxy-[(6",6"-dimethylpyrano(2",3":4',3')]-isoflav-3-ene) led us to determine the compound **20** as **glabrene** (207).

Table 131. ^{1}H and ^{13}C NMR spectroscopic data of glabrene (**20**) (CD$_3$OD, ^{1}H: 400 MHz, ^{13}C: 100 MHz)[a]

C/H atom	Multiplicity	δ$_H$ (ppm), *J* (Hz)	δ$_C$ (ppm)
2	CH$_2$	4.93 br s	69.6
3	C		129.9
4	CH	6.47 br s	121.3
5	CH	6.87 d (8.2)	128.5
6	CH	6.34 dd (8.2, 2.3)	109.6
7	C	-	159.1
8	CH	6.26 d (2.3)	103.5
9	C	-	155.8
10	C	-	117.6
1'	C	-	120.0
2'	C	-	152.4
3'	C	-	110.8
4'	C	-	154.4
5'	CH	6.35 d (8.5)	108.9
6'	CH	6.99 d (8.5)	129.0
2"	C	-	77.2
3"	CH	5.59 d (10.0)	129.3
4"	CH	6.65 d (10.0)	118.3
5"/6"	CH$_3$/CH$_3$	1.41 s	31.2

[a] Resonances were assigned by the help of 2D NMR (COSY, HSQC and HMBC) techniques.
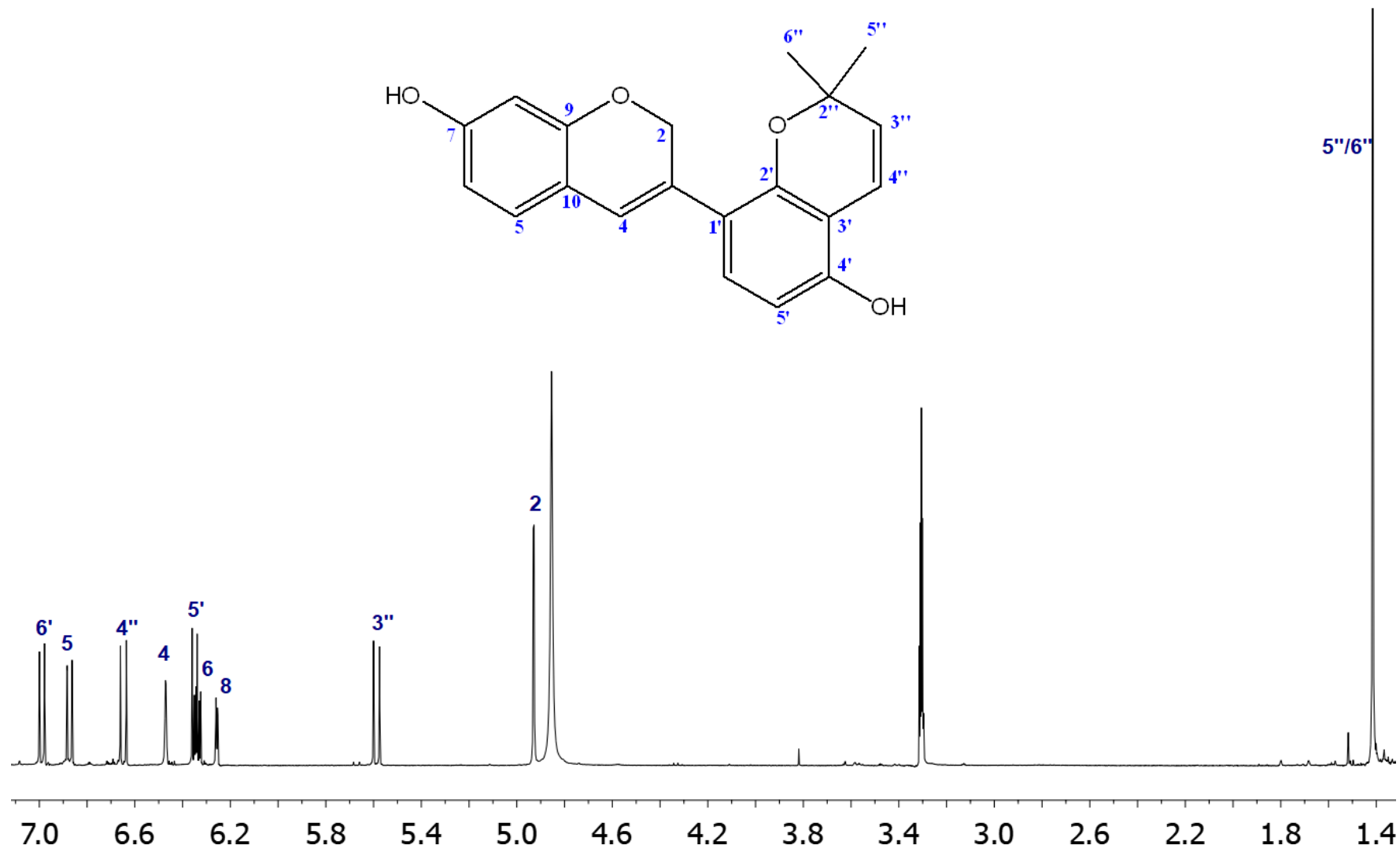
Spectrum 49. ^{1}H NMR Spectrum of Glabrene (**20**) (CD₃OD, 400 MHz)
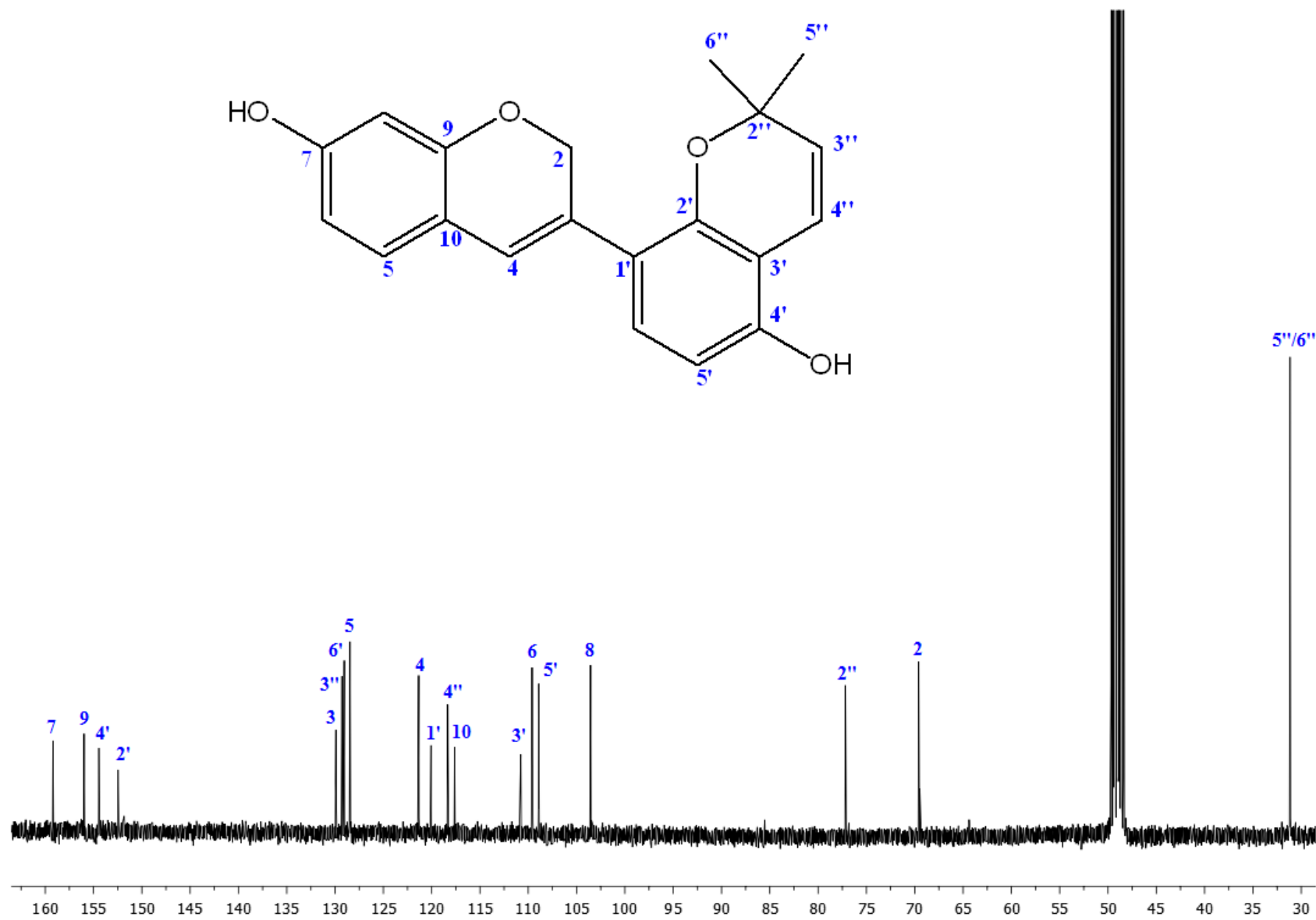
Spectrum 50. ^{13}C NMR Spectrum of Glabrene (**20**) (CD₃OD, 100 MHz)
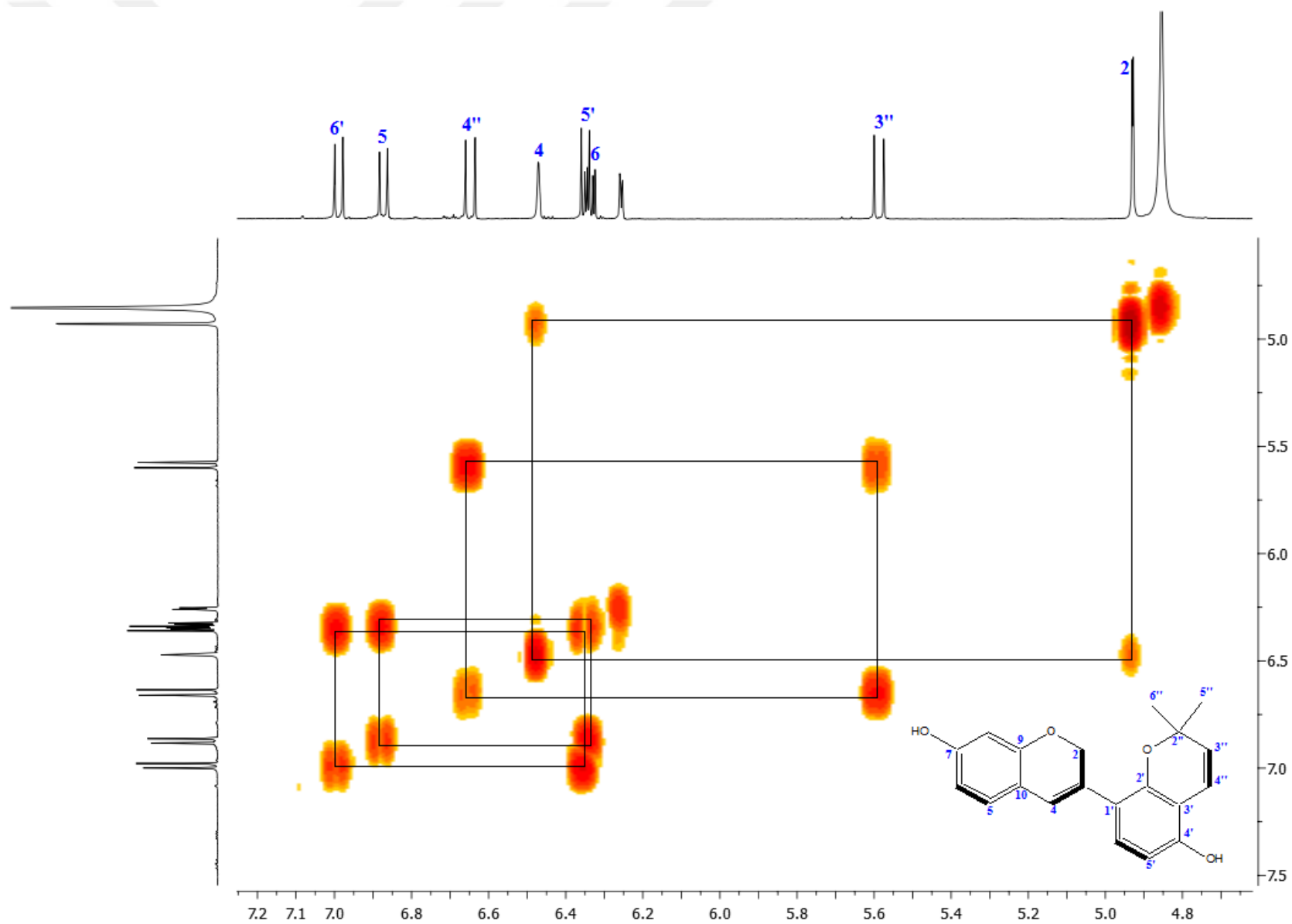
Spectrum 51. 2D-^{1}H,^{1}H-Homonuclear Correlation Spectrum (COSY) of Glabrene (**20**)
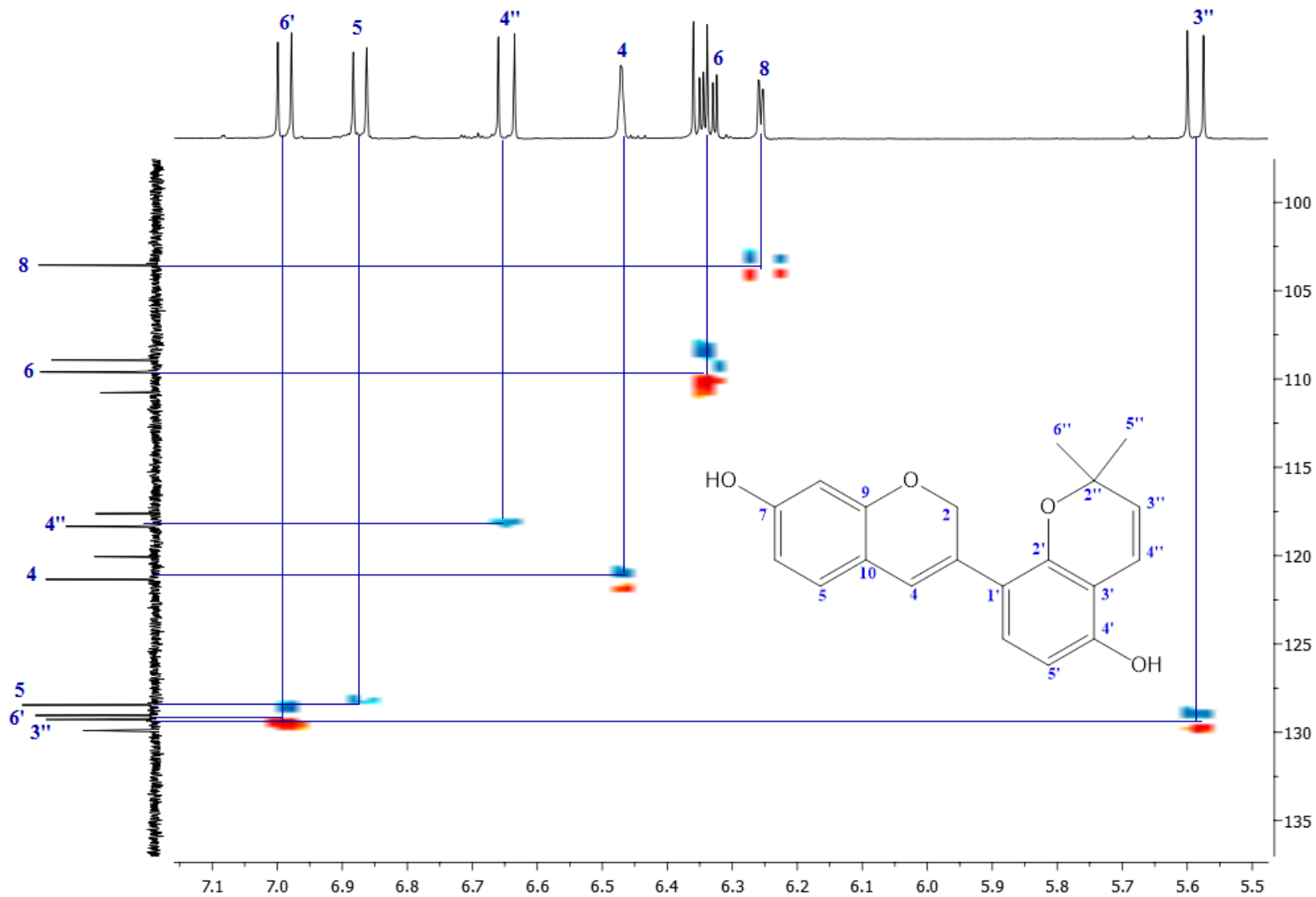
Spectrum 52. Heteronuclear 2D-^{1}H,^{13}C Correlation Spectrum (short range) of Glabrene (**20**) (HSQC)

257
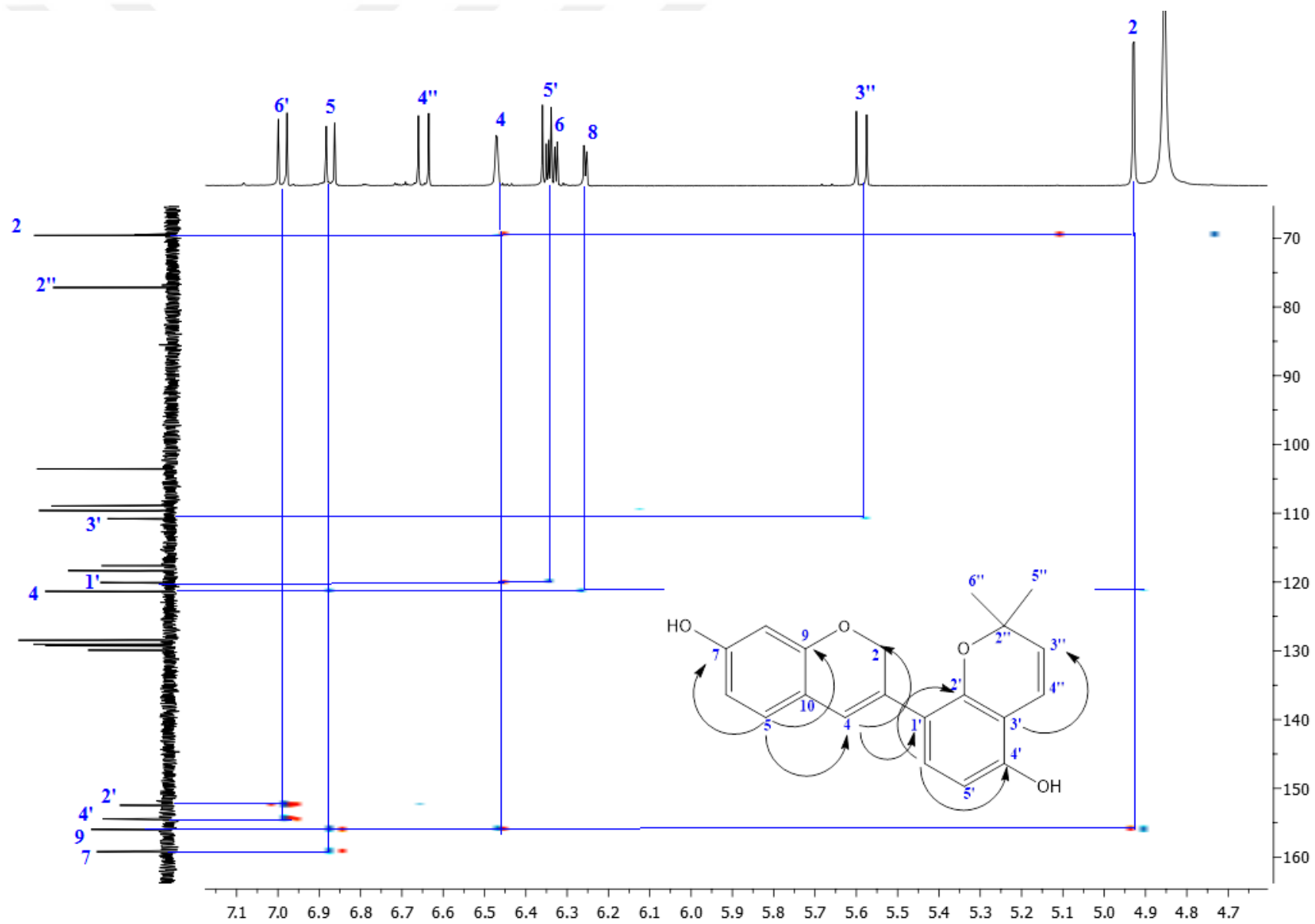
Spectrum 53. Heteronuclear 2D-^{1}H,^{13}C Correlation Spectrum (long range) of Glabrene (**20**) (HMBC)
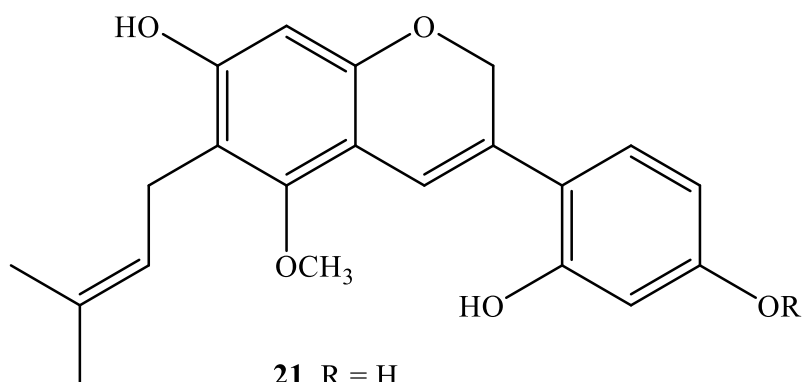
21 R = H
22 R = CH$_3$

DEHYDROGLYASPERIN C (21): C$_{21}$H$_{22}$O$_5$ (MW: 354.4)

ICONISOFLAVEN (22): C$_{22}$H$_{24}$O$_5$ (MW: 368.43)

	Dehydroglyasperin C (21)	**Iconisoflaven (22)**
UV λ$_{max}$ (MeOH) nm:	202, 330	224, 329
IR υ$_{max}$ (KBr) cm^{-1}:	3409 (OH), 1617 (conjugated C=C), 1460 (aromatic ring)	3435 (OH), 1616 (conjugated C=C), 1460 (aromatic ring)
^{1}H NMR:	Table 132 Spectrum 54	Table 132 Spectrum 59
^{13}C NMR:	Spectrum 55	-
COSY:	Spectrum 56	-
HSQC:	Spectrum 57	-
HMBC:	Spectrum 58	-

DEHYDROGLYASPERIN C (21)

Compound **21** was obtained as yellow amorphous powder from EtOAc subextract of *G. iconica* roots, showing absorption maxima at 202 and 330 nm. In IR spectrum, bands indicating hydroxyl group (3409 cm^{-1}), conjugated carbon bonds (1617 cm^{-1}) as well as aromatic ring (1460 cm^{-1}) were observed. The molecular formula of compounds were determined to be $C_{21}H_{22}O_5$.

^{1}H NMR spectrum (Table 132, Spectrum 54) of compound **21** showed trisubstituted olefinic signal at δ_H 6.66 (1H, s) and oxymethylene signal at δ_H 4.88 (2H, s) arising from H-4 and H$_2$-2 of ring C, respectively. The corresponding ^{13}C NMR resonances (Table 132, Spectrum 55) were detected at δ_C 69.3 (C-2), 129.9 (C-3) and 116.6 (C-4) which were assigned by the help of HSQC (Spectrum 57) and HMBC (Spectrum 58) indicating an isoflavene nucleus in **21**. Additionaly, one singlet aromatic signal at 6.11 ppm suggested the presence of 5,6,7-trisubstituted ring A. Moreover, an ABX system was observed and ascribed to 2',4'-disubstitution of ring B regarding the proton signals at δ_H 7.06 (d, J = 9.0 Hz), 6.30 (dd, J = 9.0, 2.3 Hz) and 6.30 (d, J = 2.3 Hz). Characteristic signals of an isoprenyl [(δ_H 5.19 (1H, m), 3.24 (2H, br d, J = 6.9 Hz), 1.76 and 1.66 (each 3H, s)] chain and a methoxy group (δ_H 3.71, 3H, s) were also elicited. COSY spectrum (Spectrum 56) displayed ^{1}H/^{1}H cross peaks between H-2/H-4, H-5'/H-6' as well as between protons of the isoprenyl unit. The attachment sites of isoprenyl and methoxy groups were established by HMBC (Spectrum 58). The cross-peaks between carbon resonances at δ_C 156.8 (C-5), 115.9 (C-6) and 157.4 (C-7) and proton signal of H-1" (δ_H 3.24) indicated the isoprenyl moiety was linked to C-6. Long-range correlations of C-5 (δ_C 156.8) to methoxy signal (δ_H 3.71), placed methoxy group at C-5. Taken together, the ^{1}H NMR resonances were similar to those of compound **17** (glyasperin C); whereas spectrum of **21** differed from that of compound **17** mainly by the presence of a tri-substituted olefinic singlet signal at δ_H 6.66 as well as the absence of the characteristic methylene and methine resonances of an isoflavan skeleton. Thus, these findings led the identification of the compound **21** as **dehydroglyasperin C** referring the previous literatures (203).

ICONISOFLAVEN (22)

Compound **22** was obtained as an orange amorphous powder from $CHCl_3$ subextract of *G. iconica* roots, having a molecular formula of $C_{22}H_{24}O_5$. The UV spectrum displayed absorption maxima at 224 and 329 nm; while its IR spectrum showed absorption bands at 3435 (OH), 1616 (conjugated C=C), 1460 (aromatic ring) cm^{-1}.

Characteristic signals of an isoflavene skeleton were observed with ^{1}H NMR spectrum (Table 132, Spectrum 59) of compound **22** including oxymethylene signal at δ_H 4.91 (2H, s, H_2-2) and a tri-substituted olefinic signal at δ_H 6.70 (1H, s, H-4). Additionally, one singlet aromatic proton resonance at 6.23 ppm was detected due to 5,6,7-trisubstitution in ring A. ABX system was observed in ring B with respect to the remaining aromatic signals [δ_H 7.18 (d, J = 8.9 Hz), 6.42 (dd, J = 8.9, 2.3 Hz) and 6.43 (d, J = 2.3 Hz)]. Furthermore, ^{1}H NMR spectrum showed signals at δ_H 5.23 (1H, m), 3.36 (2H, br d, J = 7.0 Hz) as well as at δ_H 1.82 and 1.75 (each 3H, s) assigned to a prenyl unit. Additionally, proton resonances at δ_H 3.79 and 3.74 (each 3H, s) corresponding to two methoxy groups were detected. The ^{1}H NMR spectrum of **21** and **22** exhibited very similar resonances, but the presence of an additional methoxy group in the spectrum of **22** differed from that of **21**. Thus, the above data were superimposible with those of 7,2'-dihydroxy-5,4'-dimethoxy-6-prenylisoflavene, which is also known as **iconisoflaven** (47).

Table 132. ^{1}H and ^{13}C NMR spectroscopic data of dehydroglyasperin C (**21**) (CD$_3$OD, ^{1}H: 400 MHz, ^{13}C: 100 MHz)^a and iconisoflaven (**22**) (CDCl$_3$, 400 MHz)

C/H atom	Multiplicity	δ$_H$ (ppm), *J* (Hz)	δ$_C$ (ppm)	δ$_H$ (ppm), *J* (Hz)
		21		**22**
2	CH$_2$	4.88 s	69.3	4.91 s
3	C	-	129.9	-
4	CH	6.66 s	116.6	6.70 s
5	C	-	156.8	-
6	C	-	115.9	-
7	C	-	157.4	-
8	CH	6.11 s	99.8	6.23 s
9	C	-	154.5	-
10	C	-	111.0	-
1'	C	-	119.5	-
2'	C	-	159.5	-
3'	CH	6.30 d (2.3)	103.9	6.43 d (2.3)
4'	C	-	157.6	-
5'	CH	6.30 dd (9.0, 2.3)	108.2	6.42 dd (8.9, 2.3)
6'	CH	7.06 d (9.0)	130.3	7.18 d (8.9)
1"	CH$_2$	3.24 br d (6.9)	23.6	3.36 br d (7.0)
2"	CH	5.19 m	125.5	5.23 m
3"	C	-	131.2	-
4"	CH$_3$	1.66 s	26.1	1.75 s
5"	CH$_3$	1.76 s	18.1	1.82 s
5-OCH$_3$	CH$_3$	3.71 s	62.7	3.74 s
4'-OCH$_3$	CH$_3$	-	-	3.79 s

^{a} Resonances were assigned by the help of 2D NMR (COSY, HSQC and HMBC) techniques.
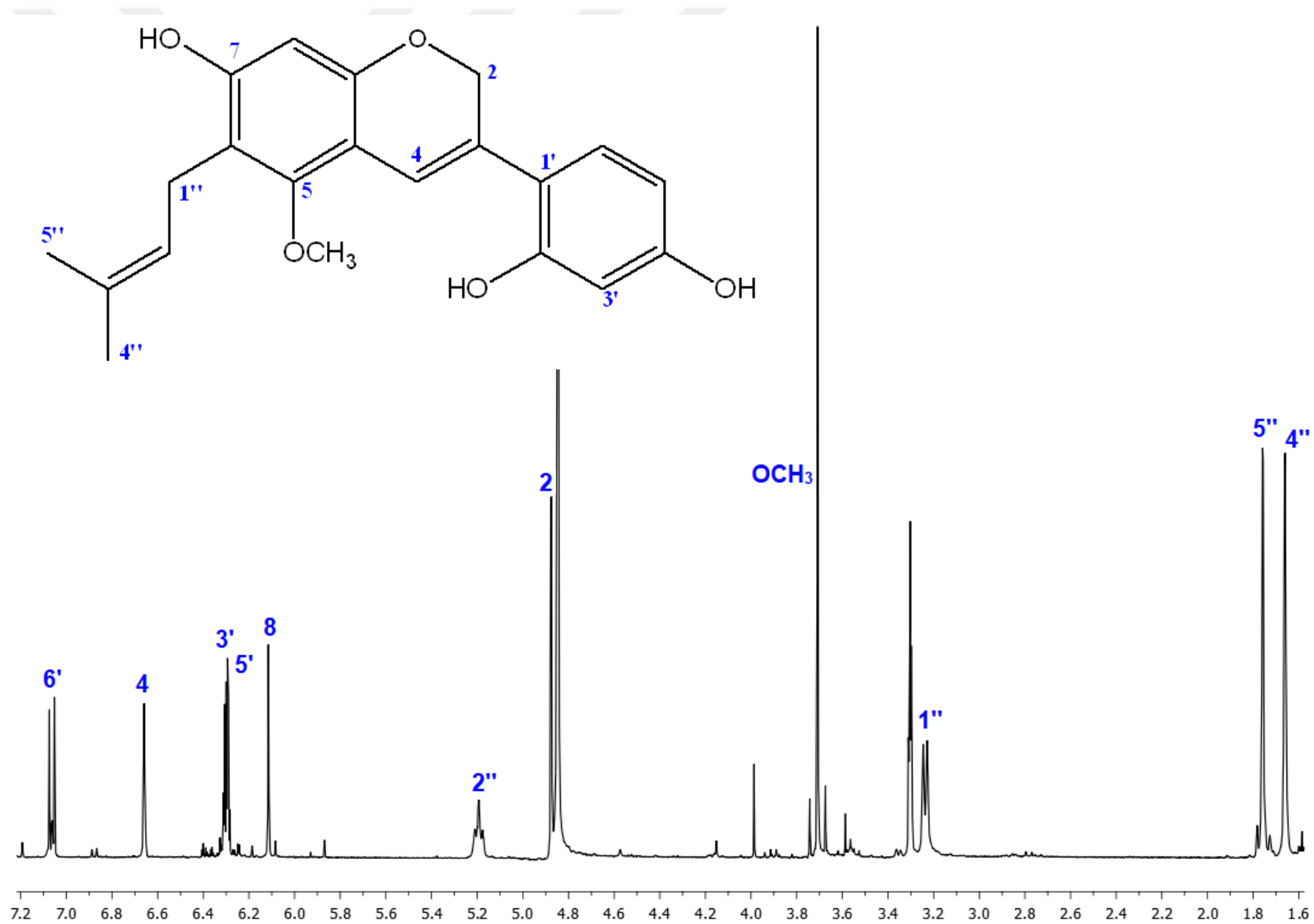
Spectrum 54. ^{1}H NMR Spectrum of Dehydroglyasperin C (**21**) (CD$_3$OD, 400 MHz)
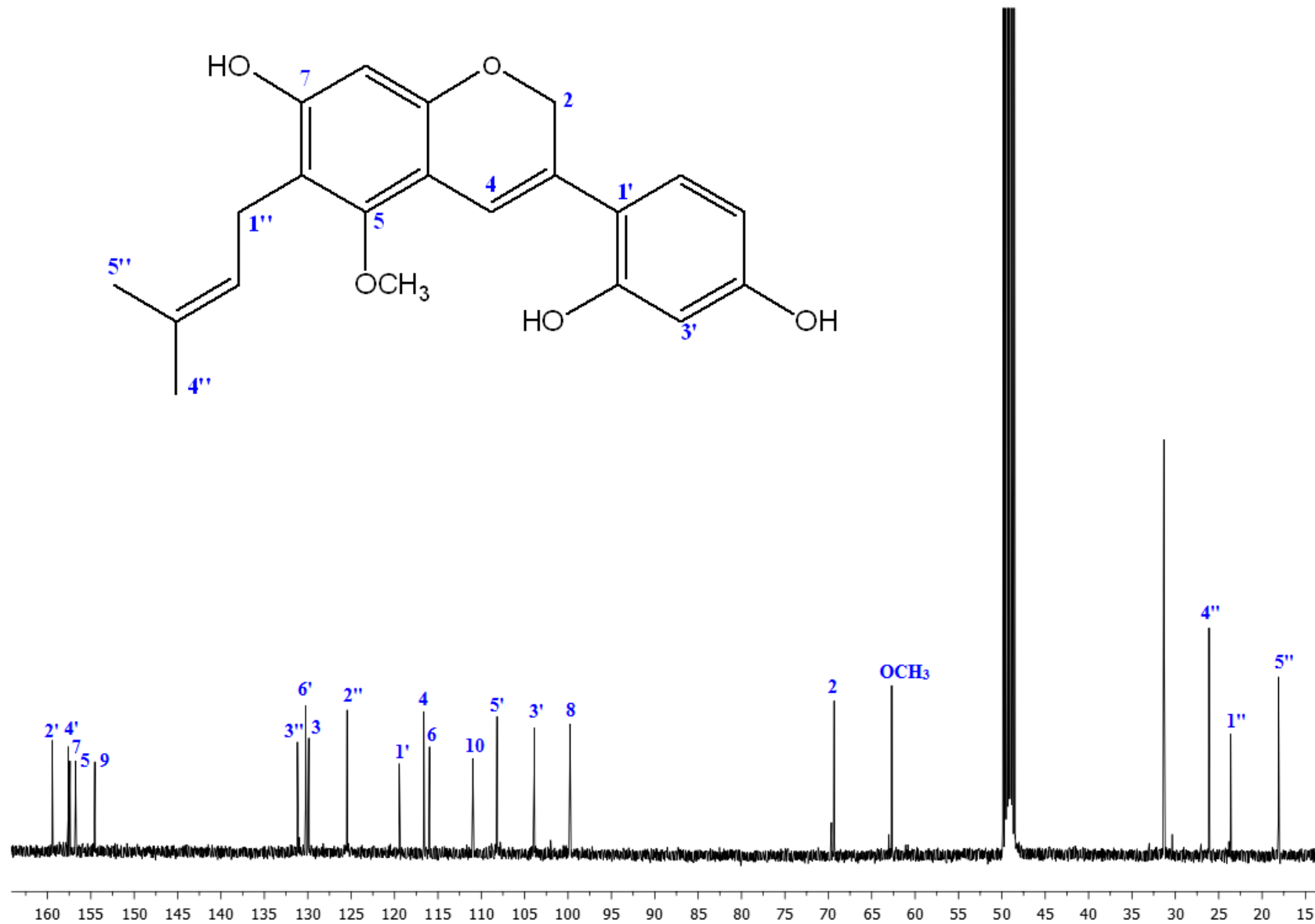
Spectrum 55. ^{13}C NMR Spectrum of Dehydroglyasperin C (**21**) (CD$_3$OD, 100 MHz)
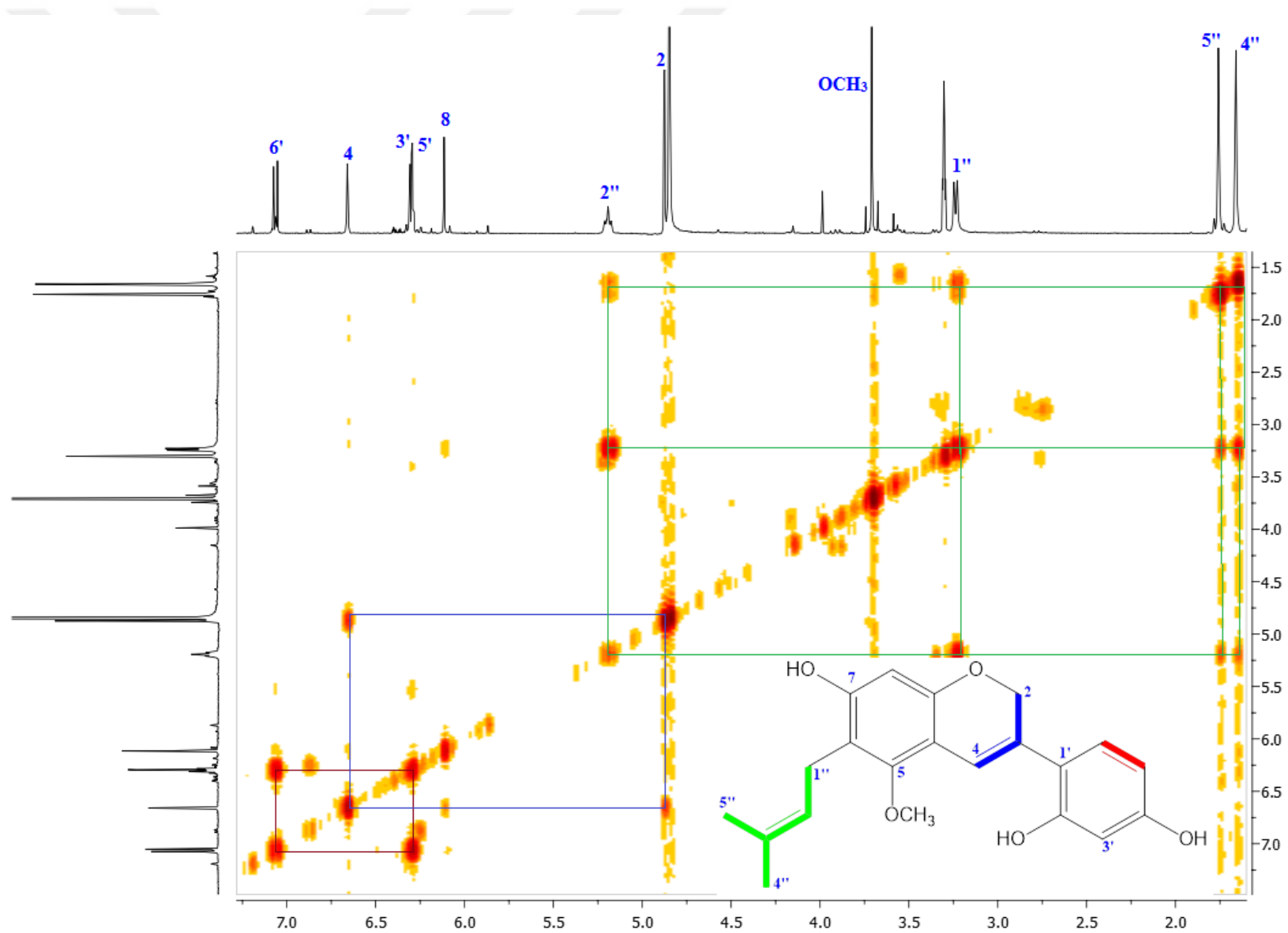
Spectrum 56. 2D-^{1}H,^{1}H-Homonuclear Correlation Spectrum (COSY) of Dehydroglyasperin C (**21**)
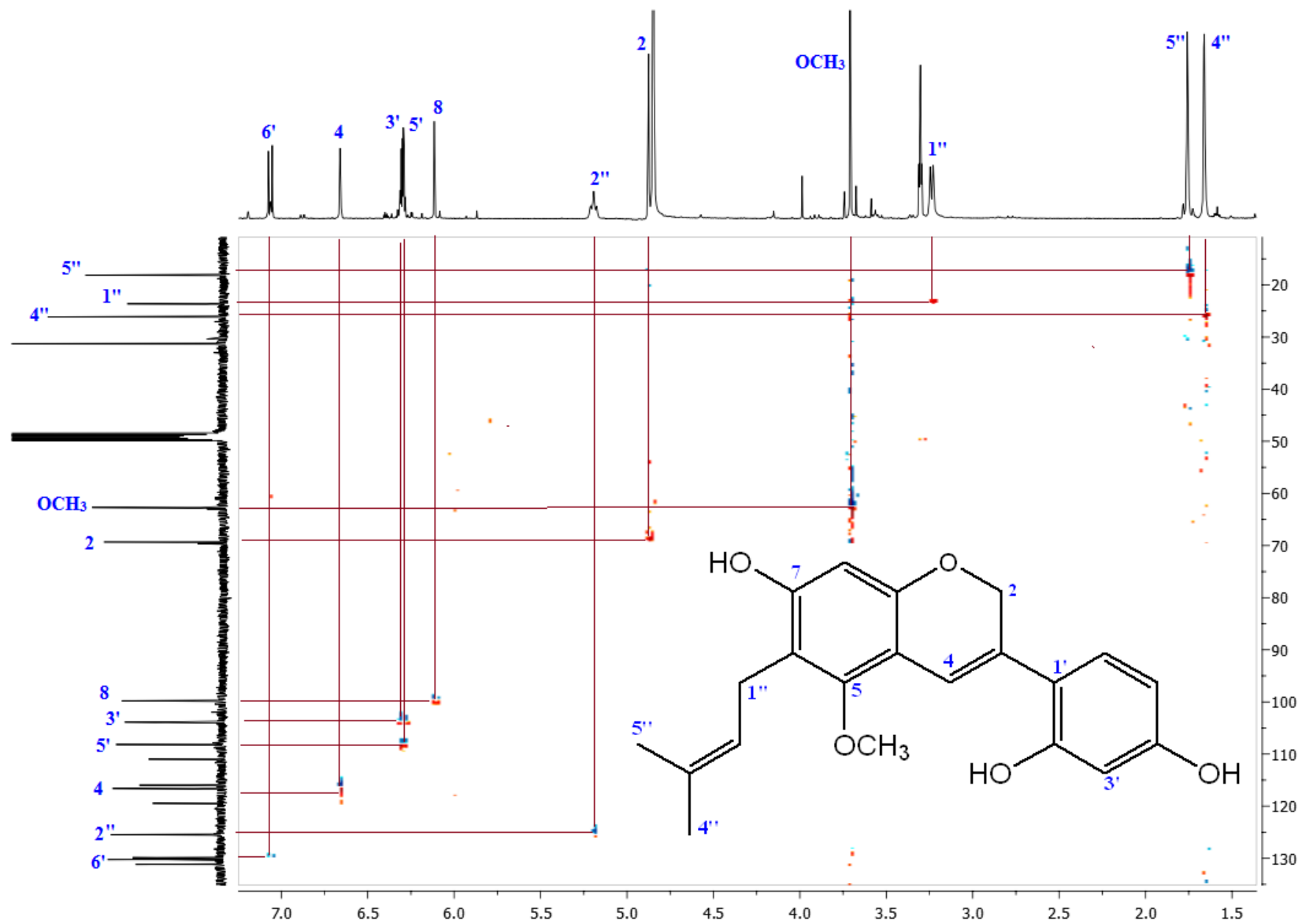
Spectrum 57. Heteronuclear 2D-^{1}H,^{13}C Correlation Spectrum (short range) of Dehydroglyasperin C (**21**) (HSQC)

266
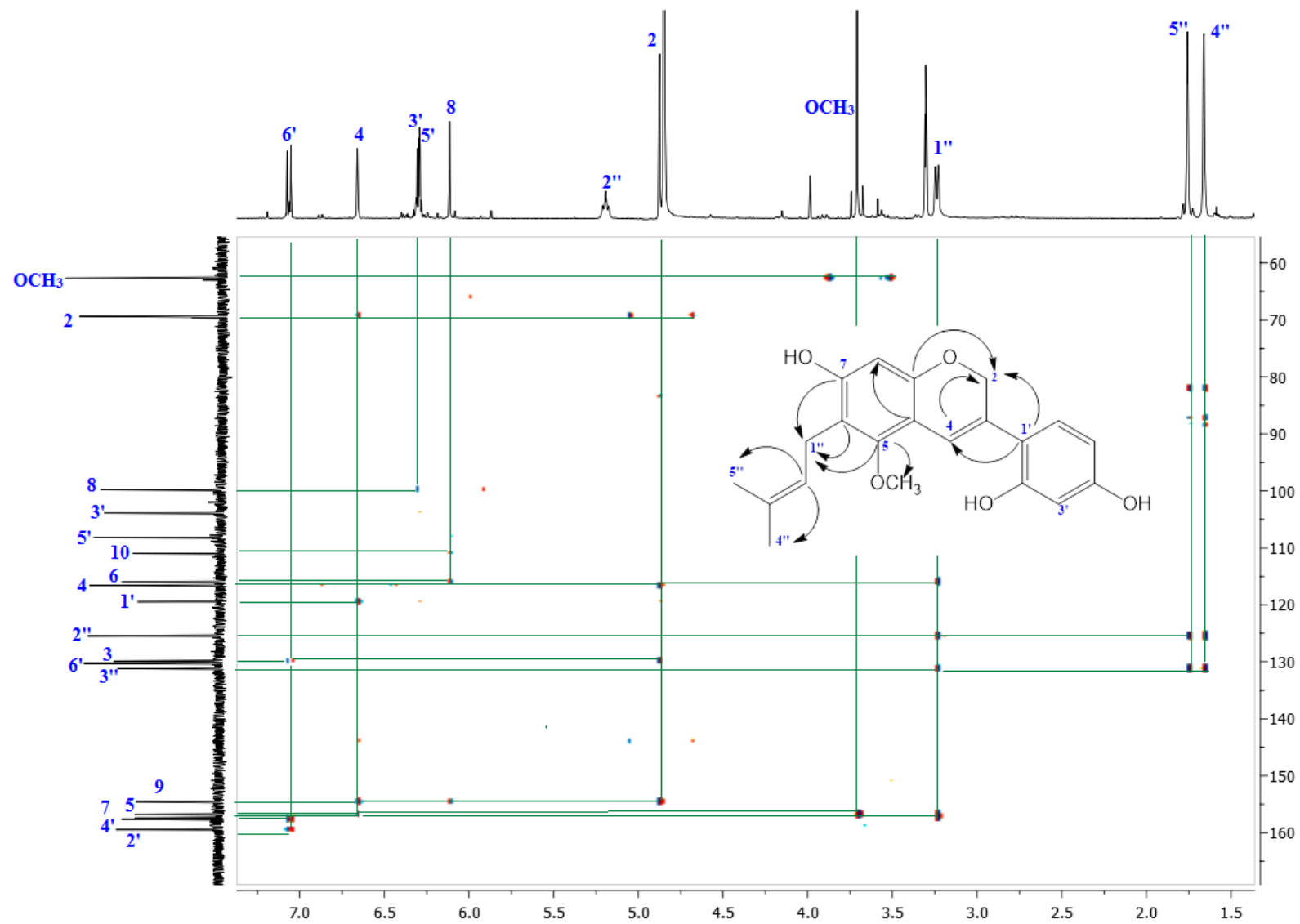
Spectrum 58. Heteronuclear 2D-^{1}H,^{13}C Correlation Spectrum (long range) of Dehydroglyasperin C (**21**) (HMBC)

267
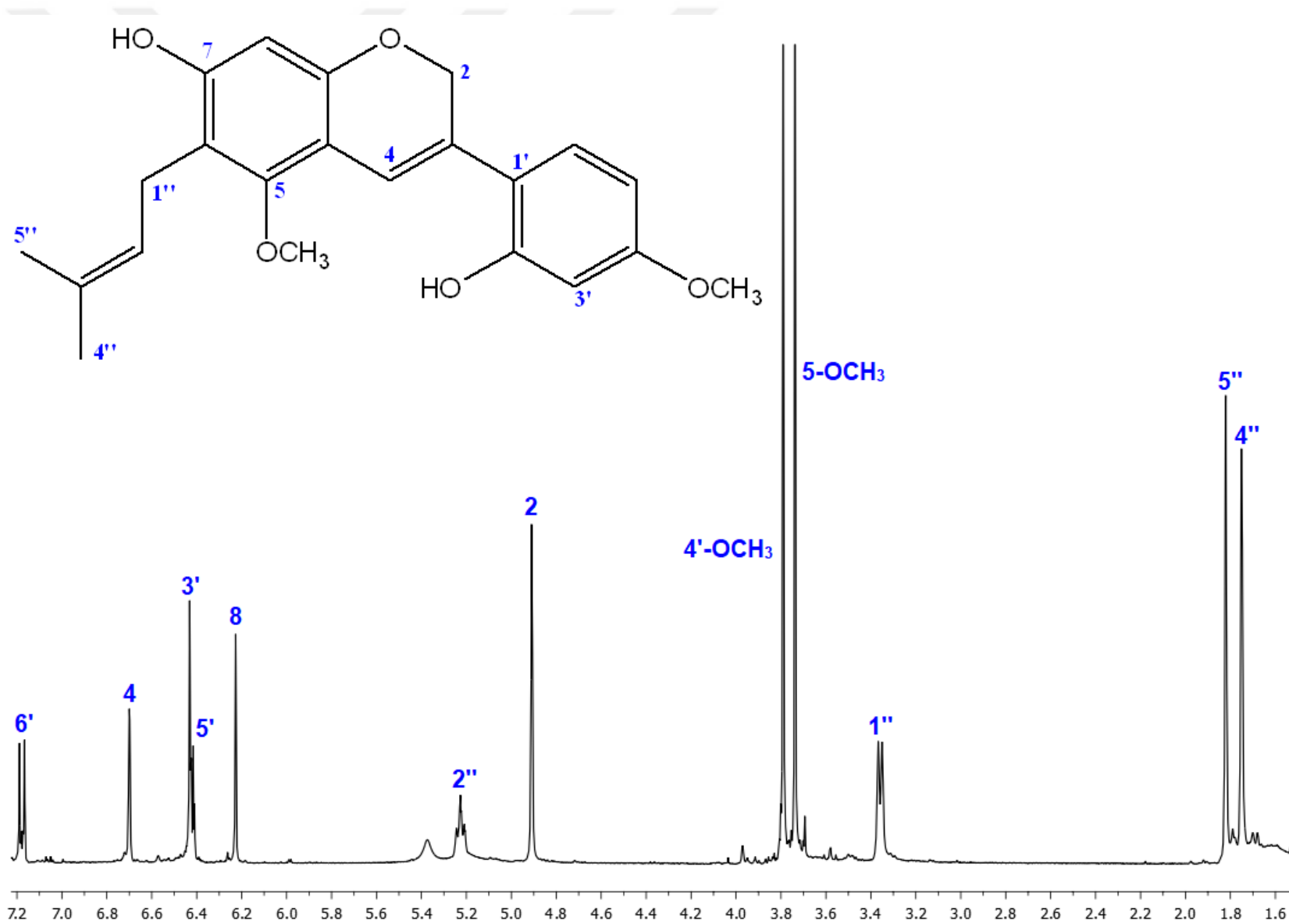
Spectrum 59. ^{1}H NMR Spectrum of Iconisoflaven (**22**) (CDCl$_3$, 400 MHz)

4.5.1.8. 2-Arylbenzofurans
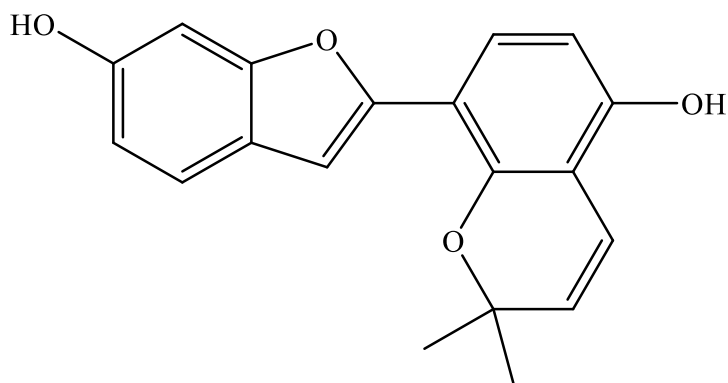
KANZONOL U (23): C$_{19}$H$_{16}$O$_4$ (MW: 308.33)

UV λ_{max} (MeOH) nm:	210 (sh), 275 (sh), 281, 289 (sh), 318
IR υ_{max} (KBr) cm^{-1}:	3392 (OH), 1601 (conjugated C=C), 1488 (aromatic ring)
HR-ESI-MS *m/z*:	309.1124 [M+H]$^+$ (calcd for C$_{19}$H$_{17}$O$_4$, 309,1127), 331.0944 [M+Na]$^+$ (calcd for C$_{19}$H$_{16}$O$_4$Na, 331.0946)
^{1}H NMR:	Table 133, Spectrum 60
^{13}C NMR:	Table 133, Spectrum 61
HMBC:	Spectrum 62

KANZONOL U (23)

Compound **23** was obtained as a yellow amorphous powder from CHCl$_3$ subextract of *G. glabra* roots. Molecular weight was calculated as 308.33 and molecular formula was established as C$_{19}$H$_{16}$O$_4$ based pseudomolecular on ion peaks at *m/z* 309.1124 [M+H]$^+$ (calcd for C$_{19}$H$_{17}$O$_4$, 309.1127) and 331.0944 [M+Na]$^+$ (calcd for C$_{19}$H$_{16}$O$_4$Na, 331.0946) in HR-ESI-MS. Bands at 210 (sh), 275 (sh), 281, 289 (sh), 318 nm on UV spectroscopy indicated the polyphenolic structure. The IR spectrum displayed bands at 3392 (OH), 1601 (conjugated C=C), 1488 (aromatic ring) cm^{-1}.

In aromatic region (7.59 - 6.44 ppm) of the ^{1}H NMR spectrum (Table 133, Spectrum 60) of compound **23**, one ABXY type olefinic and aromatic signals (H-3 and A ring) as well as one AB type *ortho*-coupled aromatic proton signals (B ring) were observed. ABXY type signals were detected at δ_H 7.08 (d, *J* = 1.0 Hz), 7.31 (br d, *J* = 8.4 Hz), 6.70 (dd, *J* = 8.4, 2.1 Hz) and 6.87 (ddd, *J* = 2.1, 1.0, 0.4 Hz), ascribed to H-3, H-4, H-5 and H-7, respectively. ^{13}C NMR spectrum (Table 133, Spectrum 61) showed five oxygenated aromatic carbon signals between 154.7-150.4 ppm assigned as C-2, C-6, C-7a, C-2' and C-4'. These findings were consistent with a 2-arylbenzofuran skeleton (23). Additionally, two conjugated doublet signals at δ_H 6.70 (*J* = 10.0 Hz) and 5.67 (*J* = 10.0 Hz) along with two overlapped methyl signals observed at 1.51 ppm (each 3H, s) in ^{1}H NMR spectrum and 26.8 (2 x C) in ^{13}C NMR spectrum were the indicator of 2,2-dimethylpyran ring. In COSY experiment, cross peaks were observed between protons of H-5'/H-6', H-4/H-5 and H-7'/H-8'. ^{13}C-^{1}H long range correlations (Spectrum 62) from C-3' (δ_C 109.5) to H-5' (δ_H 6.44) and H-8' (δ_H 5.67) and from C-4' (δ_C 153.0) to H-7' (δ_H 6.70) placed the cyclization site of isoprenyl from C-3'. HMBC spectrum also showed cross-peaks between the carbon resonance at δ_C 154.6 (C-7a) and proton resonances at δ_H 7.08 (H-3) and 7.31 (H-4), between carbon signal at 154.7 (C-6) and 7.31 (H-4) as well as between carbon signals of C-2' (δ_C 150.4)/C-4' (δ_C 153.0) and H-6' (δ_H 7.59) which pointed the oxygenated sites of the compound and confirmed the exact structure. Based on the above data, the compound was characterized as 4',6-dihydroxy-9',9'-dimethylpyrano[b-2',3']-2-arylbenzofuran, namely **kanzonol U** (171).

Table 133. ^{1}H and ^{13}C NMR spectroscopic data of kanzonol U (**23**) (CD$_3$OD, 400 MHz, ^{13}C: 100 MHz)^a

C/H atom	Multiplicity	δ_H (ppm), J (Hz)	δ_C (ppm)
2	C	-	151.4
3	CH	7.08 d (1.0)	102.8
3a	C	-	122.4
4	CH	7.31 br d (8.4)	120.2
5	CH	6.70 dd (8.4, 2.1)	111.3
6	C	-	154.7
7	CH	6.87 ddd (2.1, 1.0, 0.4)	96.8
7a	C	-	154.6
1'	C	-	111.0
2'	C	-	150.4
3'	C	-	109.5
4'	C	-	153.0
5'	CH	6.44 d (8.6)	107.4
6'	CH	7.59 d (8.6)	125.5
7'	CH	6.70 d (10.0)	116.9
8'	CH	5.67 d (10.0)	127.9
9'	C	-	76.2
10'	CH$_3$	1.51 s	26.8
11'	CH$_3$	1.51 s	26.8

^{a} Resonances were assigned by the help of HMBC experiment.
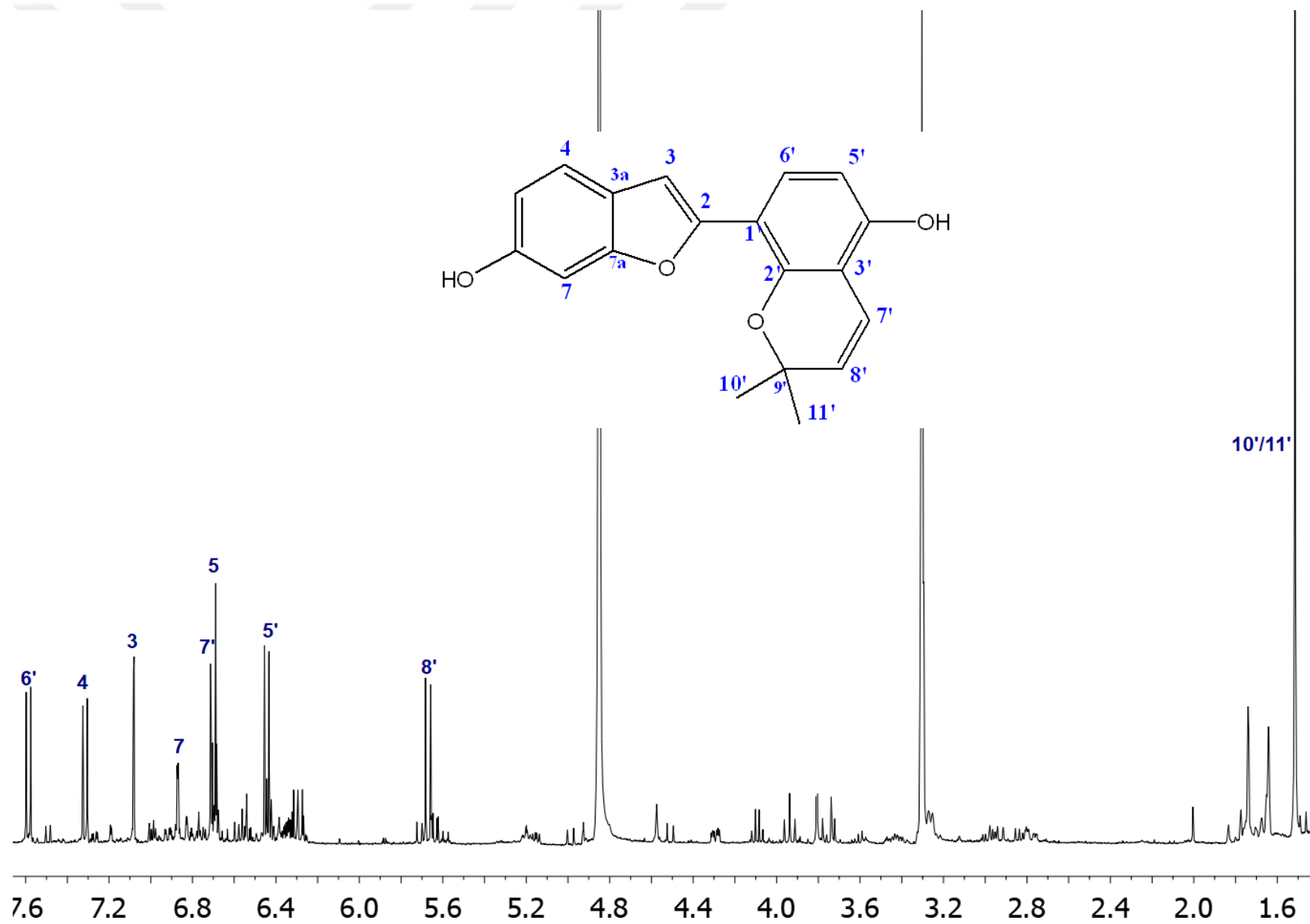
Spectrum 60. ^{1}H NMR Spectrum of Kanzonol U (**23**) (CD$_3$OD, 400 MHz)
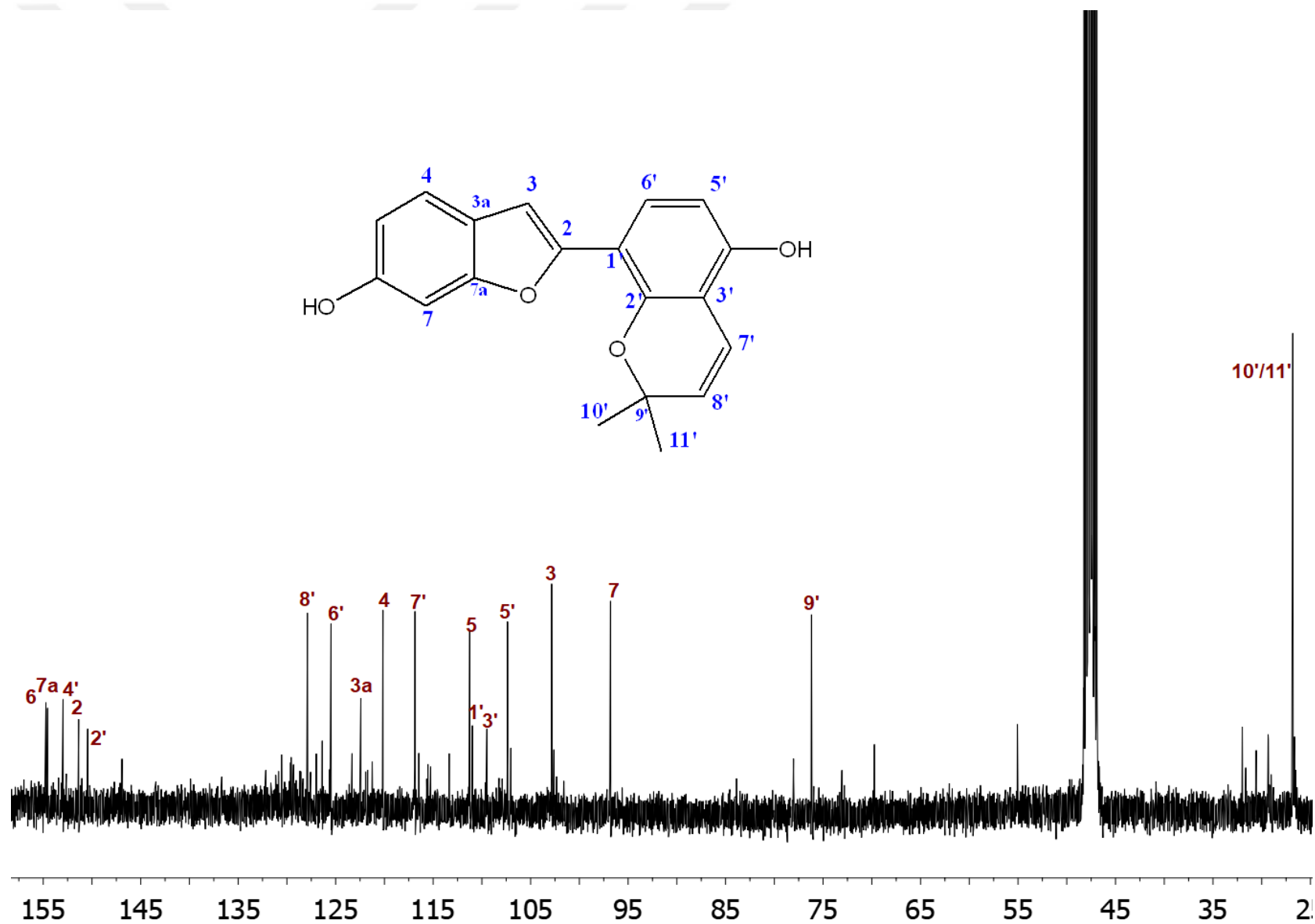
Spectrum 61. ^{13}C NMR Spectrum of Kanzonol U (**23**) (CD$_3$OD, 100 MHz)
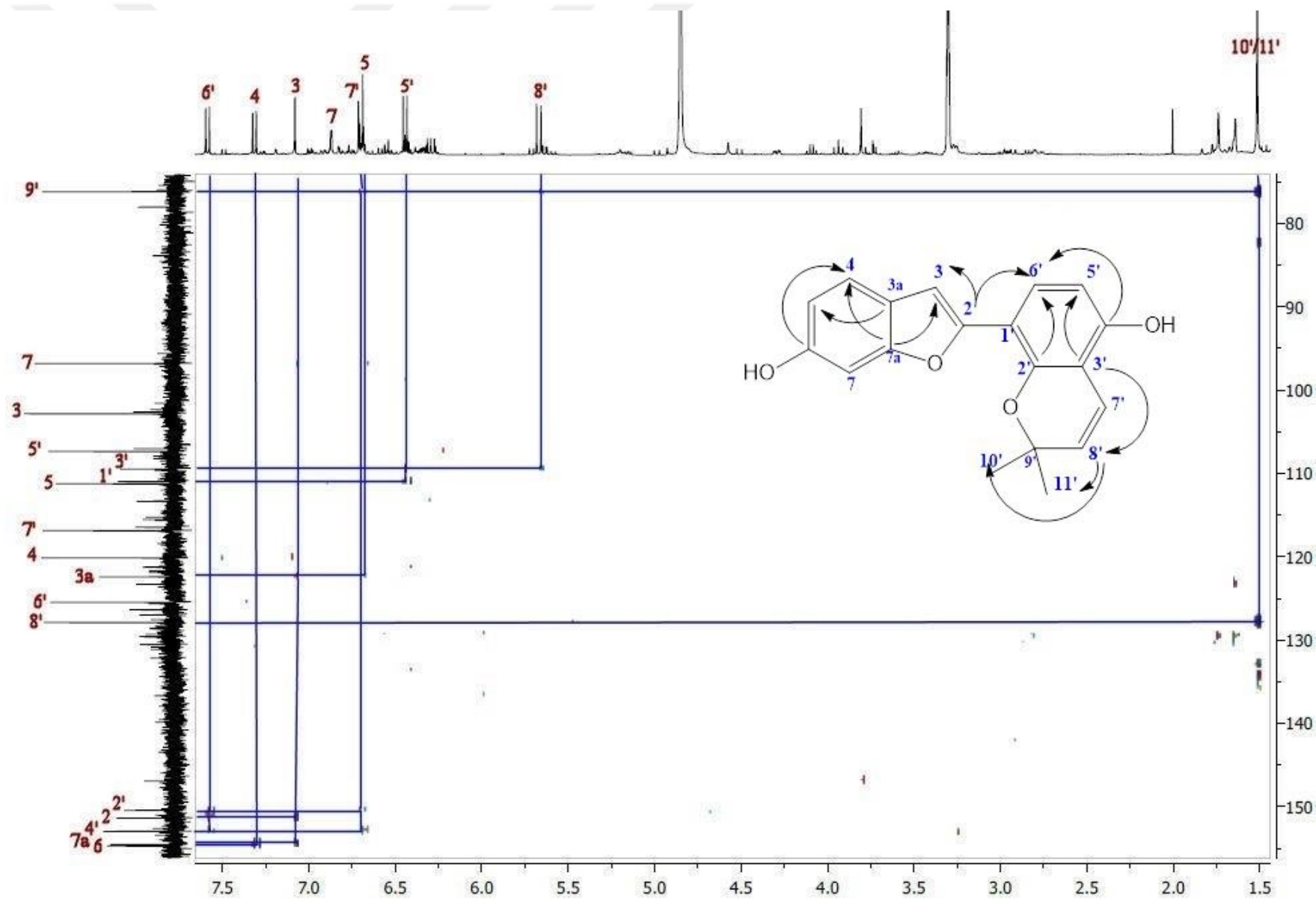
Spectrum 62. Heteronuclear 2D-^{1}H,^{13}C Correlation Spectrum (long range) of Kanzonol U (**23**) (HMBC)

274
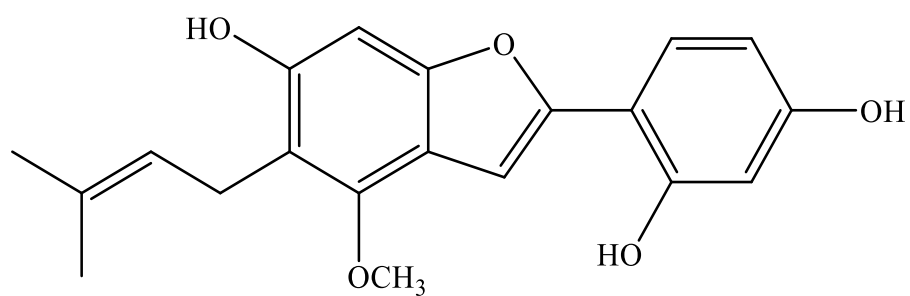
LICOCOUMARONE (24): C$_{20}$H$_{20}$O$_5$ (MW: 340.38)

UV λ_{max} (MeOH) nm:	203, 321, 336
IR υ_{max} (KBr) cm^{-1}:	3409 (OH), 1622 (conjugated C=C), 1460 (aromatic ring)
^{1}H NMR:	Table 134, Spectrum 63
^{13}C NMR:	Table 134, Spectrum 64
COSY:	Spectrum 65
HSQC:	Spectrum 66
HMBC:	Spectrum 67

LICOCOUMARONE (24)

Compound **24** was obtained as light orange colored amorphous powder from EtOAc subextract of *G. iconica* roots. Molecular weight was calculated as 340.38 and molecular formula was elucidated to be $C_{20}H_{20}O_5$. Bands at 203, 321, 336 nm were seen on UV spectroscopy. The IR spectrum displayed bands at 3409 (OH), 1622 (conjugated C=C), 1460 (aromatic ring) cm^{-1}.

^{1}H NMR spectrum (Table 134, Spectrum 63) of compound **24** contained one ABX type aromatic signals at δ_H 7.62 (d, J = 8.4 Hz), 6.37 (dd, J = 8.4, 2.3 Hz) and 6.40 (dd, J = 2.3 Hz) ascribed to H-6', H-5' and H-3' in ring B, respectively. Additionally, one aromatic singlet proton signal was observed at 6.65 ppm (s, H-7) as well as one olefinic singlet at 7.19 ppm (s, H-3). Furthermore, proton resonances of one methoxy at δ_H 3.99 (3H, s) and one isoprenyl unit at δ_H 3.35 (br d, J = 7.1 Hz, H-1"), 5.22 (m, H-2"), 1.66 and 1.78 (each 3H, s, H-4/"5") were observed. Two spins system were dedected in its COSY spectrum (Spectrum 65). These data along with the carbon resonances secured by HSQC (Spectrum 66) suggested the presence of 2-arylbenzofuran skeleton, with methoxy and isoprenyl units. According to HMBC experiments (Spectrum 67), ^{13}C-^{1}H long range correlations from C-4 (δ_C 152.3), C-5 (δ_C 116.4) and C-6 (δ_c= 154.7) to methylene signal of isoprenyl unit H-1" (δ_H 3.35) led to the location of isoprenyl unit at C-5. The attachment site of methoxy unit was determined to be at C-4 with regard to the cross-peak between C-4 (δ_C 152.3) and methoxy signal (δ_H 3.99). 2',4'-dihydroxylation of ring B was estabished by the correlations between C-2 (δ_C 152.2), C-2' (δ_C 156.9), C-4' (δ_C 159.5) and H-6' (δ_H 7.62). Furthermore, the interfragmental connections were observed with HMBC between C-3a/H-7, C-2/H-3 and C-7a/H-3 which confirmed the exact structure of the compound as 6,2',4'-trihydroxy-4-methoxy-5-prenyl-2-arylbenzofuran. All the data in published literature were overlapped with the spectral data of compound **licocoumarone** (248).

Table 134. ^{1}H and ^{13}C NMR spectroscopic data of licocoumarone (**24**) (CD$_3$OD, ^{1}H: 400 MHz, ^{13}C: 100 MHz)[a]

C/H atom	Multiplicity	δ$_H$ (ppm), J (Hz)	δ$_C$ (ppm)
2	C	-	152.2
3	CH	7.19 s	102.0
3a	C	-	115.2
4	C	-	152.3
5	C	-	116.4
6	C	-	154.7
7	CH	6.65 s	93.6
7a	C	-	155.4
1'	C	-	111.7
2'	C	-	156.9
3'	CH	6.40 d (2.3)	104.0
4'	C	-	159.5
5'	CH	6.37 dd (8.4, 2.3)	108.2
6'	CH	7.62 d (8.4)	128.2
1"	CH$_2$	3.35 br d (7.1)	23.8
2"	CH	5.22 m	125.6
3"	C	-	131.0
4"	CH$_3$	1.78 s	18.1
5"	CH$_3$	1.66 s	26.2
4-OCH$_3$	CH$_3$	3.99 s	60.8

[a] Resonances were assigned by the help of 2D NMR (COSY, HSQC and HMBC) techniques.
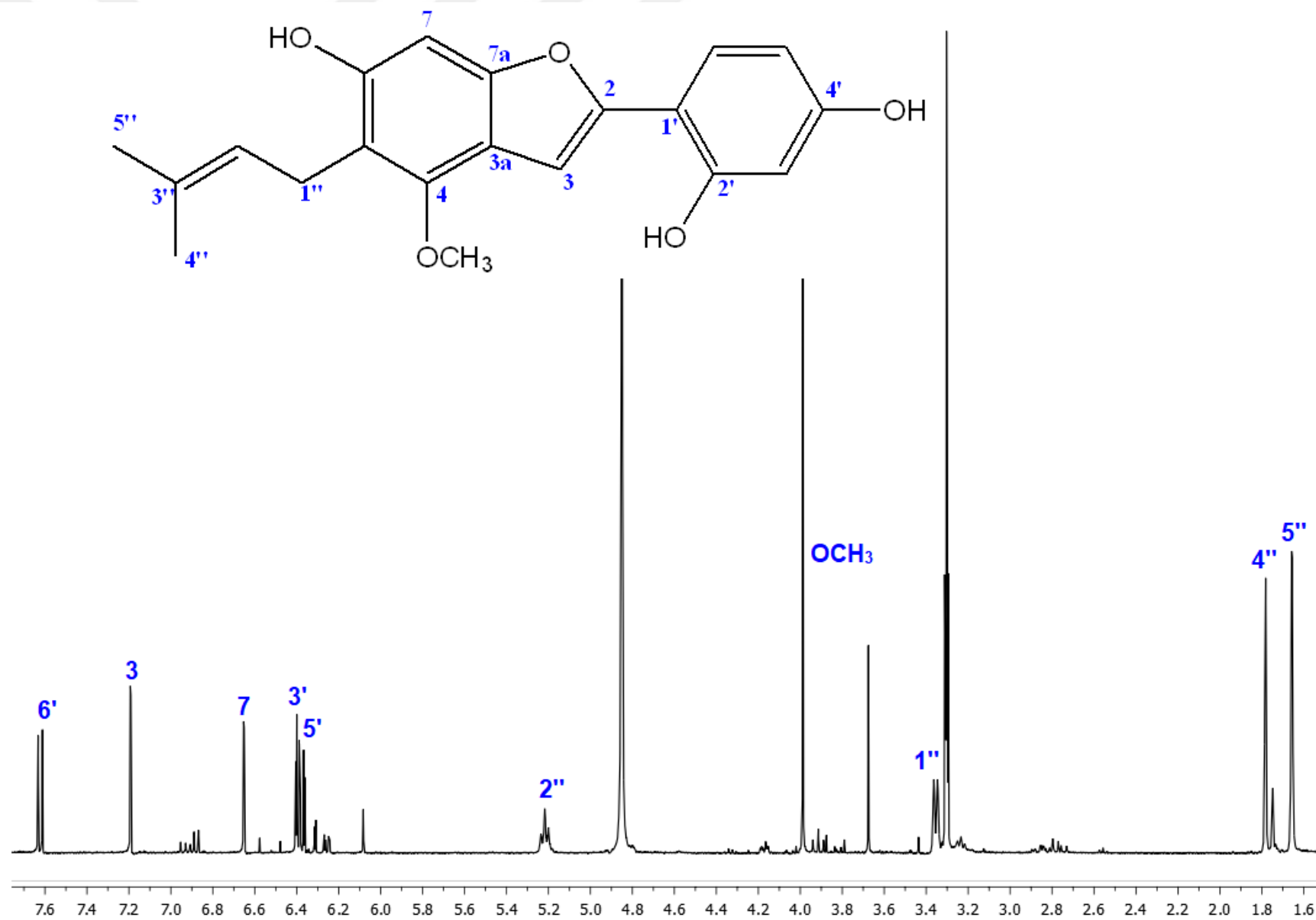
Spectrum 63. ^1H NMR Spectrum of Licocoumarone (**24**) (CD$_3$OD, 400 MHz)

278
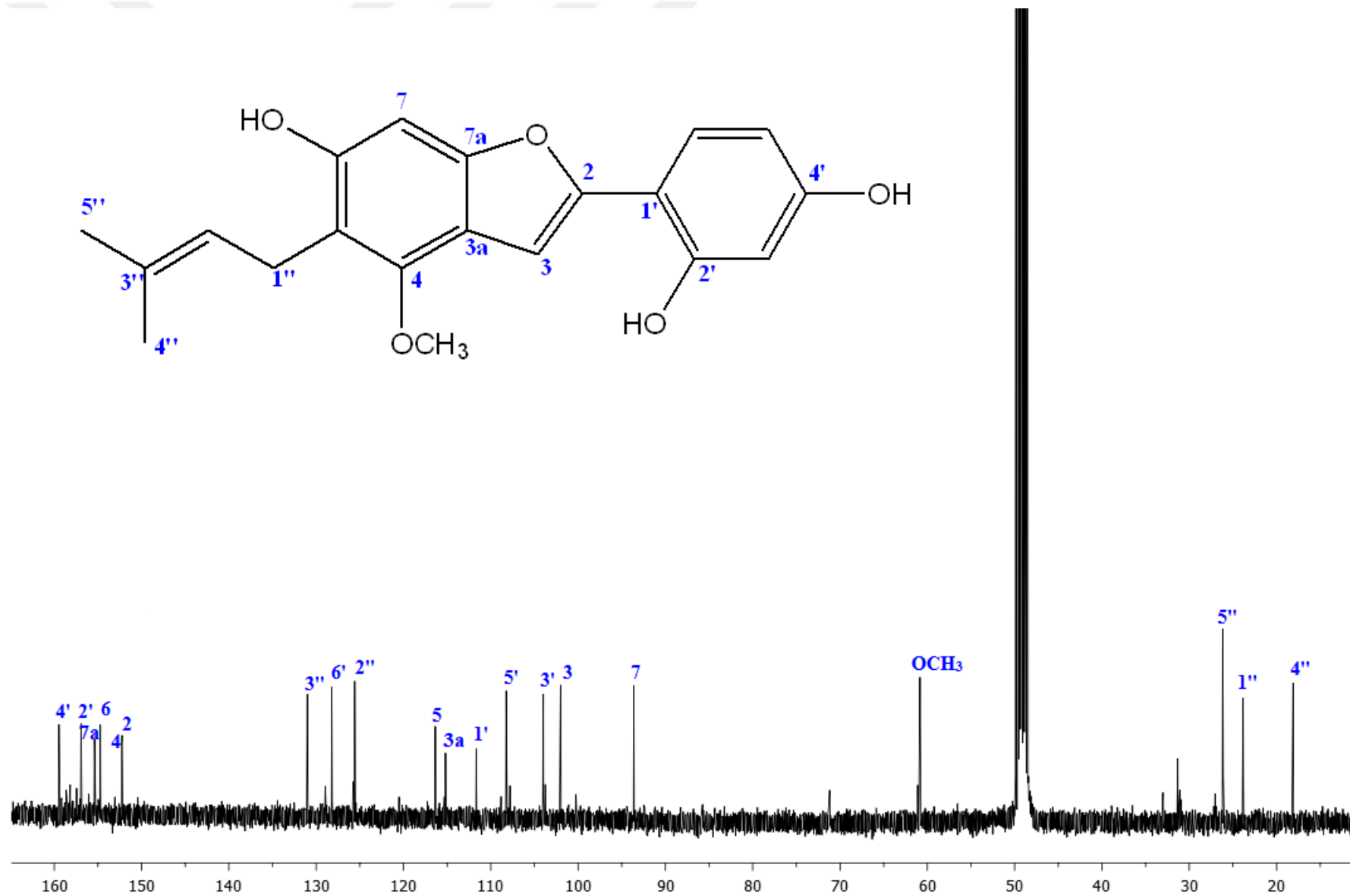
Spectrum 64. ^{13}C NMR Spectrum of Licocoumarone (**24**) (CD$_3$OD, 100 MHz)
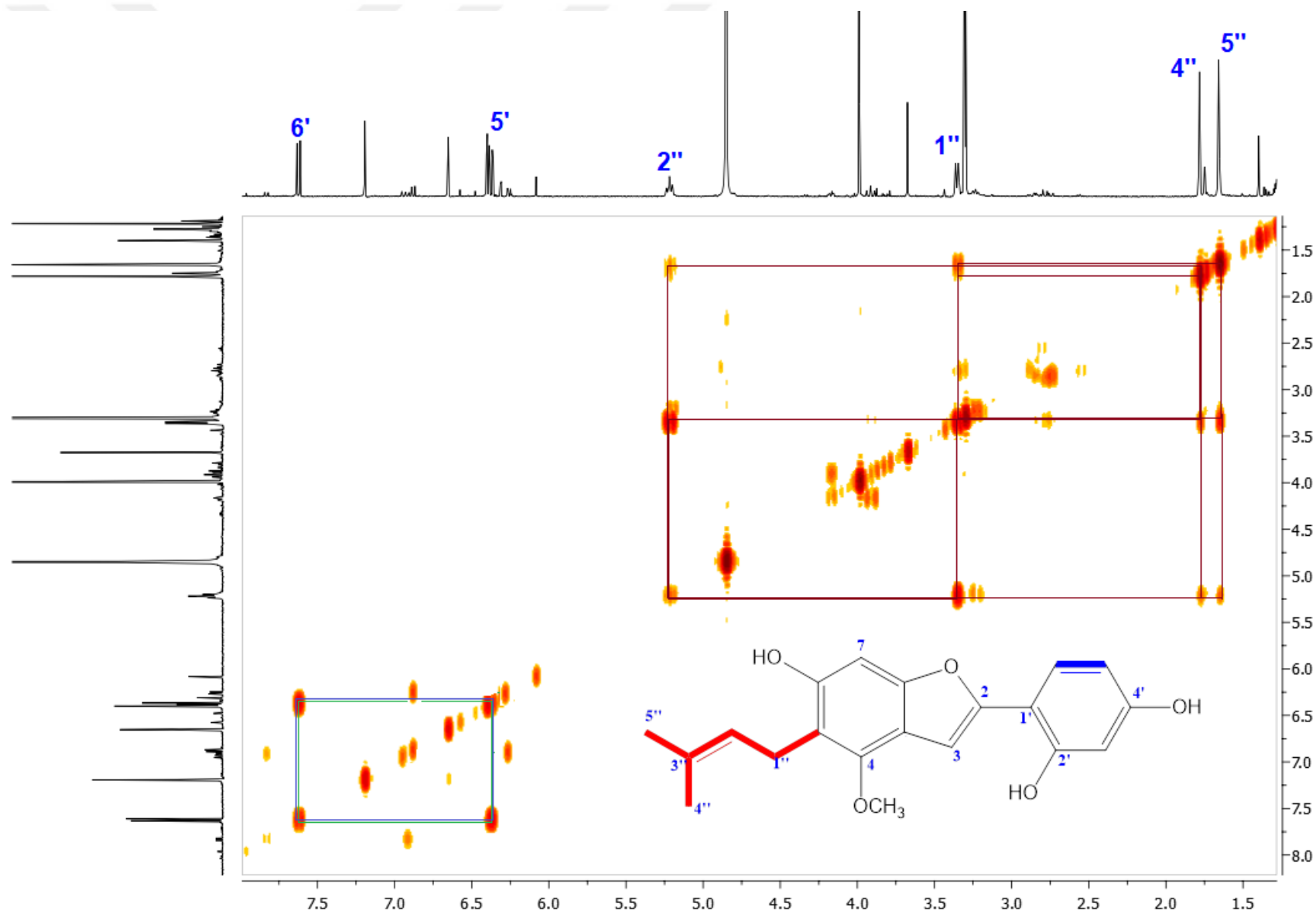
Spectrum 65. 2D-^{1}H,^{1}H-Homonuclear Correlation Spectrum (COSY) of Licocoumarone (**24**)
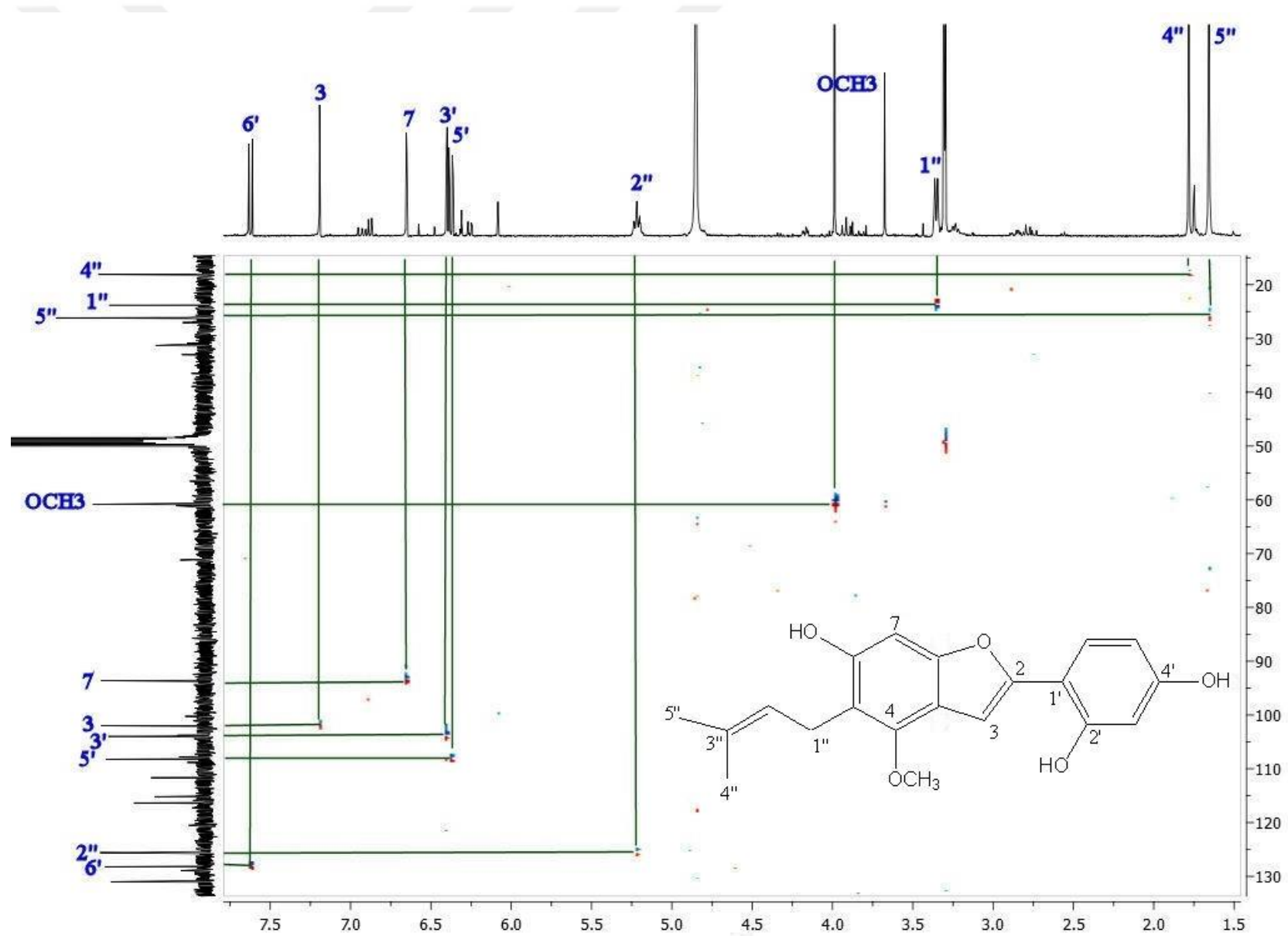
Spectrum 66. Heteronuclear 2D-^{1}H,^{13}C Correlation Spectrum (short range) of Licocoumarone (**24**) (HSQC)

281
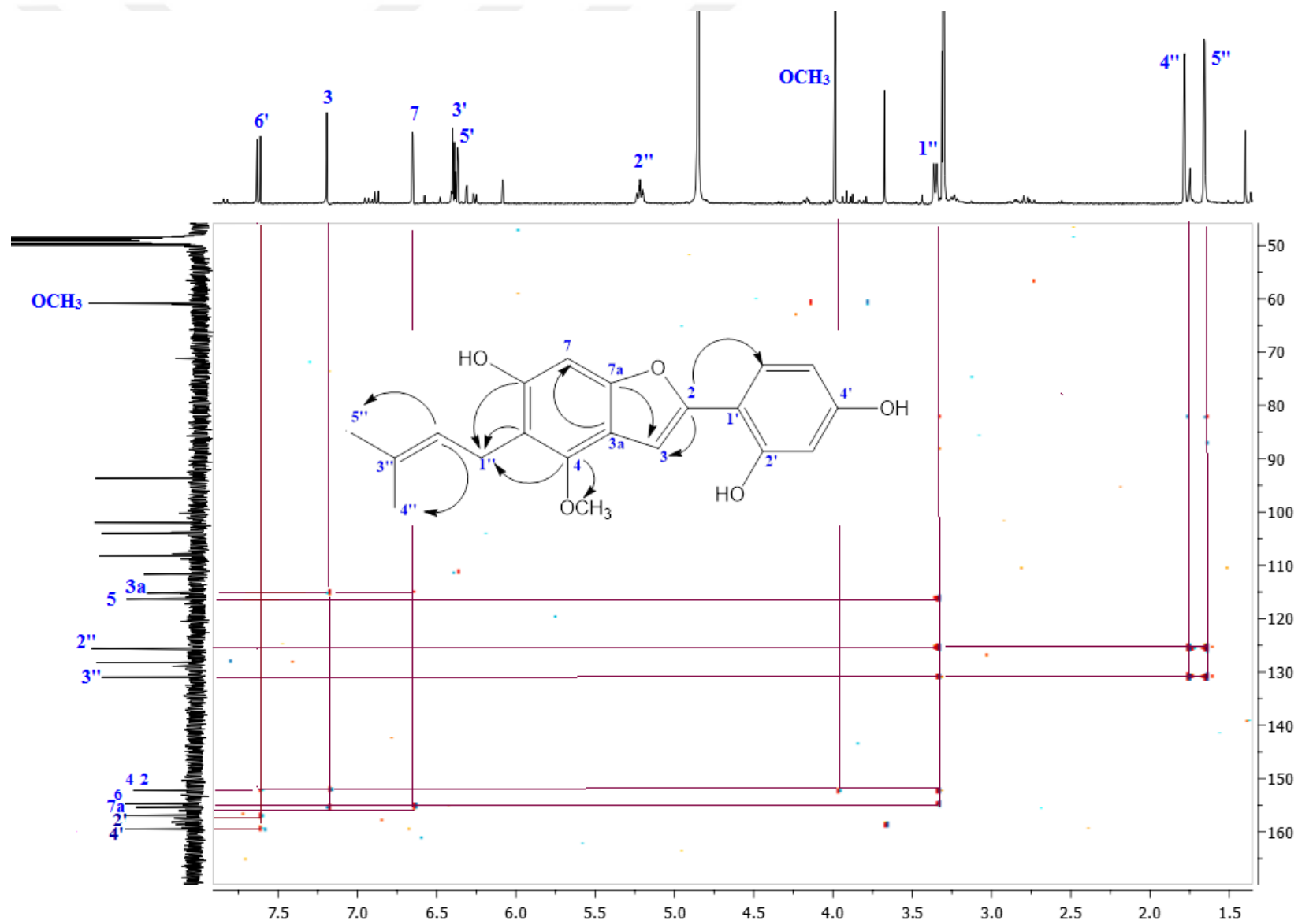
Spectrum 67. Heteronuclear 2D-^{1}H,^{13}C Correlation Spectrum (long range) of Licocoumarone (**24**) (HMBC)

4.5.1.9. 3-Arylcoumarin
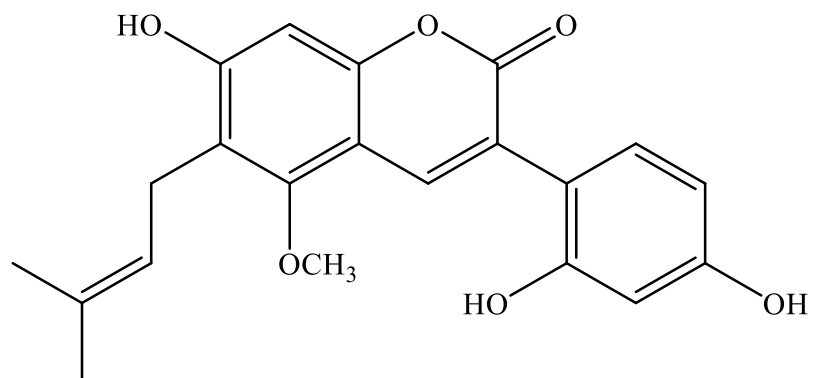
GLYCYCOUMARIN (25): C$_{21}$H$_{20}$O$_6$ (MW: 368.39)

UV λ_{max} (MeOH) nm:	206, 354
IR υ_{max} (KBr) cm^{-1}:	3339 (OH), 1609 (lactone C=O), 1461 (aromatic ring)
^{1}H NMR:	Table 135, Spectrum 68

GLYCYCOUMARIN (25)

Compound **25** was isolated as yellow amorphous powder from CHCl₃, EtOAc and *n*-BuOH subextracts of *G. iconica*, having $C_{21}H_{20}O_6$ molecular formula. UV spectra showed absorption maxima at 206 and 354 nm, while absorption bands indicating hydroxyl group (3339 cm⁻¹), lactone carbonyl group (1609 cm⁻¹) and aromatic ring (1461 cm⁻¹) were observed.

Inspection of ¹H NMR spectrum (Table 135, Spectrum 68) of compound **25** showed one sharp olefinic singlet at 7.96 ppm (H-4) and one aromatic singlet at 6.57 ppm (H-8). The H-4 signal in C ring were shifted to downfield around 1.3 ppm while H-8 signal in A ring was observed to be downshifted around 0.5 ppm when compared to dehdydroglyasperin C (**21**). Furthermore, the spectrum also lacked the signal arising from oxymethylene at around 4.9 ppm. These findings suggested that the structure of compound **25** could be a 3-arylcoumarin derivative. Besides these above mentioned signals, similar proton resonances with that of **21** were appeared in ¹H NMR of **25**. For instance, ABX type signals were observed arising from B ring at δ_H 7.14 (d, *J* = 8.2 Hz), 6.36 (dd, *J* = 8.2, 2.3 Hz) and 6.38 (d, *J* = 2.3 Hz) ascribed to H-6', H-5' and H-3', respectively. Additionally, the ¹H NMR spectrum contained signals for an isoprenyl moiety along with a methoxy group at δ_H 3.36 (d, *J* = 6.8 Hz, H-1"), 5.21 (t, *J* = 6.8 Hz, H-2"), 1.78 and 1.67 (each 3H, s, H-5"/4") and at δ_H 3.82 (3H, s, OCH₃). Based on the above findings, the structure of **25** was identifed as 7,2',4'-trihydroxy-5-methoxy-6-prenyl-3-arylcoumarin, **glycycoumarin** (150). The TLC comparision with the reference compound also supported the structure.

Table 135. ^{1}H NMR spectroscopic data of glycycoumarin (**25**) (CD$_3$OD, 400 MHz)

C/H atom	Multiplicity	δ$_H$ (ppm), J (Hz)
2	C	-
3	C	-
4	CH	7.96 s
5	C	-
6	C	-
7	C	-
8	CH	6.57 s
9	C	-
10	C	-
1'	C	-
2'	C	-
3'	CH	6.38 d (2.3)
4'	C	-
5'	CH	6.36 dd (8.2, 2.3)
6'	CH	7.14 d (8.2)
1"	CH$_2$	3.36 d (6.8)
2"	CH	5.21 t (6.8)
3"	C	-
4"	CH$_3$	1.67 s
5"	CH$_3$	1.78 s
5-OCH$_3$	CH$_3$	3.82 s
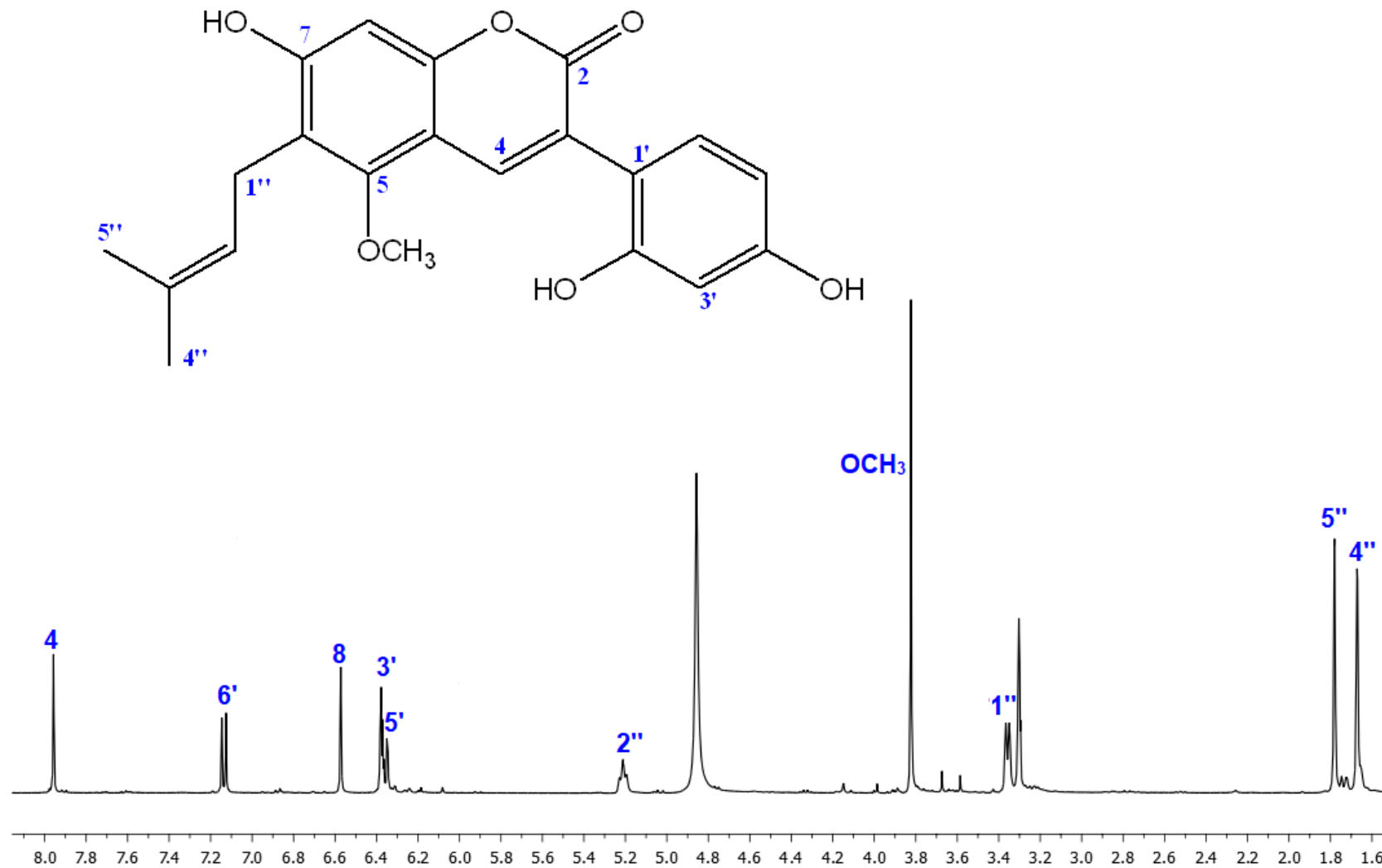
Spectrum 68. ¹H NMR spectrum of Glycycoumarin (**25**) (CD₃OD, 400 MHz)

4.5.1.10. Pterocarpans
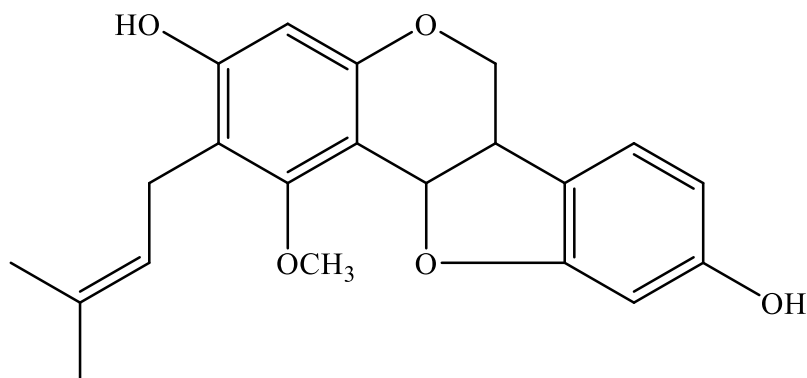
EDUDIOL (26): C$_{21}$H$_{22}$O$_5$ (MW: 354.40)

UV λ_{max} (MeOH) nm:	205 (sh), 217, 273, 334
IR υ_{max} (KBr) cm^{-1}:	3435 (OH), 2918, 2849 (aliphatic C-H), 1619 (conjugated C=C), 1461 (aromatic ring)
MS m/z:	355.5 [M+H]$^+$
^{1}H NMR:	Table 136, Spectrum 69

EDUDIOL (26)

Compound **26** was isolated from $CHCl_3$ subextract of *G. iconica* as pale orange colored amorphous powder. The MS spectrum of compound **26** gave a pseudomolecular ion peak at *m/z* 355.5 $[M+H]^+$ corresponding to the molecular formula of $C_{21}H_{22}O_5$. Its IR spectrum revealed the presence of hydroxyl (3435 cm^{-1}), aliphatic (2918, 2849 cm^{-1}), olefinic (1619 cm^{-1}) atoms and aromatic ring (1461 cm^{-1}), while its UV spectrum showed bands at 205 (sh), 217, 273 and 334 nm.

The ^1H NMR spectrum (Table 136, Spectrum 69) of compound **26** displayed proton signals at δ_H 4.16 (dd, *J* = 11.1, 5.0 Hz), 3.60 (t, *J* = 11.1 Hz), 3.38 (m) and 5.64 (d, *J* = 6.5 Hz), attributed to H$_2$-6, H-6a and H-11a of a pterocarpan core, respectively. Moreover, signals were observed which showed the presence of a methoxy unit at δ_H 3.92 (3H, s), an aromatic singlet at δ_H 6.27 (s, H-4) and aromatic proton signals as an ABX spin system at δ_H 7.07 (d, *J* = 7.9 Hz, H-7), 6.36 (dd, *J* = 7.9, 2.2 Hz, H-8) and 6.39 (d, *J* = 2.2 Hz, H-10). In addition, the ^1H NMR spectrum contained the characteristic signals for an isoprenyl moiety at δ_H 3.40 (2H, br d, *J* = 6.7 Hz), 5.25 (H, m), 1.77 and 1.84 (each 3H, s). Thus, compound **26** was identified as 3,9-dihydroxy-1-methoxy-2-prenylpterocarpan with regard to the superimposible NMR data of **26** with those of **edudiol** (249).

Table 136. ^{1}H NMR spectroscopic data of edudiol (**26**) (CDCl$_3$, 400 MHz)

C/H atom	Multiplicity	δ$_H$ (ppm), J (Hz)
1	C	-
2	C	-
3	C	-
4	CH	6.27 s
4a	C	-
6	CH$_2$	4.16 dd (11.1, 5.0)
		3.60 t (11.1)
6a	CH	3.38 m
6b	C	-
7	CH	7.07 d (7.9)
8	CH	6.36 dd (7.9, 2.2)
9	C	-
10	CH	6.39 d (2.2)
10a	C	-
11a	CH	5.64 d (6.5)
11b	C	-
1'	CH$_2$	3.40 br d (6.7)
2'	CH	5.25 m
3'	C	-
4'	CH$_3$	1.84 s
5'	CH$_3$	1.77 s
1-OCH$_3$	CH$_3$	3.92 s
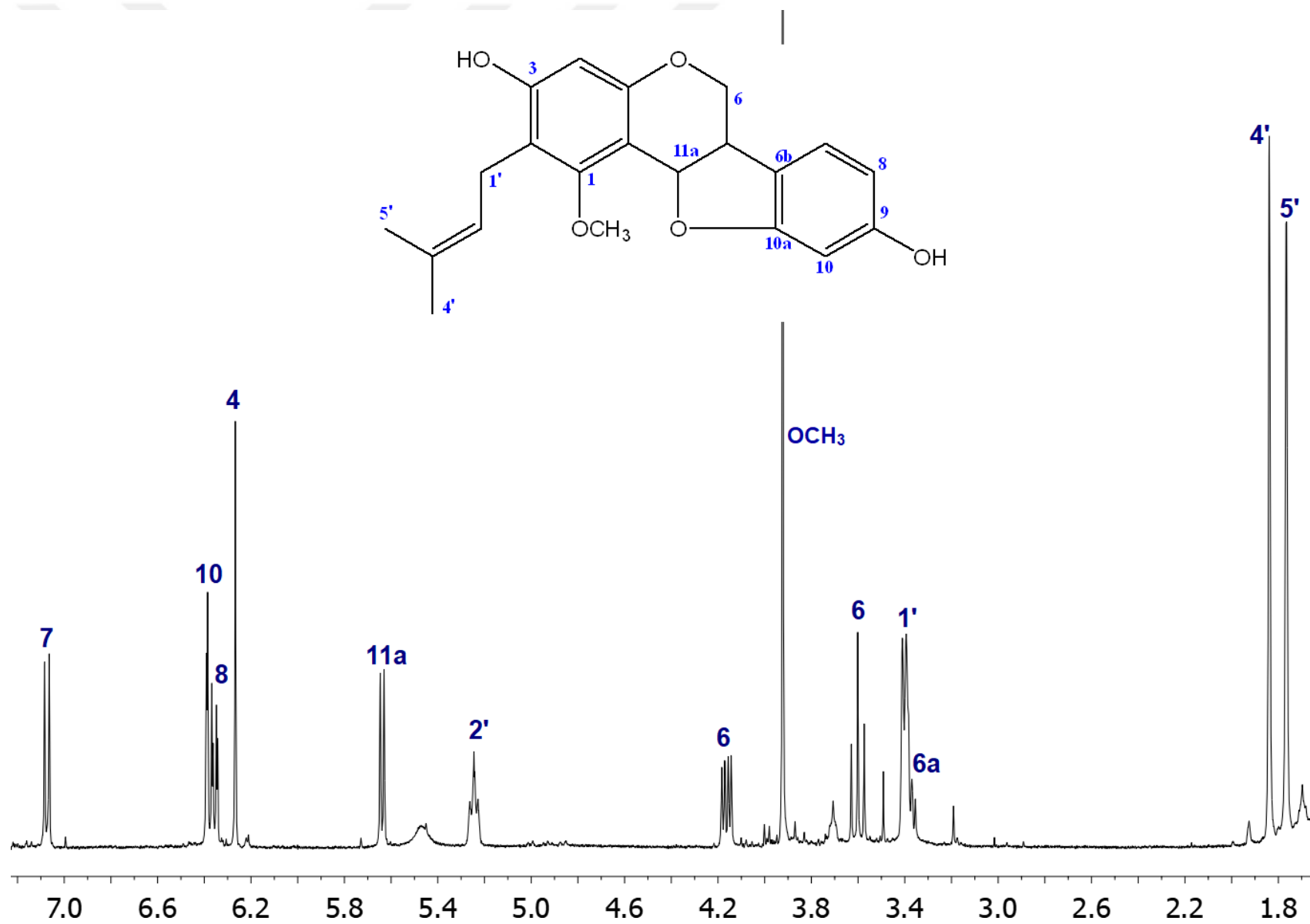
Spectrum 69. ¹H NMR Spectrum of Edudiol (**26**) (CDCl₃, 400 MHz)
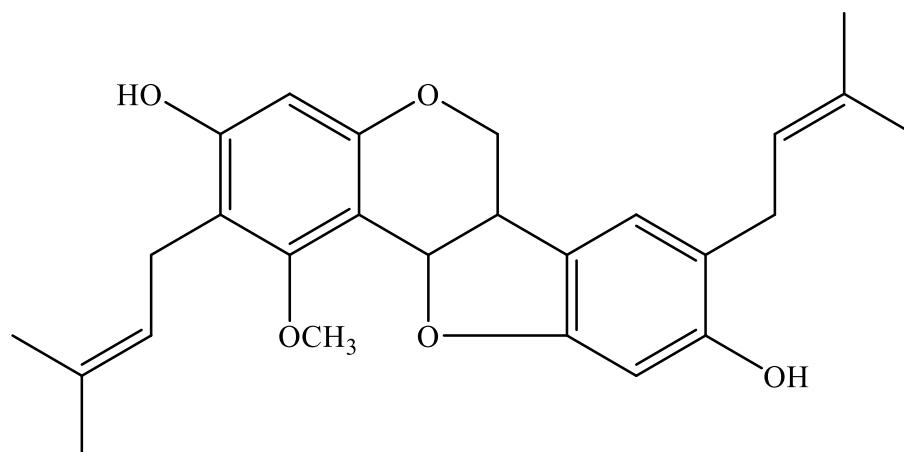
1-METHOXYFICIFOLINOL (27): C₂₆H₃₀O₅ (MW: 422.52)

UV λ$_{max}$ (MeOH) nm:	209, 289, 336
IR υ$_{max}$ (KBr) cm^{-1}:	3430 (OH), 1618 (C=C), 1456 (aromatic ring)
^{1}H NMR:	Table 137, Spectrum 70
^{13}C NMR:	Table 137, Spectrum 71

1-METHOXYFICIFOLINOL (27)

Compound **27**, an amorphous whitish colored powder, isolated from *G. iconica* CHCl$_3$ subextract. Based on the ^{1}H and ^{13}C NMR data, the molecular formula was determined to be C$_{26}$H$_{30}$O$_5$. UV spectrum exhibited bands at 209, 289 and 336 nm. IR spectrum indicated hydroxyl groups (3430 cm^{-1}), olefinic bonds (1618 cm^{-1}) and aromatic ring (1456 cm^{-1}).

The pterocarpan skeleton was deduced from ^{1}H NMR spectrum (Table 137, Spectrum 70) from non-equivalent oxymethylene signals at δ_H 4.16 (dd, J = 11.1, 5.1 Hz) and 3.60 (t, J = 11.1 Hz), one methine signal at δ_H 3.35 (m) as well as oxymethine signal at δ_H 5.60 (d, J = 6.5 Hz), corresponding to H$_2$-6, H-6a, and H-11a, respectively. ^{13}C NMR (Table 137, Spectrum 71) showed totally 26 resonances, supported the pterocarpan skeleton by exhibiting the characteristic signals for C-6, C-6a and C-11a of the pterocarpan core at 66.3, 39.2 and 75.6 ppm, respectively. Moreover, the ^{1}H NMR spectrum contained signals for three aromatic protons at δ_H 6.26 (s, H-4), 6.95 (s, H-7) and 6.38 (s, H-10) suggested trisubstitution in both A and B rings of pterocarpan. Additional signals arising from one methoxy group (δ_H 3.92, 3H, s and δ_C 63.0) and two prenyl groups [δ_H 5.24 (m), 3.29 (br d, J = 7.0 Hz), 1.76 (s), 1.78 (s) and 5.30 (m), 3.40 (br d, J = 7.0 Hz), 1.78 (s), 1.84 (s)] were seen in both ^{1}H and ^{13}C NMR spectra. According to comparison of the proton resonances of compound **27** with those of edudiol (**26**); **27** differs from **26** by possesing one additional isoprenyl group at C-8. Taken together, the structure of **27** was characterized as 3,9-dihydroxy-1-methoxy-2,8-diprenyl-pterocarpan, known as **1-methoxyficifolinol** which was confirmed by the comparasion of NMR data with those published (250).

Table 137. ^{1}H and ^{13}C NMR spectroscopic data of 1-methoxyficifolinol (**27**) (CDCl$_3$, ^{1}H: 400 MHz, ^{13}C: 100 MHz)

C/H atom	Multiplicity	δ$_H$ (ppm), J (Hz)	δ$_C$ (ppm)
1	C	-	155.3
2	C	-	119.0
3	C	-	157.3
4	CH	6.26 s	98.7
4a	C	-	155.1
6	CH$_2$	4.16 dd (11.1, 5.1) 3.60 t (11.1)	66.3
6a	CH	3.35 m	39.2
6b	C	-	113.9
7	CH	6.95 s	125.1
8	CH	-	118.6
9	C	-	159.4
10	CH	6.38 s	100.4
10a	C	-	159.2
11a	CH	5.60 d (6.5)	75.6
11b	C	-	107.0
1'	CH$_2$	3.29 br d (7.0)	23.0
2'	CH	5.24 m	122.2
3'	C	-	135.3
4'	CH$_3$	1.76 s	25.8
5′	CH$_3$	1.78 s	17.9
1"	CH$_2$	3.40 br d (7.0)	29.5
2"	CH	5.30 m	122.0
3"	C	-	134.6
4"	CH$_3$	1.78 s	25.8
5"	CH$_3$	1.84 s	17.8
1- OCH$_3$	CH$_3$	3.92 s	63.0
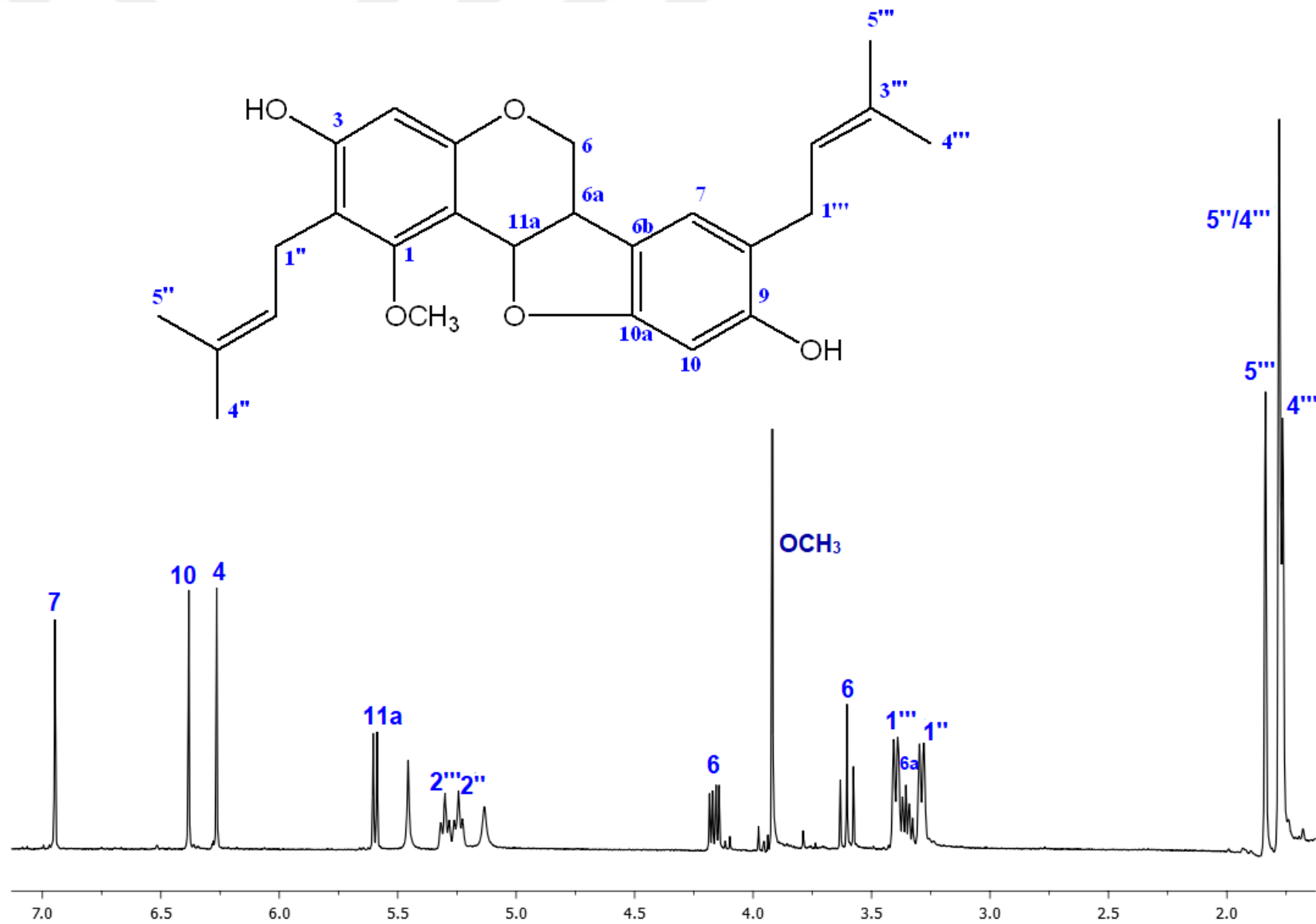
Spectrum 70. ^{1}H NMR Spectrum of 1-Methoxyficifolinol (**27**) (CDCl$_3$, 400 MHz)
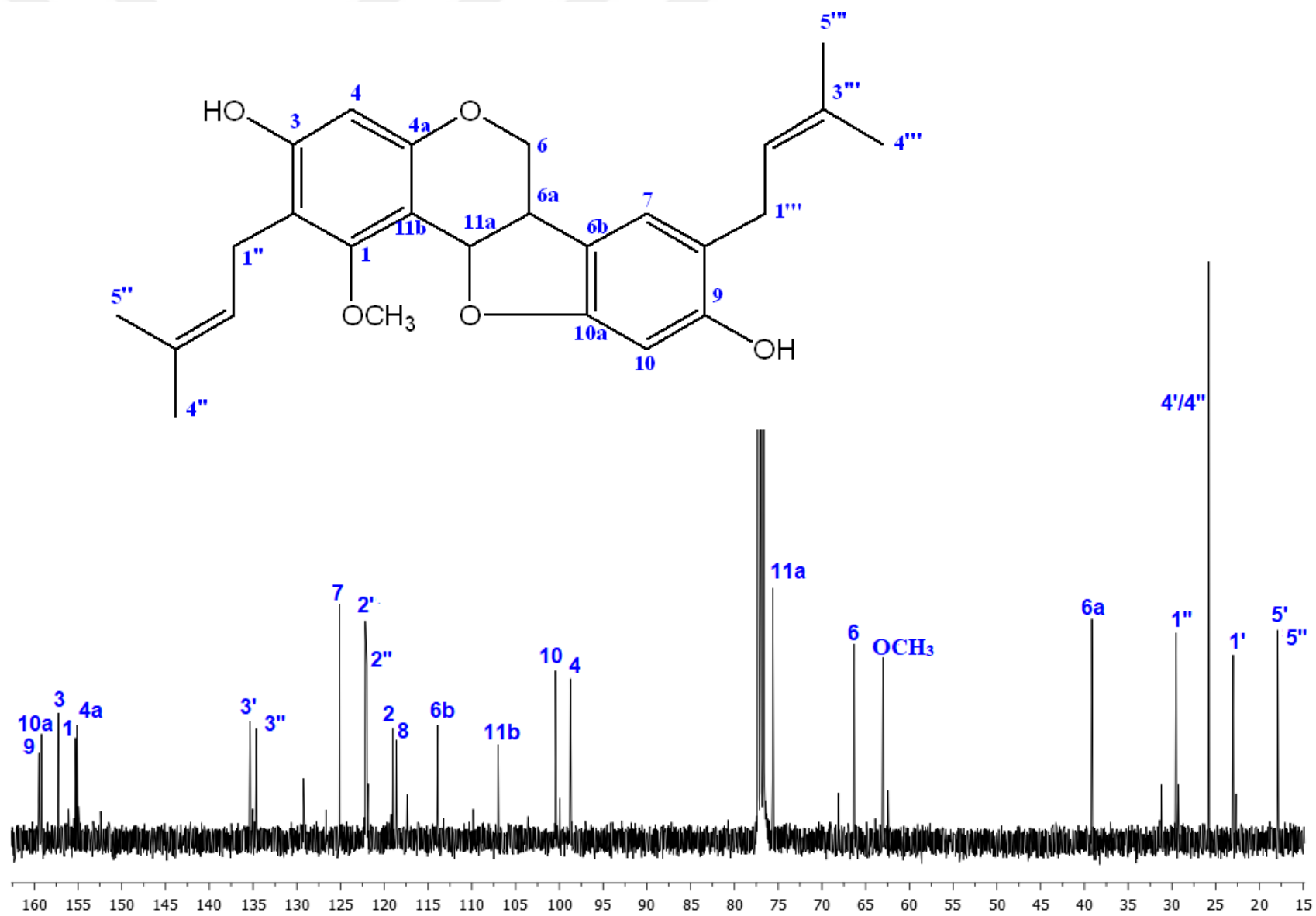
Spectrum 71. ^{13}C NMR Spectrum of 1-Methoxyficifolinol (**27**) (CDCl$_3$, 100 MHz)

4.5.1.11. Triterpene
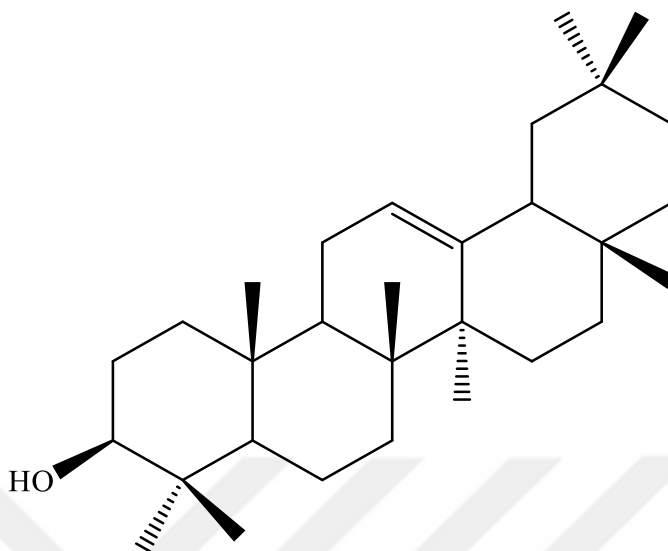
β-AMYRIN (28): C$_{30}$H$_{50}$O (MW: 426.73)

IR υ_{max} (KBr) cm^{-1}:	3306 (OH), 2930 (aliphatic C-H), 1464 (C=C)
MS *m/z*:	425.34 [M- H]$^+$
^{1}H NMR:	Table 138, Spectrum 72
^{13}C NMR:	Table 138, Spectrum 73

β-AMYRIN (28)

Compound **28** was obtained from CHCl$_3$ subextract of *G. glabra* as a white powder. It exhibited absorption bands at 3306 (OH), 2930 (aliphatic C-H) and 1464 (C=C) cm^{-1} in IR spectroscopy. According to ion peaks at *m/z*: 425.34 [M-H]$^+$ in MS spectrum, the molecular weight of **28** was calculated as 426.7, while molecular formula was determined to be C$_{30}$H$_{50}$O.

^{1}H NMR of **28** (Table 138, Spectrum 72) contained one oxymethine signal at 3.21 (dd, *J* = 11.3, 4.5 Hz, H-3) and one olefinic signal at 5.28 (t, *J* = 3.5 Hz, H-12). In the ^{13}C NMR spectrum (Table 138, Spectrum 73) of **28**, 30 carbon resonances were observed between 15.3 and 143.5 ppm, mostly methyl and methylene signals. Olefinic carbon signal at 122.6 ppm (C-12) and 143.5 ppm (C-13) along with oxygenated carbon signal at 79.0 (C-3) indicated the presence of an olean-12-en type triterpene structure with one hydroxyl group. Therefore, compound **28** was identified as 3β-hydroxy-olean-12-en and the NMR data were in complete accordance with the literature for this compound, namely **β-amirin** (251).

Table 138. ^{1}H and ^{13}C NMR spectroscopic data of β-amyrin (**28**) (CDCl$_3$, ^{1}H: 400 MHz, ^{13}C: 100 MHz)

C/H atom	Multiplicity	δ_H (ppm), J (Hz)	δ_C (ppm)
1	CH$_2$	-	38.7
2	CH$_2$	1.52 † /1.67 †	27.7
3	CH	3.21 dd (11.3, 4.5)	79.0
4	C	-	39.3
5	CH		55.2
6	CH$_2$		18.3
7	CH$_2$		33.0
8	C	-	41.0
9	CH		47.6
10	C	-	37.0
11	CH$_2$	1.87	22.9
12	CH	5.28 t (3.5)	122.6
13	C	-	143.5
14	C	-	41.6
15	CH$_2$		27.2
16	CH$_2$		29.6
17	C	-	32.6
18	CH		46.5
19	CH$_2$		45.8
20	C	-	31.2
21	CH$_2$		33.8
22	CH$_2$		38.4
23	CH$_3$	0.98 s	28.1
24	CH$_3$	0.77 s	15.5
25	CH$_3$	0.91 s	15.3
26	CH$_3$	0.75 s	17.1
27	CH$_3$	1.12 s	25.9
28	CH$_3$	1.25 s	29.7
29	CH$_3$	0.90 s	30.7
30	CH$_3$	0.92 s	23.6
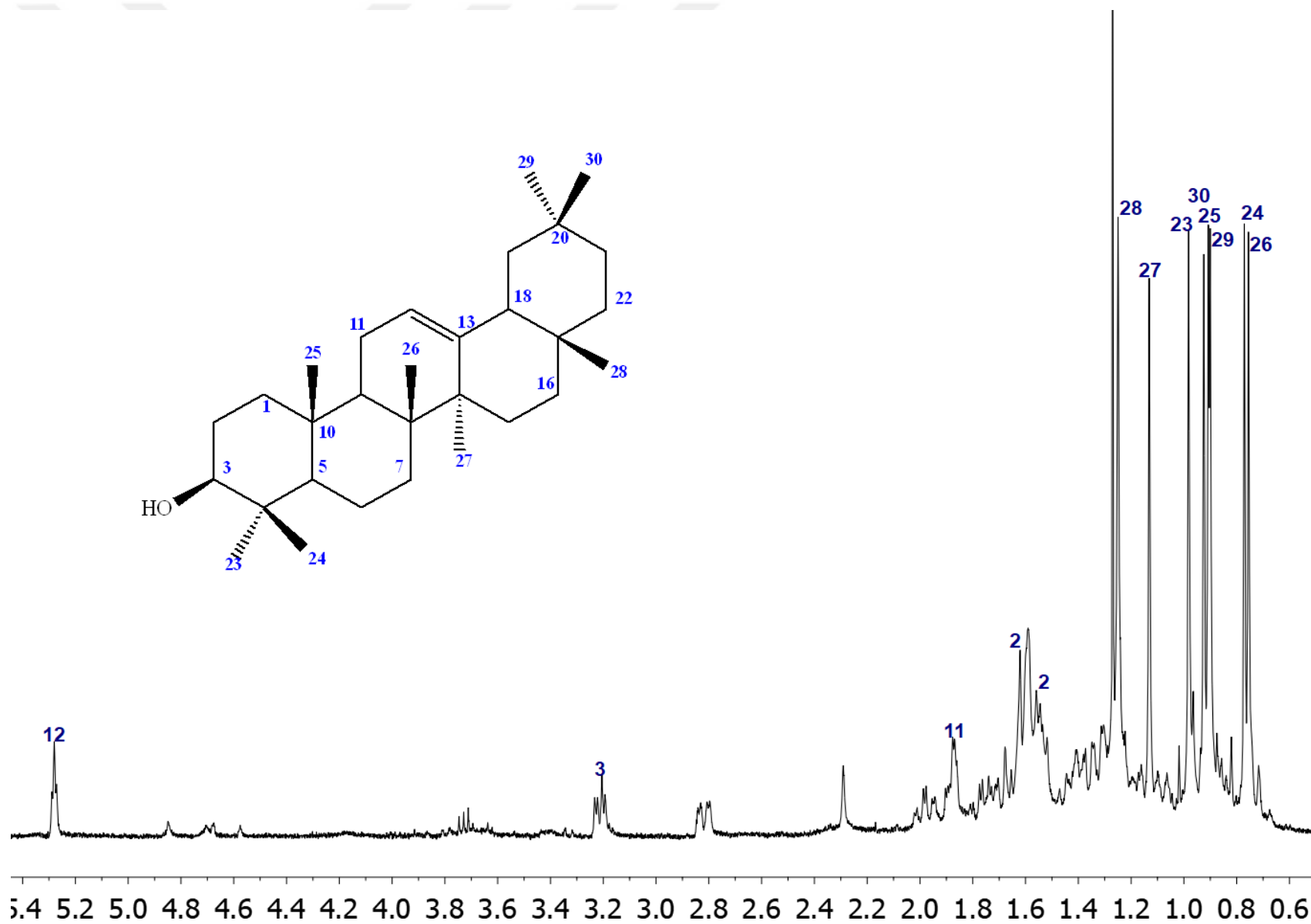
Spectrum 72. ^{1}H NMR Spectrum of β-amyrin (**28**) (CDCl$_3$, 400 MHz)
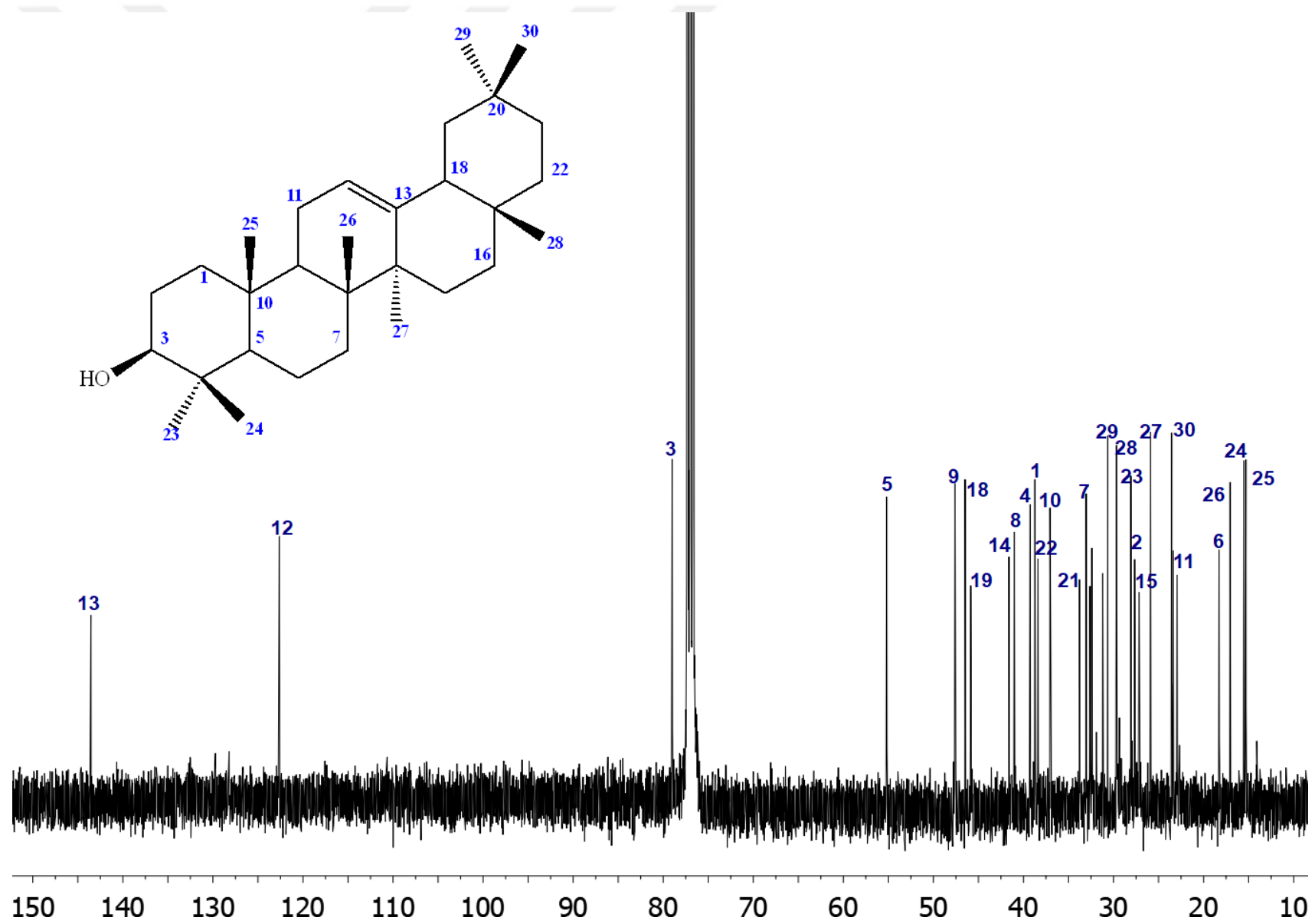
Spectrum 73. ^{13}C NMR Spectrum of β-amyrin (**28**) (CDCl$_3$, 100 MHz)

4.6. *In vitro* Cytotoxic Activity Results of Isolated Compounds

The cytotoxic activities of the purified compounds from *G. glabra* and *G. iconica* were tested on the same epithelial cancer cell lines (Huh7, MCF7 and HCT116) by using SRB assay. *In vitro* cytotoxicity results of isolated compounds with their IC_{50} (µM) and R^2 values were calculated and given in Tables 139 and 140. The compounds having IC_{50} values below 40 µM were accepted as active.

4.6.1. *In vitro* Cytotoxic Activity Results of Compounds Isolated from *G. glabra*

Table 139. Cytotoxic activity results of compounds isolated from *G. glabra* against Huh7, MCF7 and HCT116 cancer cell lines by SRB assay

Compound	Huh7		MCF7		HCT116	
	IC_{50} (µM)	R^2	IC_{50} (µM)	R^2	IC_{50} (µM)	R^2
Tetrahydroxymethoxychalcone (**2**)	8.3	0.97	13.9	0.99	13.3	0.98
Isoliquiritigenin 4′-*O*-β-glucopyranoside (**5**)	NI		NI		NI	
Licuroside + Neolicuroside (**6**+**7**)	NI		NI		NI	
Abyssinone II (**11**)	NI		NI		NI	
Glabridin (**15**)	16.7	0.9	15.1	0.9	10.5	0.9
4′-*O*-methylglabridin (**16**)	9.6	1	16.5	0.9	10.8	0.9
Glabrene (**20**)	2.3	0.99	5.0	0.7	4.9	0.92
Kanzonol U (**23**)	1.8	0.8	16.8	0.9	14.0	0.8
β-amyrin (**28**)	9.3	0.9	6.8	0.8	17.6	0.9
Camptothecin	< 1		< 1		< 1	

NI: No inhibition

Among the tested metabolites, **2**, **15**, **16**, **20**, **23** and **28** showed cytotoxic effects while **6**+**7**, **5** and **11** did not exert any activity as shown in Table 139. The active compounds (**2**, **15**, **16**, **20**, **23** and **28**) exerted cytotoxic activity against Huh7 cancer cell lines in the range of 1.8 - 16.7 µM, the most potent ones were kanzonol U (**23**) (IC_{50} = 1.8 µM) and glabrene (**20**) (IC_{50} = 2.3 µM). The same compounds displayed cytotoxic activity also against MCF7 cells in different degrees (IC_{50} = 5.0 - 16.8 µM), being glabrene (**20**) (IC_{50} = 5.0 µM) and β-amyrin (**28**) (IC_{50} = 6.8 µM) as the strongest ones. Against HCT116 cells, compounds **2**, **15**, **16**, **20**, **23** and **28** were also found to be cytotoxically active (IC_{50} = 4.9 - 17.6 µM) and glabrene (**20**) was the most potent one. Based on the SRB results, hepatocellular cancer cells (Huh7) were the most sensitive cells against the cytotoxic effects of the tested secondary metabolites except for **15** and **28** (Table 139). Since compounds **3** and **12** were obtained as a mixture with different molecular weights and compound **13** was isolated from an inactive main fraction of *G. glabra*, they were not evaluated for their cytotoxic effects.

4.6.2. *In vitro* **Cytotoxic Activity Results of Compounds Isolated from** *G. iconica*

Table 140. Cytotoxic activity results of compounds isolated from *G. iconica* against Huh7, MCF7 and HCT116 cancer cell lines by SRB assay

Compound	Huh7		MCF7		HCT116	
	IC_{50} (µM)	R^2	IC_{50} (µM)	R^2	IC_{50} (µM)	R^2
Iconichalcone (**1**)	> 40	0.78	> 40	0.88	> 40	0.65
Tetrahydroxymethoxychalcone (**2**)	8.3	0.97	13.9	0.99	13.3	0.98
2′-*O*-Methylisoliquiritigenin (**4**)	12.1	0.83	13.8	0.98	18.4	0.93
3-*O*-Methylkaempferol (**8**)	14.7	0.98	19.6	0.97	33.0	0.99
Topazolin (**9**)	7.2	0.96	10.5	0.99	11.8	0.9
Violanthin (**10**)	> 40	0.64	> 40	-	> 40	0.95
Glycyrrhisoflavone (**14**)	8.7	0.89	11.0	0.91	11.1	0.98
Glyasperin C (**17**)	17.2	0.77	16.8	0.86	20.0	0.74
Licoricidin (**18**)	4.7	0.95	9.3	0.97	9.2	0.99
Licorisoflavan A (**19**)	11.5	0.99	12.8	0.99	13.0	0.97
Dehydroglyasperin C (**21**)	5.8	0.97	6.4	0.99	9.6	0.99
Iconisoflaven (**22**)	7.1	0.98	17.1	0.91	18	0.8
Licocoumarone (**24**)	10.0	0.87	10.5	0.95	18.3	0.93
Glycycoumarin (**25**)	10.7	0.87	15.0	0.85	17.5	0.9
Edudiol (**26**)	7.5	0.86	20.0	0.91	20.0	0.96
1-Methoxyficifolinol (**27**)	2.4	0.98	4.6	0.98	5.0	0.96
Camptothecin	< 1		< 1		< 1	

As shown in Table 140, all of the isolates obtained from *G. iconica* except for iconichalcone (**1**) and violanthin (**10**) were found to be active with IC_{50} values in the range of 2.4 - 33.0 µM against all tested cancer cell lines. The active compounds (**2**, **4**, **8**, **9**, **14**, **17**, **18**, **19**, **21**, **22**, **24**, **25**, **26** and **27**) exerted considerable cytotoxic activities against Huh7 cancer cells (IC_{50} = 2.4 - 17.2 µM), most potent compounds amongst them were 1-methoxyficifolinol (**27**) (IC_{50} = 2.4 µM), licoricidin (**18**) (IC_{50} = 4.7 µM), dehydroglyasperin C (**21**) (IC_{50} = 5.8 µM), iconisoflaven (**22**) (IC_{50} = 7.1 µM), topazolin (**9**) (IC_{50} = 7.2 µM), edudiol (**26**) (IC_{50} = 7.5 µM), tetrahydroxymethoxychalcone (**2**) (IC_{50} = 8.3 µM), glycyrrhisoflavone (**14**) (IC_{50} = 8.7 µM) and licocoumarone (**24**) (IC_{50} = 10 µM). Against MCF7 cells, the compounds exhibited cytotoxic effects in different degrees (IC_{50} = 4.6 – 20.0 µM) included the strongest molecules as **27** (IC_{50} = 4.6 µM), **21** (IC_{50} = 6.4 µM) and **18** (IC_{50} = 9.3 µM). Also the same compounds **27** (IC_{50} = 5.0 µM), **18** (IC_{50} = 9.2 µM) and **21** (IC_{50} = 9.6 µM) were found to be most active compounds against HCT116 cancer cells amongst the other active isolates (IC_{50} = 5.0 – 33.0 µM). Comparing the cancer cell lines regarding their vulnerabilities, Huh7 cells were the most sensitive cells against the cytotoxic effects of active secondary metabolites obtained from *G. iconica* except for **17** (Table 140).

4.7. Mechanistic Study Results

The most active compounds based on their IC_{50} values (with IC_{50} values < 10 µM) in SRB assay, **2**, **16**, **20** and **23** from *G. glabra* and **2**, **9**, **14**, **18**, **21**, **22**, **26** and **27** from *G. iconica* were chosen for further mechanistic studies in relatively most sensitive cancer cell lines, Huh7 cells. First, time dependent cytotoxicity assay for these compounds was conducted by Real-Time cell electronic sensing (RT-CES) in Huh7 cancer cells. Regarding to the RT-CES results, compounds with IC_{50} values ≤ 10 µM at 48th hour were accepted as the most active ones that were justified to be mechanistically evaluated in further bioactivity studies including Hoechst staining, Fluorescence-activated cell sorting (FACS) and Western blot assays.

4.7.1. Real-Time Bioactivity Assay Results

4.7.1.1. Real-Time Boactivity Assay Results of Compounds Isolated from *G. glabra*

The most active isolates having IC_{50} values < 10 µM in SRB assay (Table 139) including **2**, **16**, **20** and **23** obtained from *G. glabra* were conducted to real-time bioactivity assay in Huh7 cancer cells. Based on RT-CES assay results as depicted in Table 141 and Figure 11, compounds **2**, **16** and **20** were accepted as the most potent isolates of *G. glabra* by exhibiting IC_{50} values of 4.4, 9.8 and 5.8 µM at 48th hour, respectively and choosen for further mechanistic studies in Huh7 cancer cells.

Table 141. Real-time bioactivity assay (RT-CES x CELLigence) results of active compounds obtained from *G. glabra* against Huh7 cells

Compound	24 h		48 h		72 h	
	IC_{50} (µM)	R^2	IC_{50} (µM)	R^2	IC_{50} (µM)	R^2
Tetrahydroxymethoxychalcone (**2**)	18	0.6	4.4	0.8	6.6	0.7
4′-*O*-methylglabridin (**16**)	7.31	0.9	9.8	0.9	11.4	0.9
Glabrene (**20**)	9	1	5.8	1	5.9	1
Kanzonol U (**23**)	10	0.9	13	0.8	14.7	0.9
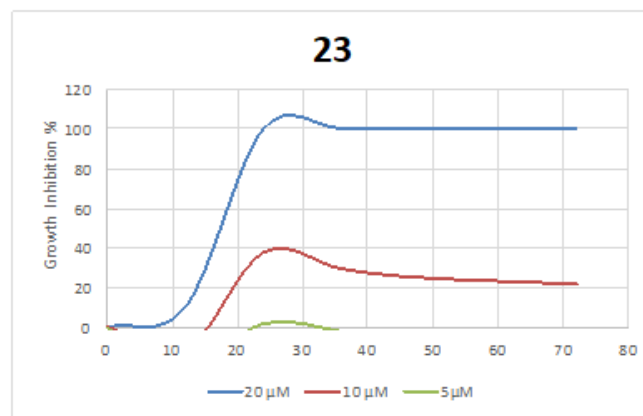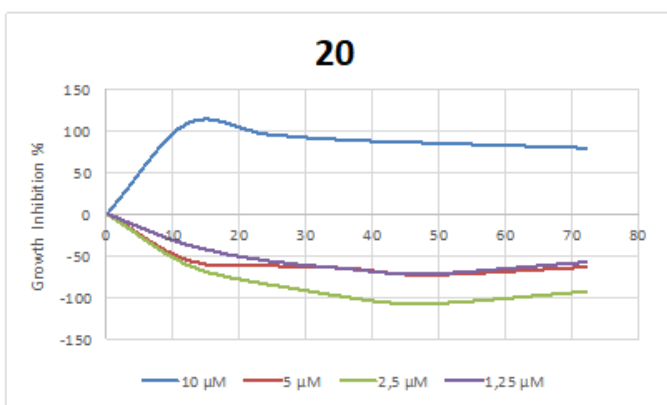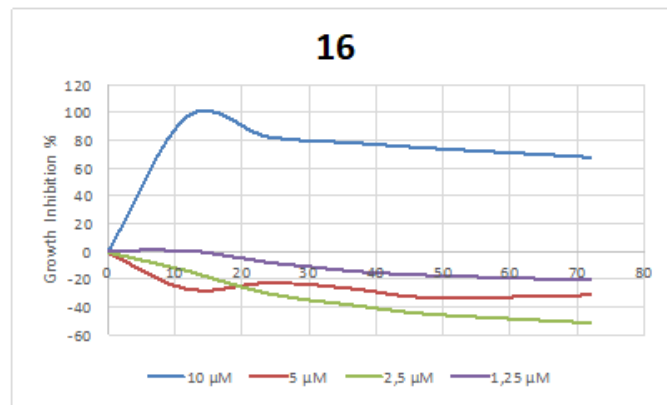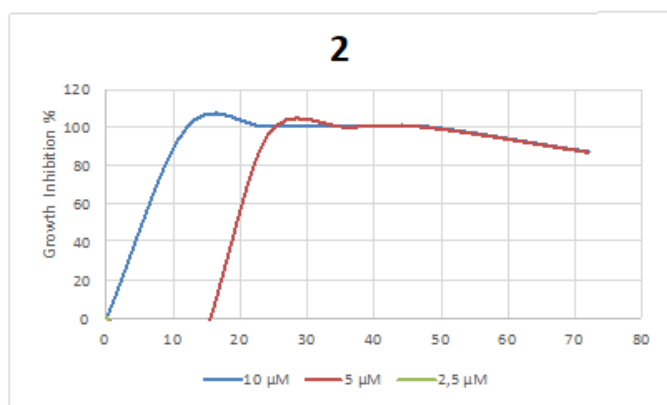
Figure 11. RT-CES xCELLigence results of active compounds obtained from *G. glabra* against Huh7 cells

4.7.1.2. Real-Time Boactivity Assay Results of Compounds Isolated from *G. iconica*

2, **9**, **14**, **18**, **21**, **22**, **26** and **27** obtained from *G. iconica* were the cytotoxically most active compounds against Huh7 cells by exerting IC_{50} values < 10 µM in SRB assay (Table 140). Therefore, these isolates were conducted to RT-CES assay in Huh7 cancer cells. According to the results as illustrated in Table 142 and Figure 12, compounds **2**, **18**, **21**, **22** and **27** displayed IC_{50} values lower than or equal to 10 µM at 48th hour and were established as the most potent isolates that deserved further mechanistic examinations.

Table 142. Real-time bioactivity assay (RT-CES xCELLigence) results of active compounds obtained from *G. iconica* against Huh7 cells

Compound	24 h		48 h		72 h	
	IC_{50} (µM)	R^2	IC_{50} (µM)	R^2	IC_{50} (µM)	R^2
Tetrahydroxymethoxychalcone (**2**)	18	0.6	4.4	0.8	6.6	0.7
Topazolin (**9**)	6.9	0.5	19	0.7	16	0.9
Glycyrrhisoflavone (**14**)	> 10	-	> 10	-	> 10	-
Licoricidin (**18**)	6.9	0.7	10	0.7	11.8	0.9
Dehydroglyasperin C (**21**)	4.2	0.7	3.5	0.7	4	0.8
Iconisoflaven (**22**)	4.8	1	6.5	1	6.3	1
Edudiol (**26**)	> 10	-	> 10	-	> 10	-
1-Methoxyficifolinol (**27**)	3.8	0.7	4.3	0.8	5.7	0.9
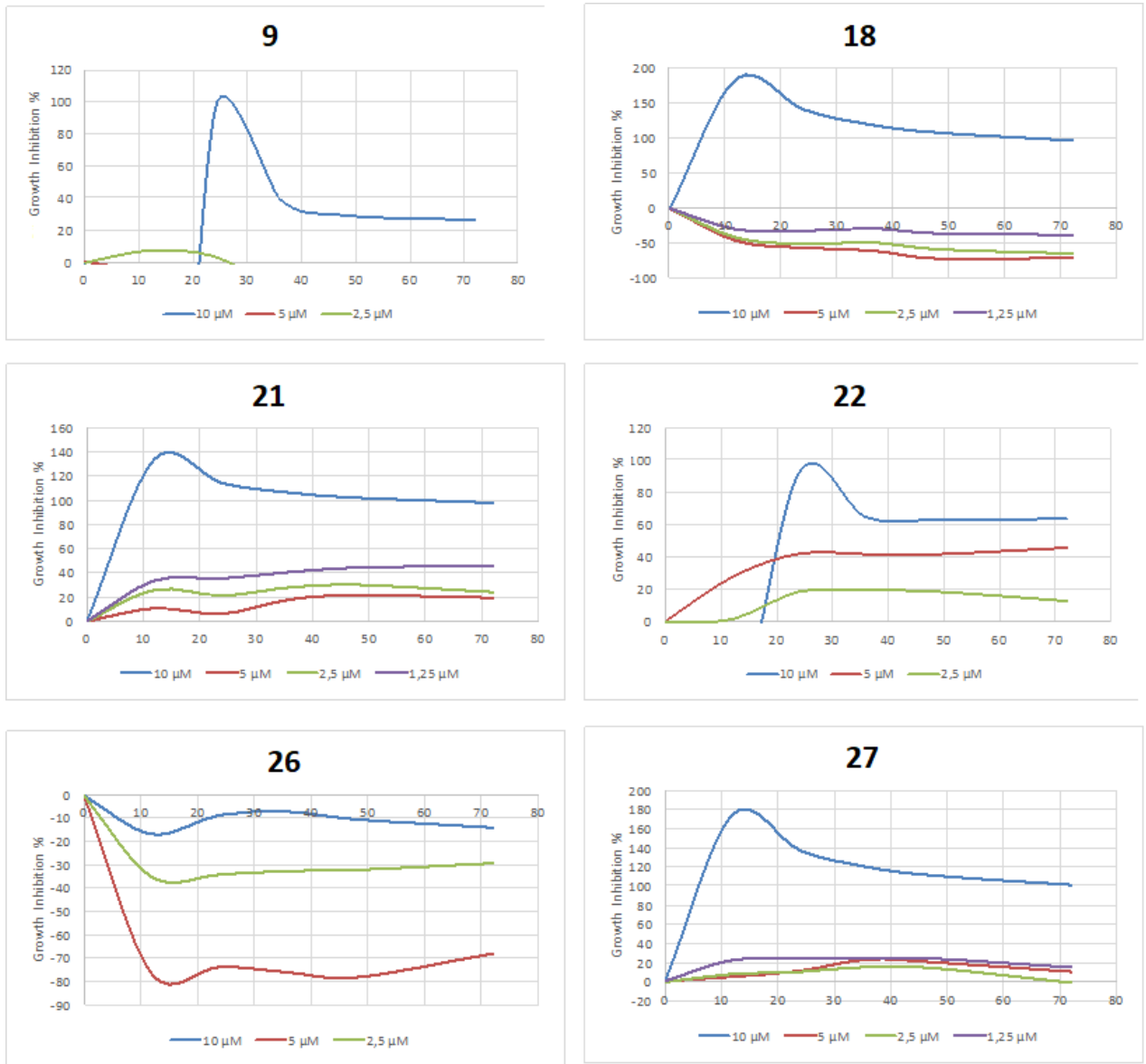
Figure 12. RT-CES xCELLigence results of active compounds obtained from *G. iconica* against Huh7 cells

4.7.2. Hoechst 33258 Staining Assay Results

Hoeschst 33258 staining was performed on the most active isolates with regard to RT-CES assay, **2**, **16** and **20** from *G. glabra* and **2**, **18**, **21, 22** and **27** from *G. iconica* in order to observe apoptotic changes morphologically.

4.7.2.1. Hoechst 33258 Staining Assay Results of Compounds Isolated from *G. glabra*

The isolates **2**, **16** and **20** obtained from *G. glabra*, having IC_{50} values ≤ 10 μM at 48th hour in RT-CES assay were determined to be evaluated by Hoechst staining assay (**2**: 5 μM, **16**: 10 μM, **20**: 6 μM). As seen in fluorescent microspcopy images of Huh7 cells in Figure 13, compared to DMSO control, cells treated with tetrahydroxymethoxychalcone (**2**) showed the characteristics of chromatin condensation in cell nuclei which were positive for Hoechst staining, indicating apoptotic cell death. Besides, glabrene (**20**) displayed slightly bright blue colored cells, which was also related to apoptosis.
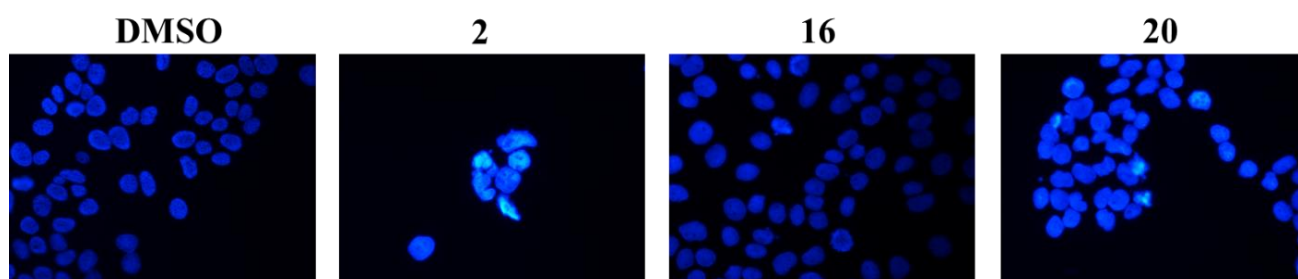
Figure 13. Fluorescent microscopy images of Huh7 cells treated with DMSO or compounds obtained from *G. glabra* for 48 hours and stained with Hoechst 33258 nuclear dye

4.7.2.2. Hoechst 33258 Staining Assay Results of Compounds Isolated from *G. iconica*

Hoechst staining assay was conducted to most active compounds isolated from *G. iconica* according to RT-CES assay results (**2**: 5 µM, **18**: 10 µM, **21**: 4 µM, **22**: 7 µM and **27**: 5 µM). Images of Hoechst 33258 dyed cells were taken by fluorescent microscopy and given in Figure 14. Results demonstrated that treatment with licoricidin (**18**) and dehydroglyasperin C (**21**) displayed slightly condensed nuclei comparing to DMSO, indicated existence of apoptotic cells. Furthermore, tetrahydroxymethoxychalcone (**2**) revealed apoptotic cell death in Huh7 cells by displaying remarkable chromatin condensation as mentioned previously (Figures 13 and 14).
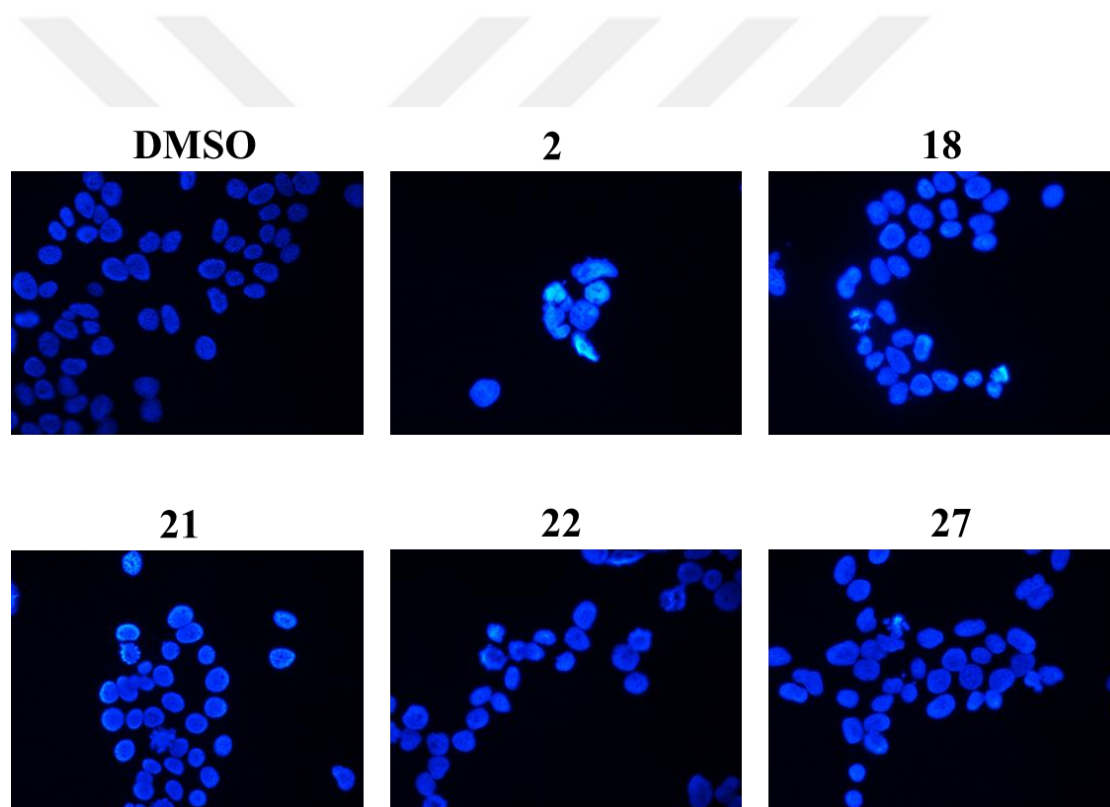
Figure 14. Fluorescent microscopy images of Huh7 cells treated with DMSO or compounds obtained from *G. iconica* for 48 hours and stained with Hoechst 33258 nuclear dye

4.7.3. Cell Cycle Assay Results

To evaluate the effects of the isolates on the cell cycle distribution (SubG$_1$, G$_1$, S, G$_2$/M) of Huh7 cells, **2**, **16** and **20** from *G. glabra* and **2**, **18**, **21**, **22** and **27** from *G. iconica* were characterized by PI staining using Fluorescence-activated cell sorting (FACS).

4.7.3.1. Cell Cycle Assay Results of Compounds Isolated from *G. glabra*

According to cell cycle assay results conducted on isolates obtained from *G. glabra* (**2**: 2.5 µM**, 16**: 10 µM, **20**: 6 µM) as shown in Figure 15, there were remarkable increases in the percentages of subG$_1$ cells of Huh7, treated with **2**, **16** and **20** indicating increased number of apoptotic cells. Furthermore, accumulation of the cells in G$_2$/M phase was observed for compounds **2**, **16** and **20**. Especially, the G$_2$/M arrest was very dramatical for the cells treated with compound **2**.
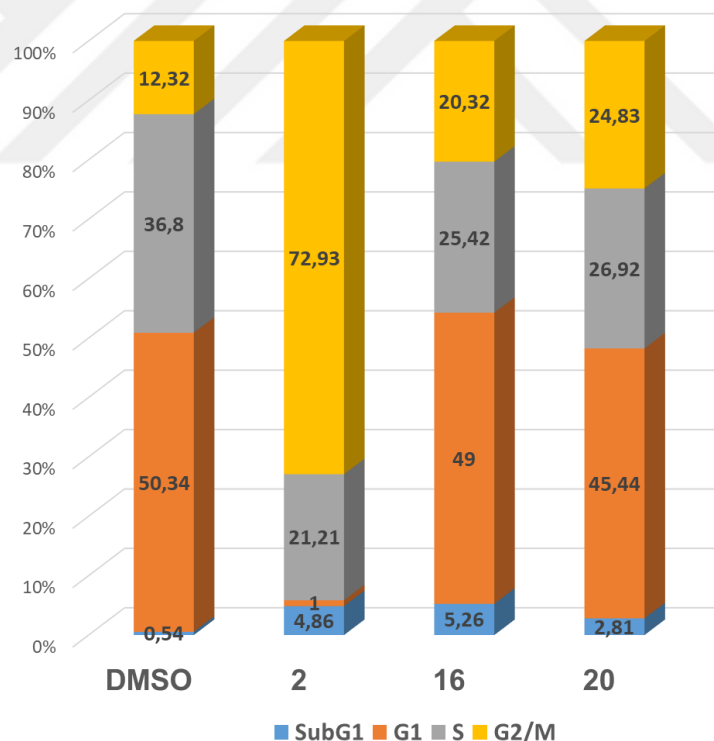
Figure 15. Cell cycle analysis of Huh7 cells upon treatment with **2**, **16**, **20** and DMSO following 48 hours of treatment

4.7.3.2. Cell Cycle Assay Results of Compounds Isolated from *G. iconica*

Cell cycle assay results of compounds from *G. iconica* (**2**: 2.5 μM, **18:** 10 μM, **21:** 4 μM, **22:** 7 μM and **27:** 5 μM) are illustrated in Figure 16. The results revealed that all of the tested compounds particularly **22** caused accumulation of cells in SubG$_1$ phase indicating apoptotic cell death. Besides, **18**, **21**, **22** and most especially **2** induced apoptosis by inducing cell cycle arrest in G$_2$/M phase. Moreover, Huh7 cells treated with **18** and **27** showed elevated G$_1$ phase cell population.
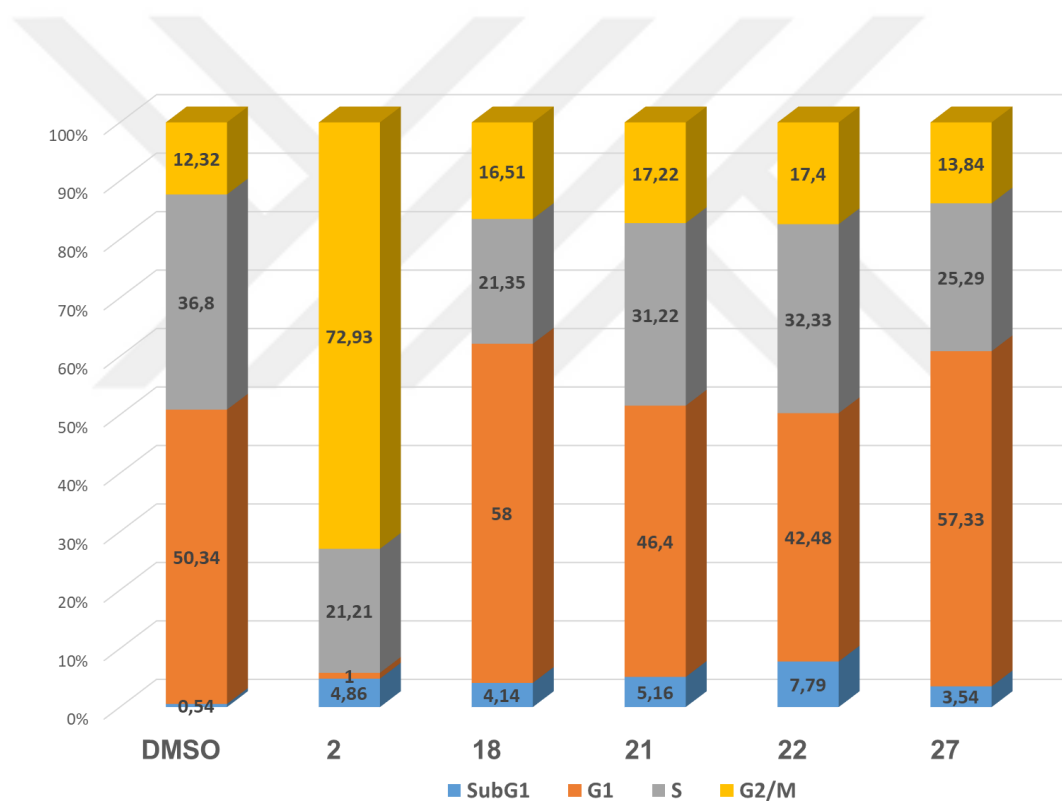
Figure 16. Cell cycle analysis of Huh7 cells upon treatment with **2**, **18**, **21**, **22**, **27** and DMSO following 48 hours of treatment

4.7.4. Western Blot Assay Results

To gain better understanding and clarify the cellular cytoxicity mechanisms of compounds **2**, **16** and **20** obtained from *G. glabra* and **2**, **18**, **21**, **22** and **27** afforded from *G. iconica* in Huh7 cells more specifically, their effects against the expressions of apoptotic (cytochrom C, cleaved caspase-3/-9 and PARP) and cell cycle regulatory proteins (Mdm2, pRb, p21 and p53) were investigated by Western blot analysis.

4.7.4.1. Western Blot Assay on Compounds Isolated from *G. glabra*

As shown in Figure 17A, cytochrome C levels were markedly raised compared to DMSO control in Huh7 cells incubated with all of the tested compounds (**2**, **16** and **20**). While treatment with these isolates (**2**, **16** and **20**) also increased cleaved caspase-9 levels in Huh7 cells, cleaved PARP protein levels were observed to be increased with compounds **2** and **20**. Phospho-Rb levels were decreased in cells incubated with **16** and **20** (Figure 17B). p21 levels were observed to be significantly decreased in all samples (**2**, **16** and **20**) compared to DMSO, indicating induction of apoptotic process by treatment with all tested compounds. On the other hand, Mdm2 levels were considerably decreased in the cells treated with the compounds (**2, 16** and **20**). Moreover, as elicited in Figure 17B, phospho-p53 level was elevated in cells incubated with compound **16**. As a result, these findings suggested that all these tested compounds particularly **20** might exert proapoptotic effects through intrinsic mitochondrial pathway of caspase cascade.
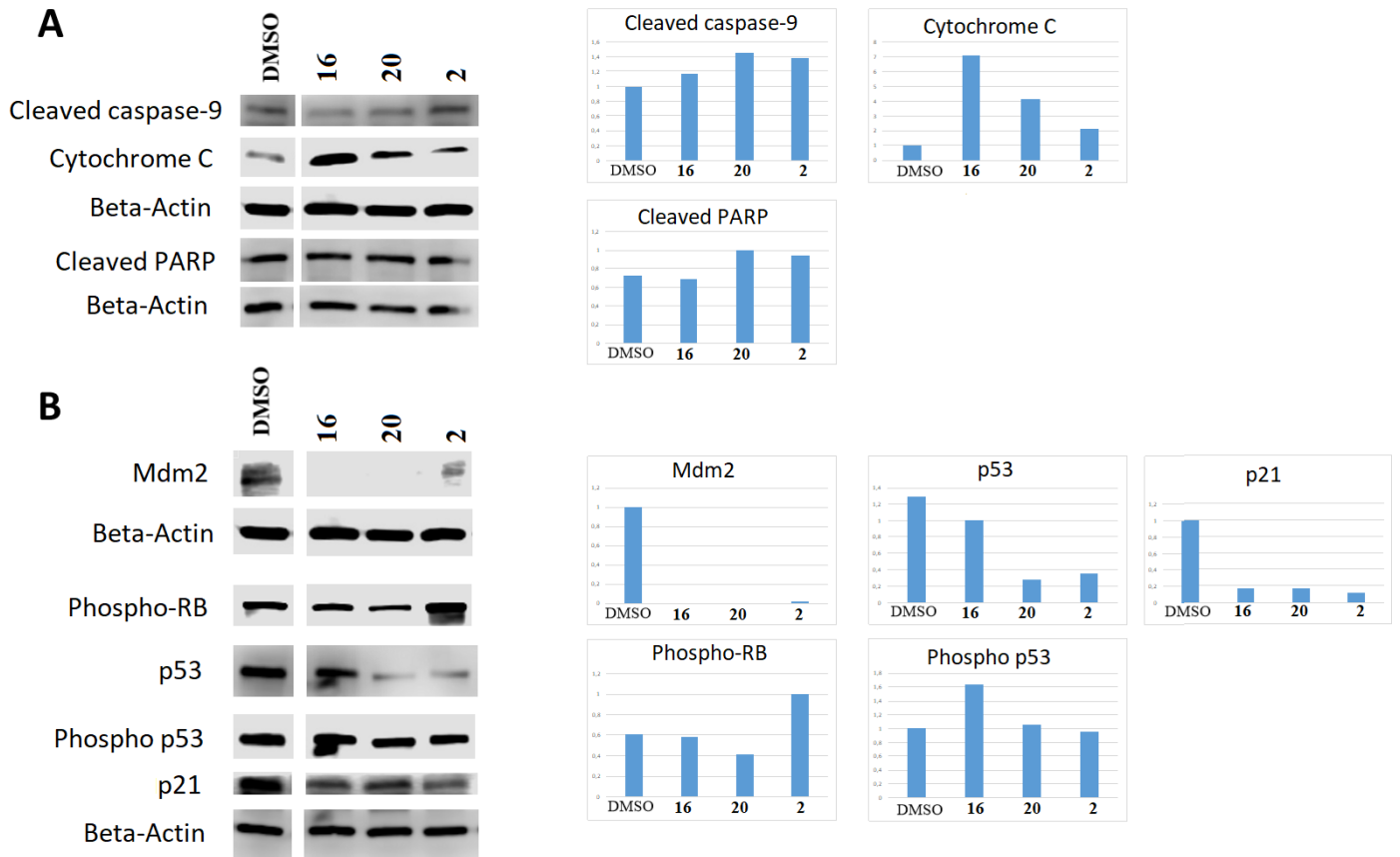
Figure 17. Effects of compounds **2**, **16** and **20** on different cell protein levels (A, B) in Huh7 cells. (**A**) Apoptotic protein levels (**B**) Cell cycle regulatory proteins

4.7.4.2. Western Blot Assay on Compounds Isolated from *G. iconica*

Compounds **2**, **18**, **21**, **22** and **27** as cytotoxically most active compounds from *G. iconica* roots were conducted to Western blot assay. Since compound **2** was obtained from both plants and the results of it were already given in Figure 17, the assay results for **2** are not presented again. As depicted in Figures 17A and 18A, treatment with all of the tested compounds (**2**, **18**, **21**, **22** and **27**) increased cytochrome C levels in Huh7 cells. Besides, **2**, **18**, **21** and **27** caused increases in cleaved caspase-9 levels, while elevated cleaved caspase-3 levels were observed in Huh7 cells treated with **21** and **22**. Moreover, increased cleaved PARP levels were detected with compounds **18** and **21**. As shown in figures 17B and 18B, phospho-Rb levels were decreased in cells treated with **22** and **27**, whereas p21 levels were supressed in all tested samples compared to DMSO. Mdm2 levels were observed to be decreased in **2**, **18**, **22** and **27** treated cells. Moreover, increased p53 levels along with increased Mdm2 levels with compound **21** were observed, indicating antitumor gene of p53 was stimulated upon **21** administration (Figure 18B). Taken together, all these tested compounds obtained from *G. iconica* particularly **21** exhibited proapoptotic effects mediated through intrinsic mitochondrial pathway of caspase cascade.
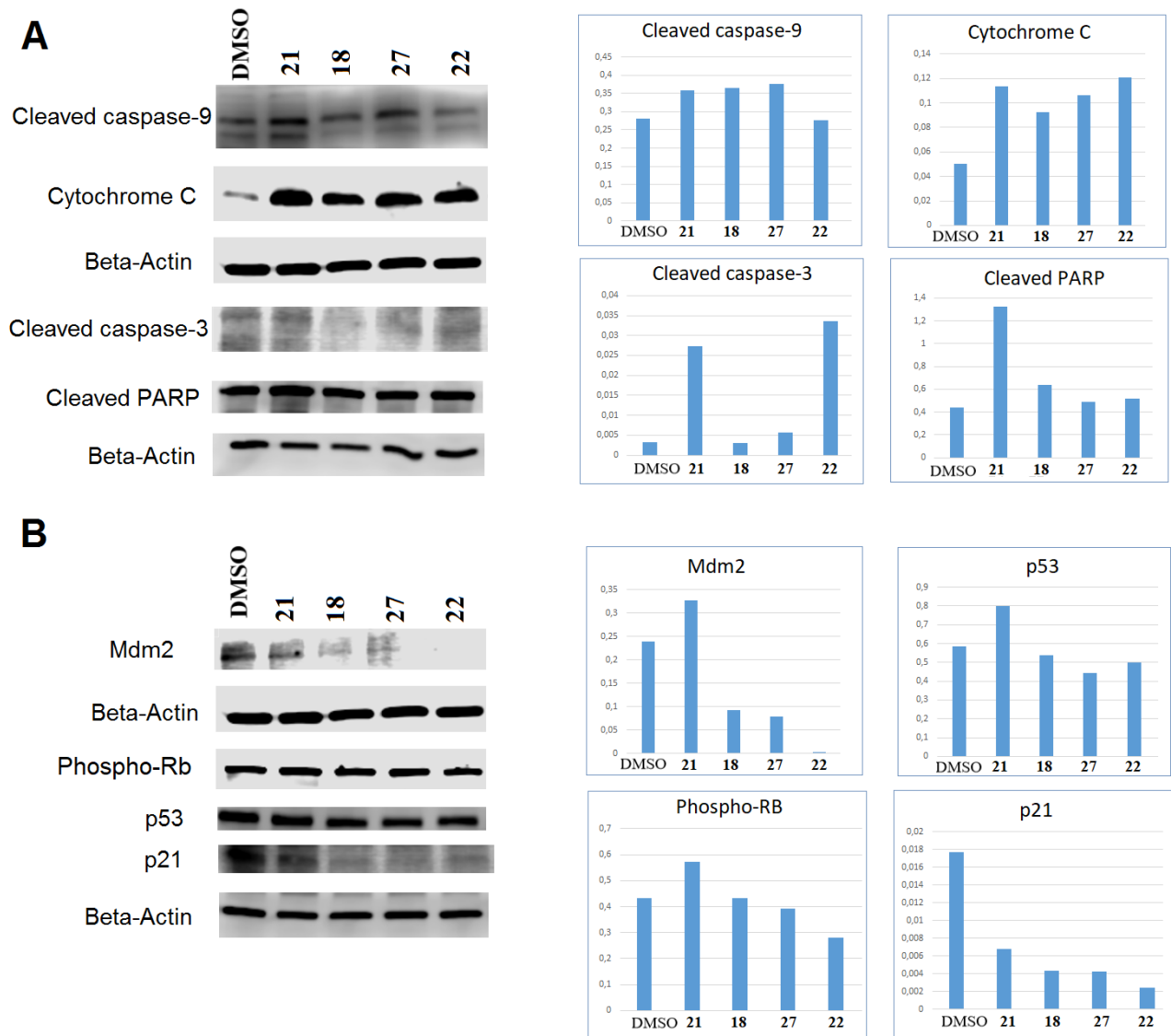
Figure 18. Effects of compounds **18**, **21**, **22** and **27** on different cell protein levels (A, B) in Huh7 cells. (**A**) Apoptotic protein levels (**B**) Cell cycle regulatory proteins

5. DISCUSSION and CONCLUSION

Cancer is a significant cause of death globally. The incidence and mortality rates of cancer are rapidly increasing around the world because of many factors related to socioeconomic development. According to cumulative risk of incidence, 1 in 8 men and 1 in 10 women will develop the disease in a lifetime (2). Severe adverse effects and multidrug resistance are the major obstacles in clinical cancer chemotherapy. More effective and selective new anticancer drug candidates with less adverse effects are needed to combat cancer which makes many researchers to turn their attentions to natural products in recent years (8). Many of natural products having interesting biological properties are known as 'lead' molecues for drug development processes (234). Since 1940s, approximately half of the total number of small anticancer drugs have been discovered from either natural resources or semi-synthesis of them (9). Four classes of plant oriented lead anticancer agents are used as therapeutic agents in the market today including the vinca alkaloids (vinblastine, vincristine and vindesine), the epipodophyllotoxins (etoposide and teniposide), the taxanes (paclitaxel and docetaxel) and the camptothecin derivatives (camptothecin and irinotecan) (252). Plants are a reservoir of natural compounds that still remains huge potential to provide newer drugs having chemoprotective potential against cancer. This project was oriented towards the exploration of new plant originated secondary metabolite candidates with anticancer properties.

The genus *Glycyrrhiza* (Fabaceae) is commonly known as licorice, contains about 30 species worldwide (14). Some of the licorice species including *G. glabra*, *G. inflata* and *G. uralensis*, have long been used traditionally as antiulcer, antiinflammatory and expectorant agent (12). Different extracts as well as the isolated secondary metabolites obtained from *Glycyrrhiza* species were shown to possess antiulcer, antimicrobial, antiviral, antiprotozoal, hepatoprotective, antiinflammatory, antidiabetic, antioxidative, memory enhancing, immunomodulatory, cytotoxic and antitumor activities based on the literature survey (15–17).

In the Flora of Turkey, the genus *Glycyrrhiza* is represented by six species, half of which are endemic (25). In recent years, *Glycyrrhiza* species are receiving much attention in terms of their significant cytotoxic and antitumor effects according to many *in vitro* and *in vivo* anticancer activity studies conducted on the extracts and isolates

317

obtained from various *Glycyrrhiza* species (22–24,115,119,253,254). Considering the wide utilization and the documented bioactivities of several *Glycyrrhiza* species, the purpose of this study was to isolate cytotoxic secondary metabolites from roots of two cultivated *Glycyrrhiza* species, namely *G. glabra* and *G. iconica* through *in vitro* cytotoxicity-guided fractionation and isolation techniques. Furthermore, the underlying mechanisms behind this cytotoxic activites of the most active isolates were also aimed to be elucidated. Besides, some of the major secondary metabolites were also isolated from the other fractions so as to make a contribution to the phytochemisty of the plant species.

The crude MeOH extracts and subextracts obtained from *G. glabra* and *G. iconica* roots were first evaluated against human hepatocellular (Huh7), breast (MCF7) and colon (HCT116) cancer cell lines by using Sulforhodamine B (SRB) assay. The SRB assay results (Table 108) revealed that crude MeOH extract of *G. glabra* showed remarkable cytotoxic activity with IC_{50} values of 18.9, 28.8 and 33.6 µg/mL against hepatocellular (Huh7), breast (MCF7) and colorectal (HCT116) cancer cell lines, respectively. Crude MeOH extract of *G. iconica* roots displayed cytotoxic activity also against Huh7, MCF7 and HCT116 cancer cell lines (IC_{50} = 12.7, 7.4 and 4.3 µg/mL, respectively) in different degrees (Table 109). Comparing the SRB assay results of these two extracts indicated that *G. iconica* extract was cytotoxically more active than *G. glabra* extract.

It is the very first report for evaluation of the cytotoxic effects of extracts and isolates obtained from *G. iconica*. On the other hand, there exist some published studies by far demonstrating the cytotoxic effects of *G. glabra* extract. For instance, Basar et al. showed that MeOH extract of *G. glabra* inhibited *in vitro* growth of HepG2 and A549 tumor cells (116). Another study conducted by Thu et al. demonstrated that MeOH extract of *G. glabra* roots exerted cytotoxic activities against five human cancer cell lines such as A549 (IC_{50} = 6.6 µg/mL), Huh7 (IC_{50} = 8.6 µg/mL), HT1080 (IC_{50} = 9.8 µg/mL), MCF7 (IC_{50} = 12.4 µg/mL) and HepG2 (IC_{50} = 15.4 µg/mL) with MTT assay (112). In a very recent study performed by Fraihat and colleagues, methanol extract of *G. glabra* supressed skin cancer melanoma (WM136-1A) proliferation in a dose-dependent manner with IC_{50} value of 35.2 µg/mL (113). Sheela et al. demonstrated that *G. glabra* methanol extract inhibited *in vivo* proliferation of Ehrlich Ascites Tumor (EAT) cell growth by 90% and water extract inhibited *in vitro* proliferation of EAT cells (122). According to a study by Hawthorne and Gallagher, crude *G. glabra* extract (70% ethanol) exhibited *in vitro*

antiproliferative activity against androgen-dependent prostate cells (LNCaP) with IC_{50} value of 10.3 mg/mL (131). Another study conducted by Zhou and Wink indicated that *G. glabra* MeOH extract displayed moderate cytotoxic activities on HCT116 cancer cell lines by MTT assay (255). These above mentioned studies revealed similar results with the results of this thesis regarding the cytotoxic activity potential of extracts obtained from *G. glabra*. However, there is no study on the *G. glabra* aiming to isolate the cytotoxic compounds from the extract through bioactivity-guided fractionation technique as well as to elucidate thier mechanisms of action.

Regarding the potential of other licorice species, Park et al. carried out a study on the ethanol extract of roasted *G. inflata* roots. The extract inhibited the growth of prostate cancer cell lines, DU145, MLL and HT-29 with the IC_{50} values in the range of 4.3 - 12.2 µg/mL). *G. inflata* extract at 30 µg/mL concentration inhibited the growth of human breast cancer cells MCF7 (88%) and MDA-MB-231 (82%), mouse melanoma cancer cells B16-F10 (80%) and human skin cancer cells A375 (94%) and A2058 (93%). But conversely, it caused increase in the growth of normal intestinal epithelial cells IEC-6 and fibroblasts CCD118SK (115). Aydemir et al. reported the cytotoxic effects of aqueous extracts prepared from the leaves and flowers of an endemic species to Turkey, *G. flavescens* subsp. *antalyensis* against mouse melanoma cell lines (B16F10, B16LNAD) and human embryo kidney cells (293T) by *in vitro* MTS test. Extracts were found to be cytotoxic against B16F10 and B16LNAD cells however, no cell toxicity was observed against human embryo kidney cells (293T) when compared to doxorubicin (119). Based on these previously published reports, *Glycyrrhiza* extracts were shown to possess cytotoxic activities against cancer cell lines without showing any cytotoxic effects on normal cells.

$CHCl_3$ and EtOAc subextracts obtained from the crude MeOH extract of *G. glabra* roots showed cytotoxic activities against Huh7, MCF7 and HCT116 cancer cell lines with IC_{50} values in the range of 5.6-29.3 µg/mL, whereas *n*-BuOH and remaining H_2O subextracts were not cytotoxic (Table 108). Comparing the subextracts of *G. glabra*, the EtOAc subextract (IC_{50} = 5.6 - 9.1 µg/mL) was found to be more cytotoxic than its crude MeOH extract (IC_{50} = 18.9 - 33.6 µg/mL) and $CHCl_3$ (IC_{50} = 8.2 - 29.3 µg/mL), *n*-BuOH (NI) and rH_2O (NI) subextracts against all three tested cell lines Huh7, MCF7 and HCT116. The difference between IC_{50} concentrations of $CHCl_3$ (29.3 µg/mL) and EtOAc

(9.1 µg/mL) subextracts was very dramatical especially against MCF7 cancer cell lines. On the other hand, $CHCl_3$, EtOAc and *n*-BuOH subextracts of *G. iconica* exhibited strong cytotoxic effects against three tested cell lines with IC_{50} values in the range of $< 0.4 – 7.7$ µg/mL, while remaining H_2O subextract was found to be active only against MCF7 cells (Table 109). EtOAc subextract of *G. iconica* showed stronger cytotoxic effects in Huh7 and HCT116 cancer cell lines (IC_{50} = 6.4, <0.4 µg/mL, respectively) comparing to crude MeOH extract (IC_{50} = 12.7, 4.3 µg/mL, respectively), $CHCl_3$ (IC_{50} = 7.0, 2.4 µg/mL, respectively), *n*-BuOH (IC_{50} = 7.7, 2.1 µg/mL, respectively) and rH_2O (NI) subextracts of *G. iconica*. However, against MCF7 cell lines, *n*-BuOH (IC_{50} = 0.6 µg/mL) and $CHCl_3$ (IC_{50} = 0.9 µg/mL) subextracts of *G. iconica* were relatively more active than EtOAc subextract (IC_{50} = 1.1 µg/mL).

In previous studies, Ji et al. demonstrated that EtOAc extract of *G. uralensis* (25 µg/mL) showed more potent *in vitro* cytotoxic effects by inhibiting cell growth by 76-99% comparing to same doses (25 µg/mL) of H_2O (12-17%), *n*-BuOH (0-15%) and EtOH (35-68%) extracts against HepG2, SW480, A549 and MCF7 cancer cells (22). In another study conducted by Lin et al., EtOAc extract (77-94% inhibition against HepG2, SW480 and MCF7 at 50 µg/mL) of *G. inflata* roots were also found to be more cytotoxic than the same doses of *n*-BuOH (4-17%), H_2O (2-14%) and EtOH (49-59%) extracts (24). Above mentioned previous studies indicated that EtOAc extracts of *Glycyrrhiza* species possessed potent cytotoxic properties which was consistent with results of our study. This might be explained by the presence of prenylated phenolic compounds in the EtOAc extracts.

The cytotoxically active $CHCl_3$ and EtOAc subextracts obtained from *G. glabra* roots were further fractionated by Sephadex LH-20 and Polyamide column chromatography, respectively in order to yield main fractions which were also submitted to SRB assay. The active main fractions (frs. B and C of $CHCl_3$ and fr. 4 of EtOAc) were selected for the isolation of the potential bioactive metabolites. As a result of bioassay-guided fractionation and isolation studies on *G. glabra*, abyssinone II (**11**), glabridin (**15**), 4'-*O*-methylglabridin (**16**), kanzonol U (**23**) and β-amyrin (**28**) were isolated from active fractions of $CHCl_3$ (frs. B and C) while tetrahydroxymethoxychalcone (**2**), isoliquiritigenin 4′-*O*-β-glucopyranoside (**5**), glabridin (**15**), glabrene (**20**) as well as a mixture of isoliquiritigenin (**3**) and (2*R*,3*R*)-3,4',7-trihydroxy-3'-prenylflavanone (**12**)

were obtained from active fraction of EtOAc (fr. 4). Moreover, the major compounds licuroside (**6**) and neolicuroside (**7**) mixture and liquiritin apioside (**13**) of the inactive fractions of the EtOAc subextract (frs. 2 and 3) were also isolated in order to make a phytochemical contribution to the plant species.

The cytotoxically active CHCl$_3$ subextract obtained from *G. iconica* was fractionated over Sephadex LH-20 while active EtOAc and *n*-BuOH subextracts were fractionated by Polyamide CC to yield main fractions. Based on the cytotoxicity assay results conducted on obtained main fractions, frs. B and C from CHCl$_3$, frs. 2-4 from EtOAc and frs. E-G from *n*-BuOH subextracts were used for isolation procedures to yield cytotoxic compounds. Thus, bioassay-guided isolation of *G. iconica* yielded to the compounds iconichalcone (**1**), tetrahydroxymethoxychalcone (**2**), 2′-*O*-methylisoliquiritigenin (**4**), 3-*O*-methylkaempferol (**8**), topazolin (**9**), glycyrrhisoflavone (**14**), glyasperin C (**17**), dehydroglyasperin C (**21**), licocoumarone (**24**) and glycycoumarin (**25**) from active main fractions of *G. iconica* EtOAc subextract (frs. 2-4). While compounds topazolin (**9**), licoricidin (**18**), licorisoflavan A (**19**), iconisoflaven (**22**), glycycoumarin (**25**), edudiol (**26**) and 1-methoxyficifolinol (**27**) were purified from active fractions of CHCl$_3$ subextract (frs. B and C), compounds 3-*O*-methylkaempferol (**8**) and glycycoumarin (**25**) were isolated from the active main fractions of *n*-BuOH subextract (frs. F and G). Furthermore, violanthin (**10**) was afforded from the less active fraction (fr. E) of *G. iconica*.

Totally 28 secondary metabolites (**1**-**28**) including a new one (**1**) were isolated from *G. glabra* and *G. iconica* roots through several sequential chromatographic methods. The structures of the isolates were determined by spectroscopic techniques including UV, IR, 1D (^{1}H and ^{13}C NMR) and 2D (COSY, HSQC, HMBC and NOESY) NMR and MS. Compounds **2**, **3**, **5-7**, **11-13**, **15**, **16**, **20**, **23** and **28** were isolated from *G. glabra* while compounds **1**, **2**, **4**, **8-10**, **14**, **17-19**, **21**, **22**, **24-27** were obtained from *G. iconica* roots. Among these compounds, **6**+**7** and **3**+**12** were afforded as inseparable mixtures while compound **2** was purified from both plants.
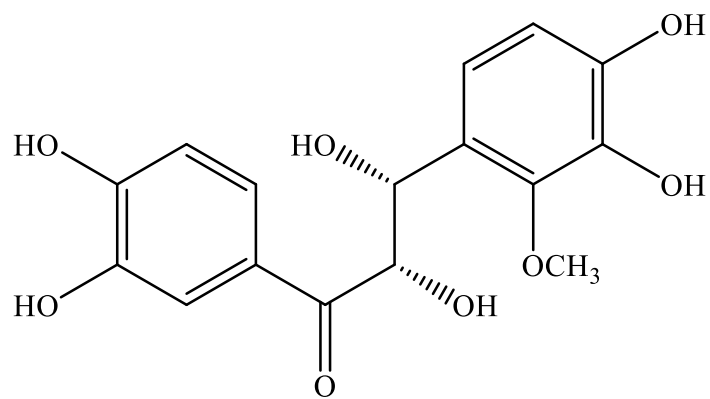
1   Iconichalcone
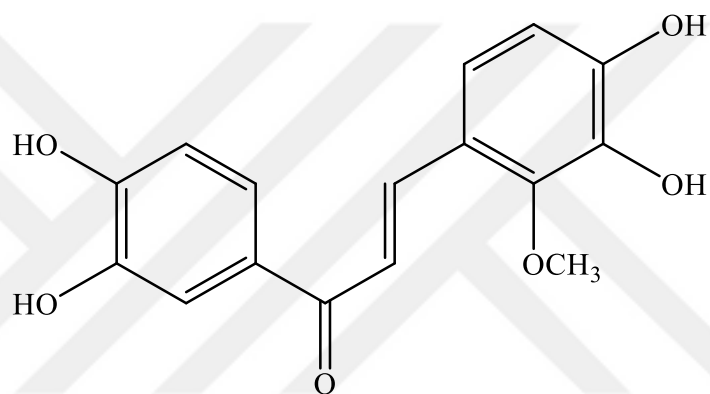
2   Tetrahydroxymethoxyhalcone
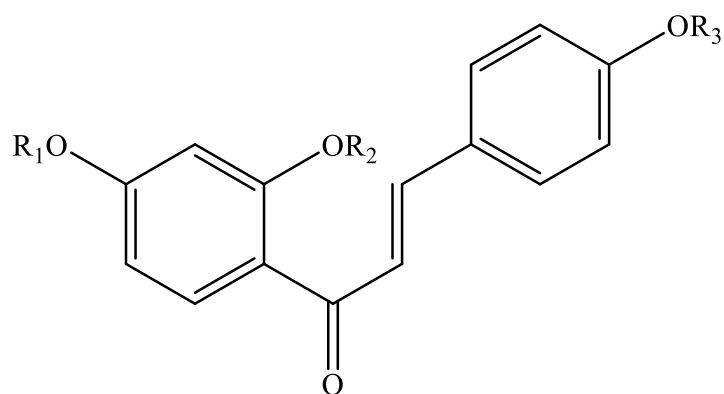
		R₁	**R₂**	**R₃**
3	Isoliquiritigenin	H	H	H
4	2'-*O*-methylisoliquiritigenin	H	CH₃	H

322

		R₁	R₂	R₃
5	Isoliquiritigenin 4'-*O*-β-glucopyranoside	β-Glc	H	H
6	Licuroside	H	H	β-Api-(1→2) -β-Glc
7	Neolicuroside	β-Api-(1→2) -β-Glc	H	H

Seven chalcone derivatives were obtained in this study namely iconichalcone (**1**), tetrahydroxymethoxychalcone (**2**), isoliquiritigenin (**3**), 2'-*O*-methylisoliquiritigenin (**4**), isoliquiritigenin 4'-*O*-β-glucopyranoside (**5**), licuroside (**6**) and neolicuroside (**7**). They all contained oxygene atom at C-4 and C-4' positions. Compound **1** was purified from *G. iconica* as a new compound and named as iconichalcone. In previous studies, α-hydoxylated chalcone derivatives were reported from the genus *Glycyrrhiza* (23,99,177). However, this is the first report of the occurrence of α,β-dihydroxychalcone nucleus in the genus *Glycrrhiza*. Thus, besides being a new compound, **1** is also established as the first α,β-dihydroxylated chalcone derivative that was isolated from *Glycyrrhiza* species. Tetrahydroxymethoxychalcone (**2**) was afforded from both *G. glabra* and *G. iconica* extracts, furthermore it was isolated from *G. iconica* for the very first time. Moreover, 2'-*O*-methylisoliquiritigenin (**4**) is new for the genus *Glycyrrhiza* which was previously obtained from *Dalbergia odorifera* and *Arachis* species (243,256). Among the purified chalcones, isoliquiritigenin 4'-*O*-β-glucopyranoside (**5**), licuroside (**6**) and neolicuroside (**7**) were chalcone glycosides that were all obtained from *G. glabra*. Licuroside (**6**) which was first isolated by Litvinenko from *G. glabra*, was found to be a non-homogenous compound by Miething and Speicher-Brinker that could be separated into two isomeric glycosides licuroside and neolicuroside by using chromatographic techniques such as HPLC and LPLC (156). Considering this, yielding **6** and **7** as a mixture was not suprising.
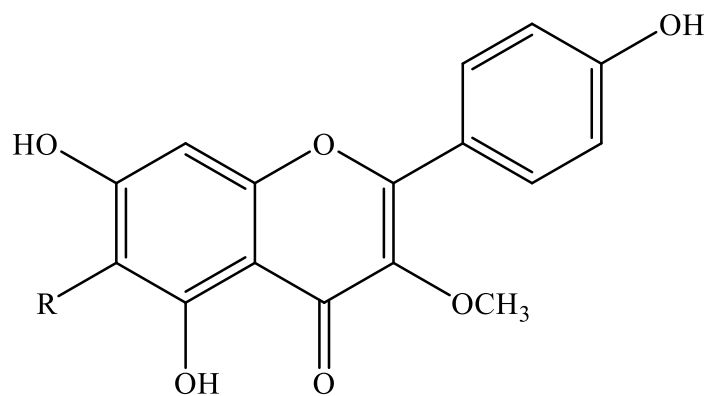
		R
8	3-*O*-Methylkaempferol	H
9	Topazolin	isoprenyl
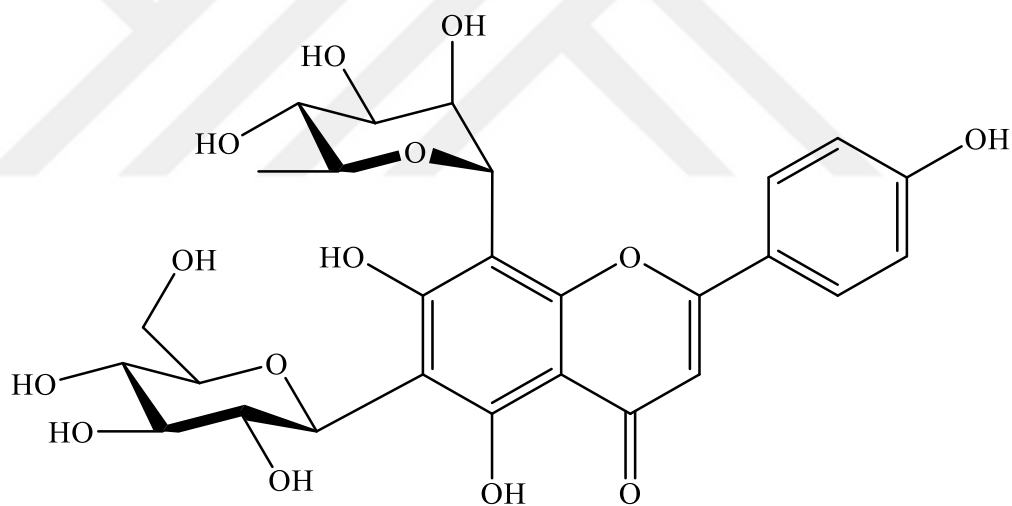
10   Violanthin

Within this study, two flavonols 3-*O*-methylkaempferol (**8**) and topazolin (**9**) as well as one flavone glycoside violanthin (**10**) were all isolated from *G. iconica* roots. They were all 5,7,4'-OH substituted. 3-*O*-methylkaempferol (**8**) was previously obtained from *G. uralensis*, while violanthin (**10**) was purified from *G. eurycarpa* previously, but it is the first report of the isolation of compounds **8** and **10** from *G. iconica* (154,257).
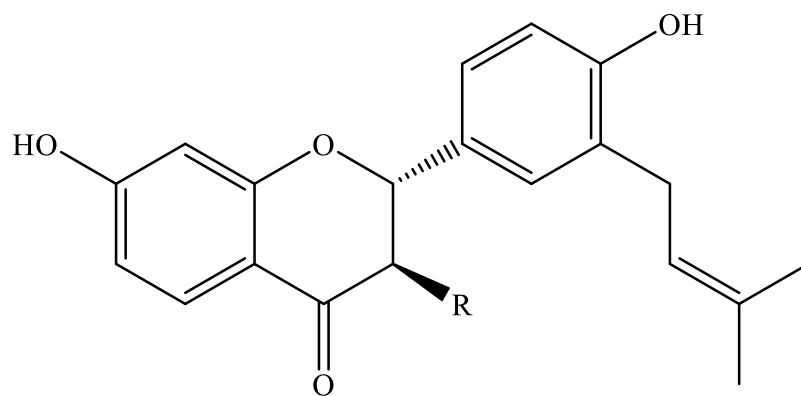
		R
11	Abyssinone II	H
12	(2*R*,3*R*)-3,4',7-trihydroxy-3'-prenylflavanone	OH
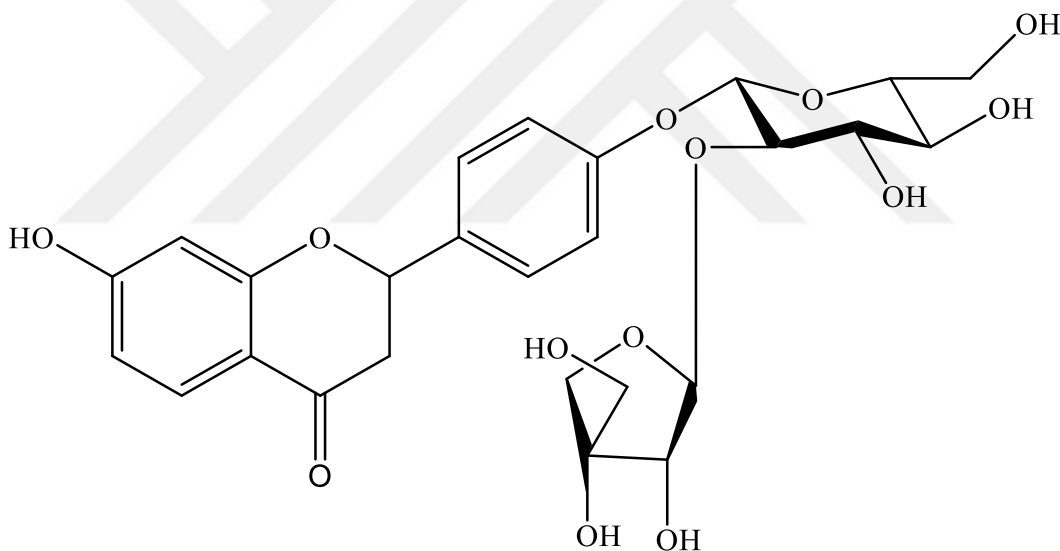
13 Liquiritin apioside

Flavanon derivatives abyssinone II (**11**), (2*R*,3*R*)-3,4',7-trihydroxy-3'-prenylflavanone (**12**) and liquiritin apioside (**13**) were isolated from *G. glabra* possesing 7-monosubstituted A ring and hydroxyl groups at C-4' as common structural features. These mentioned compounds were all previosly obtained from various *Glycyrrhiza* species as mentioned before. Abyssinone II (**11**) and (2*R*,3*R*)-3,4',7-trihydroxy-3'-prenylflavanone (**12**) had very similar chemical structures except for the presence of OH group at C-3 in **12**. Abyssinone II (**11**) was yielded from CHCl₃ subextract of *G. glabra*,

whereas (2*R*,3*R*)-3,4',7-trihydroxy-3'-prenylflavanone (**12**) was isolated from EtOAc subextract of *G. glabra* which might be due to increased polarity of compound **12**.
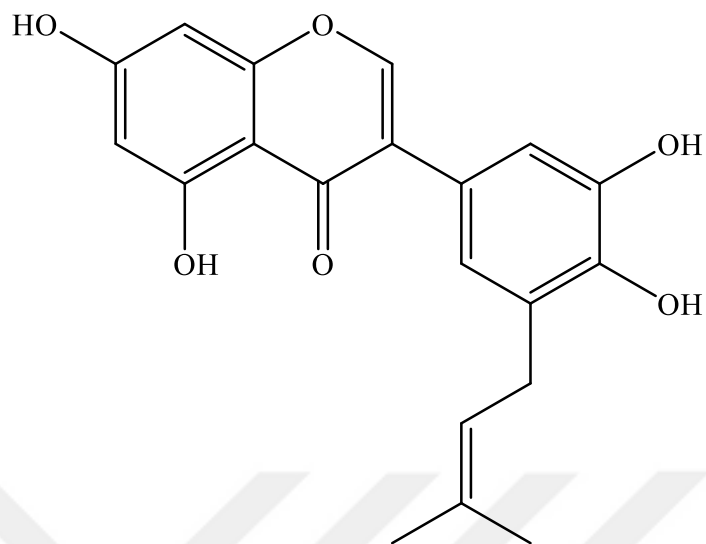
14   Glycyrrhisoflavone

Glycyrrhisoflavone (**14**) was the only isoflavone that were isolated. It was previously obtained from *G. uralensis*, *G. glabra* and *G. inflata* as mentioned before (96,109,205). But, this is the first study that compound **14** was purified from *G. iconica*.
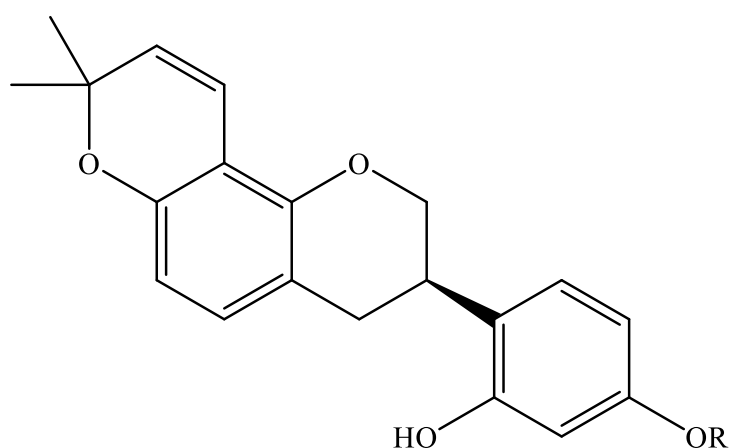
		R
15	Glabridin	H
16	4'-*O*-Methylglabridin	CH$_3$
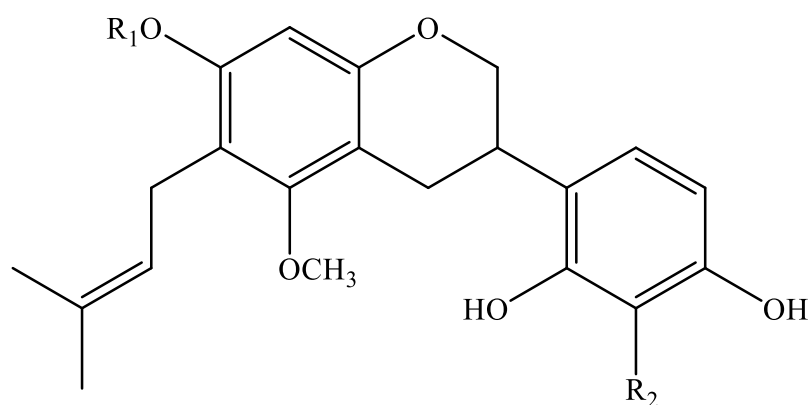
		R_1	R_2
17	Glyasperin C	H	H
18	Licoricidin	H	isoprenyl
19	Licorisoflavan A	CH$_3$	isoprenyl

Isoflavans with 2,2-dimethylpyran structure attached to ring A were isolated from *G. glabra* roots namely glabridin (**15**) and 4'-*O*-methylglabridin (**16**). On the other hand, glyasperin C (**17**), licoricidin (**18**) and licorisoflavan A (**19**) were the other isoflavans that were purified from *G. iconica*. All of the isolated isoflavans (**15-19**) were oxygenated at C-7, C-2' and C-4'. Moreover, they were all prenylated. In **15** and **16** isoprenylation occured from C-8 and cyclized through hydroxyl group in C-7. Compounds **17**, **18** and **19** were all prenylated at C-6 while **18** and **19** had additional isoprenyl chains in ring B. Compound **17** with only one isoprenyl moiety was obtained from EtOAc subextract of *G. iconica* whereas **18** and **19** having two isoprenyl chains were isolated from CHCl$_3$ subextract. This might be explained through increased lipophilicity by substitution of second prenyl groups in compounds **18** and **19** (258). It is noteworthy to mention that glyasperin C (**17**) was isolated from *G. iconica* for the first time.
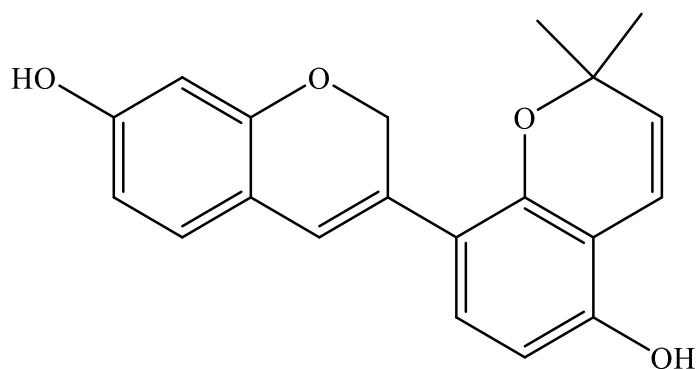
20   Glabrene
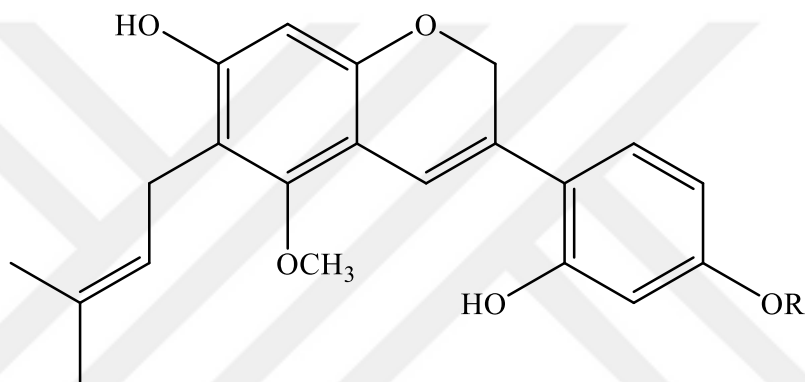
		R
21	Dehydroglyasperin C	H
22	Iconisoflaven	CH$_3$

Obtained isoflavene derivatives whose structures are given above were glabrene (**20**), dehydroglyasperin C (**21**) and iconisoflaven (**22**). These compounds were previosly reported from *Glycyrrhiza* species. Dehydroglyasperin C (**21**) was afforded from *G. aspera* and *G. uralensis* before, but isolation of **21** from *G. iconica* is firstly reported (22,177,204). Dehydroglyasperin C (**21**) might biosynthetically occured by dehydrogenation of glyasperin C (**17**) based on the similarity in their chemical stuctures. Glabrene (**20**) as the isolate of *G. glabra* possessed a cyclized prenyl ring. On the other

hand, both of the isoflavenes yielded from *G. iconica* (**21** and **22**) had methoxy units at C-5, isoprenyl moieties at C-6 and OH groups at C-2'.
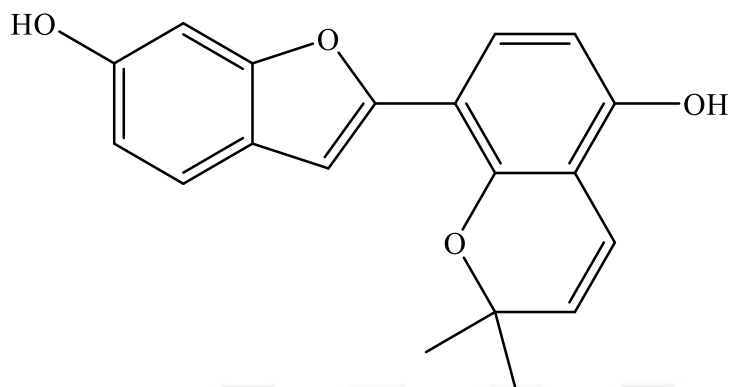
23   Kanzonol U
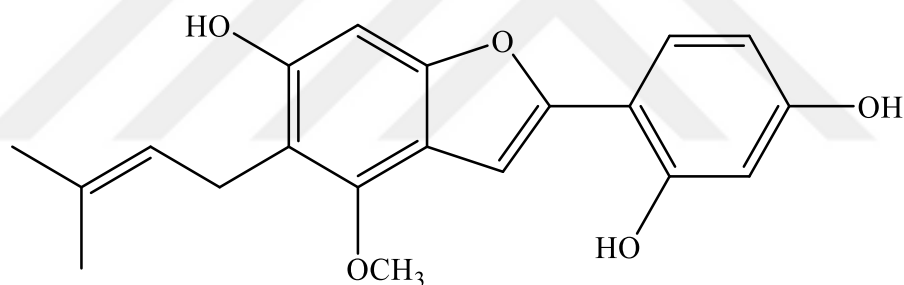
24   Licocoumarone

2-Arylbenzofuran derivatives kanzonol U (**23**) and licocoumarone (**24**) were obtained from *G. glabra* and *G. iconica*, respectively. They differed from each other, by the location and cyclization of the prenyl unit as well as the presence of OH/OCH$_3$ groups. Kanzonol U (**23**) might be biosynthetically originated from glabrene (**20**) with respect to the similarity of their substituents. Licocoumarone (**24**) is being reported for the first time from *G. iconica*.
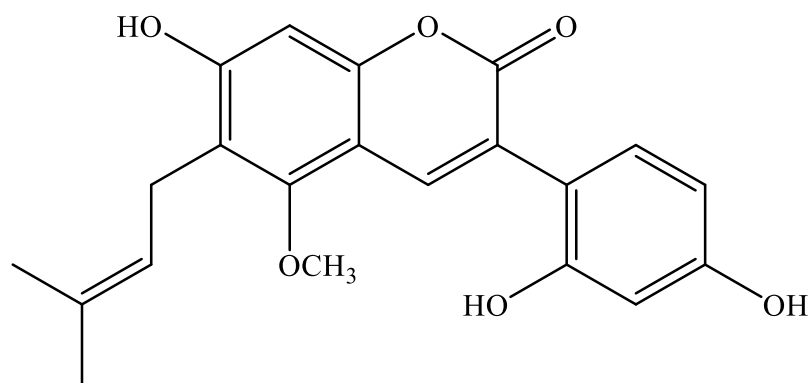
25   Glycycoumarin

Glycycoumarin (**25**), a 3-arylcoumarin type compound was isolated from CHCl₃, EtOAc and *n*-BuOH subextracts of *G. iconica* as a prenylated compound. It is widespread in the genus *Glycyrrhiza* (22,47,187). It might be biosynthetically occured by the oxidation of dehydroglyasperin C (**21**), moreover it might be the precursor of licocoumarone (**24**).
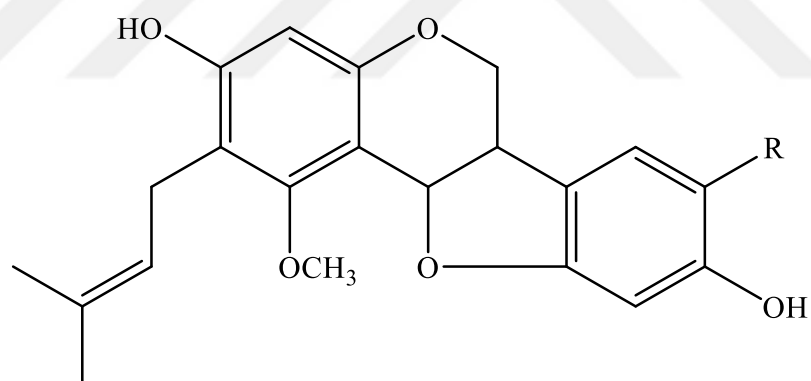
		R
26	Edudiol	H
27	1-Methoxyficifolinol	isoprenyl

Edudiol (**26**) and 1-methoxyficifolinol (**27**) belonging to pterocarpan subclass, were obtained from CHCl₃ subextract of *G. iconica*. Both compounds differed from each other by the presence of the second isoprenyl chain in C-8 of **27**. Edudiol (**26**) was

previously reported from *Desmodium uncinatum*, *G. uralensis* and *G. glabra* while 1-methoxyficifolinol (**27**) was purified from *G. uralensis* and *G. aspera* before with regard to the published literatures (13,163,177,249). However, it is the first study on the isolation of both **26** and **27** from *G. iconica*. Based on the structural similarity, edudiol (**26**) might be biosynthetically originated from glyasperin C (**17**) or *vice versa*.

28   β-amyrin
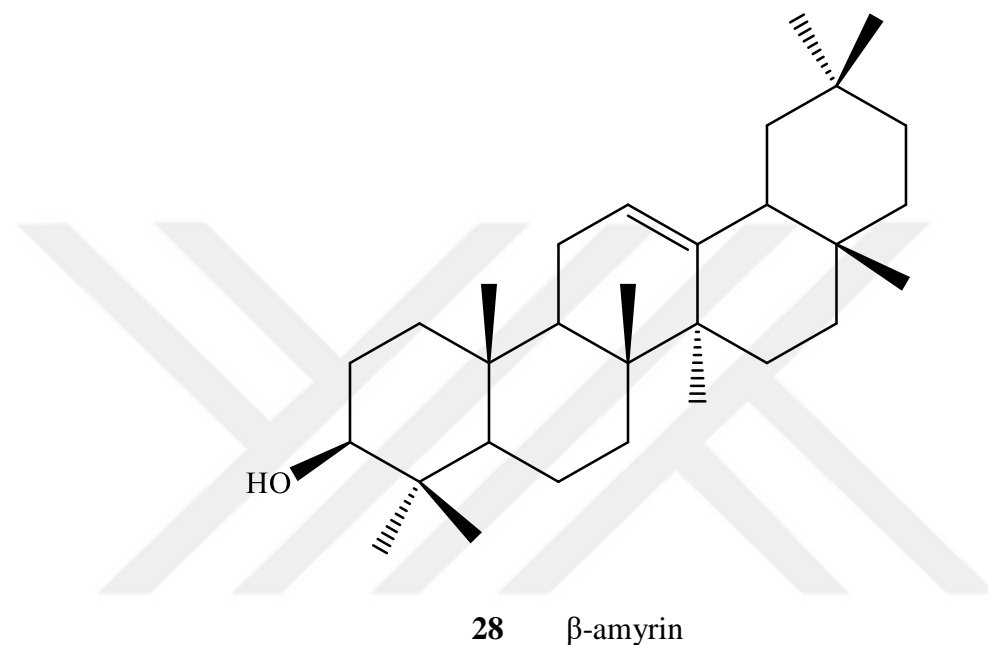
β-amyrin was the only terpenic compound that were isolated in our study. It is a olean-12-en type triterpene that was obtained from *G. glabra*.

From *G. glabra* roots, totally thirteen different compounds were obtained including two chalcones (**2** and **3**), three chalcone glycosides (**5-7**), two flavanones (**11** and **12**), one flavanone glycoside (**13**), two isoflavans (**15** and **16**), one isoflavene (**20**), one 2-arylbenzofuran (**23**) and one triterpene (**28**). Among these mentioned compounds, abyssinone II (**11**), (2R,3R)-3,4',7-trihydroxy-3'-prenylflavanone (**12**), glabridin (**15**), 4'-O-methylglabridin (**16**), glabrene (**20**) and kanzonol U (**23**) were prenylated. Furthermore, all of the isoflavonoids **15**, **16**, **20** and **23** that were isolated from *G. glabra* possessed cyclized prenyl moieties, whereas **11** and **12** flavanones had aliphatic isoprenyl chains.

Sixteen different compounds were yielded from *G. iconica* roots belonging to chalcones (**1,2** and **4**), flavonols (**8** and **9**), flavone glycoside (**10**), isoflavone (**14**),

isoflavans (**17**-**19**), isoflavenes (**21** and **22**), 2-arylbenzofuran (**24**), 3-arylcoumarin (**25**) and pterocarpans (**26** and **27**) as chemical subclasses. Eleven of these compounds contained aliphatic isoprenyl chains in either ring A or B, including topazolin (**9**), glycyrrhisoflavone (**14**), glyasperin C (**17**), licoricidin (**18**), licorisoflavan A (**19**), dehydroglyasperin C (**21**), iconisoflaven (**22**), licocoumarone (**24**), glycycoumarin (**25**), edudiol (**26**) and 1-methoxyficifolinol (**27**). Moreover, three of these above mentioned compounds (**18**, **19** and **27**) possessed two isoprenyl groups.

The Fabaceae family and most specifically Papilionoidae subfamily which includes the genus *Glycyrrhiza* is the major source of naturally occuring isoflavonoids. More than 840 new isoflavonoid derivatives were reported between 1997-2011, suggesting the high interest in this area (259). Isoflavonoid derivatives such as isoflavones, isoflavanones, isoflavans, isoflavenes, 3-arylcoumarins and pterocarpans are the characteristic secondary metabolites for the genus *Glycyrrhiza* (47).

Isoflavonoids are believed to be synthesized by aryl migration of 5-hydroxyflavanones (naringenin) and 5-deoxyflavanones (liquiritigenin) by the catalization of P450-, O_2- and NADPH- dependent isoflavone synthase enzymes which yielded to 2-hydroxyisoflavanone. Further, dehydration occured and resulted in genistein or daidzein, respectively. Based on the reaction mechanism, the enzymatic aryl migration require a C-4' or C-2' hydroxy unit. Therefore, most of the isoflavonoids are oxygenated at C-4' or C-2' position of corresponding B ring except for very few examples (260). In this study, isolated isoflavonoids (**15**-**27**) were all oxygenated at both C-4' and C-2' except for **14** which was oxygenated only at C-4', supporting the previous report.

Prenylated isoflavonoids of Fabaceae are suggested to be the phytoalexins that are synthesized by prenyltransferase enzyme in addition to above mentioned isoflavone synthase enzyme in response to a fungal attack or challenge with biotic/abiotic elicitor (258,260). In contrast to prenylated isoflavonoids, prenylated flavonoids are constitutively expressed by conjugation reaction (261). In spite of rich variety and structural diversity of prenylated flavonoids and isoflavonoids, they have a very narrow distribution in the plant kingdom (260,261). It is noteworthy to mention that, in this study all of the isoflavonoid derivatives (**14**-**27**) obtained from both species contained at least one prenyl moiety in their structures. Furthermore, among six isolated flavonoids (**8**-**13**),

half of them (**9**, **11** and **12**) had isoprenyl moieties. These were important findings regarding the chemotaxonomic evaluation of *Glycyrrhiza* species.

Based on the *in vitro* cytotoxicity results conducted on isolates by using SRB assay (Table 139), tetrahydroxymethoxychalcone (**2**), glabridin (**15**), 4'-*O*-methylglabridin (**16**), glabrene (**20**), kanzonol U (**23**) and β-amyrin (**28**) were identified as the bioactive secondary metabolites that are responsible for *in vitro* cytotoxicity of *G. glabra*. The active compounds of *G. iconica* (Table 140) were found to be tetrahydroxymethoxychalcone (**2**), 2'-*O*-methylisoliquiritigenin (**4**), 3-*O*-methylkaempferol (**8**), topazolin (**9**), glycyrrhisoflavone (**14**), glyasperin C (**17**), licoricidin (**18**), licorisoflavan A (**19**), dehydroglyasperin C (**21**), iconisoflaven (**22**), licocoumarone (**24**), glycycoumarin (**25**), edudiol (**26**) and 1-methoxyficifolinol (**27**).

Comparing all the tested compounds, against Huh7 cancer cell lines kanzonol U (**23**) ($IC_{50} = 1.8$ µM) was the strongest compound, followed by glabrene (**20**) ($IC_{50} = 2.3$ µM) and 1-methoxyficifolinol (**27**) ($IC_{50} = 2.4$ µM). Among the tested compounds, glabrene (**20**) and 1-methoxyficifolinol (**27**) were the cytotoxically most potent compounds against MCF7 cells with IC_{50} values of 5.0 and 4.6 µM, respectively. Compounds **20** ($IC_{50} = 4.9$ µM) and **27** ($IC_{50} = 5.0$ µM) were also found to be most potent ones against HCT116 cancer cell lines. Furthermore, 1-methoxyficifolinol (**27**) was the most potent compound against three tested cell lines ($IC_{50} = 2.4 - 5.0$ µM) when compared to the other isolates of *G. iconica* according to SRB assay.

Although, **6**+**7** were obtained from inactive main fraction of *G. glabra* EtOAc subextract (fr. 3), the mixture was evaluated for their cytotoxic effects by SRB assay and found to be inactive against three tested cell lines. These finding indicated that the cytotoxic activity-guided fractionation was achieved. On the other hand, iconichalcone (**1**), 4'-*O*-β-glucopyranoside (**5**) and abyssinone II (**11**) which were yielded from active main fractions, did not display any growth inhibition effects against cancer cells.

With regard to SRB results, active compounds ($IC_{50} < 40$ µM) possessed chalcone (**2** and **4**), flavonol (**8** and **9**), isoflavone (**14**), isoflavan (**15-19**), isoflavene (**20-22**), 2-arylbenzofuran (**23** and **24**), 3-arylcoumarin (**25**), pterocarpan (**26** and **27**) and triterpene (**28**) skeletons. The inactive ones were α,β-dihydroxychalcone (**1**), chalcone glycosides (**5** and **6**+**7**), flavone glycoside (**10**) and flavanone derivative (**11**).

In terms of structure activity relationships, the presence of isoprenyl chain in flavonoid and isoflavonoid derivatives can enhance biological activity by increasing their lipophilicity, improving interaction with proteins and thus the affinity to the biological membranes (258). According to a previous study of Tang et al., it was shown that number of isopyrenyl groups in A and B rings, the hydroxyl groups at *ortho* position of isopyrenyl on A ring and conjugated plane of C ring were positively-correlated with anticancer activity of flavonoids and isoflavonoids (184). Lin et al. revealed that isoprenyl group remarkably improved the cytotoxic activity of compounds against MCF7, SW480 and HepG2 cells (24). An *in vitro* study conducted by Li and collegues indicated that absence of prenyl group diminished the cytotoxic activity (23). Another study by Ji et al. demonstrated that flavonoid glycosides did not cause any *in vitro* cytotoxicity whereas prenylated phenolics were found to be active against cancer cell lines (22).

According to SRB assay results of this study, licoricidin (**18**) (IC_{50} = 4.7 - 9.3 μM) which contained two isoprenyl units in both A and B rings, was found to be more active than glyasperin C (**17**) (IC_{50} = 16.8 - 20 μM) which had only one isoprenyl in A ring. Similarly, the number of isoprenyl moieties in the structures of pterocarpan derivatives (**26** vs. **27**) effected their cytotoxic activities significantly. As 1-methoxyficifolinol (**27**) (IC_{50} = 2.4 - 5.0 μM) having two isoprenyl units was found to be cytotoxically more active than edudiol (**26**) (IC_{50} = 7.5 - 20.0 μM) having only one isoprenyl unit. SRB assay results of two afforded flavonol derivatives (**8** and **9**) revealed that the presence of isoprenyl moiety in **9** (IC_{50} = 7.2 - 11.8 μM) caused a remarkable increase in cytotoxicity when compared to 3-*O*-methylkaempferol (**8**) (IC_{50} = 14.7 - 33.0 μM). Furthermore, dehydrogenation between C-3/C-4 position of C ring as in dehydroglyasperin C (**21**) (IC_{50} = 5.8 - 9.6 μM) increased the cytotoxic activity when compared with glyasperin C (**17**) (IC_{50} = 16.8 - 20.0 μM). Besides, **21** was also found to be more active than glycycoumarin (**25**) (IC_{50} = 10.7 - 17.5 μM). This phenomenon could be explained by the introduction of ketone function at C-2 on isoflavenes caused around 2-fold decrease in the activity. These findings highlighted the advantages of prenylated flavonoids and isoflavonoids over unprenylated ones in *in vitro* cytotoxic activity assays. Furthermore, increased number of isoprenyl moieties in ring A and B and presence of a conjugated plane between C-3/C-4 could enhance the cytotoxicity of compounds based on above information.

Presence of a second methoxy group in the structure as seen in licorisoflavan A (**19**) (IC$_{50}$ = 11.5 - 13.0 µM) and iconisoflaven (**22**) (IC$_{50}$ = 7.1 - 18.0 µM) showed a decrease in the cytotoxic activity when compared to licoricidin (**18**) (IC$_{50}$ = 4.7 - 9.3 µM) and dehydroglyasperin C (**21**) (IC$_{50}$ = 5.8 - 9.6 µM), respectively which lack the second methoxy moieties. From another point of view, **18** had hydroxy group in *ortho* position of isoprenyl unit in ring A which might be another possible reason for having relatively high cytotoxic activity than **19**. On the other hand, presence of only one methoxy unit as observed in 4'-*O*-methylglabridin (**16**) (IC$_{50}$ = 9.6 µM) increased the cytotoxicity in Huh7 cells comparing to glabridin (**15**) (IC$_{50}$ = 16.7 µM).

According to a study by Ohno et al., chalcones were demonstrated to be cytotoxically more active and to have more tumor specificity than flavanones (262). Moreover, number of phenolic hydroxyl groups in chalcones was shown to have positively-correlated with *in vitro* cytotoxicity. Results of this thesis indicated that tetrahydroxymethoxychalcone (**2**) which had a chalcone nucleus with four OH groups (IC$_{50}$ = 8.3 - 13.9 µM) showed better cytotoxic activity than 2'-*O*-methylisoliquiritigenin (**4**) (IC$_{50}$ = 12.1 - 18.4 µM) with two OH groups while abyssinone II (**11**) that had a flavanone core did not exert any cytotoxic effects, showing similar results with previous study. Furthermore, if we compare iconichalcone (**1**) and tetrahydroxymethoxychalcone (**2**), it can be concluded that presence of α,β-dihydroxychalcone nucleus abolished the cytotoxic activity.

Based on the previous *in vitro* screening models, flavonoid glycosides displayed only weak to moderate activities (21,22,24). Addition of sugar units in the molecule was shown to cause a decrease in cytotoxic activity (22,262). In this study, none of tested glycosides (**6**+**7**, **5** and **10**) exerted any *in vitro* cytotoxic activity against any of the tested cell lines which were consistent with previous reports. However, these compounds might be metabolized to their bioactive free forms in gastrointestinal system after oral administration, and thus may play an important role in therapeutic effects of licorice.

Within this study, the *in vitro* cytotoxic effects of tetrahydroxymethoxychalcone (**2**), 2'-*O*-methylisoliquiritigenin (**4**), neolicuroside and licuroside (**6**+**7**), 3-*O*-methylkaemferol (**8**), violanthin (**10**), licorisoflavan A (**19**), iconisoflaven (**22**), edudiol (**26**) and 1-methoxyficifolinol (**27**) were studied for the first time against Huh7, MCF7

and HCT116 cancer cell lines. Moreover, among these compounds **2**, **4**, **6**, **7**, **10, 19**, **22** and **26** were evaluated for the very first time regarding their cytotoxic properties.

In vitro cytotoxicity of isoliquiritigenin 4'-*O*-β-glucopyranoside (**5**), topazolin (**9**), glycyrrhisoflavone (**14**), 4′-*O*-methylglabridin (**16**), glyasperin C (**17**), glabrene (**20**), dehydroglyasperin C (**21**), kanzonol U (**23**), licocoumarone (**24**) and glycycoumarin (**25**) against MCF7 cells were demonstrated in previous studies (22–24). However, their cytotoxic effects against Huh7 and HCT116 cell lines are reported for the first time within this study.

Ji et al. evaluated cytotoxic effects of licorice compounds including topazolin, licocoumarone, glycycoumarin, glyasperin C, dehydroglyasperin C, licoricidin, liquiritin apioside and isoliquiritigenin 4'-*O*-glucopyranoside obtained from *G. uralensis* against liver (HepG2), colorectal (SW480), lung (A549) and breast (MCF7) cancer cell lines by using MTS assay (22). Results of the mentioned study showed that licoricidin was the most potent compound among other tested isoflavans with IC_{50} values of 0.3, 7.1, 6.9 and 5.2 µM against HepG2, SW480, A549 and MCF7, respectively. Against liver cancer cells (HepG2) cytotoxic effect of licoricidin was in submicromolar level. Ji et al. also demonstrated that topazolin was the most cytotoxic compound among tested flavones by displaying IC_{50} values of 10.8 (HepG2), 16.1 (SW480), 23.1 (A549) and 7.3 (MCF7) µM. Furthermore, licocoumarone (10 µM) and dehydroglyasperin C (10 µM) were found to be cytotoxic against liver cancer cells by inhibiting HepG2 cells by 70% and 88%, respectively. On the other hand, the other compounds (glycycoumarin, glyasperin C, liquiritin apioside and isoliquiritigenin 4'-*O*-glucopyranoside) did not show significant cytotoxic effects against tested cell lines at doses of 10 µM (22). Based on SRB results in this study, licoricidin (**18**) exhibited considerable cytotoxic activities against hepatocellular (Huh7), breast (MCF7) and colorectal (HCT116) cancer cells with IC_{50} values of 4.7, 9.3 and 9.2 µM, respectively, while topazolin (**9**) exerted activity with IC_{50} values of 7.2 (Huh7), 10.5 (MCF7) and 11.8 (HCT116) µM. On the other hand, licocoumarone (**24**) (IC_{50} = 10 µM) and dehydroglyasperin C (**21**) (IC_{50} = 5.8 µM) also exhibited marked cytotoxic effects against liver cancer (Huh7) cells. In addition, chalcone glycoside isoliquiritigenin 4'-*O*-glucopyranoside (**5**) was not found to be cytotoxic against Huh7, MCF7 and HCT116 cancer cells. Taken together, compounds **9**, **18**, **21** and **24** elicited considerable cytotoxic effects against liver, breast and colorectal cancer cell lines,

while **5** was found to be inactive. These results were in accordance with the previous study of Ji and team except for activity results of glycycoumarin (**25**) and glyasperin C (**17**), even though different methods were used. In addition, in our study liquiritin apioside (**13**) was not assesed for its cytotoxic activity by SRB assay since it was isolated from an inactive main fraction of *G. glabra* (fr. 2, EtOAc subextract). As observed in the previous study, it was found to be cytotoxically inactive which might be explained by its glycosidic structure.

In a study conducted by Ji and colleagues, licoricidin was also investigated regarding its effects against different colorectal cancer cell lines namely SW480, HCT116, SW620 and LoVo cells with MTT assay. Licoricidin (IC$_{50}$ = 5.4 µM) was found to be active against HCT116 and also demonstrated as a potential chemopreventive and chemoprotective agent according to following *in vivo* antitumor experiments by inducing cell cycle arrest, apoptosis and autophagy in SW480 cells (121). Within this study, licoricidin (**18**) (IC$_{50}$ = 9.2 µM) showed marked cytotoxic effects against HCT116 cells according to SRB assay results which is consistent with the previous study. Thus, cytotoxic effects of licoricidin (**18**) against MCF7 and HCT116 were evaluated previously as mentioned above, but it is the first report demonstrating the cytotoxic activity of licoricidin (**18**) against Huh7 cells.

Zhang et al. demonstrated that combination therapy of glycycoumarin improved the *in vitro* anticancer efficacy of ABT-737 compound against liver (Huh7) cancer cells. Furthermore, the pharmacokinetic study conducted by Ye's group showed that glycycoumarin had promising oral bioavailability (263). However, there is no published report about its cytotoxic activitity against Huh7 and HCT116 cancer cells alone which is firstly reported with this study.

In another study performed by Lin et al., abyssinone II along with 66 other compounds isolated from *G. inflata* were assessed for their cytotoxic activity against HepG2, SW480 and MCF7 cancer cells by MTS assay. Results demonstrated that treatment with abyssinone II (10 µM) did not inhibit the cell proliferation of any tested cancer cells (24). In our study, abyssinone II (**11**) was not cytotoxic in the SRB tests which was in line with the previous study. On the other hand, cytotoxicity of compound **11** is being reported for the first time against Huh7 cancer cell lines.

Li et al. investigated the cytotoxic effects of glabridin, 4'-O-methylglabridin, glabrene and kanzonol U together with 52 compounds obtained from *G. glabra* in HepG2, SW480, A549 and MCF7 cancer cells. Results demonstrated that glabridin, 4'-O-methylglabridin, glabrene and kanzonol U inhibited cell proliferation in MCF7 cells by 8.8%, 5.3%, 17.6% and 9.7% at 10 µM doses according to MTS assay (23). In the current study, SRB assay results showed that glabridin (**15**) (IC_{50} = 15.1 µM), 4'-O-methylglabridin (**16**) (IC_{50} = 16.5 µM) and kanzonol U (**23**) (IC_{50} = 16.8 µM) exhibited IC_{50} values above 10 µM in MCF7 cells. These findings as well as the previous study could conclude that the doses of **15**, **16** and **23** must be > 10 µM in order to exert their *in vitro* cytotoxic effects against breast cancer cells. In contrast, glabrene (**20**) showed cytotoxicity with IC_{50} value of 5.0 µM in MCF7 cells which might be explained by different cytotoxicity methods used in both studies.

In a very recent study, glabridin, a key biological and chemical marker of *G. glabra*, was reported to induce Huh7 cell death (50 µM) by inducing autphagy and apoptosis through caspase cascade and accumulating the cell population (100 µM) in the subG$_1$ and G$_0$/G$_1$ phases (264). Furthermore, glabridin (10 mg/kg) inhibited tumor growth in the hepatoma xenograft model (123). Tamir and colleagues evaluated the effects of glabridin on human estrogen receptors and growth of breast cancer cells. Results indicated that glabridin acted like a phytoestrogen, at doses of 10 nm-10 µM. It showed estrogen-receptor dependent growth promoting effect on breast tumor cells, whereas it showed estrogen receptor-independent antiproliferative effects at doses of >15 µM. Furthermore, it inhibited colony formation of anchorage-independent MCF7 breast cancer cells at concentrations of ≥ 25 µM (125). On the other hand, against HCT116 cell lines, glabridin found to be cytotoxic with the IC_{50} value of lower than 25 µM (197). In our study, glabridin (**15**) showed cytotoxic effects against Huh7 (IC_{50} = 16.7 µM), MCF7 (IC_{50} = 15.1 µM) and HCT116 (IC_{50} = 10.5 µM) similar to previous studies.

Cytotoxicity of β-amyrin (**28**) was reported before by Halawany et al. against HCT116 (IC_{50} = >100 µM) and MCF7 (IC_{50} = 10.1 µM) cell lines using MTT assay, while this study presents the first report on cytotoxic effect of **28** in Huh7 cells (265).

In order to determine the underlying cytotoxicity mechanisms of the most active compounds based on their IC_{50} values (<10 µM) in SRB assay, tetrahydroxymethoxychalcone (**2**), 4′-O-methylgrabridin (**16**), glabrene (**20**) and

kanzonol U (**23**) obtained from *G. glabra* and **2**, topazolin (**9**), glycyrrhisoflavone (**14**), licoricidin (**18**), dehydroglyasperin C (**21**), iconisoflaven (**22**), edudiol (**26**) and 1-methoxyficifolinol (**27**) obtained from *G. iconica*, were chosen for further mechanistic studies.

Liver cancer is estimated to be the sixth most commonly diagnosed cancer and the fourth leading cause of cancer-related mortality with 841.080 new cases and 781.631 deaths per year across globe for both sexes according to GLOBOCAN 2018 statics. Moreover, liver cancer has two to three times higher incidence and mortality rates among men than women in most of the regions while it is ranked second in terms of deaths for males (2). Primary liver cancer mostly includes hepatocellular carcinoma (HCC) by consisting 75-80% of cases. The major risk factors of HCC are chronic infection of Hepatitits B or Hepatitis C virus, aflatoxin explosure, heavy alcohol intake, obesity, type-2 diabetes and smoking. Surgery and liver transplant are the therapeutic methods for the treatment of HCC which have limiting difficulties because of the scarcity of donor organs (266). Therefore, new alternative treatment methods are needed to combat HCC. Among the cancer cell lines used in this study, especially liver cancer cells (Huh7) were the most sensitive cells to the cytotoxic effects of the tested compounds except for glabridin (**15**), glyasperin C (**17**) and β-amyrin (**28**). Hence, mechanistic studies were determined to be carried on with hepatocellular (Huh7) cancer cell lines. First, time dependent cytotoxicity assay for above mentioned compounds (**2**, **9**, **14**, **16**, **18**, **20**, **21**, **22**, **23**, **26** and **27**) was conducted by Real-Time cell electronic sensing (RT-CES) in Huh7 cells. Compounds with IC$_{50}$ values ≤ 10 μM at 48th in hour in RT-CES assay were accepted as the most active ones that were justified to be mechanistically evaluated in further bioactivity studies including Hoechst staining, Fluorescence-activated cell sorting (FACS) and Western blot assays.

The most active compounds that deserved further mechanistic studies were established as **2**, **16** and **20** from *G. glabra* and **2**, **18**, **21**, **22** and **27** from *G. iconica* with regard to RT-CES results. These compounds were conducted to Hoechst staining assay and observed for their morphological changes. One of the most outstanding changes in apoptotic cells is the chromatin condensation and fragmentation and hence increase in concentration of the chromosomes. Apoptotic cells become brighter blue color, while normal cells become milder after staining with Hoechst dye which can be more invasive to cell nucleus and bound to DNA in apoptotic cells due to chromatin condensation (267).

According to the images taken by fluorescent microscopy, most particularly tetrahydroxymethoxychalcone (**2**) showed condensed nuclei remarkably, indicating apoptotic cell death as evidenced by an intense pycnotic bluish fluorescence in the nuclei of Huh7 cells. Besides, licoricidin (**18**), glabrene (**20**) and dehydroglyasperin C (**21**) induced relatively milder chromatin condensation in Huh7 cells, also revealed the existence of apoptotic cells by exhibiting slightly bright blue colored cells.

Dysregulation of cell cycle is a key feature of tumor cells and an important target in cancer therapies (225). Effects of **2**, **16** and **20** from *G. glabra* and **2**, **18**, **21**, **22** and **27** from *G. iconica* on cell cycle were further characterized by FACS analysis. The obtained results revealed that all of the tested compounds particularly iconisoflaven (**22**) caused accumulation of cells in $SubG_1$ phase which is the indicator of extensive DNA fragmentation and hence apoptotic cell death (240). Furthermore, **2**, **16**, **18**, **20**, **21** and **22** induced apoptosis also by the cell cycle arrest in G_2/M phase. Especially, the G_2/M arrest was very dramatical for the cells treated with tetrahydroxymethoxychalcone (**2**). Moreover, elevated cell population in G_1 also revealed apoptosis in licoricidin (**18**) and 1-methoxyficifolinol (**27**) treated Huh7 cells.

In order to clarify the cellular cytoxicity mechanisms of these compounds more specifically in Huh7 cells, their effects against the expressions of apoptotic (cytochrom C, cleaved caspase-3/-9 and PARP) and cell cycle regulatory proteins (Mdm2, pRb, p21 and p53) were investigated with Western blot analysis.

Caspases are cysteine protease enzymes, accepted to be central mechanisms of apoptosis, activation of them consists of both intrinsic and extrinsic pathways (4,225). The intrinsic pathway is initiated within the cell as a result of increased mitochondrial permeability and release of pro-apoptotic molecules such as cytochrome C. It is released from mitochondria into cytosol by induction of apoptosis (228). Cytosolic cytochrome C expression activates caspase-9 early during the apoptotic process. The activated caspase-9 subsequently stimulates proteolytic activity of other downstream caspases including caspase-3 which leads to cleavage of various proteins such as PARP and results in cell death (5,227). According to our findings, all of the tested compounds (**2**, **16** and **20** from *G. glabra* and **2**, **18**, **21**, **22** and **27** from *G. iconica*) might cause an increase in mitochondrial membrane permeability and thus released cytochrome C into cytosol as understood from marked cytochrome C levels. Among these compounds, **2**, **16**, **18**, **20**,

21 and **27** caused increased cleaved caspase-9 levels in Huh7 cells while increased cleaved caspase-3 levels were observed in the cells treated with **21** and **22**. In accordance with these results, increase in cleaved PARP protein levels were seen for compounds **2**, **18**, **20** and **21**. Based on these above mentioned findings, all these tested compounds most particularly **21**, might exert proapoptotic effects through intrinsic mitochondrial pathway of caspase cascade.

A tumor supressor gene p53 is a DNA-binding phosphoprotein, which plays an important role in several aspects of cell cycle arrest, apoptosis, DNA repair etc. and regulates the cell mechanisms by trans activating various genes including p21 and Mdm2 (231). Chen et al. demonstrated that silencing of p21 significantly promoted apoptosis, supressed the cellular proliferation and increased G_2/M phase arrest. In addition, it was reported that p53 expression usually mimics the p21 expression (236). Based on these findings, the remarkable decreases in p21 levels in Huh7 cells treated wih the compounds **2**, **16**, **18**, **20**, **21**, **22** and **27** indicated induction of apoptotic response. Furthermore, along with decreased p21 levels, the accumulation of cells in G_2/M phase were also observed with **2**, **16**, **18**, **20**, **21** and **22**. Moreover, the expression profiles of p53 and p21 were found to be parallel in all of the samples except for **21** which showed similar results with the previous study.

Retinoblastoma (Rb) protein (pRb) is neccesary for the continuation of cell cycle and decrease in phosphorylation of this protein (phospho-Rb) is an indicator of the suppression in cell cycle. It is also an anti-apoptotic factor and cleaved during apoptotic pathways. This fragmentation impairs the interaction of pRb with Mdm2 which is also an apoptosis inhibitor, working together with pRb. Rb proteins function in G_1 phase for the phosphorylation of transcriptional genes and phosphorylated Rb (phospho-Rb) is key for the entering the cell in the G_1 phase of cell cycle. Thus, decrease in the phospho-Rb levels indicates cell cycle arrest in G_1 phase (231). According to our results, phosphorylation of retinoblastoma proteins (phospho-Rb levels) were decreased especially in cells incubated with **16**, **20**, **22** and **27**. These results were in accordance with cell cycle assay results in which increase in $subG_1$ phase population also with the same compounds (**16**, **20**, **22** and **27**) and G_1 arrest with **27** were observed.

In normal conditions of cells p53 gene remains in "standby" mode (233). Whereas activation of it causes increasing levels of p53 protein induce variety of cellular responses,

most notably in cell cycle arrest and apoptosis pathways. Activity of p53 can be regulated by multiple cellular proteins particularly by mouse double minute 2 (Mdm2) (230). Levels of Mdm2, an apoptosis inhibitor were decreased with all of the tested compounds except for **21** (dehydrogyasperin C). Besides being a potent physiological antagonist of p53, Mdm2 can also be a direct target for the transcriptional activation by p53, thus establishing a negative autoregulatory feedback loop in which p53 activates its own inhibitor (230). In our present study, increased p53 levels along with increased Mdm2 levels with compound **21** were observed, indicating anti-tumor gene of p53 was stimulated upon **21** administration. It is known that p53 plays an important role in G_1 and G_2 phases of cell cycle (234). Overexpression of p53 inhibits the cells entrying to mitosis by causing cell cycle arrest in G_1 and G_2/M (231,232). Upregulation of p53 in Huh7 cells treated with compound **21** might be the another possible explanation for the higher percentage of cells in subG_1 and G_2/M phases. On the other hand, induction of p53 is a multistep phenomena that involves phosphorylation of p53 in the N- terminus might be occured by dissociation of p53-Mdm2 interaction (268). Phoshorylation of p53 was observed with compound **16** indicating the induction of p53 protein. In addition, p53 regulates expression of pro-apoptotic genes including Bad, Bax and anti-apoptotic protein Bcl-2 (234). The relative levels of these proteins are crucial for apoptosis. Bcl-2 is known to prevent apoptosis by inhibiting proapoptotic protein Bax. p53 transcriptionally activates Bad protein which further inhibitis anti-apoptotic Bcl-2 by directly binding to it. Inactivation of Bcl-2 rescues pro-apoptotic protein Bax. Bax increases the permeability of mitochondrial membrane causing cytochrome C release and finally leads to p53 mediated and caspase dependent apoptosis (232,234,235). Caspase dependent apoptosis was observed with dehydrogyasperin C (**21**) as mentioned above, might be mediated by p53 activation. The further studies regarding the alterations in the transcription of pro- and anti-apoptotic members of Bcl-2 family can be conducted in future.

Table 143. Summary of the mechanistic studies of **2**, **16**, **18**, **20**, **21**, **22** and **27** on Huh7 cancer cell lines

	RT-CES	Hoechst Staining	FACS	Western Blot
Tetrahydroxymethoxychalcone (**2**)	IC_{50}= 4.4 µM at 48th h	Condensed nuclei	SubG$_1$ ↑ G$_2$/M arrest	Cytochrome C, cleaved caspase-9 and PARP ↑
				p21 and Mdm2 ↓
4'-*O*-Methylglabridin (**16**)	IC_{50}= 9.8 µM at 48th h	-	SubG$_1$ ↑ G$_2$/M arrest	Cytochrome C and cleaved caspase-9 ↑
				Phospho-Rb, p21 and Mdm2 ↓
				↑ Phospho-p53 → Induction of p53
Licoricidin (**18**)	IC_{50}= 10 µM at 48th h	Mild chromatin condensation	SubG$_1$ ↑ G$_1$, G$_2$/M arrest	Cytochrome C, cleaved caspase-9 and PARP ↑
				p21 and Mdm2 ↓
Glabrene (**20**)	IC_{50}= 5.8 at 48th h	Mild chromatin condensation	SubG$_1$ ↑ G$_2$/M arrest	Cytochrome C, cleaved caspase-9 and PARP ↑
				Phospho-Rb, p21 and Mdm2 ↓
Dehydroglyasperin C (**21**)	IC_{50}= 3.5 µM at 48th h	Mild chromatin condensation	SubG$_1$ ↑ G$_2$/M arrest	Cytochrome C, cleaved caspases -9/-3 and PARP ↑
				p21 ↓
				↑ p53 and Mdm2 → p53 activation
Iconisoflaven (**22**)	IC_{50}= 6.5 µM at 48th h	-	SubG$_1$ ↑ G$_2$/M arrest	Cytochrome C, cleaved caspase-3 ↑
				Phospho-Rb, p21 and Mdm2 ↓
1-Methoxyficifolinol (**27**)	IC_{50}= 4.3 µM at 48th h	-	SubG$_1$ ↑ G$_1$ arrest	Cytochrome C, cleaved caspase-9 ↑
				Phospho-Rb, p21 and Mdm2 ↓

343

To sum up (Table 143), tetrahydroxymethoxychalcone (**2**) induced apoptosis by increasing cytochrome C, cleaved caspase-9 and PARP levels as well as decreasing p21 and Mdm2 levels, increased the percentage of cells at $subG_1$ and caused very remarkable G_2/M arrest and showed nuclei with condensed chromatin as the morphological indicator of apoptosis in Huh7 cells. 4′-*O*-methylgrabridin (**16**) caused apoptosis through caspase cascade by releasing cytochrome C into cytosol and increasing cleaved caspase-9 level. Furthermore, it caused p53 protein induction and decrease in phospho-Rb as well as p21 levels and hence accumulated the Huh7 cells in $subG_1$ and G_2/M phases. Licoricidin (**18**) and glabrene (**20**) induced caspase-dependent apoptosis by increasing cytochrome C, cleaved caspase-9 and PARP levels in Huh7 cells. While **18** caused increase in cell population at $subG_1$, G_1 and G_2/M phases and decrease in p21 level, **20** showed elevation of cells in apoptotic $subG_1$ phase and caused cell cycle arrest in G_2/M by decreasing phospho-Rb and p21 levels. Dehydroglyasperin C (**21**) caused apoptosis by increasing the p53 protein expression and also through caspase activation by increasing cytochrome C, cleaved caspase-9/-3 and PARP levels in Huh7 cells. Furthermore, it caused increase in the Huh7 cell populations at $subG_1$ and G_2/M phases. Iconisoflaven (**22**) caused caspase-dependent apoptosis by increasing levels of cytochrome C and cleaved caspase-3. Moreover, it caused elevation in $subG_1$ cell population and cell cycle arrest in G_2/M phase by inhibiting phosphorylation of pRb and alleviating Mdm2 and p21 levels. 1-Methoxyficifolinol (**27**) led to the activation of caspases by increasing cytochrome C release and activating caspase-9 and thus induced apoptosis through caspase cascade. Moreover, it showed increase in $subG_1$ cell percentage and caused cell cycle suppression at G_1 phase by decreasing the phosphorylation of Rb protein.

The characteristics of cancer commonly are uncontrolled growth, angiogenesis and apoptosis evasion by numerous mutations in both extrinsic and intrinsic pathways independent with the cause or type of cancer (5). Apoptosis can be considered as a double edged sword, besides being a causative it might also be a treatment (4). The current strategies for the anticancer drug development relies on inducing apoptosis which provide more universal cancer therapy regardless of the cancer type. New drugs target different aspects of apoptosis including apoptotic genes or pathways (6). Because utilizing the cell's own death mechanism is a very efficient method (5). Therefore, apoptosis is a very critical target for clinical anticancer chemotherapeutic agents.

There are many plant-derived promising compounds that have been shown to trigger apoptosis such as evodiamine (229), curcumin (266), liquiritin (269), licochalcone A (7,124), isoliquiritigenin (120), licoricidin (121), glabridin (264), isoangustone A (128) etc. in variety of cancer cells. Lin et al., tested cytotoxic effects of twenty-five compounds isolated from *G. inflata* including glabridin (**15**) in LO2 and HEK293T human normal cell lines and demonstrated that compounds were selective to the cancer cells by displaying potent cytotoxic actions on cancer cells but only little effect on the normal cells (24). Jung et al. showed that isoliquiritigenin induced apoptosis in human prostate cancer cells however no effect was detected on the growth of normal intestinal epithelial cells (120). Another study performed by Sharma et al. demonstrated that 18β-glycyrrhetinic acid exerted potent cytotoxic effects against MCF7 cancer cells, while it did not affect normal mamary epithelial cell line (MCF10A). He et al. indicated that liquiritin supressed the growth of human cervical cancer cells whereas the effect of liquiritin to human normal liver cells, L02, and human primary renal epithelial cells, HREpiC did not cause any significant difference (269). Although we did not conduct any cytotoxicity assay on normal epithelial cells, these above mentioned published reports revealed that licorice compounds were found to be non-toxic to normal cells to the best of our knowledge.

In conclusion, totally 13 secondary metabolites (**2**, **5**, **6**+**7**, **3**+**12**, **11**, **13**, **15**, **16**, **20**, **23** and **28**) were isolated and identified from *G. glabra*. Amongst the isolates, tetrahydroxymethoxychalcone (**2**), glabridin (**15**), 4'-*O*-methylglabridin (**16**), glabrene (**20**), kanzonol U (**23**) and β-amyrin (**28**) were established to be responsible for the *in vitro* cytotoxic effects of *G. glabra* against Huh7, MCF7 and HCT116 cancer cells. Furthermore, the mechanisms behind the cytotoxic activities of the most active compounds were also elucidated by Hoechst staining, cell cycle assay and Western blot analyses in most sensitive Huh7 cells. Tetrahydroxymethoxychalcone (**2**), 4'-*O*-methylglabridin (**16**) and glabrene (**20**) contributed to the *in vitro* cytotoxic activity of *G. glabra* against Huh7 cancer cell lines by inducing apoptosis via caspase cascade, causing cell cycle arrest at G_2/M phase and increasing the percentage of cells in apoptotic $subG_1$ phase through different mechanisms such as inducing p53 (**16**), decreasing the phospho-Rb (**16** and **20**) and/or p21 (**2**, **16** and **20**) levels. We have recently published our above mentioned results on *G. glabra* (270).

In vitro cytotoxic activity guided fractionation and isolation of *G. iconica* roots led to the isolation of 16 secondary metabolites including a new one, iconichalcone (**1**). The known compounds, tetrahydroxymethoxychalcone (**2**), 2′-*O*-methylisoliquiritigenin (**4**), 3-*O*-methylkaempferol (**8**), topazolin (**9**), glycyrrhisoflavone (**14**), glyasperin C (**17**), licoricidin (**18**), licorisoflavan A (**19**), dehydroglyasperin C (**21**), iconisoflaven (**22**), licocoumarone (**24**), glycycoumarin (**25**), edudiol (**26**) and 1-methoxyficifolinol (**27**) were found to be responsible for the in *vitro* cytotoxic activity of *G. iconica* against Huh7, MCF7 and HCT116 cell lines. The mechanisms behind the cytotoxic activity of the most active compounds were also investigaed. The results indicated that induced apoptosis of Huh7 cells by **2**, **18**, **21**, **22** and **27** were mediated via caspase activation. Furthermore, according to FACS results, **2**, **18**, **21**, **22** and **27** caused accumulation of cells in different phases of cell cycle including subG$_1$, G$_2$/M and/or G$_1$. The underlying reasons of these cell cycle arrests might be due to decrease in phospho-Rb levels (**22** and **27**), p21 levels (**2**, **18**, **21**, **22** and **27**) or increase in p53 expression (**21**). Amongst the tested compounds, **21** which showed activation of p53 expression, increase in apoptotic subG$_1$ population and thus G$_2$/M arrest as well as a condensed nuclei, established very promising results, might cause cytotoxicity by inducing Huh7 cells to apoptosis through p53-mediated caspase cascade. Furthermore, compound **2** which was isolated from both *G. glabra* and *G. iconica*, displayed the most potent activity in Hoechst staining and cell cycle assays through dramatical condensation of chromatin and G$_2$/M arrest, caused cell death by apoptosis in Huh7 cells. Taken together, tetrahydroxymethoxychalcone (**2**), licoricidin (**18**), dehydroglyasperin C (**21**), iconisoflaven (**22**) and 1-methoxyficifolinol (**27**) were found to be cytotoxically active secondary metabolites of *G. iconica* against liver cancer by enhancing apoptosis and displaying anticancer functions via promoting pro-apoptotic factors such as cytochrom C and caspases.

As a result, all of the mechanistically tested compounds (**2**, **16**, **18**, **20**, **21**, **22** and **27**) in this study caused induction of apoptosis through caspase activation and cell cycle supression, showed very promising results. All of these aforementioned compounds most particularly tetrahydroxymethoxychalcone (**2**) and dehydroglyasperin C (**21**) could be potential anticancer drug candidates which deserve further *in vivo* and preclinical studies for the development of new anticancer drug leads especially against hepatocellular carcinoma. The isolated bioactive compounds deserve to be investigated for their potential cytotoxic activities against other human cancer cell lines. Based on these

findings on *G. glabra* and *G. iconica* as well as the other results obtained from previous studies on different *Glycyrrhiza* species put forward the potential of licorice species to afford new promising anticancer drug candidates.

6. REFERENCES

1) Jemal A, Bray F, Center MM, Ferlay J, Ward E, Forman D. Global cancer statistics. *CA Cancer J Clin*. 2011;61(2):69-90.

2) Bray F, Ferlay J, Soerjomataram I, Siegel RL, Torre LA, Jemal A. Global cancer statistics 2018 : GLOBOCAN estimates of incidence and mortality worldwide for 36 cancers in 185 Countries. *CA Cancer J Clin*. 2018;68(6):394-424.

3) International Agency for Research on Cancer. *World Cancer Report 2014*. Lyon Cedex France: World Health Organization; 2014. https://shop.iarc.fr/products/world-cancer-report-2014. Accessed January 15, 2019.

4) Wong RS. Apoptosis in cancer: from pathogenesis to treatment. *J Exp Clin Cancer*. 2011;30(1):87. doi:10.1186/1756-9966-30-87.

5) Pfeffer CM, Singh ATK. Apoptosis: A target for anticancer therapy. *Int J Mol Sci*. 2018;19(2):448. doi:10.3390/ijms19020448.

6) Jensen M, Engert A, Weissinger F, et al. Phase I study of a novel pro-apoptotic drug R-etodolac in patients with B-cell chronic lymphocytic leukemia. *Invest New Drugs*. 2008;26(2):139-49.

7) Park M-R, Kim S-G, Choa I-A, et al. Licochalcone-A induces intrinsic and extrinsic apoptosis via ERK1/2 and p38 phosphorylation-mediated TRAIL expression in Head and Neck Squamous Carcinoma FaDu Cells. *Food Chem Toxicol*. 2015;77:34-43.

8) Wu C-P, Ohnuma S, Ambudkar S V. Discovering natural product modulators to overcome multidrug resistance in cancer chemotherapy. *Curr Pharm Biotechnol*. 2011;12(4):609-20.

9) Newman DJ, Cragg GM. Natural products as sources of new drugs over the 30 years from 1981 to 2010. *J Nat Prod*. 2012;75(3):311-35.

10) Balunas MJ, Kinghorn AD. Drug discovery from medicinal plants. *Life Sci*. 2005;78:431-41.

11) Fujita T, Sezik E, Tabata M, et al. Traditional medicine in Turkey VII. Folk medicine in Middle and West Black Sea regions. *Econ Bot*. 1995;49(4):406-22.

12) Nassiri-Asl M, Hosseinzadeh H. Review of pharmacological effects of *Glycyrrhiza* sp. and its bioactive compounds. *Phytother Res*. 2008;22:709-24.

13) Gafner S, Bergeron C, Villinski JR, et al. Isoflavonoids and coumarins from *Glycyrrhiza uralensis*: Antibacterial activity against oral pathogens and conversion of isoflavans into isoflavan-quinones during purification. *J Nat Prod*. 2011;74(12):2514-9.

14) Nomura T, Fukai T, Akiyama T. Chemistry of phenolic compounds of licorice (*Glycyrrhiza* species) and their estrogenic and cytotoxic activities. *Pure Appl Chem*. 2002;74(7):1199-206.

15) Hosseinzadeh H, Nassiri-Asl M. Pharmacological effects of *Glycyrrhiza* spp. and its bioactive constituents: Update and review. *Phytother Res*. 2015;29(12):1868-86.

16) Pastorino G, Cornara L, Soares S, Rodrigues F, Oliveira MBPP. Liquorice (*Glycyrrhiza glabra*): A phytochemical and pharmacological review. *Phytother Res*. 2018;32(12):2323-39.

17) Yang R, Wang LQ, Yuan BC, Liu Y. The pharmacological activities of licorice. *Planta Med*. 2015;81(18):1654-69.

18) Wang X, Zhang H, Chen L, Shan L, Fan G, Gao X. Liquorice, a unique "guide drug" of traditional Chinese medicine: A review of its role in drug interactions. *J Ethnopharmacol*. 2013;150(3):781-90.

19) Zhang Q, Ye M. Chemical analysis of the Chinese herbal medicine gan-cao (licorice). *J Chromatogr A*. 2009;1216(11):1954-69.

20) Altundag E, Ozturk M. Ethnomedicinal studies on the plant resources of East Anatolia, Turkey. *Procd Soc Behv*. 2011;19:756-77.

21) Shults EE, Shakirov MM, Pokrovsky MA, Petrova TN, Pokrovsky AG, Gorovoy PG. Phenolic compounds from *Glycyrrhiza pallidiflora* Maxim. and their cytotoxic activity. *Nat Prod Res*. 2017;31(4):445-52.

22) Ji S, Li Z, Song W, et al. Bioactive constituents of *Glycyrrhiza uralensis* (licorice): Discovery of the effective components of a traditional herbal medicine. *J Nat Prod*. 2016;79(2):281-92.

23) Li K, Ji S, Song W, et al. Glycybridins A-K, bioactive phenolic compounds from *Glycyrrhiza glabra*. *J Nat Prod*. 2017;80(2):334-46.

24) Lin Y, Kuang Y, Li K, et al. Screening for bioactive natural products from a 67-compound library of *Glycyrrhiza inflata*. *Bioorganic Med Chem*. 2017;25(14):3706-13.

25) Chamberlain DF. *Glycyrrhiza* L. In: Davis P, ed. *Flora of Turkey and East Aegean Islands*. Edinburgh: Edinburgh University Press; 1969:260-3.

26) Siracusa L, Saija A, Cristani M, et al. Phytocomplexes from liquorice (*Glycyrrhiza glabra* L.) leaves - Chemical characterization and evaluation of their antioxidant, anti-genotoxic and anti-inflammatory activity. *Fitoterapia*. 2011;82(4):546-56.

27) Sezik E, Yesilada E, Honda G, Takaishi Y, Takeda Y, Tanaka T. Traditional medicine in Turkey X. Folk medicine in Central Anatolia. *J Ethnopharmacol*. 2001;75(2–3):95-115.

28) Honda G, Yeşilada E, Tabata M, et al. Traditional medicine in Turkey VI. Folk medicine in West Anatolia: Afyon, Kutahya, Denizli, Mugla, Aydin provinces. *J Ethnopharmacol.* 1996;53(2):75-87.

29) Armanini D, Fiore C, Mattarello MJ, Bielenberg J, Palermo M. History of the endocrine effects of licorice. *Exp Clin Endocrinol Diabetes*. 2002;110(6):257-61.

30) Fiore C, Eisenhut M, Ragazzi E, Zanchin G, Armanini D. A history of the therapeutic use of liquorice in Europe. *J Ethnopharmacol*. 2005;99(3):317-24.

31) Varshney IP, Jain DC, Srivastava HC. Study of saponins from *Glycyrrhiza glabra* root. *Int J Crude Drug Res*. 1983;21(4):169-72.

32) Rajurkar NS, Pardeshi BM. Analysis of some herbal plants from India used in the control of diabetes mellitus by NAA and AAS techniques. *Appl Radiat Isot*. 1997;48(8):1059-62.

33) Sircar NN. Pharmaco –therapeutics of Dasemani drugs. *Anc Sci Life*. 1984;3(3):132-5.

34) Ramazani A, Tavakolizadeh M, Ramazani S, Kheiri-Manjili H, Eskandari M. Antiplasmodial property of *Glycyrrhiza glabra* traditionally used for Malaria in Iran:

Promising activity with high selectivity index for malaria. *J Arthropod Borne Dis*. 2018;12(2):135-40.

35) Dafni A, Yaniv Z, Palevitch D. Ethnobotanical survey of medicinal plants in northern Israel. *J Ethnopharmacol*. 1984;10:295-310.

36) Arseculeratne SN, Gunatilaka AAL, Panabokke RG. Studies on medicinal plants of Sri Lanka. part 14: Toxicity of some traditional medicinal herbs. *J Ethnopharmacol*. 1985;13(3):323-35.

37) Jalilzadeh-Amin G, Najarnezhad V, Anassori E, Mostafavi M, Keshipour H. Antiulcer Properties of *Glycyrrhiza glabra* L. extract on experimental models of gastric ulcer in mice. *Iran J Pharm Res*. 2015;14(4):1163-70.

38) Wittschier N, Faller G, Hensel A. Aqueous extracts and polysaccharides from Liquorice roots (*Glycyrrhiza glabra* L.) inhibit adhesion of *Helicobacter pylori* to human gastric mucosa. *J Ethnopharmacol*. 2009;125(2):218-23.

39) Asha MK, Debraj D, Prashanth D, et al. *In vitro* anti-*Helicobacter pylori* activity of a flavonoid rich extract of *Glycyrrhiza glabra* and its probable mechanisms of action. *J Ethnopharmacol*. 2013;145(2):581-6.

40) Puram S, Suh HC, Kim SU, et al. Effect of Gutgard in the management of *Helicobacter pylori*: A randomized double blind placebo controlled study. *Evid Based Complement Alternat Med*. 2013;2013:263805.

41) Hajiaghamohammadi AA, Zargar A, Oveisi S, Samimi R, Reisian S. To evaluate of the effect of adding licorice to the standard treatment regimen of *Helicobacter pylori*. *Braz J Infect Dis*. 2016;20(6):534-8.

42) Sadra A, Kweon HS, Huh SO, Cho J. Gastroprotective and gastric motility benefits of AD-lico/Healthy Gut™ *Glycyrrhiza inflata* extract. *Anim Cells Syst (Seoul)*. 2017;21(4):255-62.

43) Awan T, Aslam B, Javed I, Khaliq T, Ah A, Sindhu ZUD. Histopathological evaluation of *Glycyrrhiza glabra* on aspirin induced gastric ulcer in mice. *Pak J Agric Sci*. 2015;52(2):563-8.

44) Choi YH, Kim YJ, Chae HS, Chin YW. *In vivo* gastroprotective effect along with pharmacokinetics, tissue distribution and metabolism of isoliquiritigenin in mice. *Planta Med*. 2015;81(7):586-93.

45) Yang Y, Wang S, Bao Y, et al. Anti-ulcer effect and potential mechanism of licoflavone by regulating inflammation mediators and amino acid metabolism. *J Ethnopharmacol*. 2017;199:175-82.

46) Wang Y, Wang S, Bao Y, et al. Multipathway integrated adjustment mechanism of *Glycyrrhiza* triterpenes curing gastric ulcer in rats. *Pharmacogn Mag*. 2017;13(50):209-15.

47) Kırmızıbekmez H, Uysal GB, Masullo M, et al. Prenylated polyphenolic compounds from *Glycyrrhiza iconica* and their antimicrobial and antioxidant activities. *Fitoterapia*. 2015;103:289-93.

48) Chen JC, Ho TY, Chang YS, Wu SL, Li CC, Hsiang CY. Identification of *Escherichia coli* enterotoxin inhibitors from traditional medicinal herbs by *in silico*, *in vitro*, and *in vivo* analyses. *J Ethnopharmacol*. 2009;121(3):372-8.

49) Bensch K, Tiralongo J, Schmidt K, et al. Investigations into the antiadhesive activity of herbal extracts against *Campylobacter jejuni*. *Phytother Res*. 2011;25(8):1125-32.

50) Lee JW, Ji YJ, Yu MH, et al. Antimicrobial effect and resistant regulation of *Glycyrrhiza uralensis* on methicillin-resistant *Staphylococcus aureus*. *Nat Prod Res*. 2009;23(2):101-11.

51) Badr AE, Omar N, Badria FA. A laboratory evaluation of the antibacterial and cytotoxic effect of liquorice when used as root canal medicament. *Int Endod J*. 2011;44(1):51-8.

52) Long DR, Mead J, Hendricks JM, Hardy ME, Voyich JM. 18β-glycyrrhetinic acid inhibits methicillin-resistant *Staphylococcus aureus* survival and attenuates virulence gene expression. *Antimicrob Agents Chemother*. 2013;57(1):241-7.

53) Ahn SJ, Cho EJ, Kim HJ, Park SN, Lim YK, Kook JK. The antimicrobial effects of deglycyrrhizinated licorice root extract on *Streptococcus mutans* UA159 in both planktonic and biofilm cultures. *Anaerobe*. 2012;18(6):590-6.

54) Irani M, Sarmadi M, Bernard F, Hossein G. Leaves antimicrobial activity of *Glycyrrhiza glabra* L. *Iran J Pharm Res*. 2010;9(4):425-8.

55) Gupta VK, Fatima A, Faridi U, et al. Antimicrobial potential of *Glycyrrhiza glabra* roots. *J Ethnopharmacol*. 2008;116(2):377-80.

56) Tanaka Y, Kikuzaki H, Fukuda S, Nakatani N. Antibacterial compounds of licorice against upper airway respiratory tract pathogens. *J Nutr Sci Vitaminol*. 2001;47:270-3.

57) Demizu S, Kajiyama K, Takahashi K, et al. Antioxidant and antimicrobial constituents of licorice: Isolation and structure elucidation of new benzofuran derivative. *Chem Pharm Bull (Tokyo)*. 1988;36(9):3474-9.

58) Esmaeili S, Naghibi F, Mosaddegh M, Sahranavard S, Ghafari S, Abdullah NR. Screening of antiplasmodial properties among some traditionally used Iranian plants. *J Ethnopharmacol*. 2009;121:400-4.

59) Sangian H, Faramarzi H, Yazdinezhad A, et al. Antiplasmodial activity of ethanolic extracts of some selected medicinal plants from the northwest of Iran. *Parasitol Res*. 2013;112(11):3697-701.

60) Kalani K, Agarwal J, Alam S, Khan F, Pal A, Srivastava SK. *In silico* and *in vivo* anti-malarial studies of 18β-glycyrrhetinic acid from *Glycyrrhiza glabra*. *PLoS One*. 2013;8(9):e74761.

61) Ryu YB, Kim JH, Park S-J, et al. Inhibition of neuraminidase activity by polyphenol compounds isolated from the roots of *Glycyrrhiza uralensis*. *Bioorg Med Chem Lett*. 2010;20:971-4.

62) Dao TT, Nguyen PH, Lee HS, et al. Chalcones as novel influenza A (H1N1) neuraminidase inhibitors from *Glycyrrhiza inflata*. *Bioorg Med Chem Lett*. 2011;21(1):294-8.

63) Matsumoto Y, Matsuura T, Aoyagi H, et al. Antiviral activity of glycyrrhizin against Hepatitis C virus *in vitro*. *PLoS One*. 2013;8(7):e68992.

64) Sasaki H, Takei M, Kobayashi M, Pollard RB, Suzuki F. Effect of glycyrrhizin, an active component of licorice roots, on HIV replication in cultures of peripheral blood

mononuclear cells from HIV-seropositive patients. *Pathobiology*. 2002;3(70):229-36.

65) Kwon HJ, Kim HH, Ryu YB, et al. *In vitro* anti-rotavirus activity of polyphenol compounds isolated from the roots of *Glycyrrhiza uralensis*. *Bioorg Med Chem* 2010;18(21):7668-74.

66) Alfajaro MM, Kim HJ, Park JG, et al. Anti-rotaviral effects of *Glycyrrhiza uralensis* extract in piglets with rotavirus diarrhea. *Virol J*. 2012;9(1):310. doi:10.1186/1743-422X-9-310.

67) Omer MO, AlMalki WH, Shahid I, Khuram S, Altaf I, Imran S. Comparative study to evaluate the anti-viral efficacy of *Glycyrrhiza glabra* extract and ribavirin against the Newcastle disease virus. *Pharmacognosy Res*. 2014;6(1):6-11.

68) Yeh CF, Wang KC, Chiang LC, Shieh DE, Yen MH, Chang JS. Water extract of licorice had anti-viral activity against human respiratory syncytial virus in human respiratory tract cell lines. *J Ethnopharmacol*. 2013;148(2):466-73.

69) Laconi S, Madeddu MA, Pompei R. Autophagy activation and antiviral activity by a licorice triterpene. *Phytother Res*. 2014;28(12):1890-2.

70) Wolkerstorfer A, Kurz H, Bachhofner N, Szolar OHJ. Glycyrrhizin inhibits influenza A virus uptake into the cell. *Antiviral Res*. 2009;83(2):171-8.

71) Wang J, Chen X, Wang W, et al. Glycyrrhizic acid as the antiviral component of *Glycyrrhiza uralensis* Fisch. against coxsackievirus A16 and enterovirus 71 of hand foot and mouth disease. *J Ethnopharmacol*. 2013;147(1):114-21.

72) Song W, Si L, Ji S, et al. Uralsaponins M-Y, antiviral triterpenoid saponins from the roots of *Glycyrrhiza uralensis*. *J Nat Prod*. 2014;77(7):1632-43.

73) Hendricks JM, Hoffman C, Pascual DW, Hardy ME. 18β-Glycyrrhetinic acid delivered orally induces isolated lymphoid follicle maturation at the intestinal mucosa and attenuates rotavirus shedding. *PLoS One*. 2012;7(11):e49491.

74) Kuo K, Chang J, Wang K, Chiang L. Water extract of *Glycyrrhiza uralensis* inhibited Enterovirus 71 in a human. 2009;37(2):383-94.

75) Pellati D, Fiore C, Armanini D, Rassu M, Bertoloni G. *In vitro* effects of glycyrrhetinic acid on the growth of clinical isolates of *Candida albicans*. *Phytother Res*. 2009;23:572-4.

76) Messier C, Grenier D. Effect of licorice compounds licochalcone A, glabridin and glycyrrhizic acid on growth and virulence properties of *Candida albicans*. *Mycoses*. 2011;54:e801-6.

77) Simmler C, Pauli GF, Chen SN. Phytochemistry and biological properties of glabridin. *Fitoterapia*. 2013;90:160–84.

78) Yokota T, Nishio H, Kubota Y, Mizoguchi M. The inhibitory effect of glabridin from licorice extracts on melanogenesis and inflammation. *Pigment Cell Res*. 1998;11(6):355-61.

79) Kang JS, Yoon YD, Cho IJ, Han MH, Lee CW, Song-Kyu. Glabridin, an isoflavan from licorice root, inhibits inducible nitric-oxide synthase expression and improves survival of mice in experimental model of septic shock. *J Pharmacol Exp Ther*. 2005;312(3):1187-94.

80) Thiyagarajan P, Chandrasekaran CV, Deepak HB, Agarwal A. Modulation of lipopolysaccharide-induced pro-inflammatory mediators by an extract of *Glycyrrhiza glabra* and its phytoconstituents. *Inflammopharmacol*. 2011;19(4):235-41.

81) Park SH, Kang JS, Yoon YD, et al. Glabridin inhibits lipopolysaccharide-induced activation of a microglial cell line, BV-2, by blocking NF-κB and AP-1. *Phytother Res*. 2010;24:S29–34.

82) Kim KR, Jeong C-K, Park K-K, et al. Anti-inflammatory effects of licorice and roasted licorice extracts on TPA-induced acute inflammation and collagen-induced arthritis in mice. *J Biomed Biotechnol*. 2010;2010:709378.

83) Shah SL, Wahid F, Khan N, et al. Inhibitory effects of *Glycyrrhiza glabra* and its major constituent glycyrrhizin on inflammation-associated corneal neovascularization. *Evid Based Complement Alternat Med*. 2018;2018:8438101.

84) Abd AH, Qasim BJ, Shibab SA, Dawood JO. Effect of *Glycyrrhiza glabra* on antigen induced arthritis in mice model. *Iraqi J Med Sci*. 2015;13(2):129-36.

85) Uto T, Morinaga O, Tanaka H, Shoyama Y. Analysis of the synergistic effect of glycyrrhizin and other constituents in licorice extract on lipopolysaccharide-induced nitric oxide production using knock-out extract. *Biochem Biophys Res Commun* 2012;417(1):473-8.

86) Furusawa J, Funakoshi-Tago M, Tago K, et al. Licochalcone A significantly suppresses LPS signaling pathway through the inhibition of NF-κB p65 phosphorylation at serine 276. *Cell Signal*. 2009;21(5):778-85.

87) Furusawa J, Funakoshi-Tago M, Mashino T, et al. *Glycyrrhiza inflata*-derived chalcones, licochalcone A, licochalcone B and licochalcone D, inhibit phosphorylation of NF-κB p65 in LPS signaling pathway. *Int Immunopharmacol*. 2009;9(4):499-507.

88) Chandrasekaran C V., Deepak HB, Thiyagarajan P, et al. Dual inhibitory effect of *Glycyrrhiza glabra* (GutGard^{TM}) on COX and LOX products. *Phytomedicine*. 2011;18(4):278-84.

89) Ohuchi K, Kamada Y, Levine L, Tsurufuji S. Glycyrrhizin inhibits prostaglandin E_2 production by activated peritoneal macrophages from rats. *Prostaglandins Med*. 1981;7:457-63.

90) Wu T-Y, Khor TO, Saw CLL, et al. Anti-inflammatory/anti-oxidative stress activities and differential regulation of Nrf2-mediated genes by non-polar fractions of tea *Chrysanthemum zawadskii* and licorice *Glycyrrhiza uralensis*. *AAPS J*. 2011;13(1):1-13.

91) Wang W, Luo M, Fu Y, Wang S, Efferth T, Zu Y. Glycyrrhizic acid nanoparticles inhibit LPS-induced inflammatory mediators in 264.7 mouse macrophages compared with unprocessed glycyrrhizic acid. *Int J Nanomedicine*. 2013;8:1377-83.

92) Wang CY, Kao TC, Lo WH, Yen GC. Glycyrrhizic acid and 18β-glycyrrhetinic acid modulate lipopolysaccharide-induced inflammatory response by suppression of NF-κB through PI3K p110δ and and p110γ inhibitions. *J Agric Food Chem*. 2011;59(14):7726-33.

93) Sasaki H, Suzuki N, AlShwaimi E, et al. 18beta-glycyrrhetinic acid inhibits periodontitis via glucocorticoid-independent NF–κB Inactivation in IL-10 deficient mice. *J Periodontal Res*. 2010;45(6):757-63.

94) Kuroda M, Mimaki Y, Honda S, Tanaka H, Yokota S, Mae T. Phenolics from *Glycyrrhiza glabra* roots and their PPAR-γ ligand-binding activity. *Bioorg Med Chem*. 2010;18(2):962-70

95) Gaur R, Yadav KS, Verma RK, Yadav NP, Bhakuni RS. *In vivo* anti-diabetic activity of derivatives of isoliquiritigenin and liquiritigenin. *Phytomedicine*. 2014;21(4):415-22.

96) Li S, Li W, Wang Y, Asada Y, Koike K. Prenylflavonoids from *Glycyrrhiza uralensis* and their protein tyrosine phosphatase-1B inhibitory activities. *Bioorg Med Chem Lett*. 2010;20(18):5398-401.

97) Li W, Li S, Higai K, et al. Evaluation of licorice flavonoids as protein tyrosine phosphatase 1B inhibitors. *Bioorg Med Chem Lett*. 2013;23(21):5836-9.

98) Yoon G, Lee W, Kim SN, Cheon SH. Inhibitory effect of chalcones and their derivatives from *Glycyrrhiza inflata* on protein tyrosine phosphatase 1B. *Bioorg Med Chem Lett*. 2009;19(17):5155-7.

99) Kuang Y, Lin Y, Li K, et al. Screening of hepatoprotective compounds from licorice against carbon tetrachloride and acetaminophen induced HepG2 cells injury. *Phytomedicine*. 2017;34:59-66.

100) Hajiaghamohammadi AA, Ziaee A, Samimi R. The efficacy of licorice in decreasing transaminase activities in non-alcoholic fatty liver disease: A randomized controlled clinical trial. *Phytother Res*. 2012;26(9):1381-4.

101) Zheng YF, Wei JH, Fang SQ, et al. Hepatoprotective triterpene saponins from the roots of *Glycyrrhiza inflata*. *Molecules*. 2015;20(4):6273-83.

102) Rasool M, Iqbal J, Malik A, et al. Hepatoprotective effects of *Silybum marianum* (silymarin) and *Glycyrrhiza glabra* (glycyrrhizin) in combination: A possible synergy. *Evid Based Complement Alternat Med*. 2014;2014: 641597.

103) Ikeda K, Arase Y, Kobayashi M, et al. A long-term glycyrrhizin injection therapy reduces hepatocellular carcinogenesis rate in patients with interferon-resistant active chronic hepatitis C: A cohort study of 1249 patients. *Dig Dis Sci*. 2006;51(3):603-9.

104) Yin G, Cao L, Xu P, Jeney G, Nakao M, Lu C. Hepatoprotective and antioxidant effects of *Glycyrrhiza glabra* extract against carbon tetrachloride (CCl_4)-induced

hepatocyte damage in common carp (*Cyprinus carpio*). *Fish Physiol Biochem*. 2011;37:209-16.

105) Chen HJ, Kang SP, Lee IJ, Lin YL. Glycyrrhetinic acid suppressed NF-κB activation in TNF-α-induced hepatocytes. *J Agric Food Chem*. 2014;62(3):618-25.

106) Zong L, Qu Y, Xu MY, Dong YW, Lu LG. 18α-glycyrrhetinic acid extracted from *Glycyrrhiza* radix inhibits proliferation and promotes apoptosis of the hepatic stellate cell line. *J Dig Dis*. 2013;14(6):328–36.

107) Xiao Y, Xu J, Mao C, et al. 18β-glycyrrhetinic acid ameliorates acute *Propionibacterium acnes*-induced liver injury through inhibition of macrophage inflammatory protein-1α. *J Biol Chem*. 2010;285(2):1128-37.

108) Orazizadeh M, Fakhredini F, Mansouri E, Khorsandi L. Effect of glycyrrhizic acid on titanium dioxide nanoparticles-induced hepatotoxicity in rats. *Chem Biol Interact*. 2014;220:214-21

109) Lin Y, Kuang Y, Li K, et al. Nrf2 activators from *Glycyrrhiza inflata* and their hepatoprotective activities against CCl_4-induced liver injury in mice. *Bioorg Med Chem*. 2017;25(13):5522-30.

110) Jung JC, Lee YH, Kim SH, et al. Hepatoprotective effect of licorice, the root of *Glycyrrhiza uralensis* Fischer, in alcohol-induced fatty liver disease. *BMC Complement Altern Med*. 2016;16:19. doi:10.1186/s12906-016-0997-0.

111) Jo EH, Kim SH, Ra JC, et al. Chemopreventive properties of the ethanol extract of chinese licorice (*Glycyrrhiza uralensis*) root: Induction of apoptosis and G_1 cell cycle arrest in MCF-7 human breast cancer cells. *Cancer Lett*. 2005;230(2):239-47.

112) Thu NB, Trung TN, Ha DT, et al. Screening of Vietnamese medicinal plants for cytotoxic activity. *Nat Prod Sci*. 2010;16(1):43-9.

113) Fraihat A, Alatrash L, Abbasi R, et al. Inhibitory effects of methanol extracts of selected plants on the proliferation of two human melanoma cell lines. *Trop J Pharm Res*. 2018;17(6):1081-6.

114) Rasul A, Ma T. *In vitro* cytotoxic screening of 300 selected Chinese medicinal herbs against human gastric adenocarcinoma SGC-7901 cells. *Afr J Pharm Pharmacol*. 2012;6(9):592-600.

115) Park SY, Kim EJ, Choi HJ, et al. Anti-carcinogenic effects of non-polar components containing licochalcone A in roasted licorice root. *Nutr Res Pract*. 2014;8(3):257-66.

116) Basar N, Oridupa OA, Ritchie KJ, et al. Comparative cytotoxicity of *Glycyrrhiza glabra* roots from different geographical origins against immortal human keratinocyte (HaCaT), lung adenocarcinoma (A549) and liver carcinoma (HepG2) cells. *Phytother Res*. 2015;29(6):944-8.

117) Yoon G, Jung YD, Cheon SH. Cytotoxic allyl retrochalcone from the roots of *Glycyrrhiza inflata*. *Chem Pharm Bull*. 2005;53(6):694-5.

118) Yoon G, Kang BY, Cheon SH. Topoisomerase I inhibition and cytotoxicity of licochalcone A and E from *Glycyrrhiza inflata*. *Arch Pharm Res*. 2007;30(3):313-6.

119) Aydemir EA, Oz ES, Göktürk RS, Ozkan G, Fiskin K. *Glycyrrhiza flavescens* subsp. *antalyensis* exerts antiproliferative effects on melanoma cells via altering TNF-α and IFN-α levels. *Food Chem Toxicol*. 2011;49(4):820-8.

120) Jung JI, Lim SS, Choi HJ, et al. Isoliquiritigenin induces apoptosis by depolarizing mitochondrial membranes in prostate cancer cells. *J Nutr Biochem*. 2006;17(10):689-96.

121) Ji S, Tang S, Li K, et al. Licoricidin inhibits the growth of SW480 human colorectal adenocarcinoma cells *in vitro* and *in vivo* by inducing cycle arrest, apoptosis and autophagy. *Toxicol Appl Pharmacol*. 2017;326:25-33.

122) Sheela ML, Ramakrishna MK, Salimath BP. Angiogenic and proliferative effects of the cytokine VEGF in Ehrlich ascites tumor cells is inhibited by *Glycyrrhiza glabra*. *Int Immunopharmacol*. 2006;6(3):494-8.

123) Hsieh M-J, Lin C-W, Yang S-F, Chen M-K, Chiou H-L. Glabridin inhibits migration and invasion by transcriptional inhibition of matrix metalloproteinase 9 through modulation of NF-κB and AP-1 activity in human liver cancer cells. *Br J Pharmacol*. 2014;171(12):3037-50.

124) Yo Y-Y, Shieh G-S, Hsu K-F, Chao-Liang W, Shiau A-L. Licorice and licochalcone-A induce autophagy in LNCaP Prostate Cancer Cells by suppression of Bcl-2 expression and the mTOR pathway. *J Agric Food Chem*. 2009;57(18):8266-73.

125) Tamir S, Eizenberg M, Somjen D, et al. Estrogenic and antiproliferative properties of glabridin from licorice in human breast cancer cells. *Cancer Res*. 2000;60(20):5704-9.

126) Lee CK, Park KK, Lim SS, Park JHY, Chung WY. Effects of the licorice extract against tumor growth and cisplatin-induced toxicity in a mouse xenograft model of colon cancer. *Biol Pharm Bull*. 2007;30(11):2191-5.

127) Choi HJ, Seon MR, Lim SS, Kim J-S, Chun HS, Park JHY. Hexane/ethanol extract of *Glycyrrhiza uralensis* licorice suppresses doxorubicin-induced apoptosis in H9c2 rat cardiac myoblasts. *Exp Biol Med*. 2008;233(12):1554-60.

128) Seon MR, Lim SS, Choi HJ, et al. Isoangustone A present in hexane/ethanol extract of *Glycyrrhiza uralensis* induces apoptosis in DU145 human prostate cancer cells via the activation of DR4 and intrinsic apoptosis pathway. *Mol Nutr Food Res*. 2010;54(9):1329-39.

129) Seon MR, Park SY, Kwon SJ, et al. Hexane/ethanol extract of *Glycyrrhiza uralensis* and its active compound isoangustone A induce G1 cycle arrest in DU145 human prostate and 4T1 murine mammary cancer cells. *J Nutr Biochem*. 2012;23(1):85-92.

130) Huang W, Tang S, Qiao X, et al. Isoangustone A induces apoptosis in SW480 human colorectal adenocarcinoma cells by disrupting mitochondrial functions. *Fitoterapia*. 2014;94:36-47.

131) Hawthorne S, Gallagher S. Effects of glycyrrhetinic acid and liquorice extract on cell proliferation and prostate-specific antigen secretion in LNCaP prostate cancer cells. *J Pharm Pharmacol*. 2008;60(5):661-6.

132) Hibasami H, Iwase H, Yoshioka K, Takahashi H. Glycyrrhetic acid (a metabolic substance and aglycon of glycyrrhizin) induces apoptosis in human hepatoma, promyelotic leukemia and stomach cancer cells. *Int J Mol Med*. 2006;17(2):215-9.

133) Khan R, Khan AQ, Lateef A, et al. Glycyrrhizic acid suppresses the development of precancerous lesions via regulating the hyperproliferation, inflammation, angiogenesis and apoptosis in the colon of wistar rats. *PLoS One*. 2013;8(2): e56020.

134) Zheng Y-F, Qi L-W, Cui X-B, et al. Oleanane-type triterpene glucuronides from the roots of *Glycyrrhiza uralensis* Fischer. *Planta Med*. 2010;76:1457-63.

135) Takahashi T, Takasuka N, Iigo M, et al. Isoliquiritigenin, a flavonoid from licorice, reduces prostaglandin E_2 and nitric oxide, causes apoptosis, and suppresses aberrant crypt foci development. *Cancer Sci*. 2004;95(5):448-53.

136) Zheng H, Li Y, Wang Y, et al. Downregulation of COX-2 and CYP 4A signaling by isoliquiritigenin inhibits human breast cancer metastasis through preventing anoikis resistance, migration and invasion. *Toxicol Appl Pharmacol*. 2014;280(1):10-20.

137) Chueh F, Hsiao Y, Chang S, Wu P. Glycyrrhizic acid induces apoptosis in WEHI-3 mouse leukemia cells through the caspase- and mitochondria-dependent pathways. *Oncol Rep*. 2012;28(6):2069-76.

138) Sharma G, Kar S, Palit S, Das PK. 18β-Glycyrrhetinic acid induces apoptosis through modulation of Akt/FOXO3a/Bim pathway in human breast cancer MCF-7 Cells. *J Cell Physiol*. 2012;227:1923-31.

139) Hajirahimkhan A, Mbachu O, Simmler C, et al. Estrogen receptor (ER) subtype selectivity identifies 8-prenylapigenin as an ERβ agonist from *Glycyrrhiza inflata* and highlights the importance of chemical and biological authentication. *J Nat Prod*. 2017;81(4):966-975.

140) Simons R, Vincken JP, Mol LAM, et al. Agonistic and antagonistic estrogens in licorice root (*Glycyrrhiza glabra*). *Anal Bioanal Chem*. 2011;401(1):305-13.

141) Dhingra D, Sharma A. Antidepressant-like activity of *Glycyrrhiza glabra* L. in mouse models of immobility tests. *Prog Neuropsychopharmacol Biol Psychiatry*. 2006;30(3):449-54.

142) Parle M, Dhingra D, Kulkarni SK. Memory-strengthening activity of *Glycyrrhiza glabra* in exteroceptive and interoceptive behavioral models. *J Med Food*. 2004;7(4):462-6.

143) Cho S, Park JH, Pae AN, et al. Hypnotic effects and GABAergic mechanism of licorice (*Glycyrrhiza glabra*) ethanol extract and its major flavonoid constituent glabrol. *Bioorganic Med Chem*. 2012;20(11):3493-501.

144) Hoffmann KM, Beltrán L, Ziemba PM, Hatt H, Gisselmann G. Potentiating effect of glabridin from *Glycyrrhiza glabra* on $GABA_A$ receptors. *Biochem Biophys Rep*. 2016;6:197-202.

145) Nerya O, Vaya J, Musa R, Izrael S, Ben-Arie R, Tamir S. Glabrene and isoliquiritigenin as tyrosinase inhibitors from licorice roots. *J Agric Food Chem.* 2003;51(5):1201-7.

146) Adhikari A, Devkota HP, Takano A, et al. Screening of Nepalese crude drugs traditionally used to treat hyperpigmentation: *In vitro* tyrosinase inhibition. *Int J Cosmet Sci.* 2008;30(5):353-60.

147) Ammosov AS, Litvinenko VI. Phenolic compounds of the genera *Glycyrrhiza* L. and *Meristotropis* Fisch. et Mey. (review). *Pharm Chem J.* 2007;41(7):372-95.

148) Hatano T, Shintani Y, Aga Y, Shiota S, Tsuchiya T, Yoshida T. Phenolic constituents of licorice. VIII. Structures of glicophenone and glicoisoflavanone, and effects of licorice phenolics on methicillin-resistant *Staphylococcus aureus*. *Chem Pharm Bull (Tokyo).* 2000;48(9):1286-92.

149) Dey S, Deepak M, Setty M, S'Souza P, Agarwal A, Snagli GK. Bioactive caffeic acid esters from *Glycyrrhiza glabra*. *Nat Prod Res*. 2009;23(18):1657-63.

150) Hatano T, Kagawa H, Yasuhara T, Okuda T. Two new flavonoids and other constituents in licorice root: Their relative astringency and radical scavenging effects. *Chem Pharm Bull (Tokyo).* 1988;36(6):2090-7.

151) Tao W-W, Duan J-A, Yang N-Y, Tang Y-P, Liu M-Z, Qian Y-F. Antithrombotic phenolic compounds from *Glycyrrhiza uralensis*. *Fitoterapia*. 2012;83(2):422-5.

152) Kajiyama K, Hiraga Y, Takahashi K, et al. Flavonoids and isoflavonoids of chemotaxonomic significance from *Glycyrrhiza pallidiflora* (Leguminosae). *Biochem Syst Ecol.* 1993;21(8):785-93.

153) Hatano T, Fukuda T, Liu YZ, Noro T, Okuda T. Phenolic constituents of licorice. III. Structures of glicoricone and licofuranone, and inhibitory effects of licorice constituents on monoamine oxidase. *Yakugaku Zasshi*. 1991;111(6):311-21.

154) Liu Q, Liu YL. Studies on chemical constituents of *Glycyrrhiza eurycarpa* P. C. Li. *Yao Xue Xue Bao*. 1989;24(7):525-31.

155) Kaur P, Kaur S, Kumar N, Singh B, Kumar S. Evaluation of antigenotoxic activity of isoliquiritin apioside from *Glycyrrhiza glabra* L. *Toxicol In Vitro*. 2009;23(4):680–6.

156) Miething H, Speicher-Brinker A. Neolicurosid - ein neues Chalkonglykosid aus der SuBholzwurzel. *Arch Pharm (Weinheim)*. 1989;322:141-3.

157) Lee JE, Lee JY, Kim J, Lee K, Choi SU, Ryu SY. Two minor chalcone acetylglycosides from the roots extract of *Glycyrrhiza uralensis. Arch Pharm Res.* 2015;38(7):1299-303.

158) Kajiyama K, Demizu S, Hiraga Y, et al. Two prenylated retrochalcones from *Glycyrrhiza inflata. Phytochemistry*. 1992;31(9):3229-32.

159) Bai H, Li W, Koike K, et al. A novel biflavonoid from roots of *Glycyrrhiza uralensis* cultivated in China. *Chem Pharm Bull*. 2003;51(9):1095-7.

160) Furuya T, Matsumoto K, Hikichi M. Echinatin, a new chalcone from tissue culture of *Glycyrrhiza echinata*. *Tetrahedron Lett*. 1971;12(27):2567-9.

161) Kitagawa I, Chen W-Z, Hori K, Harada E, Yasuda N, Yoshikawa M, et al. Chemical studies of Chinese licorice-roots. I. Elucidation of five new flavonoid constituents from roots of *Glycyrrhiza glabra* L. collected in Xinjiang. *Chem Pharm Bull (Tokyo)*. 1994;42(5):1056-62.

162) Ayabe S-I, Kobayashi M, Hikichi M, Matsumoto K, Furuya T. Flavonoids from the cultured cells of *Glycyrrhiza echinata*. *Phytochemistry.* 1980;19:2179-83.

163) Kitagawa I, Chen W-Z, Hori K, Ren J. Chemical studies of Chinese licorice-roots. II. Five new flavonoid constituents from the roots of *Glycyrrhiza aspera* PALL. collected in Xinjiang. *Chem Pharm Bull*. 1998;46(10):1511-7.

164) Feng K-P, Chen R-D, Li J-H, et al. Flavonoids from the cultured cells of *Glycyrrhiza uralensis*. *J Asian Nat Prod Res*. 2016;18(3):253-9.

165) Hamed MM, El-Amin SM, Refahy LA, et al. Isolation of some chemical constituents from licorice and their evaluation as anticancer and antiviral agents. *Pharmacol Online*. 2013;3:95-109.

166) Li W, Asada Y, Yoshikawa T. Flavonoid constituents from *Glycyrrhiza glabra* hairy root cultures. *Phytochemistry*. 2000;55:447-56.

167) Asada Y, Li W, Yoshikawa T. Isoprenylated flavonoids from hairy root cultures of *Glycyrrhiza glabra*. *Phytochemistry*. 1998;47(3):389-92.

168) Asada Y, Li W, Yoshikawa T. The first prenylated biaurone, licoagrone from hairy root cultures of *Glycyrrhiza glabra. Phytochemistry*.1999;50(6):1015-9.

169) Iwasaki N, Baba M, Aishan H, Okada Y, Okuyama T. Studies of traditional folk medicines in Xinjiang Uighur Autonomous. Ⅱ. Research for chemical constituents of Xinjiang licorice. *Heterocycles*. 2009;78(6):1581-7.

170) Hatano T, Takagi M, Ito H, Yoshida T. Phenolic constituents of liquorice. VII. A new chalcone with a potent radical scavenging activity and accompanying phenolics from liquorice. *Chem Pharm Bull*. 1997;45(9):1485-92.

171) Fukai T, Sheng CB, Horikoshi T, Nomura T. Isoprenylated flavonoids from underground parts of *Glycyrrhiza glabra. Phytochemistry*. 1996;43(5):1119-24.

172) Fukai T, Nomura T. Isoprenoid-substituted flavonoids from roots of *Glycyrrhiza inflata. Phytochemistry*. 1995;38(3):759-65.

173) Fukai T, Wang QH, Inami R, Nomura T. Structures of prenylated dihydrochalcone, gancaonin J and homoisoflavanone, gancaonin K from *Glycyrrhiza pallidiflora. Heterocycles*. 1990;31(4):643-50.

174) Demizu S, Kajiyama K, Hiraga Y, et al. Prenylated dibenzoylmethane derivatives from the root of *Glycyrrhiza inflata* (Xinjiang licorice). *Chem Pharm Bull (Tokyo).* 1992;40(2):392-5.

175) Zeng L, Fukai T, Kaneki T, Nomura T, Zhang RY, Lou ZC. Four new isoprenoid-substituted dibenzoylmethane derivatives, glyinflanins A, B, C, and D from the roots of *Glycyrrhiza inflata. Heterocycles*. 1992;34(1):85-97.

176) Kajiyama K, Demizu S, Hiraga Y, et al. New Prenylflavones and dibenzoylmethane from *Glycyrrhiza inflata. J Nat Prod*. 1992;55(9):1197-203.

177) Fukai T, Cai B, Maruno K, Miyakawa Y, Konishi M, Nomura T. An isoprenylated flavanone from *Glycyrrhiza glabra* and rec-assay of licorice phenols. *Phytochemistry*. 1998;49(7):2005-13.

178) Li W, Koike K, Asada Y, et al. Flavonoids from *Glycyrrhiza pallidiflora* hairy root cultures. *Phytochemistry*. 2002;60:351-5.

179) Martins N, Ferreira ICFR, Henriques M, Silva S. *In vitro* anti-*Candida* activity of *Glycyrrhiza glabra* L. Ind Crops Prod. 2016;83:81-5.

180) Fukai T, Wang QH, Takayama M, Nomura T. Structures of five new prenylated flavonoids, gancaonins L, M, N, O, and P from aerial parts of *Glycyrrhiza uralensis*. *Heterocycles.* 1990;31(2):373-82.

181) Fukai T, Qing-Hua W, Nomura T. Six prenylated phenols from *Glycyrrhiza uralensis*. *Phytochemistry*. 30(4):1245-50.

182) Li J-R, Wang Y-Q, Deng Z-Z. Two new compounds from *Glycyrrhiza glabra*. *J Asian Nat Prod Res*. 2005;7(4):677-80.

183) Yahara S, Nishioka I. Flavonoid glucosides from licorice. *Phytochemistry.* 1984;23(9):2108-9.

184) Tang S, Huang W, Ji S, Wang Y, Pei D, Ye M, et al. Prenylated flavonoids from *Glycyrrhiza uralensis* as promising anti-cancer agents: a preliminary structure-activity study. *J Chin Pharm Sci*. 2016;25(1):23-9.

185) Hatano T, Aga Y, Shintani Y, Ito H, Okuda T, Yoshida T. Minor Flavonoids from licorice. *Phytochemistry*. 2000;55:959-63.

186) Manfredi KP, Vallurupalli V, Demidova M, Kindscher K, Pannell LK. Isolation of an anti-HIV diprenylated bibenzyl from *Glycyrrhiza lepidota*. *Phytochemistry*. 2001;58:153-7.

187) Fukai T, Zeng L, Nishizawa J, Wang Y-H, Nomura T. Four isoprenoid-substituted flavonoids from *Glycyrrhiza aspera*. *Phytochemistry*. 1994;36(1):233-4.

188) Jia SS, Liu D, Wang HQ, Suo ZX. Isolation and identification of gancaonin P-3'-methylether from the leaves of *Glycyrrhiza uralensis* Fisch. *Acta Pharm Sin*. 1993;28:623-5.

189) Bharadwaj DK, Murari R, Seshadri TR, Singh R. Occurrence of 2-methylisoflavones in *Glycyrrhiza glabra*. *Phytochemistry.* 1976;15:352-3.

190) Jia SS, Ma CM, Wang JM. Studies on flavonoid constituents isolated from the leaves of *Glycyrrhiza uralensis* Fisch. *Acta Pharm Sin*. 1990;25(10):758-62.

191) Fukai T, Zeng L, Nomura T, Zhang R-Y, Lou Z-C. Phenolic constituents of aerial parts of *Glycyrrhiza eurycarpa*. *Nat Med*. 1996;50(3):247-51.

192) Hayashi H, Hiraoka N, Ikeshiro Y, Yamamoto H. Organ specific localization of flavonoids in *Glycyrrhiza glabra* L. *Plant Sci*. 1996;116(2):233-8.

193) Hayashi H, Yasuma M, Hiraoka N, et al. Flavonoid variation in the leaves of *Glycyrrhiza glabra*. *Phytochemistry*. 1996;42(3):701-4.

194) Biondi DM, Rocco C, Ruberto G. New dihydrostilbene derivatives from the leaves of *Glycyrrhiza glabra* and evaluation of their antioxidant activity. *J Nat Prod*. 2003;66(4):477-80.

195) Yuldashev MP, Batirov EK, Vdovin AD, Abdullaev ND. Structural study of glabrisoflavone, a novel isoflavone from *Glycyrrhiza glabra* L. *Russ J Bioorg Chem*. 2000;26(8):784-6.

196) Mitscher LA, Park YH, Clark D, Beal JL. Antimicrobial agents from higher plants. Antimicrobial isoflavanoids and related substances from *Glycyrrhiza glabra* L. var. *typica*. *J Nat Prod*. 1980;43(2):259-69.

197) Park J-H, Wu Q, Yoo K-H, et al. Cytotoxic effect of flavonoids from the roots of *Glycyrrhiza uralensis* on human cancer cell lines. *J Appl Biol Chem*. 2011;54(1):67-70.

198) Fukai T, Wang QH, Nomura T. Four new prenylated flavonoids from aerial parts of *Glycyrrhiza uralensis*. *Heterocycles*. 1989;29(7):1369-78.

199) Montoro P, Maldini M, Russo M, Postorino S, Piacente S, Pizza C. Metabolic profiling of roots of liquorice (*Glycyrrhiza glabra*) from different geographical areas by ESI/MS/MS and determination of major metabolites by LC-ESI/MS and LC-ESI/MS/MS. *J Pharm Biomed Anal*. 2011;54(3):535-44.

200) Fukai T, Tantai L, Nomura T. Isoprenoid-substituted flavonoids from *Glycyrrhiza glabra*. *Phytochemistry*. 1996;43(2):531-2.

201) Vaya J, Belinky PA, Aviram M. Antioxidant constituents from licorice roots: Isolation, structure elucidation and antioxidative capacity toward LDL oxidation. *Free Radic Biol Med*. 1997;23(2):302-13.

202) Fukai T, Marumo A, Kaitou K, Kanda T, Terada S, Nomura T. Anti-*Helicobacter pylori* flavonoids from licorice extract. *Life Sci*. 2002;71(12):1449-63.

203) Shibano M, Hemni A, Matsumoto Y, Kusano G, Toshio M, Hatakeyama Y. Studies on the index compounds for HPLC analysis of *Glycyrrhiza uralensis*. *Heterocycles*. 1997;45(10):2053-60.

204) Kuroda M, Mimaki Y, Sashida Y, et al. Phenolics with PPAR-γ ligand-binding activity obtained from licorice (*Glycyrrhiza uralensis* roots) and ameliorative effects of glycyrin on genetically diabetic KK-A^y mice. *Bioorg Med Chem Lett*. 2003;13(24):4267-72.

205) Matsui T, Lallo S, Nisa K, Morita H. Filamenting temperature-sensitive mutant Z inhibitors from *Glycyrrhiza glabra* and their inhibitory mode of action. *Bioorg Med Chem Lett*. 2017;27(6):1420-4.

206) Villinski JR, Bergeron C, Cannistra JC, et al. Pyrano-isoflavans from *Glycyrrhiza uralensis* with antibacterial activity against *Streptococcus mutans* and *Porphyromonas gingivalis*. *J Nat Prod*. 2014;77(3):521-6.

207) Kinoshita T, Tamura Y, Mizutani K. Isolation and synthesis of two new 3-arylcoumarin derivatives from the root of *Glycyrrhiza glabra* (licorice), and structure revision of an antioxidant isoflavonoid glabrene. *Nat Prod Lett*. 1997;9(4):289-96.

208) Zeng L, Fukai T, Nomura T, Zhang R-Y, Lou Z-C. Four new prenylated flavonoids, glyasperin A, B, C, and D from the roots of *Glycyrrhiza aspera*. *Heterocyles*. 1992;34(3):575-87.

209) Kinoshita T, Tamura Y, Mizutani K. The isolation and structure elucidation of minor isoflavonoids from licorice of *Glycyrrhiza glabra* origin. *Chem Pharm Bull (Tokyo)*. 2005;53(7):847-9.

210) Zeng L, Fukai T, Nomura T, Zhang R-Y, Lou Z-C. Five new isoprenoid-substituted flavonoids, glyasperins F, G, H, I, and J from the roots of *Glycyrrhiza aspera*. *Heteroycles*. 1992;34(9):1813-28.

211) Shibata S, Saitoh T. The chemical studies on the oriental plant drugs. XIX. Some new constituents of licorice root. (1). The structure of licoricidin. *Chem Pharm Bull*. 1968;16(10):1932–6.

212) Fukai T, Nishizawa J, Yokoyama M, Tantai L, Nomura T. Five new isoprenoid-substituted flavonoids, kanzonols M-P and R, from two *Glycyrrhiza* species. *Heterocycles.* 1994;38(5):1089-98.

213) Fukai T, Nishizawa J, Yokoyama M, Nomura T. Five new isoprenoid-substituted flavonoids, kanzonols F-J, from *Glycyrrhiza uralensis*. *Heterocycles.* 1993;36(11):2565-76.

214) Hatano T, Yasuhara T, Fukuda T, Noro T, Okuda T. Phenolic constituents of licorice. II. Structures of licopyranocoumarin, licoarylcoumarin and glisoflavone, and inhibitory effects of licorice phenolics on xanthine oxidase. *Chem Pharm Bull.* 1989;37(11):3005-9.

215) Xu M-Y, Kim YS. Antitumor activity of glycyrol via induction of cell cycle arrest, apoptosis and defective autophagy. *Food Chem Toxicol*. 2014;74:311-9.

216) Shiozawa T, Urata S, Kinoshita T, Saitoh T. Revised structures of glycyrol and isoglycyrol, constituents of the root of *Glycyrrhiza uralensis*. *Chem Pharm Bull*. 1989;37(8):2239-40.

217) Fukai T, Wang Q-H, Kitagawa T, Kusano K, Nomura T, Iitaka Y. Structures of six isoprenoid-substituted flavonoids, gancaonins F, G, H, I, glycyrol, and isoglycyrol from Xibei licorice (*Glycyrrhiza* sp.). *Heterocycles*. 1989;29(9):1761-72.

218) He J, Chen L, Heber D, Shi W, Lu Q. Antibacterial compounds from *Glycyrrhiza uralensis*. *J Nat Prod*. 2006;69(1):121-4.

219) Schmid C, Dawid C, Peters V, Hofmann T. Saponins from European licorice roots (*Glycyrrhiza glabra*). *J Nat Prod*. 2018;81(8):1734-44.

220) Kitagawa I, Zhou JL, Sakagami M, Taniyama T, Yoshikawa M. Licorice-saponins A3, B2, C2, D3, and E2, five new oleanene-type triterpene oligoglycosides from Chinese Glycyrrhizae radix. *Chem Pharm Bull.* 1988;36(9):3710-3.

221) Kitagawa I, Zhou JL, Sakagami M, Uchida E, Yoshikawa M. Licorice-saponins F3, G2, H2, J2, and K2, five new oleanene-triterpene oligoglycosides from the root of *Glycyrrhiza uralensis*. *Chem Pharm Bull*. 1991;39(1):244-6.

222) Shibano M, Takahashi T, Tlaniguchi M, et al. Three new saponins as index compounds of *Glycyrrhiza flavescens* BOISS. growing in Turkey. *Nat Med*. 2004;58(4):150-5.

223) The Global Cancer Observatory. *Cancer Fact Sheets GLOBOCAN 2018*. Geneva, Switzerland: World Health Organization; 2018. http://gco.iarc.fr/today/data/factsheets/populations/900-world-fact-sheets.pdf Published September 2018. Accessed January 15, 2019.

224) Kroemer G, Galluzzi L, Vandenabeele P, et al. Classification of cell death. *Cell Death Differ*. 2009;16(1):3-11.

225) Liu Y, Liu G, Mei J, Wang J. The preventive effects of hyperoside on lung cancer *in vitro* by inducing apoptosis and inhibiting proliferation through caspase-3 and p53 signaling pathway. *Biomed Pharmacother*. 2016;83:381-91.

226) Thorburn A. Death receptor-induced cell killing. *Cell Signal*. 2004;16(2):139-44.

227) Shyu MH, Kao TC, Yen GC. Oleanolic acid and ursolic acid induce apoptosis in HuH7 human hepatocellular carcinoma cells through a mitochondrial-dependent pathway and downregulation of XIAP. *J Agric Food Chem*. 2010;58(10):6110-8.

228) Hengartner MO. The Biochemistry of apoptosis. *Nature*. 2000;407:770-6.

229) Mohan V, Agarwal R, Singh RP. A novel alkaloid, evodiamine causes nuclear localization of cytochrome-c and induces apoptosis independent of p53 in human lung cancer cells. *Biochem Biophys Res Commun*. 2016;477(4):1065-71.

230) Oren M, Rotter V. Introduction : p53 – the first twenty years. *Cell Mol Life Sci*. 1999;55:9-11.

231) Pucci B, Kasten M, Giordano A. Cell cycle and apoptosis. *Neoplasia*. 2000;2(4):291-9.

232) Bai L, Zhu W-G. p53 : Structure, function and therapeutic applications. *J Cancer Mol*. 2006;2(4):141-53.

233) Gasco M, Shami S, Crook T. The p53 pathway in breast cancer. *Breast Cancer Res*. 2002;4(2):70-6.

234) Sagar S, Esau L, Moosa B, Khashab NM, Bajic VB, Kaur M. Cytotoxicity and apoptosis induced by a plumbagin derivative in estrogen positive MCF-7 breast cancer cells. *Anticancer Agents Med Chem*. 2014;14(1):170-80.

235) Basu A, Haldar S. The relationship between BcI2, Bax and p53: consequences for cell cycle progression and cell death. *Mol Hum Reprod*. 1998;4(12):1099-109.

236) Chen A, Huang X, Xue Z, et al. The role of p21 in apoptosis, proliferation, cell cycle arrest, and antioxidant activity in UVB-irradiated human HaCaT keratinocytes. *Med Sci Monit Basic Res*. 2015;21:86-95.

237) Hawash MMA, Kahraman DC, Eren F, Cetin Atalay R, Baytas SN. Synthesis and biological evaluation of novel pyrazolic chalcone derivatives as novel hepatocellular carcinoma therapeutics. *Eur J Med Chem*. 2017;129:12-26.

238) Vichai V, Kirtikara K. Sulforhodamine B colorimetric assay for cytotoxicity screening. *Nat Protoc*. 2006;1(3):1112-6.

239) Ke N, Wang X, Xu X, Abassi YA. The xCELLigence system for real-time and label-free monitoring of cell viability. In: Stoddart MJ, ed. *Mamalian Cell Viability: Methods and Protocols, Methods in Molecular Biology*. Springer Science Business Media: Humana Press; 2011;740:33-43.

240) Riccardi C, Nicoletti I. Analysis of apoptosis by propidium iodide staining and flow cytometry. *Nat Protoc*. 2006;1(3):1458-61.

241) Gallagher S, Winston SE, Fuller SA, Hurrel JGR. Immunoblotting and immunodetection. *Curr Protoc Immunol*. 2008;83:8.10.1-8.10.28.

242) Sato Y, He J-X, Nagai H, Tani T, Akao T. Isoliquiritigenin, one of the antispasmodic principles of *Glycyrrhiza ularensis* roots, acts in the lower part of intestine. *Biol Pharm Bull*. 2007;30(1):145-9.

243) Yahara S, Ogata T, Saijo R, et al. Isoflavan and related compounds from *Dalbergia odorifera*. I. *Chem Pharm Bull (Tokyo)*. 1989;37(4):979-87.

244) Tahara S, Hashidoko Y, Mizutani J. New 3-methoxyflavones in the roots of yellow lupin (*Lupinus luteus* L. cv. Topaz). *Agric Biol Chem*. 1987;51(4):1039-44.

245) Carnat A-P, Carnat A, Didier F, Lamaison J-L. Violarvensin, a new flavone di-C-glycoside from *Viola arvensis*. *J Nat Prod*. 1998;61(2):272-4.

246) Kamat VS, Chuo F, Kubo I, Nakanishi K. Antimicrobial agents from an East African medicinal plant *Erythrina abyssinica*. *Heterocycles*. 1981;15(2):1163-9.

247) Shih TL, Wyvratt MJ, Mrozik H. Total synthesis of (±)-5-*O*-methyllicoricidin. *J Org Chem.* 1987;52(10):2029-33.

248) Watanabe M, Hayakawa S, Isemura M, et al. Identification of licocoumarone as an apoptosis-inducing component in licorice. *Biol Pharm Bull*. 2002;25(10):1388-90.

249) Guchu SM, Yenesew A, Tsanuo MK, et al. C-methylated and C-prenylated isoflavonoids from root extract of *Desmodium uncinatum*. *Phytochemistry*. 2007;68:646-51.

250) Ahn SJ, Park SN, Lee YJ, et al. *In vitro* antimicrobial activities of 1-methoxyficifolinol, licorisoflavan A, and 6,8-diprenylgenistein against *Streptococcus mutans*. *Caries Res*. 2015;49:78-89.

251) Martins LR, Takahashi JA. Rearrangement and oxidation of β-amyrin promoted by growing cells of *Lecanicillium muscarinium. Nat Prod Res*. 2010;24(8):767-74.

252) Desai AG, Qazi GN, Ganju RK, et al. Medicinal plants and cancer chemoprevention. *Curr Drug Metab*. 2008;9(7):581-91.

253) Tang ZH, Li T, Tong YG, et al. A systematic review of the anticancer properties of compounds isolated from licorice (gancao). *Planta Med*. 2015;81(18):1670-87.

254) Vlaisavljević S, Šibul F, Sinka I, Zupko I, Ocsovszki I, Jovanović-Šanta S. Chemical composition, antioxidant and anticancer activity of licorice from Fruska Gora locality. *Ind Crops Prod*. 2018;112:217–24.

255) Zhou J-X, Wink M. Reversal of multidrug resistance in human colon cancer and human leukemia cells by three plant extracts and their major secondary metabolites. *Medicines (Basel)*. 2018;5(4):123. doi:10.3390/medicines5040123.

256) Deng L, Shi AM, Wang Q. Sedative–hypnotic and anxiolytic effects and the mechanism of action of aqueous extracts of peanut stems and leaves in mice. *J Sci Food Agric*. 2018;98(13):4885-94.

257) Wang Q, Miao W, Xiang C, Guo D, Ye M. Chemical constituents in flavonoids from root of *Glycyrrhiza uralensis*. *Zhongcaoyao*. 2014;45(1):31-6.

258) Botta B, Vitali A, Menendez P, Misiti D, Monache GD. Prenylated flavonoids: pharmacology and biotechnology. *Curr Med Chem*. 2005;12(6):717-39.

259) Veitch NC. Isoflavonoids of the Leguminosae. *Nat Prod Rep*. 2013;30(7):988-1027.

260) Tahara S, Ibrahim RK. Prenylated isoflavonoids. *Phytochemistry*. 1995;38(5):1073-94.

261) Barron D, Ibrahimt RK. Isoprenylated flavonoids- A survey. *Phytochemistry*. 1996;43(5):921-82.

262) Ohno H, Araho D, Uesawa Y, et al. Evaluation of cytotoxiciy and tumor-specificity of licorice flavonoids based on chemical structure. *Anticancer Res*. 2013;33(8):3061-8.

263) Zhang E, Yin S, Lu X, Ye L, Fan L, Hu H. Glycycoumarin sensitizes liver cancer cells to ABT-737 by targeting De Novo lipogenesis and TOPK-survivin axis. *Nutrients.* 2018;10(3):353. doi:10.3390/nu10030353.

264) Hsieh M-J, Chen M-K, Chen C-J, et al. Glabridin induces apoptosis and autophagy through JNK1/2 pathway in human hepatoma cells. *Phytomedicine*. 2016;23(4):359-66.

265) El-Halawany AM, Osman SM, Abdallah HM. Cytotoxic constituents from *Vicia monantha* subsp. *monantha* seeds. *Nat Prod Res*. 2018;7:1-4.

266) Montazeri M, Sadeghizadeh M, Pilehvar-Soltanahmadi Y, et al. Dendrosomal curcumin nanoformulation modulate apoptosis-related genes and protein expression in hepatocarcinoma cell lines. *Int J Pharm*. 2016;509(1–2):244-54.

267) Kasibhatla S, Amarante-Mendes GP, Finucane D, Brunner T, Bossy-Wetzel E, Green DR. Staining of Suspension Cells with Hoechst 33258 to Detect Apoptosis. *Cold Spring Harb Protoc*. 2006;2006(3):prot4492.

268) Agrawal S, Dhruv K, Meshram S. P53 : The guardian of genome, apoptosis, and its role in carcinogenesis. *Eur J Biomed Pharm Sci*. 2018;4(2):161-6.

269) He S, Liu H, Zhou Y, Yue Q. Liquiritin (LT) exhibits suppressive effects against the growth of human cervical cancer cells through activating caspase-3 *in vitro* and xenograft mice *in vivo*. *Biomed Pharmacother*. 2017;92:215-28.

270) Çevik D, Yılmazgöz ŞB, Kan Y, et al. Bioactivity-guided isolation of cytotoxic secondary metabolites from the roots of *Glycyrrhiza glabra* and elucidation of their mechanisms of action. *Ind Crops Prod*. 2018;124:389-96.

7. CURRICULUM VITAE

Personal Information

Name	Dicle	**Surname**	Çevik
Place of birth	Zonguldak	**Date of birth**	01/01/1991
Nationality	TR	**ID No**	59107495752
E-mail	dicledemir@windowslive.com	**Phone**	+905375817631

Education

Level	Proficiency	Institution	Graduation Year
Ph.D.	Pharmacognosy	Yeditepe University	2019
B.A.	Faculty of Pharmacy	Yeditepe University	2014
	Faculty of Economics and Administrative Sciences –Business Administration Minor Programme	Yeditepe University	2014
High School	-	TED Zonguldak College	2009

Language Skill

Language	Exam Degree
English	YÖKDİL (17/03/2018): 96,250

Work Experience

Position	Institution	Dates
Research and teaching assistant	Yeditepe University Faculty of Pharmacy	2014-2018

Computer Skills

Programs	Degree
Microsoft Office	Very good
MestReNova	Very good
Mendeley	Very good
ChemOffice	Very good

Scientific Works

Publications in SCI, SSCI, AHCI Indexed Journals

Kırmızıbekmez H, Demir D. "Iridoid Glycosides and Phenolic Compounds from the Flowers of *Vitex agnus-castus." Helvetica Chimica Acta.* 2016; 99: 518 – 522.
Çevik D, Yılmazgöz ŞB, Kan Y, Güzelcan EA, Durmaz I, Çetin-Atalay R, Kırmızıbekmez H. "Bioactivity-Guided Isolation of Cytotoxic Secondary Metabolites From the Roots of *Glycyrrhiza glabra* and Elucidation of Their Mechanisms of Action." *Industrial Crops & Products.* 2018; 124: 389 – 396.
Çevik D, Kan Y, Kırmızıbekmez H. "Mechanisms of Action of Cytotoxic Phenolic Compounds from *Glycyrrhiza iconica* Roots." *Phytomedicine.* In press.

International Conference Proceedings

Dicle Demir, Yüksel Kan, Hasan Kırmızıbekmez. "Cytotoxic Phenolic Compounds from *Glycyrrhiza iconica."* Trends in Natural Product Research – Phytochemical Society of Europe (PSE) Young Scientists' Meeting, Lille, 2017.
Dicle Demir, Ş. Burçin Yılmazgöz, Yüksel Kan, Irem Durmaz, Rengül Çetin-Atalay, Hasan Kırmızıbekmez. "Bioactivity-Guided Isolation of Cytotoxic Secondary Metabolites From the Roots of *Glycyrrhiza glabra.*" Trends in Natural Product Research – Phytochemical Society of Europe (PSE) Young Scientists' Meeting, Lille, 2017.

Projects & Certificates

Scholarship in 1001 TUBİTAK Project (115S433) *"Glycyrrhiza glabra* ve *G. iconica* bitkilerinden sitotoksik etkili bileşiklerin izolasyonu ve etki mekanizmalarının araştırılması",* 2015- 2017.
Certificate of Participitation to Trends in Natural Product Research – Phytochemical Society of Europe (PSE) Young Scientists' Meeting – *Lille, June 2017*
Certificate of Participation to 5th EPSA Science Day – *Catania, April 2013*
Certificate of Participation to 36th EPSA Annual Congress in Catania – *Catania, April 2013*
Certificate of Participation to IPSF Student Exchange Programme – *Hungary, August 2012*
Certificate of Participation to 35th EPSA Annual Congress in Istanbul – *İstanbul, Reception committee member, April 2012*